Western University
Scholarship@Western

Digitized Theses | Digitized Special Collections

1984

Geochemistry And Petrogenesis Of Some Granitoids In The Grenville Province Of Ontario And Their Tectonic Implications

Tsai-way Wu

Follow this and additional works at: https://ir.lib.uwo.ca/digitizedtheses

Recommended Citation
Wu, Tsai-way, "Geochemistry And Petrogenesis Of Some Granitoids In The Grenville Province Of Ontario And Their Tectonic Implications" (1984). *Digitized Theses*. 1385.
https://ir.lib.uwo.ca/digitizedtheses/1385

This Dissertation is brought to you for free and open access by the Digitized Special Collections at Scholarship@Western. It has been accepted for inclusion in Digitized Theses by an authorized administrator of Scholarship@Western. For more information, please contact tadam@uwo.ca, wlswadmin@uwo.ca.

The author of this thesis has granted The University of Western Ontario a non-exclusive license to reproduce and distribute copies of this thesis to users of Western Libraries. Copyright remains with the author.

Electronic theses and dissertations available in The University of Western Ontario's institutional repository (Scholarship@Western) are solely for the purpose of private study and research. They may not be copied or reproduced, except as permitted by copyright laws, without written authority of the copyright owner. Any commercial use or publication is strictly prohibited.

The original copyright license attesting to these terms and signed by the author of this thesis may be found in the original print version of the thesis, held by Western Libraries.

The thesis approval page signed by the examining committee may also be found in the original print version of the thesis held in Western Libraries.

Please contact Western Libraries for further information:
E-mail: libadmin@uwo.ca
Telephone: (519) 661-2111 Ext. 84796
Web site: http://www.lib.uwo.ca/

CANADIAN THESES ON MICROFICHE

I.S.B.N.

THESES CANADIENNES SUR MICROFICHE

National Library of Canada
Collections Development Branch

Canadian Theses on
Microfiche Service

Ottawa, Canada
K1A 0N4

Bibliothèque nationale du Canada
Direction du développement des collections

Service des thèses canadiennes
sur microfiche

NOTICE

The quality of this microfiche is heavily dependent upon the quality of the original thesis submitted for microfilming. Every effort has been made to ensure the highest quality of reproduction possible.

If pages are missing, contact the university which granted the degree.

Some pages may have indistinct print especially if the original pages were typed with a poor typewriter ribbon or if the university sent us a poor photocopy.

Previously copyrighted materials (journal articles, published tests, etc.) are not filmed.

Reproduction in full or in part of this film is governed by the Canadian Copyright Act, R.S.C. 1970, c. C-30. Please read the authorization forms which accompany this thesis.

THIS DISSERTATION
HAS BEEN MICROFILMED
EXACTLY AS RECEIVED

AVIS

La qualité de cette microfiche dépend grandement de la qualité de la thèse soumise au microfilmage. Nous avons tout fait pour assurer une qualité supérieure de reproduction.

S'il manque des pages, veuillez communiquer avec l'université qui a conféré le grade.

La qualité d'impression de certaines pages peut laisser à désirer, surtout si les pages originales ont été dactylographiées à l'aide d'un ruban usé ou si l'université nous a fait parvenir une photocopie de mauvaise qualité.

Les documents qui font déjà l'objet d'un droit d'auteur (articles de revue, examens publiés, etc.) ne sont pas microfilmés.

La reproduction, même partielle, de ce microfilm est soumise à la Loi canadienne sur le droit d'auteur, SRC 1970, c. C-30. Veuillez prendre connaissance des formules d'autorisation qui accompagnent cette thèse.

LA THÈSE A ÉTÉ
MICROFILMÉE TELLE QUE
NOUS L'AVONS REÇUE

GEOCHEMISTRY AND PETROGENESIS OF SOME GRANITOIDS IN THE GRENVILLE PROVINCE OF ONTARIO AND THEIR TECTONIC IMPLICATIONS

(VOLUME I)

by

Wu Tsai-Way

Department of Geology

Submitted in partial fulfillment
of the requirements for the degree of
Doctor of Philosophy

Faculty of Graduate Studies
The University of Western Ontario
London, Ontario

May, 1984

© Wu Tsai-Way 1984.

ABSTRACT

Samples taken from eight granitic bodies (Algonquin Batholith, Union Lake Pluton, Elphin Complex, Cheddar Granite, Mulock Batholith, Coe Hill Granite, Deloro Pluton and Barber's Lake Granite) from the Grenville Province of Ontario have been petrographically and geochemically studied. It is believed that these granitoids were associated with the Grenville Orogeny and have recorded a history of about 300 million years of magmatism in this region.

Modal compositions of sampled granitoids range from diorite-gabbro, quartz diorite - tonalite - trondhjemite, monzonite - syenite and granite (adamellite). Except for the riebeckite-bearing hypersolvus granite of the Deloro Pluton, hornblende and biotite are major mafic minerals for the other subsolvus granitoids.

Chemically, as expected from the mode, most of the sampled granitoids are metaluminous with the exceptions of the Deloro Pluton (peralkaline) and the Barber's Lake Granite (peraluminous). Although chemical compositions are varied from one pluton to the other (eg. enrichment of thorium and uranium in Barber's Lake Granite, HFS elements anomalies of the Cheddar Granite and Deloro Pluton and high concentrations of F - Cl in Elphin Complex), the Grenville granitoids are characterized, in general, by high agpaitic indices and oxidation ratios.

Except that the Union Lake Pluton (tonalite - trondhjemite suite) is consistently I-type granite and the Barber's Lake Granite is close to S-type granite, the remaining Grenville granitoids fall within both I- and S-type categories. However, the peralkaline Deloro Pluton is an A-type analoque. It is reasonable to assume that the source rocks, P-T conditions and geological settings of the Grenville granitoids differ from those granites of the Lachlan Mobile Belt of eastern Australia. Particularly, the abundances of syenitic - monzonitic phases in the Grenville granitoids are uncommon for granitoids from an orogenic belt. REE modelling indicates most Grenville granitoids were from a deep source, either lower crust (granulite) or upper mantle (quartz eclogite). This is consistent with their lower $^{87}Sr/^{86}Sr$ initial ratios (< 0.706, in general) and higher K/Rb ratios.

The similarities between New England plutonic rocks, mainly alkaline granite, and sampled Grenville granitoids suggest a comparable geological setting, either zones of transform fault or zones of rifting. Further, the close resemblance with the Younger Granite of Nigeria from an extensional environment may imply the existence of a long term extensional regime during the development of Grenville plutonism. This hypothesis agrees well with the Grenville evolution model of opening and closing of the Bancroft - Renfrew aulacogen; thus, the Grenville granitic terrain may be interpreted as products of Proterozoic "extension - contraction" cycles.

ACKNOWLEDGEMENTS

I am sincerely indebeted to Dr. N. D. MacRae, my thesis supervisor, for suggesting this topic and providing constant encouragement, simulation and finacial support. I am grateful to Dr. S. B. Lumbers for providing thin sections, rock samples and valuable discussions of the Algonquin Batholith. I specially thank Dr. C. Pride for much appreciated guidance and assistance in constructing the intrumental neutron activation lab, Dr. A. Hayatsu and Dr. A. Beck for permission to use the gamma-ray spectrometry facilities, Dr. S. Haynes for expertise in obtaining accurate F - Cl analyses and Dr. R. Kerrich for carrying out oxygen isotope analyses. I also thank Mr. G. W. Camero for helping calibrate the portable scintilator, Mr. R. L. Barnett for assistance in electron microprobe analyses, and Mr. J. Forth for preparation of thin and probe sections. I also would like to thank many of my fellow graduate students, particularly R. Epstein, G. Somers, D. Barbery and R. Tronnes for contributing to my understanding of granitic magmatism.

I especially thank Oi-Lun Wu, my wife, for her patience, encouragement and diligence in typing this manuscript. I would also like to remember my parents who provided a particular sense of purpose to my study.

TABLE OF CONTENTS

* * * * * * * * * * * * *

LIST OF TABLES

* * * * * * * * * * *

LIST OF FIGURES

Chapter I. INTRODUCTION

1.0 REGIONAL GEOLOGY

1.1 General Statement

The Grenville Province is the southernmost structural provinces of the Canadian Shield (Fig. 1-1). The northeast-trending Grenville Front Boundary Fault of both ductile and brittle deformation (Lumbers, 1978), separates the relatively lower grade metamorphic supercrustal rocks of the Superior and Southern Provinces to the northwest from the high grade gneisses of the Grenville Province to the southeast. The Grenville Province is unconformably overlain by the undeformed Paleozoic rocks of the St. Lawrence Plateform; but it extends across the international boundary into New York State along the Frontenac Axis (Fig. 1-2).

The Grenville Province has long been recognized as a structural entity, on the basis of its uniform isotopic ages, patterns of deposition and erosion, pervasive plutonism, as well as penetrative metamorphic and structural imprints of its unique tectonic evolution (Wynne-Edwards, 1972).

As Lumbers (1982) stated, "The Grenville Province of Ontario is underlain by a variety of supercrustal and

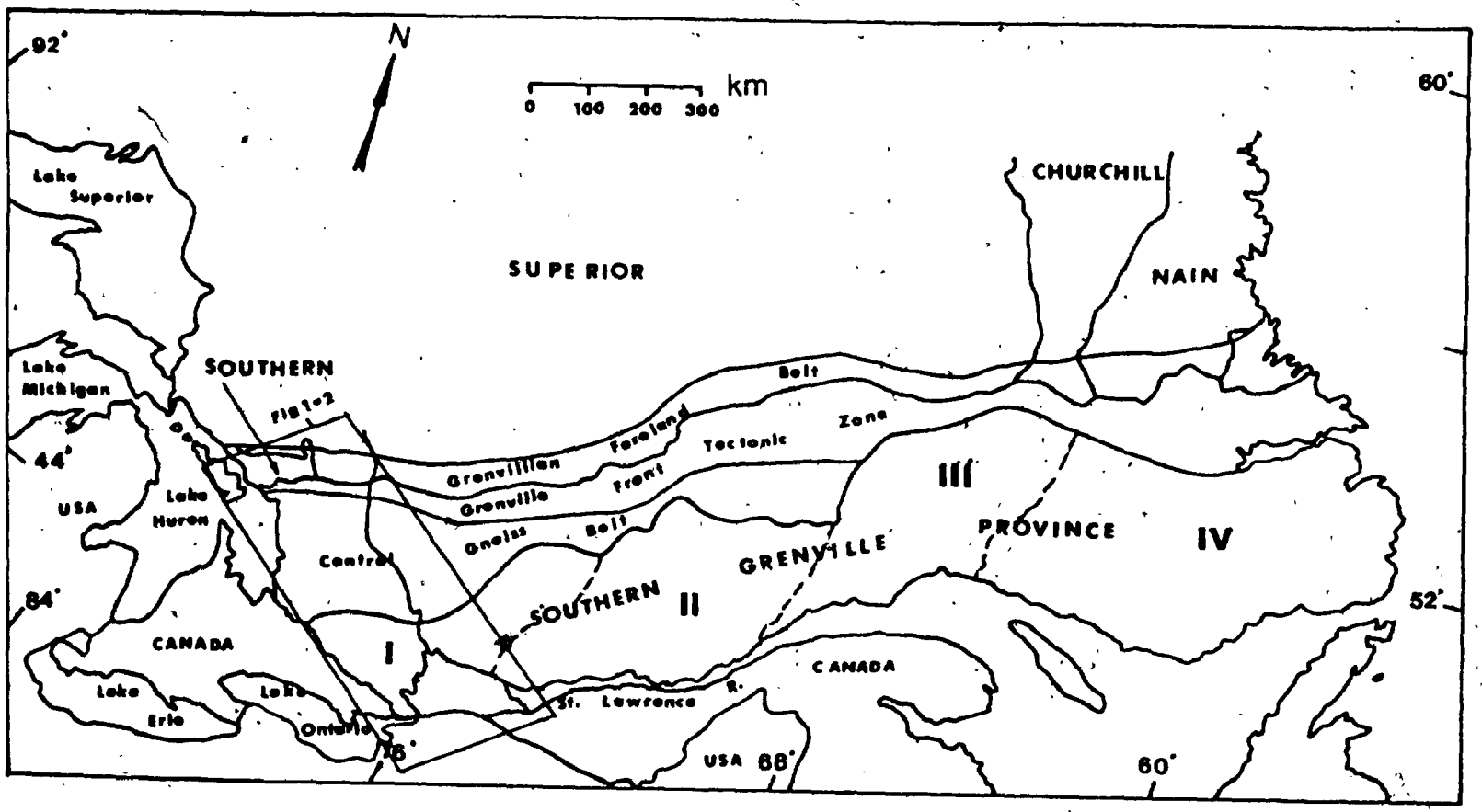

Figure 1-1. Major tectonic subdivisions of the Grenville Province of Canada (Wynne-Edwards, 1972).

Southern Grenville Province : I. Central metasedimentary belt

II. Central granulite terrain

III. Baie Comeau Segment

IV. Eastern Grenville Province

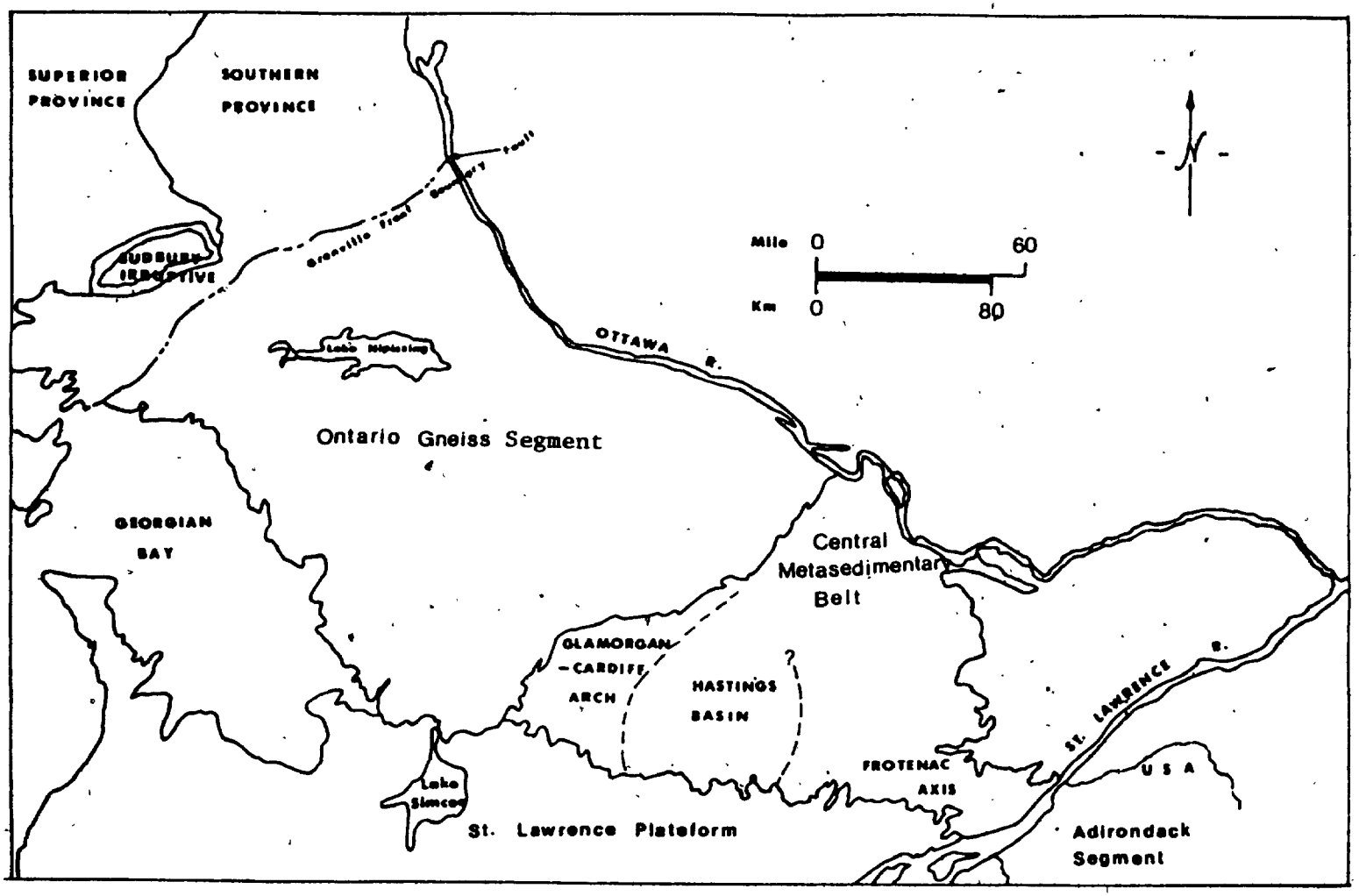

Figure 1-2. Major geological features of the Grenville Province of Ontario (Wynne-Edwards, 1972).

plutonic rocks that reflect a long, complex geological history spanning more than 2.0 Ga".

Southeast of the boundary fault zone, the Grenville Province can be divided into two distinct lithological and structural complexes, namely: (1) the Ontario Gneiss Segment, (2) the Central Metasedimentary Belt, which includes the Glamorgan - Cardiff Segment, the Hastings Basin and the Frontenac Axis (Wynne-Edwards, 1972).

Based on recent detailed mapping and stratigraphic correlation in eastern Ontario, Moore (1982) proposed that the Central Metasedimentary Belt is a "discrete orogen", which can be further subdivided into:

1. the Bancroft Terrain (mainly carbonates),
2. the Elzevir Terrain (dominately volcanic rocks overlain by carbonates),
3. the Sharbot Lake Terrain (mainly carbonates),
4. the Frontenac Terrain (heterogeneous gneisses and marbles).

Boundaries between terrains are abrupt and probably tectonic; they are oriented north-northeasterly and are not parallel to the Grenville Front.

1.2 Deposition And Stratigraphy

Although most of the supercrustal rocks of the Grenville Province have been entirely eroded, two main accumulations of contrasting age and lithology have been identified in Ontario (Lumbers, 1982).

The older accumulation, deposited during Middle Precambrain time (2.5 Ga to 1.8 Ga), occupied the northern two-thirds of the Province and consisted mainly of clastic siliceous metasediments with a possible submarine fan environment (Lumbers, 1982). Coarse deep water turbidite deposits, which overlie the Archean basement unconformably, gradually change southeasterly into well-sorted arkose and orthoquarzite of shallow water environment. Some of these supercrustal rocks are correlated with the lower part of the Huronian Supergroup in Southern Province (eg. the Sudbury-Espanola area). The original stratigraphic sequence and regional correlation could not be established due to Late Precambrian high grade metamorphism and recrystallization.

The younger accumulation associated with the major volcanism, which is referred to the "Grenville Supergroup", was deposited during the early Late Precambrain about 1300 Ma ago (Lumbers, 1967). It is exposed in eastern Ontario and western Quebec and is composed predominantly of marbles, calcareous

metasediments, subordinate clastic siliceous metasediments and local thick metavolcanic sequences. The thickest accumulation of this kind is exposed in the Hastings Basin and surrounding areas, which coincides with the only region of low grade metamorphism so far identified in the Grenville Province (Lumbers, 1967; Sampson, 1972).

Five major stratigraphic sequences have been verified and correlated on a regional scale. In ascending order, they are:

1. the Anstruther Lake Group (Bright, 1976) consisting mainly of arenaceous metasediments, with minor biotite-rich quartzofeldspathic gneiss;

2. the Hermon Group (Hewitt and James, 1955) consisting of units of pelitic schist, paragneiss, calcareous metasediments and thick formations of metavolcanic rocks of mafic pillow lavas and silicic pyroclasts;

3. the Mayo Group (Hewitt and James, 1955) is composed dominantly of marbles, siliceous limestones with minor calcareous arenite;

4. the Flinton Group (Moore and Thompson, 1972) is composed of a basal formation of red beds, quarztite conglomerate and shale following

upwards with predominant dolostone and limestone, as well as thin-bedded black shale and calcareous sandstone.

The boundary between the Anstruther Lake Group and the Hermon Group is thought to be concordant (Bright, 1980); the contact between the Hermon Group and the Mayo Group is locally interfingered and thought to be age-equivalent within the Hastings Basin (Lumbers, 1967).

The Flinton Group truncates contacts between metavolcanics of the Hermon Group and the metamorphosed Elzevir and Northbrook plutons. The relationship between the Mayo and Flinton Groups is not clear; however, "there is a close association of dolostone conglomerate with a thick carbonate unit below the uncomformity" (Moore and Thompson, 1972).

For most of the area, the Frontenac Axis of Ontario is underlain by high grade metamorphic rocks assigned to the Grenville Supergroup on the basis that one of the most abundant lithologies is marble. It is associated with quartzite, diopside granulite and grey, quartz-oligoclase gneiss which is thought to be the basement of the Grenville Supergroup (Wynne-Edwards, 1967) in the Frontenac Axis region. The Algonquin Batholith underlies the central portion of the Grenville

Province of Ontario. It intruded rocks of the older accumulation and is overlain unconformably by rocks of the Grenville Supergroup (eg. the Anstruther Lake Group of Bright, 1976) along its southern flank.

The Parry Sound Domain, adjacent to the western flank of this Batholith , consists of continuous zones of various tectonites of possible allochthonous origin. There are relatively higher pressure mineral assemblages in the inclusions indicating that shearing and thrusting occurred at a deep crustal level (Davison and Morgan, 1981; Davison et al., 1982).

A second, thinner accumulation of metavolcanics and marble existing within the Middle Precambrian Gneiss Segment extends northward from Parry Sound to south of Lake Nipissing and may be correlative with those of the carbonate-rich phase in the Hastings Basin.

1.3 Metamorphic And Structural Style

Nearly all the structural fabrics and metamorphic style in the Grenville Province are the product of the Late Precambrian tectono-metamorphic event (Grenville Orogeny). Although most of the Grenville Province is characterized by a prevailing regional metamorphism up to almandine amphibolite facies, there are differences in degree and type of metamorphism among the segments.

The Grenville Front Boundary Fault itself marks an abrupt metamorphic discontinuity, the predominant aluminosilicate kyanite indicating high pressure metamorphism. Barrovian-type (intermediate pressure) metamorphism with sillimanite as the common aluminosilicate occurs throughout most of the Grenville Province.

Metamorphic grade in the Ontario Gneiss Segment is generally upper amphibolite facies. Some evidence has suggested that the older accumulation near the northwest margin of this segment was affected by the Penokean event (Lumbers, 1978). Local hypersthene-bearing rock in the Algonquin Batholith contains primary igneous texture and is interpreted to be intrusive in origin rather than to be indicative of granulite facies metamorphism (Lumbers, 1982).

In the Central Metasedimentary Belt of Ontario, metamorphic grade decreases southeastward from amphibolite facies in the Glarmorgan - Cardiff Segment to greenschist facies in the Hastings Basin, and increases sharply again towards the Frontenac Axis, reaching two-pyroxene granulite facies.

The average temperature of metamorphism was about 700 ^{o}C; and the common mineral assemblages in the amphibolite facies suggest a pressure of 6 kb, equivalent to a depth of 15 km prior to erosion

(Wynne-Edwards, 1972).

Both the gneiss terrain and supercrustal rocks have been penetratively deformed. Strong northeast-trending foliations and zones of cataclasis are evident along the Grenville Front, but not always apparent in other segments of the Province. Northwesterly foliations and structures are common in the northwestern part of the Ontario Gneiss Segment; while north to northeasterly foliations and fold axes predominate in the Central Metasedimentary Belt.

2.0 TIMING OF THE GRENVILLE OROGENY

The "Grenville Orogeny" is defined as a major metamorphic, tectonic and plutonic event that took place within the Greville Province around 1000 Ma ago. Although the Grenville Province has prevailing mineral K-Ar closure dates of 900 ± 100 Ma (MacIntyre et al., 1967), the U-Pb isotopic measurements on zircons (Silver and Lumbers, 1966) and the Rb-Sr whole-rock isochron studies (Krogh and Hurley, 1968) have shown that the time of Grenvillian tectono - metamorphism is consistently about 150 Ma older than the corresponding K-Ar values. Therefore, the reliable age of the culmination of the Grenville Orogeny would be around 1000 ± 100 Ma ago. However, "Grenville Orogeny does not define a time-interval, but an event or events that occurred within a time-interval" (Wynne-Edwards, 1967).

The older accumulation, likely the prolongation of the Huronian Supergroup, overlies the Archean Basement and deposited during the Aphebian time, prior to 1800 Ma. It was intruded by the Algonquin Batholith which appears to be associated with a major magmatic event throughout the North American continent at about 1400 - 1500 Ma (Lumbers, 1982). The younger supercrustal rocks were deposited unconformably on the southern edge of the batholith and did not start until about 1300 Ma ago (Mid-Helikian) (Lumbers, 1967).

About 1300 Ma ago major volcanism occurred along the northwestern portion of the southern (mio)geosyncline. Mafic to intermediate pillow lavas, and volcaniclastic debris formed aprons of turbidite deposits around the volcanic highland (Lumbers, 1982). The metavolcanic rocks of the Tudor Formation (the lower part of Hermon Group) were dated by U-Pb method on zircons at about 1310 $\pm$ 15 Ma (Silver and Lumbers, 1966). Rhyolites from the Burnt Lake Formation (the top of Hermon Group) have a model U-Pb zircon age of 1250 $\pm$ 25 Ma (Lumbers, 1967). The carbonate facies was deposited both during and after the volcanism.

The major metamorphic and tectonic event of the Grenville Orogeny affected the Province, especially the region of Grenville Supergroup, around 1150 Ma ago (Silver and Lumbers, 1965, U-Pb zircon date). It produced amphibolite facies regional metamorphism, pervasive plutonism and the northerly to northeasterly structural grains in southeastern Ontario.

Based upon geochronological data, four periods of Grenvillian tectonic activity occurred during the time from 1400 Ma to 700 Ma ago: (1) around 1300 Ma marked the peak for the pre-tectonic stage, (2) 1150 Ma for the syn-tectonic stage and (3) 950 Ma for the late-tectonic stage (Baer, 1981a). The post-Grenvillian tectonism may be recognized as late activity along the Ottawa - Bonnechere Graben of the St. Lawrence Rift System which was probably initiated earlier in Archean time (Lumbers, 1982).

Except for the post-tectonic stage, each period is characterized by its own "structural regim" suggested by the structural elements present in the Province. In the pre-Grenvillian history prior to 1800 Ma, an early deformation (Hudsonian) along the northeast-trending axis parallel to the Grenville Front, caused development of tight overturned folding and local high grade metamorphism. A second phase of this deformation produced north to nothwest-trending fold axes in the Grenville Province (Baer, 1981a).

The pre-tectonic activity of the Grenville Orogeny corresponds to an extensional regime and is characterized by the intrusion of alkaline plutons, and the formation of rift-systems (eg. the nepheline-syenite of Bancroft). At the syn-tectonic stage, a north to northeast-trending fabric at high angle to the Grenville Front was produced by northwesterly shortening. The third phase corresponds to thrusting and block uplift in the Grenville Front zone and a

general thickening of the crust. About 800 Ma ago, the differential stress was no longer able to deform the Canadian Shield on a regional scale (Baer, 1981a).

The systematically lower values of K-Ar mineral dates than the corresponding Rb-Sr whole-rock isochrons have been explained by the different blocking temperatures for ^{40}Ar and ^{87}Sr loss from different minerals. Most Grenville geologists favour the interpretation of a slow cooling history (6 - 10°C per Ma) after the orogenic event of around 1100 Ma ago. In addition, Harper (1967) used K-Ar dates of biotite from granitic gneisses of the Grenville Province to construct the "metamorphic veil" (Amstrong, 1966). He interpreted the subparallel and southeasterly dipped contours (or "thermochrons") as being due to different times of uplifting and cooling of the Grenville craton and not the age of metamorphism.

Baer (1981a) argued that the K-Ar dates in the 900 - 950 Ma range are widely distributed in the Province, but 1050 - 1100 Ma Rb-Sr whole-rock ages and U-Pb zircon dates are concentrated only in the southern part of the Province. The absence of 1100 Ma dates in the northern portion of the Province may indicate that 950 Ma dates represent an independent thermotectonic event rather than the end of a long cooling phase.

In addition, uraniferous pegmatites from Bancroft, Mont Laurin and Johan Beetz areas yielded Rb-Sr isochron ages of

950 ± 25 Ma, whereas the surrounding syntectonic granitic plutons dated from 1200 to 1100 Ma (Fowler and Doig, 1979, 1983) by the same method. Fowler (1980) excluded the possibility that the uraniferous granite pegmatites were formed by in-situ anatexis of the pre-existing Grenville Supergroup during the peak of the Grenville Orogeny. Therefore, two Grenvillian events are proposed by Baer (1981b):

1. the older event, the Morin Event (named after the deformation of Morin anorthosite about 1100 to 1050 Ma), would be of more restricted extent but greater intensity to give a common north to northeasterly structural grain in the Central Metasedimentary Belt;

2. the younger event, the Grenvillian Event (sensu stricto, about 950 Ma), would have affected the whole province but of lesser intensity.

3.0 IGNEOUS ROCKS AND PLUTONISM

A great variety of igneous rocks, from non-granitic to granitic intrusions and from mafic to felsic volcanic rocks, are exposed within the Province. There are differences of spatial distribution, variations of temporal magmatism, contrasts in degree of deformation and complexity of genetic relationship.

The major igneous rocks in the Grenville Province can be generally grouped into: (1) volcanic rocks, (2) anorthosite massives, (3) alkalic intrusions, (4) granitic plutons. Gabbroic and dioritic rocks are less important and form smaller discrete bodies or are associated with larger plutonic complexes.

3.1 Volcanic Rocks

The stratified (meta)volcanic rocks of the Grenville Supergroup extend from southeastern Ontario to southwestern Quebec for more than 200 miles. This extensive metavolcanic-metasedimentary belt has been referred to as the "Ottawa River Remnant" (Lumbers, 1967).

The volcanic rocks extruded into a carbonate marine basin in which the metasediments were deposited. Extrusion, erosion and deposition activities may have continuously carried on for a span of 50 Ma and to a maximum thickness of 27,000 ft around the Hastings Basin area (Lumbers, 1967). The limited extent of volcanic sequences of the Grenville Province as a whole may indicate a local volcanic event in which the volcanic terrain was concentrated in southeastern Ontario and southwestern Quebec.

The composition of the Grenville volcanic rocks range from mafic pillow basalt to pyroclastic rocks of

rhyolitic, dacitic composition. A detailed geochemical study of stratified volcanic sequence in the vicinity of Bishop Corners, Ontario has been reported by Condie and Moore (1977). The lower section is composed of low-K, pillowed tholeiite and the upper part consists mainly of andesites and dacites (classification of Condie, 1976).

Geochemical data indicate that the Grenville tholeiites are similar to Archean counterparts both in major and trace element compositions, except that the former has higher FeO/Fe_2O_3 and K/Rb ratios. They are interpreted to represent an immature, emerging arc system associated with a convergent plate boundary (Condie and Moor, 1977; Brown et al., 1975; Sethuraman and Moore, 1973). Average compositions of Grenville andesite and dacite bear a strong resemblance to modern calc-alkaline andesite from a mature arc system.

3.2 Anorthosite Massives

In addition to the coherent radiometric dates, the high grade regional metamorphism and pervailing structural grain, the anorthosite massives are another distinctive feature of the Grenville Province. However, anorthosites do not occur in all parts of the Province; the Chibougamau - Gatineau lineament coincides with the western limit of extensive outcrops of anorthosite bodies (Baer, 1981a).

In Ontario the smaller, discrete anorthosite plutons are confined to the northwestern portion of the Ontario Gneiss Segment, in particular the Parry Sound Domain. In addition, anorthositic and related mafic rocks occur in the Algonquin Batholith.

Emplacement of anorthosite suites in Laborador and eastern Grenville Province is well dated at about 1400 to 1500 Ma by the U-Pb method on zircons (Krogh and Davis, 1973), while the time of emplacement of anorthositic plutons in central and western portions of the Province is about 1100 to 1150 Ma as related by both Rb-Sr isochron and U-Pb zircon ages (Silver, 1969; Barton and Doig, 1977). Thus, relative to the culmination of the Grenville Orogeny, the anorthosite plutonism is a pre-tectonic (pre-Grenvillian) to perhaps early syn-tectonic event.

3.3 Alkaline Intrusions

Nepheline-bearing syenite and nepheline-bearing gabbros occur in a narrow zone along the boundary between the Ontario Gneiss Segment and the Central Metasedimentary Belt which is well-documented in the Haliburton-Bancroft area. Small bodies of carbonatite are also scattered in the area.

The igneous vs. metamorphic origin of the nepheline-bearing rocks in the Haliburton-Bancroft

region has been argued for years. Adams and Barlow (1910) noted an intimate relation between the nepheline-bearing syenite, granite and crystalline limestone and suggested that the nepheline rocks are products of assimilation between the granite intrusion and the limestone wallrock. Later detailed remapping of these classic area found a group of igneous-textured nepheline rocks including types of theralite and canadite not previously recognized. These discoveries favour the recent view that the nepheline rocks are crystallized from an undersaturated magma (Gittins, 1967).

The Blue Mountain nepheline syenite has been dated at 1285 ± 41 Ma by Rb-Sr whole-rock isochron (Krogh and Hurley, 1968); the mafic nepheline gneiss of the Haliburton-Bancroft area at 1225 ± 3 Ma (U-Pb zircon age), and the nepheline syenite of the same region yielded 1187 ± 20 Ma by Rb-Sr isochron age (Miller and Gittins, 1982). Time of emplacement of nepheline plutons in southern Ontario is likely pre-orogenic and/or continued just before the syn-Grenvillian event.

Alkalic complexes of Cambrian age (K-Ar dates of 560 Ma, Currie, 1976) are also abundant and extend throughout the entire Grenville Province; for example, the Nipissing Alkaline Province (Ontario) consists of at least seven distinct plutonic complexes. These complexes are characterized by vigorous fenitization

with the country rocks and strong enrichment of Nb, U, rare elements and Fe. By contrast, the pre-tectonic alkaline province in the Haliburton-Bancroft area is characterized by its mineralogical simplicity rather than by rare mineral or element concentrations.

3.4 Granitic Plutons

In a broad sense, granite is "a holocrystalline coarse-grained rock of plutonic aspect composed of essentially quartz, potash feldspar and/or sodic plagioclase and subordinate biotite" (Turner and Verhoogan, 1969) or "any holocrystalline, quartz-bearing plutonic rocks" (AGI, 1972). Thus, granite (sensu lato) will consist of plutonic rocks ranging from quartz diorite, trondhjemite, tonalite, granodiorite to granite (sensu stricto).

An unusual geological feature of the Grenville Province is the great abundance of granitic intrusions --- "a sea of granite", according to Wynne-Edwards (1972).

Based upon recent compiled data on plutonic rocks in Ontario (McCrank et al., 1980), the 266 identified plutons in the Grenville Province, Ontario classified by rock type : granite (sensu lato) comprises 62% of the plutons, gabbro 18%, alkalic rocks 15% and anorthosite 5%.

Although granitic plutons vary greatly in composition and relative age, Lumbers (1982) has divided most of the granitic rocks in the Grenville Province, Ontario, into five major suites based on petrologic observation and average modal composition. Genetic implications are also reflected by the variation of chemistry and mineralogy within each suite.

In the order of ascending age of intrusion, they are:

1. the <u>biotite diorite suite</u> is characterized by larger plutonic complexes predominantly of trondhjemite, granodiorite and sodic granite-syenite. It may be further subdivided into (1) albite granite-syenite group, (2) diorite group, and (3) trondhjemite and sodic granite group (Lumbers, 1967). This suite forms a distinct age group at about 1250 $\pm$ 25 Ma (Silver and Lumbers, 1966).

2. the <u>anorthosite suite</u> is composed of anorthositic and tonalitic rocks and associated monzonitic and syenitic rocks. Most of the discrete anorthosite plutons are distributed in the northwestern portion of the Ontario Gneiss Segment, ranging in age from 1500 to 1100 Ma (Lumbers, 1975; Lumbers and Krogh, 1977).

3. the quartz monzonite suite is characterized by abundant quartz monzonite (adamellite) and a minor phase of calc-alkaline intrusive rocks. The plutons of this suite were emplaced mainly within the carbonate-rich younger accumulation of the Central Metasedimentary Belt. Some massive plutons of this suite may postdate the culmination of the intense metamorphism. Therefore, the time for the emplacement of the quartz monzonite suite in southern Ontario may extend from 1125 ± 25 Ma (Silver and Lumbers, 1966) to about 1059 ± 12 Ma (Loon Lake Pluton, Heaman et al., 1980).

4. the alkalic suite is dominated by alkalic syenite and granite, with minor alkalic gabbro and nepheline syenite. These intrusions are mainly concentrated in the "alkalic belt" which marks the approximate nothwestern margin of the present extent of the Grenville Supergroup. The syn-tectonic quartz monzonite suite may overlap in age with this suite.

5. the syenite-monzonite suite is characterized by abundant calc-alkalic syenite and minor monzonite, quartz monzonite and mafic rocks. The rocks of this suite are generally quartz-poor and K-feldspar-rich and postdate the regional metamorphism in their host rocks

(Lumbers,1967).

Relatively younger dykes of pegmatite are dated at 1050 ± 20 Ma old (Silyer and Lumbers, 1966) and the uraniferous granite pegmatites are 950 ± 25 Ma (Fowler and Doig, 1983); both were emplaced when the plutonic activity and regional metamorphism were on the wane.

In addition, the only plutonic bodies, mainly quartz mozonite and granodiorite, older than the anorthosite suite in the Ontario Gneiss Segment were emplaced about 1800 Ma ago (Lumbers, 1982). The Algonquin Batholith intruded the older accumulation about 1400 to 1500 Ma ago and was reactivated, becoming diapiric toward the overlying rocks during the Grenville Orogeny (Schwerdtner and Lumbers, 1980).

According to the petrographic and chemical studies, two distinct types of granitic plutons can be classified in the Frontenac Axis:

1. the Frontenac-type monzonite-quartz monzonite group;

2. the Rockport-type granite group.

The former might be equivalent to the quartz monzonite suite of Lumbers (1967, 1982), which is most common in the Central Metasedimentary Belt. However,

the alternating intruding and including contact relationships between these two types of granitic rocks suggested that both rocks were mobile at the same age, but their relative mobility varied temporally and spatially (Wynne-Edwards, 1967).

Relative to the culmination of the Grenville Orogeny and the degree of deformation (recrystallization) within the granitic rocks, Davison et al., (1979) intended to classify plutonic rocks of the southern Ontario and western Quebec into pre-, syn-, late- and post-tectonic categories.

4.0 PETROGENESIS MODELS OF GRANITOIDS IN THE GRENVILLE PROVINCE

4.1 Assimilation And Magmatic Differentiation

The so-called "granite dispute" has gone on for almost a century. Prior to the sixties, studies of granites of the Grenville Province concentrated on whether these granitic bodies were produced in situ by metasomatic replacement of pre-existing country rocks, or whether they crystallized by magmatic differentiation.

On the basis of detailed mapping, petrographic observations and partial chemical analyses of three

"post-tectonic" granitic plutons (the Wollaston Granite, Chandos Lake Pluton and Deloro Pluton), a classic study by Saha (1957, 1959) suggested that:

1. diffusion of silica and soda in aqueous solution from the surrounding paragneiss into the granite magma at the early stage of crystallization accounted for the mineralogical and chemical variations in the Wollaston Granite;

2. assimilation of various country rocks may cause the variation in the Chandos Lake Pluton;

3. in the composite Deloro Pluton, assimilation of gabbro and diabase by granite magma accounted for the syenitic western border zone, but magmatic differentiation by fractional crystallization caused a systematic trend of silicification towards the centre of the pluton.

4.2 Partial Melting And Anatexis

Following successful experiments on melting of natural rocks (eg. greywacke, Winkler, 1961), partial melting of pre-existing rocks, either sedimentary or igneous, with excess water could be expected at depth of 2[illegible]km in the crust (Wyllie, 1963). Thereafter, the concept of anatexis has been widely employed to

interpret various granitic plutons in the Shield area associated with high grade regional metamorphism.

Sauerbrei (1966) studied the intrusive relations and origin of the two major types of granites in the Frontenac Axis of Ontario, and concluded that both of them were produced by anatexis.

1. The normative compositions of the Rockport-type granite fall close to the ternary minimum of the "petrogeny residua system" of Tuttle and Bowen (1958). The abundance of "mortar texture" supports the idea that the Rockport-type granite originated from the anatectic melting of hydrous Grenville Supergroup metasediments during the Grenville Orogeny.

2. The Frontenac-type quartz monzonite was usually emplaced in structural sites of low pressure or dilatant zones developed during deformation. Their origin was then interpreted to be the remobilized anhydrous basement rocks, moved diapiricly into the Grenville Supergroup by folding.

Bright (1976, 1980) reported that the basement gneiss of the Grenville Supergroup has been found in the Cavendish-Anstruther township area. The Cheddar dome in the Cardiff-Monmouth Townships is interpreted to be an

anatectic body developed by a high degree of partial melting of the basal arenaceous Anstruther Lake Group.

4.3 Origin Of Alkalic And Peralkaline Granitoids

The nepheline-bearing suite of the Haliburton-Bancroft area forms a long sinuous belt that divides two portion of the Grenville Province of contrasting lithological and structural character. This prominant feature led earlier geologists to suggest that the nepheline-bearing rocks were products of metamorphism of analcime-rich sediments. Adams and Barlow (1910) suggested that nepheline rocks are products of assimilation around the margins of granitic magma and crystalline limestone. However, recent studies have found the truely igneous-textured nepheline suites that have survived from the regional metamorphism because of the "cushioning effects" of surrounding marbles (Tilley and Gittins, 1961).

According to Gittins (1967), the nepheline-bearing rocks in the Haliburton - Bancroft area can be classified into three groups of rock with different origins.

1. The igneous-textured suite is a typical hypersolvus assemblage or one feldspar nepheline syenite, indicative of magmatic origin.

2. Nepheline-bearing gneisses, the majority rock type in the area, are probably metamorphosed nepheline syenite, or due to nephelinization of a variety of pre-existing rock by high grade metamorphism.

3. Nepheline pegmatites are probably of two types of origin: the crystallization of residual fluids derived from the feldspathoidal magma, and/or the partial melting of earlier-formed nepheline rocks, of both igneous and sedimentary origin, during regional metamorphism.

Kuehnbaum (1973) re-evaluated the origin of the Deloro Pluton (Madoc) through detailed petrochemical studies. The presence of perthitic, hypersolvus feldspar, riebeckite, normative sodium metasilicate and high agpaitic index confirmed that the Deloro Pluton is peralkaline in composition with epizonal emplacement.

Three hypotheses have been suggested for the origin of the peralkaline granite (Kuehnbaum, 1973):

1. fractional crystallization of syenite liquid (Upton, 1960);

2. partial melting of oversaturated syenite (Bailey and Schairer, 1966);

3. partial melting of continental crust with excess alkali-rich volatile flux (Bailey and MacDonald, 1970).

4.4 Geochemical Modelling

Since the early seventies, the advancing analytical techniques for trace-element in rocks and the increased understanding of the behaviour of elements in magmatic processes have made it possible to use trace-element geochemistry for evaluating the nature of igneous rocks.

During the study of geochemistry and petrology of the Loon Lake Pluton (or Chandos Lake Pluton), Dostal (1973, 1975) observed the chemical variations, especially the alkaline-earth and rare-erath elements, in the monzonitic core and the quartz monzonitic rim. Trends of chemical variations in the pluton are consistent with fractional crystallization dominated by feldspar, with lesser mafic mineral and possible accessory minerals. This fractionation also involves "flowage differentiation". The origin of the monzonitic melt is believed to be by partial melting of lower crust/upper mantle rocks, or by differentiation of deep-seated, basic magma The quartz monzonite was probably generated by a "mixing" of monzonitic magma with the granitic melt produced by partial melting of

the basement of the Grenville Supergroup.

Fowler (1980) precluded that the uraniferous granite pegmatites in the Grenville Province were derived from in-situ anatexis at the base of the Grenville Supergroup, due to their younger ages and lower initial $^{87}Sr/^{86}Sr$ ratios. He further suggested a deep-seated basaltic magma produced by partial melting of Rb-depleted peridotite source, under a "tensional environment". Later water-saturated granitic melt which was enriched in the incompatible elements (eg. U, Th) is produced by magmatic differentiation aided by a flux of volatiles.

Pride and Moore (1983) studied the trondhjemite suite (the biotite diorite suite of Lumbers') in eastern Ontario and suggested that the chemical differences between the pluton itself and surrounding metavolcanic sequences can be explained by accumulation of plagioclase in the plutonic environment. Therefore, the parental magma of the trondhjemite suite is similar to that of dacites in the nearby metavolcanic rocks. Such magma was formed at the mature arc system by partially melting the crustal material (Condie and Moore, 1977).

4.5 Isotopic Data Interpretation

In addition to trace-element geochemistry, the isotopic composition of the granitic rocks, particularly the $^{18}O/^{16}O$ and initial $^{87}Sr/^{86}Sr$ ratios, may possible constrain the inferred parental sources.

Shieh (with Schwarcz, 1974; 1978, 1980) has suggested three isotopically distinct groups of granitic and syenitic plutons between the Harvey-Cardiff Arch and the Frontenac Axis of Ontario, based upon their whole-rock $^{18}O/^{16}O$ ratios. The characteristic $^{18}O/^{16}O$ ratios observed in plutons from each group may reflect the unique isotopic fingerprint of the source material from which the plutons were derived, if they are primary.

The most possible source for the low- $\delta^{18}O$ group is the basement gneisses of the Grenville Supergroup, while for the high- $\delta^{18}O$ group is the supercrustal metasediments. The intermediate $\delta^{18}O$ group plutons been may have been derived from mixing of both.

In interpretation of their Rb-Sr isotope data, Davis et al.(1967), Krogh and Hurley (1968), Bell and Blenkinsop (1980), Heaman et al. (1980) and Fowler and Doig (1983) have considered that the granitic bodies in southeastern Ontario emplaced between 1300 and 900 Ma were not derived from an ancient sialic basement, because of the low projected $^{87}Sr/^{86}Sr$ ratios (ranging

from 0.699 to 0.706).

5.0 TECTONIC MODELS OF THE GRENVILLE PROVINCE

According to Baer (1981a), "A model of evolution of the Grenville Province is by necessity a temporary figment of controlled scientific imagination". Such models have been developed into two main frames for the Grenvillian evolution.

(A) Uniformitarian Models :

1. The Basement-Reactivation Model proposed by Dewey and Burke (1973). They suggested that the Tibetan Plateu is a modern analogue of the Grenville Province, and that it presents crustal thickening following continental collision. The suture in this case would be somewhere in or under the Appalachians.

   This collision model has been supported by paleomagnetic data (Donaldson and Irving, 1972; Palmer and Carmicheal, 1973; Irving et al., 1974) which shows that Grenville paleopoles in pre-Grenvillian time do not lie on the remainder of the North American polar track. Consequently, it has been interpreted that the Grenville Province was not part of the North American craton prior to about 1100 Ma.

2. Recently, Baer (1981a) proposed a mechanism of intra-continental (intra-plate) deformation by "plate-jams" to explain the existing stress-fields and to accommodate the known geology in the Grenville Province. Such deformation will occur whenever the plates are held under high directed stress for a long period. The essential difference from the plate-edge type deformation of Phanerozoic plate tectonics is no subduction of oceanic plates being involved in the intra-plate deformation. Thus, the Grenville Province is inferred as being part of the North American plate prior to 1350 Ma (cf. Morris and Roy, 1977).

(B) Non-uniformitarian Models :

1. The Millipede Model proposed by Wynne-Edwards (1976). The major concept in this model is that of a deformable plate drifting over a chain of hot spots. At any given time, domains above a hot spot are in extension whereas those farther off to the side are under compression. As the plate moves, each point in the plate passes successively from extensional to contractional domains.

2. The Mega-Shear Model proposed by Baer (1977) in which he considered the Grenville Province as a large zone of dextrial simple shear. In this

interpretation, a northeasterly trending shear zone following the Grenville Front and another, less developed, parallel zone along the southern margin of the Province outline the Grenville "mega-shear". Between these two main marginal shear zones, the Province is broken into a number of blocks separated by north-northeasterly trending shear "belts", such as the Chibougamau - Gatineau lineament.

6.0 AIMS OF THE PRESENT STUDY

The purpose of the present study is :

1. to present some geochemical and petrological data of sampled granitic plutons in the Grenville Province of Ontario;

2. to reveal the distribution and variation of trace elements in Grenville granites;

3. to assess the classification of the Grenville granitic plutons into S-, I- and A-type scheme;

4. to evaluate or re-evaluate the origin and evolution of the sampled granitic plutons;

5. to model the sampled granitic plutons quantitatively under proper constraints;

6. to contribute to the understanding of the Grenvillian tectonics on the basis of the petrochemistry of the Grenville granites, in general.

Chapter II. GEOCHEMISTRY AND PETROGRAPHY OF SAMPLED GRANITOIDS

1.0 GENERAL STATEMENT

Eight granitic bodies, ranging from single to composite phase stocks and batholiths, have been selected for this study (Fig. 2-1-1). Some of these granitoids have been petrologically investigated by previous workers during regional reconnaissance surveys, however detailed petrographic and geochemical studies are needed to completely understand their place in the regional development.

The selected granitoids are well-distributed across the Grenville Province of Ontario, except in the area of the Frontenac Axis. Rocks sampled are equigranular, medium- to coarse-grained, showing little deformation and recrystallization. All samples selected are holocrystalline with a massive, gneissic, or slightly porphyritic appearance.

The riebeckite-bearing phase of the Deloro Pluton, characterized by perthite as the only feldspar, can be classified as "hypersolvus granite" of Tuttle and Bowen (1958); whereas the other sampled granites, consisting of both plagioclase and microcline or perthitic alkaline feldspar, are "subsolvus granites".

Figure 2-1-1. Locations of sampled granitoids of the Grenville Province of Ontario.

(A) Algonquin Batholith
(B) Union Lake Pluton
(C) Elphin Granite-Syenite Complex
(D) Cheddar Granite
(E) Mulock Batholith
(F) Coe Hill Granite
(G) Deloro Pluton
(H) Barber's Lake Granite

Previous Work :

(1) Glamorgan Complex (Chesworth, 1967)
(2) Elzevir Batholith (Pride and Moore, 1983)
(3) White Lake Pluton (Somers, 1984)
(4) Westport Pluton (Sauerbrei, 1966)
(5) Rockport-type granite (Sauerbrei, 1966)
(6) Loon Lake Pluton (Dostal, 1973)

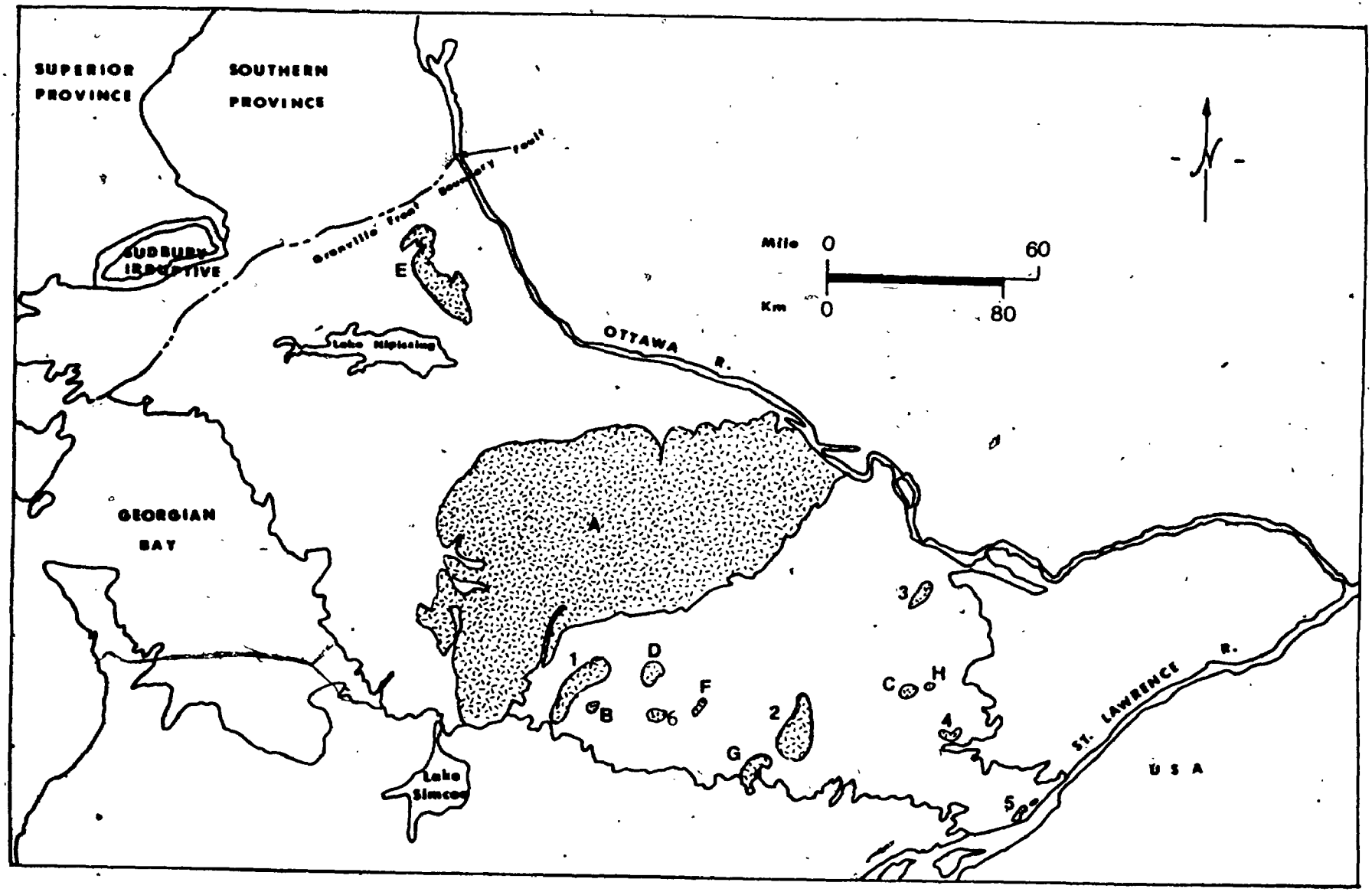
SUPERIOR PROVINCE
SOUTHERN PROVINCE
SUDBURY IRRUPTIVE
Grenville Front
Boundary Fault
E
Lake Nipissing
OTTAWA R.
Miles 0 60
Km 0 80
N
GEORGIAN BAY
A
1
B
D
6
F
2
G
3
C
H
4
5
Lake Simcoe
ST. LAWRENCE R.
U S A

Since recorded geochronological information of these granites is sketchy, the ages of some granites in the study area are estimated indirectly from a nearby dated granitic body of similar rock type. In addition, the sequence of plutonic events in the Grenville Province, proposed by Lumbers (1982) is used as a determining factor. The following descriptions of general characters, petrography and geochemistry of individual granites are in the order of ascending age. The outline of characteristic mafic and accessory minerals of the sampled granitoids is summarized in Table 2-1-1.

Evidence for identifying primary and secondary muscovite are used according to Miller et al. (1981): the primary muscovite grains must

1. have relatively larger grain size, comparable to obviously primary phases;

2. have a sharp termination with subhedral to euhedral form;

3. not be enclosed by or enclose any mineral from which the muscovite may have formed by alteration (e.g. feldspar).

Modal compositions of representative rocks of sampled granitoids are given in Appendix C-1. The modal classification of Streckeison (1976) is used in this study;

Table 2-1-1. Summary of sampled granitoids of the Grenville Province, Ontario

Pluton	Location	Rock-type	Characteristic Mafic and Accessory Minerals	Age
1. Algonquin Batholith	Pembroke-Renfrew area westward to eastern Parry Sound District	a. Tonalite-diorite and related mafic rocks.	Hb, Biot, ±Px, Ap, Zir, Sph, ±Gt, Fe-oxides; secondary Mus, Ep.	1400-1500 Ma (Lumbers and Krogh, 1977) U-Pb Zircon.
		b. Monzonitic-syenitic rocks.	Hb, Biot, ±Px, Ap, Sph, Zir, ±Gt, ±All, Fe-oxides, secondary Mus, Ep, Cc.	
		c. Granitic rocks.	Biot, ±Hb, Ap, Zir, Sph, All, ±Gt; secondary Ep, Cc.	
2. Union Lake Pluton	Galway - Snowdon Townships	Quartz diorite.	Hb, Biot, ±Px, Sph, Ap, Zir, Fe-oxides; secondary Ep, Cc.	Biotite-diorite Suite of Lumbers(1967). i.e. 1250 ± 25 Ma
3. Elphin Granite -Syenite Complex	N. Sherbrooke-Palmerston Townships	a. Granite-granodiorite.	Biot, Sph, Ap Zir; secondary Ep, Mus, Carb.	No quantitative data.
		b. Quartz monzonite-syenite.	Biot, Hb, Sph, Ap, Zir; secondary Ep, Mus, Cc.	
		c. Quartz diorite (hybrid phase).	Biot, Hb, ±Px, Ap, Sph; secondary Mus, Ep, Cc, Tm, ±Gt, ±Topaz.	
4. Cheddar Granite	Cardiff-Monmouth Townships	a. Granite-Gneiss.	Biot, Hb, ±Px, Ap, Sph, Zir, All, ±Gt, ±Fl, ±Tm, Fe-oxides; secondary Mus, Ep, Cc.	1207 ± 46 Ma (Fowler and Doig,1983). Rb-Sr whole-rock.
		b. Green Monzonite.	Px, Hb, Biot, Sph, Zir, Ap, All; secondary Mus.	
		c. Tonalitic Xenolith.	Biot, Hb, Ap, Sph, Zir, All, ±Gt, Spinel.	

(Table 2-1-1, cont'd)

5. Mulock Batholith	North Bay Area	Gneissic to porphyritic granite	Biot, Hb, Sph, Zir, Ap, All, Fe-oxides; secondary Mus, Ep.	1175 Ma (Baer, 1980). Rb-Sr whole-rock.
6. Coe Hill Granite	Wollaston Township	Massive to gneissic granite.	Biot, Hb, ±Px, Sph, Ap, Zir, All, Fl, Fe-oxides; secondary Mus, Ep, Cc.	Similar rock-type as Loon Lake Pluton, 1059 ± 12 Ma (Heaman et al., 1980). Rb-Sr whole-rock.
7. Deloro Pluton	Madoc-Marmora Townships	a. Peralkaline granite b. Granophyric granite c. Calc-syenite.	Riebeckite, Biot, Zir, Fl, Il. Biot, Zir, Fl, Mag. Hb, Biot, Sph, ±Gt, ±All, ±Ep.	1059 Ma (Stockwell, 1972) or 1096 Ma (Davison et al., 1979). Rb-Sr whole-rock.
8. Barber's Lake	Dalhousie Township	a. Granite. b. Basic rocks.	Biot, Mus, Sph, Zir, All, ±Ap, Fl, Fe-oxide; secondary Ep, Cc, Spinel. Hb, Biot, Px, Sph, Ap, Zir; secondary Cc, Chl, Spinel.	Equivalent to uraniferous granite of the region, 937-980 Ma (Fowler and Doig, 1983). Rb-Sr whole-rock.

Abbreviations:

Biot = biotite,	Hb = hornblende,	Px = pyroxene,
Sph = sphene,	Ap = apatite,	Zir = zircon,
All = allanite,	Fl = fluroite,	Mus = muscovite,
Mag = magnitite,	Il = ilmenite.	
Ep = epidote,	Cc = calcite,	Tm = tourmaline,
Chl = chlorite,	Gt = garnet.	

however, classification of non-feldspathoidal plutonic rocks used by Lumbers (1982) for Grenville granitoids is also listed in Table 2-1-2 for reference.

Although various Harker diagrams were constructed during the preliminary studies, for simplicity and clarity, only limited ones are presented in the text. However, some conclusions reached may be directly related to the preliminary Harker plots. Complete chemical and normative compositions of sampled granitoids are given in Appendix C-2 and C-3. In addition, the degree of variation of individual elements as a function of SiO_2 can be estimated from the correlation coefficients; the sign of the coefficient illustrates positive or negative slope of the trend. Arbitrarily, in this study, a correlation (R) > 0.45 is considered to yield an interpretable trend and R > 0.70 indicates a strong correlation.

The oxygen isotopic data are reported in terms of the quantity δ as defined by:

$$\delta\ (o/oo) = \left[\frac{(^{18}O/^{16}O)_{sample}}{(^{18}O/^{16}O)_{standard}} - 1 \right] * 1000$$

The standard used is Standard Mean Ocean Water (SMOW). Further, the isotopic fractionation between two co-existing phases, such as quartz and feldspar, is defined as $\Delta_{q-f} \cong \delta_q - \delta_f$.

Table 2-1-2 Modal classification of non-feldspathoidal plutonic rocks

QUARTZ	ESSENTIAL FELDSPAR				
	Plagioclase / Total Feldspar	Composition of Plagioclase: Albite An_{0-10}	Oligoclase An_{10-30}	Andesine An_{30-50}	Labradorite and Bytownite An_{50-90}
> 10%	< 0.33	Alkalic Granite	Quartz Monzonite		
	0.67-0.33				
	0.87-0.67	Sodic Granite	Granodiorite		
	> 0.87	Albite Granite	Trondhjemite	Tonalite	Quartz Gabbro
< 10%	< 0.33	Alkalic Syenite	Calc-alkalic Syenite		
	0.67-0.33		Monzonite		
	0.87-0.67	Sodic Syenite	Syenodiorite		
	> 0.87	Albite Syenite	Oligoclase Diorite	Diorite	Gabbro

Notes: 1. Quartz content of tonalite is rarely >20%, and of quartz gabbro, rarely >10%.
2. Granites, quartz monzonite, granodiorite, and trondhjemite generally contain > 20% quartz.
3. Quartz syenite refers to syenite containing between 10 to 20% quartz.

(modified after Lumbers, 1982)

2.0 ALGONQUIN BATHOLITH

2.1 General Characters And Intrusive Relations

The Algonquin Batholith suggested by Lumbers (with Schwerdtner, 1980; 1982) is a major gneiss dome at the southern portion of the Ontario Gneiss Segment. It extends from the Pembroke - Renfrew area westwards to east of the Parry Sound District and may trace farther west to the southeast shore of Georgian Bay (S.B. Lumbers, 1983, pers. comm.). The entire outcrop area may well be over one-third of the Ontario Gneiss Segment (Fig. 2-2-1).

It has been suggested that the batholith was emplaced along the "continental margin" about 1400-1500 Ma. ago (Lumbers and Krogh, 1977). Subsequently, it was reactivated, becoming diapiric toward the overlying gneiss terrain during the climax of the Grenville Orogeny. It is overlain unconformably by the younger Grenville Supergroup. Both the surrounding gneisses and the batholith itself have been subjected to high grade regional metamorphism of upper amphibiolite facies.

The Algonquin Batholith consists mainly of gneissic granitic rocks, pink to pale greenish monzonitic to syenitic rocks; small units of tonalite and trondhjemite, scattered anorthositic masses and related mafic rocks also occur in the southwestern part of the batholith. Local pyroxene-bearing phases contain

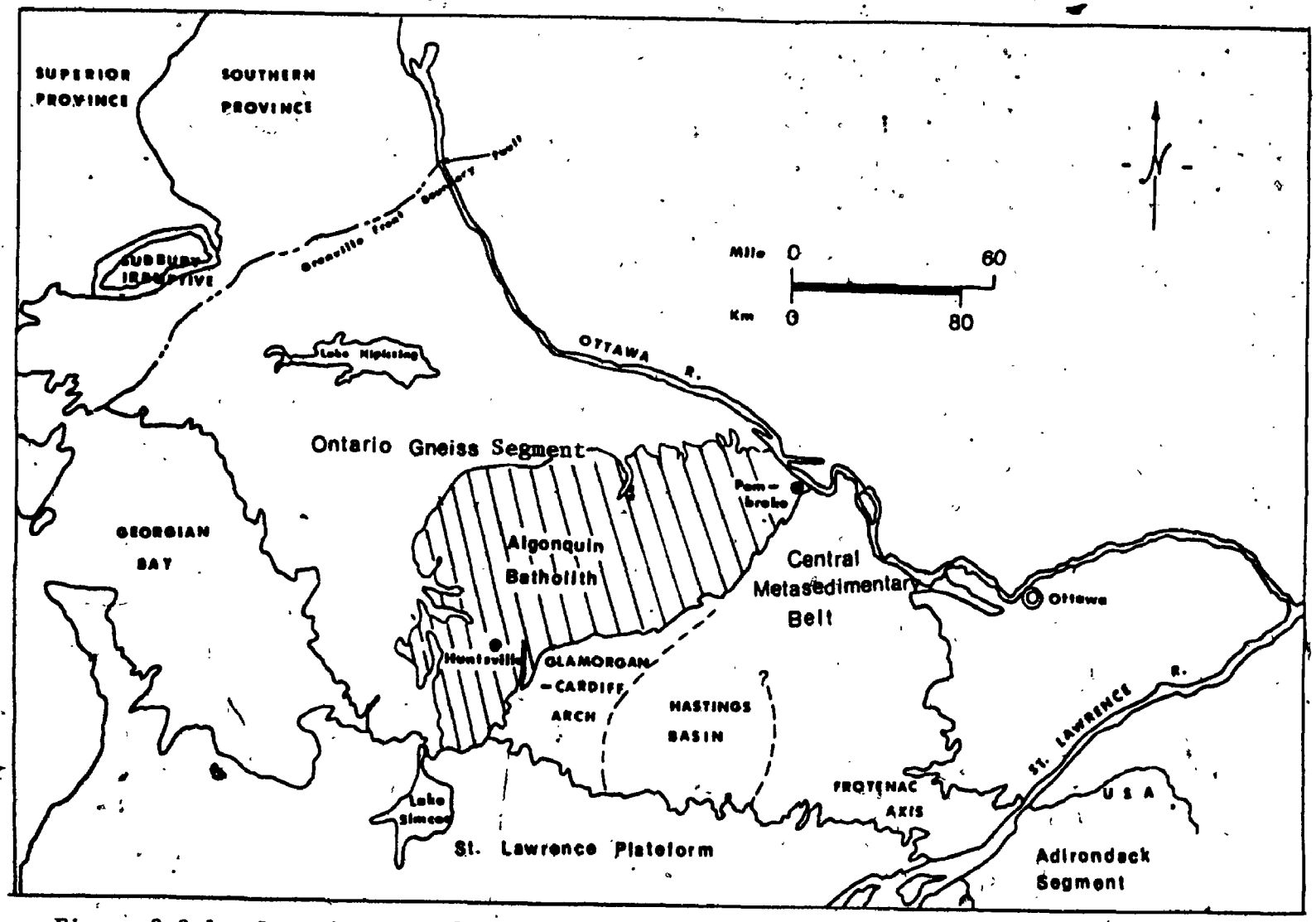

Figure 2-2-1. Location map of the Algonquin Batholith (modified from Lumbers, 1982).

primary igneous texture and are interpreted to have an intrusive origin rather than to be indicative of granulite facies metamorphism (Lumbers, 1982).

The term batholith is used to indicate a large area of moderately homogeneous granitic rocks, which is tectonically distinct from the surroundings. On the basis of cross-cutting and inclusion relations at the contact between phases, it has been suggested that the tonalitic and mafic rocks are the oldest, followed by the monzonitic - syenitic rocks and the youngest granitic rocks. Besides, within each category the potash-poor varieties are thought to be earlier than the potash-rich ones. Rock names used in this batholith are field terms.

2.2 Petrography

2.2.1 Tonalite, Trondhjemite And Related Mafic Rocks -

Rocks of the oldest phase of the Algonquin Batholith can be classified as diorite (or gabbro $An_{>50}$), quartz diorite and tonalite in Figure 2-2-2. The rocks are medium-grained with slight to strong foliations. Their colour is light buff grey , dark grey to dark brown - largely due to the proportion of dark minerals and light plagioclase in the rocks.

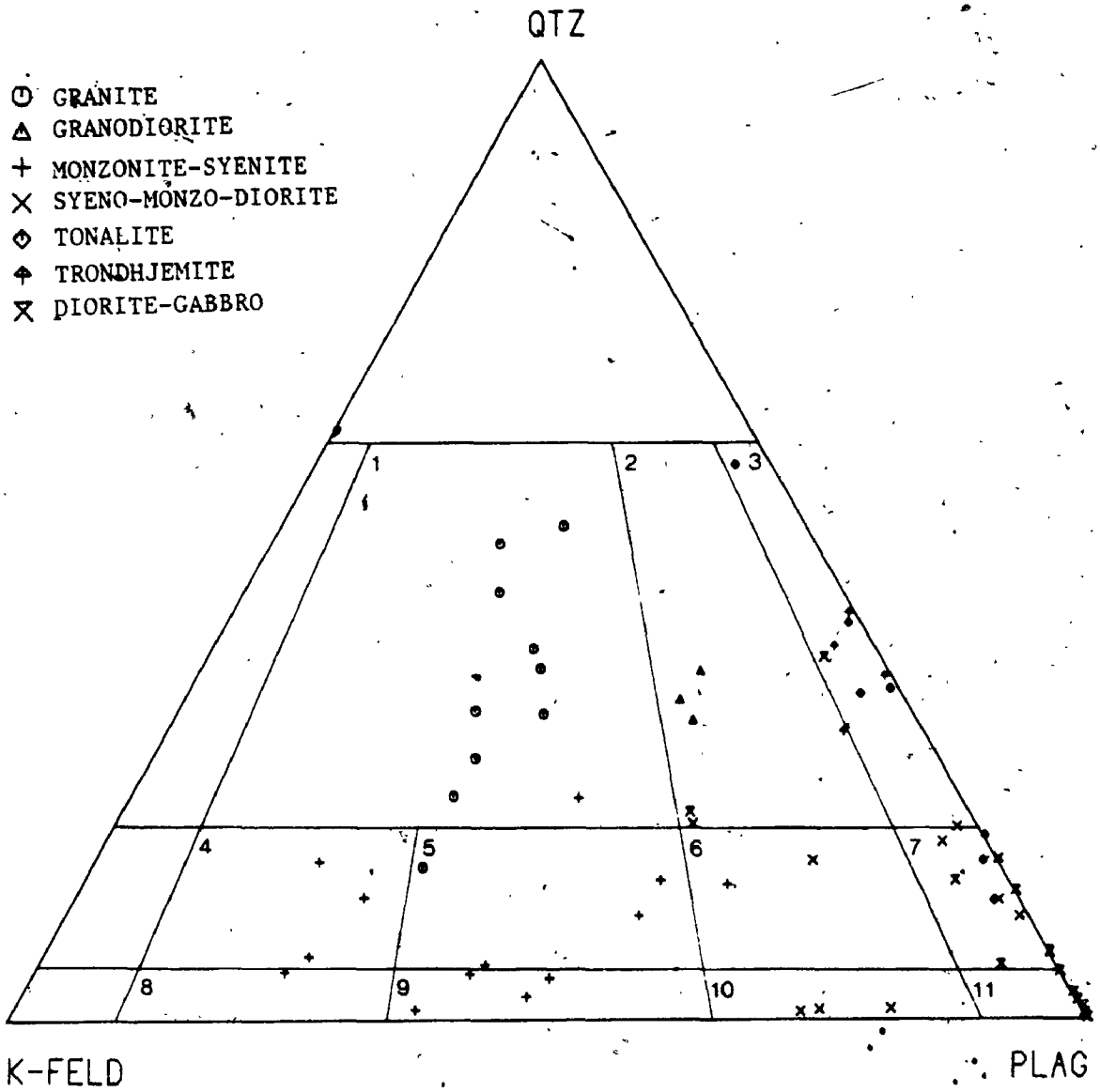

Figure 2-2-2. Modal classification of the Algonquin Batholith. Classification scheme is after Streckeisen (1976).

1. Granite (Adamellite),
2. Granodiorite,
3. Tonalite,
4. Quartz syenite,
5. Quartz monzonite,
6. Quartz monzodiorite,
7. Quartz diorite,
8. Syenite,
9. Monzonite,
10. Monzodiorite,
11. Diorite.

Tonalite and quartz diorite are composed mainly of plagioclase, hornblende and biotite with variable amounts of quartz and lesser K-feldspar. A subordinate amount of pyroxene is also observed in one sample. Accessory minerals include iron oxides (magnetite), apatite, sphene, zircon, trace garnet, secondary muscovite, epidote and calcite.

The texture is hypidiomorphic granular with features of mosaic texture and augen structure locally. Preferred dimensional orientation of biotite flakes and prismatic hornblende are responsible for the foliation which is visible in hand specimens.

Plagioclase, the predominant component of this rock unit, forms euhedral to subhedral crystals with a composition ranging from An_{70} to An_{28}. Chemical compositions and calculated formulae of representative samples are given in Table 2-2-1. Both albite and pericline twinning are common and no zoning was found in any samples investigated. Vermicular intergrowth was often seen along the contact between plagioclase and K-feldspar. The potassium feldspar is microcline and untwinned oligoclase; microperthite and micro-antiperthite are also present. Locally, microcline is intergrown with quartz.

Table 2-2-1. Chemical compositions and calculated formulae of feldspars from the Algonquin Batholith

(a) Plagioclase

Sample No.	75-L-25	75-L-76	76-L-58	75-L-40	75-L-77	75-L-29	75-L-43	78-L-53
Rock-type	G	G	G	M	M	Sy	T	D
(wt%)								
SiO_2	60.91	64.52	65.45	63.30	63.72	63.06	61.21	61.65
Al_2O_3	24.50	22.29	22.29	23.[illegible]8	22.82	22.99	24.77	24.15
CaO	6.42	3.12	2.25	4.43	4.32	4.01	5.72	5.34
Na_2O	7.93	9.69	10.04	8.69	8.79	9.38	8.00	8.64
K_2O	0.24	0.16	0.16	0.14	0.20	0.46	0.29	0.26
Total	100.00	99.78	100.19	99.84	99.85	99.90	99.99	100.04
Si (Z)	10.837	11.389	11.473	11.190	11.261	11.183	10.864	10.944
Al (Z)	5.136	4.636	4.604	4.849	4.752	4.804	5.181	5.052
	15.973	16.025	16.077	16.039	16.014	15.987	16.054	15.996
Na (X)	2.735	3.316	3.412	2.978	3.012	3.225	2.753	2.974
Ca (X)	1.224	0.590	0.423	0.839	0.818	0.762	1.088	1.016
K (X)	0.054	0.036	0.036	0.032	0.045	0.104	0.066	0.059
	4.014	3.942	3.870	3.849	3.875	4.091	3.906	4.048
O	32	32	32	32	32	32	32	32
(mol%)								
Ab	68.15	84.12	88.16	77.38	77.[illegible]73	78.83	70.47	73.46
An	30.49	14.97	10.92	21.80	22.11	18.62	27.85	25.09
Or	1.36	0.91	0.92	0.82	1.16	2.54	1.68	1.45

(b) K-feldspar

(wt%)					
SiO_2	65.31	65.51	64.93	65.28	65.47
Al_2O_3	18.06	17.91	18.68	18.47	18.31
CaO	0.03	0.00	0.09	0.06	0.00
Na_2O	1.27	1.24	0.79	1.29	1.33
K_2O	14.85	14.83	15.60	14.29	14.69
Total	99.52	99.51	100.09	99.39	99.80
Si (Z)	12.060	12.091	11.961	12.030	12.042
Al (Z)	3.930	3.895	4.055	4.011	3.968
	15.990	15.986	16.016	16.040	16.010
Na (X)	0.455	0.444	0.282	0.461	0.47[illegible]
Ca (X)	0.006	0.004	0.018	0.012	0.000
K (X)	3.498	3.491	3.665	3.359	3.446
	3.958	3.939	3.965	3.831	3.921
O	32	32	32	32	32
(mol%)					
Ab	11.49	11.27	7.12	12.03	12.10
An	0.15	0.10	0.45	0.31	0.00
Or	88.36	88.63	92.44	87.66	87.90

G - granite; M - monzonite; Sy - syenite;
T - tonalite; D - diorite.

Subhedral and anhedral quartz grains occupy the interstitial positions between early formed minerals. Elongated crystals, usually with strong undulose extinction, show their elongation parallel to the foliation. Mosaic quartz-subgrains along larger quartz or plagioclase phenocrysts may indicate a secondary origin.

Hornblende makes up 4% to 29% of the mode; the representative analyses suggest they correspond to the calcic amphibole of Leake (1968; See Table 2-2-2). The general pleochroic scheme of the hornblende is X < Y < Z; X = pale greenish yellow to yellowish green, Y = olive green, Z = green to dark green. Subhedral crystals commonly show poikilitic texture with inclusions of quartz and apatite; embayment of quartz and plagioclase between hornblende grains indicates the interference from the former during growth of hornblende. In places, hornblende forms rims around the pyroxene relicts, while oxidation rims of magnetite occur around the hornblende subhedra.

Biotite is subhedral and pleochroic from Y = Z = reddish to dark brown to X = pale to dark straw yellow. Small flakes are intergrown with hornblende; poikilitic texture is common with inclusions of quartz, sphene, apatite and zircon.

Table 2-2-2. Chemical compositions and calculated formulae of amphibole from the Algonquin Batholith

Sample No.	75-L-25	75-L-77	75-L-40	75-L-29	75-L-43	78-L-53
Rock-type	G	M	M	Sy	T	D
(wt%)						
SiO_2	40.85	41.02	41.84	41.08	44.19	41.84
TiO_2	0.67	1.74	1.81	1.64	0.66	1.53
Al_2O_3	11.63	11.08	10.18	10.38	9.77	10.55
FeO	22.54	22.49	20.02	24.26	16.28	18.42
MnO	0.61	0.63	0.38	0.64	0.84	0.37
MgO	7.60	6.32	8.05	6.35	11.07	9.62
CaO	11.40	11.17	11.35	11.01	11.41	11.52
Na_2O	1.29	1.45	1.73	1.52	1.30	1.61
K_2O	1.52	1.48	1.51	1.43	1.18	1.65
Total	97.74	97.38	96.87	[illegible].31	96.70	97.11
Si (Z)	6.328	6.401	[illegible]	6.404	6.699	6.426
Al^{iv} (Z)	1.672	1.599	[illegible]	1.596	1.301	1.574
	8.000	8.000	8.000	8.000	8.000	8.000
Al^{vi} (Y)	0.450	0.438	0.347	0.311	0.445	0.336
Ti (Y)	0.078	0.204	0.211	0.192	0.075	0.177
Fe (Y)	2.920	2.935	2.596	3.163	2.064	2.366
Mg (Y)	1.755	1.470	1.860	1.475	2.501	2.202
Mn (Y)	0.080	0.083	0.050	0.085	0.108	0.048
	5.283	5.130	5.064	5.226	5.193	5.129
Ca (X)	1.892	1.867	1.887	1.839	1.853	1.896
Na (X)	0.387	0.439	0.520	0.459	0.382	0.479
K (X)	0.300	0.295	0.299	0.284	0.228	0.323
	2.579	2.601	2.704	2.582	2.463	2.698
O	23	23	23	23	23	23

Table 2-2-3. Chemical compositions and calculated formulae of biotite from the Algonquin Batholith

Sample No.	75-L-25	75-L-26	76-L-58	75-L-40	75-L-77	75-L-29	75-L-43	78-L-53
Rock-type	G	G	G	M	M	Sy	T	D
(wt%)								
SiO_2	34.96	36.45	36.27	36.10	35.01	34.42	36.80	36.27
TiO_2	4.13	4.17	3.29	4.62	6.09	4.65	3.90	4.44
Al_2O_3	14.20	13.83	14.89	13.09	13.38	13.69	13.95	13.74
Fe_2O_3	2.88	2.68	2.68	3.89	4.66	4.79	4.81	5.16
FeO	19.68	18.31	18.31	17.30	20.70	21.26	13.08	14.04
MnO	0.41	0.79	0.34	0.22	0.34	0.27	0.60	0.23
MgO	9.29	9.70	8.72	9.81	4.84	7.56	11.54	11.85
CaO	0.07	0.05	0.06	0.03	0.04	0.02	0.01	0.01
Na_2O	0.00	0.01	0.08	0.01	0.01	0.00	0.02	0.00
K_2O	9.64	9.85	9.66	9.66	9.56	9.27	9.92	10.03
Total	95.58	96.12	94.60	95.16	95.17	96.48	95.16	96.35
Si (Z)	5.443	5.591	5.632	5.589	5.541	5.386	5.603	5.492
Al^{iv} (Z)	2.557	2.409	2.368	2.387	2.459	2.523	2.397	2.450
	8.000	8.000	8.000	7.976	8.000	7.909	8.000	7.942
Al^{vi} (Y)	0.047	0.091	0.355	0.000	0.035	0.000	0.104	0.000
Ti (Y)	0.483	0.481	0.384	0.537	0.724	0.547	0.446	0.505
Fe^{3+} (Y)	0.337	0.309	0.313	0.453	0.555	0.564	0.551	0.588
Fe^{2+} (Y)	2.560	2.348	2.376	2.238	2.738	2.780	1.664	1.777
Mg (Y)	2.154	2.217	2.016	2.262	1.141	1.762	2.616	2.672
Mn (Y)	0.054	0.103	0.045	0.029	0.046	0.036	0.077	0.029
	5.635	5.550	5.488	5.519	5.238	5.687	5.458	5.571
Ca (X)	0.012	0.008	0.010	0.005	0.007	0.003	0.002	0.002
Na (X)	0.000	0.003	0.024	0.003	0.003	0.000	0.006	0.000
K (X)	1.913	1.927	1.912	1.906	1.929	1.849	1.925	1.936
	1.925	1.938	1.946	1.914	1.939	1.852	1.933	1.938
O	22	22	22	22	22	22	22	22
mole % of annite	0.427	0.391	0.396	0.373	0.456	0.463	0.277	0.296

indicate they classify as the Mg-biotite of Foster (1960; See Fig. 2-2-3). Subhedral pyroxene grains were found only in one sample; both orthopyroxene and clinopyroxene are fractured and replaced at their rims by later hornblende.

Magnetite is the most common iron-oxide constituting up to 4% in the rock, although the amount is variable from sample to sample. Apatite forms either as euhedral individual grains or as subhedral inclusions of biotite, hornblende and plagioclase. One apatite inclusion in biotite shows a corona of sphene, indicating apatite crystallized before sphene in at least this sample. Sphene and zircon occur frequently as inclusions in biotite, rarely as individual aggregates. Secondary epidote and calcite occur as alteration of plagioclase; garnet is also present.

2.2.2 Monzonite And Syenite -

Rocks of the second phase of the Algonquin Batholith are, with few exceptions, clustered in the quartz syenite and monzonite fields of Streckeisen's classification (1976; See Fig. 2-2-2). They are medium in grain size and greyish buff to greenish grey in colour. Frequently, they are foliated with "strips" of biotite, hornblende and opaques.

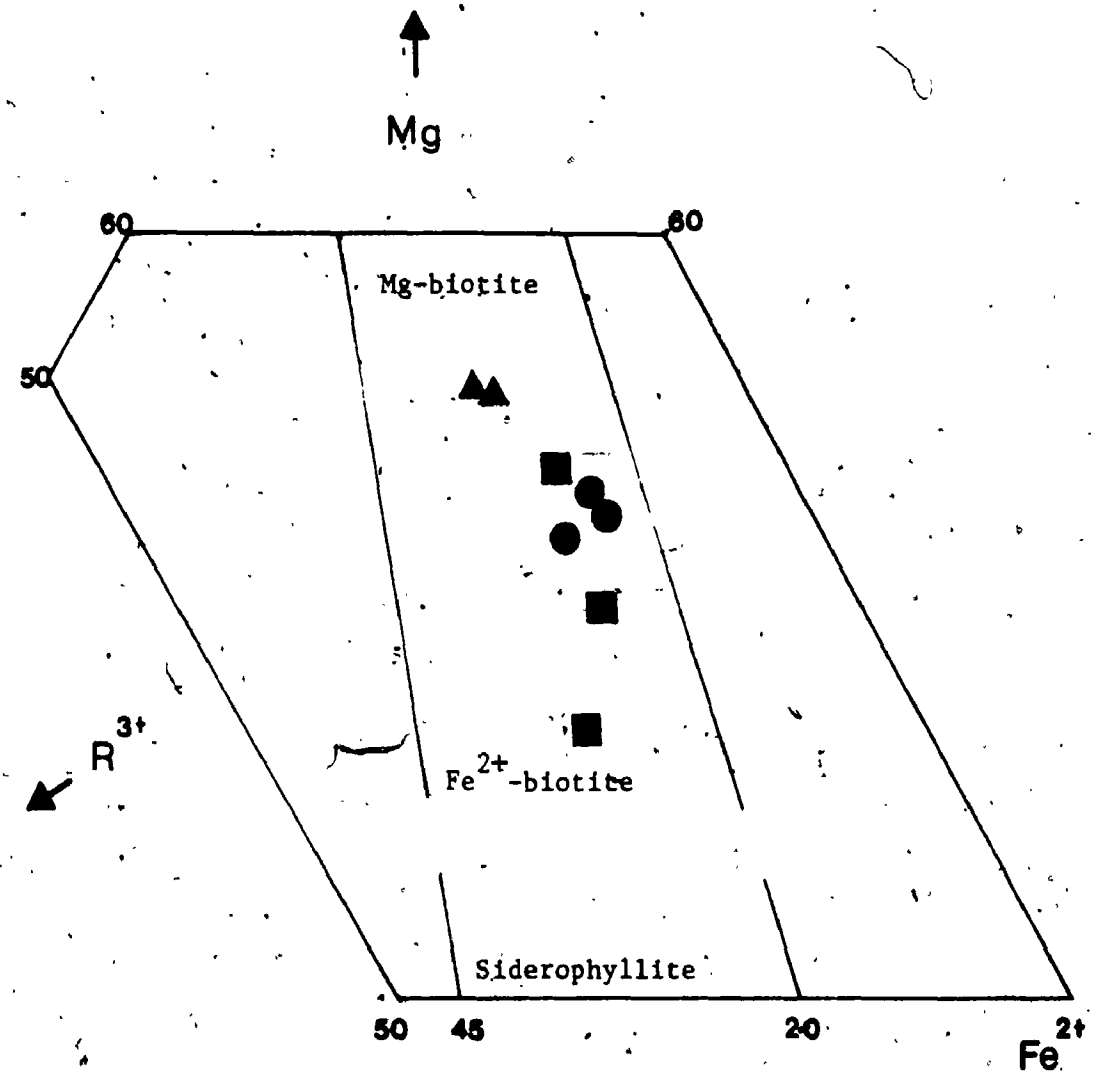

Figure 2-2-3. The $Mg-Fe^{2+}-R^{3+}$ relations in trioctahedral micas of the Algonquin Batholith (after Foster, 1960).

$R^{3+} = Al^{vi} + Fe^{3+} + Ti^{4+}$

● Granite

■ Monzonite-syenite

▲ Tonalite-diorite

The monzonitic-syenitic rocks consist predominantly of K-feldspar and plagioclase, lesser amount of quartz and variable amounts of mafic minerals (4% - 20%). Accessory sphene, apatite, zircon, iron oxides, garnet, allanite, secondary muscovite, calcite and epidote are common. Under the microscope, the texture of these rocks is hypidiomorphic granular with a pronounced porphyritic variety locally.

Microcline and microperthite, up to 68% of the modal composition, form large phenocrysts among the finer-grained quartz-feldspar "matrix", locally. The chemical analyses and structural formulae are summarized in Table 2-2-1. Plagioclase, either with albite twinning or untwinned, ranges in composition from An_{14} to An_{34} (Table 2-2-1). No zoning is developed within the crystal; however, strong sericitization occurs in the core of the plagioclase, leaving an unaltered rim.

Quartz occurs as anhedral and interstitial crystals, indicating a later crystallization product. Myrmekite intergrowths occur frequently among plagioclase, microperthite and quartz grains. In addition to elongated grains in the foliated zones, mosaic secondary quartz was also noted along the corroded boundaries.

Hornblende is calcic in composition (Table 2-2-2) with a pleochroic scheme of X = light greenish yellow to light green, Y = olive green and Z = green to dark green. Biotite flakes (X = light greenish yellow to pale straw yellow, Y = Z = greenish or yellowish brown to dark brown) are intergrown with hornblende and associated with magnetite and garnet (if any) to constitute the rock foliations. The biotite has a wide range of annite content (Table 2-2-3) and can be classified as Fe^{2+}-biotite (Foster, 1960; See Fig. 2-2-3). Chloritization frequently occurs in both; the clusters of opaques and sphene aggregates associated with the mafic minerals are products of oxidation and Fe-Ti ion redistribution. Besides, apatite, zircon, allanite and quartz are common inclusions; graphic intergrowth of microcline with quartz was also observed.

Although pyroxene is the dominant mafic mineral in some samples (eg. 75-L-77 and 74-L-50), it is accessory or absent from most rocks of this type. Euhedral olinopyroxene crystals show exsolution lamellae of orthopyroxene and oxidation rims of magnetite. Frequently, it is completely replaced by chlorite and/or occurs as a relict core in hornblende or biotite.

Apatite and zircon also occur as individual grains; brownish allanite is commonly altered to a yellowish brown mineraloid due to radioactive damage. In one sample (75-L-59), garnet contains magnetite in the core and is intergrown with hornblende and biotite.

2.2.3 Granite And Granodiorite -

The youngest phase of the Algonquin Batholith is the granitic rock, which plots in the fields of granite and granodiorite of Streckeisen (1976; See Fig. 2-2-2) or falls within the definition of quartz monzonite of Lumbers (1982). Generally, these rocks are pinkish in colour, medium- to coarse-grained and foliated. The texture is mainly hypidiomorphic with subordinate cataclastic and porphyritic features locally.

The granitic rocks are commonly composed of 18 to 35% quartz, and roughly equal amounts of plagioclase and K-feldspar. Felsic minerals constitute more than 90% modal composition in most samples. Biotite is the major ferromagnesian mineral; more rarely, hornblende is present as well. Muscovite, with a biotite core is thought to be of secondary origin by replacement of biotite. Apatite, zircon, sphene, allanite and iron-oxide are

common accessory minerals. Garnet, secondary calcite and epidote occur locally.

Granulation of quartz is common in the foliation zone. Myrmekite or vermicular intergrowth occurs frequently along the contact between microcline and plagioclase. Feldspar unmixing texture occurs in microcline more often in the granitic rocks than that in monzonite - syenite phases. Plagioclase ($An_{< 30}$) is highly sericitized in the core with secondary calcite and epidote aggregates. Compositions and calculated formulae of selected feldspars are given in Table 2-2-1.

Biotite is the chief and, in some, the only mafic mineral in these rocks. It is pleochroic from X = pale straw yellow to Y = Z = light to dark brown with greenish tint; the composition of the biotite is Fe^{2+}-biotite (Fig. 2-2-3) with a relatively lower mole fraction of annite (Table 2-2-3). Minor hornblende (X = light green, Y = olive green, Z = dark green with bluish tint) is calcic amphibole in composition (Table 2-2-2). Both are commonly chloritized and partly oxidized to opaques or amorphous ferruginous material. Zircon, apatite and sphene are common inclusions.

2.2.4 Syeno-monzo-dioritic Rocks -

Rocks of this category are characterized by their plagioclase of oligoclase composition and can be classified as syenodiorite and oligoclase diorite of Lumbers, (1982). They are, with one exception, located in the monzodiorite and quartz diorite fields of Streckeisen (1976; See Fig. 2-2-2) and are considered to be hybrid phases between monzonite-syenite and mafic rocks of the batholith.

The syeno-monzo-dioritic rocks are generally composed of less than 15% quartz, 45 to 75% plagioclase (An_{20-35}) and variable amounts of K-feldspar. Biotite and hornblende are the major mafic components, while apatite, zircon, sphene, iron-oxides and allanite are common accessories.

2.3 Whole-rock Geochemistry

2.3.1 Major-oxides -

With respect to SiO_2, monzonite-syenite rocks of the Algonquin Batholith plot in the saturated and undersaturated fields of Thornton and Tuttle (1960; See Fig. 2-2-4), except for two quartz-rich monzonitic samples. Granite, granodiorite, trondhjemite and tonalite are silica - oversaturated; while dioritic-gabbroic rocks are

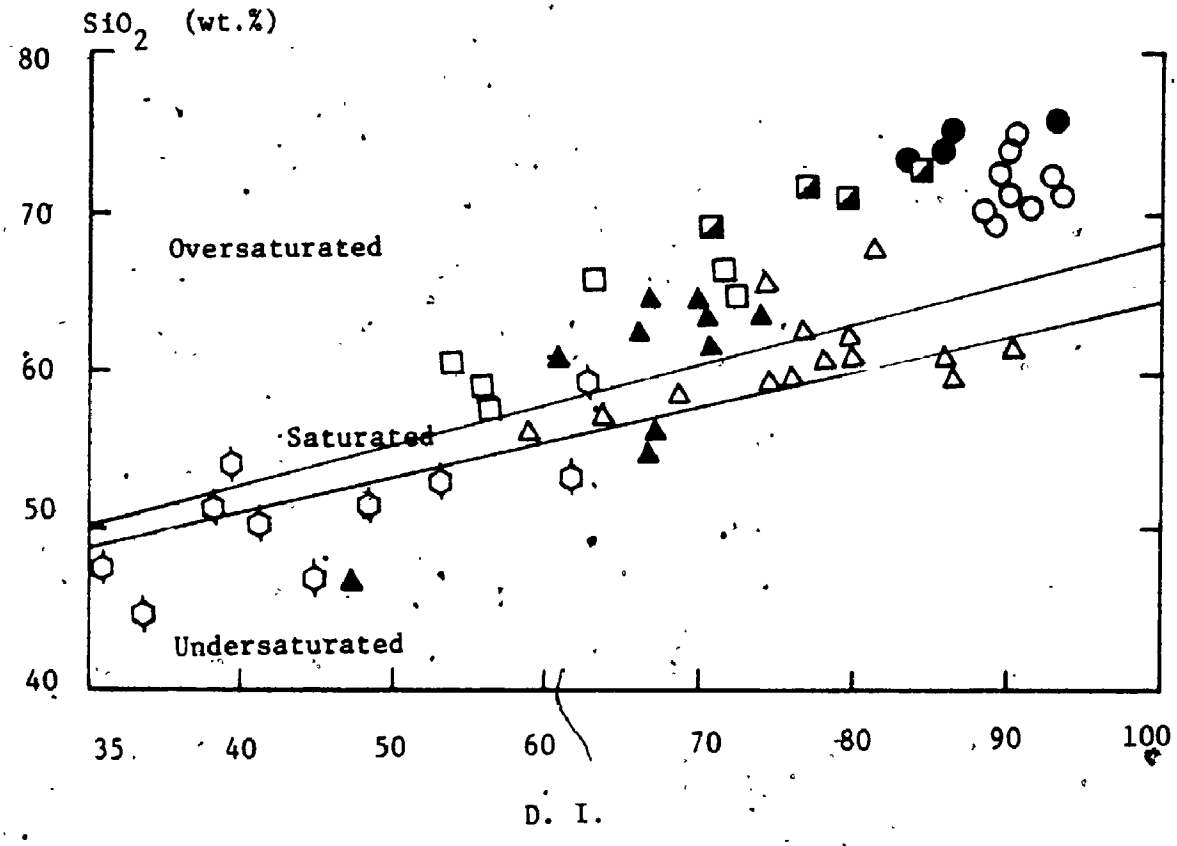

Figure 2-2-4. Variation of SiO_2 as a function of D.I.
Solid-lines separate the oversaturated, saturated and undersaturated fields of Thornton and Tuttle (1960).

○ Granite
● Granodiorite
△ Monzonite-syenite
▲ Syeno-monzo-diorite
□ Tonalite
◪ Trondhjemite
⬡ Diorite-gabbro

scattered in all three fields. Excluding diorite and gabbro, the average molar $Al_2O_3/(Na_2O+K_2O+CaO)$ of the batholith ranges from 1.09 to 0.95 indicating a peraluminous to metaluminous composition.

The mean compositions of various rock-types from the Algonquin Batholith are summarized in Table 2-2-4. There are general trends of increasing Na_2O/K_2O ratios and decreasing agpaitic indices from granite to diorite-gabbro. Granodiorite contains higher SiO_2 than granite, which is a reverse trend of the normal igneous differentiation; besides, granodioritic rocks have the highest oxidation indices of the batholith indicating a more oxidizing environment during crystallization. Comparatively, average granite of the batholith is similar to the calc-alkaline granite of Nockolds (1954; See Table 2-2-4); the monzonite-syenite is similar to quartz syenite from the Gardar Province (Watt, 1966) and from the Pikes Peak Bahtolith (Barker et al, 1975), except that the former has relatively lower SiO_2, total alkali and agpaitic index (0.72; 0.92 - 0.95 for the latter). Trondhjemitic rocks of the batholith are similar to those of the Elzevir Batholith (Pride and Moore, 1983), except for their lower agpaitic index; while tonalite and diorite agree with those average compositions of Nockolds (1954).

Table 2-2-4. Comparison of mean compositions of the Algonquin Batholith with other similar rock-types

	1 (n=10)	2 (n=4)	3 (n=14)	4 (n=10)	5 (n=7)	6 (n=4)	7 (n=14)	8 (n=72)	9 (n=3)	10 (n=6)	11 (n=16)	12 (n=58)	13 (n=50)
(wt%)													
SiO_2	72.49	74.27	60.90	60.77	62.30	71.28	51.29	72.08	64.70	63.77	70.12	66.15	51.86
TiO_2	0.33	0.38	0.81	0.78	0.61	0.33	1.63	0.37	0.30	0.75	0.37	0.62	1.50
Al_2O_3	13.80	12.60	17.96	18.88	17.33	14.32	17.93	13.86	17.60	15.73	15.68	15.56	16.40
Fe_2O_3	0.91	1.38	1.76	1.81	1.46	1.84	2.50	0.86	1.30	2.07	* 2.57	1.36	2.73
FeO	1.30	1.27	3.46	3.18	3.68	1.81	7.66	1.67	1.90	4.01	-	3.42	0.97
MnO	0.04	0.04	0.10	0.09	0.09	0.07	0.15	0.06	0.20	0.15	~~0.07~~	0.08	0.18
MgO	0.53	0.40	1.10	2.07	2.33	1.36	5.62	0.52	0.20	0.33	0.92	1.94	6.12
CaO	1.24	1.52	2.98	4.45	5.10	2.76	7.80	1.33	1.30	1.60	2.73	4.65	8.40
Na_2O	3.47	2.85	4.68	4.62	4.66	4.05	3.26	3.08	6.20	5.52	4.57	3.90	3.36
K_2O	5.06	5.89	4.93	2.09	1.11	1.32	1.21	5.46	5.50	5.39	2.57	1.42	1.33
P_2O_5	0.08	0.01	0.21	0.37	0.21	0.17	0.44	0.18	0.10	0.14	0.10	0.21	0.35
LOI	0.36	0.34	0.56	0.51	0.31	0.83	0.45	0.53	0.05	0.54	-	0.69	0.80
Na_2O/K_2O	0.68	0.48	0.95	2.21	4.20	3.07	2.69	0.56	1.13	1.02	1.78	2.75	2.53
O.I.	54.03	67.49	50.86	55.15	43.32	61,28	38.71	50.74	57.78	50.80	-	44.30	43.92
A.I.	0.81	0.73	0.72	0.52	0.51	0.57	0.35	0.79	0.92	0.95	0.83	0.51	0.42
Al/CNK	1.03	1.09	0.98	1.05	0.95	1.09	0.85	-	-	-	-	-	-

Average compositions of the Algonquin Batholith (this study) :

1. Granite, 2. Granodiorite, 3. Monzonite-syenite, 4. Syeno-monzo-diorite,
5. Tonalite, 6. Trondhjemite, 7. Diorite-gabbro.
8. Average calc-alkaline granite of Nockolds (1954).
9. Average quartz-syenite from the Pike Peak Batholith (Barker et al., 1975).
10. Average quartz-syenite from the Gardar Province, Greenland (Watt, 1966).
11. Average composition of the Elzevir Batholith, Ontario (Pride and Moore, 1983).
12. Average tonalite of Nockolds (1954).
13. Average diorite of Nockolds (1954).

* Total iron as Fe_2O_3.
O.I. = oxidation index; A.I. = agpaitic index.
Al/CNK = molar Al_2O_3/ (Na_2O+K_2O+CaO).

The normative Qtz-Plag-Or projection of the batholith (Fig. 2-2-5) shows the quartz-rich nature of the granodioritic and trondhjemitic rocks; on the other hand, tonalitic rocks have less quartz than the average tonalite of Nockolds (1954). In terms of normative An-Ab-Or composition (Fig. 2-2-6), granite, granodiorite and most monzonite-syenite are in the granite field of O'Connor (1965), while trondhjemite, tonalite and dioritic rocks are in the tonalite field. Rocks of syeno-monzo-diorite are scattered in both the granodiorite and tonalite field, while gabbroic rocks form a distinct group near the An-apex. Although granite and granodiorite are both enclosed in a 2% contour of granitic rocks (Tuttle and Bowen, 1958), only granitic rocks fall within the low temperature trough of Kleeman (1965) which is indicative of a magmatic origin. In addition, granitic rocks are closely associated with the eutectics of Ab/An = 2.9 in the Qtz-Ab-Or plot (Fig. 2-2-7), and the monzonite-syenite rocks lie within the syenite field of Gardar Province (Watt, 1966). Two quartz-rich monzonite samples are related to the granitic trend. It is also noteworthy that projections of gabbros were away from Ab-apex in Qtz-Ab-Or diagram as compared to Qtz-Plag-Or plot, which may reflect their high normative An-compositions; two gabbroic samples plotted in

2

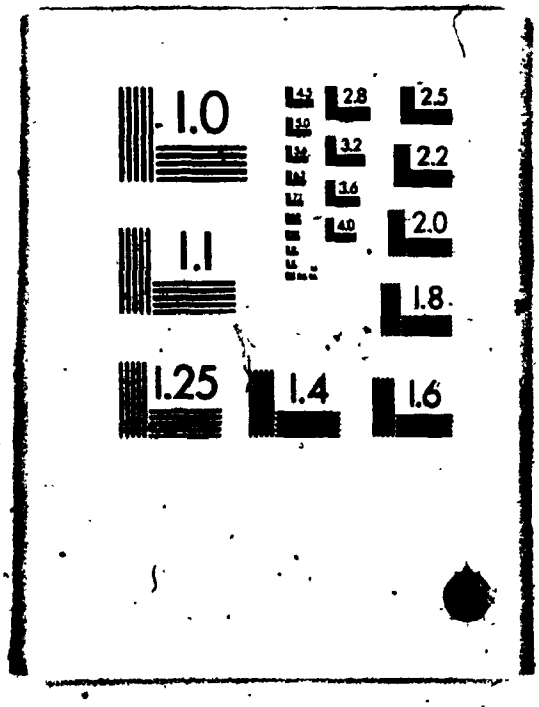

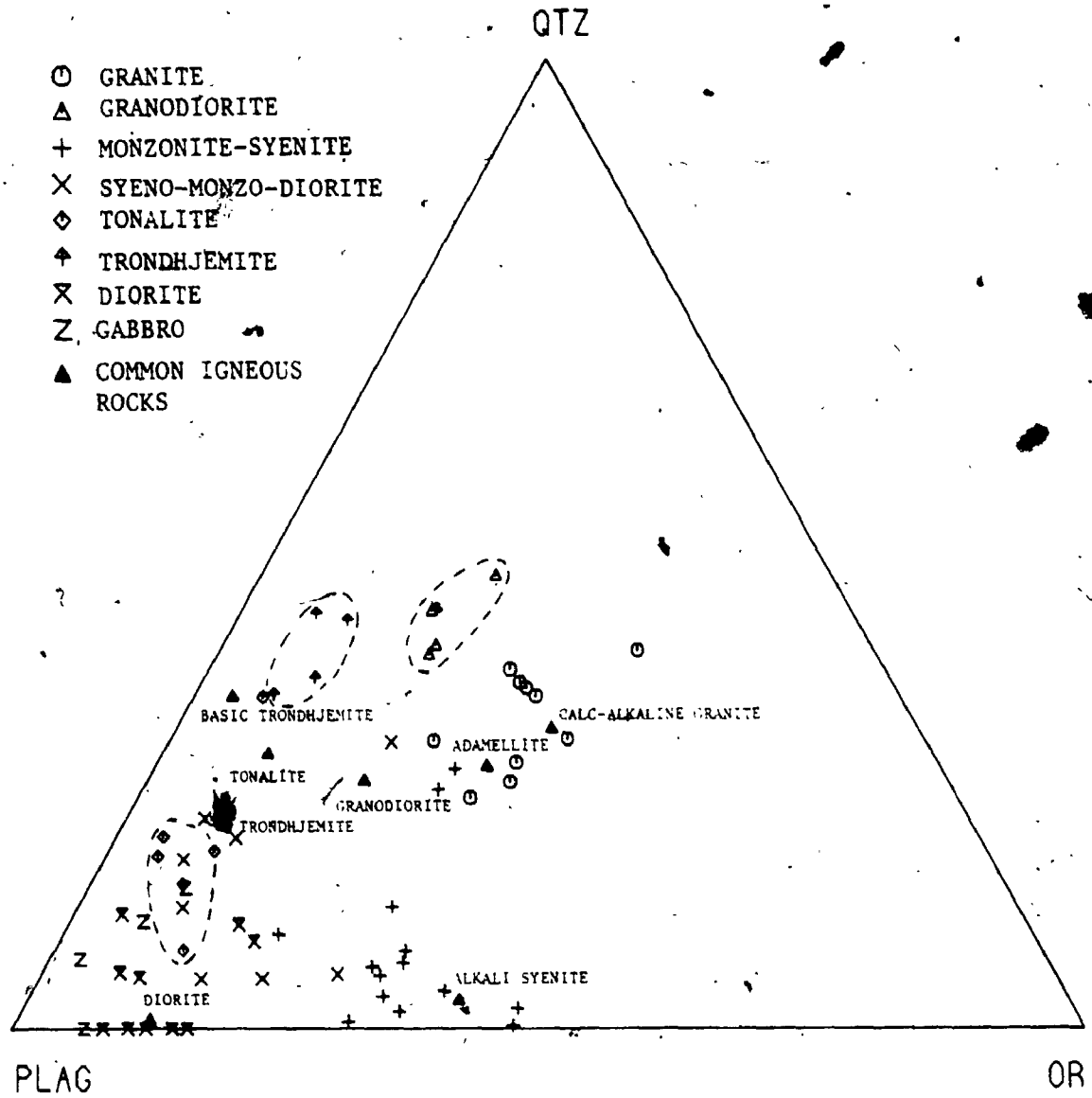

Figure 2-2-5. Normative Qtz-Or-Plag ratios of the Algonquin Batholith and common igneous rocks. Compositional fields of the tonalite, trondhjemite and granodiorite of the Algonquin Batholith are enclosed by dashed lines. Compositions of common igneous rocks are taken from Nockolds (1954).

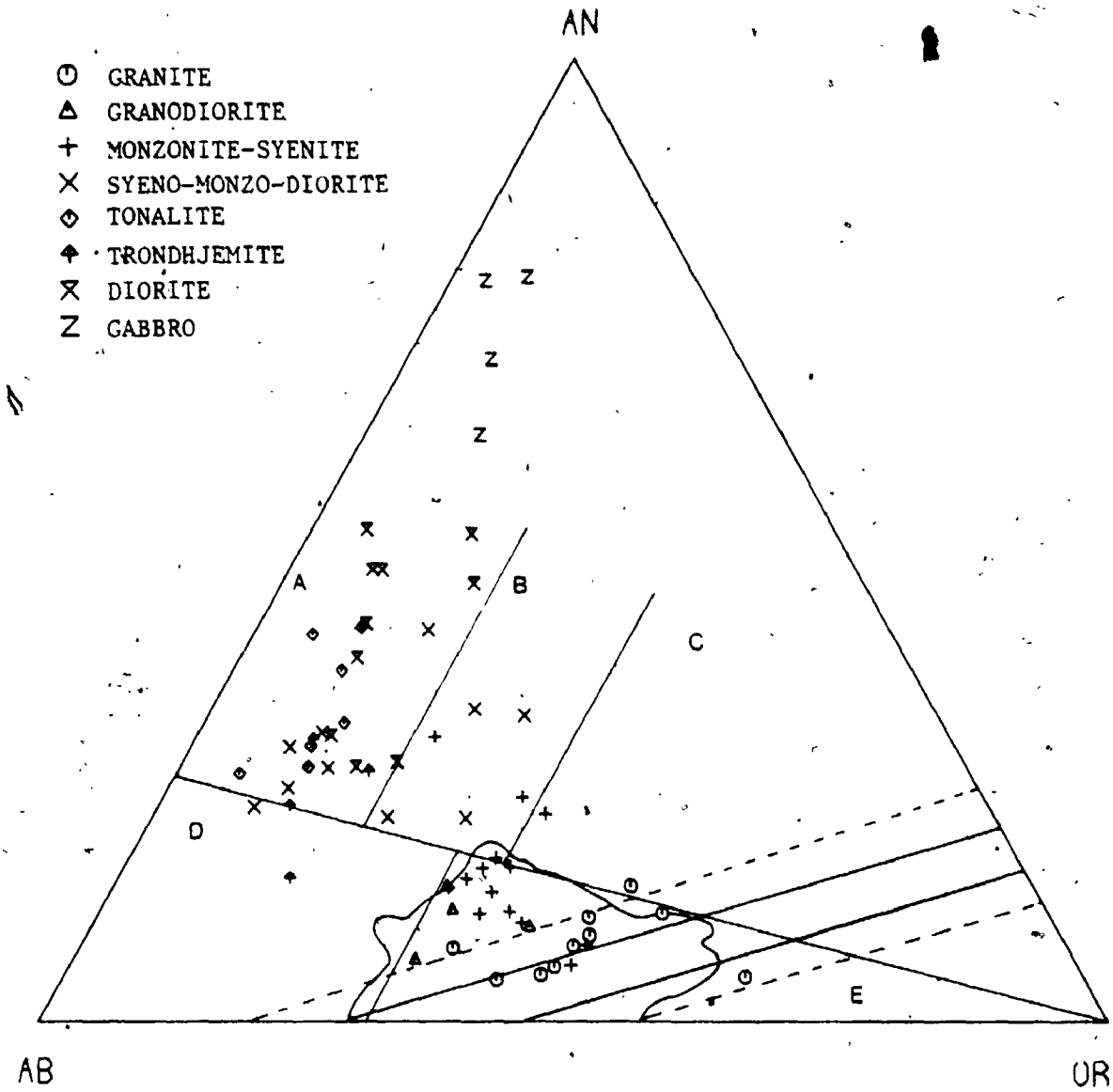

Figure 2-2-6, Normative Ab-An-Or ternary diagram of the Algonquin Batholith. The irregular solid boundary is the 2% contour of Tuttle and Bowen (1958) enclosing most of granitic rocks that contain 80% or more normative Ab+An+Or+Qtz. Solid-lines indicate the boundaries of low temperature trough; dashed-lines show uncertainty due to analytical errors (Kleeman, 1965). Classification scheme is after O'Connor (1965) : A. Tonalite B. Granodiorite C. Quartz monzonite D. Trondhjemite E. Granite

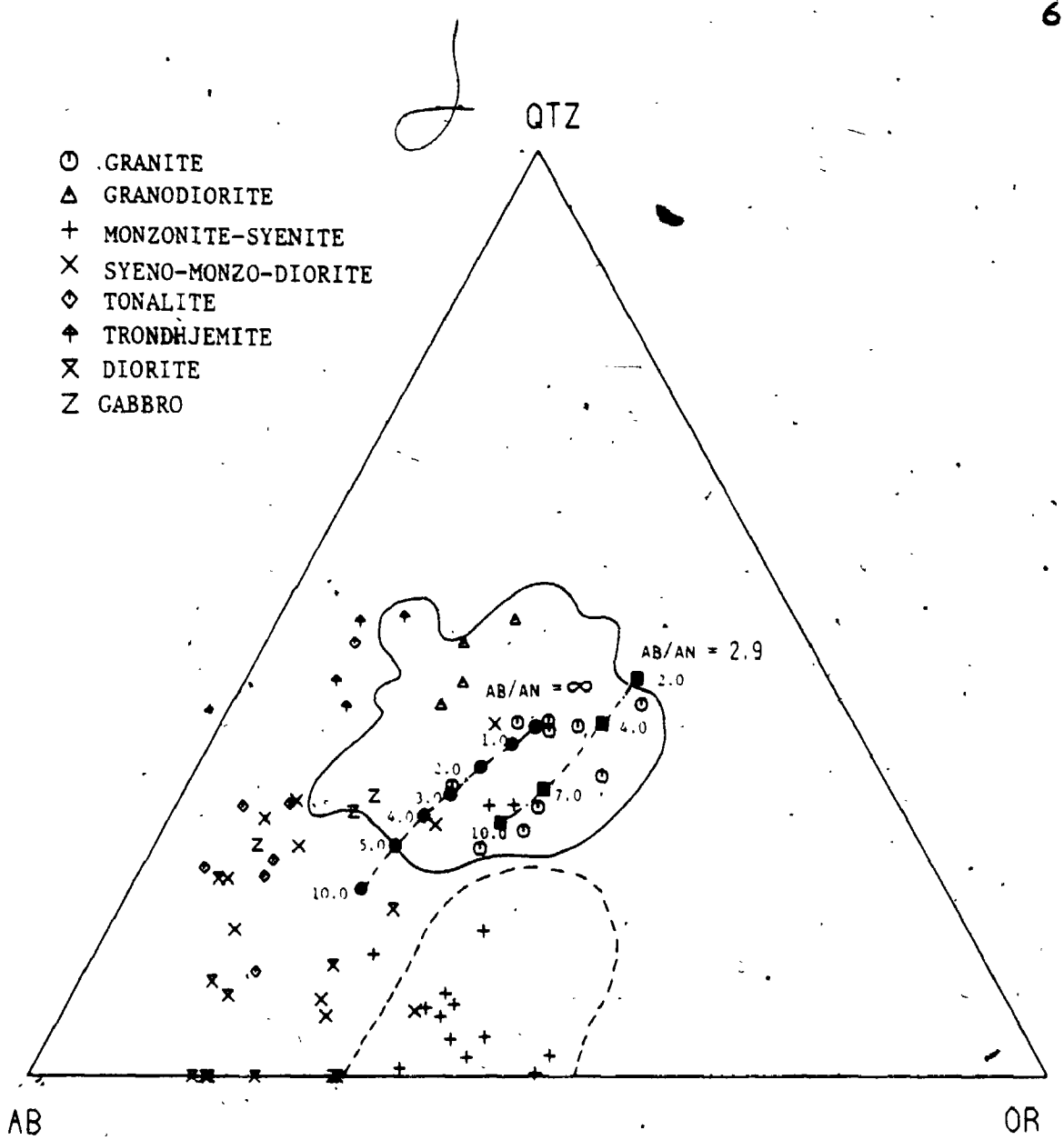

Figure 2-2-7. Normative Qtz-Ab-Or ternary diagram of the Algonquin Batholith. The solid irregular boundary encloses analyses of 1190 granitic rocks (Winkler and Von Platen, 1961). The irregular dashed-line shows the compositional field of syenitic rocks from Gardar Province of Greenland (Watt, 1966). Experimentally determined ternary minima (Tuttle and Bowen, 1958; Luth et al., 1964) and minima in An - bearing systems (James and Hamilton, 1969) are shown by solid circles and solid squares, respectively.

the granite field (Winkler and Von Platen, 1961) can be explained by exaggeration of the plotting method used. Furthermore, the diorite - tonalite - trondhjemite rocks show an Ab-enriched trend similar to that of gabbro - trondhjemite of southwest Finland (Barker and Arth, 1976).

The K_2O-Na_2O-CaO ternary diagram (Fig. 2-2-8) is one of the most informative methods for illustrating compositional trends of the Algonquin Batholith. The diorite - tonalite - trondhjemite again show a Na_2O-enrichment trend with relatively lower K_2O abundances as compared to the trend outlined by Barker and Arth (1976), whereas syenitic and granitic rocks show a K_2O-enrichment trend similar to the typical calc-alkaline series of the Southern California Batholith (Nockolds and Allen, 1956). Granodiorite follows the calc-alkaline trend. Similar results were also obtained from the AFM ternary plot (Fig. 2-2-9). Scattered data of syeno - monzo - diorite in both diagrams may reflect their heterogeneous origin.

Therefore, for further discussions, rocks of the Algonquin Batholith are chemically grouped into: (1) the sodic, diorite -tonalite - trondhjemite association, and (2) the potassic, syenite - monzonite - granodiorite - granite association. Gabbroic rocks are considered to be cumulates.

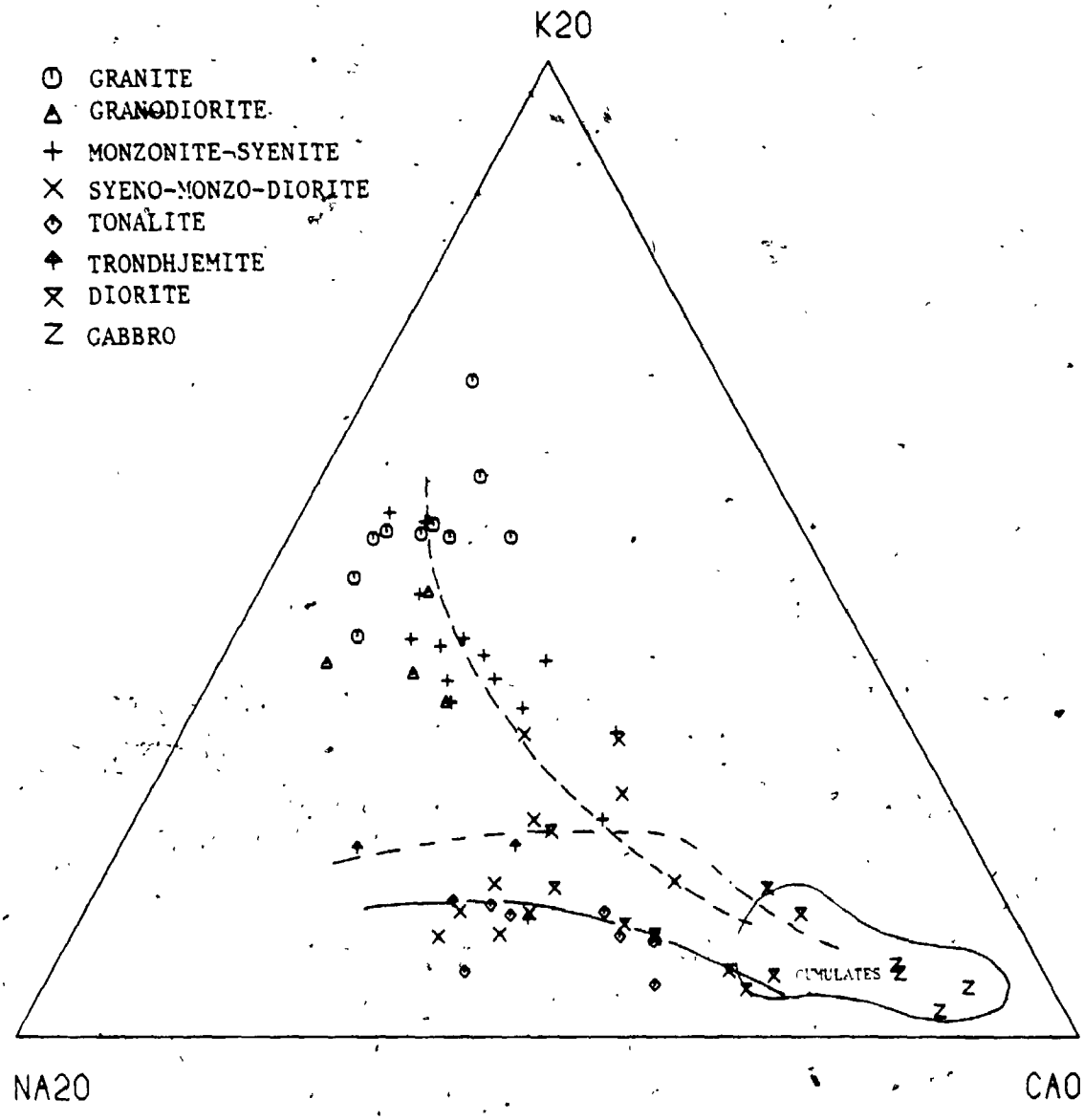

Figure 2-2-8. Na_2O-K_2O-CaO variation diagram of the Algonquin Batholith.

---- Calc-alkaline trend of Southern California Batholith (after Nockolds and Allen, 1956)

—·—·— Typical trondhjemite trend of Barker and Arth (1976).

——— Tonalite-trondhjemite trend of the Algonquin Batholith (this study).

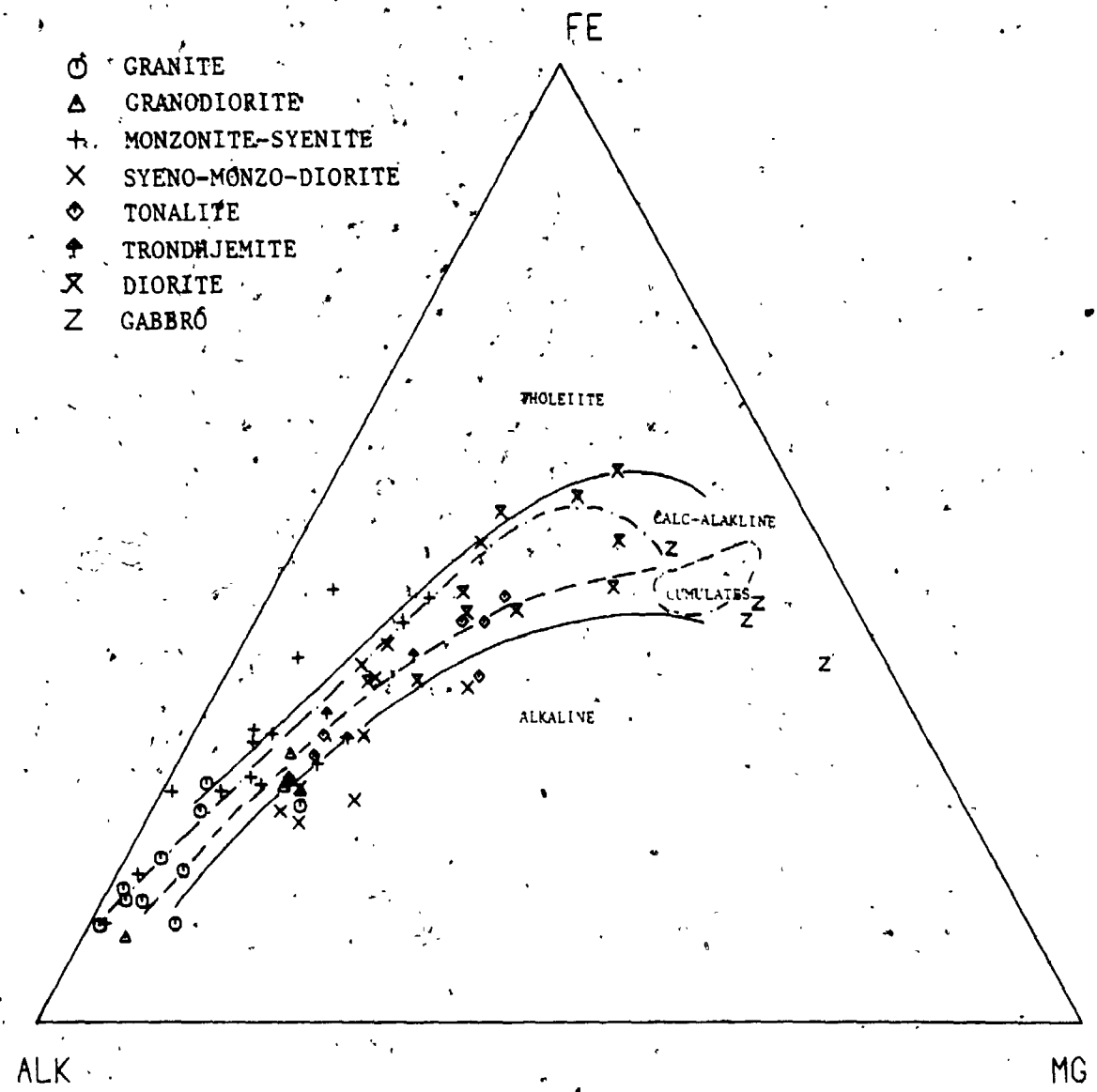

Figure 2-2-9. AFM diagram of the Algonquin Batholith.
Solid lines separate the tholeiite, calc-alkaline and alkaline fields (Barker and Arth, 1976).

-·-·- Calc-alkaline trend of Southern California Batholith (Nockolds and Allen, 1956).

---- Typical trondhjemite trend (Barker and Arth, 1976).

However, these compositional trends are not necessarily the results of differentiation.

Correlation coefficients of major-oxides as a function of SiO_2 for both sodic and potassic rock-associations are given in Table 2-2-5. For sodium-rich rocks, there are strong negative correlations of TiO_2O, MnO, MgO, CaO and P_2O_5 with SiO_2, while Al_2O_3 shows a trend with a mild negative slope. For potassium-rich rocks, all major-oxides (except for K_2O) show negative correlations with SiO_2. Moreover, during the preliminary studies, it was found that, in syenitic and monzonitic rocks, Al_2O_3 increases with increasing SiO_2 which is the reverse of the general trend of potassium-rich rocks of the batholith. In addition, two quartz-rich monzonitic rocks retaining the syenitic composition are closely associated with the trend of granitic rocks.

2.3.2 Trace-elements -

The mean concentrations of trace-elements of the Algonquin Batholith are summarized in Table 2-2-6. Both granitic and syenitic rocks are higher in Zr, Ba, Ba/Rb, K/Rb, Sr/Ca and Zr/Nb, but lower in Nb and S in comparison with average granite (Taylor, 1964) and syenite (Turenkian and Wedepohl,

Tabel 2-2-5. Correlation coefficients of inter-element variations for the Algonquin Batholith

Correlation		Sodic* rocks	Potassic** rocks	Correlation		Sodic rocks	Potassic rocks
SiO_2 vs.	TiO_2	-0.7135	-0.7632	SiO_2 vs.	U	-0.3773	0.3469
	Al_2O_3	-0.5695	-0.8496		Th	0.6725	0.3104
	Fe_2O_3	-0.9070	-0.7716		F	-0.7112	-0.2755
	MnO	-0.8594	-0.7622		Cl	-0.9881	-0.4915
	MgO	-0.8179	-0.5322		S	-0.4846	-0.4840
	CaO	-0.9221	-0.8054		Ga/Al	-0.7582	-0.1795
	K_2O	0.0066	0.1151		K/Rb	0.3775	-0.5418
	P_2O_5	-0.7147	-0.5948		Rb/Sr	0.3671	0.6672
	Na_2O	0.2308	-0.6358		Sr/Ba	-0.3190	0.1293
	Rb	-0.3151	0.6232		Sr/Ca	0.2761	0.2113
	Sr	-0.5311	-0.6070		Zr/Y	0.0027	-0.2963
	Ba	-0.2439	-0.7286		Y/Ca	0.4316	0.4705
	Zr	-0.5486	-0.6012		Cr/Mg	-0.3675	0.2868
	Nb	-0.6128	-0.4347		V/Mg	-0.6014	0.3329
	Y	-0.5332	-0.7692		Ni/Mg	-0.1601	0.3396
	Ga	-0.8952	-0.7692		Fe/Mg	0.2190	-0.0159
	Pb	0.1726	0.0181		Cr/Fe	-0.3763	0.7309
	Zn	-0.7245	-0.5485		V/Fe	-0.7681	0.4641
	Cu	-0.8762	-0.6099		Ni/Fe	-0.3129	0.7940
	Ni	-0.8541	-0.1104	Nb vs.	Ga/Al	0.6445	0.8194
	Cr	-0.7510	-0.4072	Nb vs.	Y	0.8624	0.8188
	V	-0.9092	-0.3016	Al_2O_3 vs.	Ga	0.3330	0.4777

* Sodic rocks = tonalite + trondhjemite + diorite.

** Potassic rocks = granite + syenite-monzonite.

Table 2-2-6 Average trace-element concentrations of the Algonquin Batholith and similar rock-types

	1 (n=10)	2 (n=4)	3 (n=14)	4 (n=10)	5 (n=7)	6 (n=4)	7 (n=4)	8	9	10
(ppm)										
Nb	11	9	19	15	9	11	18	20	35	-
Zr	257	209	437	208	135	105	173	180	500	196
Y	22	20	30	23	16	19	27	40	20	-
Sr	224	162	398	630	642	280	697	285	200	629
Rb	145	62	95	57	25	43	45	150	110	60
Ba	1013	1170	2270	1165	571	395	636	600	1600	566
Ga	20	18	26	26	23	20	28	18	30	-
Pb	27	18	25	19	13	15	13	20	12	-
Zn	45	70	81	69	58	59	96	40	130	-
Cu	8.9	9.1	10.3	10.0	11.5	9.1	13.1	10	5	36
Ni	4.6	4.4	4.7	8.0	6.0	5.8	18.4	0.5	4	26
Cr	6.1	5.5	7.9	11.7	13.9	7.3	42.3	4	2	43
V	26	23	31	51	71	30	128	20	30	151
S	82	126	194	139	116	71	204	270	300	-
Rb/Sr	0.86	0.42	0.30	0.10	0.04	0.18	0.07	0.53	0.55	0.09
Ba/Sr	5.28	7.32	6.60	1.79	0.84	1.74	0.92	2.10	8.00	0.90
Ba/Rb	7.86	20.21	29.17	21.15	24.84	9.28	15.12	4.00	14.54	9.43
K/Rb	305	431	485	331	402	267	227	223	436	263
Sr/Ca	271	198	212	203	181	138	130	180	111	173
Ga/Al	2.75	2.76	2.82	2.57	2.52	2.58	3.01	2.60	3.41	-
Zr/Nb	32	25	30	13	17	13	12	9	14	-

1. Granite, 2. Granodiorite,
3. Syenite-monzonite, 4. Syeno-monzo -diorite,
5. Tonalite, 6. Trondhjemite,
7. Diorite + Gabbro, 8. Average granite (Taylor, 1964),
9. Average syenite (Turekian and Wedepohl, 1961).
10. Average of 38 tonalite and quartz diorite (Ermanovics et. al., 1979).

1961), respectively. Relatively, Algonquin trondhjemite has lower Zr, Sr, Ba, Ba/Rb, K/Rb and Sr/Ca, and higher Rb, Rb/Sr, Ba/Sr than tonalite of this batholith. As compared to tonalite-quartz diorite of Manitoba (Ermanovics et al., 1979), Algonquin tonalite has similar Sr, Ba abundances but lower Zr, Rb and transition metals to those of Manitoba tonalite. Compositions of granodiorite and syeno - monzo - diorite are somewhat intermediate among granite, syenite and tonalite.

Both sodic and potassic compositional trends of the Algonquin Batholith are again illustrated in the K/Rb vs. Rb plot (Fig. 2-2-10). The syenitic and granitic rocks form a coherent trend with depletion of K/Rb ratios as increasing differentiation, in spite of some compositional overlaps; the diorite - tonalite - trondhjemite members consist of another fractionation trend. Granodiorite and syeno - monzo - dioritic rocks lying between the above two trends may suggest their mixed or hybrid origin.

Correlation coefficients of trace-element variations of the Algonquin Batholith are summarized in Table 2-2-5. For sodic rocks of the batholith, Ga, V, F, Cl and transition metals have strong negative correlations with increasing SiO_2 ($R > -0.70$), while Sr, Nb, Zr and Y are mildly correlated with SiO_2 ($R > -0.50$). Depletion of Sr, high-field

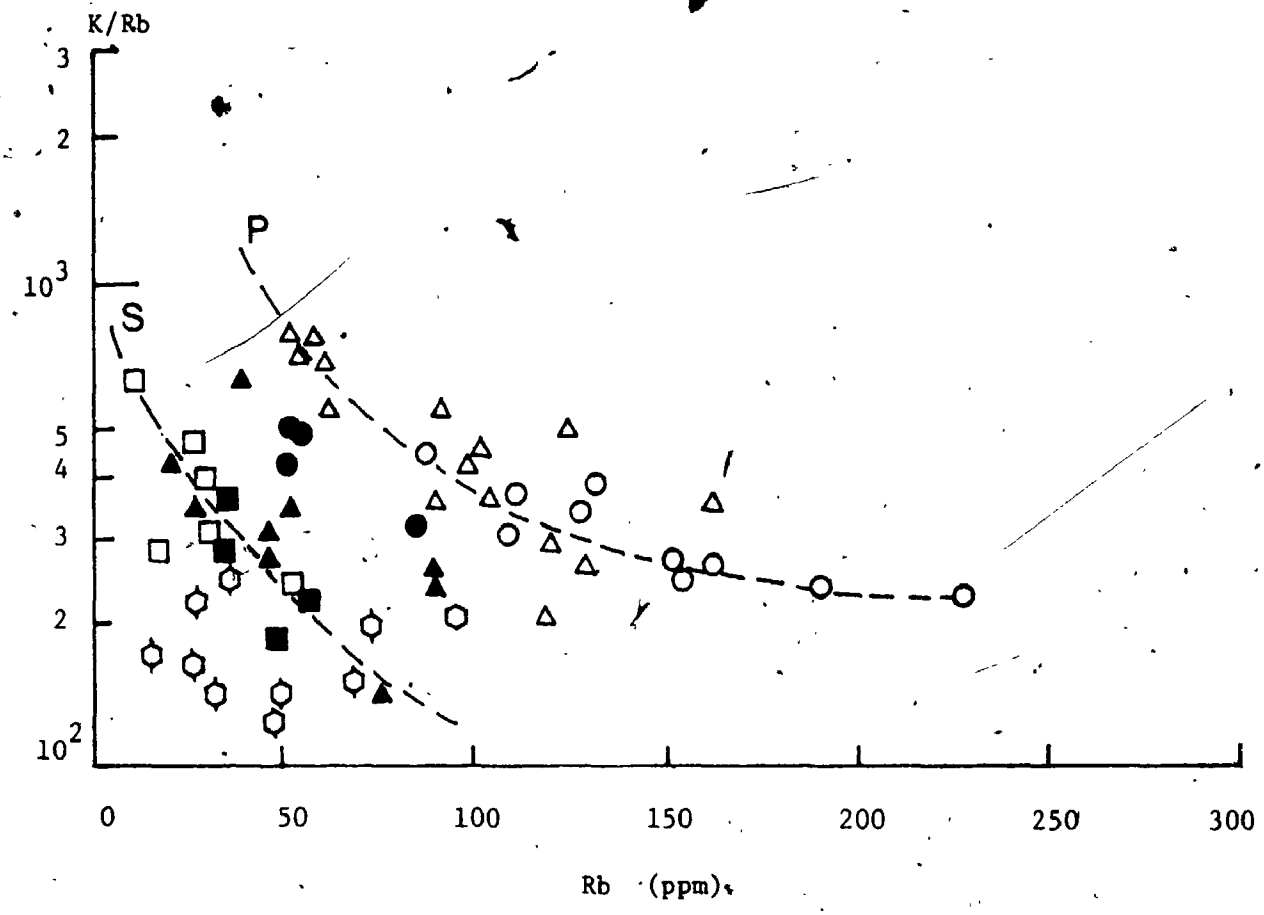

Figure 2-2-10. K/Rb ratio vs. Rb variation diagram of the Algonquin Batholith.

P - Differentiation trend of the potassic rock suite.

S - Differentiation trend of the sodic rock suite.

○ Granite
● Granodiorite
△ Monzonite-syenite
▲ Syeno-monzo-diorite
□ Tonalite
■ Trondhjemite
⬡ Diorite-gabbro

strength (HFS) elements and transition metals in the sodic rocks may be explained by fractionation of plagioclase, minor phases (eg. zircon) and mafic minerals (eg. hornblende), respectively. The decrease of Ga and Ga/Al with increasing SiO_2 are the reverse of crystal-chemical prediction and not readily explained. For potassic rocks, in addition to Ba and Ga having high negative coefficients (> -0.70), there are interpretable trends for Rb, Sr, Zr, Nb, Zn, Cu, Cl and S. In addition, the increases of Rb, Rb/Sr and decreases of Sr, K/Rb with increasing differentiation are consistent with feldspar fractionation in a normal igneous suite. However, in the Rb-Ba-Sr ternary diagram (Fig. 2-2-11), the syenitic and granitic rocks are in both the anomalous and normal granite fields, while the sodic rocks are scattered from diorite to granodiorite fields.

2.3.3 Rare-earth Elements -

Compositions of rare-earth elements and chondrite-normalized element ratios of representative samples from the Algonquin Batholith are given in Table 2-2-7. Their distribution patterns, normalized to average chondritic meteorite (Haskin et al., 1968), are shown in Figure 2-2-12 and 2-2-13. There is a general correlation of total

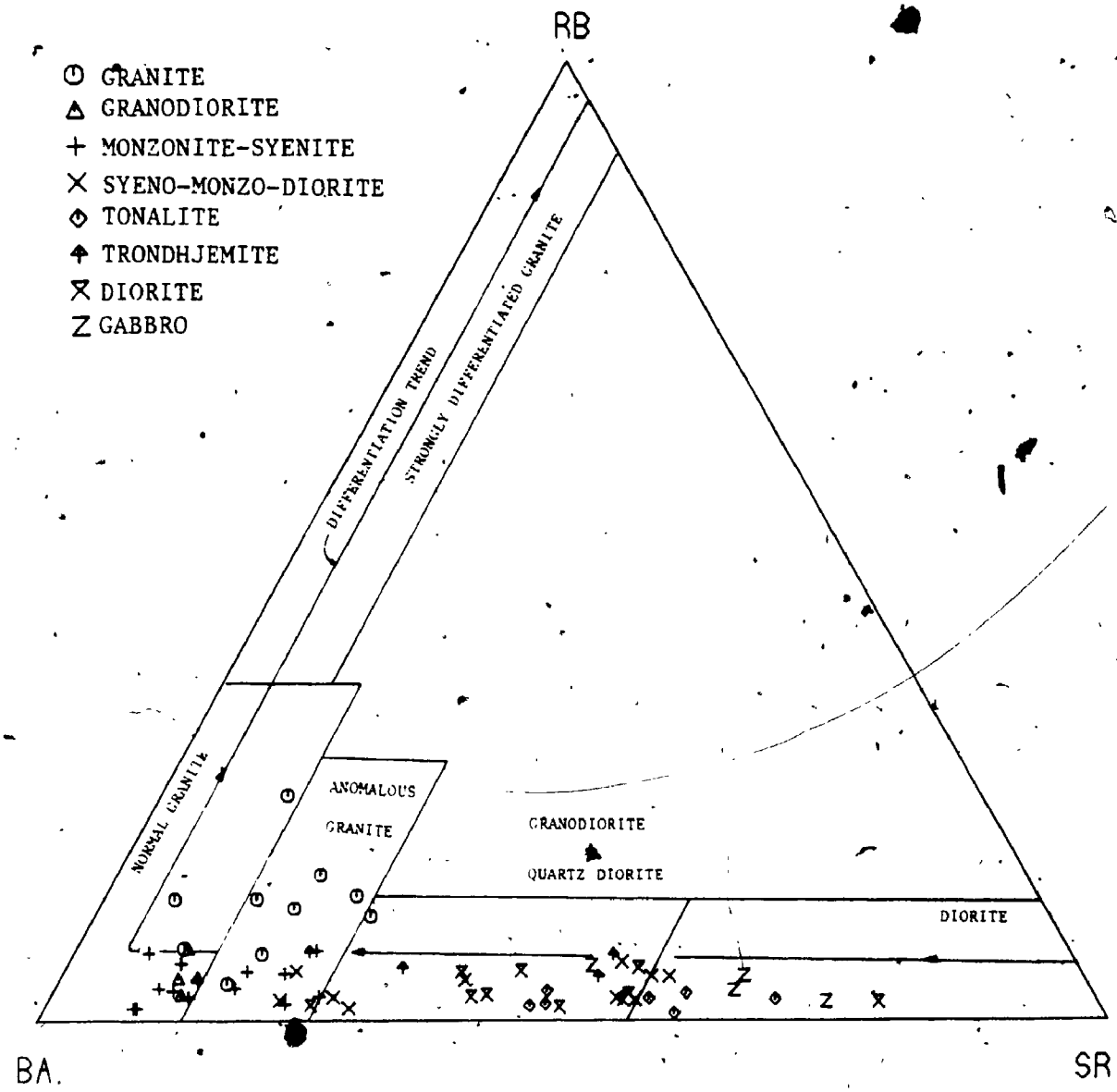

Figure 2-2-11. Rb-Ba-Sr ternary variation diagram of the Algonquin Batholith. Classification scheme is after Bouseily and Sokkary (1975).

Table 2-2-7. Rare-earth elements, Ta, Hf and Cs compositions of the Algonquin Batholith

	1	2	3	4	5	6	7	8	9	10	11	12	13
Sample No.	76-L-138	76-L-58	76-L-52	76-L-46	82-L-65	75-L-40	74-L-50	75-L-29	75-L-75	74-L-146	74-L-149	76-L-65	78-L-54
Rock-type	1	1	1	1	1	2	2	2	2	2	2	3	4
La (ppm)	86.15	244.71	41.41	15.56	17.15	45.94	46.56	24.73	53.67	38.99	42.28	26.83	49.90
Ce	201.45	248.68	83.62	22.83	34.18	111.94	99.97	63.97	116.29	72.59	103.12	60.40	126.92
Sm	14.70	17.19	5.04	1.73	3.99	12.20	10.68	6.05	7.22	4.55	11.64	4.53	12.60
Eu	2.30	2.03	0.79	1.23	0.83	3.34	2.81	2.83	2.26	2.40	2.69	1.05	5.69
Tb	1.92	3.27	0.57	0.15	1.24	1.46	1.18	0.85	1.02	0.38	2.41	0.53	1.42
Yb	9.29	4.33	1.59	0.69	4.99	6.63	6.12	3.74	1.95	1.92	14.84	1.58	5.09
Lu	0.74	0.78	0.28	0.16	0.29	0.53	0.64	0.54	0.42	0.20	1.16	0.28	0.40
ΣREE	316.55	520.99	133.30	42.35	62.67	182.04	167.96	102.71	182.83	121.03	178.14	95.20	202.02
Ta	4.61	4.13	4.19	4.07	0.33	1.80	2.63	2.09	1.44	2.44	5.23	4.24	1.22
Hf	10.05	23.24	7.23	5.29	5.47	11.98	9.95	16.31	14.07	8.07	10.91	5.29	2.84
Cs	0.31	0.73	0.47	0.73	2.17	0.32	0.37	0.49	0.28	0.26	0.42	0.14	0.18
Eu/Eu*	0.52	0.34	0.52	2.57	0.52	0.92	0.84	1.58	0.97	1.94	0.67	0.79	1.58
$(Ce/Yb)_N$	4.98	12.82	11.88	6.50	1.56	3.85	3.68	3.84	13.20	8.20	1.58	8.63	5.76
$(Ce/Sm)_N$	2.83	2.97	3.39	2.60	1.77	1.90	1.93	2.21	3.30	3.28	1.83	2.76	2.06
$(Tb/Yb)_N$	0.89	3.18	1.50	0.75	1.04	0.94	0.81	0.95	2.20	0.80	0.69	1.38	1.20
SiO_2	70.17	71.58	72.44	74.38	74.85	57.18	58.66	58.90	61.78	61.88	67.68	76.97	55.80

(Table 2-2-7 cont'd)

	14	15	16	17	18	19	20	21	22	23	24	25	26
Sample No.	82-L-107	81-L-68	80-L-437	76-L-41	82-L-74	75-L-42	75-L-43	80-L-440	82-L-35	75-L-82	82-L-70	82-L-108	82-L-71
Rock-type	4	4	[illegible]	5	5	5	5	6	7	7	7	7	8
La (ppm)	31.44	19.18	15.52	25.76	10.20	[illegible].67	19.25	11.88	11.32	9.49	18.04	36.31	7.61
Ce	54.95	37.92	30.87	55.05	21.11	29.85	34.85	8.44	12.50	20.37	21.65	45.70	4.89
Sm	6.98	3.95	3.59	5.32	1.89	2.82	2.70	1.57	4.58	2.68	5.47	9.90	1.17
Eu	1.46	0.76	0.94	1.38	0.69	0.90	0.94	1.09	1.01	1.07	1.29	1.03	0.55
Tb	1.29	0.51	0.69	0.51	0.32	0.23	0.36	0.13	0.75	0.37	0.53	1.20	0.17
Yb	5.20	2.52	1.95	2.57	0.57	1.06	1.23	0.76	3.02	1.53	2.89	6.12	1.47
Lu	0.36	0.17	0.15	0.21	0.10	0.35	0.20	0.04	0.19	0.24	0.17	0.48	0.08
ΣREE	101.68	65.01	53.71	90.80	34.88	50.88	59.63	23.91	33.37	35.75	50.04	100.74	16.50
Ta	0.54	0.34	0.11	1.29	0.36	2.04	1.73	0.05	0.65	0.66	0.36	0.30	0.14
Hf	5.91	3.36	3.84	3.73	2.66	1.87	1.30	3.71	1.63	1.23	1.20	2.47	0.71
Cs	0.79	0.39	0.31	0.08	0.16	0.16	0.10	0.33	0.35	0.07	0.07	0.55	0.17
Eu/Eu^*	0.64	0.65	0.72	0.95	1.11	1.18	1.17	2.67	0.68	1.33	0.90	0.36	1.48
$(Ce/Yb)_N$	2.42	3.31	3.50	4.85	8.00	6.80	5.71	2.50	0.93	2.88	1.79	1.68	0.76
$(Ce/Sm)_N$	1.66	1.95	1.75	2.17	2.40	2.13	2.67	1.11	0.56	1.53	0.83	0.95	0.86
$(Tb/Yb)_N$	1.04	0.85	1.50	0.85	2.33	1.00	1.14	0.75	1.07	1.00	0.79	0.81	0.49
SiO_2	60.63	62.07	64.16	57.87	63.18	64.44	65.74	72.05	45.09	50.42	51.78	54.03	50.50

Rock-type - 1. Granite, 2. Syenite-monzonite, 3. Granodiorite, 4. Syeno-monzo-diorite, 5. Tonalite, 6. Trondhjemite, 7. Dioritic rocks, 8. Gabbro.

Eu/Eu^* - Observed Eu value / value obtained by interpolating between Sm and Tb.

$(Ce/Yb)_N$ - Degree of fractionation of REE as a whole.

$(Ce/Sm)_N$ - Degree of LREE fractionation.

$(Tb/Yb)_N$ - Degree of HREE fractionation.

REE with rock-type in that the potassic rocks have relatively higher REE abundances and more fractionated patterns, while the gabbro has the lowest REE concentration and less fractionated curve with a large positive Eu-anomaly (Fig. 2-2-12B).

Except for one dioritic rock (82-L-108), sodic rocks contain less than 100 ppm of total REE and have mild fractionation patterns ($(Ce/Yb)_N$ = 8.00 to 0.93, chondrite-normalized Ce/Yb ratio as an indicator of overall REE fractionation) (Fig. 2-2-12). Comparatively, the tonalite-trondhjemite members of this batholith are less fractionated than those of continental margin and interior trondhjemites (Arth, 1979; See Fig. 2-2-12A). However, they have similar REE compositions to tonalite-trondhjemite rocks from southwest Finland (Arth et al., 1978). Additionally, REE contents of the dioritic rocks increase with increasing SiO_2, while the total REE decrease and Eu/Eu* ratios increase (from 0.95 to 2.67) as SiO_2 increases in the tonalite-trondhjemite. Such a sympathetic variation of REE with SiO_2 from tonalite to trondhjemite is similar to that of the diorite-tonalite-trondhjemite suite of Finland (Arth et al., 1978), which can result through continuous crystallization of hornblende from a gabbroic melt (Arth and Barker, 1976). On the other hand,

Figure 2-2-12. Chondrite-normalized REE distribution patterns for diorite-tonalite-trondhjemite association of the Algonquin Batholith.

(A) REE distributions for tonalite-trondhjemite.

(B) REE distributions for diorite-gabbro.

(REE concentrations of the gabbro-tonalite-trondhjemite suite of Finland were from Arth et. al, 1978)

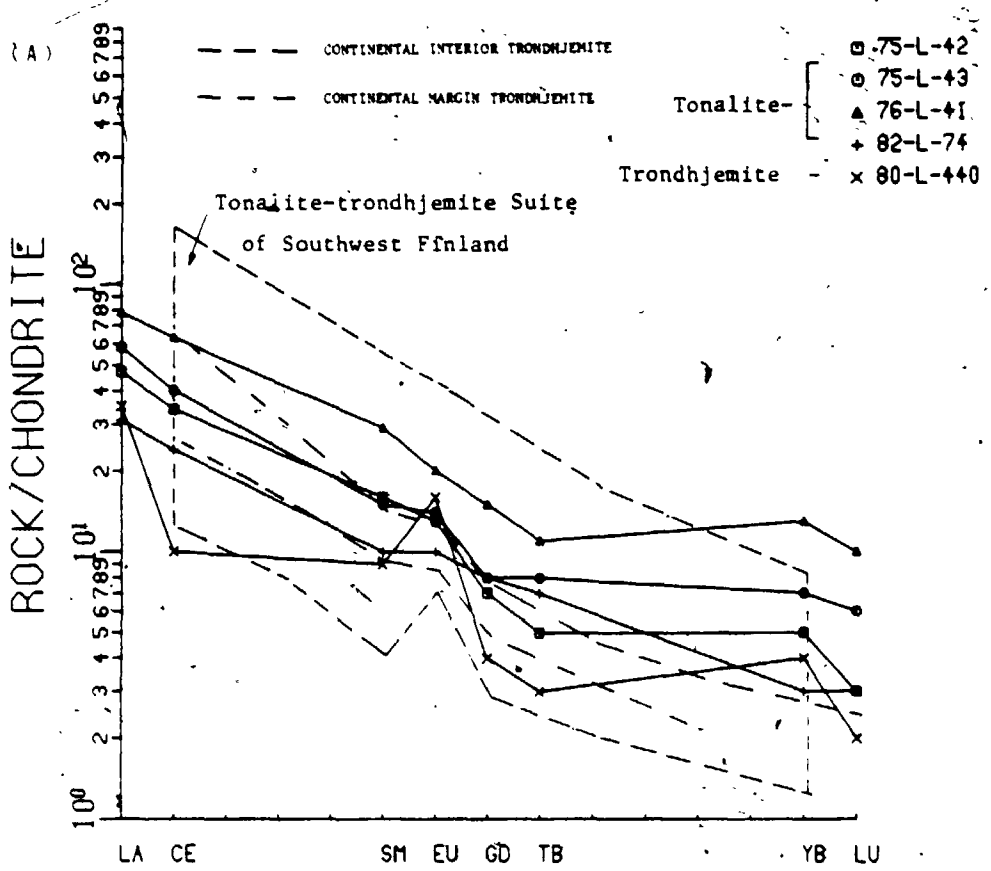
(A)
CONTINENTAL INTERIOR TRONDHJEMITE
CONTINENTAL MARGIN TRONDHJEMITE
Tonalite-
75-L-42
75-L-43
76-L-41
82-L-74
Trondhjemite -
80-L-440
Tonalite-trondhjemite Suite
of Southwest Finland
ROCK/CHONDRITE
LA CE SM EU GD TB YB LU

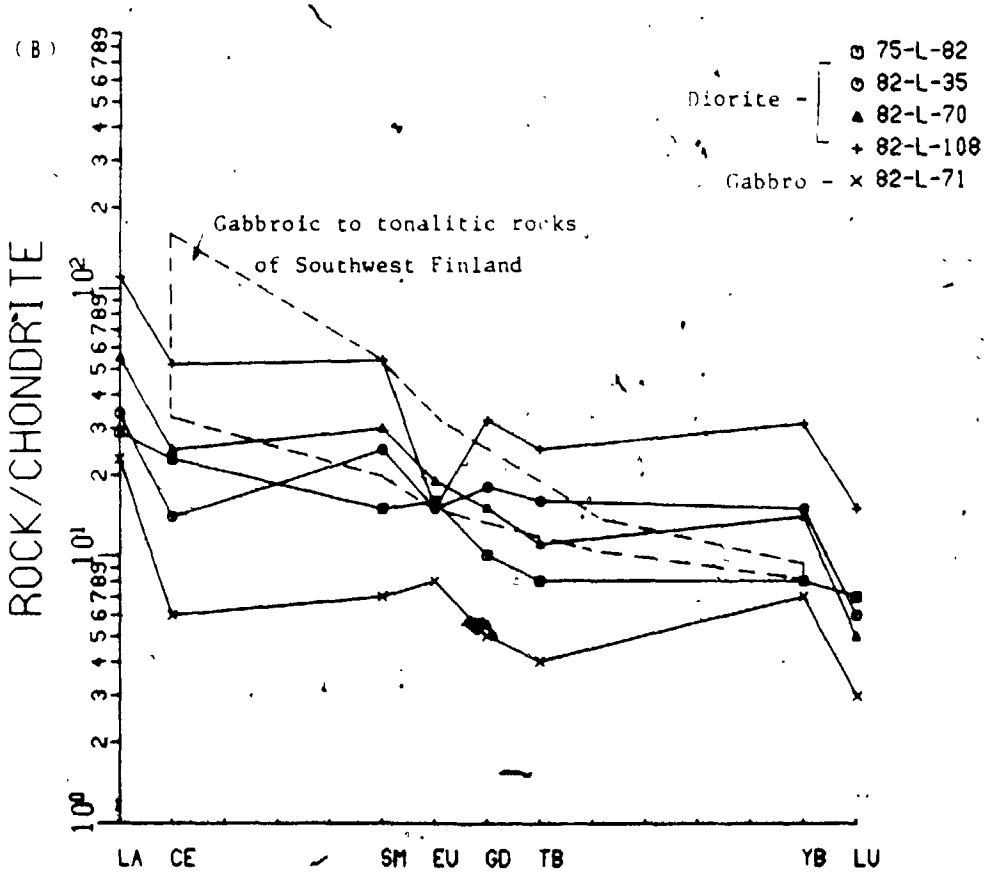
(B)
Diorite -
75-L-82
82-L-35
82-L-70
82-L-108
Gabbro -
82-L-71
Gabbroic to tonalitic rocks
of Southwest Finland
ROCK/CHONDRITE
LA CE SM EU GD TB YB LU

dioritic rocks of this batholith are less fractionated and with mild positive or negative Eu-anomalies, which are different from the gabbro-diorite of Arth et al (1978). Gabbro with pronounced positive Eu-anomaly and lower REE abundances than those of diorites is not considered to be cogenetic with the diorite - tonalite - trondhjemite suite of this batholith.

The granitic rocks (Fig. 2-2-13A) are LREE-enriched with strongly to moderately fractionated patterns ($(Ce/Yb)_N$ = 12.86 - 1.56). Except for 76-L-46, all granites have large negative Eu-anomalies with a constant Eu/Eu* about 0.52. Comparatively, granitic rocks of the Algonquin Batholith have higher REE abundances and less fractionated patterns than those of the Giant Range Granites (Arth, 1973; See Fig. 2-2-13A). Furthermore, there is a general trend of decreasing REE concentrations, particularly LREE, with increasing SiO_2 contents; such a depletion of overal REE abundances without significant changes of the Eu-anomaly may be expected by the continuous fractionation of REE-enriched minor phases and less significant fractionation of feldspars.

Sample 76-L-46, modally a quartz monzonite of Streckeisen (1976; a quartz poor rock), shows a moderately fractionated curve with a large positive

Figure 2-2-13. Chondrite-normalized REE distribution patterns for granite-monzonite-syenite association of the Algonquin Batholith.

(A) REE distributions for granite (Giant Range Granite, Arth, 1973).

(B) REE distributions for monzonite-syenite (syenite of Linden Pluton, Arth, 1973; Monzonite of California, Miller, 1977).

(C) REE distributions for syeno-monzo-diorite.

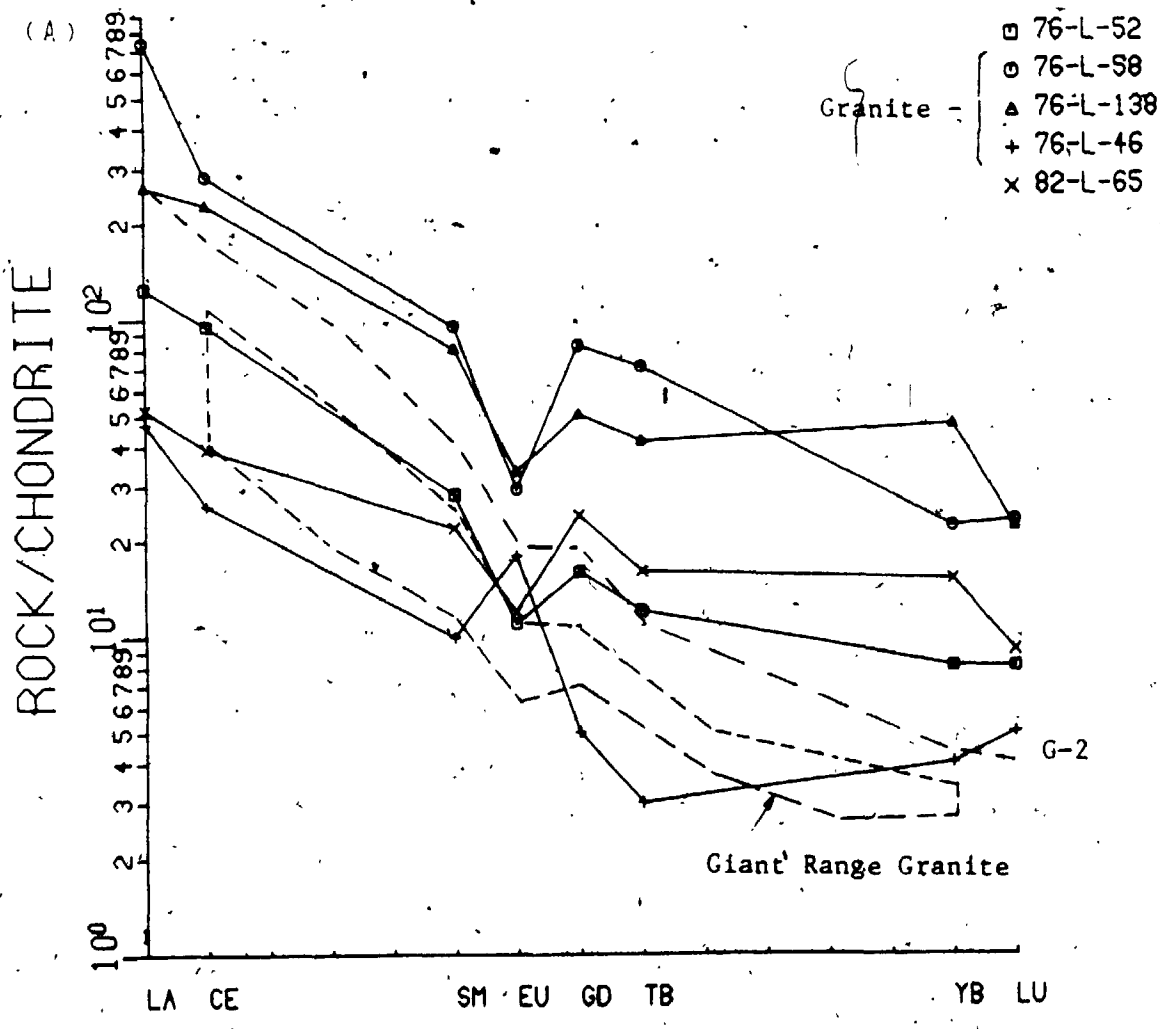

(Figure 2-2-13. Cont'd)

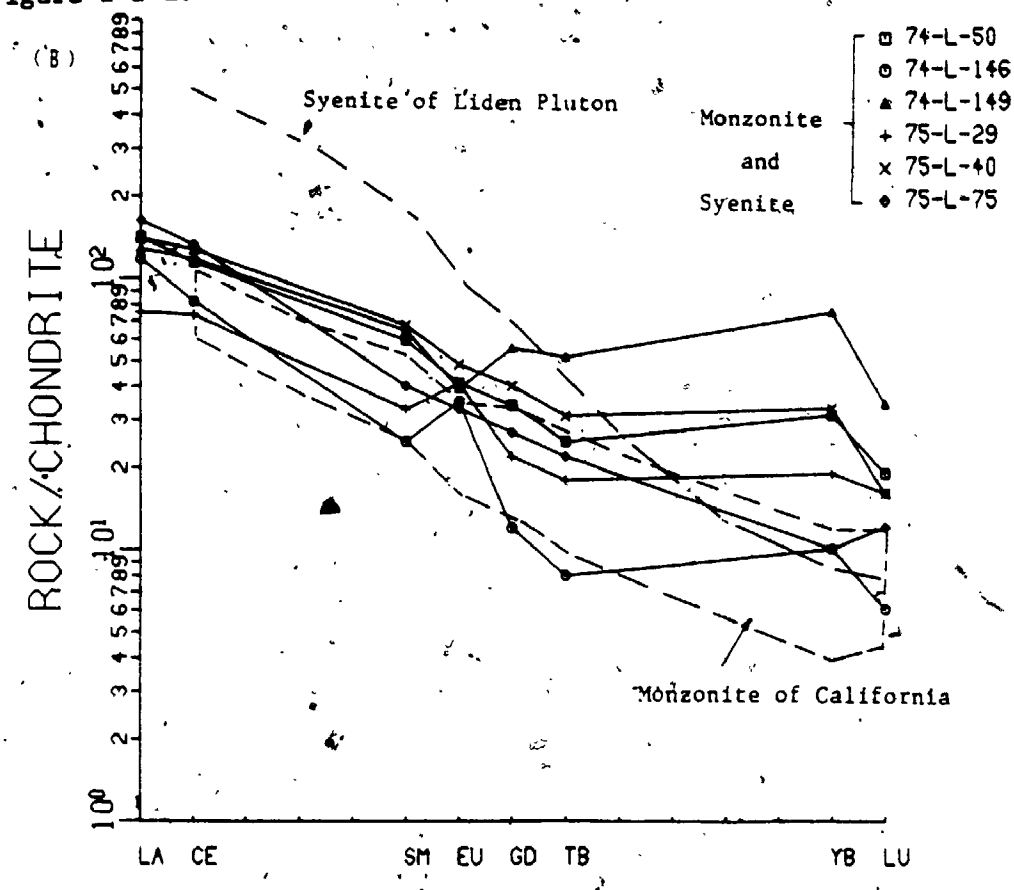

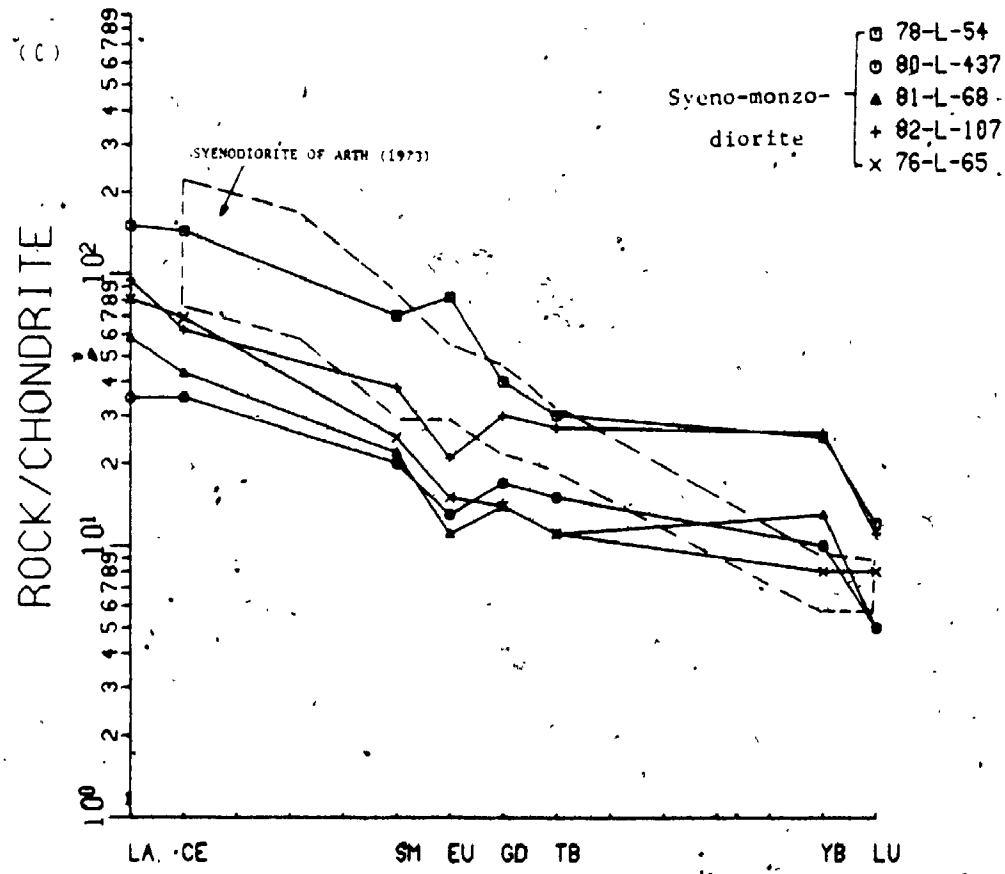

Eu-anomaly (Eu/Eu* = 2.67), which is similar to that of trondhjemitic rock of the batholith (Fig. 2-2-12A). However, according to Streckeisen (1976), trondhjemite is a leucocratic tonalite with colour index < 10 and plagioclase of oligoclase - andesine composition; comparison of sample 76-L-46 with typical trondhjemite is given in Table 2-2-8. Because of its mineralogy and geochemistry, sample 76-L-46 is not thought to be one of the trondhjemitic suite. Nevertheless, its large positive Eu-anomaly and strong depletion of middle REE may indicate an intensive fractionation of hornblende and/or apatite rather than a cumulative origin.

Monzonitic-syenitic rocks with moderately fractionated patterns ($(Ce/Yb)_N$ = 1.58 - 1.32) contain a relatively narrower range of REE compositions (7REE = 102.7 - 182.8) than those of the Algonquin granites. There is a general trend of decreasing Eu/Eu* ratios with increasing SiO_2, which may indicate feldspar fractionation; the positive Eu-anomaly of the less evolved samples suggests a partial cumulative sign in the early differentiation phase. Comparatively, the Algonquin syenite - monzonite have similar REE abundances to those of the California monzonites (Miller, 1978), but less abundant than syenite of the Linden Pluton (Arht,

Table 2-2-8. Comparison of sample 76-L-46 with typical trondhjemite

Typical Trondhjemite *	Sample 76-L-46
A. Mineralogy	
1. leucocratic tonalite,	1. quartz monzonite of Streckeisen (1976),
2. colour index >10, feldsapr ratio >0.80,	2. colour index = 4.1, feldspar ratio = 0.36,
3. plagioclase of oligoclase-andesite composition,	3. plagioclase An_{28-34},
4. K-feldspar <10%,	4. K-feldspar >50%,
5. biotite is the typical dark mineral with rarely hornblende and diopsidic pyroxene.	5. biotite, hornblende are main dark minerals.
B. Major-oxide Concentrations	
1. SiO_2 >68%, usually <75%,	1. SiO_2 74.38%, Al_2O_3 13.58%,
2. Al_2O_3 >15% at 70% SiO_2, but <14% at 75% SiO_2,	2. total iron + MgO = 1.49, total iron / MgO = 17.6,
3. total iron + MgO <3.4%, commonly total iron / MgO =2-3,	
4. CaO 1.5-3.0%, K_2O <2%.	3. CaO 1.41%, Na_2O 3.18%, K_2O 4.82%.

* Limits of chemical compositions of common trondhjemite are taken from Barker (1979).

1973) (Fig. 2-2-13B). However, the striking feature of the Algonquin monzonite - syenite is their less HREE fractionated patterns which may suggest a less intensive crystallization or a sufficient partial melting of HREE-retained mineral phases (eg. zircon and hornblende).

Syeno-monzo-dioritic rocks contain relatively less abundant REE than those of monzonite-syenite of the batholith, and have less fractionated REE patterns than syenodiorite of Arth (1973, See Fig. 2-2-13C). There are trends of decreasing total REE and Eu/Eu* with increasing SiO_2 indicating a continuous removal of feldspars and REE-enriched (esp. LREE) accessory minerals (eg. sphene and allanite; Mittlefehdt and Miller, 1983). Granodiorite has a similar REE composition to the syeno-monzo-diorite, except that the former has relatively strongly fractionated pattern ($(Ce/Yb)_N$ = 8.63, Fig. 2-2-13C).

2.4 Isotopic Geochemistry

Oxygen isotope analyses of whole-rocks and co-existing quartz-feldspar fractionations of representative samples from this batholith are given in Table 2-2-9. There is no correlation between rock-types and their oxygen isotope compositions; except for

Table 2-2-9. Oxygen isotope analyses of whole-rock and co-existing minerals from the Algonquin Batholith

Rock-type	Sample No.	$\delta^{18}O$ whole-rock	$\delta^{18}O$ quartz	$\delta^{18}O$ feldspar	$\Delta q-f$
Granite	75-L-76	7.95			
	82-L-65	4.29	5.97	4.25	+ 1.72
Syenite-monzonite	75-L-58	8.36			
	75-L-40	9.34			
Granodiorite	82-L-85	6.68			
Syenodiorite	82-L-38	8.90			
Trondhjemite	79-L-135	8.33			
Tonalite	79-L-337	6.30			
Diorite	78-L-53	7.92			
Gabbro	82-L-71	6.41			

$\Delta q-f \cong \delta q - \delta f$ = isotopic fractionation between co-existing quartz and feldspar.

granitic rock 82-L-65, all samples have $\delta^{18}O$ values of 6.30 to 9.34, which are compatible to those of isotopically "normal" granites (6.0 to 10 o/oo; Taylor, 1978). Sodium-rich rock samples have $\delta^{18}O$ values of 6.30 to 8.33, averaging 7.50, which is consistent with isotopically undisturbed trondhjemites, ranging from 5.2 to 8.9 (Barker et al., 1976). Granitic sample 82-L-65 contains the lowest $\delta^{18}O$ value (4.29 o/oo) and is considered to be a low-^{18}O granite of Taylor (1978). In order to determine whether the low $\delta^{18}O$ value of the sample reflects a magmatic condition or was produced by low temperature alteration after solidification (eg. interchange with meteoric water), oxygen isotopes of co-existing quartz and feldspar are also analyzed to measure their isotopic fractionation.

Isotopic fractionation between co-existing quartz-feldspar has been defined as $\Delta_{q-f} \cong \delta^{18}O_{quartz} - \delta^{18}O_{feldspar}$; the equilibrium values of Δ_{q-f} for "normal" igneous rocks fall within the range of 0.8 to 2.5 (Taylor and Epstein, 1962; O'Neil and Tayor, 1967; Margaritz and Taylor, 1976; Taylor, 1978). Values outside this range indicate meteoric and/or hydrothermal alterations at sub-solidus temperature (Taylor and Turi, 1976; O'Neil et al., 1977). The Δ_{q-f} value + 1.72 of the sample 82-L-65 suggests a high-temperature fingerprint; in other words, some of the granitic rocks of the Algonquin Batholith were crystallized from a low

^{18}O magma.

Such an ^{18}O depleted magma may be derived from: (1) the deep mantle directly; (2) an ordinary granitic melt with a large quantity of assimilated low ^{18}O country rocks (metasediments) which have been altered by meteroic water; (3) a granitic magma by partial melting of a source which was subjected to intensive oxygen isotope exchange with meteoric water prior to melting. On the other hand, the high-temperature fingerprint may only reflect the processes of metamorphism; that is, an isotopically normal granite may has been altered by meteoric water before metamorphism took place.

There is no Rb-Sr isotope data available at present; however, it has been suggested that the Algonquin Batholith was intruded about 1,500 to 1,400 Ma. (Lumbers and Krogh, 1977; U-Pb date on zircon) and remobilized during the Grenville Orogeny (Lumbers, 1982; Schwerdtner and Lumbers, 1980).

2.5 Petrogensis And Source Rocks

Based on variations of major-oxides, rocks of the Algonquin Batholith can be chemically grouped into : (1) the sodic rock-association (gabbro, diorite, tonalite and trondhjemite), and (2) the potassic rock-association (syenite, monzonite, granite and granodiorite). Compositions of syeno-monzo-dioritic

rocks are somewhat intermediate. Additionally, alkaline trace-element variations deciphered two comagmatic series in the batholith: (1) the diorite - tonalite - trondhjemite suite of the soda-rich rock-association, and (2) the syenite - monzonite - granite suite of the potash-rich rock-association. However, overlaps of composition and different slopes of variation trends between granitic and syenitic rocks suggest that they originated from a single magma but may have diffentiated independently. Further, granodioritic rocks with similar REE patterns to those of syeno-monzo-dioritic rocks are considered to have a similar parent. Gabbroic rocks with hornblende - plagioclase - rich mineralogy and unique chemical characters are considered to be cumulative.

2.5.1 Diorite-Tonalite-Trondhjemite Suite -

The diorite-tonalite-trondhjemite suite of the Algonquin Batholith can be classified as the high-Al_2O_3, low-Yb continental type trondhjemite of Arth (1979; See Fig. 2-2-14), although some of them are not depleted in HREE. Petrogenesis of trondhjemite - tonalite and related mafic rocks has been summarized by Barker and Arth (1976). Based on their low initial strontium ratios, most geochemists agree that these magmas were generated in the upper mantle or lower crust. In general, the high-Al_2O_3,

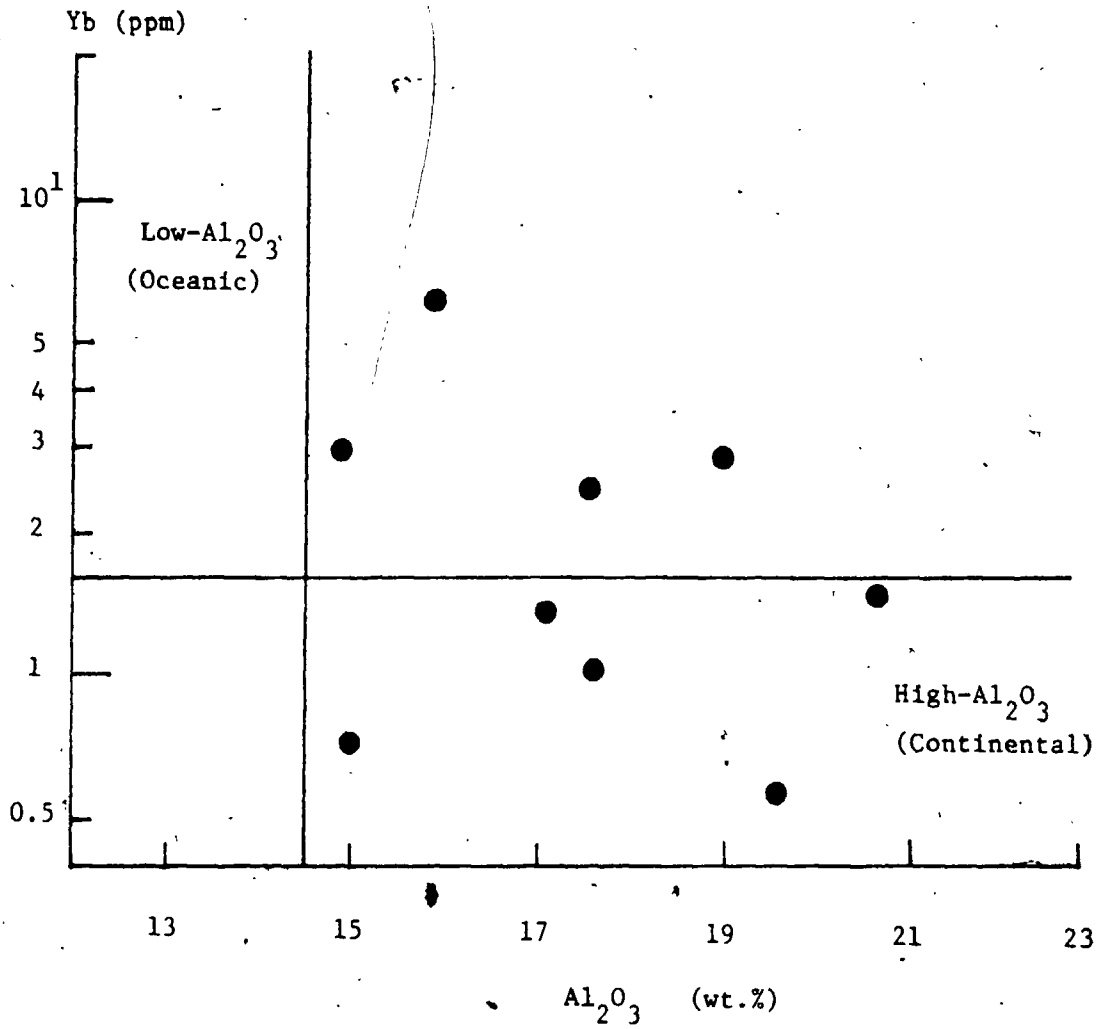

Figure 2-2-14. Al_2O_3 vs. Yb plot for tonalite-trondhjemite suite of the Algonquin Batholith. Solid-lines separate the high-Al_2O_3, HREE-depleted continental trondhjemites from the low-Al_2O_3, HREE-undepleted oceanic ones (Arth, 1979).

low-Yb type trondhjemite - tonalite was derived either by differentiation of wet basalt leaving hornblende as a major cumulate phase, or by partial melting of hydrous metabasalt (eg. quartz eclogite or amphibolite).

Sympathetic variation of REE with SiO_2 of the Algonquin tonalite - trondhjemite suite (Fig. 2-2-12A), which is compatible to that of diorite-tonalite-trondhjemite of Finland (Arth et al., 1978), suggests similar petrogenetic processes for the Algonquin counterparts. Based on partition coefficients of hornblende of various rock-types, Arth et al., (1978) proposed that a continuous removal of hornblende from a dacitic melt would produce a depletion of HREE and a positive Eu-anomaly in the tonalite - trondhjemite differentiates. Variations of CaO vs. Al_2O_3 and MgO vs. CaO (Fig. 2-2-15) illustrate that in addition to hornblende, plagioclase and biotite are also fractionated during differentiation from tonalite to trondhjemite in this batholith.

Mass balance calculations by means of a least squares method (Stormer and Nicholls, 1978) were used to verify the feasibility of the crystal fractionation models. Only minerals identified in tonalite - trondhjemite were used in modelling; mineral compositions of hornblende, biotite and

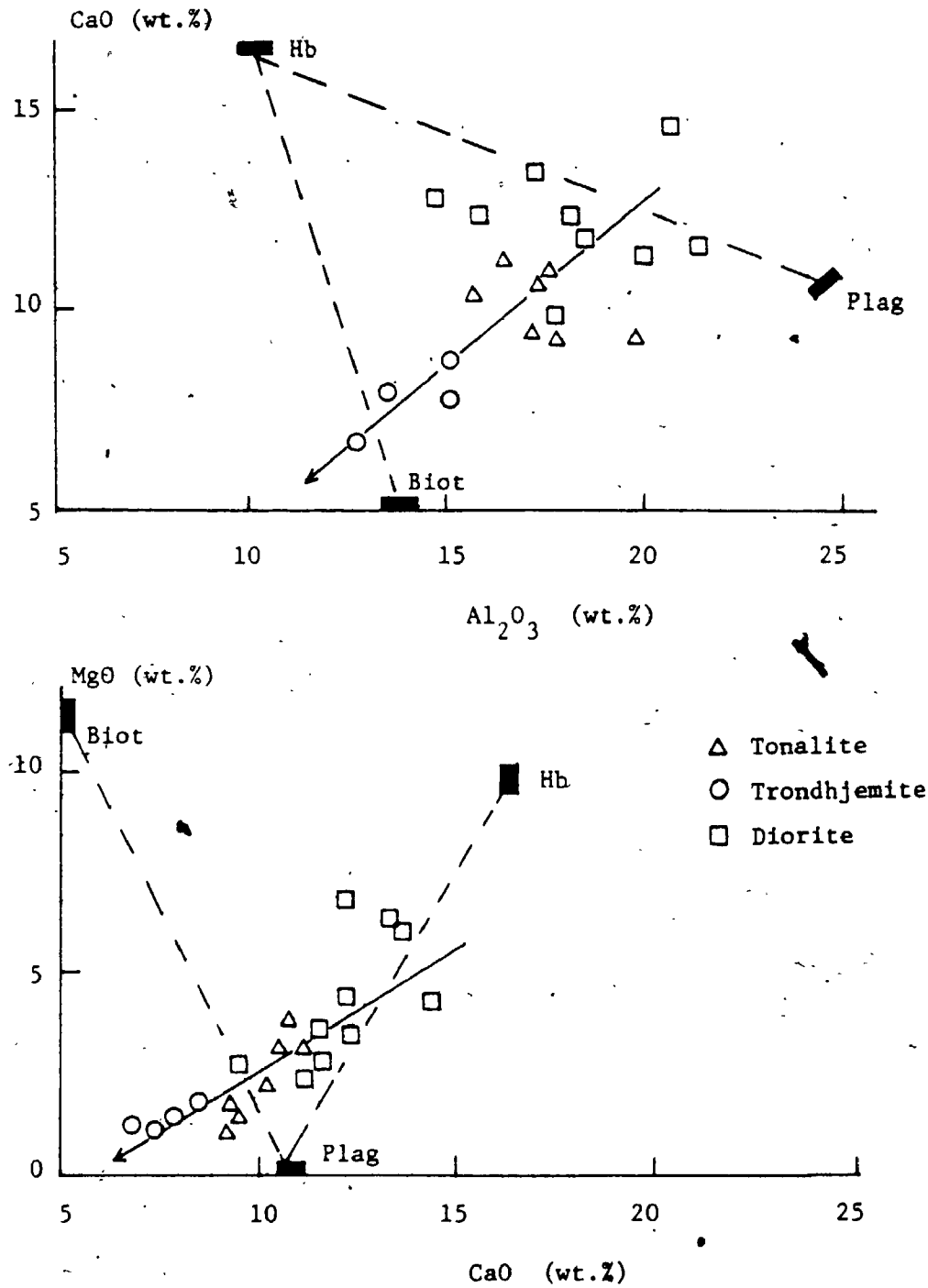

Figure 2-2-15. Inter-elemental variation plots of the diorite-tonalite-trondhjemite suite of the Algonquin Batholith. (A) CaO vs. Al_2O_3 (B) MgO vs. CaO with relations to the composition of major mineral components. Dashed-lines indicate the possible fractionation mineral pairs (eg. Cox et al., 1979). Solid-lines illustrate the differentiation trend of the tonalite-trondhjemite suite.

plagioclase were determined by electron microprobe, while sphene, apatite and iron-oxides were chosen from the literature (Deer et al., 1966). It is suggested that differentiation from the least evolved tonalite sample (76-L-41, 57.87% SiO_2) to the most differentiated trondhjemite (75-L-73) required removal of a modal solid of 30% hornblende, 58% plagioclase (An_{30}), 10% biotite, 0.4% apatite, 0.9% sphene and 0.4% magnetite. The proportion of precipitates to evolved liquid is about 76:24; the sum of squares of residuals of 0.134 indicates a good fit between the modal and observed data. It is interesting to note that similar calculations performed by Arth et al. (1978) gave the same proportion of trondhjemitic melt versus precipitates, except for more hornblende (52%) and less plagioclase (23%) in their modal precipitates. Besides, the least fractionated tonalite (76-L-41) can be derived by 80% fractional crystallization of a basaltic magma with similar composition to sample 82-L-35; that is, 100 units of basaltic melt (82-L-35, 45.09% SiO_2) = 16 unit tonalite (76-L-41) + 27% hornblende + 36% plagioclase (An_{60}) + 15% biotite + 6% magnetite. Variation of REE and overlaps of composition (eg. the most differentiated diorite of 58.47% SiO_2 is in the range of tonalite) suggest dioritic and tonalitic rocks are cogenetic but differentiated separately.

Furthermore, the complementary REE patterns between the gabbro and evolved diorite would also suggest a plagioclase-rich cumulate (gabbro) and a residual melt (diorite) produced by fractional crystallization of an undifferentiated Archean basalt with REE concentration of about 10 times chondritic values (Basaltic Volcanism Study Project, 1981, p.23, average of ACH-13 and ACH-14).

2.5.2 Granite-Syenite-Monzonite Suite -

Arth (1973) suggested that the Linden Syenite was probably derived from partial melting of a peridotite in the mantle, while Miller (1977) proposed a partial melting of quartz eclogite with similar composition to continental basalt would produce a near - silica -saturated melt for California monzonites. The contrast of REE patterns between Linden Syenite and Algonquin monzonite - syenite precludes a common origin between them, whereas the similar REE abundances to California monzonites suggest a comparable source for the Algonquin monzonite-syenite.

The model for partial melting using equations of Shaw (1970) and solid/liquid partition coefficients for dacitic rocks (Arth, 1976) is shown in Figure 2-2-16. The Algonquin monzonite-syenite

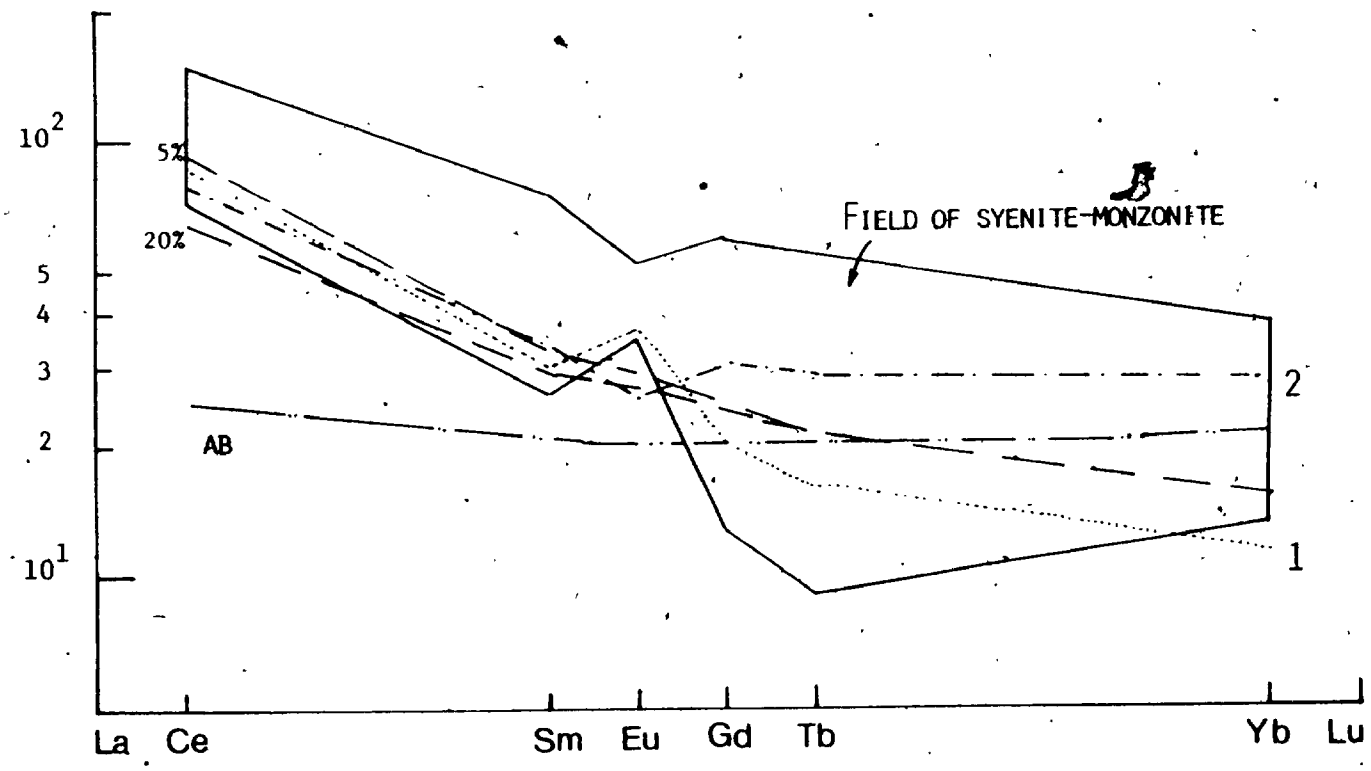

Figure 2-2-16. REE modelling of the monzonite-syenite rocks of the Algonquin Batholith. The monzonite-syenite rocks could be derived from less than 20% partial melting of a quartz elcogite with similar composition to Archean basalt (AB).

1. Initial composition with 60% OPX, 20% CPX, 5% Garnet and 0% Plagioclase.
2. Initial composition with 60% OPX, 20% CPX, 1% Garnet and 15% Plagioclase.

could be derived by less than 20% partial melting of a quartz eclogite ($Opx_{60}Cpx_{20}Plag_{10}Gt_3Qtz_7$) with similar REE composition to that of Archean Fe-rich basalt (Basaltic Volcanic Study Project, 1981, p.23, Fig. 1.2.1.18, ACH-10) at great depths. The general trend of decreasing Eu/Eu* ratios and increasing HREE contents can be expained by progressively increasing plagioclase and decreasing garnet in the residue (See Fig. 2-2-16).

It has been suggested that the Algonquin Batholith was intruded into the older clastic siliceous metasedimentary sequences of possible Huronian Supergroup, which uncomformably overlie the Archean basement (Lumbers, 1982). Partial melting of such a greywacke at crustal depths would produce a granitic melt, leaving a residue predominantly composed of plagioclase, amphibole, garnet and pyroxene or biotite (Arth, 1973; Winkler, 1967). However, the relatively higher HREE abundances and correspondingly less fractionated REE patterns of the Algonquin granites preclude the possible sources of Archean greywacke (Arth, 1973) or Huronian metasediments (McLennan et al., 1979) for partial melting, due to their lower HREE contents.

In addition to major-oxide and trace-element data, the sympathetic variation of REE in the granitic rocks and similarity of REE patterns

between the evolved syenite and the least differentiated granite support the possibility that the Algonquin granites were differentiated from a near - silica - saturated alkalic magma by fractional crystallization. The gradual decrease of total REE with increasing SiO_2, which is the reverse to the normal igneous trend, may be explained by the continuous crystallization of REE-enriched accessory mineral phases (Mittlefehdt and Miller, 1983) and/or the increase of partition coefficients (Mahood and Hildreth, 1983) in the strongly differentiated siliceous melt. Furthermore, there is speculation that those granitic rocks with extremely low oxygen isotope compositions originated in the upper mantle or lower crust may be associated with the Grenville Orogeny (W.S. Fyfe, pers. comm., 1984).

2.5.3 Syeno-monzo-dioritic Rock -

Arth (1973) proposed that partial melting at mantle depths of a near-silica-saturated eclogite derived from an olivine basalt would produce the high-Al and high-Na syenodioritic rocks in general. The sympathetic variation of Eu/Eu* ratios and the less fractionated REE patterns of the syeno - monzo - dioritic rocks of this batholith suggest that more plagioclase and less garnet were retained in the residue than those of Arth (1973).

On the other hand, the intermediate geochemistry of the Algonquin syeno - monzo - diorite suggest an orgin of assimilation of tonalitic rocks by later syenitic magma or hybridization of syenitic melt with lower crust of mafic mineralogy.

2.6 Summary

The Algonquin Batholith is predominantly composed of granitic gneisses, monzonitic to syenitic rocks, small units of tonalite - trondhjemite and other related mafic masses; the batholith as a whole was assigned to the anorthositic intrusive rock category by Lumbers (1982). Based on field relationships, it is suggested that the tonalite - trondhjemite and related mafic rocks are the earlier phases, followed by monzonite-syenite and the youngest granite. They intruded the older metasedimentary sequences of possible Huronian age at about 1,500 to 1,400 Ma; and were subsequently reactivated during the Grenville Orogeny. Both the batholith and surrounding country rocks were subjected to regional metamorphism to upper amphibolite facies.

Two distinct compositional trends are identified in the batholith in terms of Na_2O-K_2O-CaO ternary variations : (1) the soda-rich, diorite - tonalite - trondhjemite association, and (2) the potash-rich,

syenite - monzonite - granite association. Further, alkaline trace-element variations verify these rocks to be two comagmatic series, respectively. Granodiorite with anomalously high SiO_2 content and syeno-monzo-dioritic rocks are somewhat intermediate in composition and are scattered between the above two rock-groups.

Based on REE variations, the origin of dioritic rocks of this batholith is consistent with fractional crystallization from an undifferentiated Archean basalt with REE of about 10 times chondrite. Further differentiation of this melatonalitic melt would subsequently produce the entire composition range of tonalite-trondhjemite observed; mass balance calculations suggest that it required about 75% crystallization of a modal solid of 30% hornblende, 58% plagioclase, 10% biotite, 0.4% apatite, 0.9% sphene and 0.4% magnetite to form the most evolved trondhjemite.

REE compositions of Algonquin monzonite - syenite are consistent with less than 20% partial melting of a quartz eclogite ($Opx_{60}Cpx_{20}Plag_{10}Gt_3Qtz_7$) with REE concentrations of about 20 to 25 times chondritic values. Variations of major- and trace-elements between granite and monzonite-syenite support the possibilty that the Algonquin granites were derived from crystal fractionation of the syenitic melt. However, overlaps of compositions and variable slopes of variation trends

between syenitic and granitic rocks suggest a more complicate mechanism was involvedd during their differentiation. A similar conclusion can also apply to the relations between diorite and tonalite.

Although syenodioritic magma can be derived by partial melting of an olivine basalt at mantle depths, the intermediate geochemistry and heterogeneous nature of the Algonquin syeno - monzo - dioritic rocks favour an origin of either assimilation of diorite - tonalite by later syenitic melt, or by hybridization of syenitic liquid with mafic lower crust.

3.0 UNION LAKE PLUTON

3.1 General Characters And Intrusive Relations

The Union Lake Pluton is located between Galway and Snowden townships (Fig. 2-3-1), where access is by logging roads and recreation routes to the northern portion of the pluton; fluvial and swamp deposits associated with the Union Lake drainage system cover large areas of the southern region. The pluton is subrounded in plan form and is discordant with the surrounding marbles and siliceous limestone layers. The contact aureole, which may be obscured by the amphibolite facies regional metamorphism, has not been found in the field. Mafic-rich metasedimentary schlieren and clots are occassionally observed and they

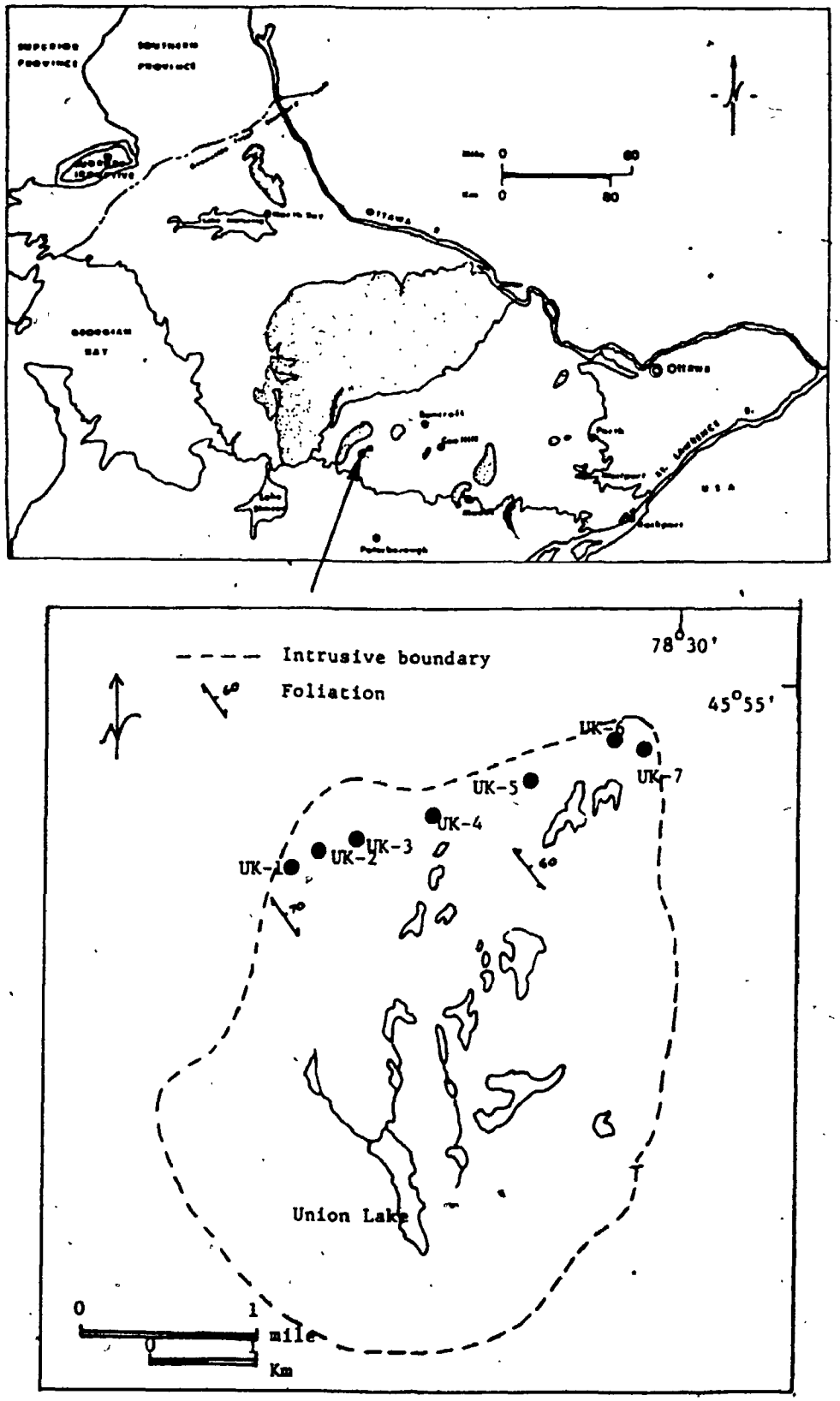

Figure 2-3-1. Sample location map of the Union Lake Pluton.

are noted to deflect the rock foliations.

This pluton, with a generally homogeneous mineral composition, can be classified as quartz diorite of Streckeisen (1976; See Fig. 2-3-2). It has a pronounced metamorphic fabric which strikes NW and dips NE, indicating a pre-tectonic emplacement.

3.2 Petrography

The quartz diorite of Union Lake Pluton is of medium grain size and is dark to light grey in colour with a pinkish tint due to local enrichment of K-feldspar.

Plagioclase, up to 65% of the mode, is the dominant phase. Quartz and K-feldspar are subordinate and vary from 4 to 12% and 3 to 6%, respectively. The main ferromagnesian mineral is hornblende, ranging from 12 to 24%, which is subordinate to biotite and rarer orthopyroxene. Magnetite, sphene, apatite, zircon, secondary epidote and calcite are common accessories. Under the microscope, rocks of this pluton are hypidiomorphic-granular with foliation defined by the preferred dimensional alignment of hornblende prisms and biotite flakes.

Euhedral to subhedral plagioclase crystals with albite-twinning have compositions ranging from An_{15} to

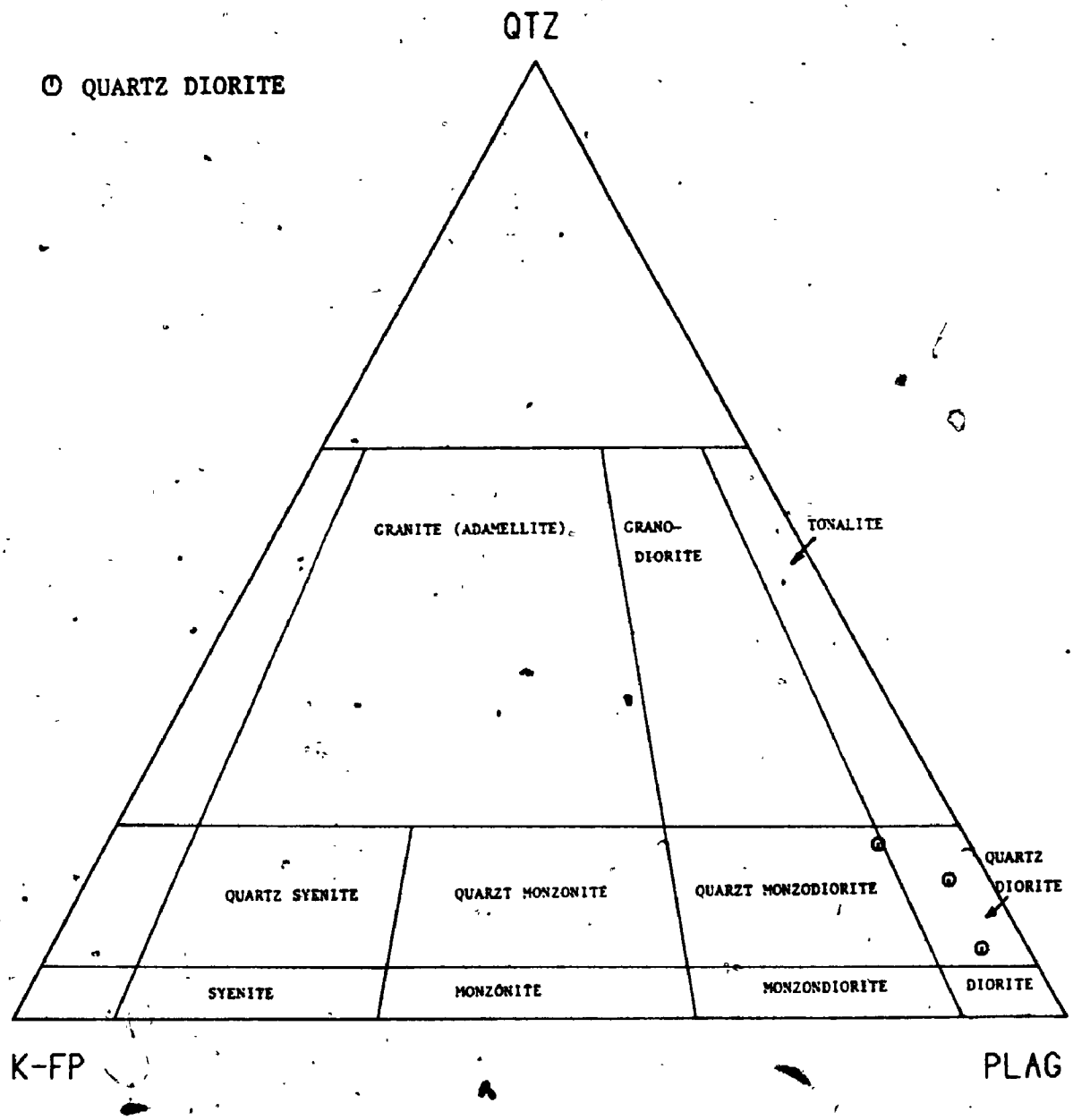

Figure 2-3-2. Modal classification of the Union Lake Pluton. (after Streckeisen, 1976)

An_{26}; no zoning has been observed. Sericitization occurs in some grains, producing patches of secondary calcite, white mica and epidote aggregates. Microcline, the only K-feldspar, is less abundant and smaller in size than plagioclase. The chemical analyses and mole fraction of Ab-An-Or of representative feldspars are given in Table 2-3-1. Quartz occurs as subhedral grains and as interstitial fillings or inclusions in mafic minerals.

Hornblende (X = earthy yellow, Y = olive green, Z = leaf green), the most abundant mafic mineral phase of the pluton, is calcic amphibole (Leake's classification, 1968), i.e. (Ca+Na) $\geq$ 1.34, Na < 0.67 (See Table 2-3-2A). It is similar to typical hornblende of tonalite (Deer et al., 1966), except for lower Al_2O_3 and TiO_2 and higher alkali contents. Subhedral to anhedral biotite flakes (1 to 10% of the mode) have a pleochroic scheme from X = light greenish yellow to pale orange, to Y = Z = reddish to dark brown. Chemical composition and calculated formaulae of biotite are listed in Table 2-3-2B. The sum of octahedral group elements is approximately 5.5, which is deficient in comparison with the ideal trioctahedral micas (6.0). It can be classified as the Mg-biotite of Foster (1960), in terms of $Mg-Fe^{2+}-R^{3+}$ (Fig. 2-3-3). Poikilitic texture is common in both hornblende and biotite with inclusions of apatite, sphene, quartz, microcline and rarer zircon.

Table 2-3-1. Chemical compositions and calculated formulae of feldspars from the Union Lake Pluton

Sample No. Mineral	UK-3-3 Plagioclase	UK-6 Plagioclase	UK-3-3 K-feldspar	UK-6 K-feldspar
(wt%)				
SiO_2	63.53	64.82	65.42	65.00
Al_2O_3	23.51	22.74	18.42	18.93
CaO	4.12	3.21	0.00	0.01
Na_2O	8.86	9.39	0.76	0.63
K_2O	0.22	0.34	15.26	15.39
Total	100.24	100.50	99.86	99.96
Si] Z	11.184	11.359	12.039	11.960
Al] Z	4.877	4.696	3.994	4.104
	16.061	16.055	16.034	16.064
Na] X	3.024	3.190	0.271	0.225
Ca] X	0.777	0.603	0.000	0.002
K] X	0.049	0.076	3.582	3.612
	3.851	3.869	3.853	3.839
O	32	32	32	32
(mol%)				
AB	78.54	82.46	7.04	5.85
AN	20.18	15.58	0.00	0.05
OR	1.28	1.96	92.96	94.09

Table 2-3-2. Chemical compositions and calculated formulae of amphibole and biotite from the Union Lake Pluton

(a) Sample No. Mineral		Tonalite Hornblende	UK-3-3 Amphibole	UK-6 Amphibole	(b) UK-3-3 Biotite	UK-6 Biotite
SiO_2		44.99	43.85	44.65	37.50	38.16
TiO_2		1.46	0.83	0.67	1.67	1.50
Al_2O_3		11.21	9.47	9.09	14.68	14.55
Fe_2O_3		3.33	-	-	4.65	4.51
FeO		13.17	*17.33	*17.77	12.81	12.41
MnO		0.31	0.35	0.34	0.26	0.21
MgO		10.41	10.44	11.07	12.66	13.32
CaO		12.22	11.91	11.65	0.05	0.06
Na_2O		0.97	1.67	1.68	0.06	0.53
K_2O		0.76	1.25	1.16	9.88	9.25
Total		98.72	97.10	98.08	94.22	94.50
Si	Z	6.669	6.660	6.705	5.695	5.741
AL^{iv}	Z	1.331	1.340	1.295	2.305	2.259
		8.000	8.000	8.000	8.000	8.000
Al^{vi}	Y	0.629	0.355	0.314	0.320	0.320
Ti	Y	0.163	0.095	0.076	0.191	0.170
Fe^{3+}	Y	0.370	-	-	0.531	0.510
Fe^{2+}	Y	1.633	2.201	2.232	1.626	1.560
Mg	Y	2.300	2.363	2.478	2.863	2.984
Mn	Y	0.039	0.045	0.043	0.033	0.027
		5.134	5.059	5.143	5.563	5.571
Ca	X	1.923	1.938	1.875	0.008	0.010
Na	X	0.278	0.492	0.489	0.018	0.154
K	X	0.144	0.242	0.222	1.913	1.774
		2.355	2.672	2.586	1.938	1.938
O		23	23	23	22	22
$Mg/Fe^t+Mg+Mn$		0.530	0.513	0.521	0.567	0.587
$Fe^t/Fe^t + Mg$		0.465	0.482	0.474	0.430	0.410
mole of annite		-	-	-	0.271	0.260

* Total iron as FeO

$Fe^t = Fe^{3+} + Fe^{2+}$ in unit cell

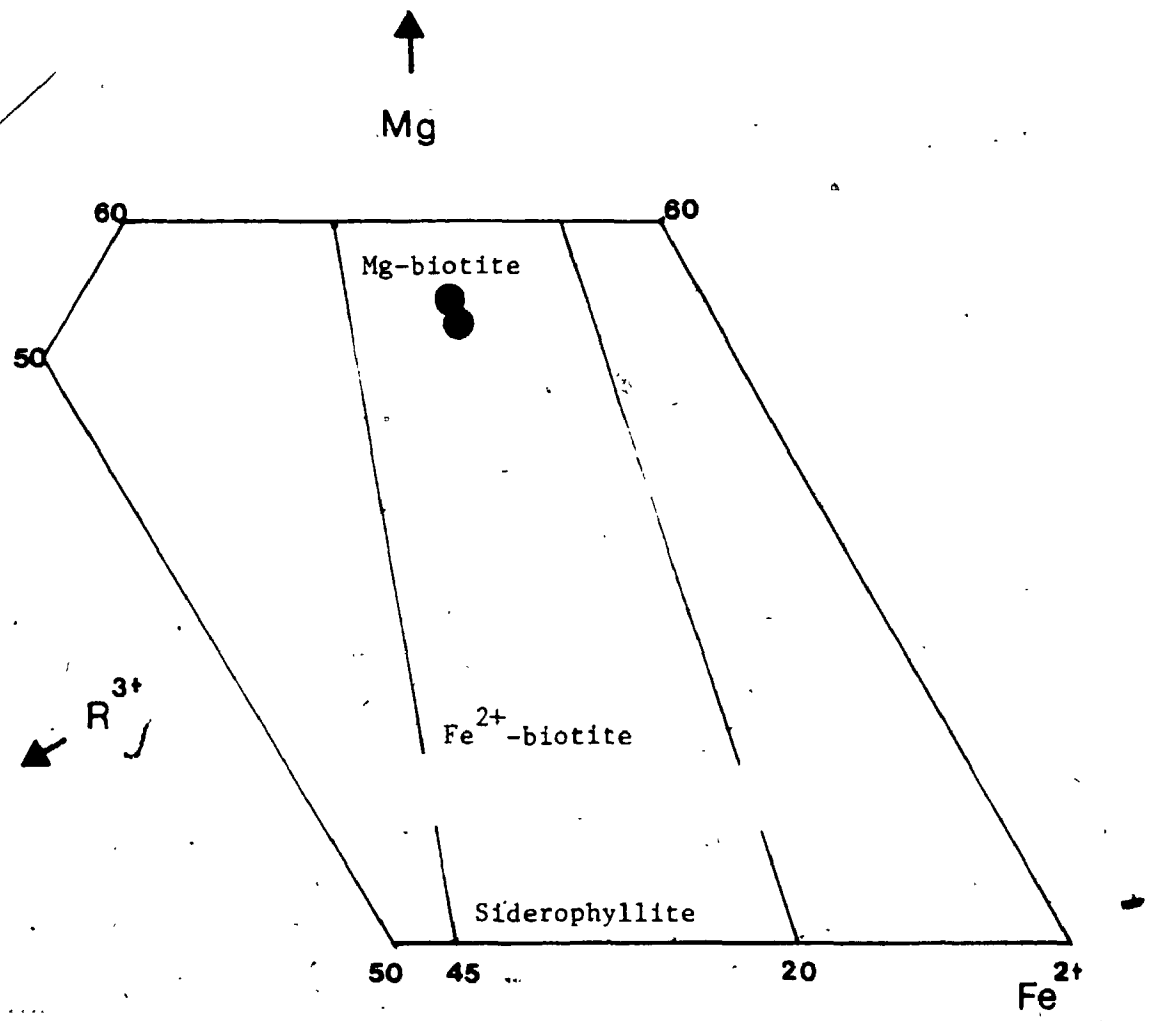

Figure 2-3-3. The Mg-Fe^{2+}-R^{3+} relation in trioctahedral micas of the Union Lake Pluton (after Foster, 1960).

$$R^{3+} = Al^{vi} + Fe^{3+} + Ti^{4+}$$

Locally, biotite and hornblende are clustered together indicating a contemporaneous crystallization. Pyroxene (if any) is frequently replaced by hornblende along the edge.

3.3 Whole-rock Geochemistry

3.3.1 Major-oxides -

Although only seven unevenly distributed samples have been chemically analyzed, the data are probably sufficient to represent and to illustrate the general chemical features of the pluton because of its homogeneous mineralogy. This homogeneity is also reflected by the small composition variation between samples relative to the mean (See Table 2-3-3).

The Union Lake Pluton lies within the fields of trondhjemite and tonalite of the normative An-Ab-Or diagram of O'Connor (1965, See Fig. 2-3-4). It is metaluminous with an average agpaitic index of about 0.68. The alkali-lime index of Peacock (1931) of this pluton is around 58% SiO_2, indicating a calc-alkalic affinity (Fig. 2-3-5).

In general, the mean composition of the pluton is richer in Al_2O_3, CaO, Na_2O and poorer in SiO_2 than the average tonalite of Nockolds (1954).

Table 2-3-3. Comparison of average composition of trondhjemitic rocks in Grenville Province, Ontario

	1 (n=7)	s.d.	2 (n=58)	3 (n=12)	4 (n=16)	5 (n=7)	6 (n=10)	7 (n=2)
SiO_2 (wt%)	61.05	1.31	66.15	65.30	70.12	67.49	69.17	64.40
TiO_2	0.74	0.05	0.62	0.48	0.37	0.44	0.28	0.44
Al_2O_3	16.54	0.67	15.56	17.10	15.68	16.03	16.36	16.30
TFe_2O_3	5.53	0.49	-	-	2.57	3.33	2.69	3.84
Fe_2O_3	1.59	0.46	1.36	0.16	-	-	-	0.40
FeO	3.41	0.23	3.42	3.08	-	-	-	3.10
MnO	0.08	0.01	0.08	0.03	0.07	0.05	0.04	-
MgO	2.88	0.40	1.94	1.92	0.92	1.40	1.11	2.20
CaO	5.14	0.64	4.65	2.53	2.73	3.79	3.38	3.20
Na_2O	5.50	0.43	3.90	5.07	4.57	4.81	5.34	4.00
K_2O	2.01	0.60	1.42	2.06	2.57	1.78	1.14	2.40
P_2O_5	0.27	0.03	1.21	0.12	0.10	0.16	0.03	-
LOI	0.54	0.14	0.69	-	-	-	0.58	-
Na_2O/K_2O	2.74	-	2.75	2.46	1.78	2.70	4.68	1.67
Sr (ppm)	843.9	179.5	-	398 *	336	614	400.6	256
Rb	56.4	15.9	-	61	62	46	27.9	30
Ba	553.0	147.1	-	346	391	395	271.5	-
Zr	140.5	36.5	-	99	127	161	87.3	-
K/Rb	296	34.2	-	280	344	466	339	664
Sr/Ca	230	49.5	-	220	172	227	166	112
Ba/Sr	0.66	.14		0.87	1.16	0.64	0.68	-

1. Average of the Union Lake Quartz Diorite (this study).
2. Average tonalite of Nockolds (1954).
3. Trondhjemite from Weslemkoon Batholith, Ontario (Lumbers, 1968).
4. Average composition of the Elzevir Batholith, Ontario (Pride and Moore, 1983).
5. Average composition of the Northbrook Pluton, Ontario (Pride and Moore, 1983).
6. Average composition of White Lake Pluton, Ontario (Somers, 1984).
7. Average composition of the Grenville dacite (Codle and Moore, 1977).

* Trace-element data are taken from Pride and Moore (1983).

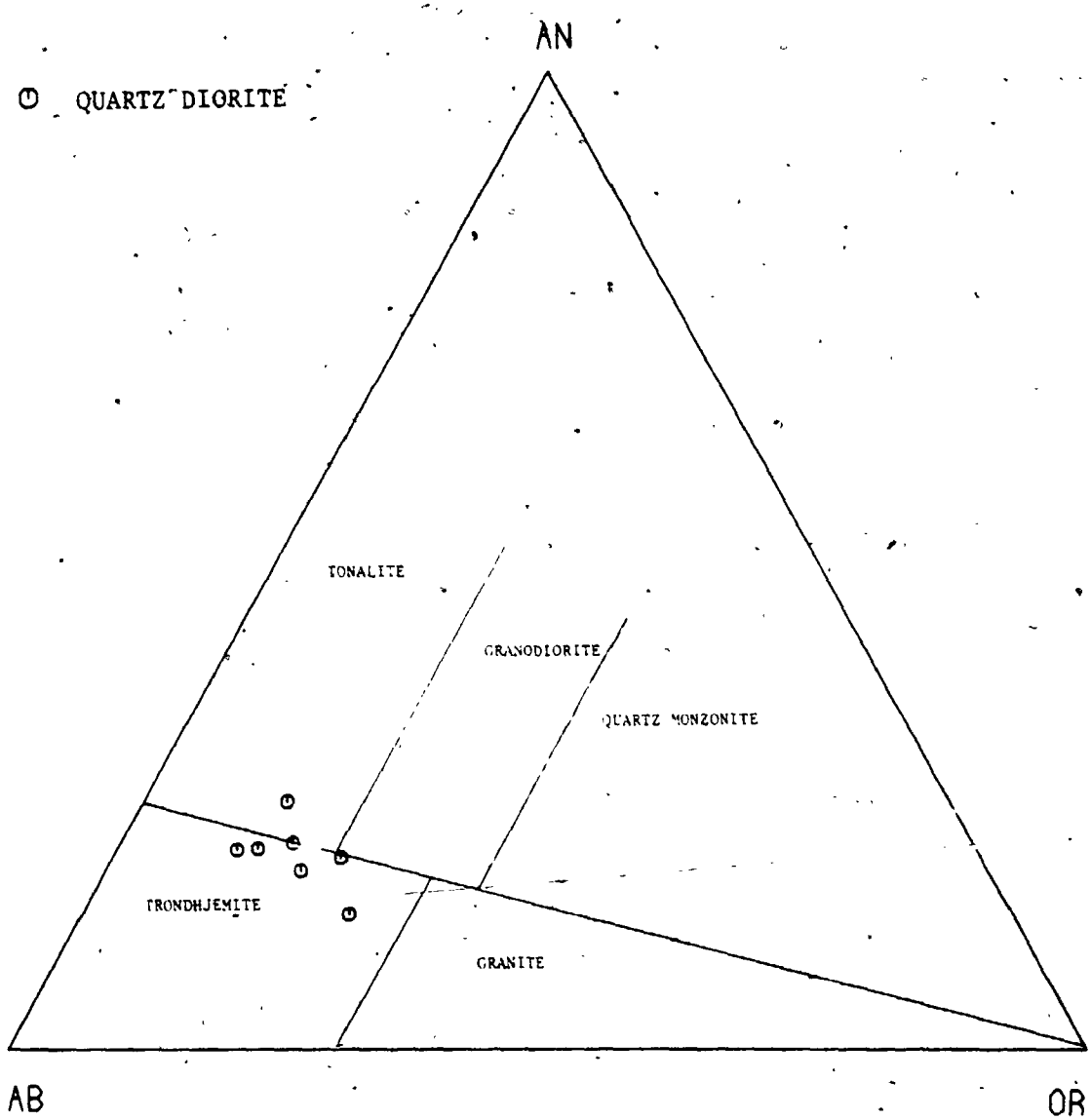

Figure 2-3-4. Normative Ab-An-Or ternary diagram of the Union Lake Pluton. Classification scheme is after O'Connor (1965).

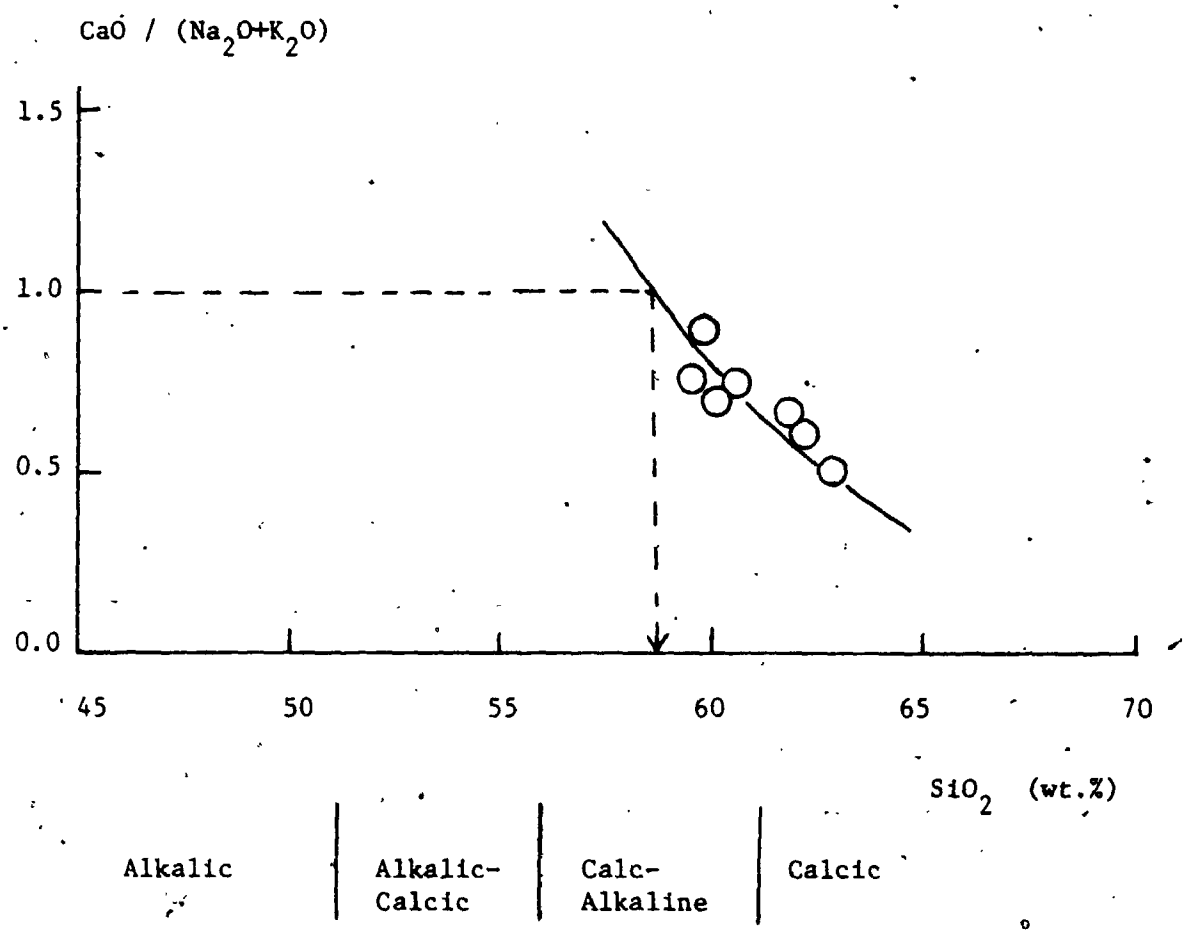

Figure 2-3-5. The alkali-lime ratio vs. SiO_2 plot of the Union Lake Pluton. Solid-line indicates the chemical variation trend of the pluton. Classification is from Peacock (1931).

However, except for low SiO_2 and high CaO and total iron contents, it is similar to the trondhjemite of the Weslemkoon Batholith (Lumbers, 1968) and other trondhjemitic suites (Pride and Moore, 1983) from this part of the Grenville Province (Table 2-3-3).

Correlation coefficients of major-oxides as a function of SiO_2 are given in Table 2-3-4. As SiO_2 increases, TiO_2, Al_2O_3, MgO, CaO and P_2O_5 decrease, while K_2O increases. Total iron as Fe_2O_3 and Na_2O exhibit weak correlations with SiO_2. The decreases in Al_2O_3, CaO, Fe_2O_3 and MgO with increasing SiO_2, and the presence of plagioclase and hornblende as the major mineral phases, suggest that differentiation of the pluton was mostly controlled by plagioclase and hornblende fractionations.

In terms of Na_2O-K_2O-CaO (Fig. 2-3-6), the variation trend of the Union Lake Pluton is comparable to the differentiation trends of the Elzevir Batholith (Pride and Moore, 1983) and other calc-alkaline igneous suites (eg. Southern California Batholith and Klamath Mountain Series). However, it deviates from the normal trondhjemitic trend, defined by a typical gabbro - tonalite - trondhjemite suite of Finland (Barker and Arth, 1976), or trondhjemitic rocks associated with calc-alkaline suites. In the normative, Qtz-Ab-Or diagram (Fig. 2-3-7), the Union Lake Pluton

Table 2-3-4. Correlation coefficients of inter-element variation for the Union Lake Pluton

SiO_2 vs.	TiO_2	-0.6727	SiO_2 vs.	Th	0.2891
	Al_2O_3	-0.7514		F	0.3544
	Fe_2O_3	-0.5298		Gl	0.9410
	MnO	-0.1878		S	-0.3524
	MgO	-0.8059		Ga/Al	0.0835
	CaO	-0.9320		K/Rb	0.4269
	K_2O	0.9518		Rb/Sr	0.5003
	P_2O_5	-0.8458		Sr/Ba	-0.8231
	Na_2O	-0.5046		Sr/Ca	0.4637
	Rb	0.8561		Zr/Y	0.6537
	Sr	-0.1146		Y/Ca	0.3429
	Ba	0.5519		Cr/Mg	0.3972
	Zr	0.5649		V/Mg	0.3671
	Nb	-0.2090		Ni/Mg	0.5683
	Y	-0.4596		Fe/Mg	0.8166
	Ga	-0.0677		Cr/Fe	0.1629
	Pb	-0.2123		V/Fe	0.1191
	Zn	-0.5468		Ni/Fe	0.3148
	Cu	-0.6171	Nb vs.	Ga/Al	0.9106
	Ni	0.0816	Nb vs.	Y	0.7724
	Cr	-0.0329	Al_2O_3 vs.	Ga	0.6750
	V	-0.0809	K_2O vs.	Rb	0.9265
	U	0.4179	Sr vs.	Ba	0.6580

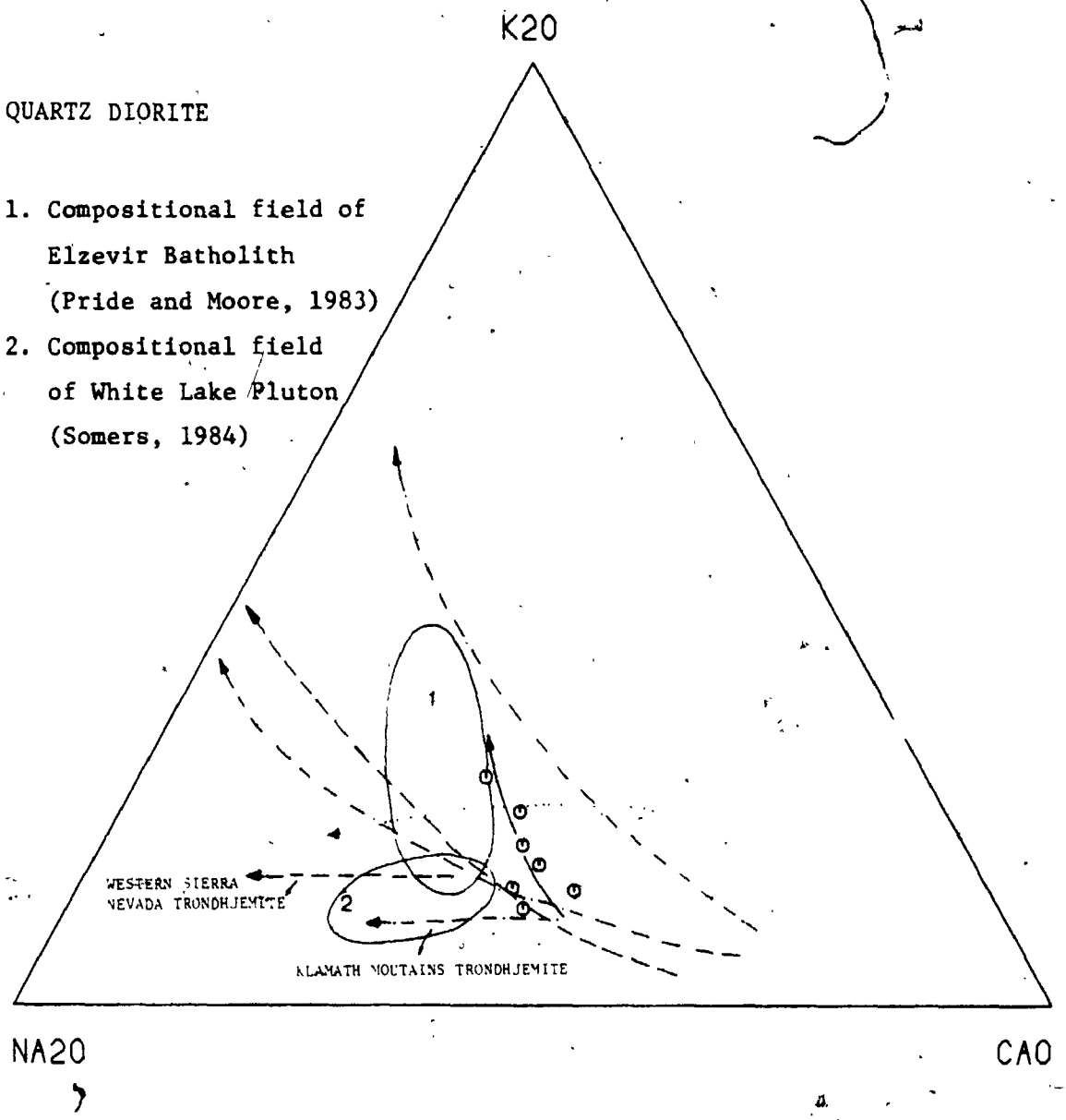

Figure 2-3-6. Na_2O-K_2O-CaO variation diagram of the Union Lake Pluton.

— · — · — Calc-alkaline trend of Southern California Batholith (Nockolds and Allen, 1956).

— · — · — Differentiation trend of Klamath Mountains Series (Hotz, 1971).

— — — — Chemical trend of Western Sierra Nevada (Nockolds and Allen, 1956).

····· Typical trondhjemite trend of Barker and Arth (1976).

——— Differentiation trend of Union Lake Pluton (this study).

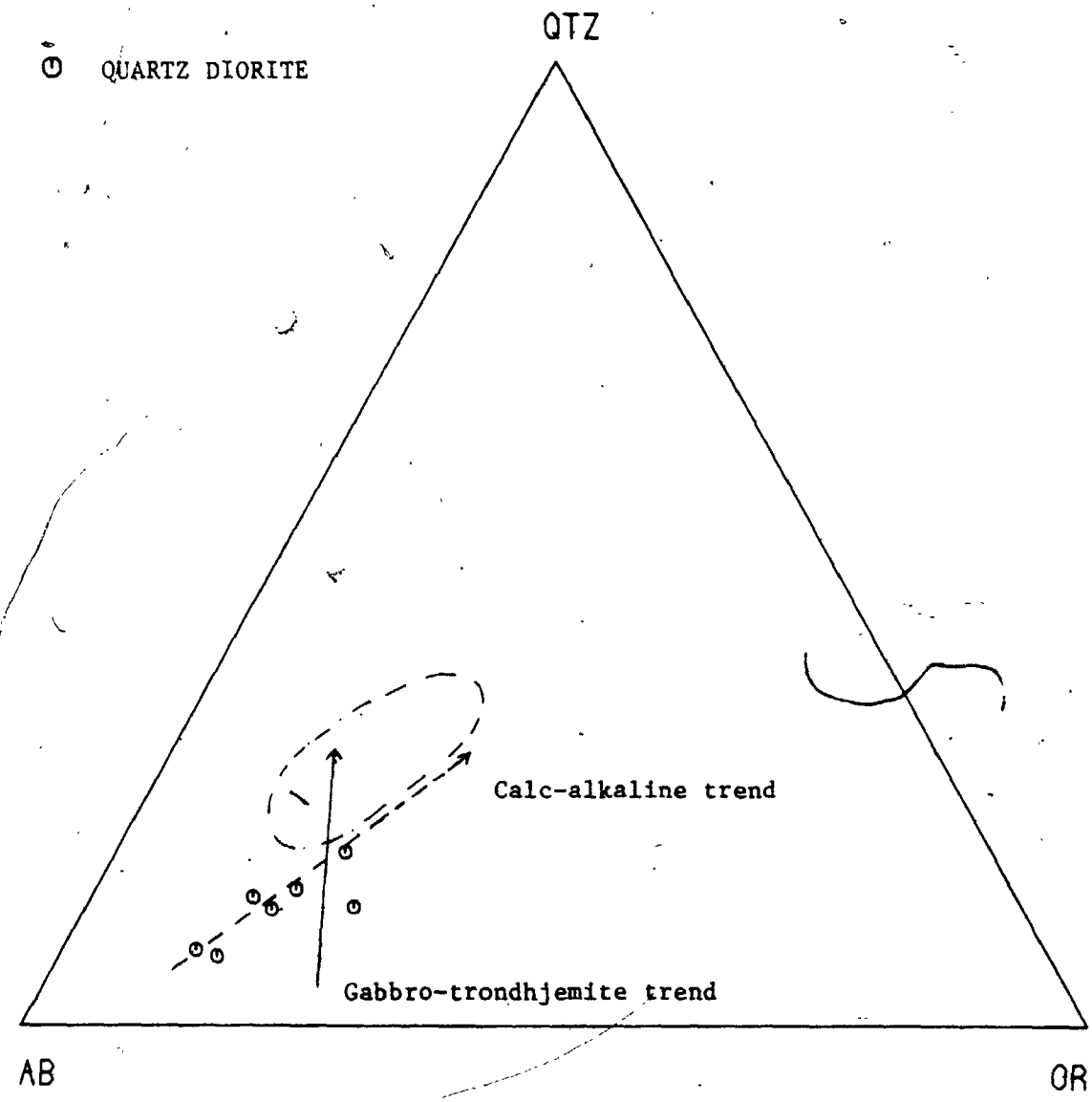

Figure 2-3-7. Normative Qtz-Ab-Or ternary diagram of the Union Lake Pluton. The calc-alkaline and trondhjemite trends are from Barker and Arth (1976). Compositional field of the Elzevir Batholith (Pride and Moore, 1983) is enclosed by dash-dot line.

illustrates a calc-alkaline differentiation trend and shows the important role of the plagioclase (Ab) during formation of this pluton. The ratios of total alkali, FeO (as total iron) and MgO are plotted in Figure 2-3-8; it shows a partially differentiated and less Fe-rich trend as compared with typical calc-alkaline rocks.

3.3.2 Trace-elements -

Correlation coefficients of trace-element variations as a function of SiO_2 for the Union Lake Pluton are summarized in Table 2-3-4. Except that Rb, Ba, Zr, Cl (positive coefficients) and Y, Zn, Cu (negative coeffients) indicate consistent trends, most trace-elements do not show any significant correlation with increasing differentiation..

The Union Lake Pluton shows the characteristics of continental high-Al_2O_3 trondhjemites (Barker and Arth, 1976), with low Rb and moderate to high Sr contents. It is also comparable to other trondhjemitic suites in this part of the Grenville Province, despite the higher Sr and Ba contents (Table 2-3-3).

In terms of the ternary relations of Rb-Ba-Sr (Bouseily and Sokkary , 1975; See Fig. 2-3-9), the Union Lake Pluton rocks plot mainly in the diorite

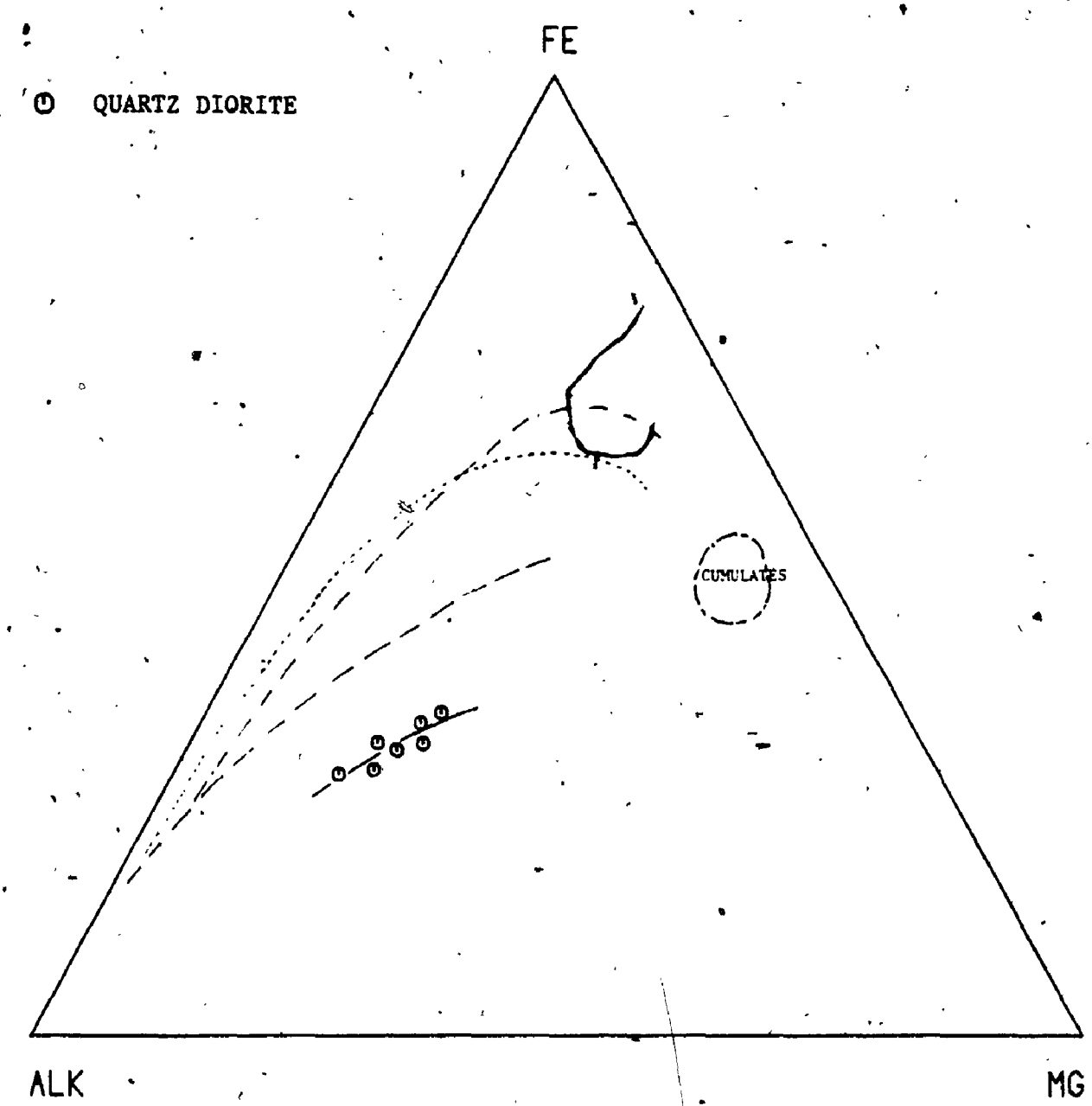

Figure 2-3-8. AFM diagram of the Union Lake Pluton.

- - - - - Calc-alkaline trend of Southern California Batholith (Nockolds and Allen, 1956).

—·—·— Chemical trend of Hakone P-series tholeiite lava (Nockolds and Allen, 1953).

---·--- Differentiation trend of Scottish alkaline basalt (Nockolds and Allen, 1953).

——— Variation trend of Union Lake Pluton (this study).

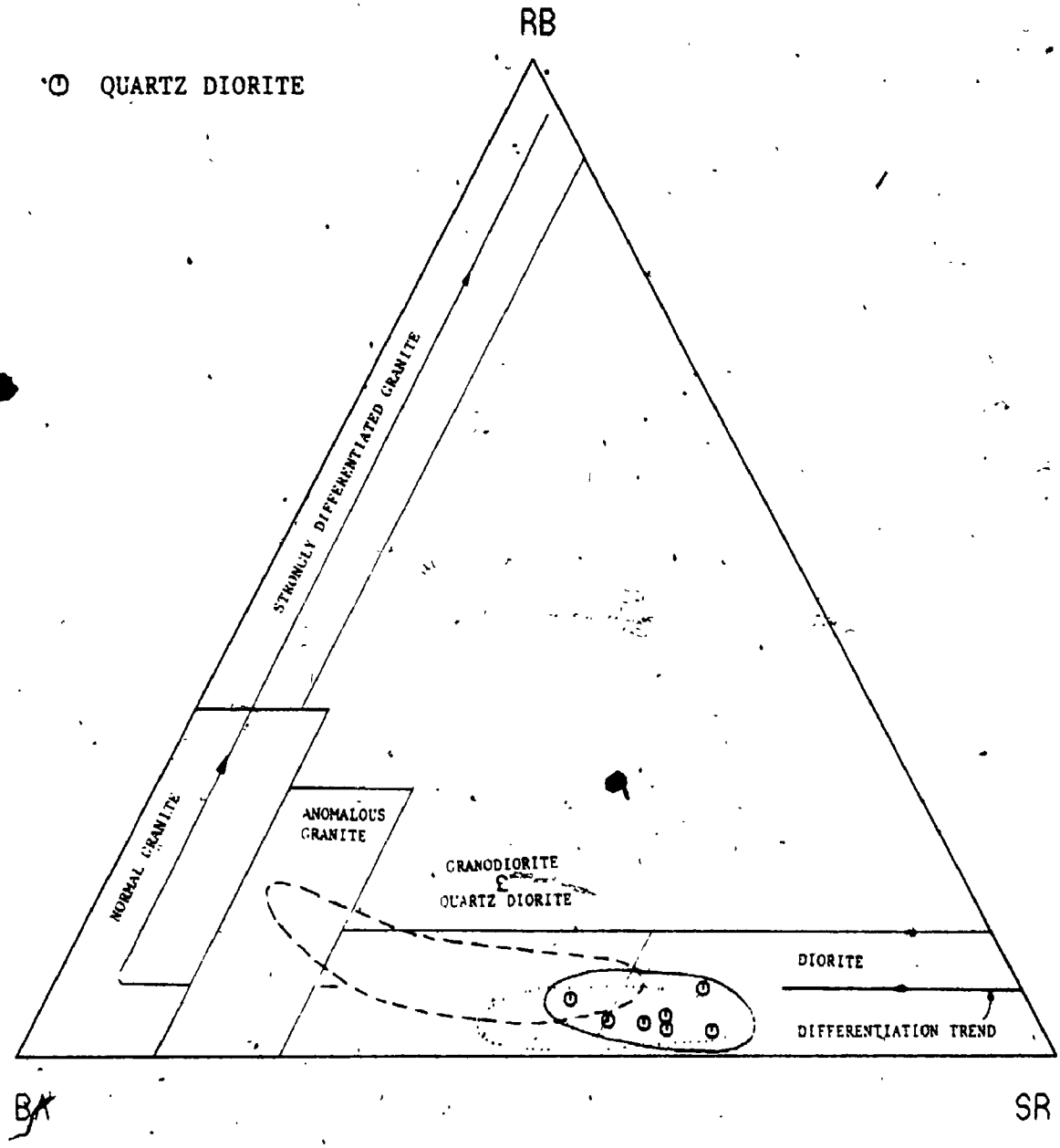

Figure 2-3-9. Rb-Ba-Sr ternary variation diagram of the Union Lake Pluton (after Bouseily and Sokkary, 1975). Compositional fields of Elzevir Batholith (Pride and Moore, 1983), White Lake Pluton (Somers, 1984) and Union Lake Pluton (this study) are enclosed by dashed-line, dotted-line and solid-line, respectively.

field with an average Ba/Sr ratio of 0.66. The Elzevir Batholith, by comparison, plots predominantly in the granodiorite field with a wide range of Ba/Sr ratios, whereas the White Lake Pluton straddles the diorite and granodiorite fields with Ba/Sr ratios similar to the Union Lake Pluton.

Furthermore, the positive correlations of K_2O with Rb (R = 0.9265) and Sr with Ba (R = 0.6580) are consistent with the normal differentiation trends of common igneous rocks. The increase of Rb/Sr and decrease Sr/Ba ratios with increasing SiO_2 indicate Sr is gradually depleted due to removal of early-formed (calcic) plagioclase. In addition, the positive correlations of Zr/Y, Fe/Mg and Ni/Mg with SiO_2 (See Table 2-3-4) reflect the fractionation of mafic phases, namely hornblende and bitotite. Moderate enrichment of Zr with increasing differentiation indicates no significant fractionation of zircon.

3.3.3 Rare-earth Elements -

Rare-earth element data for representative samples of the Union Lake Pluton and other trondhjemitic intrusions in the area are presented in Table 2-3-5. Chondrite-normalized curves (Fig. 2-3-10) show a moderate fractionation pattern with

Table 2-3-5. Rare-earth elements, Ta, Hf and Cs of representatives of the Union Lake Pluton and comparison with other trondhjemitic suites

	1 UK-3-3	2 UK-6	3 EL-6	4 EL-9	5 EL-14	7 GS-12	8 GS-16	9 Dacite
La (ppm)	28.12	27.02	39.40	5.92	23.50	11.50	20.00	20.00
Ce	64.84	59.48	77.30	11.80	45.70	22.70	28.70	37.00
Sm	5.79	5.10	4.44	1.98	3.01	2.24	3.11	2.80
Eu	1.74	1.25	1.57	0.28	1.12	0.64	0.81	0.29
Tb	0.55	0.42	0.45	0.28	0.37	0.18	0.32	0.40
Tm	-	-	-	-	-	0.10	0.12	-
Yb	1.14	1.11	0.88	0.89	0.85	-	-	1.20
Lu	0.24	0.19	0.13	0.15	0.13	0.10	0.11	0.20
7REE[a]	102.42	94.57	124.17	21.30	74.68	37.46	53.17	62.39
Ta	2.17	1.23	-	-	-	-	-	-
Hf	3.76	3.44	6.40	2.10	4.20	-	-	-
Cs	0.51	1.13	-	-	-	-	-	-
Eu/Eu* [b]	1.09	0.90	1.17	0.44	1.18	0.99	0.96	0.90
(Ce/Yb)N [c]	12.33	11.33	20.00	2.89	12.09	10.00	10.65	7.00
(Ce/Sm)N [d]	2.31	2.43	3.52	1.18	3.06	2.17	1.94	2.69
(Tb/Yb)N [e]	2.00	1.67	2.18	1.33	1.84	1.39*	2.00	1.35

1,2 Union Lake Pluton of this study.
3,4,5 Elzevir Batholith of Pride and Moore (1983, EL-6 and 14, the least fractionated samples; EL-9, the most fractionated sample).
7,8 White Lake Pluton of Somers (1984).
9 Dacite of Grenville Province (Condie and Moore, 1977).

a 7REE - sum of the REEs.
b Eu/Eu* - observed Eu value/value obtained by interpolating between Sm and Tb.
- degree of Eu-anomaly.
c (Ce/Yb)N - degree of fractionation of REE as a whole.
d (Ce/Sm)N - degree of LREE fractionation.
e (Tb/Yb)N - degree of HREE fractionation.

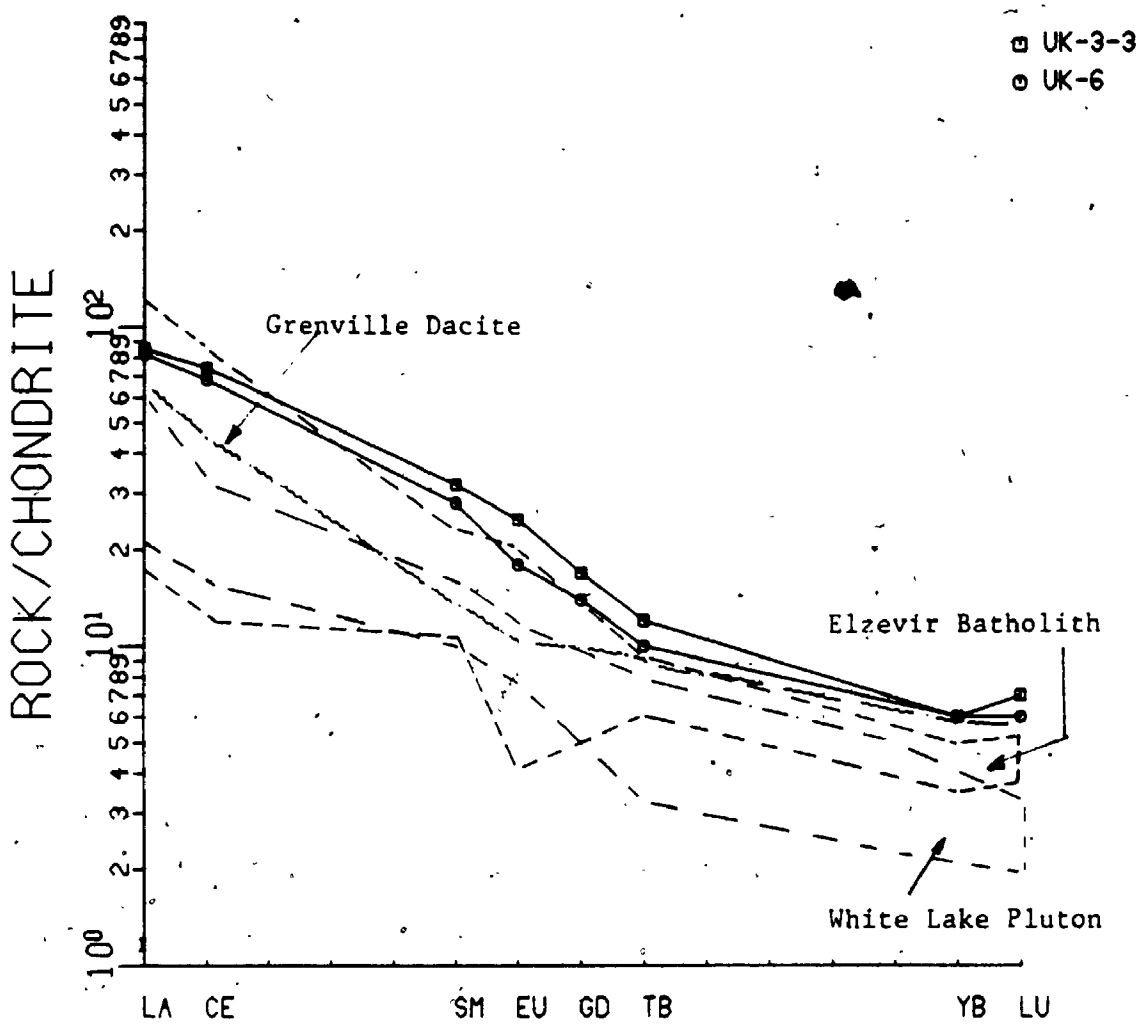

Figure 2-3-10. Chondrite-normalized REE distribution patterns for the Union Lake Pluton.

Grenville Dacite (Condie and Moore, 1977), Elzevir Batholith (Pride and Moore, 1983), White Lake Pluton (Somers, 1984).

mild negative slope and small Eu anomalies. By comparison, the REE composition of the Union Lake Pluton is similar to the least fractionated rocks of the Elzevir Batholith (Pride and Moore, 1983) with slightly higher HREE contents. Furthermore, the Union Lake Pluton has more than a 2-fold greater abundance of total REE than the White Lake Pluton, although both have similar normalized patterns.

Various REE plots are shown in Figure 2-3-11. Total REE abundances in these trondhjemites display a tendency to decrease with increasing SiO_2 (Fig. 2-3-11A), which reflects the fractionation of hornblende and apatite during differentiation. In the Eu/Eu* vs. total REE plot (Fig. 2-3-11B), the Union Lake Pluton and Elzevir Batholith show a positive correlation, while the White Lake Pluton illustrates a negative trend. However, the Eu/Eu* ratios have a strong tendency to decrease with decreasing Sr contents (Fig. 2-3-11C); this can be explained by removal of significant amounts of plagioclase during crystallization.

3.4 Isotopic Geochemistry

Two samples, UK-3-3 and UK-6, have been analyzed for whole-rocks oxygen isotope compositions; the $\delta^{18}O$ values are 8.54 and 8.34 respectively. These are

Figure 2-3-11. Various REE plots for Union Lake Pluton and similar rock-types in this part of Grenville Province. (A) total REE vs. SiO_2 (B) Eu/Eu* vs. total REE (C) Eu/Eu* vs. Sr

Visual variation trends are shown by dashed-lines.

○ Union Lake Pluton (this study)

△ Elzevir Batholith (Pride and Moore, 1983)

□ White Lake Pluton (Somers, 1984)

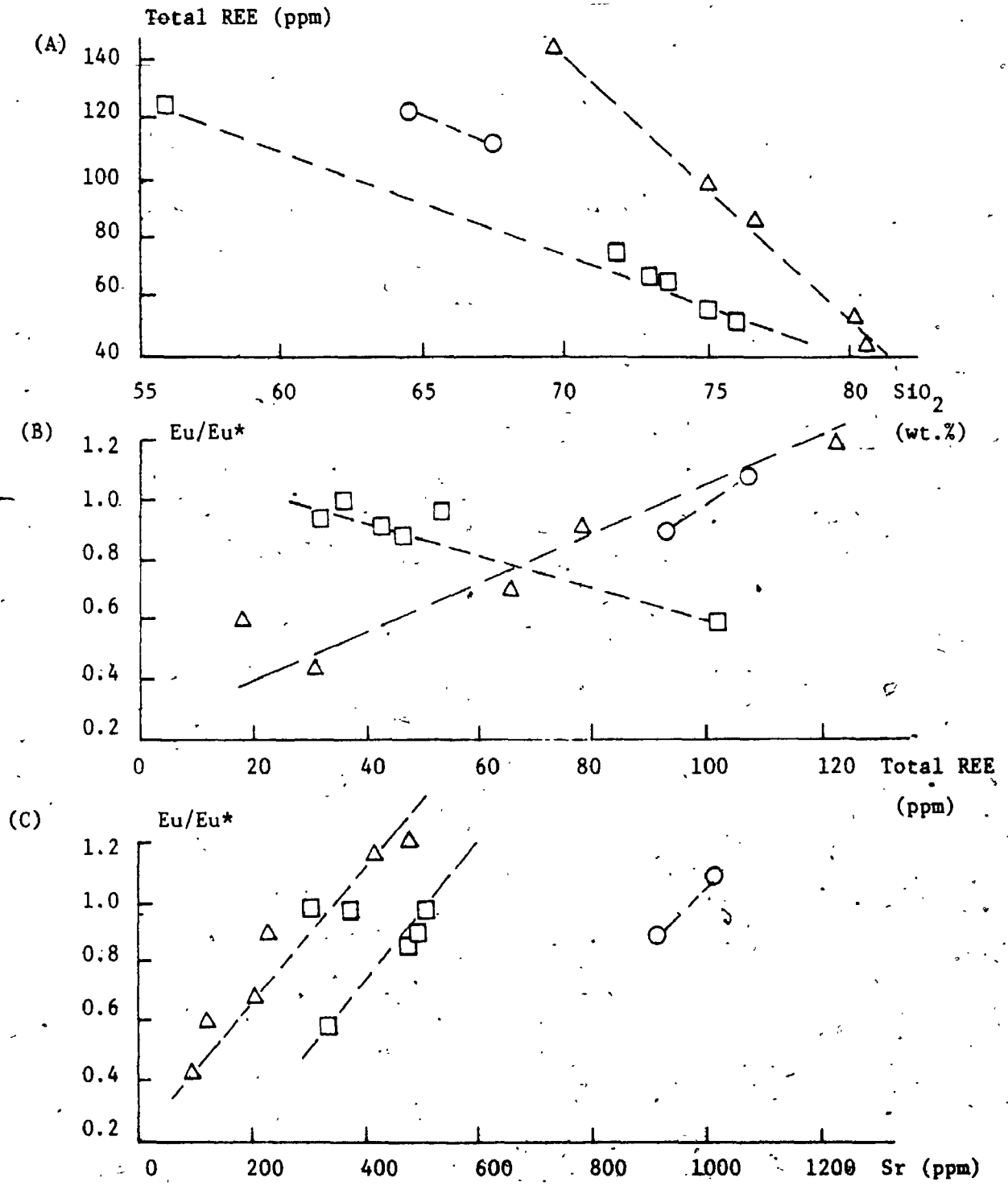
(A)
Total REE (ppm)
140
120
100
80
60
40
55
60
65
70
75
80
SiO2 (wt.%)
(B)
Eu/Eu*
1.2
1.0
0.8
0.6
0.4
0.2
0
20
40
60
80
100
120
Total REE (ppm)
(C)
Eu/Eu*
1.2
1.0
0.8
0.6
0.4
0.2
0
200
400
600
800
1000
1200
Sr (ppm)

comparable with other trondhjemitic - tonalitic intrusions in this part of the Grenville Province, which are characterized by $\delta^{18}O$ values ranging from 7.0 to 9.5 (Shieh, 1980). Such low ^{18}O concentrations of these plutons may suggest a parental source from either the lower crust or the basement gneisses of the Grenville Supergroup ($\delta^{18}O$ = 6 to 9 o/oo; Shieh, 1980).

Although no Rb-Sr isotopic dat a is available for the Union Lake Pluton, several trondhjemite intrusions of eastern Ontario have been dated by Bell and Blenkinsop (1980). A whole-rock Rb-Sr isochron for the Elzevir Batholith yields an age of about 1240 $\pm$ 50 Ma and an initial $^{87}Sr/^{86}Sr$ ratio of 0.7020. In addition, the surrounding Tudor metavolcanic rocks have a coherent age of 1250 $\pm$ 90 Ma and an initial ratio of 0.7029. These authors (above) have suggested a cogenetic relation between the trodhjemitic intrusions and the volcanic rocks due to their similarity in both age and initial isotope ratios. Besides, the relatively low initial ratios rule out the possibility of any significant involvement of continental crust in the generation of these trondhjemitic magmas.

3.5 Petrogenesis And Source Rocks

Variation plots of CaO vs. MgO, Al_2O_3 vs. CaO and MgO vs. total iron (Fig. 2-3-12) suggest that the internal chemical variations of the Union Lake Pluton can be explained by fractionation of plagioclase, hornblende and lesser biotite. The decreases in TiO_2 and P_2O_5 are likely caused by sphene and apatite fractionation, respectively. It is noteworthy that the Grenville dacite and other trondhjemitic suites of the province plot at the more fractionated end of the Union Lake Pluton differentiation trend, reflecting the primitive nature of this pluton.

The role of plagioclase fractionation is strengthened by the decrease of Sr contents and Sr/Ca ratio, and increase of Rb/Sr ratio with increasing SiO_2, as well as the strong negative correlation of Sr vs. Eu/Eu* during differentiation of the Union Lake magma. Similarly, the significant increase in Fe/Mg and Ni/Mg ratios support a Mg-biotite fractionation. Enrichment of Zr and Zr/Y ratio imply no significant fractionation of zircon and/or significant removal of hornblende or apatite (both have greater K_d for Y) during differentiation. However, the total REE abundances decrease with increasing SiO_2, which is reverse to the general trend of magmatic differentiation (eg. Mason, 1966), and may be explained by apatite fractionation for LREE (Miller and Mittlefeldt, 1982) and hornblende

Figure 2-3-12. Inter-elemental variation plots of the Union Lake Pluton. (A) CaO vs. MgO (B) Al_2O_3 vs. CaO (C) MgO vs. Fe_2O_3 with relations to the compositions of major mineral components. Solid-lines indicate the differentiation trend of the Union Lake Pluton. Dashed-lines show the possible extract mineral pairs during fractionation (Cox et al., 1979).

Δ_1 - Grenville dacite (Condie and Moore, 1977)
Δ_2 - Elzevir Batholith (Pride and Moore, 1983)
Δ_3 - Grenville andesite (Condie and Moore, 1977)

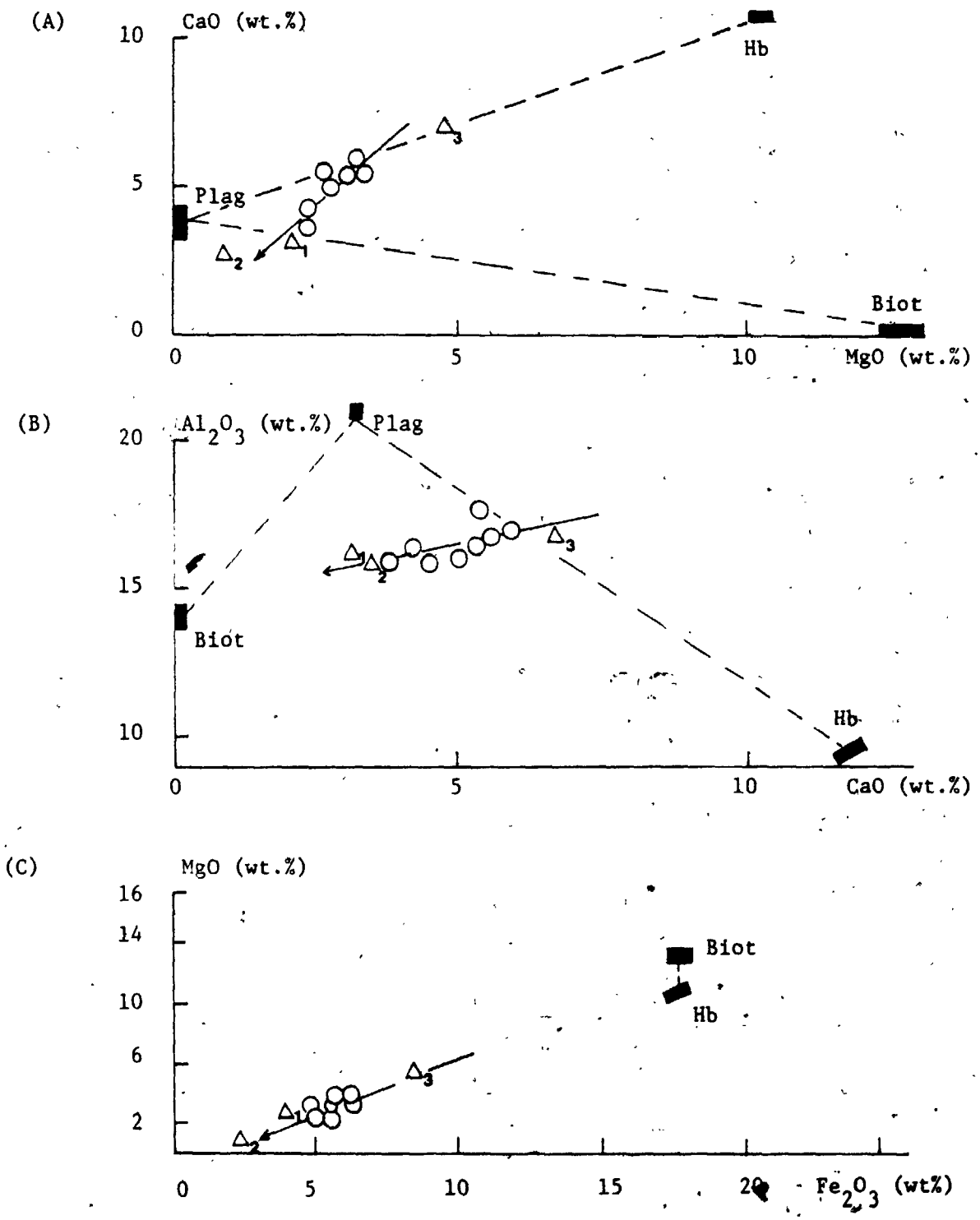
(A)
CaO (wt.%)
10
5
0
Hb
Plag
Biot
0
5
10
MgO (wt.%)
(B)
Al_2O_3 (wt.%)
Plag
20
15
10
Biot
Hb
0
5
10
CaO (wt.%)
(C)
MgO (wt.%)
16
14
10
6
2
Biot
Hb
0
5
10
15
20
Fe_2O_3 (wt%)

fractionation for HREE.

Quantitatively, the variation trends require removal of 18% hornblende, 30% plagioclase and 0.4% sphene from the least differentiated sample (UK-3-3) to form the more siliceous one (UK-1) (See Table 2-3-6A). This mass balance calculation was checked by comparison with trace-elements, for instance, a more than 2-fold enrichment of Rb from UK-3-3 to UK-1 suggests that about 50% liquid remained after differentiation, assuming no Rb was fractionated in the solid phase; the observed alkali concentrations are in excellent agreement with the calculated ones after 55% fractional crystallization.

Pride and Moore (1983) rejected current models (i.e fractional crystallization of hornblende from a wet basalt or partial melting of hydrous metabasalt for trondhjemitic rocks of the Grenville Province) and favoured a cogenetic relationship with the surrounding Grenville dacite, which was produced by about 50% partial melting of siliceous garnet granulite according to model dependent calculations of Condie and Moore (1977). However, in the study of White Lake Pluton, Somers (1984) found by quantitative modelling that the REE pattern of the pluton is similar to that of a magma produced by about 30% to 50% partial melting of mafic granulite with a composition similar to Archean basalt at the lower crust.

Table 2-3-6. Mass balance calculations for differentiation of Union Lake Puton and mixing dacitic magma with wallrock

(A) Differentiation from UK-3-3 to UK-1

Comp. (wt.%)	Parent UK-3-3	Product UK-1	Bulk comp. of added or subt. material	Obs. diff. between magmas	Calc. diff. between magmas	Residuals
SiO_2	59.91	62.84	56.46	2.936	2.958	-0.163
TiO_2	0.75	0.70	0.63	-0.054	-0.048	-0.089
Al_2O_3	16.93	16.13	18.27	-0.800	-0.821	0.240
TFe_2O_3	5.73	5.01	6.53	-0.724	-0.868	0.013
MnO	0.08	0.07	0.13	-0.010	-0.031	0.019
MgO	3.33	2.31	3.92	-1.020	-0.792	-0.237
CaO	5.60	4.16	7.28	-1.442	-1.447	0.072
Na_2O	6.02	5.47	6.17	-0.555	-0.600	-0.215
K_2O	1.34	3.07	0.61	1.732	1.697	0.536
P_2O_5	0.30	0.24	0.00	-0.062	-0.047	-0.178

Sum of the squares of the residuals = 0.5193

100 unit, UK-3-3 = 51.6 % UK-1 + 18 % Hornblende + 30 % plagioclase + 0.4 % sphene

(B) Assimilation of amphibolite and limestone by a trondhjemitic melt

Comp.	Initial (EL-6)	5% Ls+5% Amph.	5% Ls+7.5% Amph.	5% Ls+10% Amph.	Ave. of UK
SiO_2 (wt. %)	65.49	62.12	61.81	61.51	61.21
TiO_2	0.05	0.11	0.41	0.61	0.74
Al_2O_3	17.73	16.86	16.83	16.79	16.58
TFe_2O_3	4.03	4.25	4.42	4.59	5.54
MnO	0.05	0.06	0.07	0.07	0.08
MgO	1.37	2.27	2.42	2.56	2.89
CaO	3.85	7.37	7.49	7.58	5.15
Na_2O	5.17	4.81	4.76	4.71	5.51
K_2O	1.98	1.85	1.81	1.78	2 02
P_2O_5	0.28	0.27	0.27	0.26	0.27

Although the composition of the Union Lake Pluton is similar to average Grenville dacite and other trondhjemite suites in the area, the significance of enriched CaO, MgO, total iron and Sr and low SiO_2 needs to be explained. In addition, hornblende ranging from 12 to 25 vol.% in the Union Lake Pluton, is rare or absent from other trodhjemites (cf. Pride and Moore, 1983; See Table 2-3-7).

Two hypotheses could explain such chemical and mineralogical peculiarities : (A) the rocks of the Union Lake Pluton represent cumulates from which the wet basalt fractionated; (B) the differences observed are caused by assimilation of limestone and amphibolite wallrocks by the trondhjemitic melts.

(A) Accumulation of hornblende in the pluton seems to be consistent with a model of fractionation of wet basalt (in this case, Grenville tholeiite) to produce the trondhjemitic - tonalitic magmas. If so, evolution of the pluton itself would represent a "rock path" rather than a liquid path. Presumably the liquid that precipitated the Union Lake quartz diorite would be much more siliceous than those of trondhjemitic (or dacitic) composition. Besides, in the inter-element variation diagrams (Fig. 2-3-12), rocks of the pluton do not show "cumulate-differentiate" relations with other trondhjemite intrusions of the area. Further, differentiation of Grenville tholeiite to form dacitic

Table 2-3-7. Modal composition of the Union Lake Pluton and other trondhjemitic rocks

Sample No.	1 UK-1	2 UK-2	3 UK-7-2	4 Trond.	5 Trond.	6 Biot-Diorite	7 Trond.	8 Tonalite
Qtz (vol.%)	11.9	4.6	11.9	26.4	29	15	20.2	22.2
Plag	66.3	55.4	47.0	54.5	49	38	68.9	62.1
K-feld	4.3	3.7	6.4	0.8	tr	-	0.2	0.1
Biot	0.1	7.3	9.6	13.0	3	24	10.0	15.6
Hb	12.6	24.7	19.1	-	-	12	-	-
Px	2.1	-	-	-	-	-	-	-
Chlorite	-	-	-	0.4	-	4	-	-
Opaque	-	0.1	0.1	0.8	-	-	-	-
Ap	0.6	1.7	1.7	-	tr	tr	-	-
Sph	1.1	1.1	2.7	-	tr	tr	-	-
Zir	0.5	0.3	tr	-	-	-	-	-
Mus	-	-	-	tr	9	-	-	-
Calcite	-	-	-	2.0	-	-	-	-
Epidote	tr	tr	tr	0.6	9	7	-	-
Others	0.3	1.0	1.4	1.5*	-	-	0.7	tr

4 Average of 12 trondhjemites from Wadsworth trondhjemitic complex (Lumbers, 1967)
5 High Al_2O_3 type trondhjemite from southwestern Trondheim region, Norway (Barker and Millard, 1979)
6 Biotite-diorite from southwestern Trondheim region, Norway (Barker and Millard, 1979)
7 Tronhjemite from the Weslemkoon Batholith (Lumbers, 1967)
8 Tonalite from the Weslemkoon Batholith (Lumbers, 1967)

* Others = Ap + Sph + Zir

melts has been rejected by Condie and Moore (1977) due to rapid depletions of Y, Zr, Cr and HREE.

(B) Assimilation of trondhjemitic melt with limestone might explain the enrichment of CaO and the depletion of SiO_2, while incorporation of mafic rocks (amphibolite) in the magma would expect the increase of total iron and magnesium. The enrichment of hornblende and minor plagioclase in this pluton compared with other trondhjemitic suites of the area may also be the result of the above processes. In Table 2-3-6B, the average composition of the Union Lake Pluton is similar to the calculated composition after mixing trondhjemitic magma (EL-6, Elzevir Batholith) with 5% limestone and 10% amphibolite, although the increase of CaO is more rapid than that of total iron and MgO. However, if the trondjemitic melt did evolve by partial melting of mafic granulite, a relative Fe-Mg-rich magma would be expected.

Assimilation of trondhjemitic melt with limestone and amphibolite agrees generally with field relations. The local mafic clots or schlieren may represent, as "residue", undigested amphibolite wallrocks. However, such mixing processes have not significantly affected the oxygen isotope signature of the trondhjemitic melt.

3.6 Summary

Despite its relatively higher concentrations of CaO, MgO and total iron and lwoer SiO_2, geochemical data place the Union Lake Pluton into the trondhjemite suite of Pride and Moore (1983) or biotite diorite series of Lumbers (1967), in this part of the Grenville Province.

The internal variations of the pluton can best be interpreted by processes of fractional crystallization. The mass balance calculations indicate that they account for removal of about 18% hornblende, 30% plagioclase and 0.4% sphene during the course of differentiation.

The chemical and mineralogical differences between this pluton and other Grenville trondhjemite suites can be explained by assimilation of trondhjemitic melt with limestone and amphibolite wallrocks during ascent of the magma. The possible Fe-Mg-rich origin of the trondhjemitic melt for the Union Lake Pluton supports the model of 30% to 50% partial melting of mafic granulite in this part of the Grenville Province.

4.0 ELPHIN GRANITE-SYENITE COMPLEX

4.1 General Characters And Intrusive Relations

The Elphin Granite-Syenite Complex is located in the North Sherbrooke and southern corner of Palmerston Townships (Fig. 2-4-1). It intruded the southern tip of the Dalhousie Lake Diorite-Gabbro Complex, which is surrounded by crystalline limestone-dolomite, metavolcanic rocks (amphibolite) and the Lavant gneisses (ODM, Map No. 1956-4). The direct contact between the granite-syenite complex and the diorite-gabbro host was not found in the field.

The oval-shaped body consists of two major rock types : (1) pinkish, fine- to medium-grained, biotite-muscovite granite; and (2) reddish, coarse-grained biotite syenite with porphyritic to pegmatitic texture. In addition, biotite-hornblende-rich metadioritic xenoliths occur frequently inside the complex and/or around its margin.

A pegmatitic dyke of the syenitic variety cutting across fine-grained granite indicates that the latter was the early phase of the body. The sample distribution illustrates that the porphyritic syenite phases occur mostly in the central and northern portions of the pluton, whereas the fine-grained granite is dominant to its south. The presence of abundant metadioritic xenoliths in the granite-syenite suggests

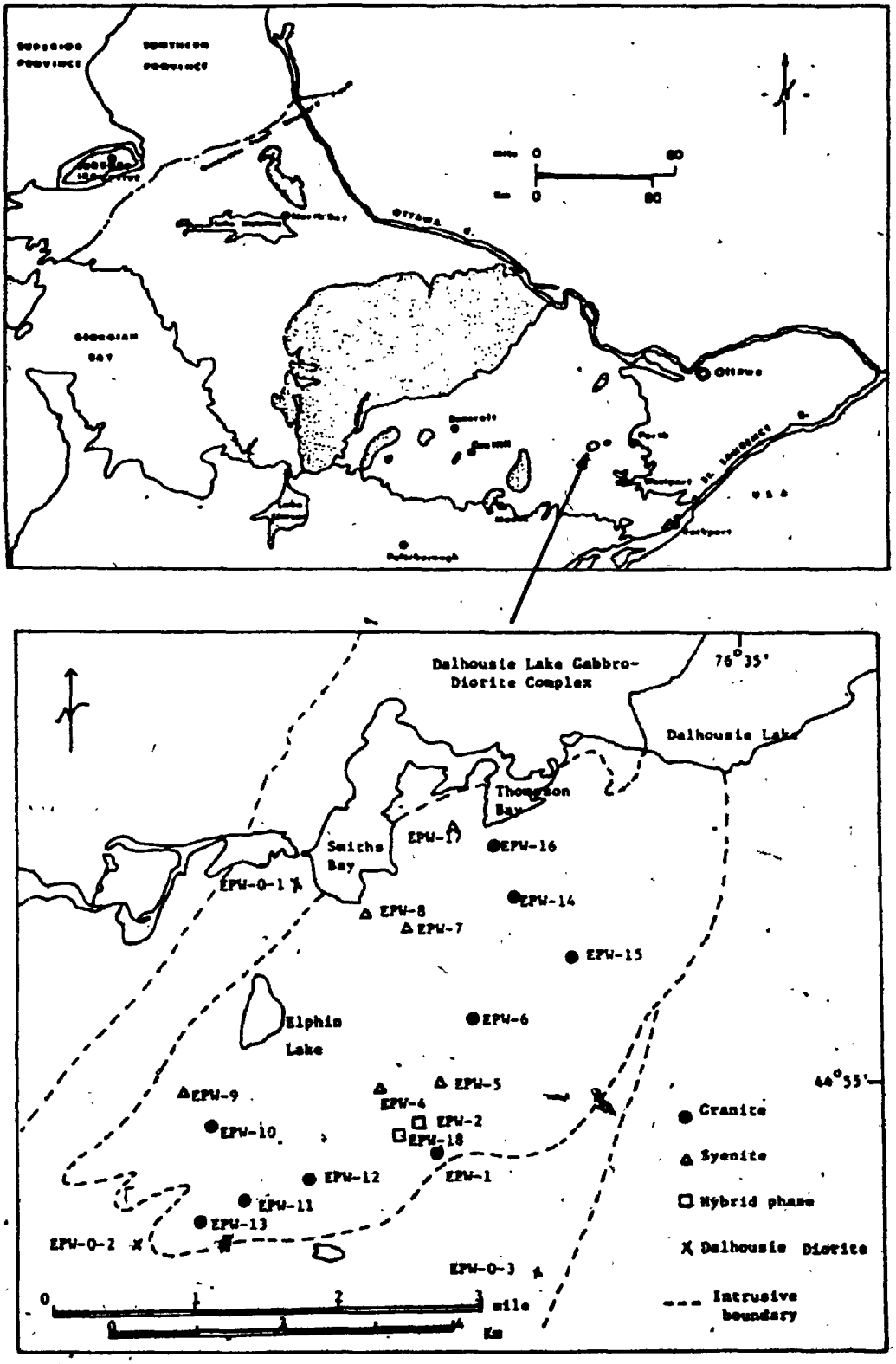

Figure 2-4-1. Sample location map of the Elphin Complex.

that stoping was the mechanism of intrusion. The contact between metadioritic xenolith and granite-syenite is commonly gradational, possibly indicative of assimilation processes. However, the genetic relationships between the Elphin Granite-Syenite Complex and the host diorite-gabbro require further study.

4.2 Petrography

Petrographically, the Elphin Granite-Syenite Complex can be classified as granite - granodiorite, quartz monzonite - syenite and quartz diorite or monzodiorite (the xenoliths) according to Streckeisen (1976, See Fig. 2-4-2; note that quartz monzonite is a quartz-poor rock). There is one exception, which is classified as coarse-syenite, falling into the lower part of the granite field. Rocks are holocrystalline and hypidiomorphic - granular; clusters of mafic minerals and porphyritic K-feldspar give the syenite a reddish colour. Chemical compositions of two feldspars and biotite from the Elphin Complex are given in Table 2-4-1 and 2-4-2, respectively.

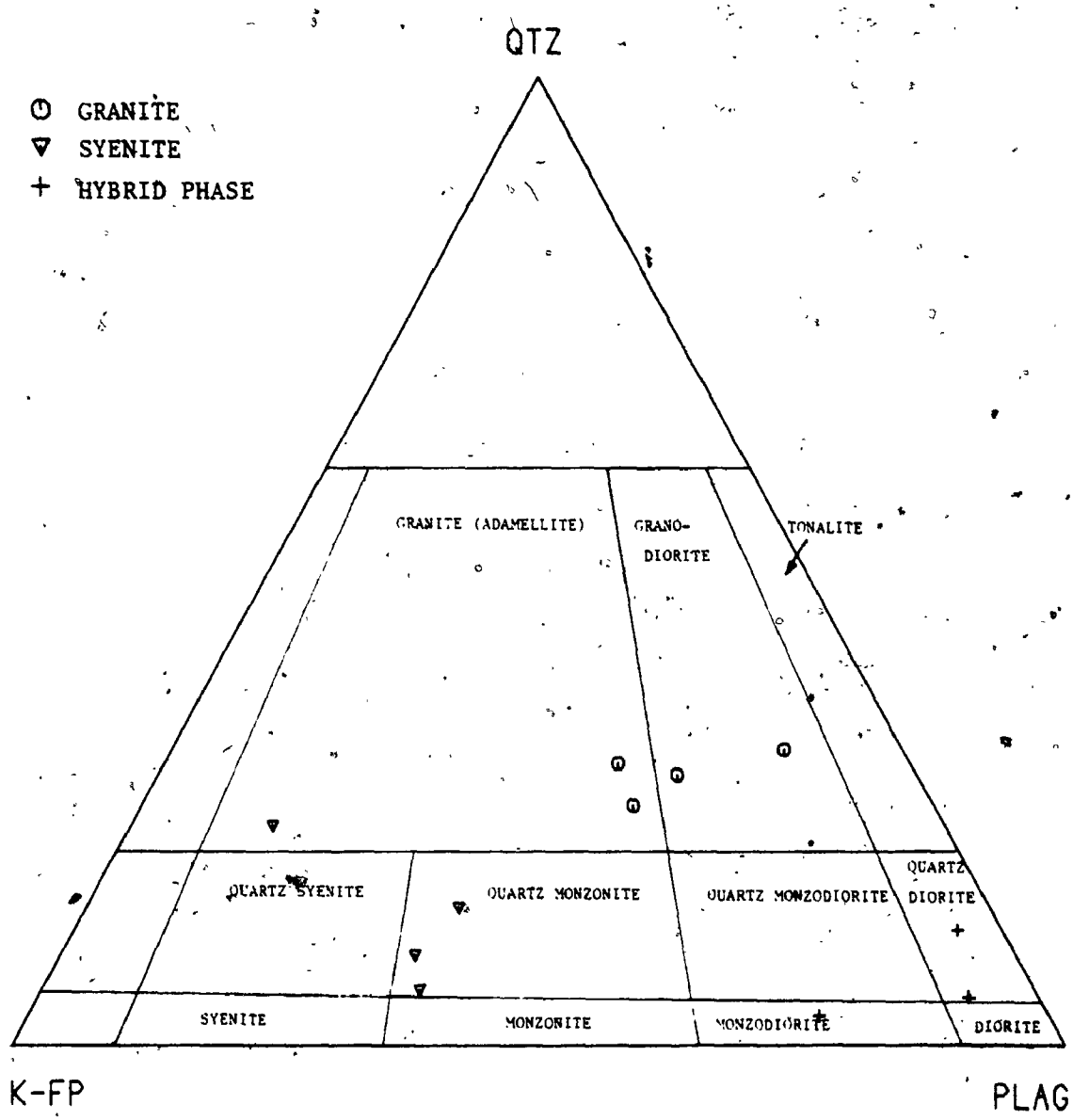

Figure 2-4-2. Modal classification of the Elphin Complex (Streckeisen, 1976).

Table 2-4-1. Chemical compositions and calculated formulae of feldspars from the Elphin Granite-Syenite Complex

(a) Plagioclase				(b) K-feldspar		
Sample No.	EPW-1	EPW-15-2	EPW-7-2	EPW-1	EPW-15-2	EPW-7-2
Rock-type	Granite	Granite	Syenite	Granite	Granite	Syenite
(wt%)						
SiO_2	67.64	67.32	65.83	64.63	65.05	65.11
Al_2O_3	20.37	20.94	20.73	18.56	18.36	18.69
CaO	0.40	1.27	1.76	0.02	0.17	0.00
Na_2O	11.66	10.73	8.64	0.52	0.60	0.61
K_2O	0.15	0.21	3.18	15.93	15.84	15.96
Total	100.22	100.47	100.14	99.66	100.02	100.37
Si (Z)	11.820	11.736	11.664	11.971	12.002	11.971
Al (Z)	4.194	4.302	4.328	4.051	3.992	4.049
	16.014	16.037	15.992	16.021	15.994	16.021
Na (X)	3.950	3.627	2.968	0.187	0.215	0.217
Ca (X)	0.075	0.237	0.334	0.004	0.034	0.000
K (X)	0.033	0.047	0.719	3.763	3.728	3.743
	4.059	3.911	4.021	3.954	3.976	3.960
O	32	32	32	32	32	32
(mol%)						
Ab	97.33	92.74	73.82	4.72	5.40	5.49
An	1.85	6.07	8.31	0.10	0.85	0.00
Or	0.82	1.19	17.87	95.18	93.76	94.51

Table 2-4-2. Chemical compositions and calculated formulae of biotite from the Elphin Granite-Syenite Complex

Sample No. Rock-type	EPW-1 Granite	EPW-15-2 Granite	EPW-7-2 Syenite
(wt%)			
SiO_2	36.52	37.57	37.11
TiO_2	2.61	1.19	1.62
Al_2O_3	14.36	13.45	14.60
Fe_2O_3	2.38	2.52	3.41
FeO	17.56	18.55	15.17
MnO	0.12	0.11	0.65
MgO	10.97	11.50	11.79
CaO	0.01	0.02	0.00
Na_2O	0.08	0.04	0.05
K_2O	9.64	9.73	10.01
Total	94.25	94.68	94.41
Si (Z)	5.644	5.800	5.689
Al^{iv} (Z)	2.356	2.200	2.311
	8.000	8.000	8.000
Al^{vi} (Y)	0.257	0.245	0.325
Ti (Y)	0.303	0.133	0.187
Fe^{3+} (Y)	0.277	0.293	0.393
Fe^{2+} (Y)	2.268	2.393	1.943
Mg (Y)	2.524	2.644	2.691
Mn (Y)	0.016	0.014	0.084
	5.645	5.727	5.624
Ca (X)	0.002	0.003	0.000
Na (X)	0.024	0.012	0.015
K (X)	1.899	1.915	1.956
	1.925	1.930	1.971
O	22	22	22
$Mg/Fe^t+Mg+Mn$	0.496	0.495	0.527
Fe^t/Fe^t+Mg	0.502	0.504	0.465
mole of annite	0.378	0.399	0.324

$Fe^t = Fe^{3+} + Fe^{2+}$ in unit cell

4.2.1 Granitic Rocks -

Granitic rocks of the pluton generally contain > 20% quartz with colour index less than 10 and feldspar ratio (= plagioclase/total feldspar) about 0.60. Biotite is the only ferromagnesian mineral associated with subordinate (secondary) muscovite. Sphene, apatite, zircon and secondary epidote and carbonate are common accessory minerals.

Plagioclase ($An_{< 10}$, Table 2-4-1), constituting more than 40% of the felsic component, forms euhedral to subhedral crystals with extensive sericitization in the cores. In addition to secondary white mica, carbonate patches and epidote aggregates are commonly enclosed. Vermicular intergrowth is also present. K-feldspar locally forms phenocrysts and is surrounded by finer quartz and plagioclase. Quartz euhedra show strong wavy extinction with subgrain boundaries, while the anhedra have mosaic or sugary texture associated with fine-grained plagioclase.

Biotite (Mg-rich; See Fig. 2-4-3), is subhedral and pleochroic from Y = Z = greenish brown to X = light straw yellow. It is partly to completely chloritized. Sphene and zircon are commonly enclosed, while associated opaques and epidote are due to alteration. Muscovite is

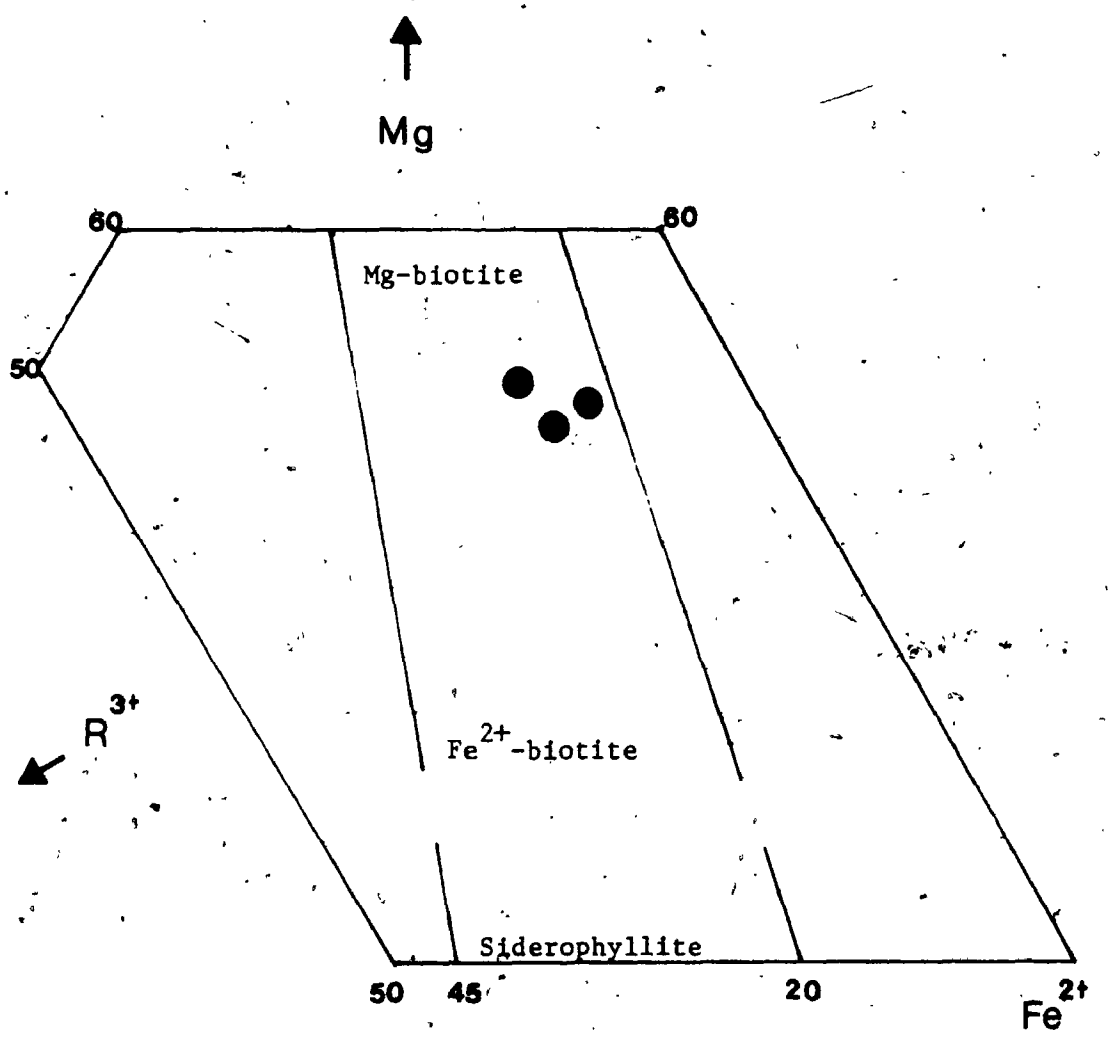

Figure 2-4-3. The Mg-Fe^{2+}-R^{3+} relation in trioctahedral micas of the Elphin Complex (after Foster, 1960).

$$R^{3+} = Al^{vi} + Fe^{3+} + Ti^{4+}$$

considered to be of secondary origin, replacing either plagioclase or biotite.

Secondary epidote (sausserite) is associated with carbonate patches and sericite in the core of an altered plagioclase. Later sphene aggregates as rims around opaques may be due to Fe-Ti oxides exsolved during the deuteric stage. Opaque minerals are mainly magnetite and rarer sulfide minerals (eg. chalcopyrite).

4.2.2 Syenitic Rocks -

In general, rocks of this category contain < 15% quartz and have a colour index ranging from 2.5 to 8.5, and feldspar ratio < 0.60. Both biotite and hornblende are common mafic minerals. Accessory minerals are sphene, apatite, zircon, secondary muscovite, epidote and carbonate, and tourmaline.

K-feldspar (microcline and microperthite) makes up 40% to 55% of the modal composition. In most samples, it forms phenocrysts which are commonly fractured and deposited with later fine-grained quartz. Later unmixing with plagioclase and intergrowth with quartz form microperthite and granophyre respectively. One sample (EPW-10) shows that euhedral microcline crystals with characteristic cross-hatch twinning have been

partially "replaced" by plagioclase and myrmekite. In addition to secondary muscovite and carbonate, small tourmaline prisms are frequently found in microperthite.

Plagioclase is highly altered in the core with a mixture of sericite, carbonate and epidote; large crystals have a core of An_{13} and a rim of An_5. In one sample (EPW-9), both microperthite and plagioclase form phenocrysts in a quartz-plagioclase groundmass. It is also noted that the average composition of the syenitic rocks suggests a "ternary" feldspar of Or-content > 15 mole% (Table 2-4-1).

Biotite (X = straw yellow to greenish yellow, Y = Z = brownish yellow to greenish brown) is the major mafic mineral associated with a subordinate amount of hornblende in some samples. Both are subhedral to anhedral with poikilitic texture and graphic intergrowth with quartz. Chloritization is a common post-magmatic alteration. Biotite of the syenite phase, classified as Mg-biotite of Foster (1960, Fig. 2-4-3), contains relatively higher MgO and lower total iron than those of the granite (Table 2-4-2).

Epidote crystals commonly occur at the rims of biotite where in contact with plagioclase or,

secondarily, as alteration product after plagioclase. Apatite forms euhedral to subhedral individual grains or inclusions in biotite. In one sample, euhedral sphene contains apatite inclusion. Sphene aggregates are associated with biotite flakes and form inclusions in hornblende. Opaques are associated with biotite and sphene. Anhedral tourmaline prisms with light green to blue-green pleochroism are often observed in slightly altered microperthite, indicative of possible tourmalinization at the expense of alkaline feldspars.

4.2.3 Xenolithic Hybrid Phases -

Quartz diorite and monzodiorite are believed by the author to be the hybrid phases of assimilation of diorite-gabbro xenoliths. They are characterized by higher colour index, up to more than 45, and feldspar ratios ranging from 0.75 to 0.94. The rock is greenish black to pinkish grey in colour due to the high content of feldspar. Rocks of this hybrid phase are massive with medium- to coarse-grain size in general.

With increasing degree of assimilation (hybridization), the amount of mafic minerals decreases, while the K-feldspar content increases.

Plagioclase is the major felsic component with various amounts of biotite, hornblende, pyroxene and lesser microcline. Apatite, sphene, secondary white mica, carbonate and epidote are common access ories; tourmaline and topaz (optical identification) are also encountered as products of pneumatolytic alteration.

4.3 Whole-rock Geochemistry

4.3.1 Major-oxides

As expected from modal classification, in the variation diagram of SiO_2 as a function of differentiation index (D.I.) (Fig. 2-4-4), the syenitic rocks of the Elphin Complex lie in the SiO_2-saturated and -undersaturated fields (Thornton and Tuttle, 1960), while the granitic rocks are, with one exception, in the oversaturated field. The overall composition of the Elphin Complex is metaluminous with an average of aluminum to total alkali-lime ratio about 0.97; the agpaitic index ranges from 0.902 of granite, 0.833 of syenite to 0.738 of xenolithic hybrid rocks. Besides, both the granitic and syenitic rocks show alkalic affinity and fall within the alkaline field of Miyashiro (1978, See Fig. 2-4-5).

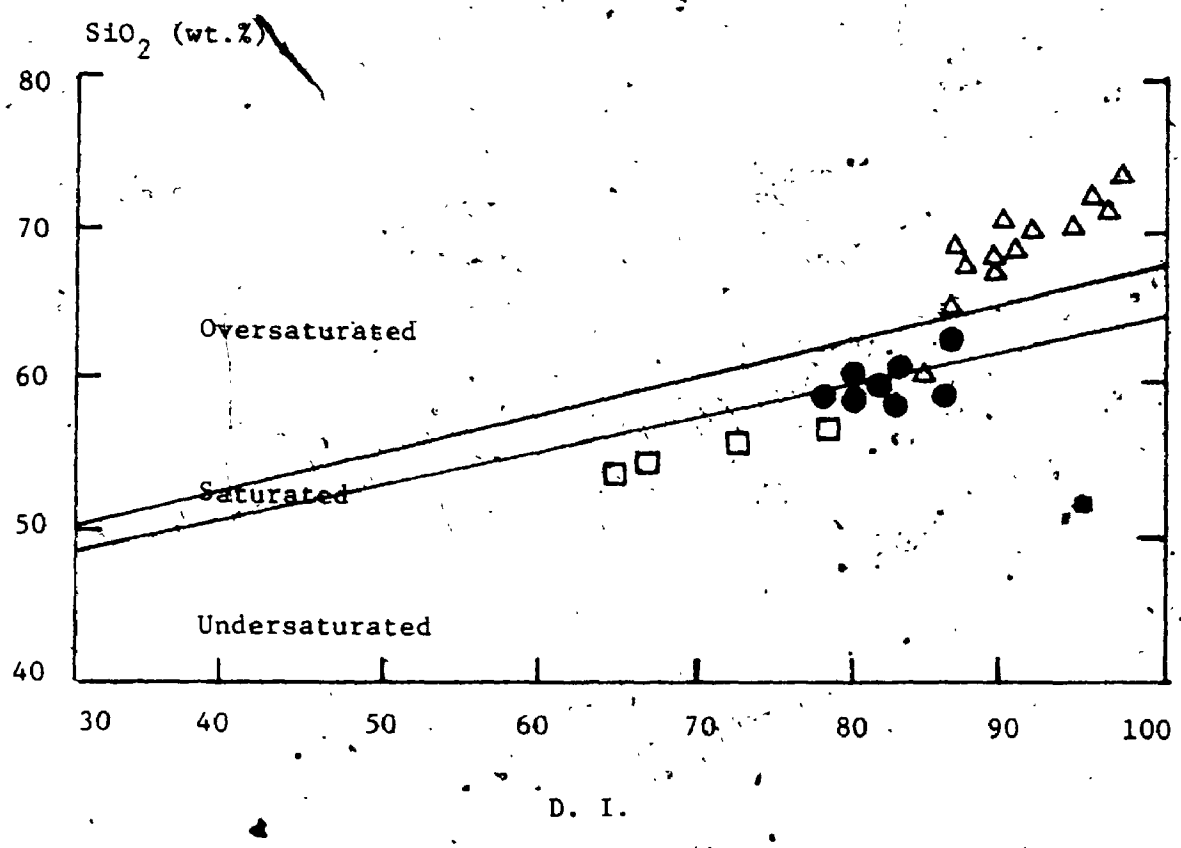

Figure 2-4-4. Variation of SiO_2 as a function of D.I. Solid-lines separate the oversaturated, saturated and undersaturated fields of Thornton and Tuttle (1960).

△ Granite ● Syenite □ Hybrid phase

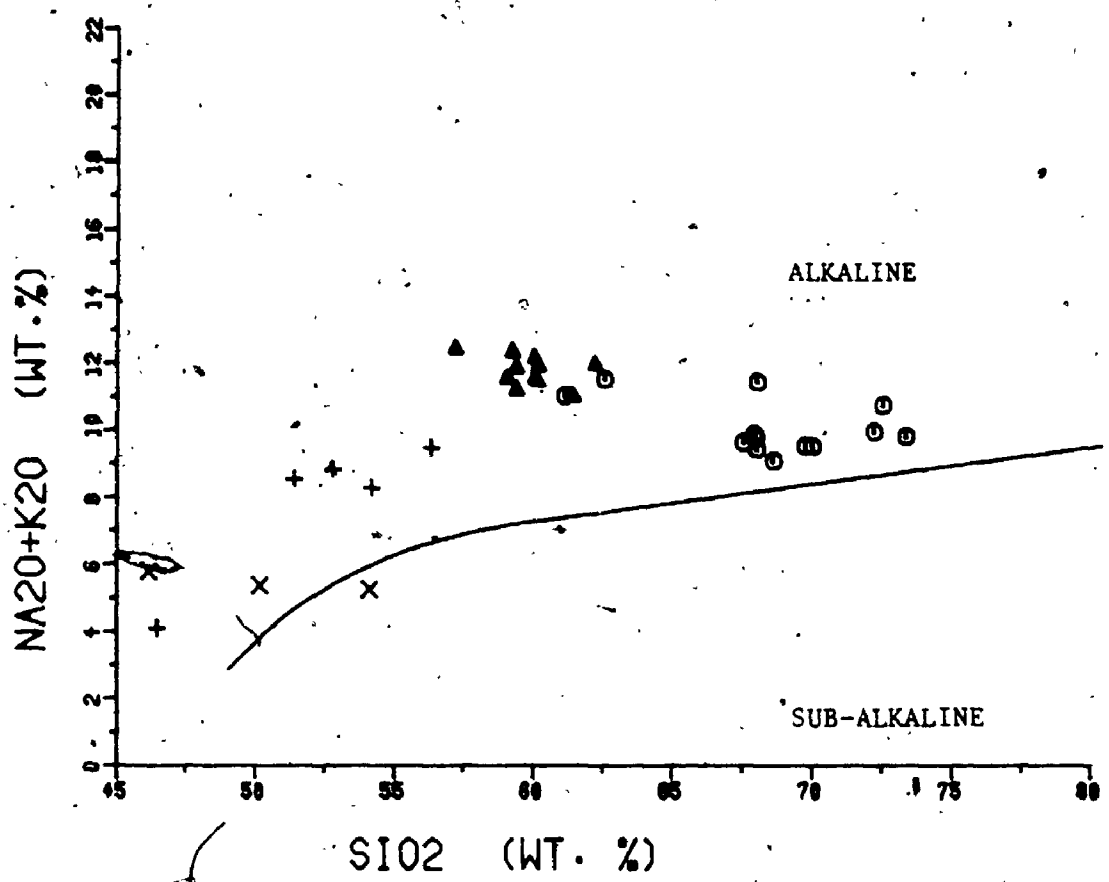

Figure 2-45. Na_2O+K_2O vs. SiO_2 plot of the Elphin Complex. Solid-line separates the alkaline and subalkaline fields of Miyashiro (1978).

⊙ GRANITE
▲ SYENITE
+ HYBRID PHASE
× METADIORITE

The mean compositions of the Elphin Granite-Syenite Complex and other similar rock-types are listed in Table 2-4-3. Generally, the major-oxide composition of the granitic rocks of this complex is similar to that of the biotite-muscovite granodiorite of Nockolds (1954), except that the former has relatively lower SiO_2, higher alkalis and much higher oxidation ratio. The syenitic rocks are close to the composition of average calc-alkali syenite (Nolckolds, 1954). In comparison with dioritic rocks of the adjacent Dalhousie Lake Diorite-Gabbro Complex (Fig. 2-4-1), the xenolithic hybrid rocks have relatively higher SiO_2, Na_2O, K_2O, lesser total iron, MgO, CaO and much lower Na_2O/K_2O ratio. Similarly, in the normative Qtz-Plag-Or plot (Fig. 2-4-6), the syenitic rocks cluster near the composition of average calc-alkaline syenite, while the granitic rocks lie close to the average of granodiorite with lesser quartz content. It is interesting to note that two granitic rocks (EPW-6 and EPW-10) have compositions near that of the alkali syenite, however they are granitic in appearance (ie. fine-grained and pinkish).

According to normative classification of O'Connor (1965, See Fig. 2-4-7), the syenitic rocks cluster in the granitic field and fall within

Table 2-4-3. Comparison of mean compostions of the Elphin Granite-Syenite Complex with other similar rock-types

(wt%)	1 (n=13)	2 (n=11)	3 (n=4)	4 (n=36)	5 (n=20)	6 (n=18)	7 (n=2)
SiO_2	68.44	59.85	53.70	68.97	70.47	59.41	52.12
TiO_2	0.32	0.33	0.96	0.45	0.30	0.83	1.43
Al_2O_3	15.36	18.17	16.47	15.47	15.50	17.12	16.84
TFe_2O_3	2.30	4.17	7.44	3.40	2.98	5.33	11.62
Fe_2O_3	1.31	2.01	2.52	1.12	0.63	2.19	4.16
FeO	0.95	1.70	4.23	2.05	2.12	2.83	7.47
MnO	0.02	0.05	0.06	0.06	0.03	0.08	0.18
MgO	0.76	1.15	3.94	1.15	0.65	2.02	4.45
CaO	1.21	2.04	4.25	2.99	1.91	4.06	7.51
Na_2O	5.70	4.47	5.31	3.69	4.12	3.92	4.45
K_2O	4.39	7.31	3.45	3.16	3.59	6.53	0.84
P_2O_5	0.08	0.20	0.59	0.19	0.16	0.38	0.33
LOI	1.03	1.45	3.03	0.70	0.52	0.63	0.60
Na_2O/K_2O	0.61	1.30	1.54	1.17	1.15	0.60	5.29
O.I.	70	73	54	52	37	60	53

(ppm)	8	9	10
Rb	75	86	150
Sr	588	1620	285
Ba	1365	3075	600
Nb	7	5	20
Zr	143	89	180
Y	10	12	40
Ga	20	20	18
Ni	2.8	4.4	0.5
Cr	5.3	5.2	4
V	24	47	20
K/Rb	497	723	-
Rb/Sr	0.16	0.06	-
Sr/Ba	0.43	0.53	-

1 Average of 13 granitic rocks of the Elphin Complex (this study).
2 Average of 11 syenitic rocks of the Elphin Complex (this study).
3 Average of 4 xenolithic hybrid rocks of the Elphin Complex (this study).
4 Average of 36 biotite granodiorite of Nockolds (1954).
5 Average of 20 biotite-muscovite granodiorite of Nockolds (1954).
6 Average of 18 calc-alkali syenite of Nockolds (1954).
7 Average of 2 diorite from the Dalhousie Lake Diorite-Gabbro Complex (this study).
8 Average trace-element compositions, in ppm, of granitic rocks of the Elphin Complex (this study).
9 Average trace-element compositions of syenitic rocks of the Elphin Complex (this study).
10 Average trace-element abundances of average granite (Taylor, 1964).

O.I. = Oxidation index = $2Fe_2O_3 \times 100 / (2Fe_2O_3 + FeO)$

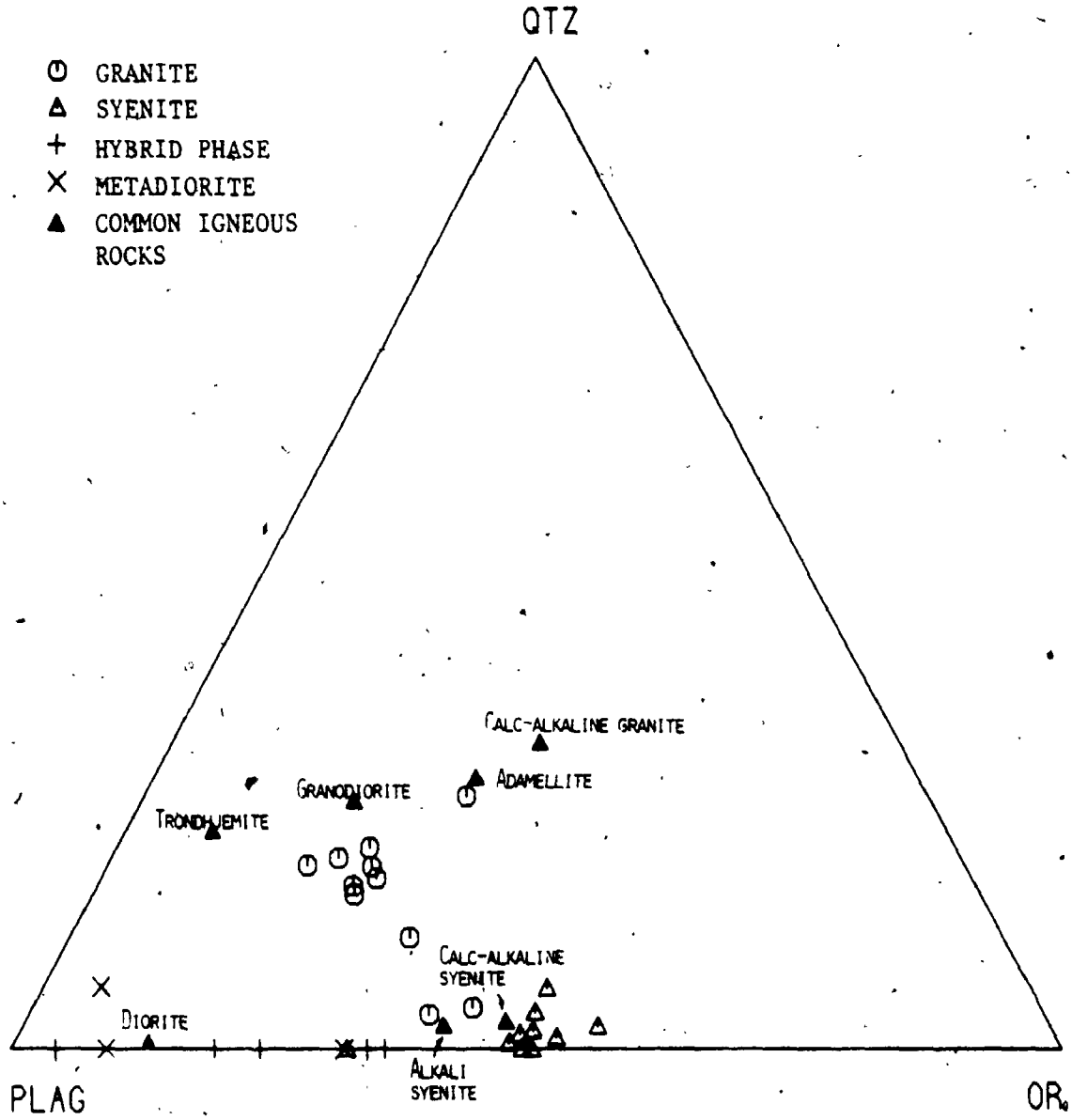

Figure 2-4-6. Normative Qtz-Or-Plag ratios of the Elphin Complex and common igneous rocks (calcualted from Nockolds, 1954).

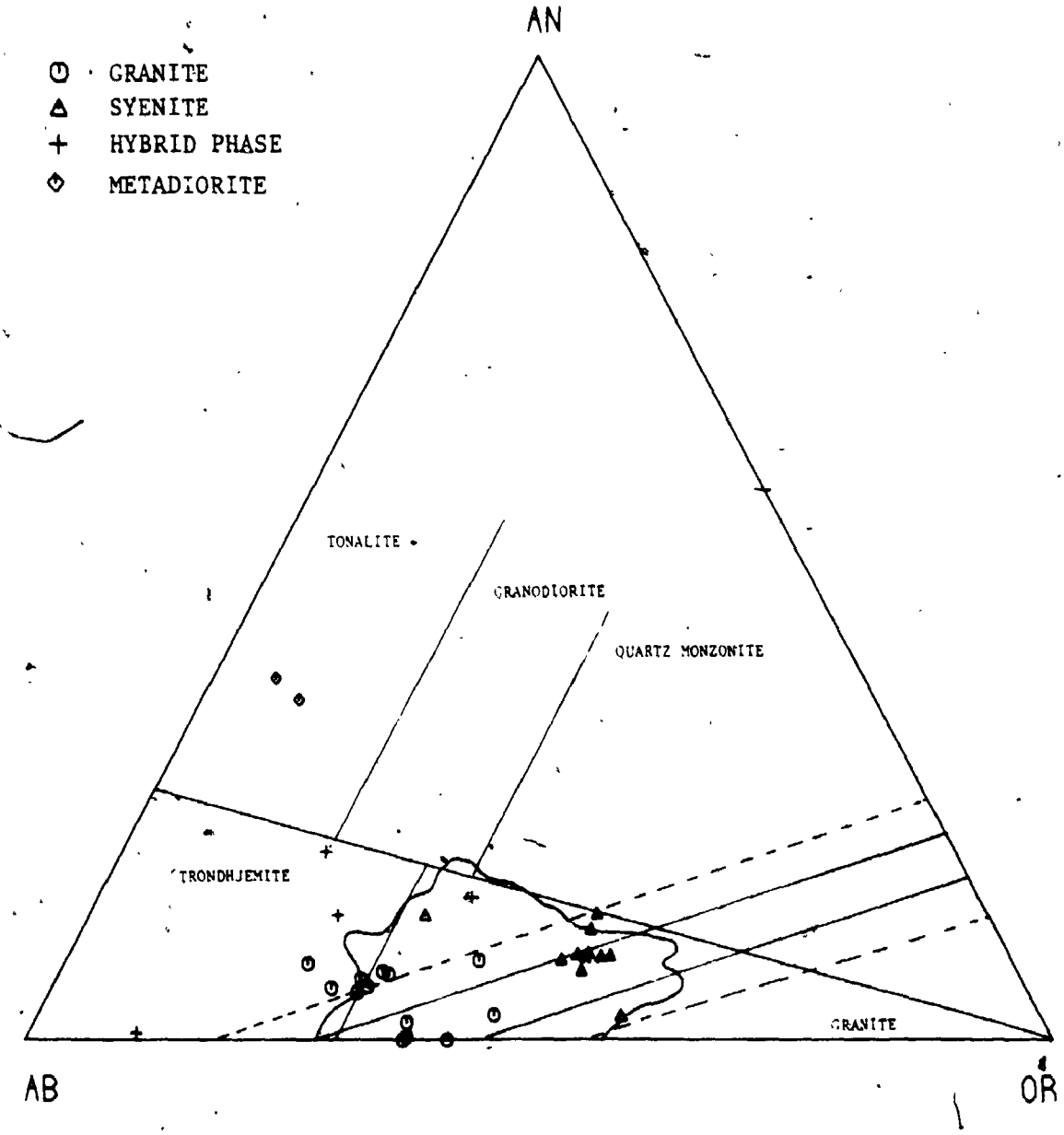

Figure 2-4-7. Normative Ab-An-Or ternary diagram of the Elphin Complex. The irregular solid boundary is the 2% contour of Tuttle and Bowen (1958) enclosing most of granitic rocks that contain 80% or more normative Ab+An+Or+Qtz. Solid-lines indicate the boundaries of low temperature trough; dashed-lines show uncertainty due to possibility of analytical error (Kleeman, 1965). Classification scheme is from O'Connor (1965).

Kleeman's (1965) low temperature trough, whereas the granitic rocks straddle the granite and trondhjemite fields and are partly located outside the low temperature trough. In addition, in the normative Qtz-Ab-Or diagram (Fig. 2-4-8), the syenitic rocks lie close to the syenitic field of the Gardar Province of Greenland (Watt, 1966); the granitic rocks again deviate from the Winkler and Von Platen's granite field (1961), but show a differentiation trend of increasing Qtz and Or contents. However, the composition of the granitic rocks lie close to the minimum melt of the Qtz-Ab-An-Or-H_2O system at about 10 Kb, with Ab/An close to infinity (Winkler, 1967).

The composition distributions in the experimental system suggest that both syenitic and granitic rocks of the Elphin Complex are of magmatic origin, however the partial deviation of the granite from the "regular" granite field (Fig. 2-4-8) may be the result of later metasomatic processes.

The intrusion relationship and internal chemical variations suggest that the granite and syenite of this complex are not comagmatic. Correlation coefficients of major-oxides as a function of SiO_2 for both rock-types are given in Table 2-4-4. In general, for both phases, TiO_2, Al_2O_3, total iron, MgO and CaO show negative

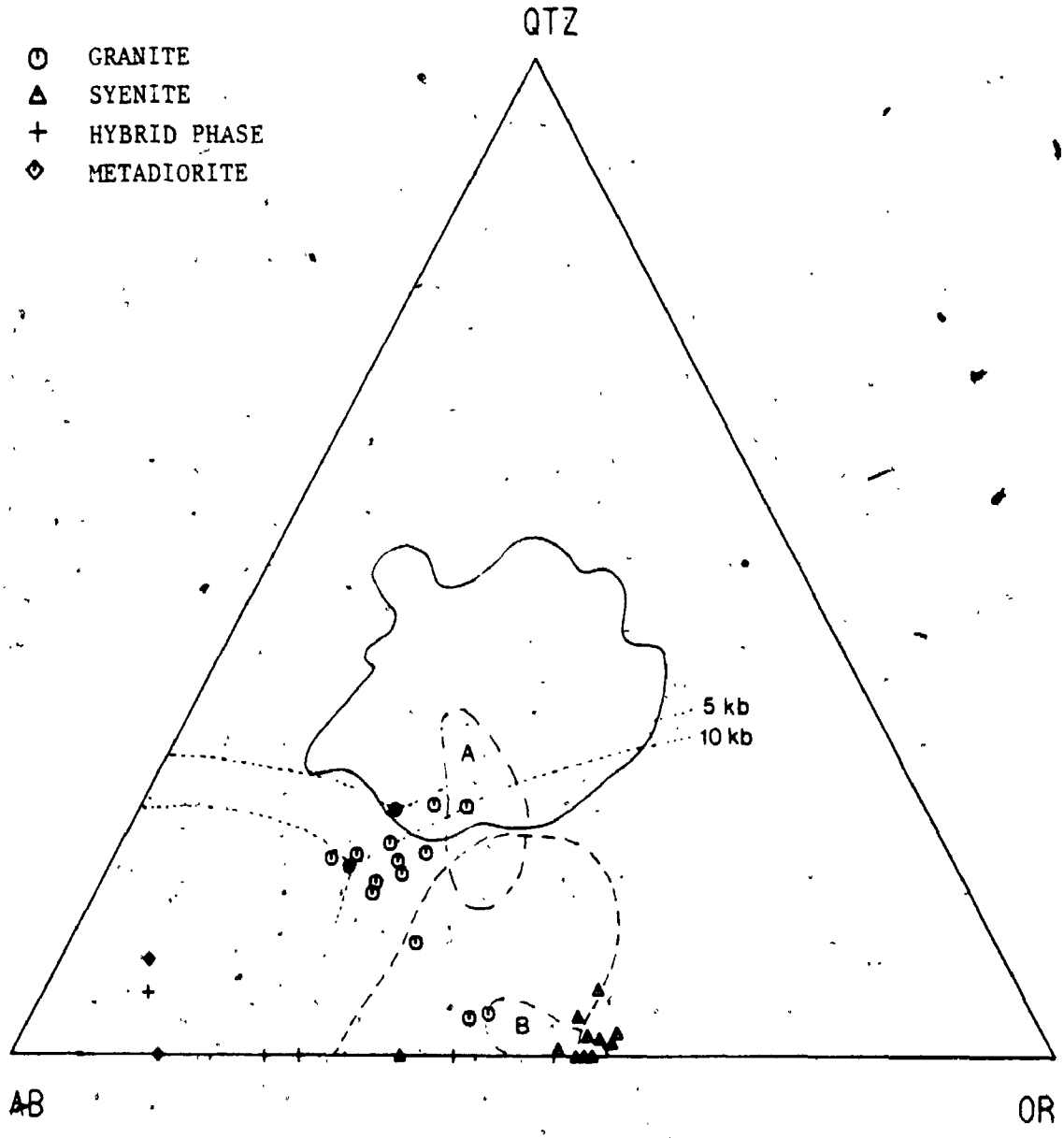

Figure 2-4-8. Normative Qtz-Ab-Or ternary diagram of the Elphin Complex. The irregular solid boundary encloses analyses of 1190 granitic rocks of Winkler and Von Platen (1961). The irregular dashed-line show the compositional field of syenitic rocks from Gardar Province of Greenland (Watt, 1966). Ternary minima at 5 kb and 10 kb in An - free system (Tuttle and Bowen, 1958) are shown by solid circles.

Field A : Coe Hill Granite

Field B : Coe Hill quartz-poor phase

Table 2-4-4. Inter-element correlation coefficients of the Elphin Granite-Syenite Complex

Correlation		Granite	Syenite	Correlation		Granite	Syenite
SiO_2 vs.	TiO_2	-0.8361	-0.6560	SiO_2 vs.	U	0.1771	0.5058
	Al_2O_3	-0.7704	-0.6471		Th	-0.3836	0.6109
	Fe_2O_3	-0.9371	-0.4068		F	-0.9687	-0.8746
	MnO	-0.5241	-0.3449		Cl	-0.6393	0.0647
	MgO	-0.5221	-0.2752		S	-0.5867	0.2235
	CaO	-0.8219	-0.5009		Ga/Al	0.4813	-0.0607
	K_2O	-0.4868	0.4124		K/Rb	-0.7271	0.0966
	P_2O_5	0.2533	-0.4786		Rb/Sr	0.3588	0.2336
	Na_2O	0.1847	-0.6299		Sr/Ba	0.2742	-0.3897
	Rb	0.5308	0.0451		Sr/Ca	0.3330	-0.0146
	Sr	-0.4153	-0.4413		Sr/(Ca+K)	-0.1561	-0.4339
	Ba	-0.8109	0.2422		Zr/Y	0.0005	0.0778
	Zr	-0.3978	-0.1315		Y/Ca	0.4906	0.1063
	Nb	-0.1937	0.0015		Cr/Mg	0.5701	0.3717
	Y	-0.5796	-0.3888		V/Mg	0.5252	0.5578
	Ga	-0.0484	-0.3136		Ni/Mg	0.5423	0.6582
	Pb	-0.0154	-0.1612		Fe/Mg	0.4338	0.3558
	Zn	-0.1616	-0.3997		Cr/Fe	0.8467	0.0770
	Cu	-0.4334	-0.1661		V/Fe	0.7181	0.3158
	[illegible]	-0.5240	-0.2781		Ni/Fe	0.6601	0.3801
	Cr	-0.5240	-0.5571				
	V	-0.6400	0.1239				

correlations with SiO_2, except that the granitic rocks retain relatively higher coefficents than those of syenite. For syenitic rocks, K_2O abundances increase with increasing SiO_2, while Na_2O shows a negative correlation with SiO_2. For the granitic rocks, K_2O decreases as SiO_2 increases. Further, such internal variations of both phases may result from fractionation of hornblende, feldspars, sphene and/or biotite during differentiation.

It was noted that there is a quasi-linear relationship among the diorite-gabbro host, the xenolithic hybrid rocks and the syenitic rocks in the preliminary Harker plots. This may be explained by assimilation of dioritic xenoliths by syenitic magma. In addition, the alkali anomaly in those granitic samples which are spatially close to the syenitic phase may also result from metasomatism of this alkali-rich melt. In terms of K_2O-Na_2O-CaO ternary variation (Fig. 2-4-9), the granitic rocks show sharply increasing K_2O and decreasing CaO and Na_2O with differentiation, whereas the syenitic rocks, similar to the Rockport-type granite of Sauerbrei (1966), show steadily decreasing CaO with constant Na_2O/K_2O ratio. The metasomatized granite samples fall between the above two groups.

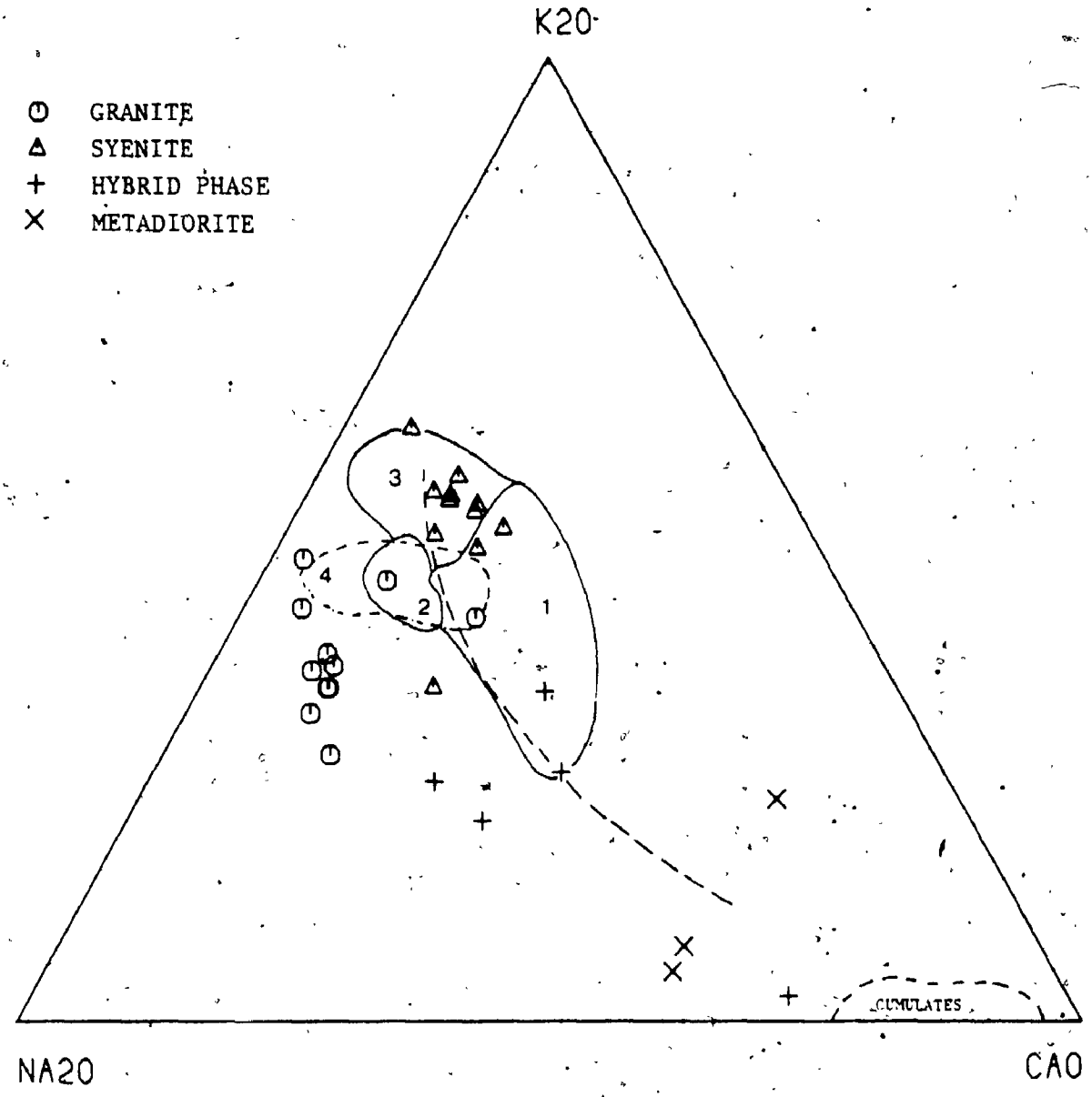

Figure 2-4-9. Na_2O-K_2O-CaO variation diagram of the Elphin Complex.

---- Calc-alkaline trend of Southern California Batholith (Nockolds and Allen, 1956).

Field 1 : Frontenac-type granite
Field 2 : Westport-type granite
Field 3 : Rockport-type granite
(Sauerbrei, 1966)

Field 4 : Coe Hill Granite (this study).

4.3.2 Trace-elements -

The mean trace-element abundances of the granite and syenite of the Elphin Complex and average granite concentrations of Taylor (1964) are summarized in Table 2-4-3. The overall composition of this complex is higher in Sr, Ba, Ni, Cr, V and lower in Rb, Nb, Zr, Y than those of average granite. In comparison with granitic rocks of this complex, the syenite has relatively abundant Rb, Sr, Ba, Y, femic elements and higher K/Rb ratio, but lesser amounts of Zr, Nb and lower Rb/Sr ratio. In terms of Rb-Ba-Sr variation (Fig. 2-4-10), syenitic rocks are scattered with a wide range of Sr, 918 to 2485 ppm, and Ba, 492 to 7173 ppm, whereas the granitic rocks are mainly located in the granodiorite field of Bouseily and Sokkary (1975). The two metasomatized granite samples are in the anomalous granite field.

Inter-element correlation coefficients for trace-elements are summarized in Table 2-4-4. As expected from variations of major-oxides, the granitic and syenitic rocks show separate trends with similar or opposite slopes. Metasomatized granite and hybrid xenoliths are close to the syenitic trends.

3

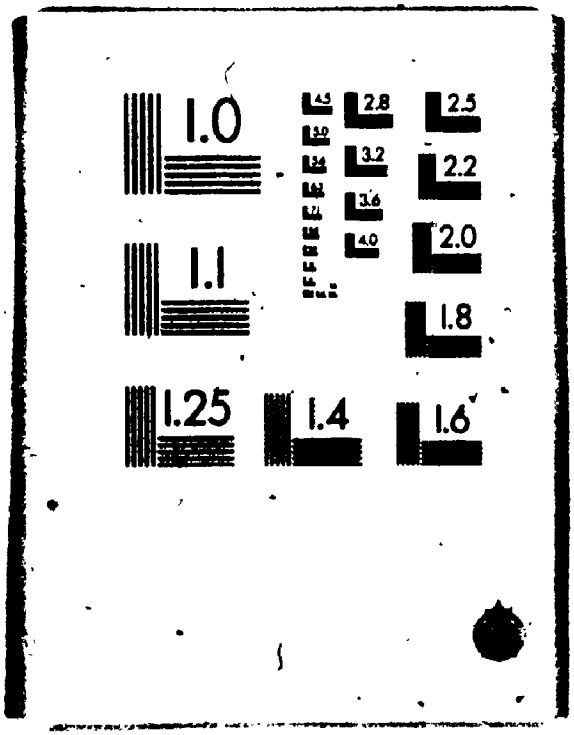

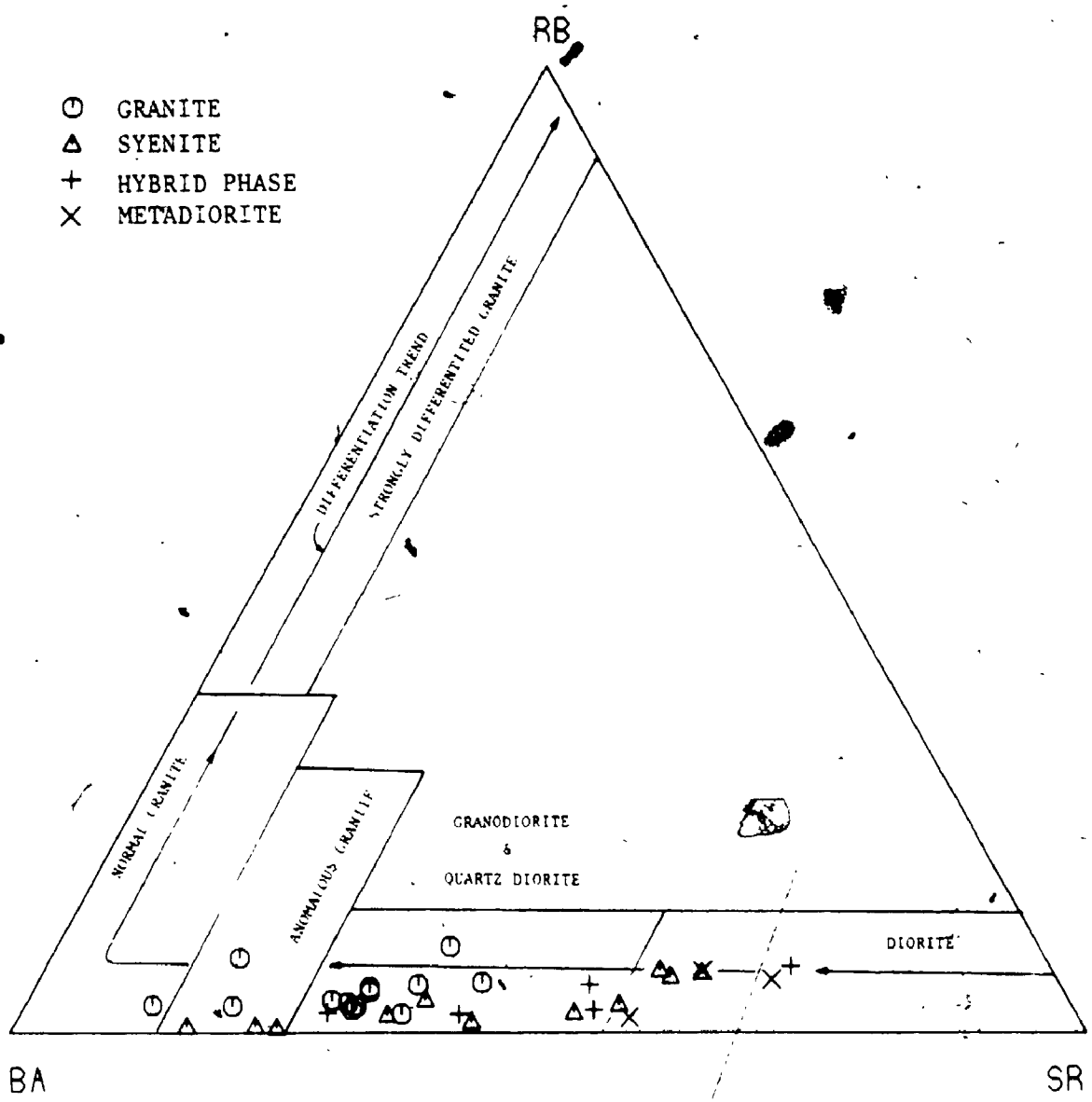

Figure 2-4-10. Rb-Ba-Sr ternary variation diagram of the Elphin Complex (after Bouseily and Sokkary, 1975).

Alkali-alkaline earth elements and their ratios are important indicators for differentiation of granitic magma. The log K/Rb vs. Rb plot (Fig. 2-4-11) illustrates again the non-comagmatic nature of the granitic and syenitic phases in this complex. The hybridized xenoliths plotted along with the evolved granite samples may indicate the possibility of alkali metasomatism at a later stage of crystallization of granite. Other alkaline element-ratios as a function of SiO_2 are plotted in Figure 2-4-12. The decrease of K/Rb and increase of Rb/Sr with increasing SiO_2 for the granitic phase (Fig. 2-4-12A,B) are consistent with removal of early Ca-rich plagioclase. Although there are poor correlation coefficients for Sr/Ba and Sr/Ca, the granitic and syenitic phases show opposite slopes (Fig. 2-4-12C, D), which may reflect fractionation of different mineral assemblages during crystallization. For instance, the negative correlation of Sr/Ba with SiO_2 in the syenitic rocks suggests a plagioclase fractionation, while the positive slope in the granitic rocks indicates a fractional crystallization of biotite. For both phases, the positive correlations of Cr/Mg, V/Mg, Ni/Mg, Fe/Mg, V/Fe, Ni/Fe with SiO_2 (Table 2-4-4) further indicate the fractionation of mafic phases, particularly biotite.

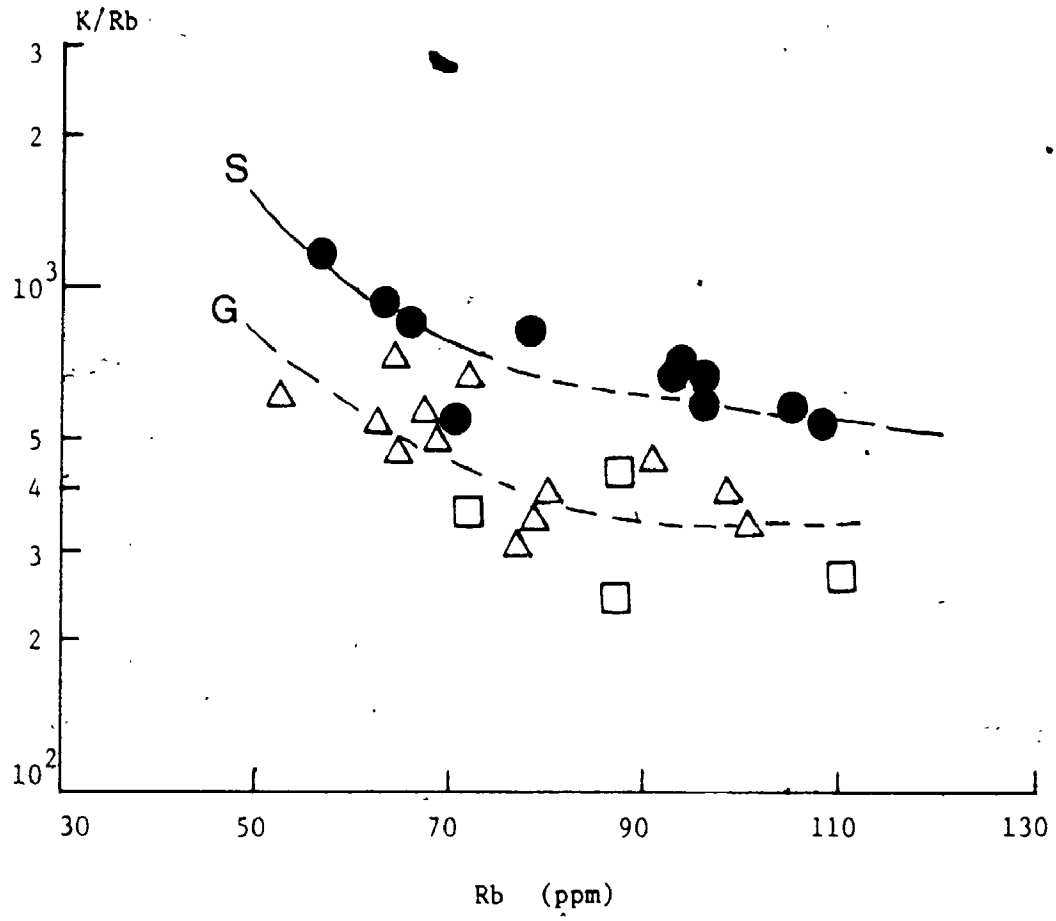

Figure 2-4-11. K/Rb ratio vs. Rb variation diagram of the Elphin Complex.

G - Differentiation trend of granitic phase.

S - Differentiation trend of syenitic phase.

△ Granite ● Syenite □ Hybrid phase

Figure 2-4-12. Plots of alkali-alkaline earth elements of the Elphin Complex.

(A) K/RB vs. SiO_2
(B) Rb/Sr vs. SiO_2
(C) Sr/Ba vs. SiO_2
(D) Sr/Ca vs. SiO_2

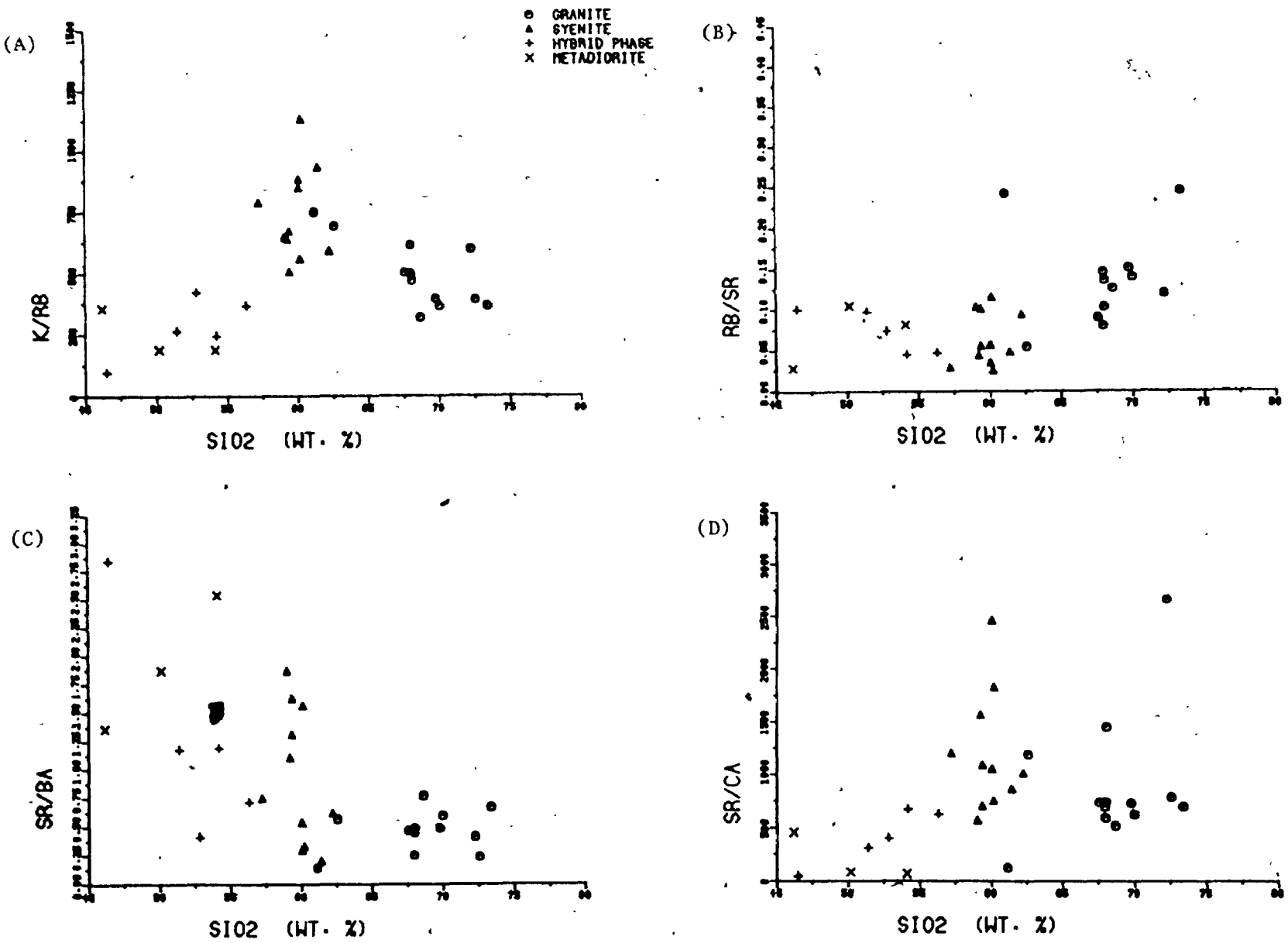
GRANITE
SYENITE
HYBRID PHASE
METADIORITE
(A)
K/RB
SIO2 (WT. %)
(B)
RB/SR
SIO2 (WT. %)
(C)
SR/BA
SIO2 (WT. %)
(D)
SR/CA
SIO2 (WT. %)

4.3.3 Rare-earth Elements -

Rare-earth element analyses for representative samples of the Elphin Granite-Syenite Complex and its country rocks are presented in Table 2-4-5. Chondrite-normalized REE curves are shown in Figure 2-4-13. Except that the syenitic rock has relatively higher absolute REE contents and small positive Eu-anomaly, both rock-types possess similar distribution patterns with negative slopes ($(Ce/Yb)_N$ = 14 to 20; Fig. 2-4-13A). The positive Eu-anomaly in the syenite may reflect either its cumulative nature at an early stage of differentiation or extensive fractionation of apatite, which retains mainly middle REE.

The REE composition and distribution curve of xenolithic hybrid rock are closely related to those of syenitic rocks. Sample EPW-14, containing clusters of biotite-hornblende and phenocrystal feldspars, has the highest REE contents and lowest $(Tb/Yb)_N$ ratio (1.45), but diorite from surrounding diorite-gabbro complex shows a flat, less fractionated pattern with no Eu-anomaly. In contrast, the country Lavant Gneiss has a well-fractionated REE pattern with large negative Eu-anomaly (Fig. 2-4-13B).

Table 2-4-5. Rare-earth elements, Ta, Hf and Cs compositions of the Elphin Granite-Syenite Complex and country rocks

	1 EPW-1	2 EPW-15-1	3 EPW-7-2	4 EPW-18-1	5 EPW-14	6 EPW-0-3	7 TYPE-6A
La (ppm)	17.77	18.22	27.95	31.62	58.83	22.24	29.06
Ce	38.12	38.24	68.36	75.46	131.15	19.29	65.07
Sm	3.48	3.25	7.45	6.26	12.76	3.95	5.67
Eu	0.62	0.87	2.71	1.97	3.34	1.25	0.94
Tb	0.22	0.30	0.54	0.49	0.77	0.57	0.78
Yb	0.40	0.10	0.14	0.14	0.34	0.68	0.39
7REE	58.69	61.53	107.88	116.70	209.40	50.38	104.32
Ta	1.34	1.88	0.95	0.91	0.35	0.88	1.70
Hf	3.41	1.97	1.32	2.28	0.66	5.03	7.51
Cs	0.61	0.54	0.67	1.45	1.24	0.13	1.29
Eu/Eu^*	0.75	1.04	1.44	1.21	1.12	1.00	0.56
$(Ce/Yb)_N$	20.50	14.33	19.50	21.50	13.55	1.83	6.17
$(Ce/Sm)_N$	2.16	2.39	1.90	2.46	2.13	1.01	2.39
$(Tb/Yb)_N$	2.50	2.00	3.00	2.75	1.45	1.00	1.42

1,2 Granitic rocks of the Elphin Complex (EPW-1, 67.97% SiO_2; EPW-15-1, 67.55% SiO_2).
3 Syenitic rocks of the Elphin Complex.
4,5 Xenolithic hybrid rocks of the Elphin Complex.
6 Diorite of the Dalhousie Lake Diorite-Gabbro Complex.
7 Lavant gneiss - country rock of the Elphin Complex.

Figure 2-4-13. Chondrite-normalized REE distribution patterns of the Elphin Complex.

(A) REE distributions for granite and syenite phases.

(B) REE distributions for hybrid phase and metadioritic xenoliths.

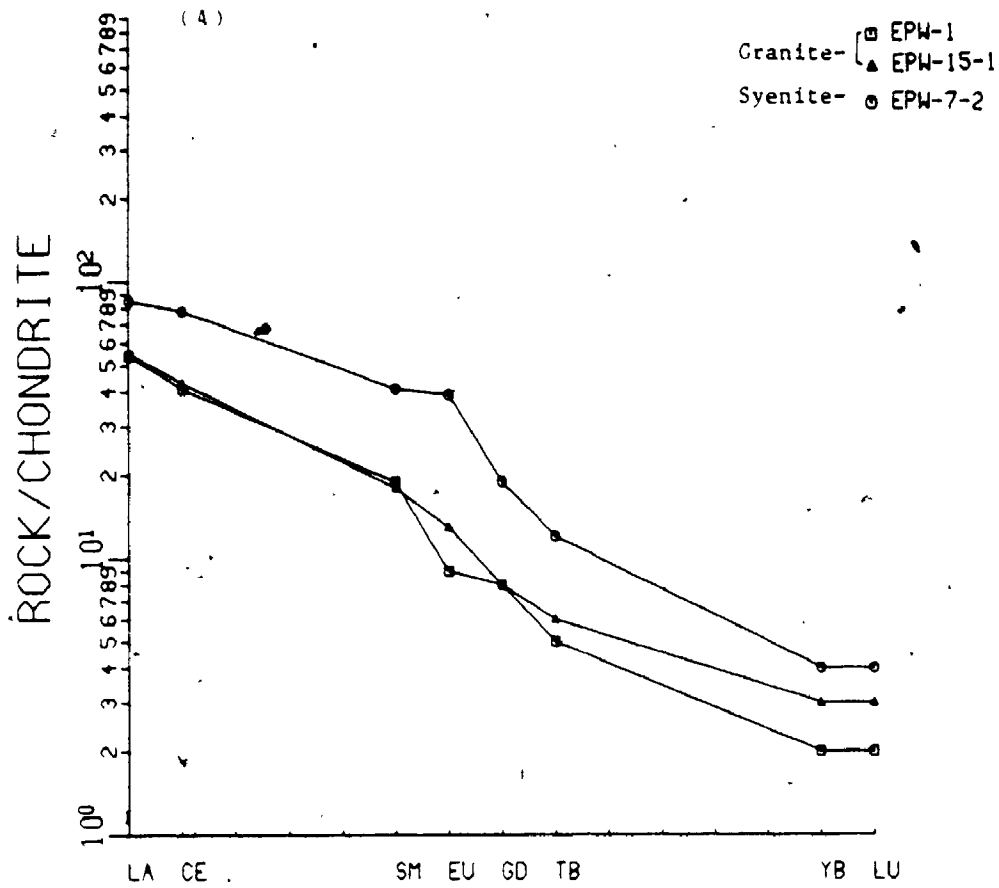
(A)
Granite- EPW-1
EPW-15-1
Syenite- EPW-7-2
ROCK/CHONDRITE
LA CE SM EU GD TB YB LU

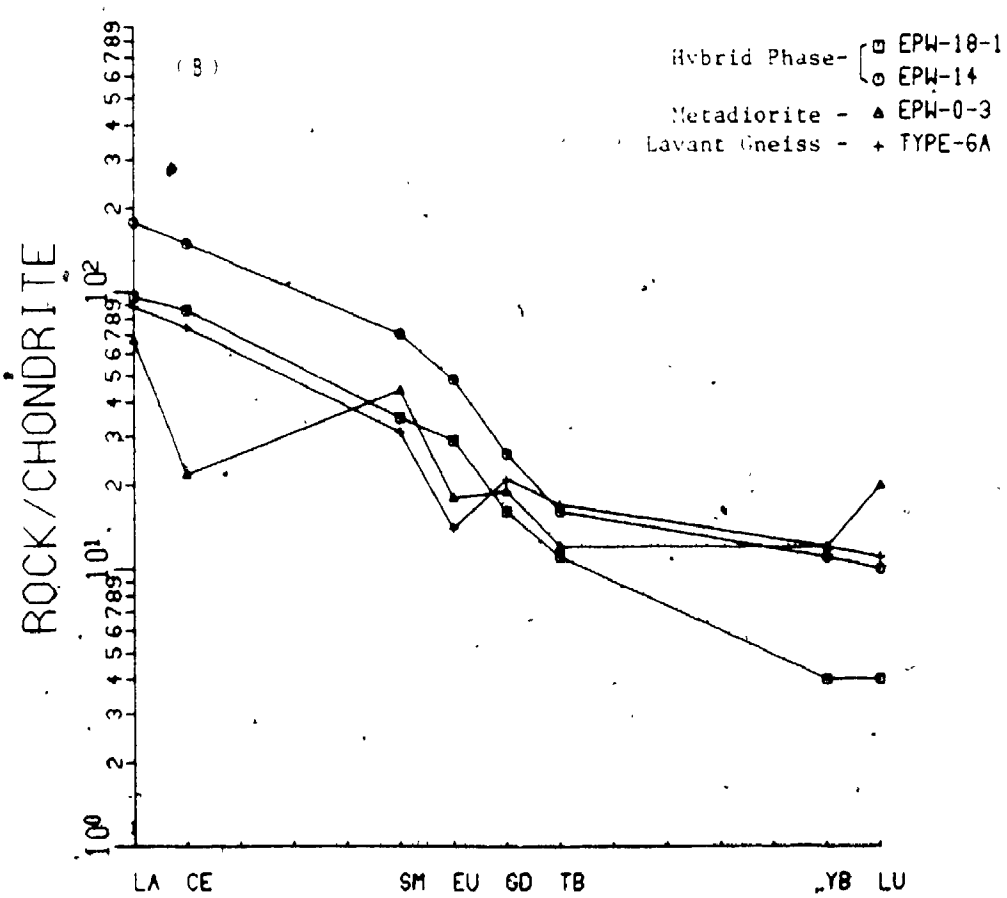
(B)
Hybrid Phase- EPW-18-1
EPW-14
Metadiorite - EPW-0-3
Lavant Gneiss - TYPE-6A
ROCK/CHONDRITE
LA CE SM EU GD TB YB LU

4.3.4 Fluorine, Chlorine And Volatiles

Analyses of F, Cl and loss of ignition for various rock-types from this complex are given in Table 2-4-6. Loss of ignition (LOI), expressed as wt%, is defined as the total of volatile components of the rock including H_2O^+, CO_2, S, F, Cl etc. In the Elphin Complex, there is a general correlation of LOI contents with rock-type; the hybrid rocks contain the highest LOI. Additionally, the subhedral tourmaline prisms occurring in the syenitic and hybrid phases may indicate an enrichment of boron in the volatile phase.

In comparison with the average granite of Taylor (1964), both granite and syenite have relatively higher Cl and comparable F concentrations (Table 2-4-6), whereas the xenolithic hybrid rocks contain anomalously high F (ave. 2447 ppm) and Cl (ave. 1188 ppm). Such an anomaly may be related to the mineralogical composition of each rock-type, particularly biotite which is the major F container in common rock-forming minerals. As shown in the modal composition, the hybrid rocks contain 12-25 vol.% biotite, while granite and syenite have only 2-8 vol.%. However, this may not be true for the Dalhousie Lake Diorite-Gabbro Complex, which contains about 20% biotite and only 880 ppm F. It is thus suggested that the enrichment of F, Cl and

Table 2-4-6. Loss of ignition (LOI), F and Cl compositions of the Elphin Granite-Syenite Complex

Sample No.	Rock-type	F (ppm)	CL (ppm)	LOI (wt%)
EPW-1	Granite	888	356	1.75
EPW-11-3	"	808	436	0.72
EPW-15-1	"	884	632	0.75
Ave.		859	475	1.07
EPW-5-1	Syenite	580	836	2.56
EPW-7-2	"	1012	508	1.11
EPW-17	"	832	536	1.18
Ave.		808	627	1.62
EPW-2	Hybrid	3660	1384	3.30
EPW-18-1	Phase	2980	1032	2.30
EPW-18-2	"	1700	1148	2.61
Ave		2447	1188	2.74
EPW-0-1	Diorite	880	1544	0.68
Ave. Granite (Taylor, 1964)		850	200	-

other volatiles in the dioritic hybrid rocks is related to the pneumatolytic alteration, such as tourmalinization, during hybridization.

4.4 Isotopic Geochemistry

Oxygen isotope analyses of whole-rocks and co-existing quartz and feldspar separates of representative samples from this complex are given in Table 2-4-7. Comparatively, the $\delta^{18}O$ values of the granitic rocks from this complex are somewhat higher than those of isotopically "normal" granites (ranging from + 6 to + 10 o/oo; Taylor, 1978). The Δ_{q-f} values of granite and syenite in the Elphin Complex, +0.96 and +1.18 respectively, suggest retention of the primary magmatic values; in other words, the high $\delta^{18}O$ of the granite was derived from anatexis of a high ^{18}O source, such as metasedimentary or altered volcanic rocks (Taylor, 1978). In addition, the hybrid rock contains the highest whole-rock $\delta^{18}O$ and the lowest Δ_{q-f} value in this complex. Such a higher $\delta^{18}O$ of the hybrid rock precludes isotopic assimilation with either granitic or syenitic melts due to their lower $\delta^{18}O$ values. It is possible that during metamorphism the "normal" dioritic - gabbroic rocks have been subjected to intensive isotope exchange with surrounding sedimentary rocks, becoming ^{18}O-rich prior to hybridization by later syenitic magma. If so, the primary magmatic Δ_{q-f} value

Table 2-4-7. Oxygen isotope analyses of whole-rock and coexisting minerals from the Elphin Granite-Syenite Complex

Rock-type	Sample No.	$\delta^{18}O$ whole-rock	$\delta^{18}O$ quartz	$\delta^{18}O$ feldspar	$\Delta q\text{-}f$
Granitic rocks	EPW-1	11.78	12.87	11.91	+0.96
	EPW-15-2	10.68	-	-	-
Syenitic rocks	EPW-7-2	9.95	11.95	10.76	+1.18
Xenolith hybrid rocks	EPW-18-2	12.70	14.07	13.30	+0.77

$\Delta q\text{-}f \cong \delta q - \delta f$ = isotopic fractionation between coexisting quartz and feldspars

of the hybrid rock can be expected from metamorphic processes during hybridization.

There is no Rb-Sr isotope data available for the Elphin Granite-Syenite Complex. The order of intrusion can only be interpreted by the field relationships and chemical variation trends. However, the overall alkalic nature and the co-existence of granite and syenite suggest this complex may be one of the syenite-monzonite suites of Lumbers (1982).

4.5 Petrogenesis And Source Rocks

Geochemistry of alkali and alkaline-earth elements preclude the possibility of comagmatic origin for the granitic and syenitic rocks in the Elphin Complex. For example, the syenitic rocks containing higher Rb, Ba and Sr than those of granite, eliminates any plausible model of magmatic differentiation from either rock-type. In addition, the separate trends in the K/Rb vs. Rb plot (Fig. 2-4-11) is consistent with the field observations that pegmatitic syenite is a later phase.

4.5.1 Granitic Magma -

The internal geochemical variations of the granitic phase can be interpreted by crystal fractionation of feldspars, biotite and minor phases

(eg. sphene). The least squares method (Stormer and Nicholls, 1978) was used to test the crystallization model by means of major-oxide variations; sample EPW-15-2 with 68.0% SiO2 was chosen as the least differentiated melt. As predicted, to form the most evolved sample EPW-16 (73.38% SiO_2) requires removal of a modal solid of 64% plagioclase, 32% biotite and 3% sphene. The proportion of solids to differentiated melt is about 30:70 and the sum of squares for the residuals are equal to 0.172, indicating a very good fit of the model to the data observed.

Although the Elphin Complex is spatially related to Dalhousie Lake Diorite-Gabbro Complex, the high $\delta^{18}O$ value of the granite and occurrence of no intermediate rock-types among them argue against the possibility that granitic magma was evolved from the dioritic melt. The granodioritic composition and relatively lower REE abundances (7REE = 60) of the ganitic phase suggest a primitive basic meta-igneous source rather than a metasedimentary origin. However, in order to explain the high $\delta^{18}O$ of the magma, such an igneous source is considered to have been subjected to intensive isotope exchange with metasediments prior to partial melting in the crust. Quantitatively, a meta-igneous source with similar REE concentrations

to the host diorite was used to test the the partial melting hypotheses. It requires about 10% residual garnet to bring down the relatively flat distribution curve of meta-diorite to the moderately fractionated REE pattern of the granite. Except that the model composition has slightly lower middle REE abundances, chondrite-normalized REE patterns of 20% to 50% equilibrium partial melting of meta-diorite are similar to average granitic rocks of this complex (Fig. 2-4-14A).

4.5.2 Syenitic Rocks -

Despite the narrow range of composition (57 to 62% SiO_2), the syenitic rocks of this complex show systematic variation trends for both major- and trace-elements. Such internal chemical variations may be explained by fractional crystallization of plagioclase, hornblende, biotite, apatite, sphene and magnetite. Mass balance calculations (Stormer and Nicholls,1978) indicate that from the least differentiated sample EPW-4-1 (57% SiO_2) to the most evolved sample EPW-8 (62% SiO_2) requires removal of a modal solid of 70% plagioclase, 25% biotite, 1% sphene and 3% apatite.

Dostal (1975) suggested the monzonitic rocks, in general, of the southern Grenville Province of

Figure 2-4-14. REE modelling of the Elphin Complex.

(A) Equilibrium partial melting of metadiorite (similar to the composition of Dalhousie Lake Diorite Complex) for generation of granitic phase of this complex.

(B) Equilibrium partial melting of basic granulite rocks (similar to Weaver, 1980) for generation of syenitic melt of this complex.

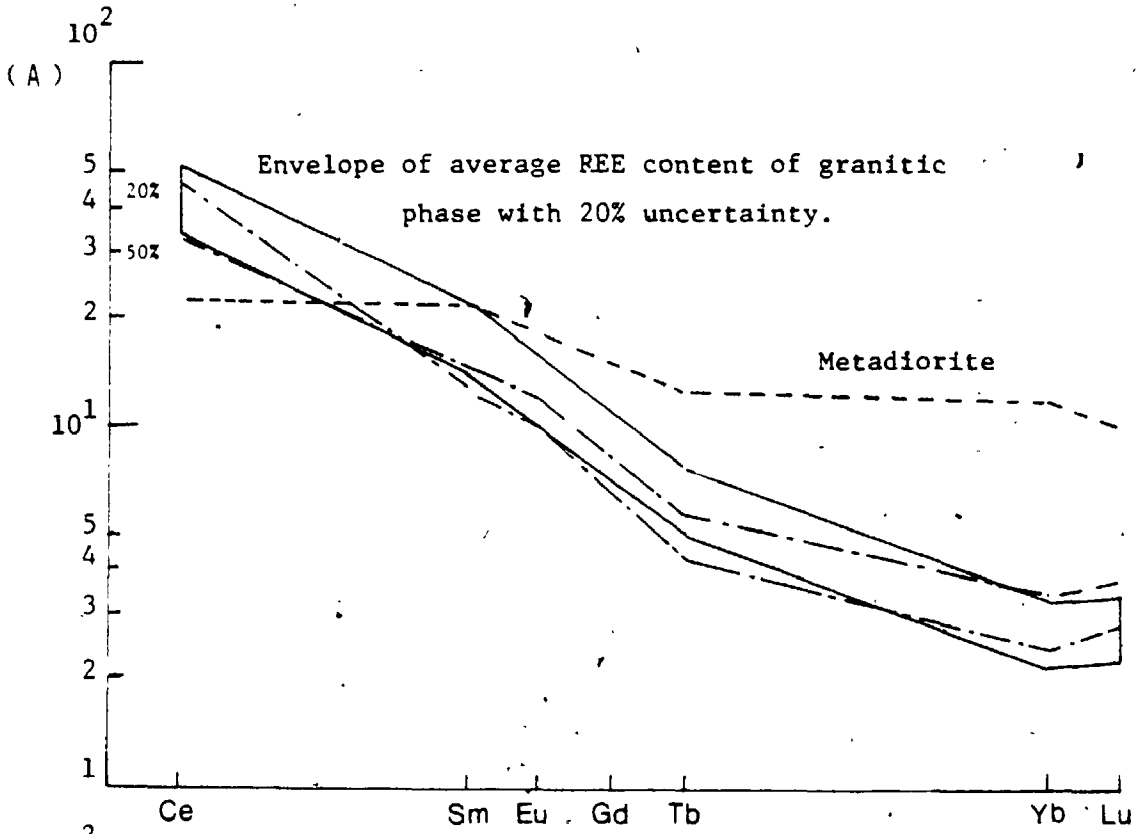
(A)
Envelope of average REE content of granitic phase with 20% uncertainty.
20%
50%
Metadiorite
Ce
Sm
Eu
Gd
Tb
Yb
Lu

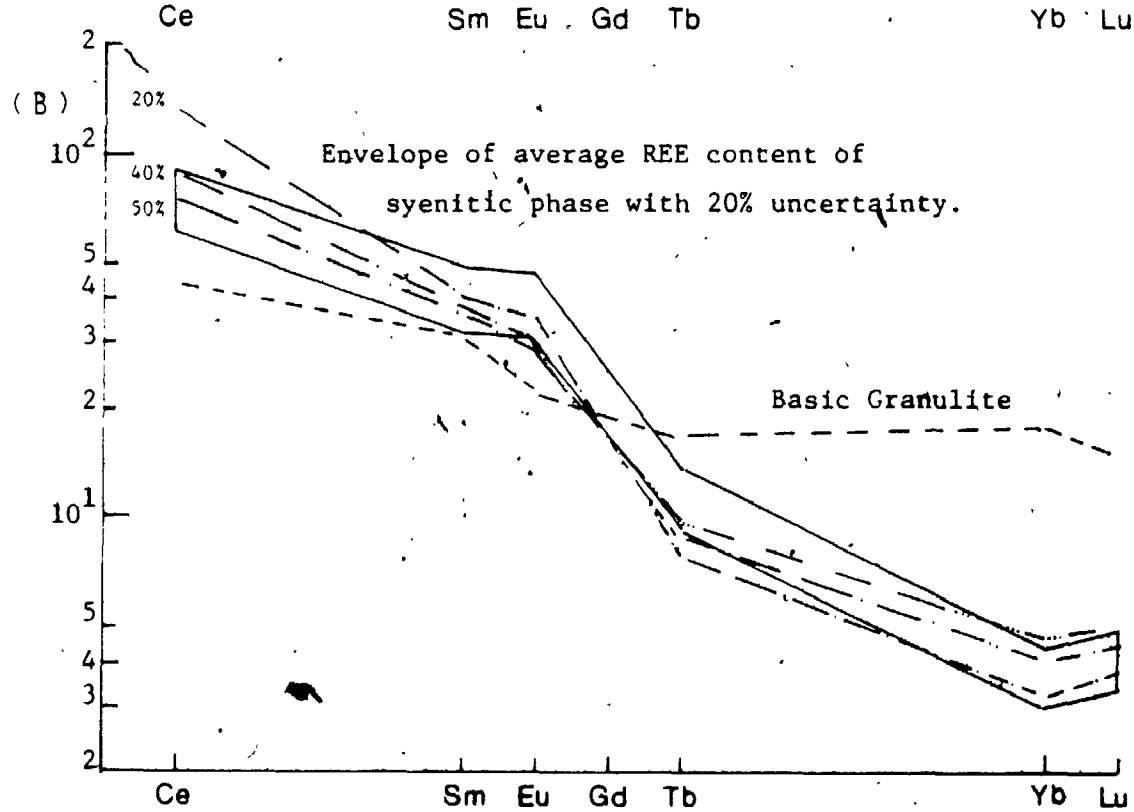
(B)
Envelope of average REE content of syenitic phase with 20% uncertainty.
20%
40%
50%
Basic Granulite
Ce
Sm
Eu
Gd
Tb
Yb
Lu

Ontario, may be derived by a high degree of partial melting of a granulite residuum with no residual feldspar, or by extensive fractionation of a primitive peridotitic magma. Based on REE fractionations, Archean peridotite ($(Ce/Yb)_N$ = 0.35, $(Ce/Sm)_N$ = 0.46, $(Tb/Yb)_N$ = 1.05; data from the Basaltic Volcanism Study Project, 1981, p.23, Fig. 1.2.1.17, ACH-1) was used for crystal fractionation model. Although extensive fractionation of clinopyroxene would raise the LREE contents from 2 to 80 times chondrite values in the melt ($(Ce/Yb)_N$ = 1.57 after 99% fractionation), it could not match the highly fractionated patterns of syenitic rocks ($(Ce/Yb)_N$ = 22.9) of this complex.

On the other hand, silicic and basic granulite (Weaver, 1980) were used for modelling of partial fusion. Basic granulite is preferred due to its overall lower concentration of REE and relatively less fractionated pattern compared to that of silicic one. Normalized-REE curves of equilibrium modal melting of 20% to 50% of basic granulite with 15% residual garnet, are shown in Figure 2-4-14B. Except that the model compositions have relatively smaller positive Eu-anomalies, they are similar to the composition of syenite. Additionally, the melting model suggests that the syenitic magma was produced in the lower crust (< 35 km) and then moved

into the crust. It is speculated by the author that the syenite phase of the Elphin Complex is possible only a large offshoot of the syenitic body which still remains below.

4.5.3 Xenolithic Hybrid Rocks -

The semi-linear relations between diorite-gabbro host, hybrid rocks and syenitic phase in various chemical variation diagrams suggest that these hybrid rocks were xenolithic diorite assimilated by later syenitic melt. It is consistent with the field occurrence in which hybrid rocks are often found within the syenite phase and/or around the contact between syenite and granite, whereas less altered dioritic xenoliths with primary igneous texture are distributed within the granite phase.

4.6 Summary

The Elphin Granite-Syenite Complex is a composite intrusive body with a granodiorite phase to the south and west, and a syenite phase to the northeast. The overall composition is metaluminous with alkalic affinity. Whole-rock geochemistry, especially the alkali-alkaline earth elements, suggests that the granitic and syenitic rocks are not consanguineous.

However, both rock-types show similar chemical variation trends, except that the syenitic rocks have relatively poor correlations with SiO_2. Internal chemical variations can be interpreted as fractional crystallization of biotite, plagioclase, sphene and apatite, for both phases.

The "normal" magmatic values of Δ_{q-f} indicate that granitic melt originated from a high-^{18}O source. Based on REE modelling, equilibrium partial melting of a basic meta-igneous source containing a similar REE composition to that of the Dalhousie Diorite-Gabbro Complex is suitable to produce the granodioritic magma in the crust.

The syenitic phase of this complex has normal $\delta^{18}O$ but an anomalously high K/Rb ratio; it is suggested that 20% to 50% partial melting of a basic granulite source is suitable to produce the syenitic melt in the lower crust. However, at the present erosional level, the syenitic phase of this complex may be interpreted as one of the offshoots of a major intrusive body beneath.

The hybrid phase is considered to be xenolithic dioritic rock assimilated by later syenitic melt and subject to pneumatolytic alterations. Otherwise, there is no direct genetic relationship between the diorite-gabbro complex and later granite-syenite intrusions. The emplacement and evolution history of

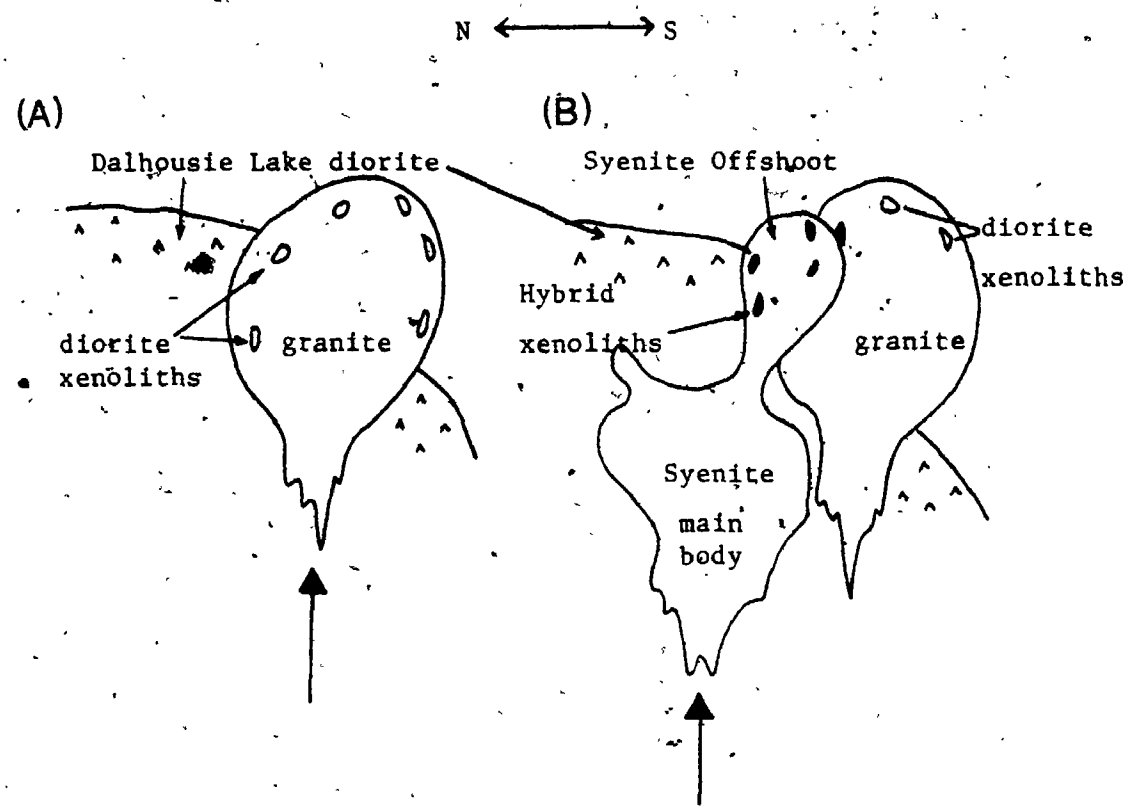

Figure 2-4-15. Schematic emplacement and crystallization history of the Elphin Complex.

(A) The granitic magma was derived by partial melting of a basic meta-igneous source with high ^{18}O content. It subsequently intruded into the Dalhousie Lake Diorite Complex leaving dioritic xenoliths around the margin. The granite was then fractionated and solidified independently.

(B) At lower crust, partial melting of basic granulite with high K/Rb ratio generated syenitic melt; it moved upward into upper crust. Late volatile-rich offshoot of this syenitic magma intruded the early granitic phase. Dioritic xenoliths were assimilated and/or metasomatised by the syenitic melt.

the Elphin Granite-Syenite Complex is summarized in Figure 2-4-15.

5.0 CHEDDAR GRANITE

5.1 General Characters And Intrusive Relations

The Cheddar Granite is a subrounded intrusive body, about 8 km E-W by 12 km N-S. It straddles the Cardiff - Monmouth Township boundary and the northeast corner of Anstruther Township (Fig. 2-5-1). Bancroft, the "mineral capital" of Canada, is located about 20 km NE of this pluton. The area has been relatively well-studied because of its potential uranium mineralization in granitic pegmatite and secondary enrichment in the surrounding metasedimentary rocks (e.g. ODM Map No. 1957-1; OGS Preliminary Map P.2205).

The granite is less gneissic and more uniform in texture than the nearby Glamorgan and Anstruther migmatitic gneiss complexes. Gneissic to massive pink biotite-hornblende granite is common; while granitic hybrid gneisses and biotite-hornblende-rich xenoliths (or schlieren) occur sporadically within the intrusion. Greenish grey coloured monzonitic rocks with pyroxene occur locally. Much of the border zone, especially along the southeast margin, is characterized by pegmatitic phases. Reddish pegmatite dykes, quartz-

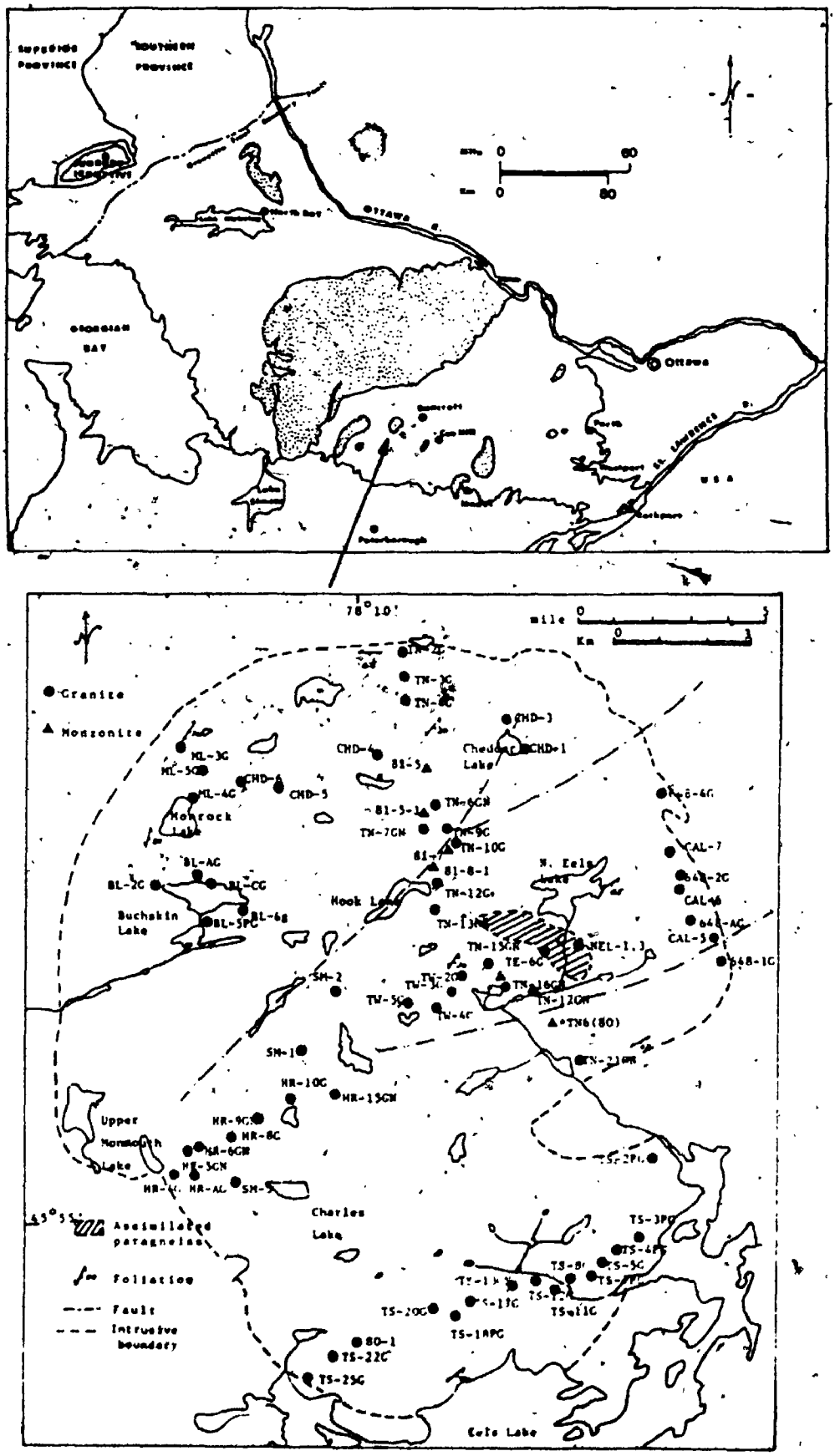

Figure 2-5-1. Sample location map of the Cheddar Granite.

feldspar-rich "pockets" and veinlets cut across both the granite and xenoliths. Aplitic and granitic dykes also occur locally.

The Cheddar Granite is concordant with the surrounding layered marble, siliceous carbonate, arenitic paragneiss, amphibolite and biotite-garnet-schist. The attitude of foliations indicates a domal structure. Contact metamorphism has either been erased by high grade regional metamorphism (up to upper amphibolite facies) or is limited only to immediately adjacent siliceous carbonate layers with skarn-type diopside-rich veins. Hypidiomorphic-granular texture, uniformity of composition and cross-cutting dykes are indicative features of magmatic origin, although migmatite and hybrid phases do occur locally.

The contact between pyroxene-bearing greenish monzonite and pinkish granite-gneiss was not found in the field. However, the biotite-hornblende-rich xenoliths and schlieren occur also in the green monzonitic rocks; a consanguineous relationship may exist between the pyroxene-bearing phase and more siliceous member of the pluton.

5.2 Petrography

On the basis of field observations and modal classification of IUGS (Streckeisen, 1976; See Fig. 2-5-2), four major lithological units can be identified in the Cheddar Granite : (1) granite-gneiss, (2) green monzonite, (3) xenoliths or schlieren and (4) granitic-pegmatitic dykes.

5.2.1 Granite-Gneiss -

Pinkish medium-grained, leucocratic granite-gneiss is the dominant phase of the pluton. With a few exceptions, all fall in the granite (adamellite) field of Streckeisen (1976) and have feldspar ratios (plagioclase/total feldspar) ranging from 0.25 to slightly over 0.60.

Texture ranges from either massive with scattered mafic mineral clusters or gneissic with prominent foliation of biotite and/or hornblende. In places, granitic gneiss has differentiated into leucocratic and melanocratic bands with both concordant and discordant veinlets. Locally, granophyric and migmatitic varieties are also encountered.

The granitic rocks are hypidiomorphic - granular with quartz content > 25% in general.

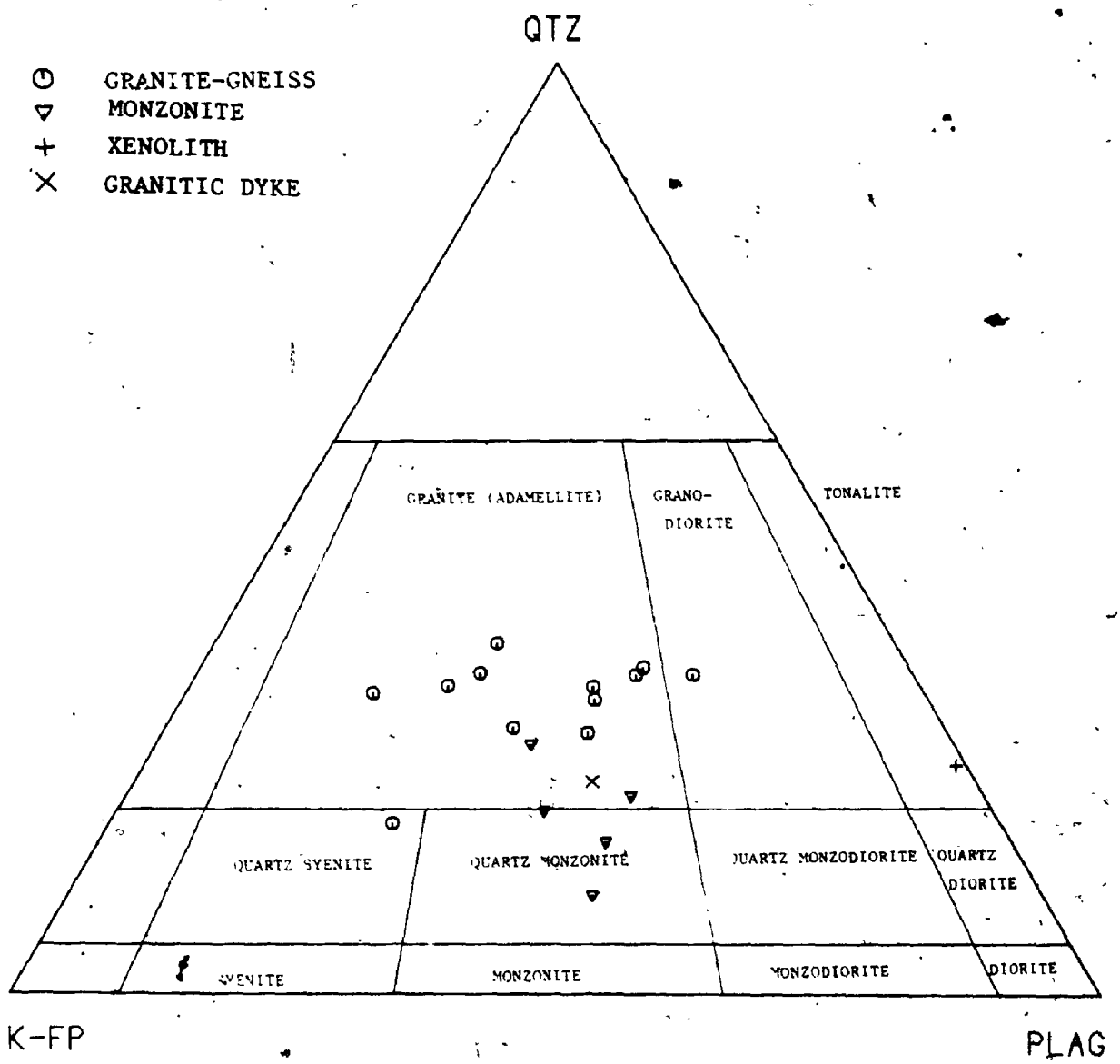

Figure 2-5-2. Modal classification of the Cheddar Granite (from Streckeisen, 1976).

Microcline and plagioclase are of approximately equal abundance, but in some specimens, microcline is twice as abundant. Microcline and microperthite are commonly surrounded and embayed by quartz and plagioclase. Partly sericitized plagioclase is well-twinned but not zoned. Vermicular intergrowth is observed locally. The composition of plagioclase is less than An_{10}. Based on these data, the Cheddar Granite can be classified as the "alkalic granite" of Lumbers (1982). Representative feldspar analyses and calculated formulae are given in Table 2-5-1.

Biotite is the chief mafic mineral with subordinate hornblende. In some specimens biotite is the only dark mineral and is subhedral to anhedral with pleochroic scheme from X = light greenish yellow to pale yellowish brown, Y = Z = brownish green to dark brown. Poikilitic texture and graphic intergrowth with quartz are also common for biotite. Hornblende (if any) is intergrown with or replaced by biotite. Both minerals are chloritized locally. The compositions and structural formulae of biotite and hornblende are given in Table 2-5-2 and 2-5-3. The annite fraction of biotite varies widely from 0.352 to 0.582; compositions of these biotite can be classified as Fe^{2+} - biotite to siderophyllite (Foster, 1960; See Fig. 2-5-3). In addition, the hornblende of the

Table 2-5-1. Chemical compositions and calculated formulae of feldspars from the Cheddar Granite

Sample No.	TS-22G	80-1	648-2G	B1-BG	BL-CG	81-5	81-6-1	NEL-2
Rock-type	1	1	1	1	1	2	2	3a
(a) Plagioclase								
(wt%)								
SiO_2	68.54	68.20	68.20	67.97	67.99	67.84	67.98	65.04
Al_2O_3	19.35	19.83	19.32	19.56	19.85	19.21	19.33	21.57
CaO	0.11	0.48	0.05	0.40	0.45	0.35	0.45	2.99
Na_2O	11.96	11.71	11.86	12.19	11.86	12.32	11.92	10.43
K_2O	0.07	0.11	0.11	0.09	0.11	0.15	0.12	0.19
Total	100.03	100.33	99.96	100.21	100.26	99.87	99.80	100.22
Si (Z)	11.982	11.900	11.998	11.897	11.881	11.924	11.936	11.457
Al (Z)	3.986	4.077	3.980	4.034	4.087	3.979	3.999	4.477
	15.968	15.977	15.978	15.931	15.968	15.903	15.935	15.935
Na (X)	4.054	3.961	4.020	4.137	4.018	4.198	4.058	3.562
Ca (X)	0.021	0.090	0.009	0.075	0.084	0.066	0.085	0.564
K (X)	0.016	0.024	0.025	0.020	0.025	0.034	0.027	0.043
	4.090	4.076	4.054	4.232	4.127	4.298	4.169	4.169
O	32	32	32	32	32	32	32	32
(mol%)								
Ab	99.11	97.20	99.16	97.75	97.36	97.68	97.33	85.44
An	0.50	2.20	0.23	1.77	2.04	1.53	2.03	13.54
Or	0.38	0.60	0.61	0.47	0.59	0.78	0.64	1.02
(b) K-feldspar								
(wt%)								
SiO_2	64.96	65.10	65.01	65.23	65.08	65.20	65.59	65.45
Al_2O_3	18.01	18.20	18.05	18.12	18.06	17.71	17.97	18.03
CaO	0.00	0.02	0.01	0.00	0.00	0.00	0.00	0.00
Na_2O	0.50	0.77	0.55	0.37	0.29	0.37	0.98	0.53
K_2O	16.16	15.81	16.10	16.03	16.14	16.35	15.21	15.74
Total	99.63	99.90	99.72	99.75	99.57	99.63	99.75	99.75
Si (Z)	12.046	12.035	12.042	12.060	12.061	12.095	12.090	12.083
Al (Z)	3.935	3.961	3.940	3.948	3.944	3.871	3.903	3.922
	15.982	15.977	15.982	16.007	16.004	15.996	15.993	16.005
Na (X)	0.180	0.276	0.198	0.133	0.104	0.133	0.350	0.190
Ca (X)	0.000	0.004	0.002	0.000	0.000	0.000	0.000	0.000
K (X)	3.822	3.725	3.804	3.780	3.815	3.868	3.576	3.706
	4.002	4.076	4.003	3.913	3.919	4.001	3.926	3.896
O	32	32	32	32	32	32	32	32
(mol%)								
Ab	4.49	6.89	4.93	3.39	2.66	3.33	8.92	4.87
An	0.00	0.10	0.05	0.00	0.00	0.00	0.00	0.00
Or	95.51	93.02	95.02	96.61	97.34	96.67	91.08	95.13

Rock-type :- 1 Granite-gneiss.
2 Green monzonite.
3a Assimilated rocks.

Table 2-5-2. Chemical compositions and calculated formulae of biotite from the Cheddar Granite

Sample No.	80-1	TS-22G	BL-CG	BL-BG	648-2G	TN4G1A	81-5	TS-19MS	37-6
Rock-type	1	1	1	1	1	1	2	3	3
(wt%)									
SiO_2	36.04	34.15	36.49	36.97	33.91	34.98	37.84	36.31	39.29
TiO_2	2.21	2.27	1.44	1.35	1.46	3.48	1.89	2.60	1.04
Al_2O_3	11.37	13.29	13.87	13.61	10.92	11.24	12.60	13.64	12.48
Fe_2O_3	7.21	9.92	6.23	6.31	9.81	9.41	6.93	3.47	2.79
FeO	21.09	22.37	15.95	16.15	25.13	24.10	17.75	16.66	13.37
MnO	0.60	0.26	1.09	1.25	0.76	0.72	1.02	0.25	0.26
MgO	6.36	2.90	8.68	8.55	3.55	1.60	8.32	12.[illegible]2	15.19
CaO	0.04	0.00	0.00	0.00	0.05	0.12	0.01	0.00	0.04
Na_2O	0.05	0.03	0.07	0.06	0.12	0.02	0.02	0.00	0.17
K_2O	9.16	9.30	9.48	9.52	7.75	8.54	9.41	9.57	10.34
Total	94.13	94.49	93.30	93.77	94.46	94.21	95.77	94.52	94.97
Si (Z)	5.781	5.542	5.736	5.787	5.636	5.731	5.833	5.599	5.914
Al^{iv} (Z)	2.148	2.458	2.264	2.213	2.137	2.169	2.167	2.401	2.086
	7.929	8.000	8.000	8.000	7.773	7.900	8.000	8.000	8.000
Al^{vi} (Y)	0.000	0.082	0.303	0.[illegible]96	0.000	0.000	0.121	0.076	0.127
Ti (Y)	0.266	0.277	0.170	0.159	0.182	0.428	0.219	0.290	0.118
Fe^{3+} (Y)	0.870	1.210	0.736	0.743	1.226	1.159	0.803	0.402	0.316
Fe^{2+} (Y)	2.827	3.034	2.095	2.113	3.490	3.299	2.287	2.147	1.682
Mg (Y)	1.519	0.701	2.032	1.993	0.874	0.390	1.910	2.783	3.405
Mn (Y)	0.081	0.036	0.145	0.166	0.107	0.100	0.133	0.033	0.033
	5.564	5.339	5.482	5.469	5.879	5.377	5.473	5.721	5.680
Ca (X)	0.007	0.000	0.000	0.000	0.009	0.005	0.002	0.000	0.006
Na (X)	0.016	0.009	0.021	0.018	0.039	0.006	0.006	0.000	0.050
K (X)	1.873	1.924	1.900	1.900	1.642	1.783	1.849	1.881	1.984
	1.895	1.933	1.921	1.918	1.689	1.795	1.857	1.881	2.040
O	22	22	22	22	22	22	22	22	22
Mg/Fe_t+Mg	0.287	0.141	0.406	0.397	0.153	0.079	0.372	0.519	0.626
Fe_t/Fe_t+Mg	0.709	0.858	0.582	0.589	0.844	0.919	0.618	0.478	0.370
mole of annite	0.471	0.506	0.349	0.352	0.582	0.550	0.381	0.358	0.280

(Rock-type:- 1 - Granite-gneiss, 2 - Monzonite, 3 - Xenoliths)

Table 2-5-3. Chemical composition and calculated formulae of amphibole from the Cheddar Granite

Sample No.	80-1	BL-CG	BL-BG	648-2G	81-6-1	37-6	81-5-3
Rock-type	1	1	1	1	2	3	3
SiO_2	42.33	42.40	42.56	42.16	40.30	41.33	45.13
TiO_2	0.89	0.44	0.35	1.18	1.15	0.77	0.71
Al_2O_3	6.88	8.16	7.84	6.29	7.85	10.66	6.86
*FeO	27.94	23.91	25.08	30.71	31.15	20.50	19.48
MnO	0.96	1.77	1.57	1.56	1.14	0.39	0.57
MgO	4.69	6.46	5.81	2.14	2.96	8.96	10.54
CaO	10.04	10.12	10.12	8.76	9.73	11.51	10.66
Na_2O	2.14	1.81	1.61	2.81	2.44	2.59	2.82
K_2O	1.39	1.46	1.48	1.50	1.65	1.74	1.48
Total	97.26	96.53	96.42	97.11	98.37	98.45	98.29
Si (Z)	6.804	6.746	6.806	6.902	6.548	6.355	6.862
Al^{iv} (Z)	1.196	1.254	1.194	1.098	1.452	1.645	1.138
	8.000	8.000	8.000	8.000	8.000	8.000	8.000
Al^{vi} (Y)	0.107	0.276	0.284	0.116	0.051	0.287	0.091
Ti (Y)	0.108	0.053	0.042	0.145	0.141	0.089	0.081
Mg (Y)	1.124	1.532	1.385	0.522	0.717	2.054	2.389
Mn (Y)	0.131	0.239	0.213	0.216	0.157	0.051	0.073
Fe (Y)	3.756	3.181	3.354	4.205	4.233	2.636	2.477
	5.226	5.281	5.278	5.204	5.299	5.117	5.111
Ca (X)	1.729	1.725	1.734	1.537	1.694	1.896	1.737
Na (X)	0.667	0.558	0.499	0.892	0.769	0.772	0.831
K (X)	0.285	0.296	0.302	0.313	0.342	0.341	0.287
	2.681	2.579	2.535	2.742	2.805	3.009	2.855
O	23	23	23	23	23	23	23
(Ca+Na)	2.396	2.283	2.233	2.429	2.463	2.668	2.568

* FeO - Total iron as FeO

Rock-type: 1 - Granite-gneiss
2 - Monzonite.
3 - Xenolith .

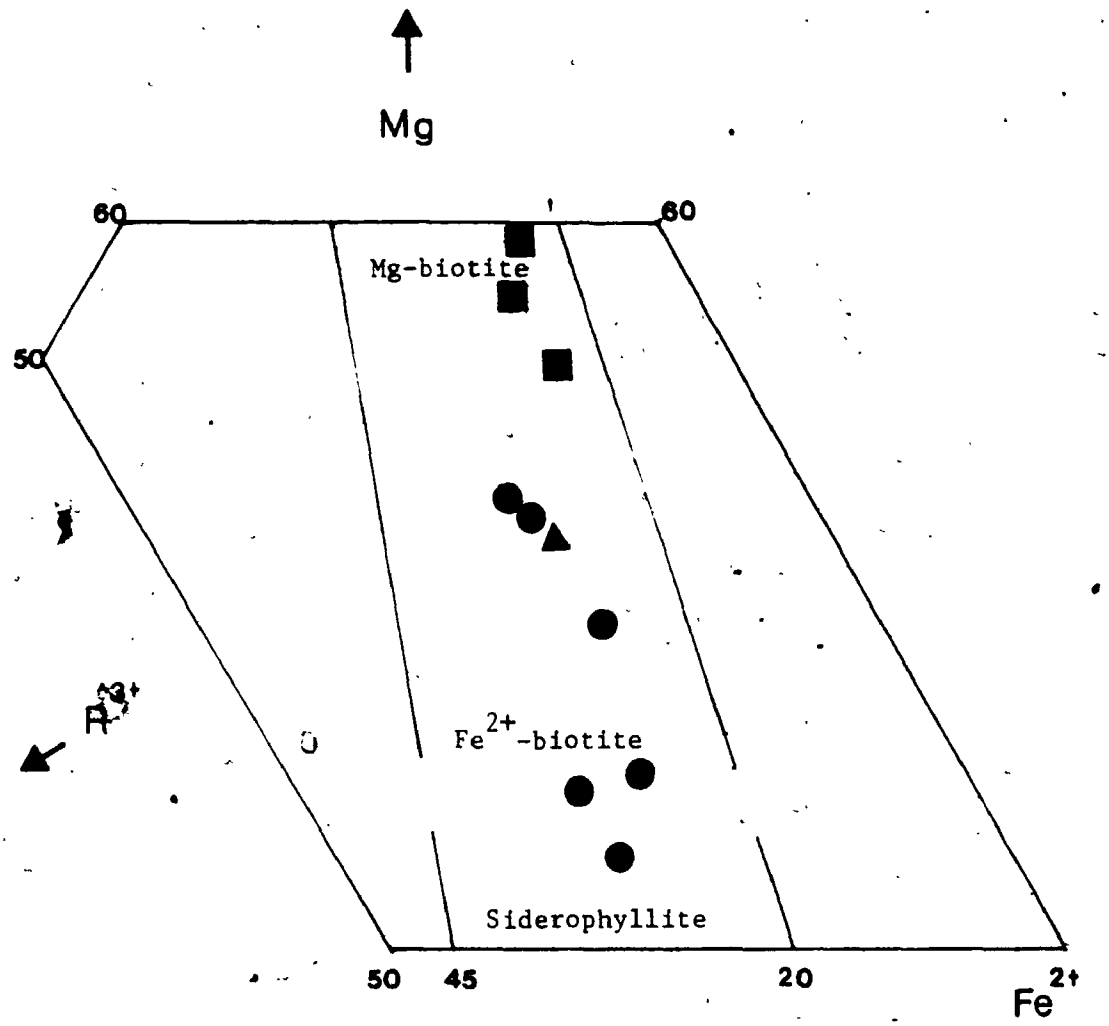

Figure 2-5-3. The Mg-Fe^{2+}-R^{3+} relation in trioctahedral micas of the Cheddar Granite. (after Foster, 1960).

$$R^{3+} = Al^{vi} + Fe^{3+} + Ti^{4+}$$

● Granite ▲ Monzonite ■ Xenolith

granitic rocks can be classified as sodic - calcic to calcic amphibole (Leake,1968).

Iron oxides, predominantly magnetite, intimately associated with biotite or hornblende may be formed by later oxidation of mafic minerals. Apatite, zircon, sphene, allanite, fluorite, secondary muscovite, epidote, garnet and trace tourmaline are common accessories. Apatite and zircon occur as inclusions of major mineral phases. Discrete zircon crystals are fractured and show lower birefringence due to radioactive damage. Epidote aggregates, considering to be of secondary origin, cluster along the boundaries between biotite and plagioclase. Also, opaques and garnet grains are rimmed by sphene aggregates.

5.2.2 Green Monzonite -

Rocks of green monzonite are characterized by their greenish-grey colour, medium grain size and massive appearance. They are composed generally of less than 20% quartz and approximately equal proportions of plagioclase and K-feldspar. They fall into the quartz monzonite field or the lower portion of the granite field of Streckeisen (1976; See Fig. 2-5-2).

The monzonitic rocks are hypidiomorphic - granular with green pyroxene as the diagnostic mineral; however, in some samples (eg. 81-6-1), pyroxene is absent and hornblende is the major mafic component with subordinate biotite. Representative pyroxene analyses are given in Table 2-5-4. Composition of the pyroxene is similar to that of the ferroaugite from syenite (Deer et al., 1966), except that the former has relatively higher SiO_2, CaO and Na_2O and lower Al_2O_3. In addition, the soda-rich nature of these pyroxene is similar to green pyroxene from metasomatized zones in the Bancroft region (S.B. Lumbers, pers. comm., 1984). Under the microscope, pyroxene grains are commonly fractured and associated with opaques, apatite and sphene. Hornblende as well as biotite is intergrown with pyroxene locally. Composition of hornblende can be categorized as sodic-calcic amphibole (Table 2-5-3), whereas biotite is Fe^{2+}-biotite with relatively lower annite content than those of granitic phase (See Fig. 2-5-3 and Table 2-5-2).

Plagioclase is commonly twinned with $An_{<5}$ (Table 2-5-1). It is relatively less altered in these rocks as compared to that in the granite-gneiss. Magnetite is closely associated with dark minerals. Sphene aggregates form corona around iron oxides and sometimes around biotite

Table 2-5-4. Chemical compositions and calculated formulae of pyroxene from the Cheddar Granite

Sample No.	81-5	81-21-1	37-6	81-5-3	**Syenite
Rock-type	2	2	3	3	
(wt%)					
SiO_2	51.34	49.89	51.48	50.56	46.61
TiO_2	0.12	0.10	0.14	0.13	1.18
Al_2O_3	0.92	1.31	1.81	1.10	3.47
Fe_2O_3	-	-	-	-	0.90
FeO	*17.63	*19.40	*13.25	*15.86	20.18
MnO	1.38	1.57	0.43	0.53	1.11
MgO	7.35	5.43	9.68	8.72	7.27
CaO	19.71	20.46	22.03	20.73	17.24
Na_2O	1.85	1.54	1.52	2.26	1.04
K_2O	0.02	0.02	0.01	0.01	0.27
Total	100.32	99.72	100.35	99.90	99.27
Si (Z)	1.996	1.978	1.960	1.961	1.859
Al^{iv} (Z)	0.004	0.022	0.040	0.039	0.141
	2.000	2.000	2.000	2.000	2.000
Al^{vi} (Y)	0.038	0.039	0.041	0.011	0.021
Ti (Y)	0.004	0.003	0.004	0.004	0.035
Mg (Y)	0.426	0.321	0.549	0.504	0.432
Mn (Y)	0.045	0.053	0.014	0.017	0.037
Fe (Y)	0.573	0.643	0.422	0.514	0.699
	1.086	1.059	1.030	1.050	1.224
Ca (X)	0.821	0.869	0.899	0.861	0.737
Na (X)	0.139	0.118	0.112	0.170	0.080
K (X)	0.001	0.001	0.000	0.000	0.014
	0.961	0.988	1.011	1.031	0.831
O	6	6	6	6	6

Rock-type: 2 - Monzonite.
3 - Xenolith.

* Total iron as FeO.
** Syenite - Ferroaugite of syenite (p.106, Deer et. al., 1966).

flakes.

5.2.3 Xenoliths And Schlieren -

5.2.3.1 Biotite-hornblende-rich Inclusions -

Biotite-hornblende-rich inclusions are frequently found in both granite-gneiss and green monzonite. They form either subrounded to subangular xenoliths or thin (max., 10 cm wide) layers of schlieren. Occassionally, "folded" schlieren are also encountered. Contacts between larger xenoliths and host rocks are usually sharp with little assimilation, while most schlieren are partly granitized with gradational contacts. Orientation of the schlieren is concordant with the foliation direction of the granite, whereas the foliation of the xenoliths frequently cuts across the preferred orientation of the host.

Because of their mafic mineral abundances, xenoliths are dark grey to black in colour with a greenish tint which comes mainly from chloritization. They fall into the tonalite field of Streckeisen (1976; See Fig. 2-5-2) with variable amounts of quartz and ferromagnesium minerals. However, the xenoliths are characterized by a constantly high fedspar ratio

(plagioclase/total feldspar > 0.97, in general).

Plagioclase is euhedral to subhedral with albite-twinning. The composition is commonly An_{13} to An_{27} with no indication of zoning. In addition to secondary muscovite and carbonate patches, zircon, corroded quartz and small biotite flakes are frequently enclosed in plagioclase.

The major mafic minerals are biotite and hornblende. Although their proportions vary from sample to sample, biotite is more abundant than hornblende. Composition of biotite can be classified as Mg-biotite (Fig. 2-5-3) with a considerably lower annite fraction (Table 2-5-2). Amphibole is sodic-calcic in composition (Table 2-5-3). Anhedral pyroxene grains are also present in some xenoliths (See Table 2-5-4).

The rarity or complete absence of iron oxides is noteworthy, compared with the host granite-gneiss. Allanite and spinel are also found in partly altered biotite. Subhedral brownish garnet was seen in only one sample.

5.2.3.2 Magnetite-garnet-rich Inclusions -

In contrast to biotite - hornblende - rich xenoliths, several samples taken along a logging road south of North Eels Lake (See Fig. 2-5-1) show abundant magnetite - garnet clusters together with zircon, sphene, epidote and altered allanite in a matrix of hornblende, microcline, quartz and subordinate plagioclase. Fluorite is another important accessory phase.

The composition of the plagioclase ($An_{> 10}$) argues against a consanguineous origin with the granite ($An_{< 10}$); besides, their peculiar chemical characteristics deviate from all the differentiation trends of the host (See Section 5.3). Instead, the magnetite - garnet - rich inclusions are thought to represent partially assimilated hornblende paragneiss of the country rocks (ODM, Map 1957-1). Three migmatitic gneiss samples with extensive hematization of feldspar are also assigned to this category.

5.2.4 Pegmatitic And Granitic Dykes -

Dykes of different varieties are abundant in the Cheddar Granite, which may indicate a hydrous magma. Fowler and Doig (1983) have demonstrated that the radioactive pegmatite dykes along the

eastern marginal zone are not consanguineous with the host Cheddar Granite, which is somewhat 200 Ma. older than the former. These dykes are commonly 1 to 5 m wide, cutting across both the granite and amphibolite country rocks. They are composed chiefly of microcline, quartz, minor hornblende and primary radioactive minerals, such as allanite, zircon, uranothorite, uranite, thorite (Fowler and Doig, 1983). In contrast to the granite-gneiss, the pegmatite dykes are massive without visible zoning. The characteristic brick red colour of the dykes is mainly due to intensive hematization.

In addition to the reddish dykes, pinkish and relatively quartz-rich pegmatitic "pockets" or veinlets, ranging from 20 cm to a few mm wide, are abundant inside the pluton. The pegmatitic veinlets cut across the foliation and penetrate the xenoliths. In places, veinlets can be traced back into "pockets"; contacts between the "pockets" and host are gradational. Frequently, concentrations of magnetite crystals are distributed along the boundaries.

Granitic and aplitic dykes are fine-grained and hypidiomorphic - granular. They usually occur in the country rocks of the border zone and are likely the "off-shoots" of the adjacent granite.

5.3 Whole-rock Geochemistry

5.3.1 Major-oxides -

The overall composition of the Cheddar Granite is metaluminous with the molar ratio of $Al_2O_3/(Na_2O+K_2O+CaO)$ ranging from 0.916 for granite, 0.809 for monzonite to 0.791 for assimilated rocks. Except for the assimilated rocks and some xenoliths which fall within the sub-alkaline field, all the granite-gneiss and later dykes are in the alkaline field of Miyashiro (1978; See Fig. 2-5-4). This classification is also reflected by their agpaitic indices; the assimilated rocks have the lowest value (0.828), following by granite (0.989) and monzonite (1.008).

Table 2-5-5 is the compilation of average major-oxide compositions for the Cheddar Granite, its inclusions and other similar rock-types. In general, the composition of granitic rocks of the pluton is similar to the hastingsite - biotite granite of the Nigeria-Niger Province, West Africa (Bowden and Turner, 1974), particularly the resemblance of Na_2O/K_2O ratio and oxidation index. In comparison with average monzonite from the North Bay Area of Ontario (Lumbers, 1971), the monzonitic phase of the Cheddar Granite is higher in SiO_2, Na_2O and ferrous iron, and lower in Al_2O_3 and CaO. The

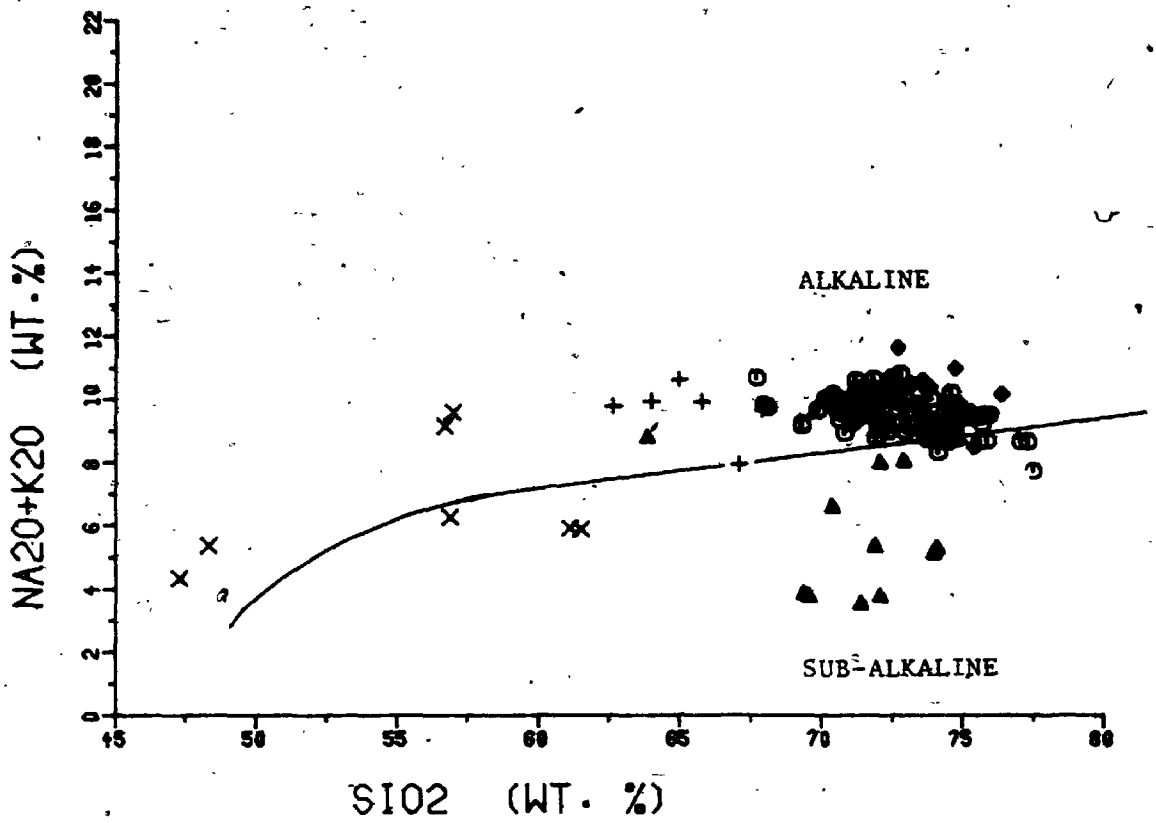

Figure 2-5-4. Na_2O+K_2O vs. SiO_2 diagram for the Cheddar Granite. Solid-line separates the alkaline and subalkaline fields of Miyashiro (1978).

- ⊙ GRANITE-GNEISS
- ▲ ASSIMILATED ROCKS
- + MONZONITE
- × XENOLITHS
- ◆ DYKES

Table 2-5-5. Comparison of average composition of the Cheddar Granite with other similar rock-types

(wt.%)	1 (n=90)	2 (n=48)	3 (n=72)	4	5 (n=7)	6 (n=6)	7 (n=11)	8 (n=7)	9 (n=16)
SiO_2	72.82	73.86	72.08	72.90	66.33	64.45	71.04	55.66	52.97
TiO_2	0.29	0.20	0.37	0.33	0.67	0.73	0.48	1.41	1.60
Al_2O_3	12.82	13.75	13.86	12.41	13.22	16.02	8.38	15.22	18.19
TFe_2O_3	3.37	*2.03	*2.62	*4.62	7.48	*6.45	10.48	10.41	*8.92
Fe_2O_3	1.68	0.78	0.86	1.80	3.40	1.16	6.74	2.95	1.97
FeO	1.53	1.13	1.67	1.71	3.13	4.77	3.70	5.80	6.29
MnO	0.06	0.05	0.06	0.09	0.18	0.12	0.40	0.16	0.13
MgO	0.26	0.26	0.52	0.34	0.50	0.76	0.37	4.44	4.75
CaO	0.57	0.72	1.33	0.89	1.86	2.63	1.65	5.14	7.61
Na_2O	4.68	3.51	3.08	4.11	4.99	3.79	1.96	3.89	3.50
K_2O	4.83	5.13	5.46	4.94	4.52	4.60	3.68	2.74	1.65
P_2O_5	0.04	0.14	0.18	0.04	0.10	0.22	0.06	0.34	0.34
LOI	0.38	0.47	0.53	0.86	0.21	1.02	0.35	0.66	1.00
Na_2O/K_2O	0.97	0.68	0.56	0.83	1.10	0.82	0.53	1.42	2.12
Oxidation Index	68.71	57.99	50.73	67.80	68.47	32.72	78.46	50.43	38.51

n - No. of analyses.
* - Calculated from ferric and ferrous values.
1 Average composition of granite-gneiss from Cheddar Granite (this study).
2 Average of 48 alkali granite (Nockolds, 1954).
3 Average of 72 calc-alkaline granite (Nockolds, 1954).
4 Composition of hastingsite-biotite granite of the Nigeria-Niger Province (Bowden & Turner, 1974).
5 Average composition of monzonitic rocks from Cheddar Granite (this study).
6 Average of 6 monzonite from North Bay Area, Ontario (Lumbers, 1971).
7 Average of 11 "assimilated rocks" from Cheddar Granite (this study).
8 Average of 7 biotite-hornblende-rich xenoliths from Cheddar Granite (this study).
9 Average of 16 biotite-hornblende diorite (Nockolds, 1954).

tonalitic xenoliths and biotite-hornblende diorite of Nockolds (1954) are similarly related. It is interesting to note that there are striking differences between the assimilated rocks and "normal" granite-gneiss of the pluton. At equivalent SiO_2 concentration, the assimilated rocks retain anomalously higher iron, MnO, CaO and lower Al_2O_3 and total alkali compared to the average granite-gneiss. Such differences were further reflected by their normative compositions: acmite (0.0 - 5.68%) and diopside (< 3.5%) for granite, hypersthene (> 3.0%) with minor acmite and diopside for monzonite, and diopside (> 3.5%) with no acmite for assimilated rocks. In addition, distinct groups are also shown in the normative Qtz-Or-Plag diagram (Fig. 2-5-5), in which monzonitic rocks lie in the low quartz end and the assimilated rocks occupy the high side. Rocks of the granite-gneiss are distributed along the trend from adamellite to alkali granite; overlaps occur with the monzonitic rocks.

According to normative classification (Fig. 2-5-6), both the monzonitic and granitic rocks, with a few exceptions, are in the granite field of O'Connor (1965). Although the data points for xenoliths and assimilated rocks are scattered, the majority of the latter is in the field of quartz

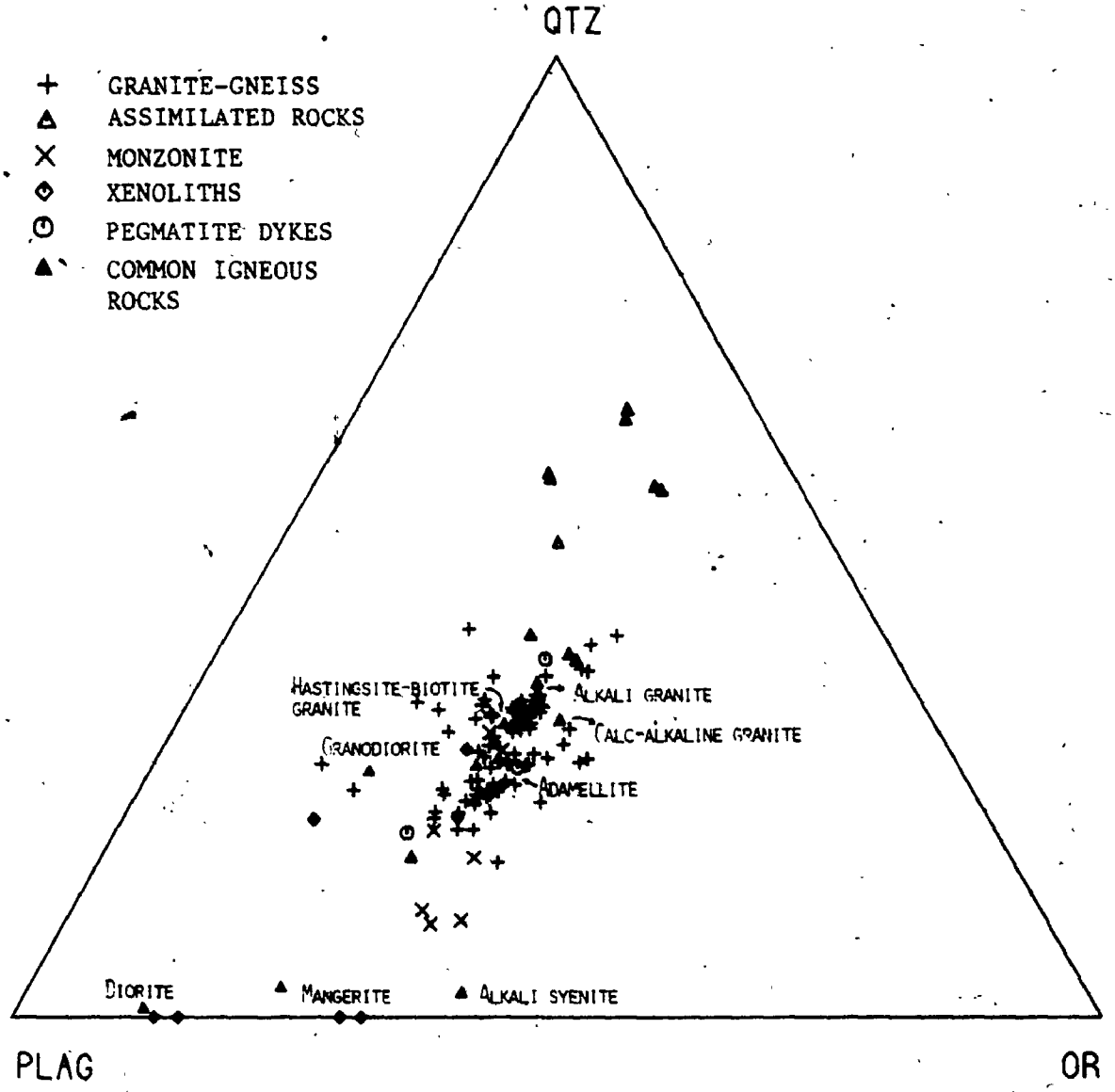

Figure 2-5-5. Normative Qtz-Or-Plag ratios of the Cheddar Granite and common igneous rocks (calculated from Nockolds, 1954).

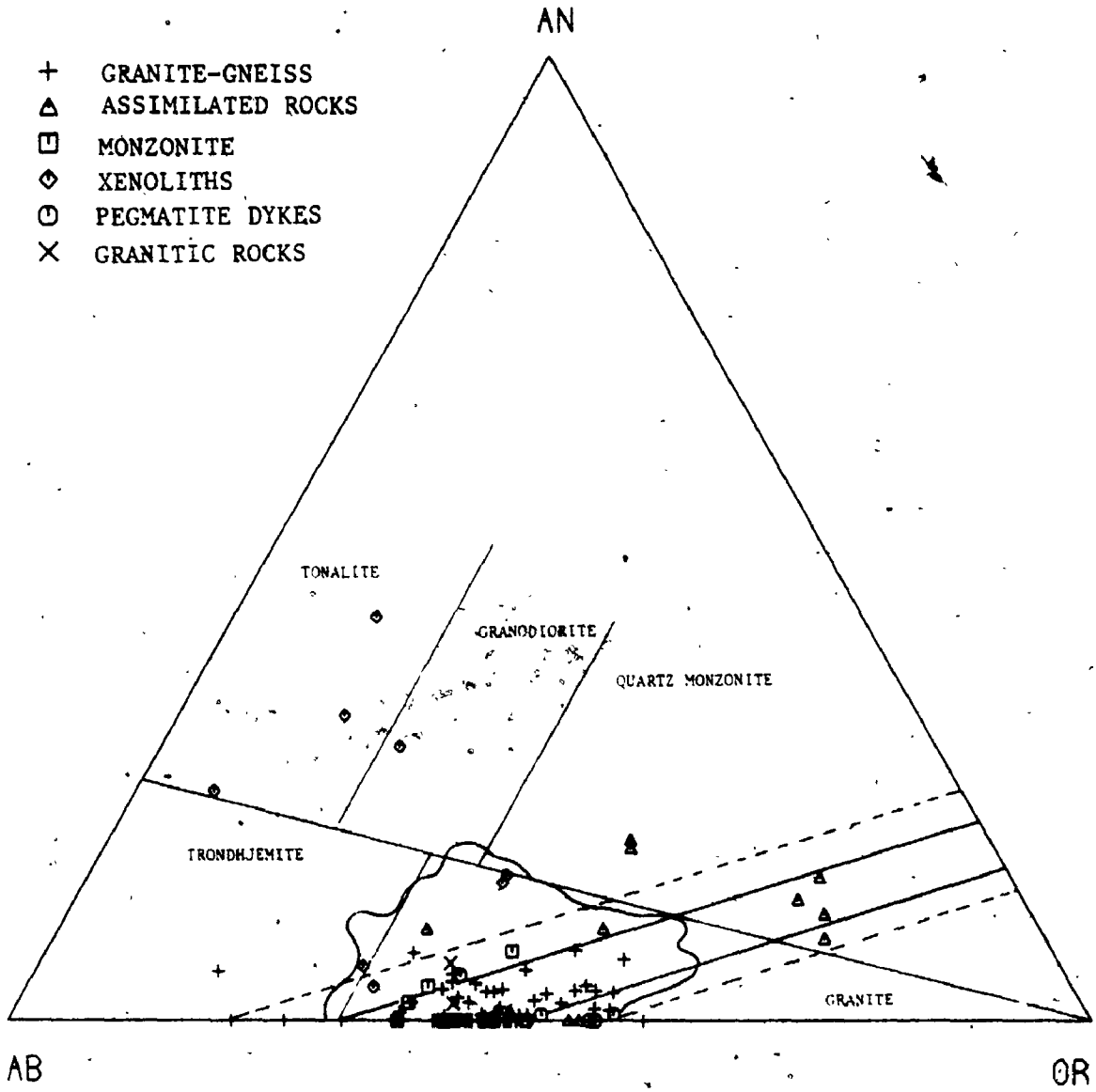

Figure 2-5-6. Normative Ab-An-Or ternary diagram of the Cheddar Granite. The irregular solid boundary is the 2% contour of Tuttle and Bowen (1958) enclosing most of granitic rocks that contain more than 80% normative Ab+An+Or+Qtz. The solid-lines indicate the boundaries of low temperature trough; dashed-lines show uncertainty due to analytical error (Kleeman, 1965). Classification scheme is from O'Connor (1965).

monzonite (O'Connor, 1965). In Figure 2-5-7, the monzonite is enclosed in the field of syenitic rocks from the Gardar Province of Greenland (Watt, 1966), while the granite-gneiss is concentrated in the granite field (Winkler and Von Platen, 1961). Distributions of the assimilation rocks in the Qtz-Ab-An-Or-H_2O system reflect their non-magmatic origin; however, samples with extensive hematization may result from metasomatism of "normal" granite-gneiss.

Correlation coefficients of major-oxides as a function of SiO_2 for granite-gneiss, monzonite and later dykes are given in Table 2-5-6. With respect to differentiation, TiO_2, Fe_2O_3, MnO, MgO, CaO and P_2O_5 show strong negative variation trends, while K_2O and Na_2O are insgnificantly correlated with SiO_2. Based on these strong negative correlations and the overlap of normative compositions (Fig. 2-5-7), it is suggested that the granite-gneiss, monzonite and later dykes are comagmatic. The overall chemical variations may thus be explained by fractionation of feldspars, mafic and accessory minerals. The assimilated rocks, which deviate from the general trends, form a distinct group. In addition, with the exception of Na_2O, there are consistent linear relationships among the granite-gneiss, monzonite, later dykes and tonalitic

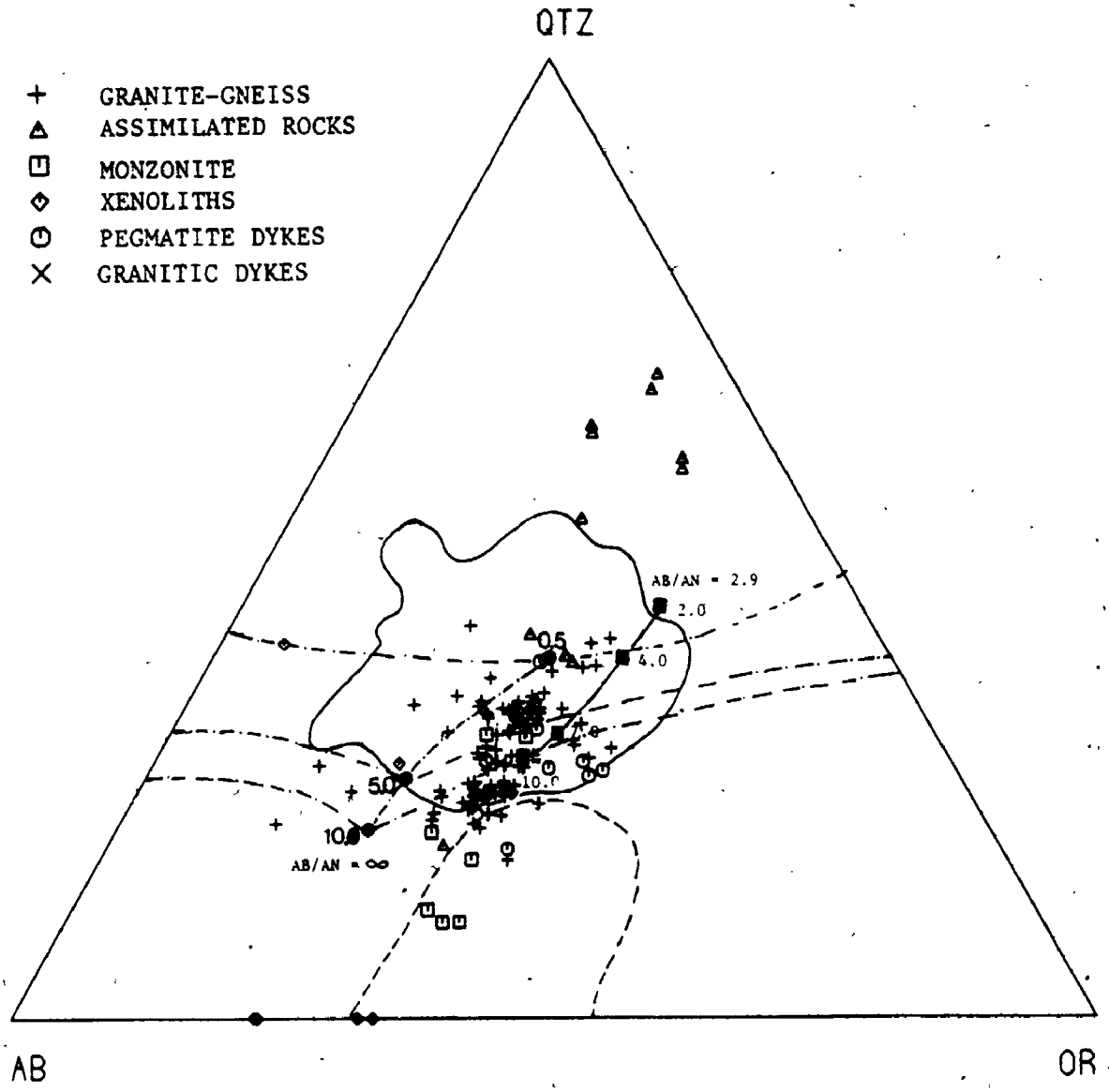

Figure 2-5-7. Normative Qtz-Ab-Or ternary diagram of the Cheddar Granite. The irregular solid boundary encloses analyses of 1190 granitic rocks of Winkler and Von Platen (1961). The irregular dashed-line shows the compositional field of syenitic rocks from Gardar Province of Greenland (Watt, 1966). Experimentally determined ternary minima (Tuttle and Bowen, 1958; Luth et al., 1964) and minima in An - bearing systems (James and Hamilton, 1969) are shown by solid circles and solid squares, respectively.

Table 2-5-6. Correlation coefficients of inter-element variations for the Cheddar Granite

Correlation		Granite + monzonite	All rock-types*	Correlation		Granite + monzonite	All rock-types
SiO_2 vs.	TiO_2	-0.7772	-0.9227	SiO_2 vs.	U	0.1204	0.1441
	Al_2O_3	-0.3953	-0.5093		Th	0.2526	0.2505
	Fe_2O_3	-0.7311	-0.8396		F	-0.0461	-0.4758
	MnO	-0.6453	-0.7201		Cl	-0.5423	-0.7301
	MgO	-0.6453	-0.8783		S	-0.3296	-0.4959
	CaO	-0.7463	-0.8789		Ga/Al	-0.3144	-0.2941
	K_2O	0.0192	0.4927		K/Rb	0.0086	0.2019
	P_2O_5	-0.5472	-0.7007		Rb/Sr	0.3112	0.5280
	Na_2O	-0.2749	0.0543		Sr/Ba	0.2179	-0.4507
	Rb	0.1266	0.1890		Sr/Ca	0.1305	0.1133
	Sr	-0.1980	-0.5639		Zr/Y	0.0715	0.0586
	Ba	-0.4299	-0.4183		Y/Ca	0.3431	0.3736
	Zr	-0.2196	0.0062		Cr/Mg	0.3638	0.2637
	Nb	-0.3173	-0.1179		V/Mg	0.4087	0.1726
	Y	-0.2992	-0.0361		Ni/Mg	0.4369	0.3757
	Ga	-0.5281	-0.5098		Fe/Mg	0.3066	0.3162
	Pb	-0.0458	-0.1536		Cr/Fe	0.2819	-0.1969
	Zn	-0.4845	-0.5003		V/Fe	0.1864	-0.5913
	Cu	-0.4448	-0.6452		Ni/Fe	0.3217	0.1686
	Ni	-0.2717	-0.6819	Nb vs.	Ga/Al	0.5572	0.5174
	Cr	-0.4629	-0.8465	Nb vs.	Y	0.6984	0.7017
	V	-0.0112	-0.7929	Al_2O_3 vs.	Ga	-0.1164	-0.0072

* All rock-types = granite + monzonite + tonalitic xenoliths + dykes.

xenoliths of the pluton.

In terms of K_2O-Na_2O-CaO ternary variation (Fig. 2-5-8), rocks of the monzonitic and granitic phases follow the differentiation trend of Scottish alkaline basalt (Nockolds and Allen, 1953), though scatter of data points is marked. Assimilated rocks are plotted away from the trend with abnormally high CaO and low Na_2O. Similarly, in the AFM diagram (Fig. 2-5-9), the monzonite and granite are consistent with the differentiation of alkaline basalt with a moderate iron enrichment trend. Again, assimilated rocks with high iron contents are plotted close to the FeO apex. It is also noted that in both diagrams, distributions of tonalitic xenoliths are associated with the calc-alkaline trend rather than the alkalic trend of the monzonite and granite-gneiss. This may rule out the possible cumulate origin for these hornblende - bitotite - rich inclusions.

5.3.2 Trace-elements -

The mean trace-element concentrations of various rock-types from the Cheddar Granite are given in Table 2-5-7. Values for average low-Ca granite and syenite (Turekian and Wedepohl, 1961) are also listed for comparison. The granite-gneiss

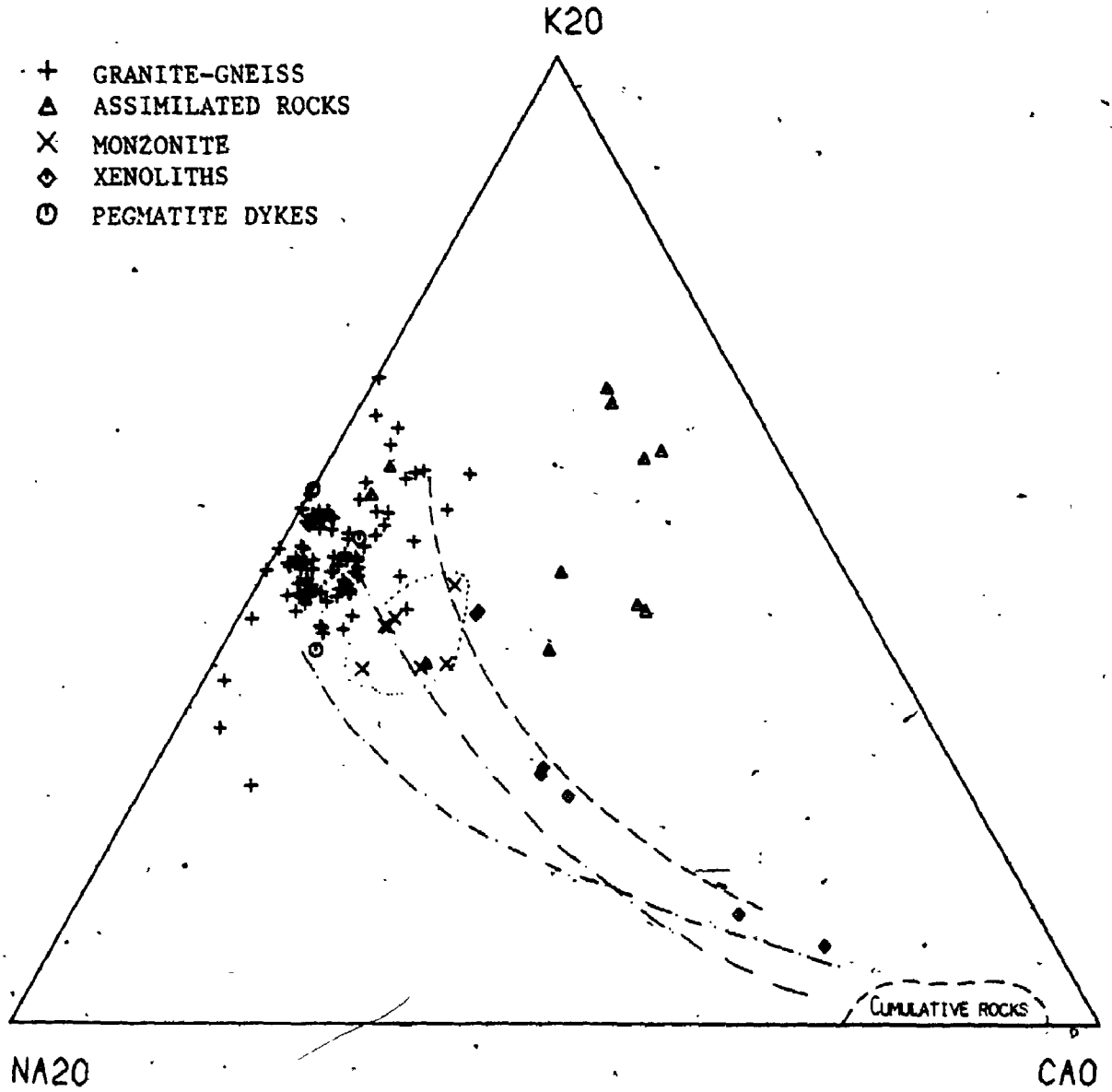

Figure 2-5-8. Na_2O-K_2O-CaO variation diagram of the Cheddar Granite. Compositional field of monzonite is enclosed by dotted-line.

- - - - Calc-alkaline trend of Southern California Batholith (Nockolds and Allen, 1956).

-·-·- Differentiation trend of Eastern Island Basalt (Nockolds and Allen, 1953).

-··-··- Differntiation trend of Scottish alkaline basalt (Nockolds and Allen, 1953).

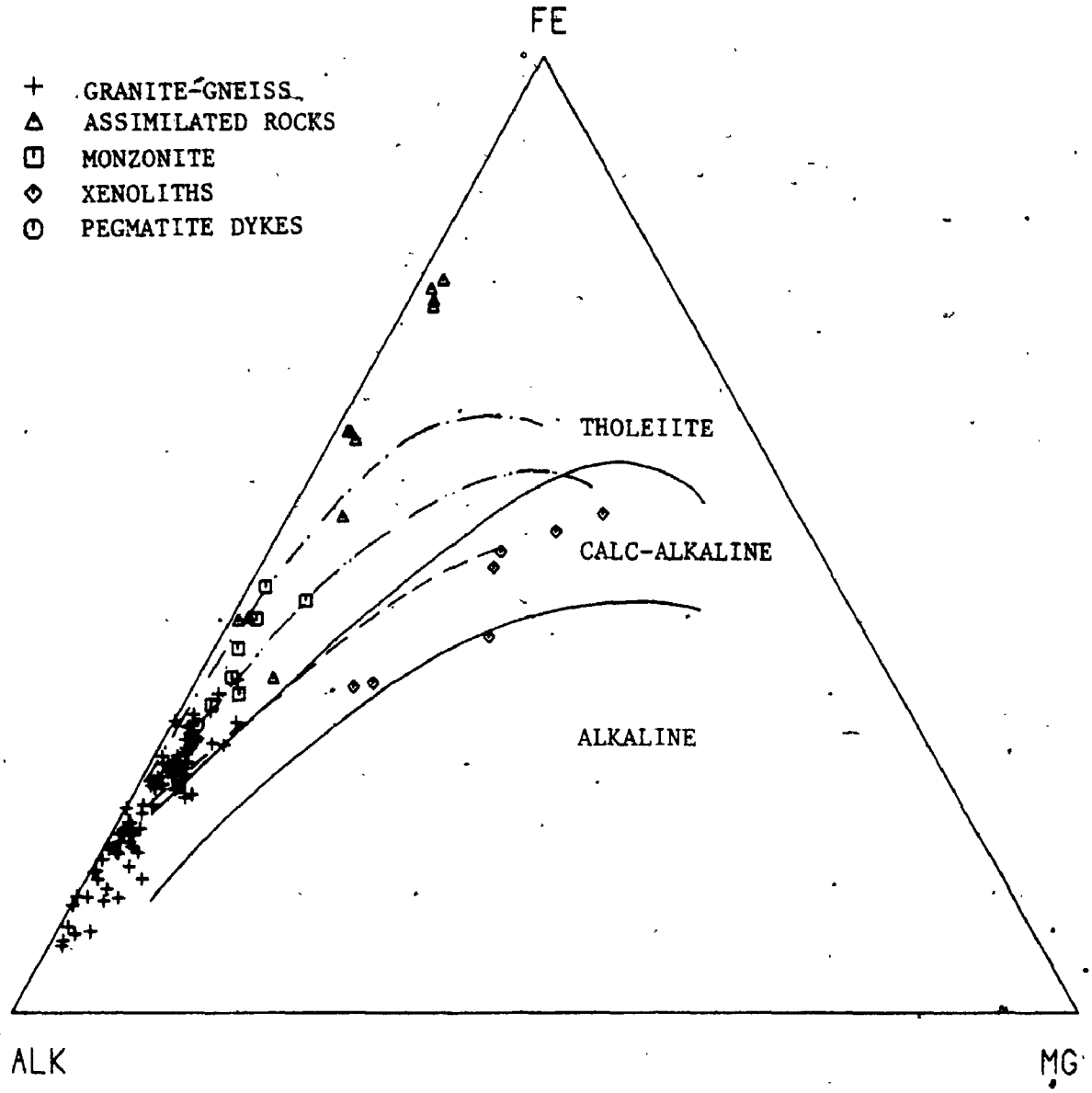

Figure 2-5-9. AFM diagram of the Cheddar Granite.
Solid-lines separate the tholeiite, calc-alkaline and alkaline fields (Barker and Arth, 1976).

-·-·-· Calc-alkaline trend of Southern California Batholith (Nockolds and Allen, 1956).

-·-·- Differentiation trend of Eastern Island Basalt (Nockolds and Allen, 1953).

-·-·- Differentiation trend of Scottish alakline basalt (Nockolds and Allen, 1953).

Table 2-5-7. Average concentrations of trace elements in the Cheddar Granite and other similar rock-types

(ppm)	1	2	3	4	5	6	7	8
Nb	33	78	46	21	9	29	21	35
Zr	448	2122	510	117	85	275	175	500
Y	73	227	92	22	10	45	40	20
Sr	83	112	111	129	164	470	100	200
Rb	141	128	116	238	193	130	170	110
Ba	209	214	565	351	392	672	840	1600
Ga	28	35	33	22	24	38	17	30
Ni	7.5	22	9.4	2.9	3.3	21	4.5	4.0
Cr	5.6	9.3	7.8	3.4	3.7	47	4.1	2.0
V	4.5	7.7	2.1	5.4	3.4	144	44	30
Agpaitic Ind.	0.989	0.828	0.809	0.992	0.926	0.615	-	-
K/Rb	297	246	344	223	223	203	*230	-
Rb/Sr	1.94	1.24	1.19	1.89	1.17	0.47	1.70	0.55

1 Granite-gneiss.
2 Assimilated rocks.
3 Monzonite.
4 Pegmatitic dykes.
5 Granitic-aplitic dykes.
6 Xenoliths.
} various rock-types from Cheddar Granite. (this study)

7 Average composition of low-Ca granite (Turekian and Wedepohl, 1961).
8 Average composition of syenite (Turekian and Wedepohl, 1961).
* Average K/Rb rotio for the crust (Heier and Adams, 1964).

of the pluton is enriched in high-field strength (HFS) elements (eg. Nb, Zr, Y and Ga) and less abundant in Ni and Cr compared with the average low-Ca granite. It is, on the other hand, markedly lower in alkali-alkaline earth elements (eg. Sr, Ba and Rb) and V. Enrichment of Nb, Zr, Ga and depletion of Sr and Ba are characteristic of a highly fractionated alkali igneous suite.

Trace-element abundances of the assimilated rocks are consistently higher by a significant amount than the "normal" granite-gneiss; such unusual Nb, Zr and Y concentrations may reflect their magnetite - garnet - zircon - rich mineralogy. Compositions of the monzonite are comparable with those of average syenite, except that the former has relatively higher Y, Ni, Cr and lower Ba, Sr and V. The K/Rb ratios of both granitic and monzonitic rocks are higher than the crustal average (230). Variation of the K/Rb ratio as a function of Rb in the pluton (Fig. 2-5-10) shows that the granite and monzonite form a comagmatic trend with few exceptions, while there is a constant K/Rb ratio among assimilated rocks.

Inter-element correlation coefficients of trace-elements are summarized in Table 2-5-6. Except for Ba, variations of alkali-alkaline earth elements and their ratios as a function of SiO_2 are

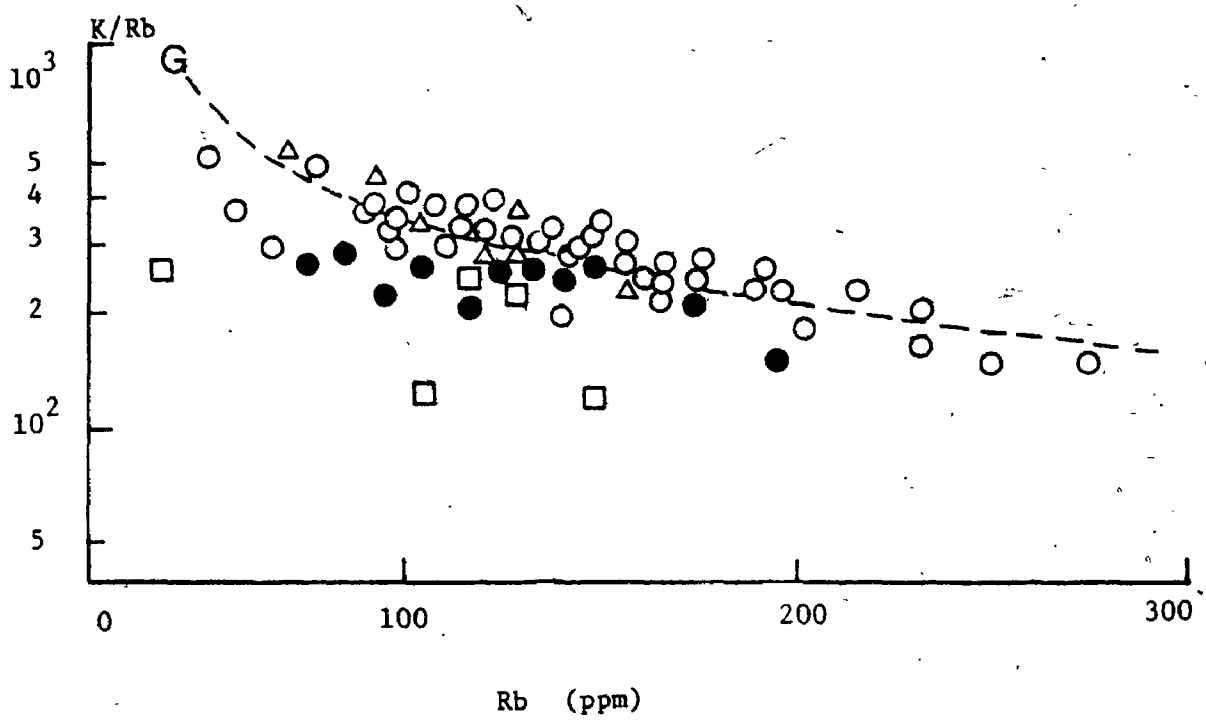

Figure 2-5-10. K/Rb ratio vs. Rb variation diagram of the Cheddar Granite.

G - Differentiation trend of the Cheddar Granite

○ Granite

△ Monzonite

● Assimilated rocks

□ Xenoliths

too poor to yield any significant trends. Ga and Ga/Al ratio show a negative correlation with SiO_2, which is opposite to the differentiation trend of common igneous rocks. The progressive enrichment of Ga over Al from basic through intermediate and felsic to alkalic rocks is predicted from crystal-chemistry (eg. Siedner, 1965). Such a reverse trend in this pluton is not readily explained.

5.3.3 Rare-earth Elements -

Analyses of rare-earth elements, Ta, Hf and Cs for the representative samples from Cheddar Granite are given in Table 2-5-8. Their chondrite-normalized distribution patterns are shown in Figure 2-5-11. In comparison with average low-Ca granite ($(Ce/Yb)_N$ = 5.23, Eu/Eu* = 0.50), the granite-gneiss of the pluton show weakly fractionated patterns with greater depletion of Eu ($(Ce/Yb)_N$ = 1.93 - 4.40, Eu/Eu* = 0.08 - 0.34; See Fig. 2-5-11A). Besides, the granite-gneiss has considerably higher total REE, Ta and Hf concentrations, which is similar to the previous analyses of Fowler (1980; See Table 2-5-8). The general trend of decreasing Eu/Eu* ratio with increasing SiO_2 may be expected by gradual removal of feldspars during differentiation. The

Table 2-5-8. Rare-earth elemets, Ta, Hf and Cs compositions of the Cheddar Granite

Sample No.	1 TS-18PG	2 648-1-1G	3 BL-1G	4 HR4G1A	5 TN4G1A	6 TE-6G	7 81-6-1	8 81-7	9 TS-19MS	10 TE-3MS	11 HR-3GD	12 54
Rock-type	1	1	1	1	1	1a	2	2	3	3	4	4
La	101.61	69.64	71.29	89.43	64.15	152.75	72.31	79.10	47.13	32.03	9.13	8.58
Ce	216.04	149.12	151.01	193.53	154.18	335.05	166.53	167.24	92.80	39.86	19.65	18.22
Sm	35.92	17.30	17.31	21.14	21.48	43.33	22.54	16.27	11.93	6.85	2.48	2.39
Eu	3.06	2.03	1.89	1.35	0.58	4.12	2.60	2.41	2.22	0.42	0.43	0.60
Tb	6.44	3.45	3.59	3.49	3.09	6.34	4.29	4.17	1.93	0.64	0.63	0.52
Yb	22.72	16.49	17.82	9.92	15.32	23.56	25.14	18.01	5.68	2.42	1.27	1.25
Lu	3.25	3.57	3.74	1.45	2.40	3.45	3.18	2.38	0.53	0.75	0.31	0.28
ΣREE	389.04	261.40	266.65	320.31	261.20	568.60	296.59	290.08	162.22	82.97	33.90	32.34
Ta	5.61	4.80	4.05	3.85	4.77	3.57	3.25	4.68	0.96	1.64	7.01	4.67
Hf	15.11	16.30	18.18	18.96	19.67	41.09	25.45	7.17	2.48	4.30	4.43	3.81
Cs	2.01	0.57	1.03	0.71	1.01	0.16	0.35	0.62	2.94	3.79	5.98	2.00
Eu/Eu*	0.26	0.34	0.30	0.19	0.08	0.31	0.34	0.39	0.58	0.22	0.05	0.69
$(Ce/Yb)_N$	2.16	2.04	1.93	4.40	2.27	3.23	1.50	2.12	3.75	3.75	3.67	3.50
$(Ce/Sm)_N$	1.24	1.76	1.79	1.88	1.48	1.59	1.51	2.05	1.59	1.18	1.57	1.62
$(Tb/Yb)_N$	1.20	0.88	0.85	1.48	0.86	1.14	0.72	0.99	1.46	1.17	2.17	1.83
F	992	2300	2740	920	2640	2600	1740	520	4440	2980	76	81
SiO_2	69.33	70.21	70.77	73.69	75.04	71.87	67.07	71.92	49.28	61.10	73.20	72.55

(Table 2-5-8. Cont'd)

Sample No.	13 Cal-8	14 Ched-3	15 Ched-9	16 CD-4	17 Ave. G	18 Ave. S
Rock-type	5	6	6	6	7	8
La	144.25	78.3	45.8	14.1	55.0	70.0
Ce	216.86	133.9	130.1	47.2	92.0	161.0
Sm	10.31	16.9	14.5	13.8	10.0	18.0
Eu	0.67	0.8	2.2	0.7	1.6	2.8
Tb	2.40	3.1	2.8	1.2	1.6	[illegible].8
Yb	5.36	16.9	12.1	8.8	4.0	7.0
Lu	0.88	1.8	1.8	-	1.2	2.1
ΣREE	380.73	251.7	209.3	-	165.4	263.7
Ta	9.76	-	-	-	4.2	2.1
Hf	2.99	-	-	-	3.9	11.0
Cs	0.80	-	-	-	4.0	0.6
Eu/Eu^*	0.18	0.14	0.44	0.19	0.50	0.49
$(Ce/Yb)_N$	9.11	1.80	2.45	1.22	5.23	5.23
$(Ce/Sm)_N$	4.32	1.63	1.85	0.70	1.89	1.85
$(Tb/Yb)_N$	1.89	0.78	0.98	0.58	1.70	1.70
F	147	-	-	-	850	1200
SiO_2	72.68	-	-	-	-	-

Rock-type:-

1. Granite-gneiss.
1a. Assimilated rock.
2. Monzonite.
3. Xenolith.
4. Granitic and Aplitic dyke.
5. Pegmatitic dyke.

6. Previous analyses of Fowler (1980).
7. Average granite (Taylor, 1964).
8. Average syenite (Turekian and Wedepohl, 1961).

Figure 2-5-11. Chondrite-normalitzed REE distribution patterns of the Cheddar Granite.

(A) REE distributions for granite-gneiss.

(B) REE distributions for monzonite and xenoliths.

(C) REE distributions for various dykes.

(D) REE distributions for average syenite (Turekian and Wedepohl, 1961), low-Ca granite (Taylor, 1964) and previous analyses from Fowler (1980, CHD-3, CHD-9 and CD-4).

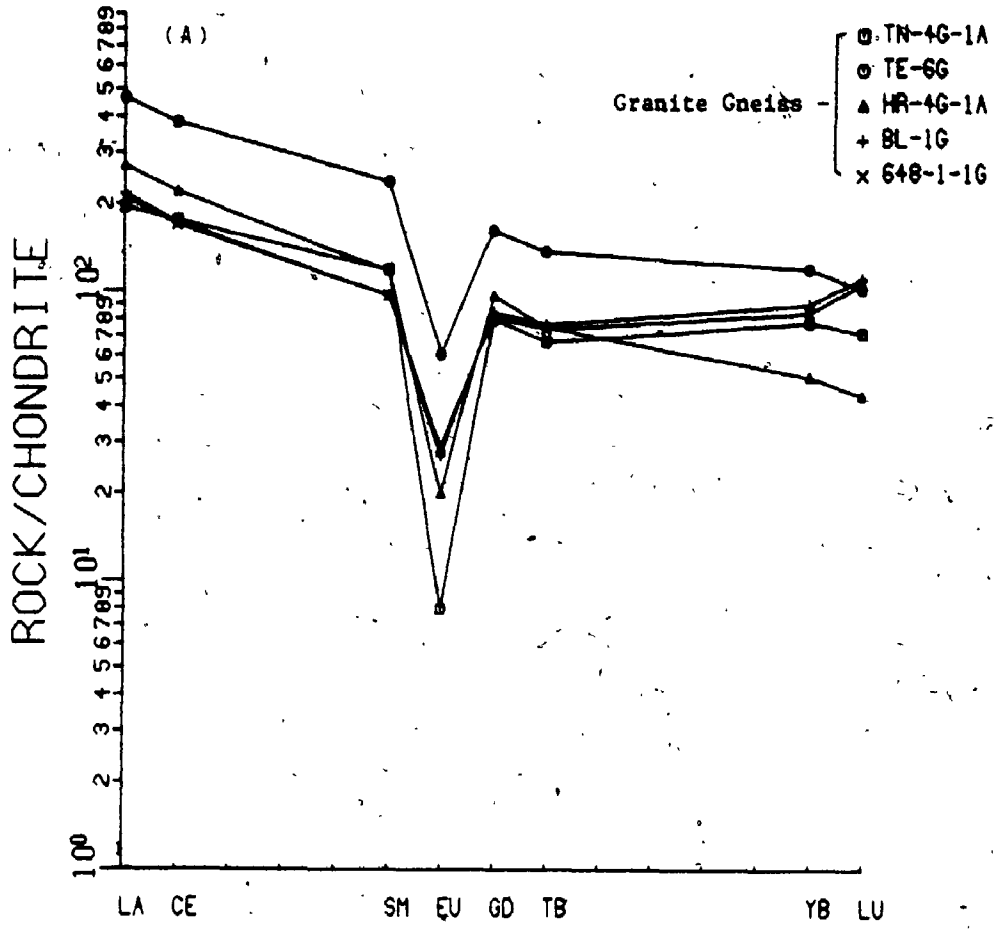
(A)
Granite Gneiss -
TN-4G-1A
TE-6G
HR-4G-1A
BL-1G
648-1-1G
ROCK/CHONDRITE
LA CE SM EU GD TB YB LU

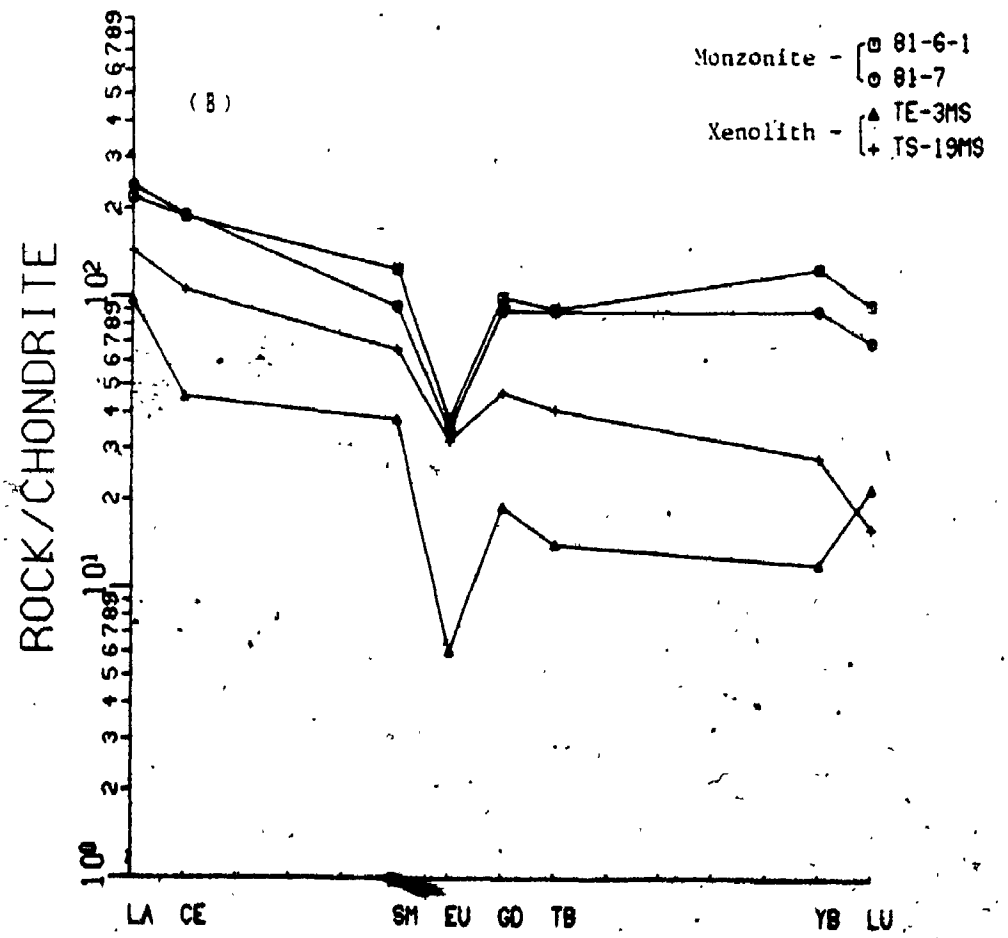
(B)
Monzonite -
81-6-1
81-7
Xenolith -
TE-3MS
TS-19MS
ROCK/CHONDRITE
LA CE SM EU GD TB YB LU

(Figure 2-5-11. Cont'd)

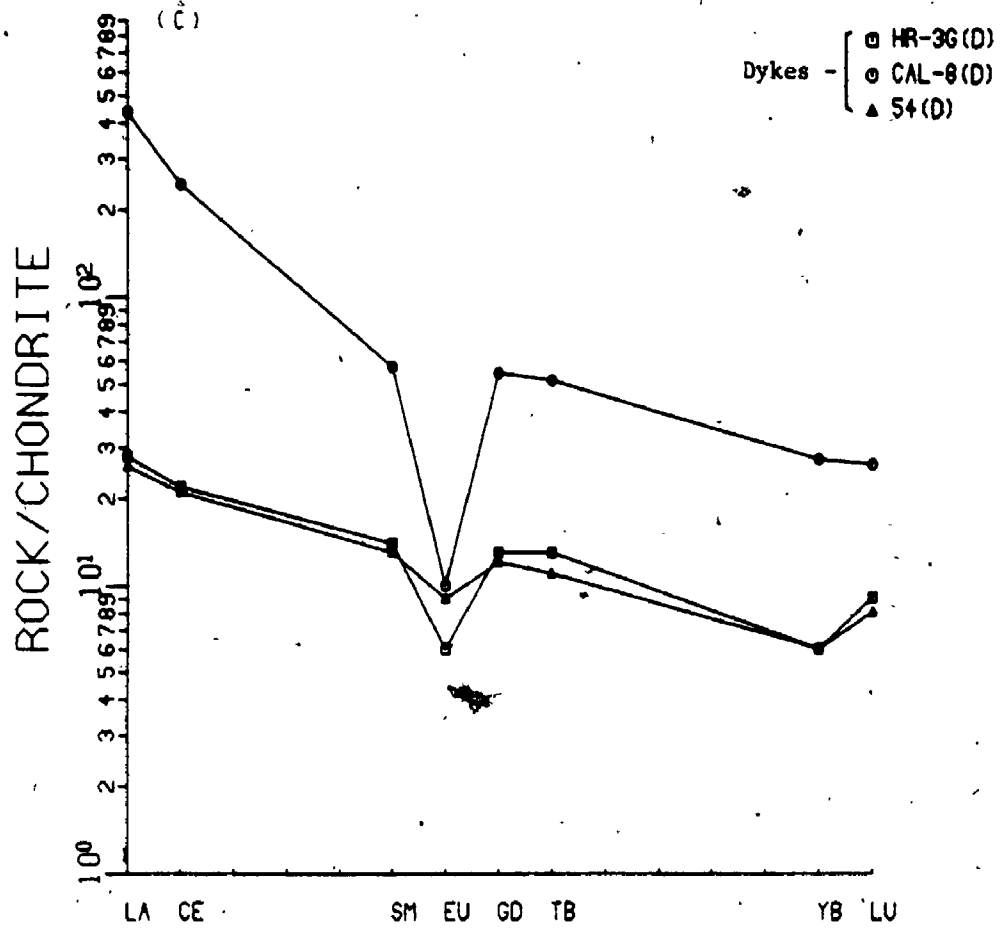

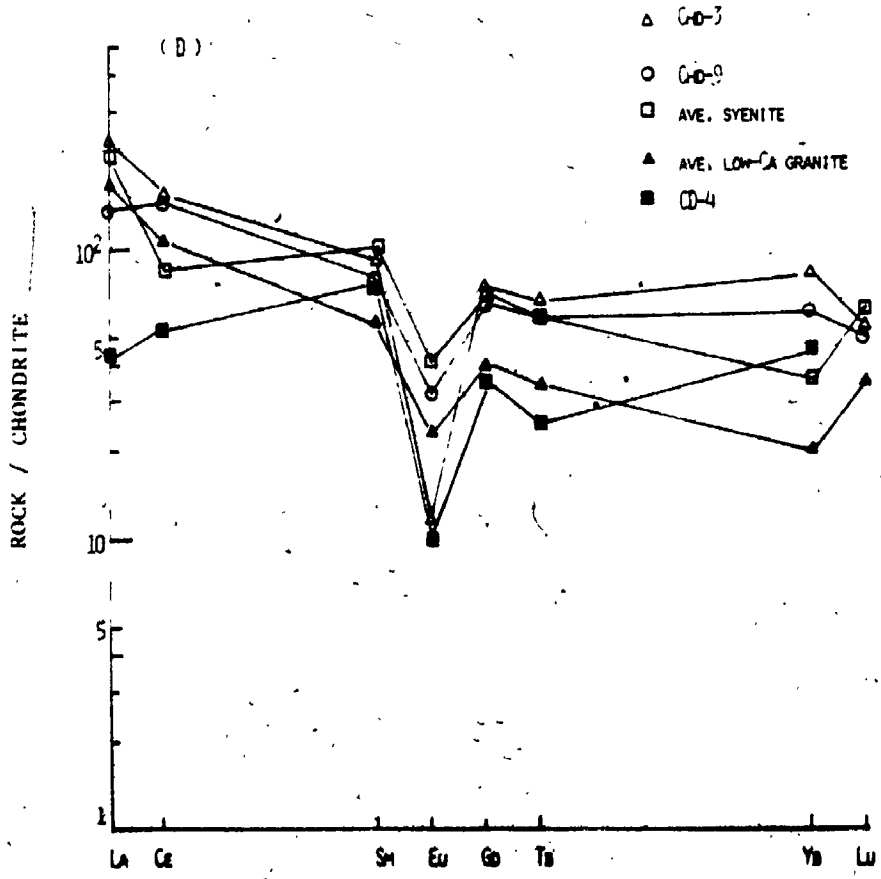

assimilated rock contains extremely high total REE and Hf abundances and shows moderately fractionated patterns. The monzonite has similar distribution curves (Fig. 2-5-11B) to those of granite-gneiss and is much less fractionated than average syenite ($(Ce/Yb)_N$ = 1.50 - 2.12 for monzonite, 5.33 for syenite; See Fig. 2-5-11D).

The horizontal or slightly concave REE distribution patterns of the Cheddar Granite, which differ completely from a normal fractionation trend of granitic rocks, suggest either a marked depletion of LREE or an anomalous enhancement in HREE relative to chondrite. The drastic depletion of LREE is likely due to fractional crystallization of LREE-enriched accessory mineral phases, such as allanite, sphene and monazite (Mittlefehdt and Miller, 1983). However, such a depletion occurs only in the highly differentiated silicic end member. In Cheddar Granite, similar REE patterns from monzonite to granite and lack of any evidence of early crystallization of LREE-enriched phases argue against the possibility of strong LREE depletion in the monzonite. On the other hand, the enhancement of heavy and middle REE is contradictory to the fractionation of HREE-enriched mineral phases (eg. zircon), which is predicted from variation of trace-elements (eg. Zr). However, Bowden and

Whitley (1964) proposed that the upward curvature in the peralkaline and associated granites of Nigeria is due to a hydrothermal volatile (mainly alkalis and fluorine) - HREE -rich residual fluid autometasomatizing the partly crystallized granite and gradually erasing the earlier magmatic patterns. The overall alkalic composition of the pluton and its considerably high F concentration (920 - 2740 ppm) favour the hypothesis of having an alkali-fluorine-rich residual fluid in the late stage of crystallization. Additionally, the general trend of increasing F content with decreasing total REE abundances indicates a possibility of mobilization of REE by fluorine-complexing (Bandurkin, 1961; Fryer and Edger, 1977). The granite-gneiss (HR4G-1A) with a moderate fractionation pattern ($(Ce/Yb)_N$ = 4.4) and less abundant F (920 ppm) reflect less REE-complexing and partly preserves the original magmatic fingerprint. Furthermore, the positive correlation of Eu/Eu* ratio with concentration of middle REE (Sm) indicates the magnitude of the Eu depletion is also related to the enrichment of middle REE (Bowden and Whitley, 1964).

The later granitic and aplitic dykes show patterns parallel to their host granite (Fig. 2-5-11C), except that the former has considerably

lower REE concentrations and relatively greater HREE fractionation. Such a depletion of overall REE concentration and similarity of distribution patterns can be expected by loss of alkali-volatile-rich fluids from the magma after crystallization of granite. In contrast, the uraniferous pegmatitic dyke (CAL-8) is not consanguineous with the host granite (Fowler and Doig, 1983) and shows a moderate fractionation pattern with enrichment of LREE. The tonalitic xenoliths have intermediate abundances of REE and show negative sloping curves (Fig. 2-5-11D).

5.4 Regional Chemical Variation

5.4.1 Analysis Of Local Variance -

A chemical variation trend in a granitic pluton can be contributed from three major sources: (1) variations among sample-sites, (2) differences between samples within the sites, (3) analytical errors. In other words, without knowledge of smaller scale variability in a pluton, it is not possible to evaluate the significance of a regional variation (eg. Baird et al., 1964, 1967). In order to test the significance of distributions of U, Th and other elements in the Cheddar Granite; a hierarchal sampling plan was carried out: six

random sampling sites were chosen and three samples were taken from each site. Duplicates were made from each sample to evaluate the analytic errors.

The conventional analysis of variance (Krumbein and Slack, 1958) was employed; the F-ratios serve as indicators for accepting or rejecting the null hypothesis (H_0) that no significant variation between sample-sites compared with variation between samples within-site. To support the null hypothesis, the calcuated F-value (F_{cal}) must be less than the tabulated value at the 99% confidence level and at the assigned degree of freedom (v_1, v_2); that is, $F_{cal} < F_{0.99;v1,v2}$. The results of analysis of variance of U, Th, Nb, Zr and Rb in the Cheddar Granite are summaried in Table 2-5-9. There are significant variations between sample-sites compared with those between samples within-site for U, Th, Nb and Zr in the Cheddar Granite. On the other hand, for Rb, $F_{cal} < F_{table}$ indicates the variation between samples in a site is more significant than that between sample-sites; that is, the regional trend will be obscured by local "noises". In addition, the variance component shown in percentage clearly indicates the contribution of variance from each level.

In order to probe spatial distribution of U and Th, seventy-five in-situ measurements by means of

Table 2-5-9. Analysis of variance of selected elements in the Cheddar Granite

Element	Source of variance	Mean square	Degree of freedom	F_{cal}	Decision	Variance Component(%)
U	Between sample-sites	81.2	4	30.07	Reject Ho**	90
	Between sample within-site	2.7	10	15.88	Reject Ho	9
	Between replicate within sample	0.17	15			
Th	Between sample-sites	2.7	4	10.72	Reject Ho	76
	Between sample within-site	0.25	10			24
Nb	Between sample-sites	4264.80	5	123.20	Reject Ho	88
	Between sample within-site	34.60	12	0.40	accept Ho	0
	Between replicate within sample	95.5	18			12
Zr	Between sample-sites	6909552.1	5	56.3	Reject Ho	94.7
	Between sample within-site	122772.1	12	31.6	Reject Ho	5.0
	Between replicate within sample	3885.0	18			0.3
Rb	Between sample-sites	2859.5	5	3.1	Accept Ho	33
	Between sample within-site	913.1	12	2.4	Accept Ho	28
	Between replicate within sample	373.7	18			39

** Ho : No significant variation between sample-sites compared with variation among sample within-site.

$F_{0.99;4,10} = 5.99$, $F_{0.99;10,15} = 3.80$, $F_{0.99;5,12} = 5.06$, $F_{0.99;12,18} = 3.37$.

portable Na(I) detector were taken at stations which are unevenly distributed in the northern half of the pluton. Forty-five samples were also taken from the above sites for Nb and Zr analyses. A modified computer program of O'Leary et al. (1966) for non-orthogonal polynomial approximations was used to separate regional trends from local effects (noises); up to sixth order polynomial surfaces were computed. The percentage reduction of sum of squares (ie. the goodness-of-fit) was used to assess which order of trend surface to rely upon; according to Davis (1973), 16 - 36% reduction of sum of squares can yield interpretable trends and residual maps. To test whether the trend surface of order k+1 gives a significant improvement over that of order k, the method of Chayes (1970) was used, except that the increment in goodness-of-fit was ratioed rather than the mean squares. It was decided to use 2nd-order surface for Nb and Zr and 4th-order for U and Th in this study.

5.4.2 Interpretation Of Areal Trends -

During their study of the Cheddar "Batholith", Ingham and Keevil (1951) proposed a generalized distribution of radioactivity (as total alpha-activity) with an impoverished core and enriched border zone for large batholiths greater

than 3 km across. The trend surfaces for U and Th of the Cheddar Granite (Fig. 2-5-12A,B) show no general patterns. The areal distribution patterns of both U and Th indicate two compositional highs at the eastern end of N. Eels Lake area and SE regions of the Monrock and Buckskin Lakes. In addition, the Th concentrations form closed contours roughly parallel to the boundary of the pluton, while the U abundances increase from the northeast corner outward to an area where uraniferous pegmatites and greisen-type uranium deposits are abundant. The differences of distribution patterns for Th and U may also illustrate the relatively high mobility of U in the granitic intrusion. Generally, its distribution is principally related to the occurrence of primary U-enriched accessory phases in the granite; however, later tectonic movement (shearing or faulting) will initiate the secondary alteration causing colloform uranyl-ion enrichment in iron-oxides along grain boundaries or microfissures (eg. Fyson et al., 1980).

The Nb variation shows a compositional high (> 50 ppm) at southeast corner of the map and forms a ridge northwesterly (Fig. 2-5-12C). On the other hand, the chemical variation of Zr forms concentric patterns with a compositional high (> 1000 ppm) between N. Eels and Hook Lakes (Fig. 2-5-12D).

Figure 2-5-12. Trend surface maps of chemical variations of the Cheddar Granite.

(A) 4th degree of trend surface of U variation

(B) 4th degree of trend surface of Th variation

(C) 2nd degree of trend surface of Nb variation

(D) 2nd degree of trend surface of Zr variation

(E) Residual map of Nb trend surface

(F) Residual map of Zr trend surface

(A)

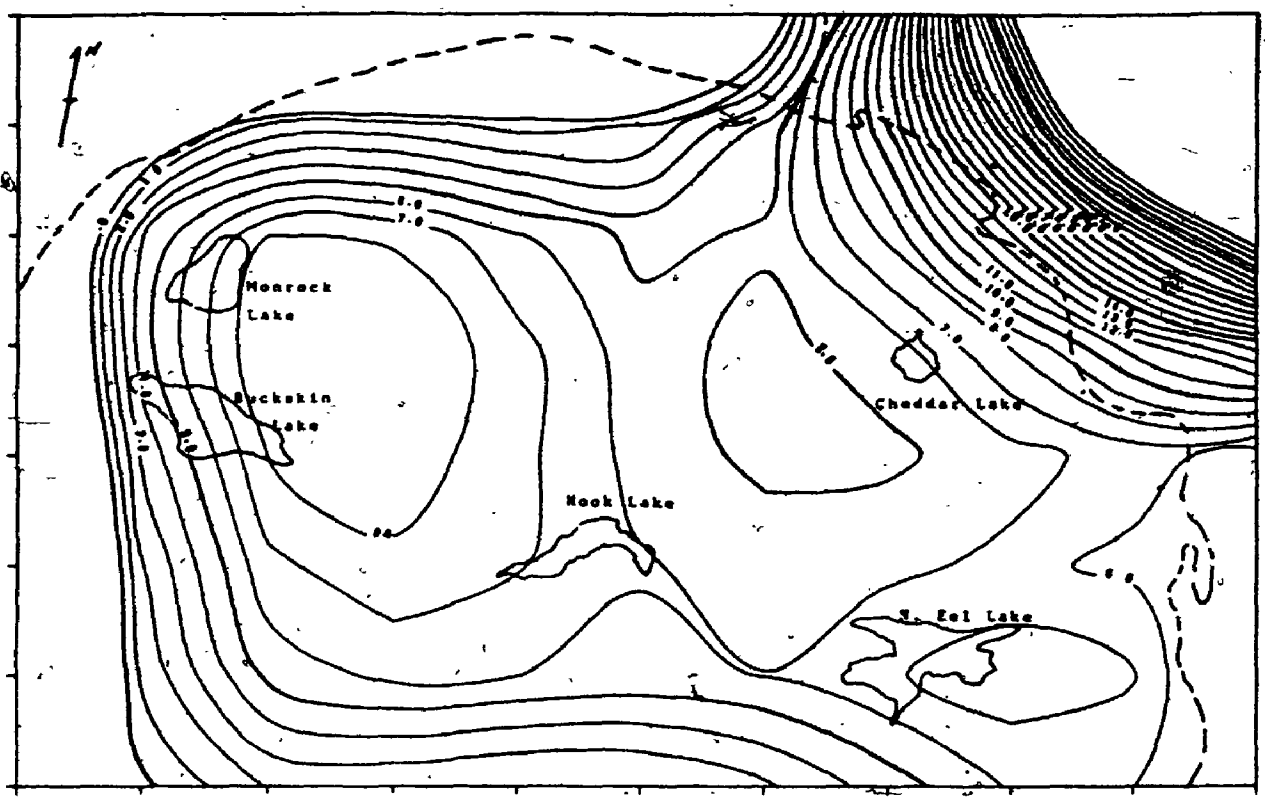
N
Monrock Lake
Buckskin Lake
Cheddar Lake
Hook Lake
N. Eel Lake

(B)

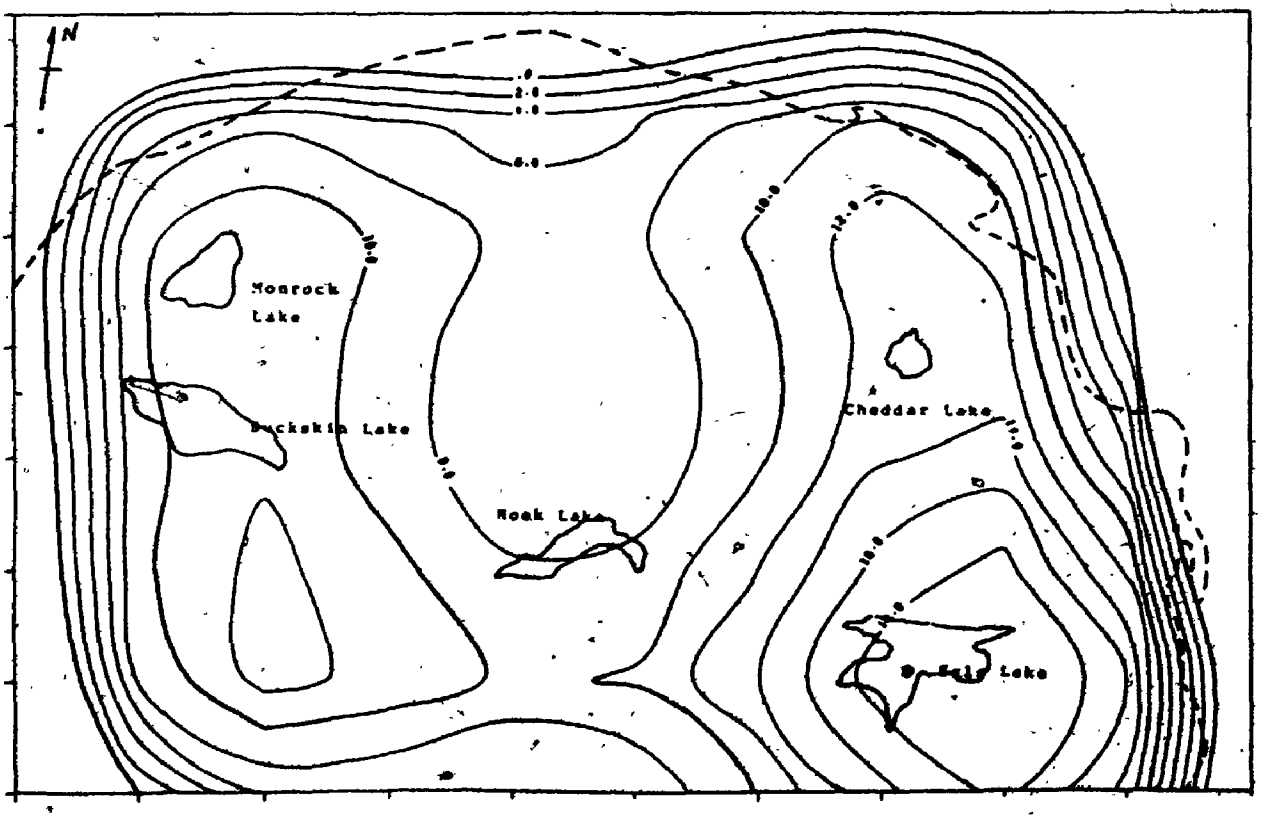
N
Monrock Lake
Buckskin Lake
Cheddar Lake
Hook Lake
N. Eel Lake

(Figure 2-5-12. Cont'd)

(C)

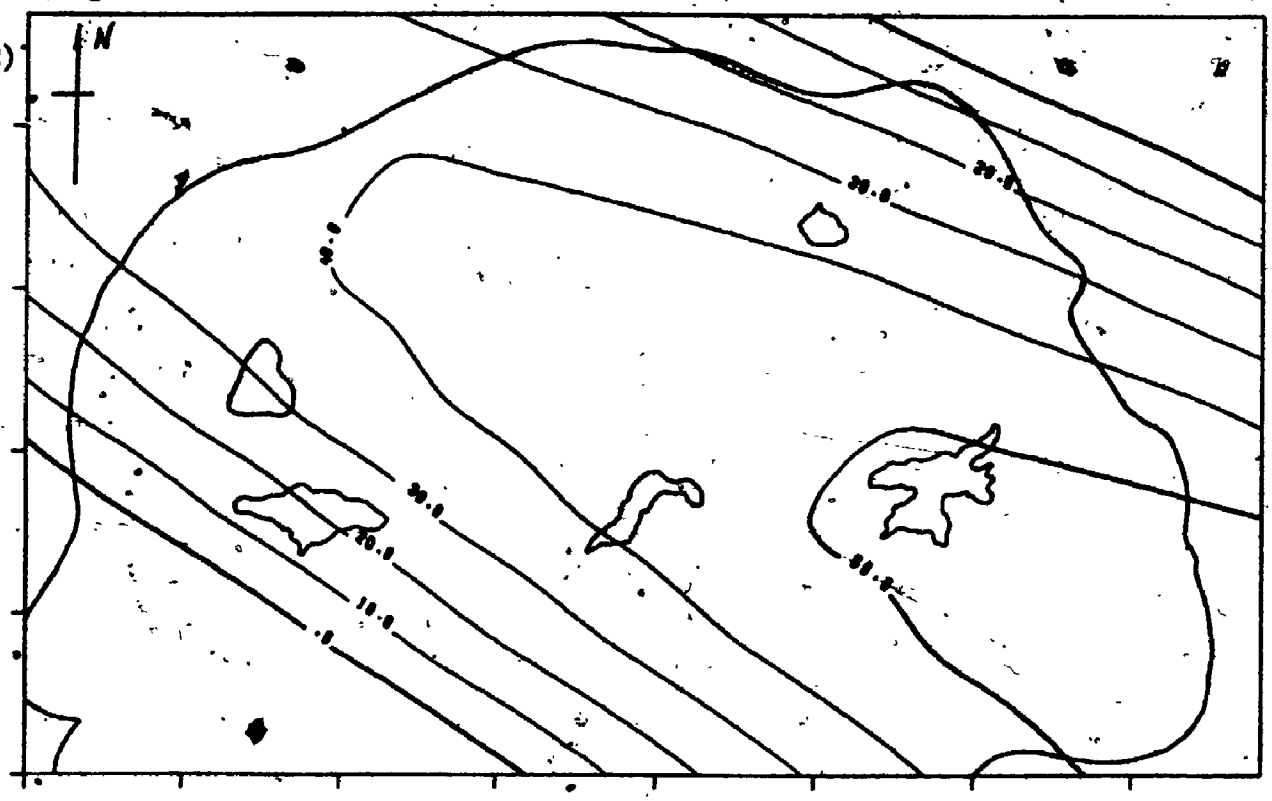

(D)

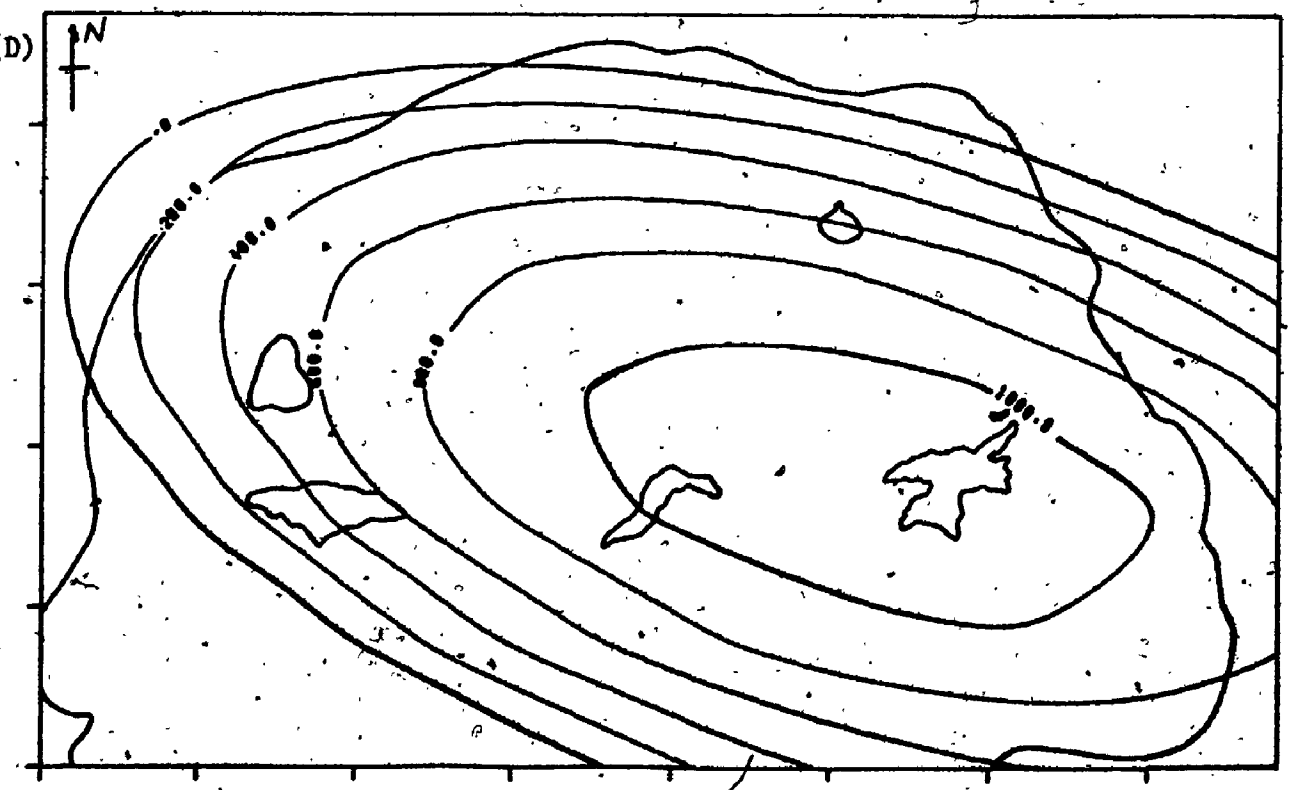

(Figure 2-5-12. Cont'd)

(E)

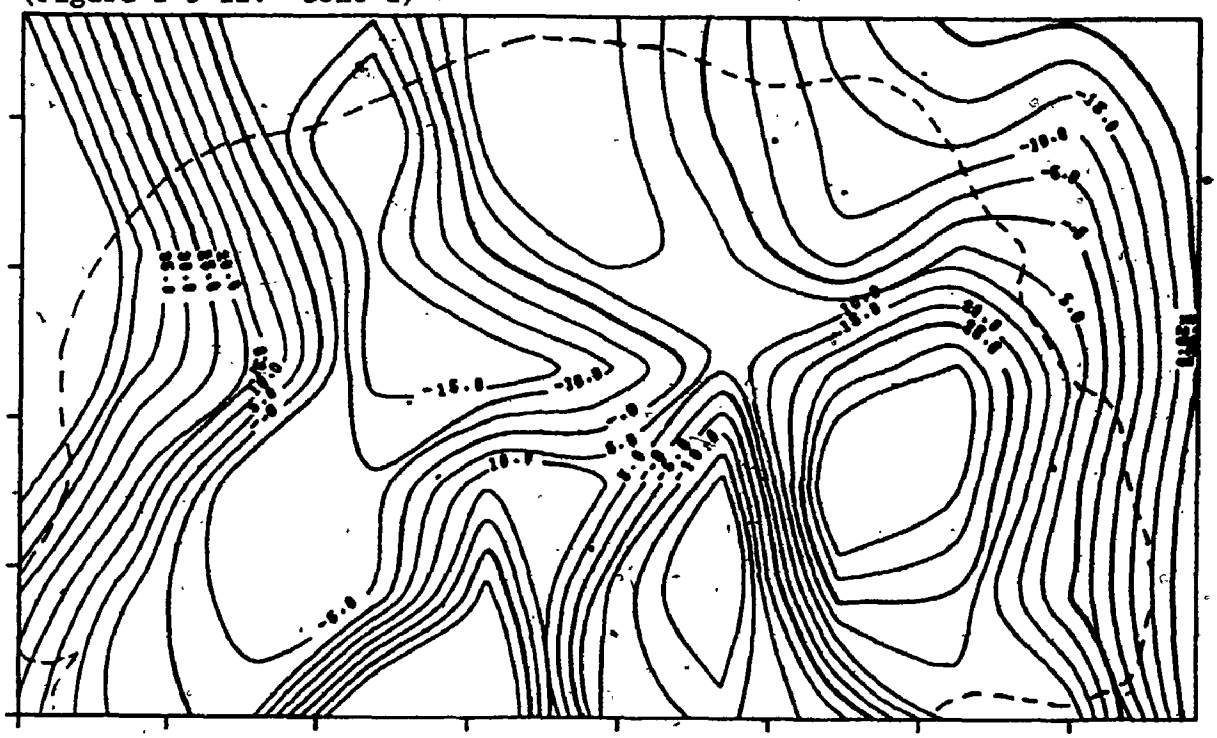

(F)

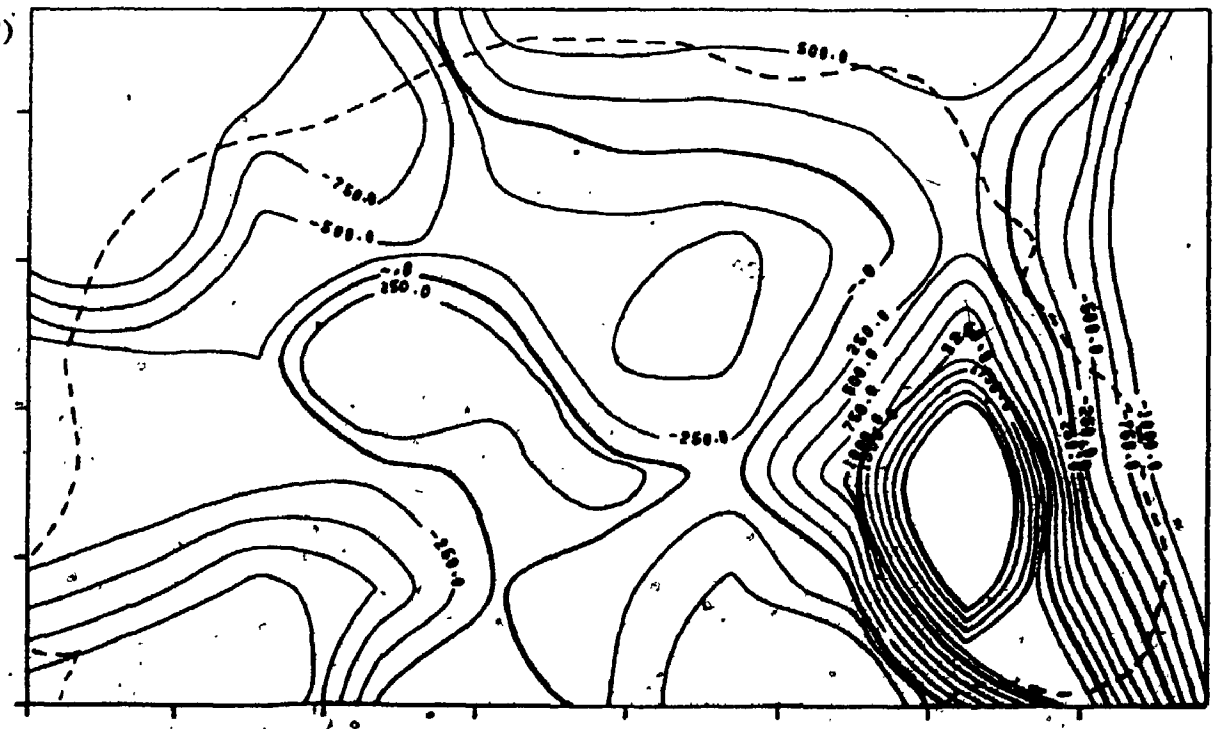

Both Nb and Zr do not readily enter the common rock-forming minerals and tend to be accumulated in the evolved melt as long as no frationation of accessory phases with large K_d for Nb or Zr occurs. The similar trends of Nb and Zr are consistent with the linear correlation in the alkaline magma.

It is also interesting to note in the residual maps (Fig. 2-5-12E,F) that the residual highs showing great enhancement of Nb and Zr are located around the N. Eels Lake area in which the large outcrop of assimilated paragneisses is sited. Although the assimilated rocks correspond to the compositional highs, the uniform decrease of Nb and Zr outward from these highs may suggest that assimilation has little effect on the overall fractionation trends of Nb and Zr during magmatic differentiation.

5.5 Isotopic Geochemistry

Oxygen isotope analyses of whole-rocks and coexisting quartz-feldspar fractions of representative samples from Cheddar Granite are given in Table 2-5-10. Except for sample HR-4G-1A with $\delta^{18}O$ of 9.28, all the others including the assimilated rocks (TE-6G) have $\delta^{18}O < 8.4$, which can be classified as low-^{18}O granites of the Grenville Province (Shieh and Schwarcz, 1974).

Table 2-5-10. Oxygen isotope analyses of whole-rock and co-existing minerals from the Cheddar Granite

Rock-type	Sample No.	$\delta^{18}O$ whole-rock	$\delta^{18}O$ quartz	$\delta^{18}O$ feldspar	$\Delta q-f$
Granite-gneiss	648-AG-1A	7.87			
	TW-4G	8.18			
	TN4G-1A	7.96	8.79	7.89	+0.90
	TS18-PG	8.12			
	HR4G1A	9.28			
Monzonite	81-5	7.93			
Xenolith	TS-19MS	5.59			
Assimilated rock	TE-6G	8.16	9.73	7.98	+1.75

$\Delta_{q-f} \cong \delta q - \delta f$ - Isotopic fractionation between coexisting quartz and feldspar.

In addition, the Cheddar Granite is comparable with the nearby Glamorgan Gneiss Complex, ranging from 6.7 to 8.8 (Shieh and Schwarcz, 1974). The Δ_{q-f} value of +0.90 suggests that the low $\delta^{18}O$ of this granite is a primary feature; however, the high-temperature fingerprint (+1.75) of the assimilated rock is the result of assimilation. It is also noteworthy that the uniform δ values among granite itself and assimilated rock may indicate an extensive oxygen isotope homogenization associated with hydrothermal autometasomatism during the late stage of solidification. If so, the higher $\delta^{18}O$ sample (HR-4G-1A) may retain the original isotopic fingerprint, in agreement with the REE data; and the precursor of the assimilated rocks should contain relatively lower $\delta^{18}O$.

The whole-rock Rb-Sr isochron of the Cheddar Granite yields an age of 1207 $\pm$ 46 Ma. (Fowler and Doig, 1983), which is interpreted to indicate syn-tectonic emplacement. Its initial $^{87}Sr/^{86}Sr$ ratio is about 0.6909, which precludes the protolith with a long term crustal history.

5.6 Petrogenesis And Source Rock

Both the whole-rock geochemistry and projections in the experimental system agree that the granite-gneiss and monzonite are genetically related and probably

comagmatic. Despite scatter of data, the continuity of their chemical variations suggests that they are products of magmatic differentiation from a single magma by accumulation of residual quartz. The internal chemical variations are consistent with extensive fractional crystallization, especially large amounts of feldspars. This crystallization model was tested by means of a least squares method (Stormer and Nicholls, 1978). As expected, it requires removal of a model solid of 64% plagioclase, 22% pyroxene, 3% sphene and 11% magnetite to form the most differentiated granite (HR-10G) from the monzonitic rock. The proportion of crystallized solid is about 27% of the initial magma, that is, about 30% fractional crystallization. A similar mechanism was required for the differentiation of later dykes as well.

The field relationships and linear nature of geochemical variation among tonalitic xenoliths, monzonitic and granitic rocks in the Cheddar Granite suggest a restite-unmixing model (White and Chappell, 1977), in that compositions of the melt, bulk restite and source rock lie on a straight line in Harker diagrams. Thus the composition of parental rock should be intermediate and must be as mafic as the most mafic granitoid of the suite. For Cheddar Granite, 61% SiO_2 is chosen for the upper limit of the parent; the abundances of other elements were then estimated by

visual estimation from extensions of variation trends between monzonite and granite. The compositional estimates of the parental rock and possible sources for Cheddar Granite are given in Table 2-5-11. Based on major-oxides, the predicted source has very similar composition to that of peralkaline syenite (Nickolds, 1954), except for higher CaO and lower K_2O. However, the latter contains anomalously high HFS elements and Rb, which are not consistent with estimations of the source. On the other hand, the source rock has trace-element abundances and element ratios similar to those of silicic granulite (Weaver, 1980), except that the former has relatively lower SiO_2 and higher Na_2O, Al_2O_3 and total iron. Furthermore, the predicted parent has a normative trondhjemite composition (O'Connor, 1965) with alkali-lime and HFS element concentrations similar to average Grenville dacite (Condie and Moore, 1977) and trondjemitic Elzevir Bahtolith (Pride and Moore, 1983).

The high K/Rb (590) of the estimated source is also consistent with the high K/Rb (344) of the monzonitic phase in the pluton. For equilibrium partial melting, the ratio (R_L) of a pair of incompatible elements in the derivative melt can be formulated as:

$$R_L = R_o * \frac{D_2 + F\,(1 - D_2)}{D_1 + F\,(1 - D_1)}$$

D_1, D_2 = bulk distribution coefficients of

Table 2-5-11. Estimations of possible sources for the Cheddar Granite

	1	2	3	4	5
SiO_2 (wt%)	61.0	70.20	64.40	61.65	72.70
TiO_2	0.9	0.37	0.44	0.52	0.58
Al_2O_3	15.0	15.68	16.30	14.73	13.00
TFe_2O_3	9.2	2.57	3.84	8.64	5.71
MnO	0.28	0.07	-	0.20	0.09
MgO	1.1	0.92	2.20	0.70	0.75
CaO	3.0	2.73	3.20	1.87	2.28
K_2O	3.2	2.57	2.40	4.65	2.26
Na_2O	6.1	4.57	4.00	6.69	3.16
P_2O_5	0.18	0.10	-	0.17	0.11
Na_2O/K_2O	1.90	1.78	1.67	1.44	1.40
Sr (ppm)	130	336	256	-	127
Rb	45	61	30	140	39
Ba	775	391	-	-	800
Zr	100	127	-	910	363
Nb	18	-	-	150	11
Y	25	-	-	120	44
K/Rb	590	344	664	230	481
Rb/Sr	0.35	0.18	0.12	-	0.31
Sr/Ca	65	172	112	-	78
Ba/Sr	5.96	1.16	-	-	6.30

1. Compositional estimates for source rock of Cheddar Granite.
2. Average composition of the Elzevir Batholith, Ontario (Pride and Moore, 1983).
3. Average composition of the Grenville dacite (Condie and Moore, 1977).
4. Average Peralkaline Syenite of Nockolds (1954).
   (trace-elements are taken from Sorensen, 1974)
5. Analysis of silica granulite (charnockite) (Weaver, 1980).

element 1 and 2;

R_o = initial ratio in the source rock;

F = fraction of partial melting.

By using the solid-liquid partition coefficients of Arth (1976), about 15% model melting of the trondhjemitic source is required to produce a monzonitic melt with K/Rb of 341, and a refractory restite with a mineralogy similar to that of the tonalitic xenolith ($Plag_{40}K\text{-}feld_{15}Biot_{10}Hb_{15}$).

For fractional crystallization, the ratio (R_L) of derivative liquid is $R_L = R_o * F^{(D1-D2)}$. As aforementioned, the granitic rock is derived from the monzonite by means of about 30% of fractional crystallization. The calculated K/Rb (291) is very close to the average granite-gneiss (K/Rb = 297) of the Cheddar Granite, indicating a reasonable petrogenetic model.

5.7 Summary

The dome-shaped Cheddar Granite is mainly composed of biotite-hornblende gneissic granite with sporadic monzonite and tonalitic xenoliths. ~~A large~~ outcrop of assimilated paragneisses is sited around N. Eels Lake area. The whole-rock Rb-Sr isochron age (1207 ± 46 Ma) indicates a syn-tectonic intrusion. The concordant orientation of foliation between the granite and country

rocks, and limited contact aureole suggest that the Cheddar Granite has subjected to a high grade (amphibolite) regional metamorphism. Chemically, the granite-gneiss and monzonitic rocks are alkalic with albitic feldspars and sodic-calcic amphiboles.

Both whole-rock geochemistry and normative projections support the hypothesis that the monzonite, granite-gneiss and later dykes are genetically related and probably comagmatic. The internal variations can be explained by extensive fractional crytallization of large amounts of feldspars, accompanied by smaller amounts of mafic and accessory minerals. Quantitatively, about 30% fractionation is required to differentiate the monzonitic melt to the most evolved granite.

The horizontal or upward curvature of normalized REE patterns are contrary to the fractionation of HREE-enriched accessory phases (eg. zircon) as predicted from variations of trace-elements. Such an enhancement of HREE is commonly found in peralkaline suites in that the magmatic REE fingerprint is autosomatized by later alkali - volatile - enriched hydrothermal fluids at the deuteric stage; F-complexing is considered to be an important mechanism.

The areal distributions of U and Th in the Cheddar Granite suggest no generalized distribution pattern of

radioactive elements as declared by Ingham and Keevil (1951). However, there are two compositional highs in the northern half of the pluton; the U contents also increase northeasterly toward the area of abundant uraniferous pegmatites and greisen-type uranium deposits. Nb and Zr show a consistent trend of decreasing outward from the compositional high. The coincidence of compositional high and residual high where the assimilation paragneiss inclusion is sited may suggest that the chemical assimilation has little effect on the overall differentiation trend of the Cheddar Granite.

The linear relationship among tonalitic xenoliths, monzonite and granite-gneiss suggest a restite-unmixing model. The estimated parent with higher contents of Na_2O, total iron and peculiar trace-element concentrations is comparable with the composition of the Grenville dacite and/or the trondhjemitic suites in this part of the Grenville Province. It requires 15% equilibrium partial melting to produce a K/Rb melt similar to the monzonitic phase of the pluton.

6.0 MULOCK BATHOLITH

6.1 General Characters And Intrusive Relations

The Mulock Batholith is an elongated complex, extending northwestwards from Widdifield Township through Mulock and Merrick Townships to north Notman Township (Fig.2-6-1). It covers an area of more than 150 km^2 and extend farther north into Gooderham and Kenny Townships (ODM Map No.2216; OGS Map 2361).

It is composed predominantly of biotite - hornblende granite, porphyritic biotite-rich gneiss with feldspar phenocrysts and minor granodiorite. All are intruded by later granitic and aplitic dykes. Metasedimentary xenoliths are common at the southeast border zone, while the migmatitic paragneisses are interfingering with this complex along the western margin. Later tectonic deformation associated with faults and shear zones is marked by mylonitization and offsetting of foliations. Augen gneisses with cataclastic texture occur locally.

The batholith is a concordant intrusion with catazonal characteristics; the prominent NW-trending foliation with steep to moderate northeasterly dip indicate a possible laccolith - like body intruded by forceful injection. Biotite-rich paragneisses derived from greywacke or immature siltstone are the major enveloping rocks. Contact metamorphism is limited or

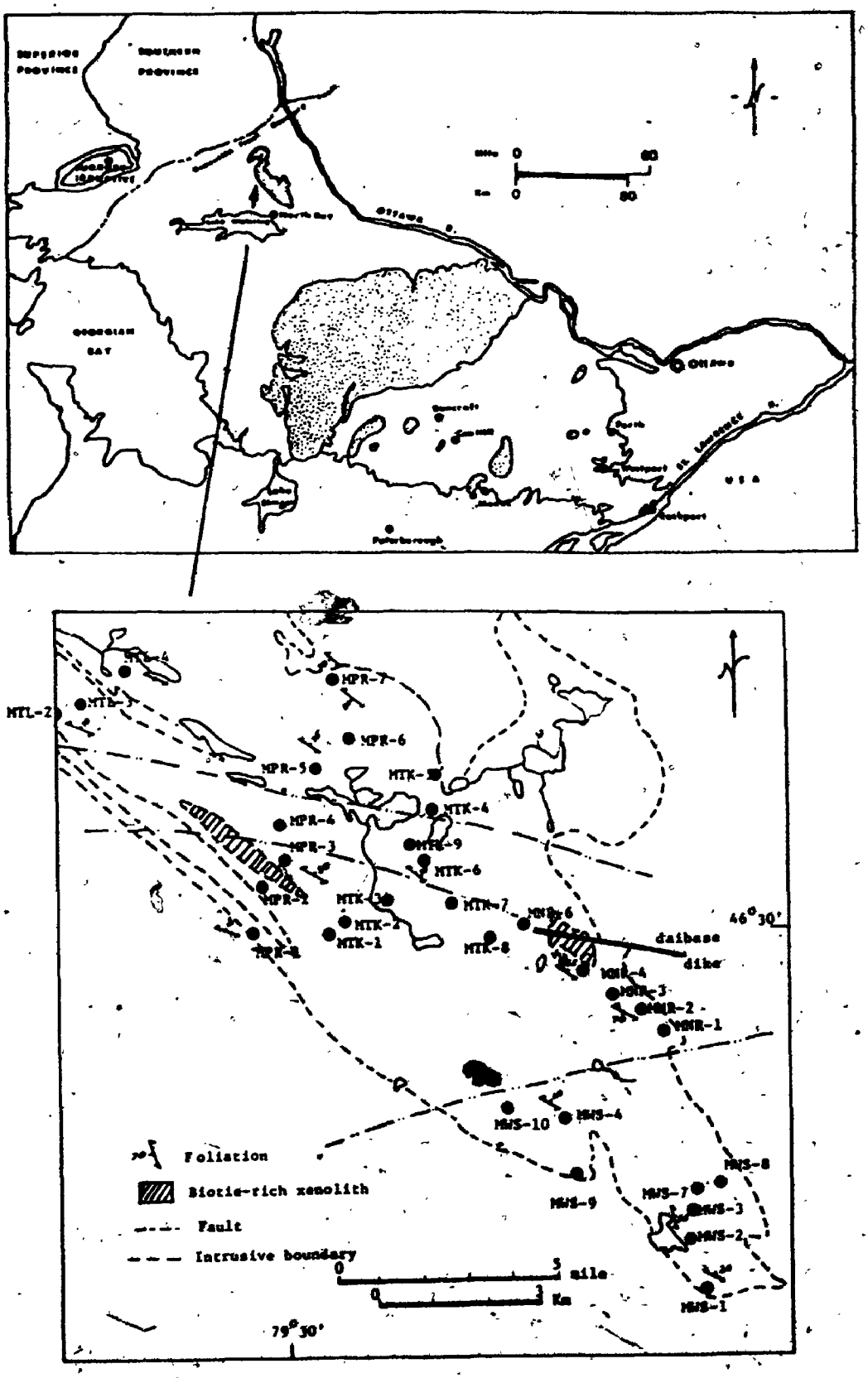

Figure 2-6-1. Sample location map of the Mulock Batholith.

obscured; only limited outcrops of biotite schist show garnet crystal, probably of hornfels origin; the regional metamorphism is in upper amphibolite facies.

6.2 Petrography

With few exceptions, most rocks of this batholith fall in the granite (adamellite) field of Streckeisen (1976, See Fig. 2-6-2). They are medium- grained with a strong planar foliation. Porphyritic varieties show mylonitization and recrystallization; mainly pinkish K-feldspar mingled with later or secondary quartz form the phenocrysts which deflect the rock foliations.

In general, samples of the granitic body have less than 15% mafic minerals (colour index ranging from 3.2 to 16.1) and about equal amounts of plagioclase and K-feldspar (average feldspar ratio = 0.55). They are hypidiomorphic-granular with a great amount of feldspar and quartz and subordinate biotite and hornblende. Sphene, zircon, apatite, allanite, epidote and muscovite are common accessories.

Both K-feldspar and plagioclase are euhedral to anhedral and mutually intergrown. Microcline with cross-hatch twinning is the chief K-feldspar; microperthite is also observed locally. Plagioclase is well-twinned with little or no alteration and no zoning has been detected. Late vermicular intergrowth is

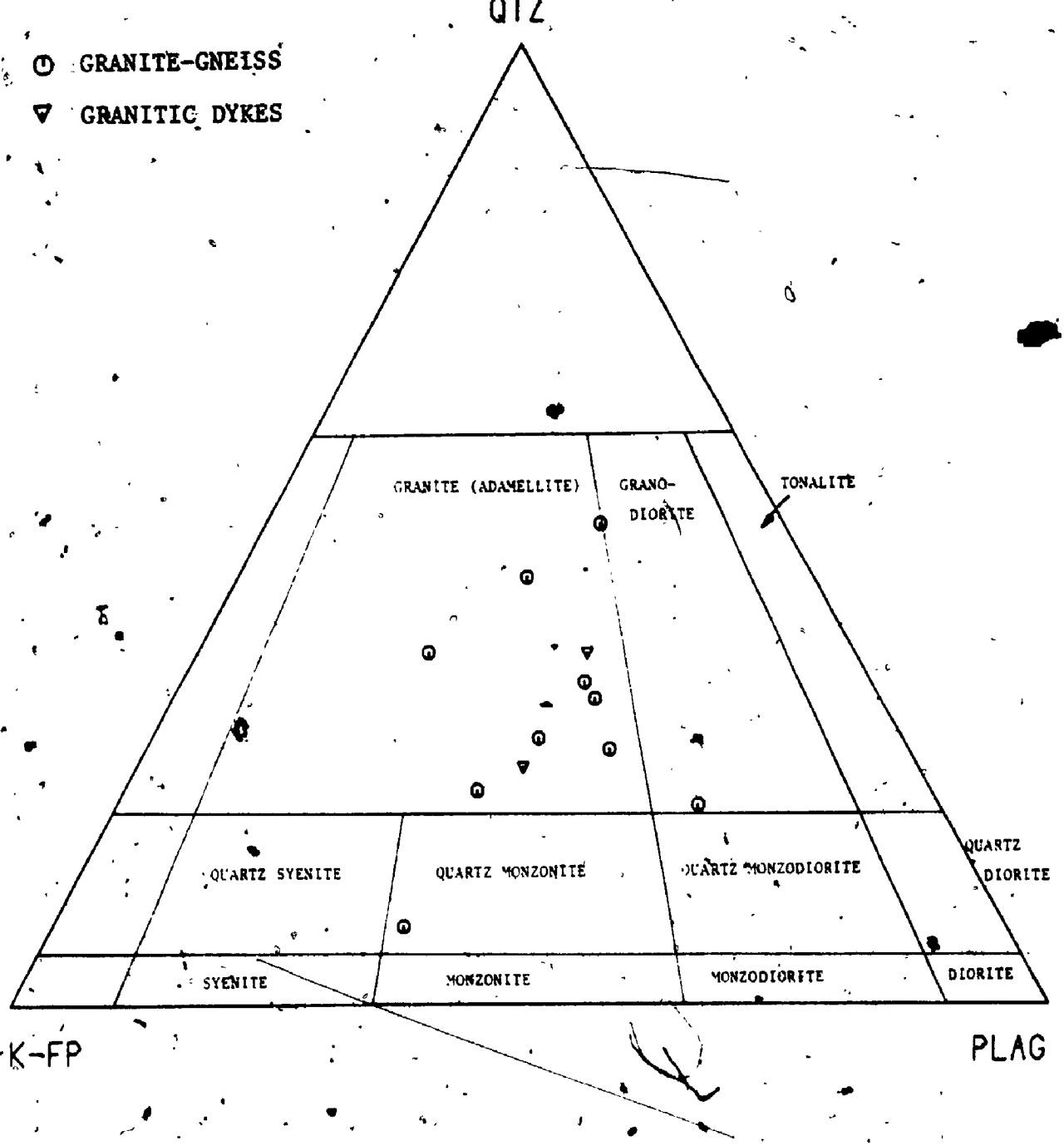

Figure 2-6-2. Modal classification of the Mulock Batholith (after Streckeisen, 1976).

present locally. Chemical compositions of representative plagioclase and K-feldspar are given in Table 2-6-1. Average composition of plagioclase is about sodic - oligoclase (An_3 to An_{15}). The lack of anorthite content in the K-feldspar reflects its microcline origin with no exsolution of plagioclase. Quartz subhedra show undulose extinction and mosaic texture which are indicative of high strain and recrystallization. Granulation and elongation of quartz are also common.

Biotite and hornblende are major minerals; relative to biotite, hornblende is less abundant or absent in most samples. Biotite occurs as euhedral to subhedral grains with a pleochroic scheme from Y = Z = dark greenish brown to X = straw yellow to greenish yellow, it is often altered to chlorite or oxidized to brownish ferruginous material. Hornblende is embayed by microcline and quartz and is usually fractured. Chemical compositions and calculated formulae of biotite and hornblende are given in Table 2-6-2. The Fe_2O_3 content of biotite was determined on concentrate from sample MTK-6 by means of titration; the Fe_2O_3/FeO ratio was then calculated for other samples. Chemically, these biotite can be classified as Fe^{2+}-biotite of Foster (1960; See Fig. 2-6-3). Hornblende is calcic in composition (Leake, 1968) and is similar to ferrohastingsite (Deer et al., 1966), except that the

Table 2-6-1. Chemical compositions and calculated formulae of feldspars from the Mulock Batholith

	(a) Plagioclase			(b) K-feldspar		
Sample No.	1 MNR-2-1	2 MTK-6	3 MTL-3-2	1 MNR-2-1	2 MTK-6	3 MTL-3-2
(wt%)						
SiO_2	67.67	67.36	65.73	65.23	65.07	65.17
Al_2O_3	20.55	20.56	21.71	18.53	18.46	18.39
CaO	0.72	1.23	2.45	0.00	0.00	0.00
Na_2O	11.15	11.01	9.95	0.38	0.77	0.62
K_2O	0.13	0.26	0.14	16.10	15.30	15.63
Total	100.22	100.42	99.98	100.24	99.60	99.81
Si] Z	11.811	11.764	11.544	12.005	12.016	12.024
Al] Z	4.227	4.231	4.493	4.019	4.017	3.998
	16.038	15.995	16.037	16.024	16.033	16.023
Na] X	3.773	3.728	3.388	0.136	0.276	0.222
Ca] X	0.135	0.230	0.461	0.000	0.000	0.000
K] X	0.029	0.058	0.031	3.779	3.604	3.678
	3.937	4.016	3.880	3.915	3.879	3.900
O	32	32	32	32	32	32
(mol%)						
Ab	95.84	92.83	87.31	3.46	7.11	5.69
An	3.42	5.73	11.88	0.00	0.00	0.00
Or	0.74	1.44	0.81	96.54	92.89	94.31

Table 2-6-2. Chemical compositions and calculated formulae of biotite and amphibole from the rocks of Mulock Batholith

(a) Biotite				(b) Amphibole		
Sample No.	MTL-3-1	MTK-6	MNR-2-1	MTK-6	MTL-3-1	Ferro-hastingsite
SiO_2	35.59	35.66	35.04	39.35	39.05	37.49
TiO_2	1.79	1.76	1.92	0.48	0.68	0.86
Al_2O_3	13.89	13.29	15.05	10.42	10.49	10.81
Fe_2O_3	6.53	6.78	6.78	-	-	7.52
FeO	21.05	21.84	21.83	28.35	27.73	25.14
MnO	0.54	0.64	0.88	0.77	0.69	0.95
MgO	5.34	5.38	3.47	3.50	3.67	1.34
CaO	0.03	0.02	0.02	10.59	10.67	9.77
Na_2O	0.04	0.04	0.02	1.93	2.04	2.06
K_2O	9.60	9.61	9.55	1.91	1.93	1.91
Total	94.58	95.02	93.56	97.30	96.95	97.85
Si (Z)	5.664	5.682	5.607	6.374	6.339	6.074
Al^{iv} (Z)	2.336	2.318	2.393	1.626	1.661	1.926
	8.000	8.000	8.000	8.000	8.000	8.000
Al^{vi} (Y)	0.268	0.176	0.444	0.363	0.346	0.138
Ti (Y)	0.236	0.211	0.231	0.058	0.083	0.105
Fe^{3+} (Y)	0.781	0.812	0.816	-	-	0.917
Fe^{2+} (Y)	2.799	2.908	2.919	3.840	3.764	3.408
Mg (Y)	1.266	1.276	0.827	0.845	0.888	0.323
Mn (Y)	0.073	0.086	0.119	0.106	0.095	0.131
	5.423	5.469	5.355	5.212	5.176	5.020
Ca (X)	0.005	0.003	0.003	1.838	1.856	1.696
Na (X)	0.012	0.012	0.006	0.606	0.642	0.648
K (X)	1.948	1.952	1.948	0.395	0.400	0.395
	1.965	1.968	1.958	2.839	2.898	2.740
O	22	22	22	23	23	23
$Mg/Fe_t+Mg+Mn$	0.257	0.176	0.177	0.176	0.187	0.068
Fe_t/Fe_t+Mg	0.739	0.745	0.819	0.821	0.809	0.931
mole of annite	0.467	0.485	0.487	-	-	-

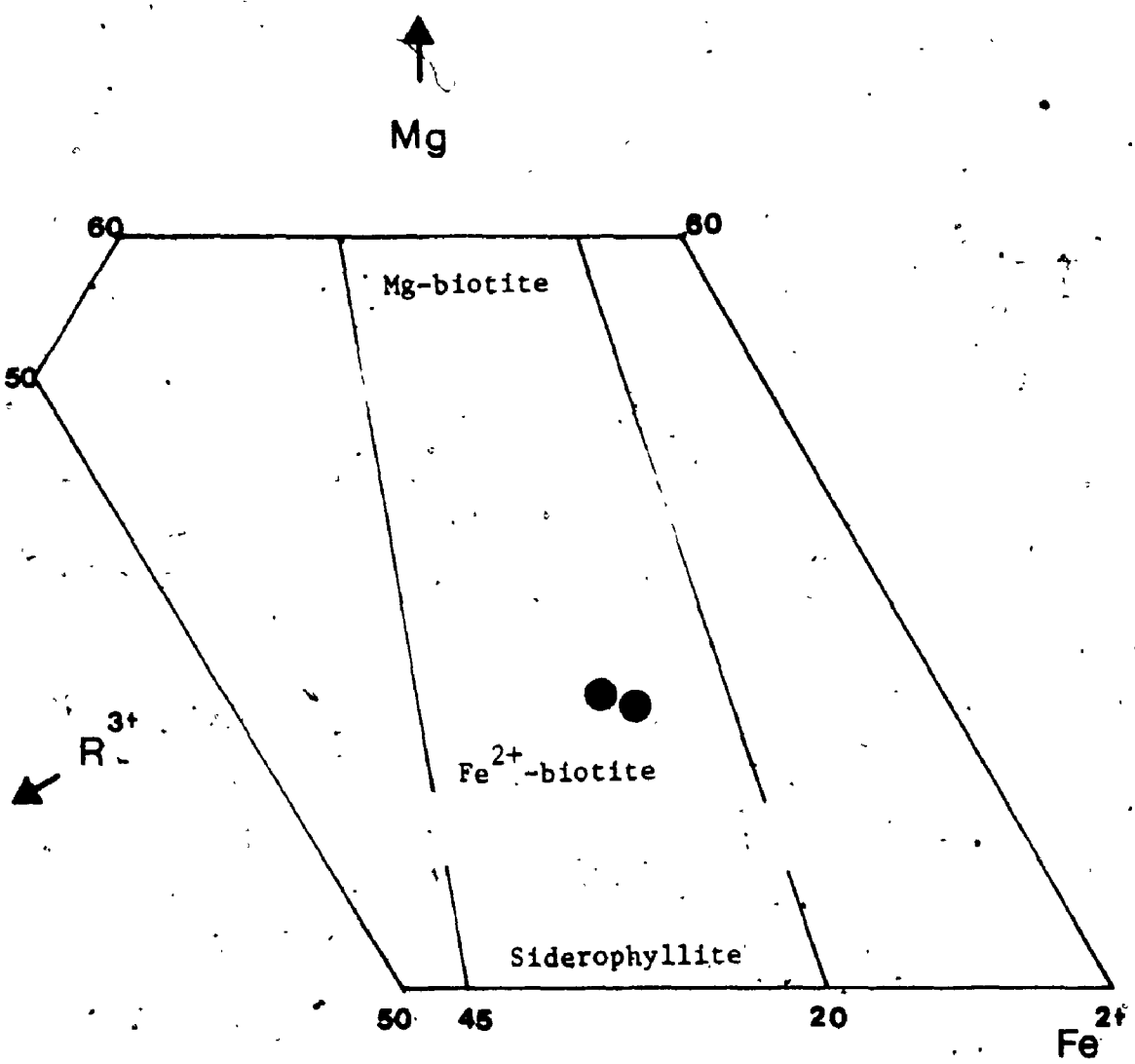

Figure 2-6-3. The Mg-Fe^{2+}-R^{3+} relation in trioctahedral micas of the Mulock Batholith (after Foster, 1960)

$$R^{3+} = Al^{vi} + Fe^{3+} + Ti^{4+}$$

former is high in SiO_2, MgO and low in FeO (Table 2-6-2).

Secondary muscovite flakes are alteration products of plagioclase or biotite. Epidote usually forms subhedral grains concentrated along the contacts between biotite and plagioclase or inside the altered plagioclase. One epidote grain associated with biotite encloses an allanite crystal at the core. Most sphene is considered to be a late mineral phase and is often associated with opaques, epidote and biotite. Zircon, apatite and allanite occur as individual grains or as inclusions of major minerals. Magnetite, the main opaque mineral, forms as discrete grains or as an oxidation product of biotite. Under reflected light, patches of exsolution ilmenite and hematite also occur within magnetite crystals.

6.3 Whole-rock Geochemistry

6.3.1 Major-oxides -

Composition of the Mulock Batholith is metaluminous with normative diopside or normative corundum < 1%. The mean molar aluminum to total alkali-lime ratio is about 0.92, ranging from 0.85 to 1.05; the overall agpaitic index is about 0.904, ranging from 0.802 to 1.05. Direct measurement of the alkali-lime index is not possible as the total

alkalies and calcium oxide trends do not intersect within the range of samples analyzed. However, rocks of the batholith fall within the alkaline field in the (Na_2O+K_2O) vs. SiO_2 plot (Fig. 2-6-4; Miyashiro, 1978).

The average composition of the batholith and other similar rock-types are summarized in Table 2-6-3. In general, the Mulock Batholith is similar to that of the biotite-hornblende granite of Nockolds (1954), except that the former has higher Na_2O/K_2O ratio and oxidation index (i.e. O.I. = $2Fe_2O_3$ * 100 / ($2Fe_2O_3$+FeO)). In comparison with the mean biotite granite of the North Bay Area (Lumbers, 1971), this batholith contains relatively higher CaO and MgO, but lower SiO_2, Al_2O_3 and total iron. In addition, the batholith shows a broad band from adamellite to calc-alkaline granite in the normative Qtz-Plag-Or plot (Fig. 2-6-5), except for one sample which lies close to the composition of calc-alkaline syenite.

According to the classification of O'Connor (1965), rocks of the Mulock Batholith cluster in the granite field and lie within the low temperature trough of Kleeman (1965; See Fig. 2-6-6). Similarly, in the Qtz-Ab-Or system (Fig. 2-6-7), most samples fall in Winkler and Von Platen's granite field (1961), while the rest lie within the

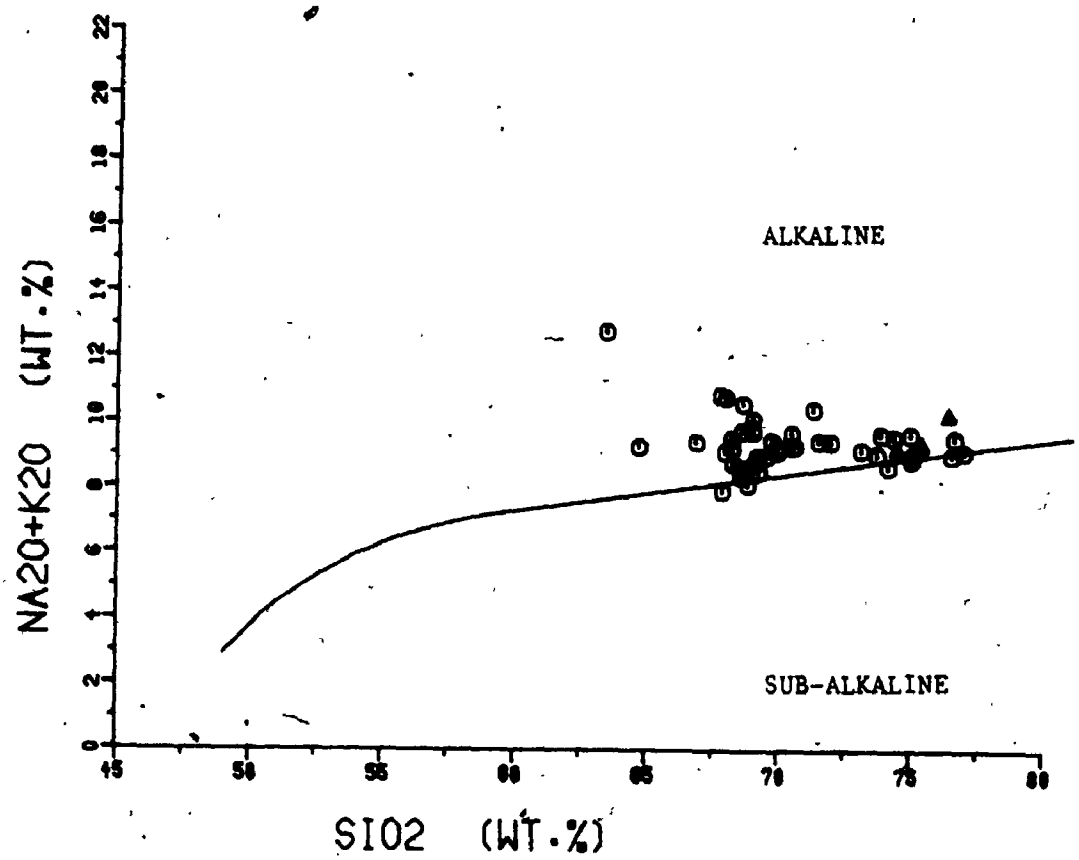

Figure 2-6-4. Na_2O+K_2O vs. SiO_2 plot of the Mulock Batholith. Solid-line separates the alkaline and subalkaline fields of Miyashiro (1978).

⊙ GRANITIC GNEISS
▲ GRANITIC-APLITIC DYKE

Table 2-6-3. Comparison of average compositions of the Mulock Batholith with other similar rock-types

(wt.%)	1 (n=41)	2 (n=6)	3 (n=121)	4 (n=72)	5 (n=3)	6 (n=6)	(ppm)	7 (n=41)	8
SiO_2	70.48	70.56	69.15	72.08	74.93	64.45	Rb	114	** 150
TiO_2	0.50	0.40	0.56	0.37	0.12	0.73	Sr	189	285
Al_2O_3	13.89	14.00	14.63	13.86	15.23	16.02	Ba	1034	600
TFe_2O_3	3.44	* 3.59	* 3.74	* 2.71	* 1.30	6.45	Nb	22	20
Fe_2O_3	1.47	0.91	1.22	0.86	0.59	1.16	Zr	348	180
FeO	1.92	2.41	2.27	1.67	0.64	4.77	Y	24	40
MnO	0.05	0.06	0.06	0.06	0.02	0.12	Ga	25	18
MgO	0.46	0.48	0.99	0.52	0.23	0.76	Ni	4.5	0.5
CaO	1.02	1.63	2.45	1.33	0.56	2.63	Cr	7.7	4
Na_2O	4.44	3.56	3.35	3.08	3.87	3.79	V	8.4	20
K_2O	4.99	5.39	4.58	5.46	4.77	4.60	Sc	4.0	5
P_2O_5	0.10	0.10	0.20	0.18	0.03	0.22			
LOI	0.40	0.50	0.54	0.53	0.49	1.02			
Na_2O/K_2O	0.89	0.66	0.73	0.56	0.81	0.82	K/Rb	389	220
							Rb/Sr	0.80	0.53
Oxidation ratio	0.60	0.43	0.52	0.51	0.65	0.33	Sr/Ca	316	-

1 Average of 41 granite-gneiss from Mulock Batholith (this study).
2 Average of 6 biotite-hornblende granite (Nockolds, 1954).
3 Average of 121 adamellite (Nockolds, 1954).
4 Average of 72 calc-alkaline granite (Nockolds, 1954).
5 Average of 3 biotite-granite from North Bay Area (Lumbers, 1971).
6 Average of 6 monzonite from North Bay Area (Lumbers, 1971).
7 Average trace elements of granite-gneiss from Mulock Batholith (this study).
8 Average trace elements of granite (Taylor, 1964).

* Calculated from FeO and Fe_2O_3.
** Rb 170, Sr 100 and Ba 840 ppm for average low-Ca granite (Turekian and Wedepohl, 1961).

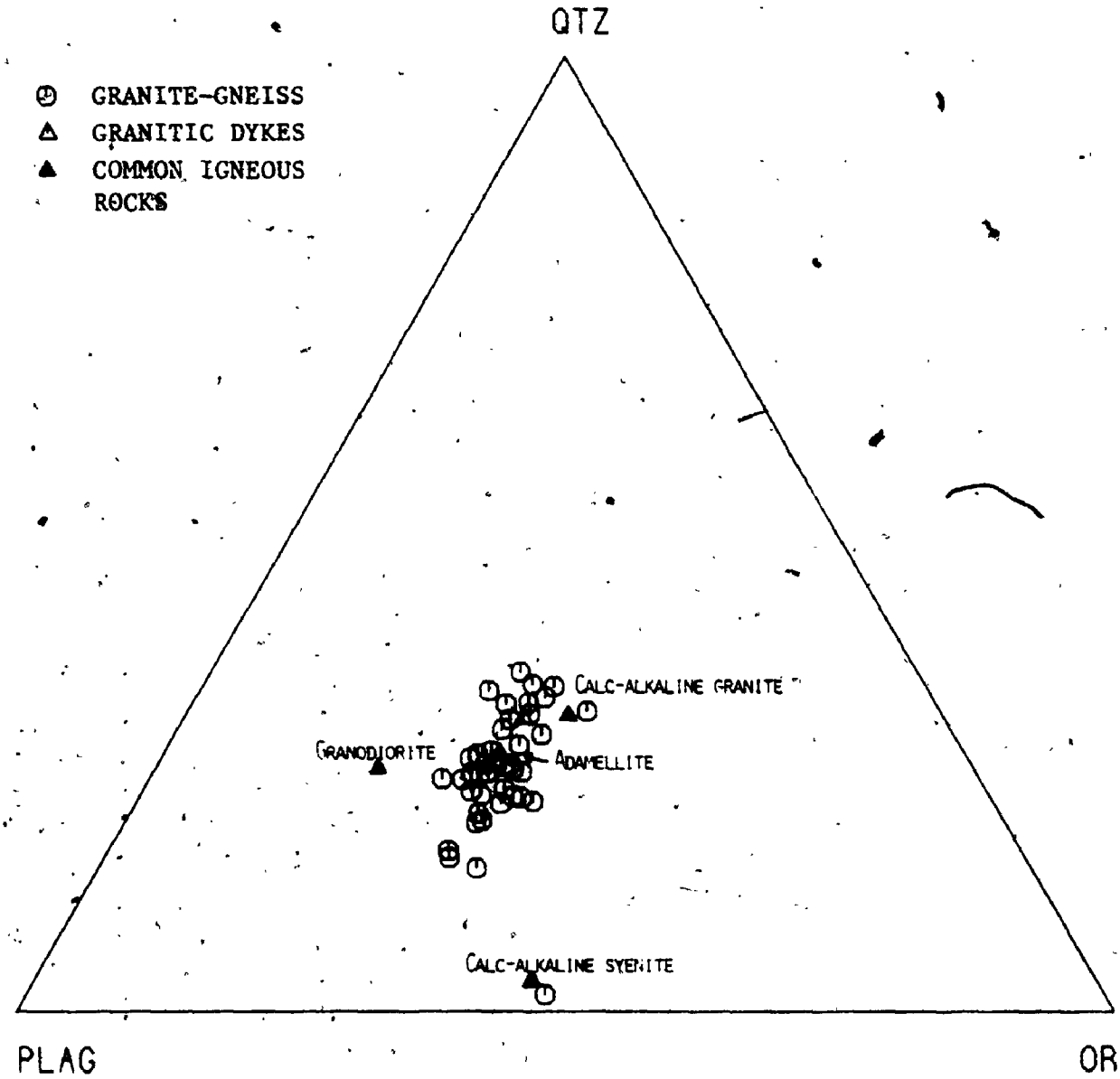

Figure 2-6-5. Normative Qtz-Or-Plag ratios of the Mulock Batholith and common igneous rocks (calculated from Nockolds, 1954).

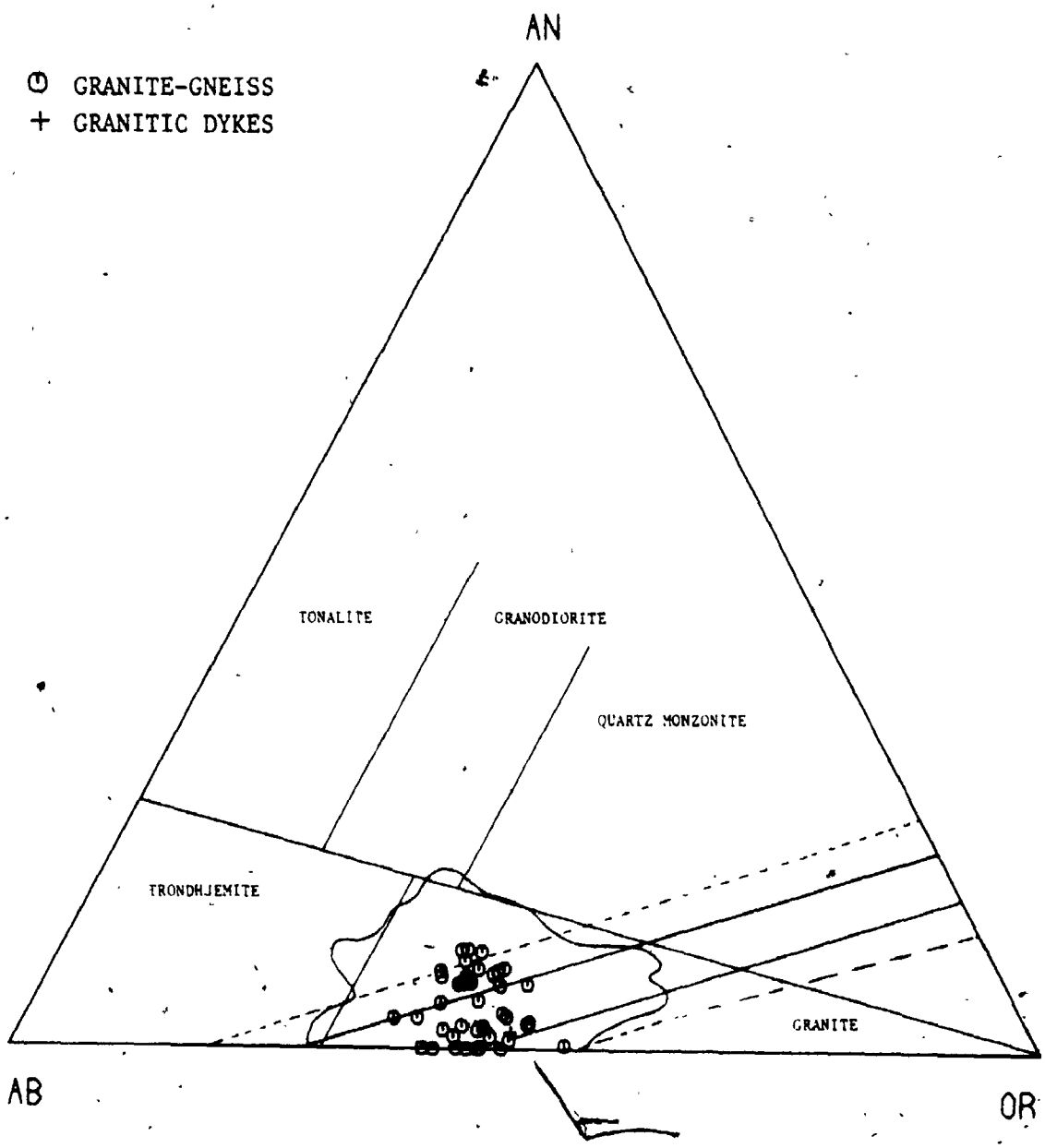

Figure 2-6-6. Normative Ab-An-Or ternary diagram of the Mulock Batholith. The irregular solid boundary is the 2% contour of Tuttle and Bowen (1958) enclosing most of granitic rocks that contain more than 80% normative Ab+An+Or+Qtz. The solid-lines indicate the boundaries of low temperature trough; dashed-lines show uncertainty due to analytical error (Kleeman, 1965). Classification scheme is from O'Connor (1965).

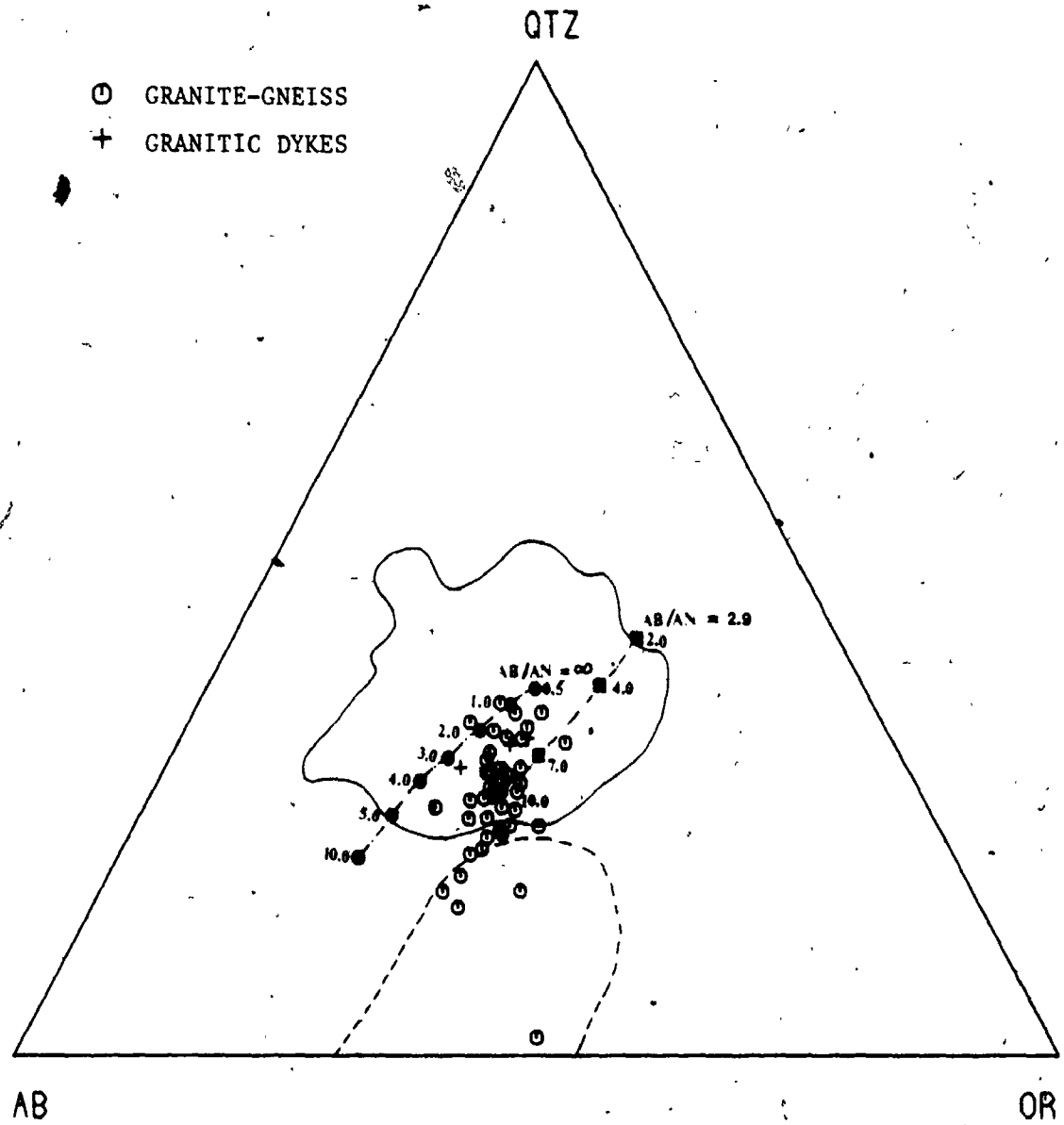

Figure 2-6-7. Normative Qtz-Ab-Or ternary diagram of the Mulock Batholith. The irregular solid boundary encloses analyses of 1190 granitic rocks of Winkler and Von Platen (1961). The irregular dashed-line shows the compositional field of syenitic rocks from Gardar Province of Greenland (Watt, 1966). Experimentally determined ternary minima (Tuttle and Bowen, 1958; Luth et al., 1964) and minima in An - bearing systems (James and Hamilton, 1969) are shown by solid circles and solid squares, respectively.

syenite field of Gardar Province (Watt, 1966) or within the transition zone.

The composition distribution in the Qtz-Ab-An-Or-H_2O system suggests that the Mulock Batholith was of magmatic origin with a general trend of increasing quartz content during differentiation. In addition, the composition of most samples corresponds to the minimum melt at about P_{H2O} = 10 Kb and Ab/An = 2.9 (Winkler, 1967; See Fig. 2-6-7), whereas the late differentiates and aplitic dykes were crystallized at lower P_{H2O} (1 - 3 Kb) and less An content condition.

As shown in Table 2-6-4, TiO_2, Al_2O_3, Fe_2O_3, MgO, MnO and CaO show strong negative correlations with SiO_2, while Na_2O and K_2O yield no significant trends. In addition, it was noted that later dykes are always located at the most evolved end of each variation trend in the Harker diagrams. It is thus suggested a comagmatic relation exists between the host granite and later dykes, the latter possibly representing the crystallized residual of the batholith. In terms of Na_2O-K_2O-CaO variation (Fig. 2-6-8), there is a trend of decreasing CaO at about constant Na_2O/K_2O ratio during differentiation. On the total alkali-FeO-MgO diagram (Fig. 2-6-9), the batholith rocks show a moderate Fe-enrichment relative to magnesium and alkalies, similar to that

Table 2-6-4. Correlation coefficients of inter-element variations for the Mulock Batholith

Correlation	Granitic rocks + dykes	Correlation	Granitic rocks + dykes
SiO_2 vs. TiO_2	-0.8907	SiO_2 vs. F	-0.4019
Al_2O_3	-0.8192	Cl	-0.2983
Fe_2O_3	-0.7489	S	-0.5011
MnO	-0.7470	Ga/Al	0.1030
MgO	-0.8062	K/Rb	-0.2907
CaO	-0.7808	Rb/Sr	0.7228
K_2O	-0.1977	Sr/Ba	0.2501
P_2O_5	-0.3823	Sr/Ca	0.4694
Na_2O	-0.1910	Zr/Y	0.3990
Rb	0.2701	Y/Ca	0.4749
Sr	-0.7740	Cr/Mg	0.5236
Ba	-0.7183	V/Mg	0.4015
Zr	-0.7557	Ni/Mg	0.5058
Nb	-0.1514	Fe/Mg	0.3756
Y	-0.4479	Cr/Fe	0.3122
Ga	-0.4467	V/Fe	0.1702
Pb	0.1954	Ni/Fe	0.3676
Zn	-0.3717	Nb vs. Ga/Al	0.5265
Cu	-0.4811	Nb vs. Y	0.7835
Ni	-0.1624	Al_2O_3 vs. Ga	0.1539
Cr	-0.7450		
V	-0.4051		
U	0.2788		
Th	0.2846		

4

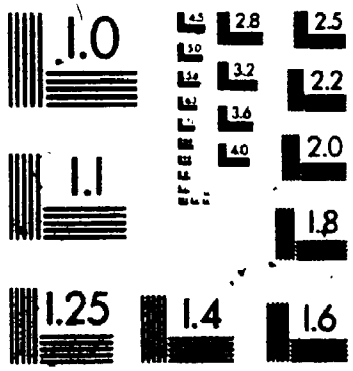

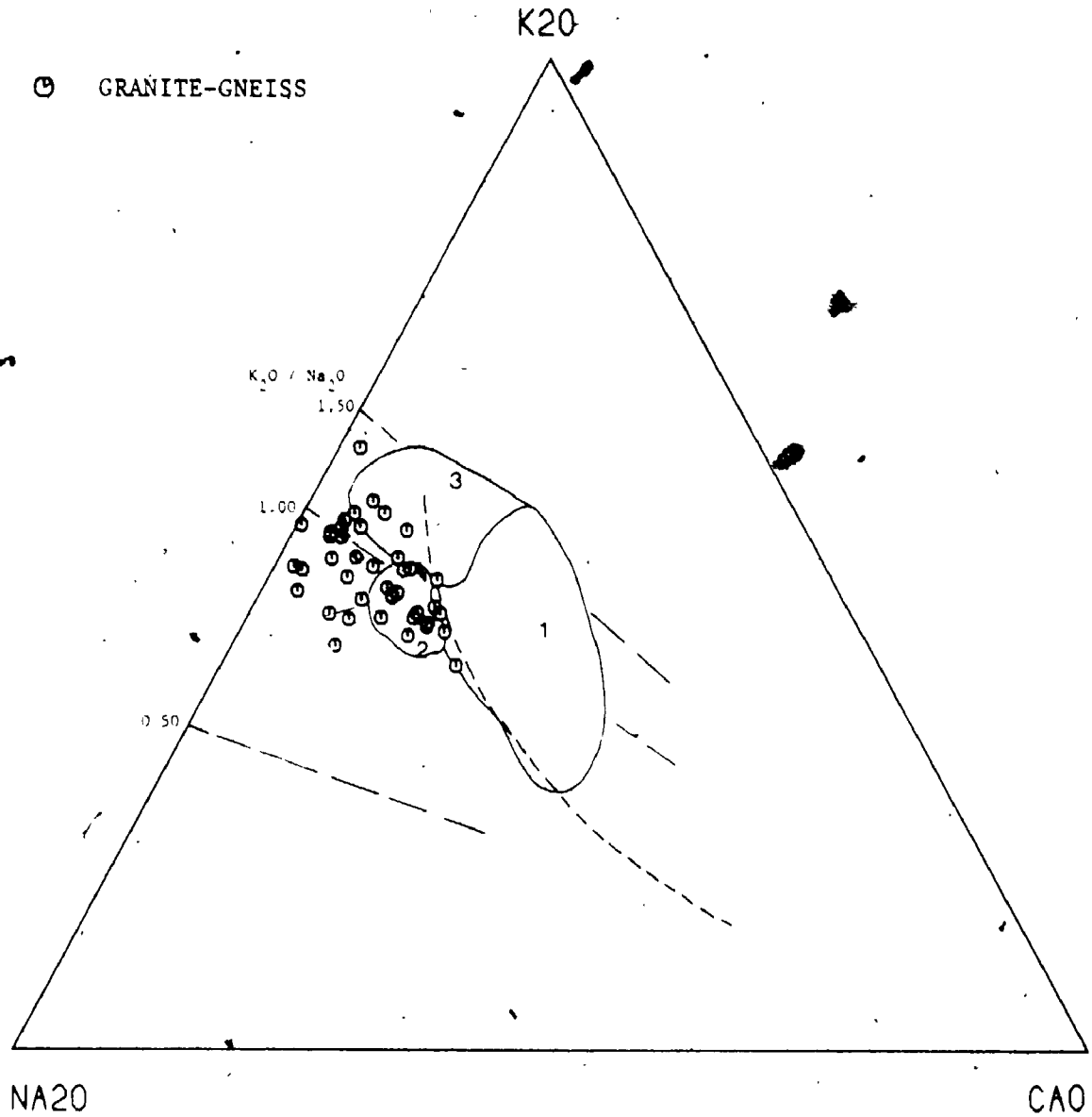

Figure 2-6-8. Na_2O-K_2O-CaO variation diagram of the Mulock Batholith.

---- Calc-alkaline trend of Southern California Batholith (Nockolds and Allen, 1956).

Field 1 : Frontenac-type granite
Field 2 : Westp[illegible]-type granite
Field 3 : Rockport-type granite
(Sauerbrei, 1966)

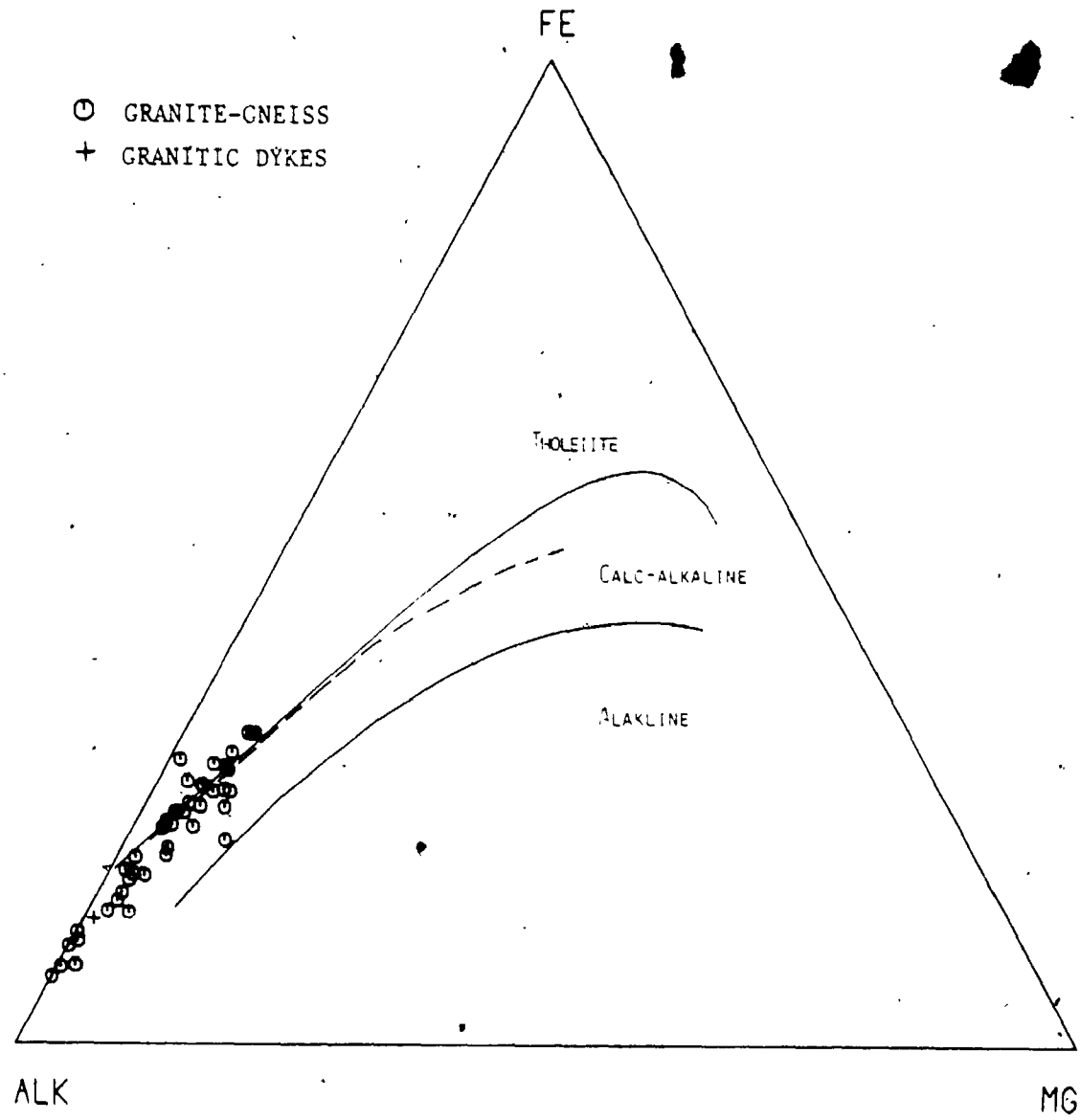

Figure 2-6-9. AFM diagram of the Mulock Batholith.
Solid-lines separate the tholeiite, calc-alkaline and alkaline fields (Barker and Arth, 1976).

---- Typical calc-alkaline trend of Souther California Batholith (Nockolds and Allen, 1956).

of a calc-alkaline trend.

6.3.2 Trace-elements -

The Mulock Batholith has relatively lower Rb, Sr, Y, V and higher Ba, Zr, Ni, Cr concentrations (Table 2-6-3) than those of average granite (Taylor, 1964,). The mean K/Rb ratio is about 389, which is higher than both the crust (230) and the "normal" igneous rocks (150-300; Taylor, 1965).

Correlation coefficients of trace-element variations as a function of SiO_2 for the batholith are given in Table 2-6-4. Sr, Ba, Zr and Cr have strong negative correlations with SiO_2, while Y, Ga, Cu and S show interpretable trends with negative slopes during differentiation. The K/Rb vs. Rb variation diagram (Fig. 2-6-10A) illustrates again the comagmatic nature of the granite and later dykes. In addition, variations of Sr/Ba, Ba/K and Sr/(Ca+K) as a function of SiO_2 (Fig. 2-6-10, B-D) support the important role of feldspar fractionation in the course of differentiation. In terms of Rb-Ba-Sr ternary relations (Fig. 2-6-11), rocks of the batholith straddle the fields of normal and anomalous granites of Bouseily and Sokkary (1975) and show a moderate Rb-enriched trend. The relatively higher Sr in the most evolved granite and

Figure 2-6-10. Plots of alkali-alkaline earth element ratios of the Mulock Batholith.

(A) K/Rb vs. Rb plots.

G - differentiation trend of the batholith.

(B) Sr/Ba vs. SiO_2.

(C) Ba/K vs. SiO_2.

(D) Sr/(Ca+K) vs. SiO_2.

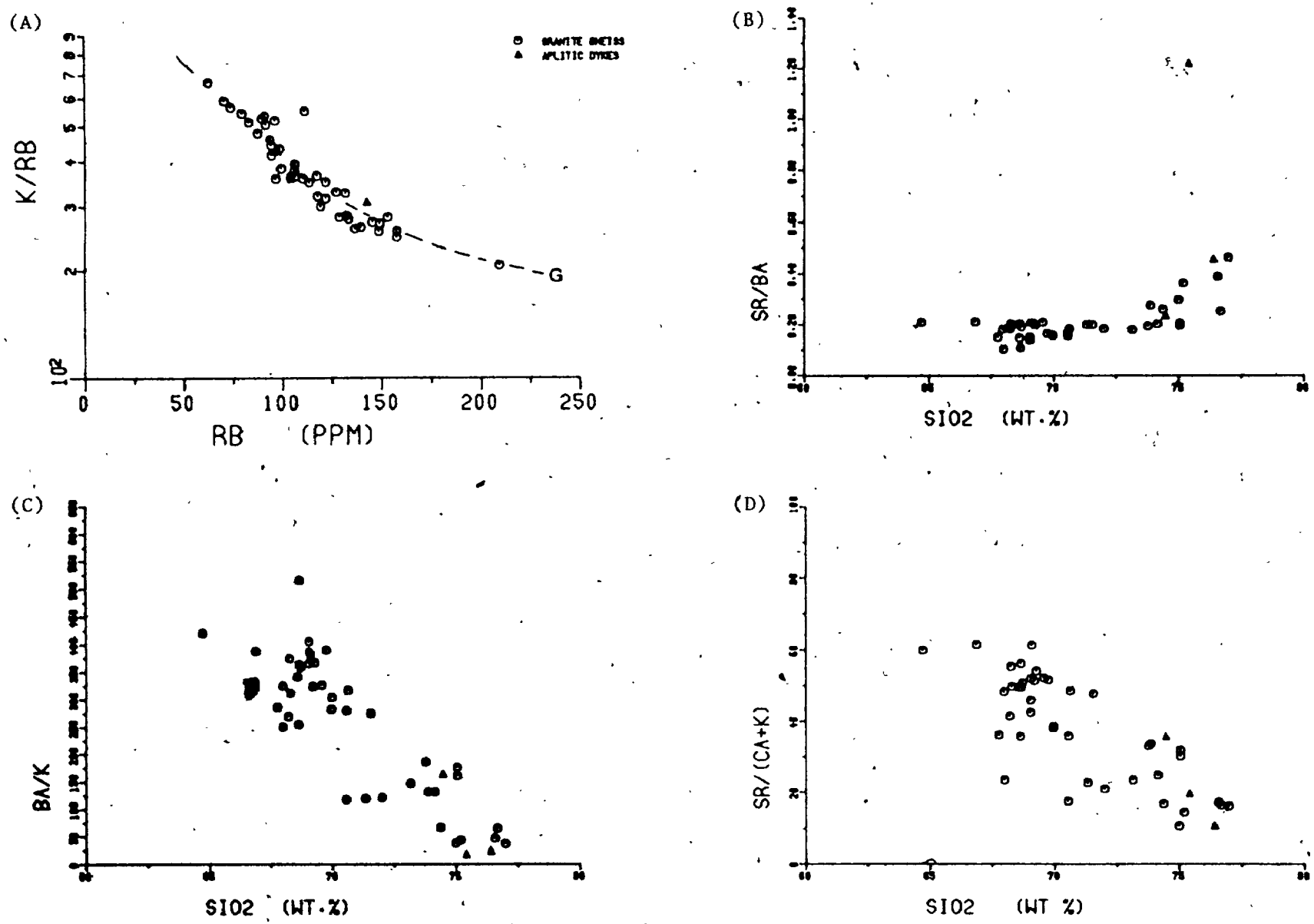
(A)
K/RB
RB (PPM)
0
50
100
150
200
250
G
(B)
SR/BA
SIO2 (WT.%)
(C)
BA/K
SIO2 (WT.%)
(D)
SR/(CA+K)
SIO2 (WT %)

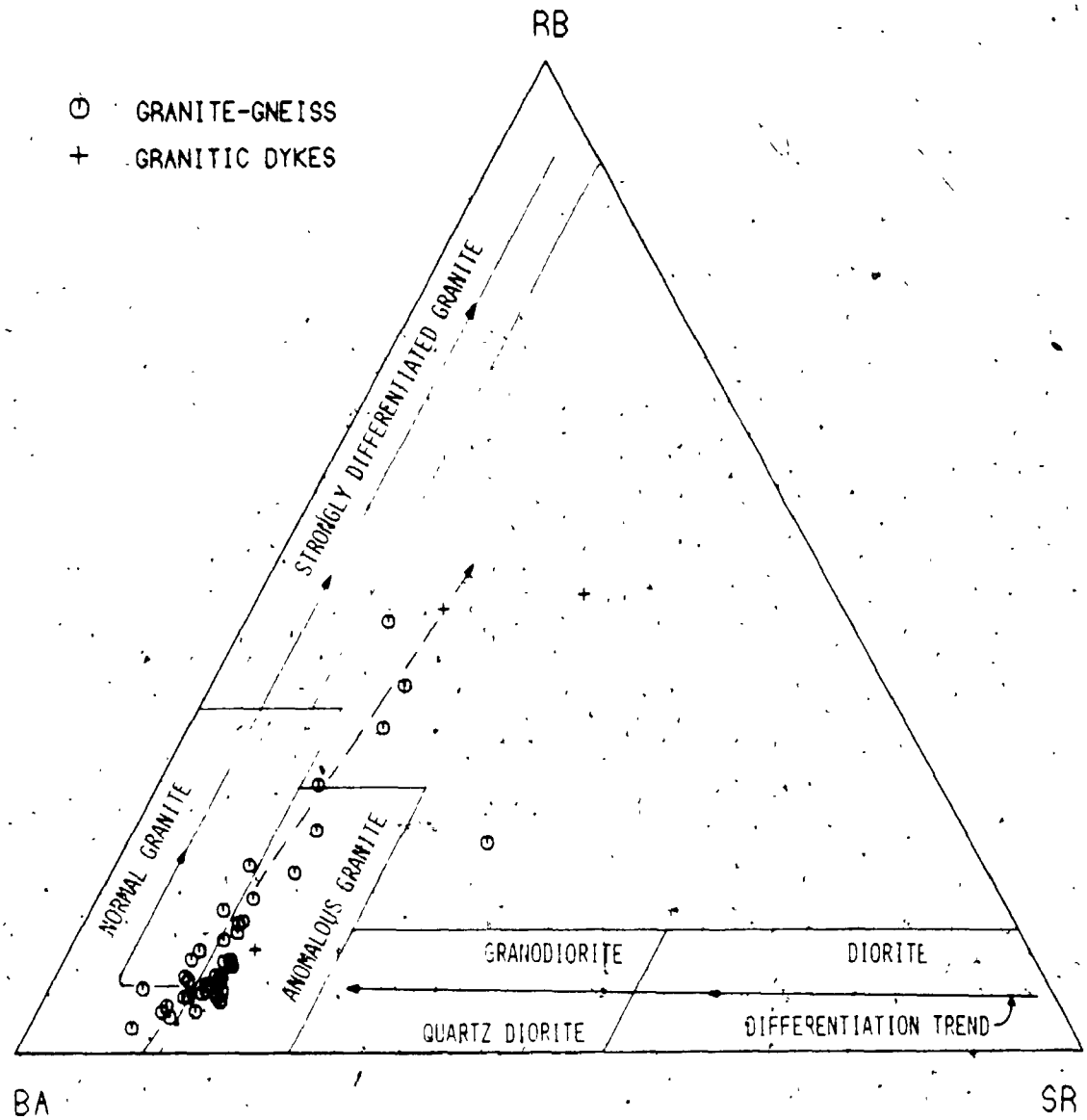

Figure 2-6-11. Rb-Ba-Sr ternary variation diagram of the Mulock Batholith. Classification scheme is from Bouseily and Sokkary (1975). Dashed-line indicates the differentiation trend of the Mulock Batholith.

aplitic dykes compared with the "strongly differentiated granite" may be due to its higher Sr source rock.

6.3.3 Rare-earth Elements -

Results of rare-earth element abundances and chondrite-normalized element ratios for the batholith and aplitic dyke are listed in Table 2-6-5. Their chondrite-normalized patterns are shown in Figure 2-6-12. All are LREE-enriched with Ce_N of 18-210, Yb_N 5.5-16 and $(Ce/Yb)_N$ of 2.25-26.25. There is a general correlation of total REE with rock type in that the aplitic dyke has the lowest REE concentrations.

The granite-gneisses of the main body display moderate REE fractionation trends with similar concentric parallel shapes. In general, the total REE abundances increase with increasing SiO_2, or the degree of defferentiation; the Eu/Eu* ratios decrease (i.e. increasing the negative Eu-anomaly) toward the more felsic rocks. Such an increase of negative Eu-anomaly can be expected by the gradual removal of feldspars (esp. plagioclase), which is consistent with variations of Sr and Ba in the batholith. In addition, the increase of $(Ce/Yb)_N$ value with increasing SiO_2 of the granite implies a

dykes were used in the modelling. Differentiation from the least differentiated sample MWS-2-2 (64.69% SiO_2) to the most evolved sample MNR-2-1 (75.18% SiO_2) required removal of a modal solid of 47% plagioclase, 22% K-feldspar, 22% hornblende, 5% biotite, 3% sphene and 0.7% apatite. A similar modal solid relates granite gneiss and the aplitic dyke. For both models, the amount of removed solid related to the initial magma is about 55%; the sum of squares of the residuals are 0.1147 and 0.4375 respectively, indicating a reasonably good fit of the model.

The large-ion-lithophile elements Rb, Sr and Ba are particularly useful for a petrogenetic study of granite, because they are almost entirely retained by major rock-forming minerals (eg. feldspars). Rb-Ba and Sr-Ba data of the batholith are plotted in Figure 2-6-14 along with the vectors showing the theoretical effects on melt composition of crystallizing a single mineral phase by means of Rayleigh fractionation. Unexpectedly, the distribution of data shows two trends with different slopes. Such inflections of the composition trend of the melt may be due to (1) a major change of liquidus mineralogy at a later stage of crystallization, or (2) loss of alkali- rich fluids from the magma after crystallization of the rocks of trend 1.

Although a relative increase in the proportions of biotite and K-feldspar in the extracted assemblage could

Figure 2-6-12. Chondrite-normalized REE distribution patterns of the Mulock Batholith.

(A) REE distributions for granite-gneiss.

(B) REE distributions for granitic and aplitic dykes.

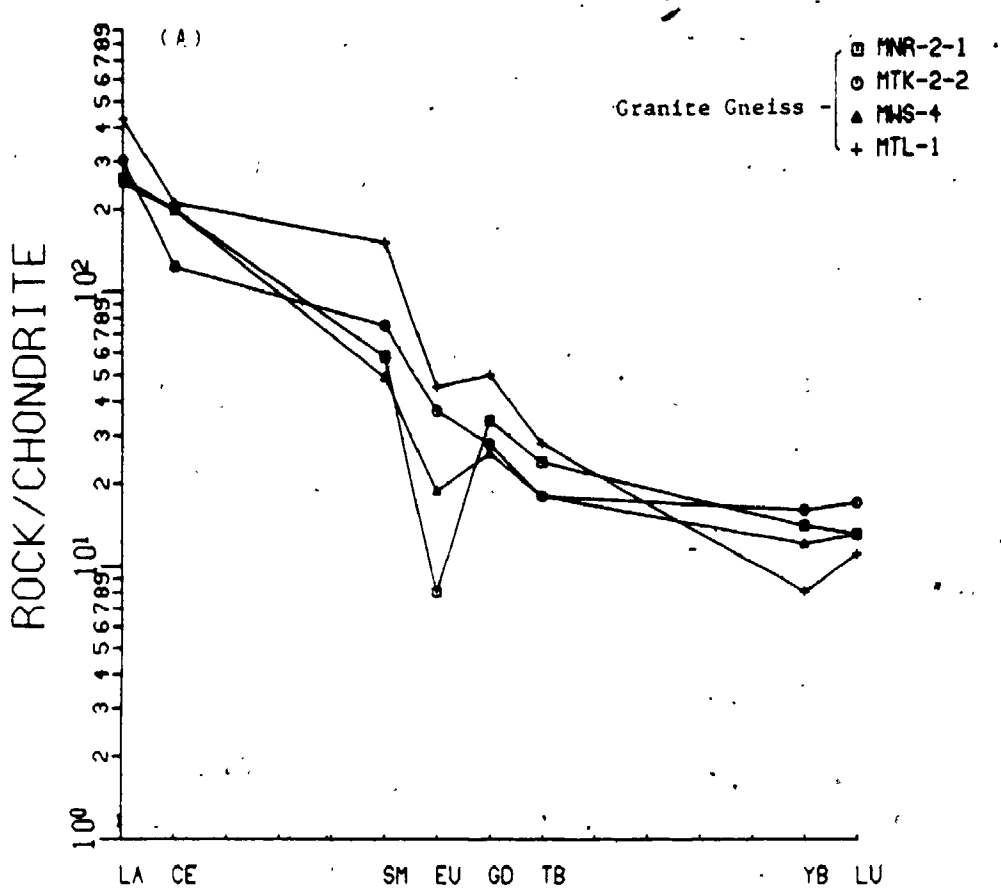
(A)
Granite Gneiss -
MNR-2-1
MTK-2-2
MWS-4
MTL-1
ROCK/CHONDRITE
LA CE SM EU GD TB YB LU

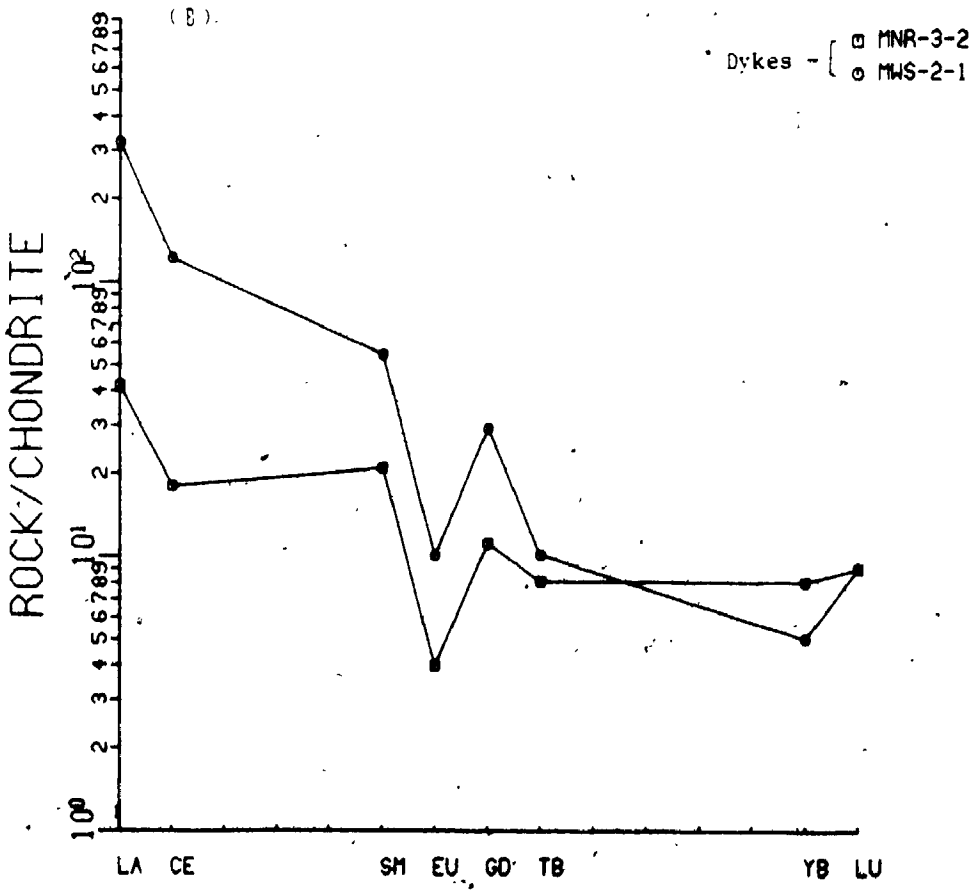
(B)
Dykes -
MNR-3-2
MWS-2-1
ROCK/CHONDRITE
LA CE SM EU GD TB YB LU

possible fractionation of zircon, which possess higher HREE partition coefficients.

Sample MTL-1, with monzonitic modal composition, contains the highest total REE contents and shows a strong REE fractionation pattern with $(Tb/Yb)_N$ = 3.5, which is double the HREE fractionation of the granite-gneiss ($(Tb/Yb)_N$ = 1.1-1.7). It is also similar to that of monzonite of the Loon Lake Pluton (Dostal, 1975), in which the granite has a less fractionated pattern and lower absolute concentrations of REE in comparison with monzonite. However, MTL-1 has a relatively larger negative Eu-anomaly and lower contents of Sr and Ba compared with Loon Lake monzonite.

The aplitic dyke (MNR-3-2) contains the lowest total REE with a flat, less fractionated pattern. This highly LREE depleted distribution curve is commonly found in later silicic veins or aplitic dykes (eg. Koljonen and Rosenberg, 1974; Mittlefehdt and Miller, 1983). It is suggested that such rapid diminishing of LREE with differentiation in the most felsic magma is likely due to early and continuing crystallization of small quantities of LREE highly enriched accessory minerals (eg. allanite, sphene and monazite).

6.4 Isotopic Geochemistry

Three representative granite-gneiss samples from the batholith have been analyzed for whole-rocks oxygen isotope; the $^{18}O/^{16}O$ ratios are 7.97, 8.18 and 8.57 o/oo (SMOW). According to the distinguish $\delta^{18}O$ values, Shieh and Schwarcz (1974) reported two types of granite in the Grenville Province of Ontario, which are correlated with the metamorphic grade and style of emplacement. Granites emplaced in the Ontario Gneiss Segment show relatively lower and uniform $\delta^{18}O$, ranging from 6.5 to 8.4. They concluded that such low values in this region may result from isotopic exchange with a low ^{18}O mafic reservior. The $\delta^{18}O$ values of the Mulock Batholith and its geological setting are comparable with Shieh and Schwarcz's conclusion. In addition, this batholith has a narrower range of $\delta^{18}O$ than their example of the Sturgeon Falls Granite (6.5 to 8.8; Shieh and Schwarcz, 1974).

The whole-rock Rb-Sr isochrons give ages of 1700 $\pm$ 150 Ma, 1330 $\pm$ 70 Ma and about 1200 Ma (or 1175 Ma adjusted by Baer, 1980) for three major plutonic events in the North Bay Area (Lumbers, 1971): (1) pre-tectonic sheet-like granitic masses (eg. Sturgeon Falls Granite), (2) pre- or syn-tectonic monzonitic intrusions (eg. Powassan-Bonfield Pluton), (3) syn-tectonic intrusions (eg. Mulock Batholith). Baer (1980) in the study of foliated and recrystallized granitic rocks from

the Timberlake Pluton, 25 km east-northeast of Mulock Batholith, suggested that the mylonitization or shearing of the plutonic rocks in the region occurred possibly as early as 1070 Ma ago and no later than 950 Ma ago. However, no quantitative data of initial $^{87}Sr/^{86}Sr$ ratio of the Mulock Batholith have been reported.

6.5 Petrogensis And Source Rocks

In addition to the strong negative correlation of most major-oxides with SiO_2, the CaO vs. MgO, Al_2O_3 vs. CaO and Al_2O_3 vs. SiO_2 plots (Fig. 2-6-13) with relation to the composition of major mineral components of the batholith, illustrate that the internal chemical variations of the Mulock Batholith can be explained by fractional crystallization of hornblende, plagioclase, biotite and, to some extent, K-feldspar. The decreases of TiO_2 and P_2O_5 with increasing SiO_2 also indicate the possible fractionations of sphene and apatite, respectively. In addition, the Al_2O_3 vs. SiO_2 (Fig. 2-6-13C) variation trend may also represent a "mixing line" of gradually increasing the proportion of quartz to total feldspar during differentiation.

The least squares method (Stormer and Nicholls, 1978) was employed to test the crystallization model for major-oxide variations in the batholith. Only mineral phases identified in the granite-gneiss and aplitic

Figure 2-6-13. Inter-elemental variation plots of the Mulock Batholith. (A) CaO vs. MgO (B) CaO vs. Al_2O_3 (C) Al_2O_3 vs. SiO_2 plot with relations to the compositions of major mineral components of the Mulock Batholith. Solid-line indicates the differentiation trend of the batholith. Dashed-lines connect the possible fractionation mineral pairs (Cox et al., 1979).

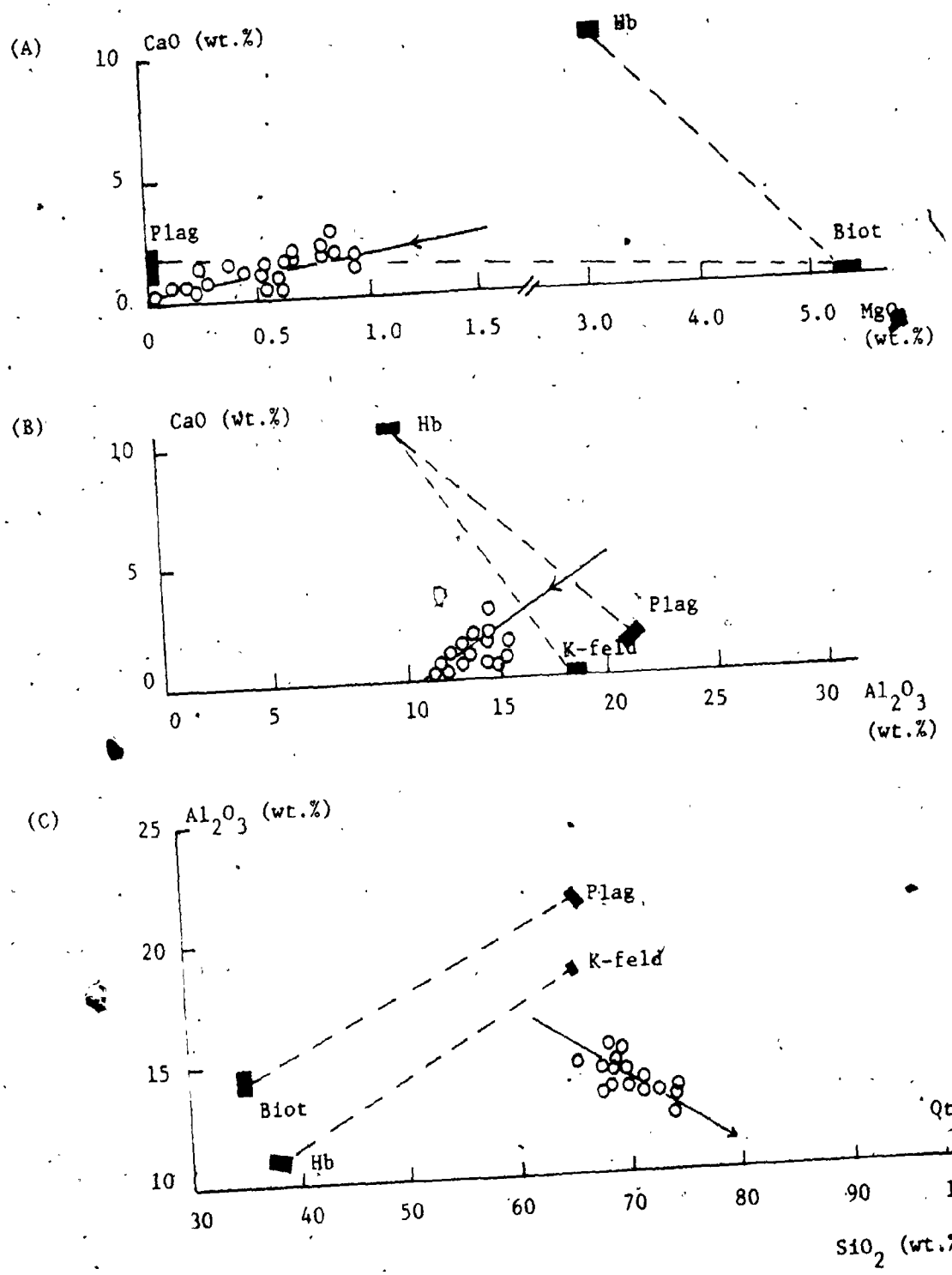
(A)
CaO (wt.%)
10
5
0
Hb
Plag
Biot
0
0.5
1.0
1.5
3.0
4.0
5.0
MgO (wt.%)
(B)
CaO (wt.%)
10
5
0
Hb
Plag
K-feld
0
5
10
15
20
25
30
Al_2O_3 (wt.%)
(C)
Al_2O_3 (wt.%)
25
20
15
10
Plag
K-feld
Biot
Hb
Qtz.
30
40
50
60
70
80
90
100
SiO_2 (wt.%)

dykes were used in the modelling. Differentiation from the least differentiated sample MWS-2-2 (64.69% SiO_2) to the most evolved sample MNR-2-1 (75.18% SiO_2) required removal of a modal solid of 47% plagioclase, 22% K-feldspar, 22% hornblende, 5% biotite, 3% sphene and 0.7% apatite. A similar modal solid relates granite gneiss and the aplitic dyke. For both models, the amount of removed solid related to the initial magma is about 55%; the sum of squares of the residuals are 0.1147 and 0.4375 respectively, indicating a reasonably good fit of the model.

The large-ion-lithophile elements Rb, Sr and Ba are particularly useful for a petrogenetic study of granite, because they are almost entirely retained by major rock-forming minerals (eg. feldspars). Rb-Ba and Sr-Ba data of the batholith are plotted in Figure 2-6-14 along with the vectors showing the theoretical effects on melt composition of crystallizing a single mineral phase by means of Rayleigh fractionation. Unexpectedly, the distribution of data shows two trends with different slopes. Such inflections of the composition trend of the melt may be due to (1) a major change of liquidus mineralogy at a later stage of crystallization, or (2) loss of alkali- rich fluids from the magma after crystallization of the rocks of trend 1.

Although a relative increase in the proportions of biotite and K-feldspar in the extracted assemblage could

Figure 2-6-14. (A) Rb vs. Ba. (B) Sr vs. Ba plots of the Mulock Batholith. Dashed-lines indicate the variation trends of the batholith. Vectors illustrate the theoretical effects on melt composition of crystallizing a single mineral phase as indicated.

○ Granite Gneiss ▲ Aplitic Dykes

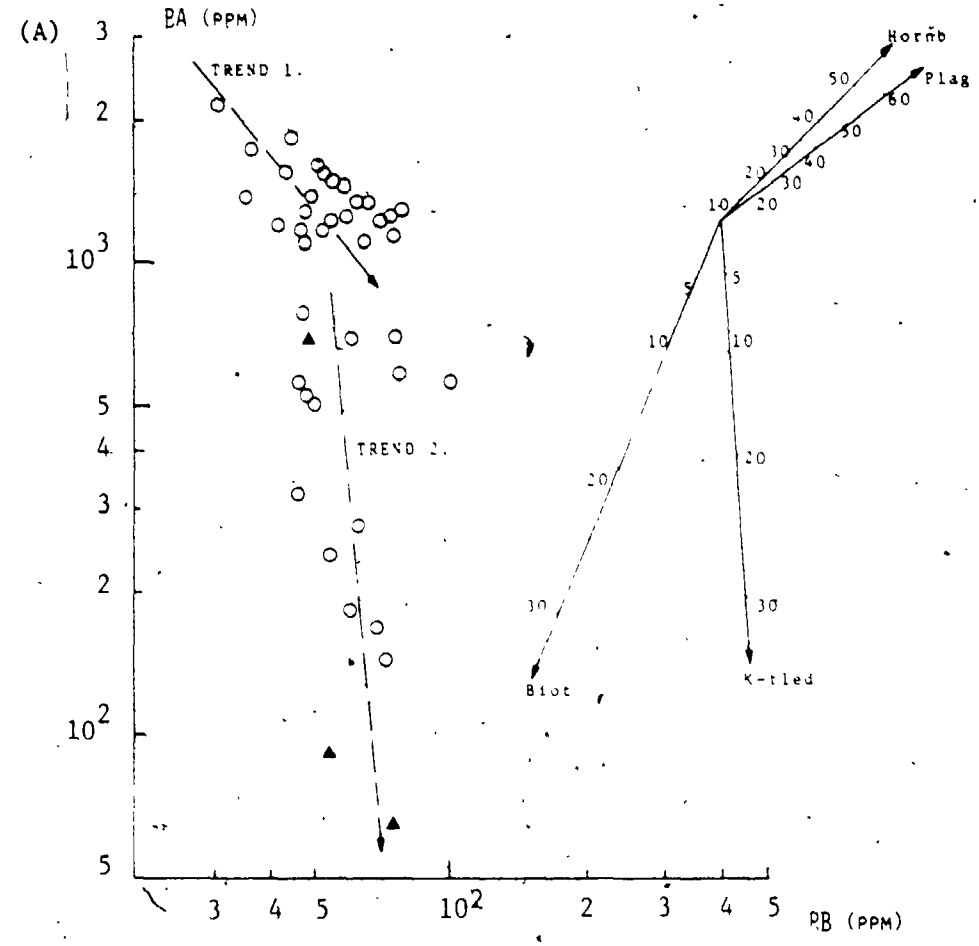
(A)
BA (PPM)
TREND 1.
TREND 2.
Hornb
Plag
Biot
K-fled
RB (PPM)

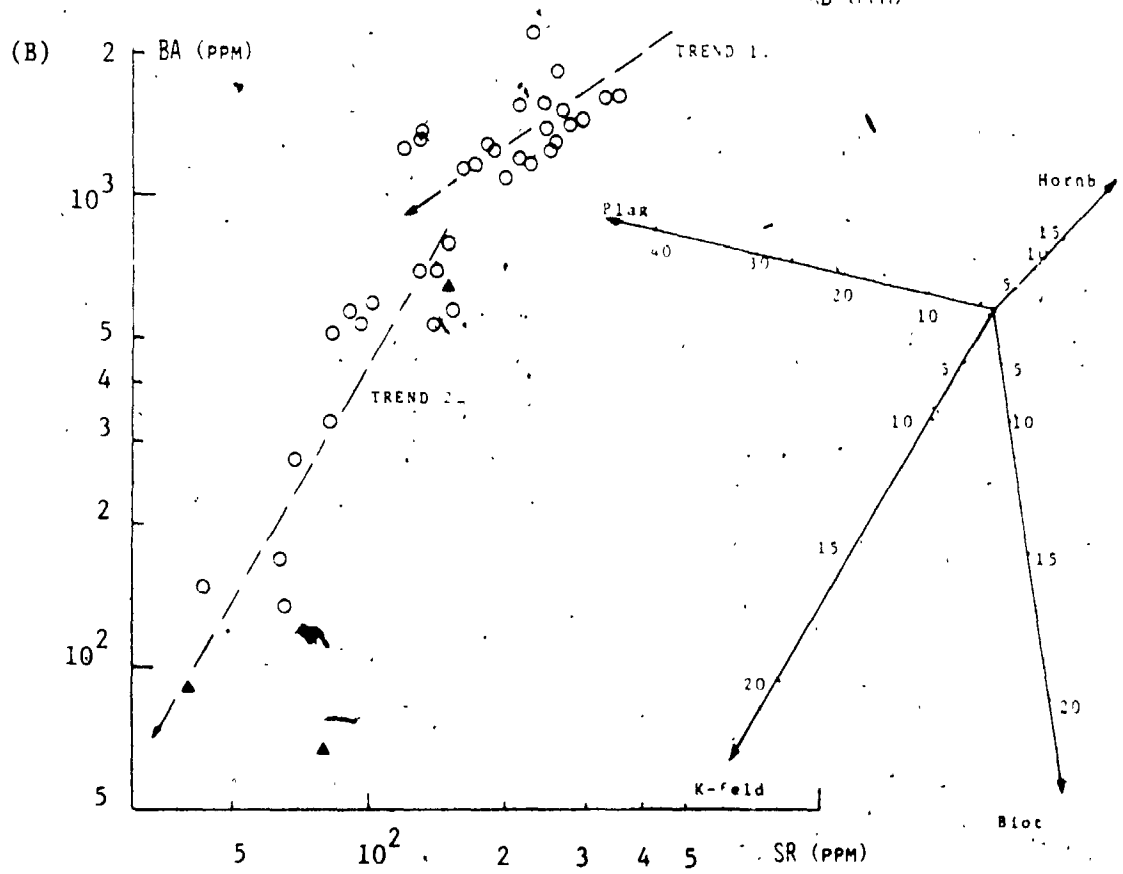
(B)
BA (PPM)
TREND 1.
TREND 2.
Hornb
Plag
K-feld
Biot
SR (PPM)

be resposible for the changing slopes of the differentiation trends, major-oxide modelling indicates no drastic change of modal solid composition throughout the path of crystallization. Therefore, a major change of liquidus mineral assemblage is unlikely to account for the inflections (cf. McCarthy and Groves, 1979). It is more likely that at the later stage of crystallization the alkali elements (Sr, Ba, Rb) are mainly controlled by volatile-rich fluids. Rocks of trend 2 may be representative of the crystallized residual melt after loss of alkali-rich fluids from magma of trend 1 (eg. Tindle and Pearce, 1981). It is also interesting to note that rocks belonging to trend 2 are mostly taken from the periphery of the batholith; this may suggest flowage differentiation for a more acidic and evolved border and less differentiated core as the magma injected from the feeder. Separation of volatile enriched liquid from the residual magma of trend 1 might be accompanied by fracturing during regional tectonic movement.

The overall higher abundances of REE (7REE = 226-360) and relatively abundant Sr and Ba suggest a slightly fractionated and REE-enriched source for the Mulock Batholith. Its mild to steep REE patterns ($(Ce/Yb)_N$ = 7.7-26.2) with marked negative Eu-anomalies (Eu/Eu* = 0.19-0.79) would be compatible with partial melting of lower crustal rock of granulite facies with

residual plagioclase and a few percent of garnet, or crystallization of hornblende and plagioclase from a basic magma with similar $(Ce/Yb)_N$ ratio. In addition, the upper amphibolite to granulite metamorphism of the Ontario Gneiss Segment supports the anatexis of crustal material, such as the Huronian metasediments, for generation of the granitic melt.

6.5.1 Crystal Fractionation From A Basaltic Magma -

Andesite of continental flood basalt (eg. Keweenawan reference suite of the North Shore Volcanic Group, Basaltic Volcanic Study Project, 1981, p.69) containing total REE 120-160 ppm and $(Ce/Yb)_N$ ranging 2.7 to 8.4 is a suitable parent for crystallization modelling. It requires a higher degree (> 50%) of crystallization of pyroxene, hornblende and plagioclase from this basaltic andesite melt to form silicic magma. However, hornblende retains a higher partition coefficent for both heavy and middle REE; it cannot induce significant HREE depletion without imparting a greater depletion of middle REE. Besides, the significant amounts of Cr and Ni in the batholith (8-1 and 11-4 ppm, respectively) argue against the possibility of fractionation from a mafic magma, since Cr and Ni would be rapidly depleted in the melt as soon as the mafic phases crystallized.

6.5.2 Partial Melting Of Mafic Granulite Of Lower Crust

The widespread Precambrian granulite terrains are commonly considered to be representative of the lower continental crust (Tarney and Windly, 1977; Weaver, 1980; Pride and Muecke, 1980). Chondrite-normalized REE curves with a low degree (< 5%) of partial melting of average mafic granulite (Weaver, 1980) with a dry pyroxene - plagioclase - garnet residue are illustrated in Figure 2-6-15A. They are located in the lower half of the REE envelope of the batholith and are consistent with its primitive nature for further differentiation of the granite. In addition, the higher Rb/Sr (0.80) and K/Rb (389) ratios support the lower degree of partial melting of granulite rocks with anomalously higher K/Rb ratios.

6.5.3 Partial Melting Of Huronian Supercrustal Rocks -

According to Lumbers (1982), rocks of the Ontario Gneiss Segment are representative of "older" supercrustal accumulations which are partly correlated with the Huronian Supergroup in the Southern Province. McLennan et al. (1979) suggested that the REE of the Gowganda Formation of the Huronian Sequence is considered to be a

Figure 2-6-15. REE modelling of the Mulock Batholith.

(A) Equilibrium modal melting of common mafic granulite (Weaver, 1980).

(B) Equilibrium partial melting of Gowganda Formation of the Huronian Sequence (McLennan et al., 1979).

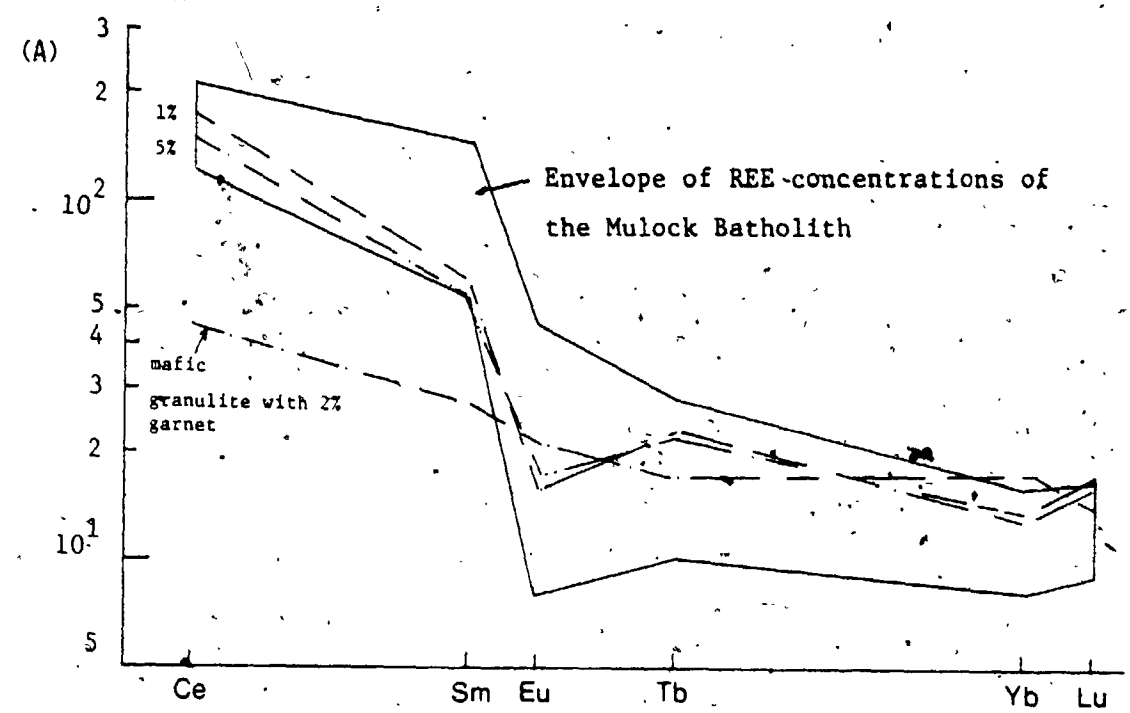
(A)
3
2
1%
5%
10^2
5
4
3
2
10^1
5
mafic
granulite with 2%
garnet
Envelope of REE concentrations of
the Mulock Batholith
Ce
Sm
Eu
Tb
Yb
Lu

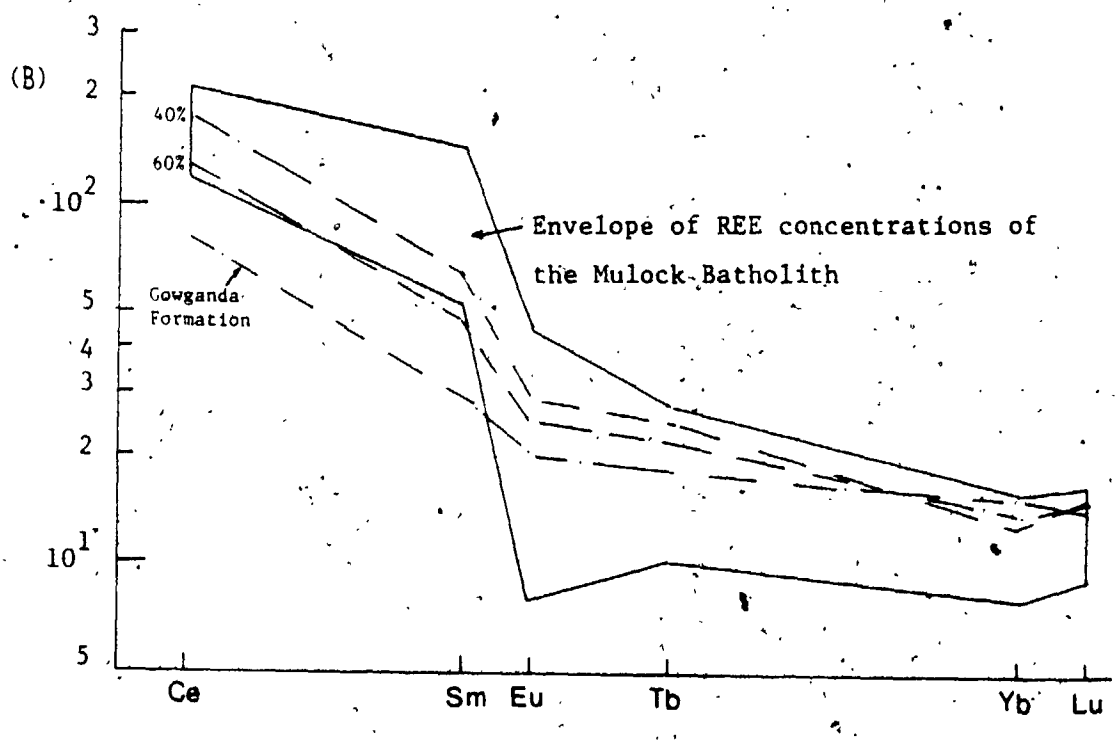
(B)
3
2
40%
60%
10^2
5
4
3
2
10^1
5
Gowganda
Formation
Envelope of REE concentrations of
the Mulock Batholith
Ce
Sm
Eu
Tb
Yb
Lu

reasonable estimation of upper crustal REE abundances of the post-Kenoran time. Figure 2-6-15B illustrates the plots of chondrite-normalized REE patterns for 40% to 60% equilibrium modal melting of average Gowganda Formation (total REE = 162, LREE/HREE = 8.9, Eu/Eu* = 0.9) with a mineral assemblage of 20% plagioclase, 15% biotite, 15% K-feldspar, 3% garnet and 40% quartz. Except for the relatively smaller Eu-anomalies and narrow ranges of HREE, the modelled REE patterns are compatible with those of the Mulock Batholith.

6.6 Summary

The Mulock Batholith can be mineralogically classified as biotite-hornblende granite and/or biotite gnessic granite with K-feldspar augens. It is metaluminous with alkaline affinity. Both major-oxide and trace-element data suggest that the granite-gneiss and later aplitic dykes are comagmatic.

Internal geochemical variations of the batholith and its differentiation to the aplitic dykes are consistent with the model of fractional crystallization of hornblende, plagioclase, biotite and K-feldspar. It is suggested that from the least evolved sample (64.69% SiO2) to the most differentiated one (75.18% SiO2) removal of a modal solid of 47% plagioclase, 22%

K-feldspar, 22% hornblende, 5% biotite, 3% sphene and 0.7% apatite is required. The rapid depletion of the LREE and its total REE abundances in the aplitic dyke can be explained by the continuous crystallization of a small amount of LREE highly enriched accessories, such as sphene and allanite. In addition, the inflections in the Rb-Ba and Sr-Ba plots suggest a flowage differentiation mechanism during injection of this laccolith-like batholith; rocks of the border zone are representative of the crystallized residual melt from the core after loss of alkali-rich fluids.

Based on REE modelling, the source of the Mulock Batholith is considered to be mildly fractionated, slightly REE enriched and with residual plagioclase and garnet. Either a low degree (< 5%) of equilibrium partial melting of common mafic granulite rocks, or 40% to 60% partial fusion of the Gowganda Formation of the Huronian Supercrustal rocks is compatible with the REE patterns of the batholith.

Due to viscosity of granitic melt, Compston and Chappell (1979) argue that it requires a minimum of 15 to 20% partial melting to allow the melt to move out of its source matrix. Thus, low degree melting of the mafic granulite rocks may not be suitable for generation of the Mulock Batholith, in terms of the volume of melt. On the other hand, based upon current understanding of anatectic melting of pre-existing supercrustal rocks,

the melt fraction (or granitic mesh) would move away gradually and solidified not far from their source; the residuum (or restite), commonly in granulite facies metamorphism, would remain behind (Fyfe, 1973; White and Chappell, 1977). The regional geology of the North Bay Area indicates that both clastic and calcareous metasedimentary gneisses contain primary sedimentary features (Lumbers, 1971); they are unlikely to be residuum after 40 to 60% partial melting of the Huronian metasediments. It is possible that the residuum of the Mulock Batholith is not exposed at the present erosional level. However, more constrains are needed, particularly isotopic compositions (eg. initial strontium and $^{18}O/^{16}O$ ratios), for determining the proper source(s) for the batholith.

7.0 COE HILL GRANITE

7.1 General Characters And Intrusive Relations

The Coe Hill Granite, located in the southewestern corner of Wollaston Township (Fig. 2-7-1), has an elongated shape with sharp and irregular contacts. Abundant inclusions of surrounding metagabbro, diorite and paragneiss in the southern half of the pluton may be indicative of the roof zone of the granite (Hewitt, 1962; ODM Map-2020).

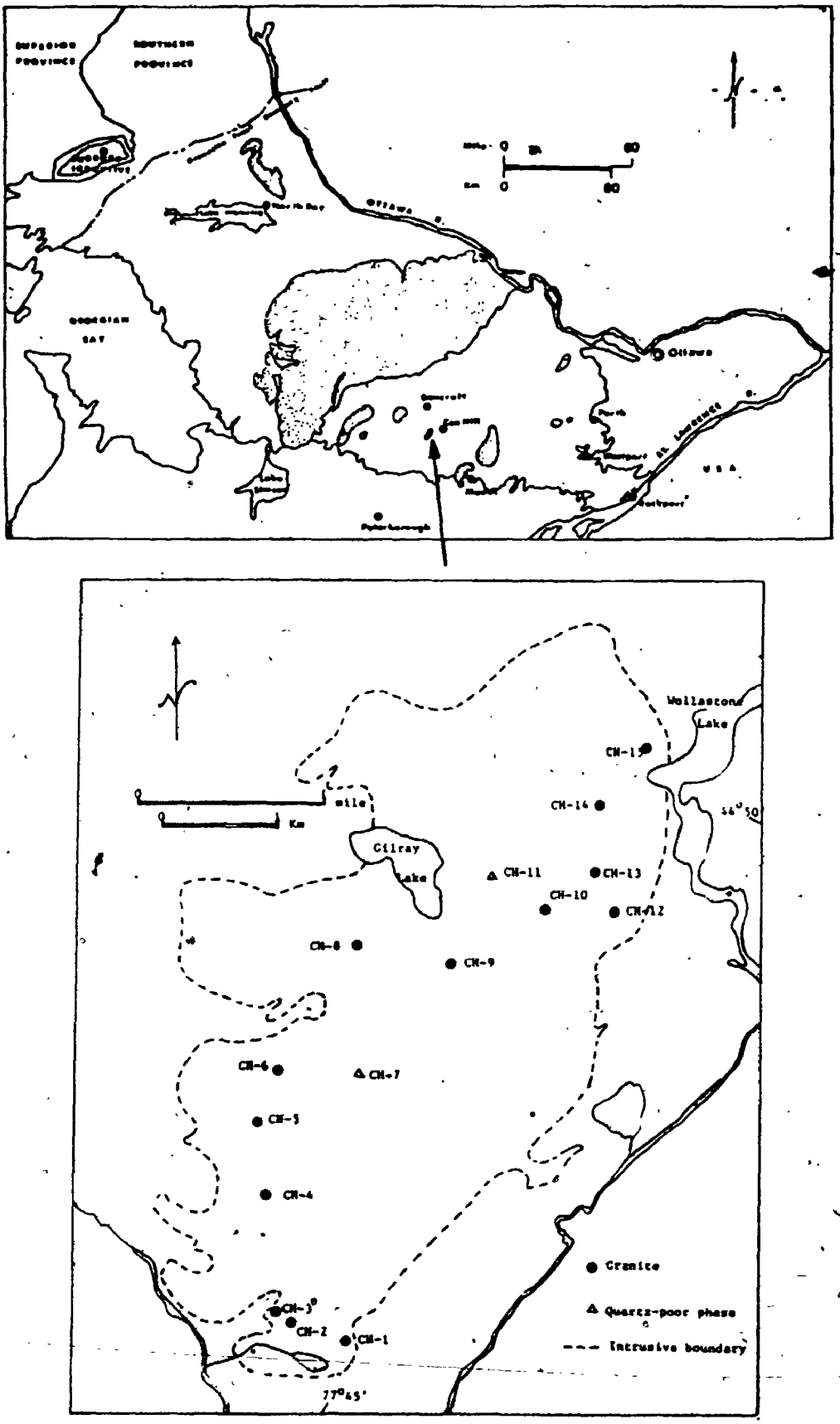

Figure 2-7-1. Sample location map of the Coe Hill Granite.

This pluton consists mainly of pink, massive to gneissic, medium- to coarse- grained biotite granite, with the exceptions of two occurrences containing less than 10% quartz and subordinate hornblende and pyroxene. The earlier gneissic augen phase is cut by a massive, coarse-grained one; however, no zonal distribution is developed inside the body. Contact metamorphism is limited to absent, and no migmatite has been mapped in the field.

7.2 Petrography

Rocks of both massive and gneissic phases can be classified as granite (adamellite) according to Streckeisen (1976), except for the quartz-poor, pyroxene - bearing ones falling into the quartz monzonite field (Fig. 2-7-2). Smaller xenoliths, ranging from 15 cm to 2 cm in length, have been completely granitized to finer-grained biotite-rich clots.

The granites are hypidiomorphic-granular with generally 20% quartz and more than 50% feldspar. The average feldspar ratio (plagioclase/total feldspar) is about 0.53. Biotite and hornblende are common dark minerals; rarer pyroxene is only present in quartz-poor phases. Sphene, opaques, apatite, zircon, secondary muscovite, carbonate and epidote are accessory minerals, with rare fluorite and allanite.

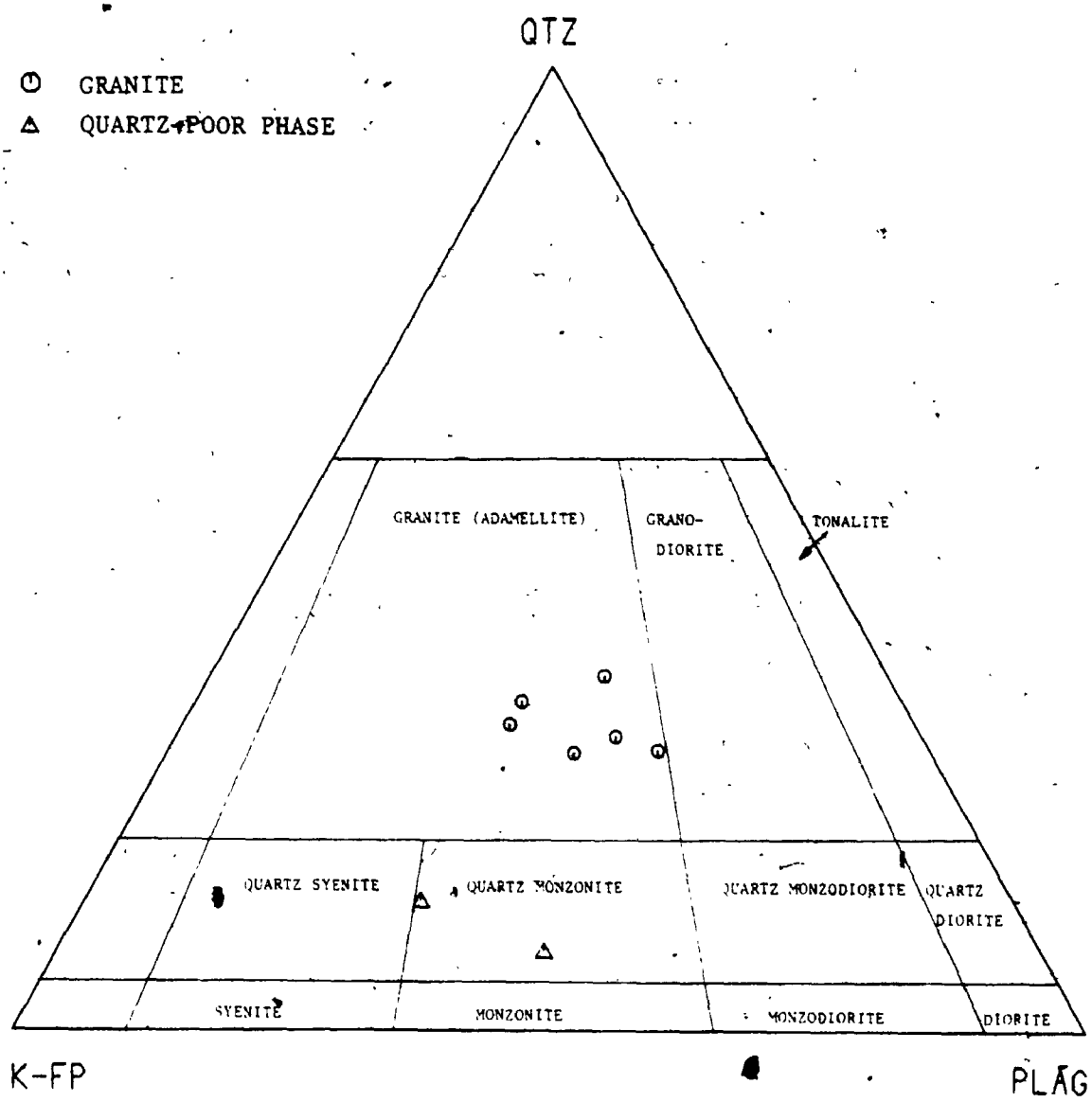

Figure 2-7-2. Modal classification of the Coe Hill Granite (after Streckeisen, 1976).

Microcline is the major alkaline feldspar in this pluton; in the gneissic variety, it occurs as phenocrysts frequently unmixed with plagioclase or quartz to form perthitic texture or granophyric intergrowth respectively. plagioclase (An_5 to An_{15}) is twinned, unzoned, but strongly altered in the core; such alterations have caused the release of Ca-component from plagioclase to form secondary epidote (eg. sample CH-2 in Table 2-7-1). The mean compositions and structural formulae of representative feldspars are given in Table 2-7-1. It was found that the mole fraction of An-content in the plagioclase decreased from south to north geographically.

Biotite and hornblende are the most common mafic minerals, but biotite is more abundant in most of the samples. They both show euhedral to subhedral shape and are strongly pleochroic (Biotite : X = straw yellow, Y = Z = dark brown with greenish tint; hornblende : X = greenish yellow, Y = olive green, Z = leave green). The relationships between them vary; in places, biotite is intergrown with hornblende, whereas in others, hornblende occurs as relict cores within the biotite euhedra. Biotite is partly chloritized and hornblende is oxidized to ferruginous material. However, biotite and hornblende are commonly associated with opaques and sphene; apatite, zircon and quartz are frequently enclosed. Chemical analyses of representative micas

Table 2-7-1. Chemical compositions and calculated formulae of feldspars from the Coe Hill Granite

	(a) Plagioclase				(b) K-feldspar		
Sample No.	CH-2A	CH-10-1	CH-13	CH-2B	CH-2	CH-10-1	CH-13
(wt. %)							
SiO_2	64.45	65.62	65.56	67.51	64.73	64.94	64.48
Al_2O_3	22.58	21.84	19.02	20.78	18.23	18.79	18.81
CaO	2.96	2.44	2.11	0.37	0.12	0.08	0.14
Na_2O	10.05	10.04	10.52	11.20	0.58	1.03	1.52
K_2O	0.16	0.16	0.14	0.17	15.74	15.08	14.46
Total	100.20	100.10	97.35	100.03	99.40	99.92	99.41
Si (Z)	11.342	11.518	11.833	11.797	12.013	11.956	11.922
Al (Z)	4.682	4.517	4.045	4.279	3.987	4.076	4.098
	16.024	16.036	15.878	16.076	15.999	16.032	16.020
Na (X)	3.429	3.417	3.681	3.795	0.209	0.368	0.545
Ca (X)	0.558	0.459	0.408	0.009	0.024	0.016	0.028
K (X)	0.036	0.036	0.032	0.038	3.726	3.541	3.410
	4.023	3.912	4.122	3.902	3.958	3.925	3.983
O	32	32	32	32	32	32	32
(mol.%)							
Ab	85.23	87.35	89.32	97.25	5.27	9.37	13.68
An	13.87	11.73	9.90	1.78	0.60	0.40	0.70
Or	0.89	0.92	0.78	0.97	94.13	90.23	85.62

(Table 2-7-2) suggest they are Fe^{2+}-biotite of Foster (1960; See Fig. 2-7-3). Pyroxene occurs only in one quartz-poor sample; it either intergrew with hornblende and biotite or formed relict core surrounded by the latter.

Secondary muscovite formed at the expense of biotite. Epidote concentrated in the altered core of plagioclase and the contacts between biotite and plagioclase. Sphene grains are commonly associated with biotite and opaques; they are intergrown with zircon crystals and enclose apatite and quartz as inclusions. Opaques are mainly magnetite grains with fine ilmenite exsolution lamellae. In places, pyrite and chalcopyrite are enclosed within the magnetite.

7.3 Whole-rock Geochemistry

7.3.1 Major-oxides -

As expected from the modal classification, rocks from the Coe Hill Granite show zonal distribution in the SiO_2 vs. Differentiation Index (D. I.) diagram (Fig. 2-7-4); the granitic rocks are in the SiO_2 oversaturated field, while the quartz-poor, monzonitic rocks fall into the saturated field of Thornton and Tuttle (1960).

Table 2-7-2. Chemical compositions and calculated formulae of biotite from the Coe Hill Granite

Sample No.		CH-2	CH-10-1	CH-13
(wt%)				
SiO_2		37.60	36.82	36.09
TiO_2		1.20	1.65	1.66
Al_2O_3		14.53	14.71	15.25
Fe_2O_3		2.08	2.49	2.59
FeO		17.81	20.30	21.13
MnO		0.95	0.81	0.91
MgO		10.54	8.55	7.49
CaO		0.05	0.03	0.03
Na_2O		0.06	0.05	0.08
K_2O		9.91	9.89	9.71
Total		94.73	95.30	94.94
Si	Z	5.972	5.717	5.655
Al^{iv}	Z	2.208	2.283	2.345
		8.000	8.000	8.000
Al^{vi}	Y	0.428	0.408	0.469
Ti	Y	0.139	0.193	0.195
Fe^{3+}	Y	0.241	0.291	0.305
Fe^{2+}	Y	2.293	2.634	2.766
Mg	Y	2.415	1.977	1.747
Mn	Y	0.124	0.106	0.121
		5.640	5.608	5.604
Ca	X	0.008	0.005	0.005
Na	X	0.018	0.015	0.024
K	X	1.946	1.958	1.939
		1.972	1.978	1.969
O		22	22	22
$Mg/Fe^t+Mg+Mn$		0.476	0.395	0.353
Fe^t/Fe^t+Mg		0.512	0.598	0.637
mole of annite		0.382	0.439	0.461

$Fe^t = Fe^{3+} + Fe^{2+}$ in unit cell

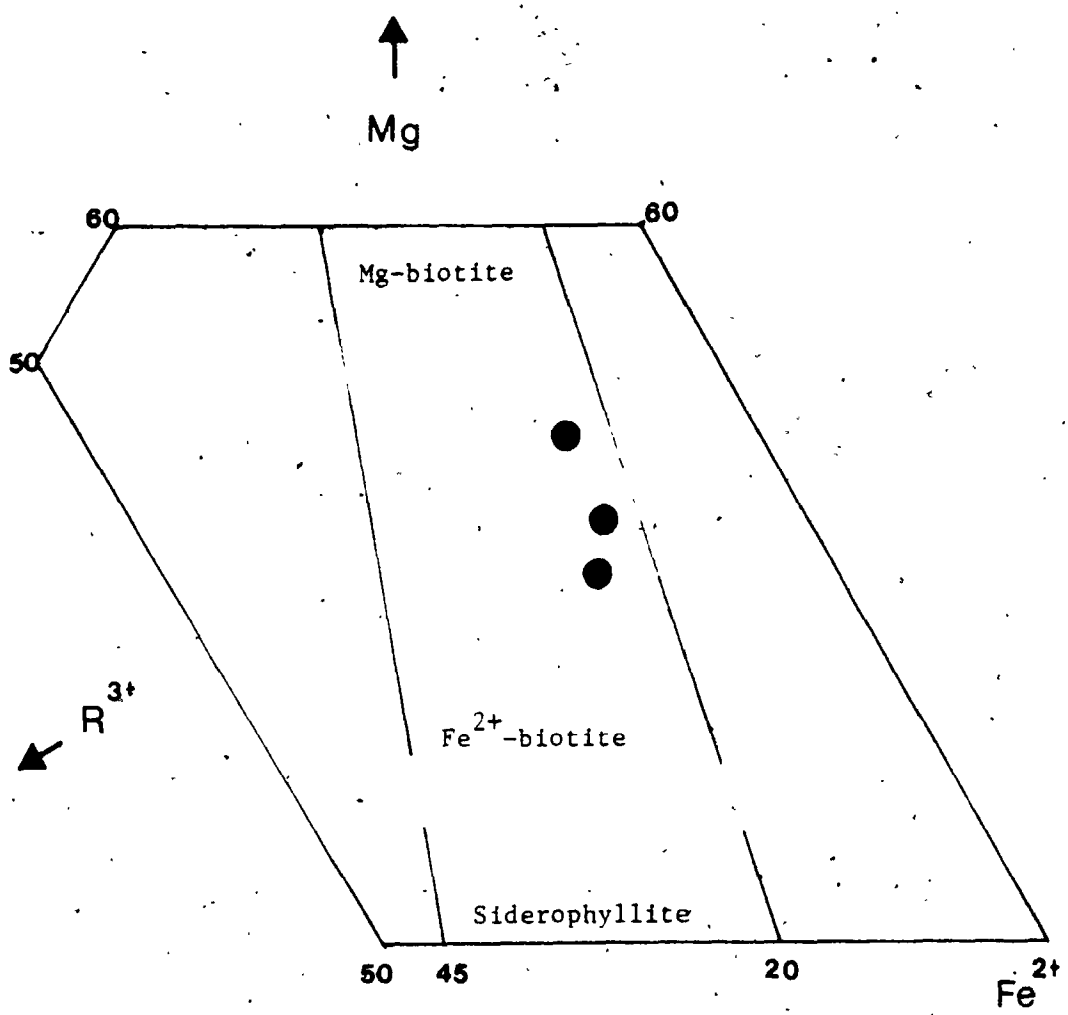

Figure 2-7-3. The Mg-Fe^{2+}-R^{3+} relation in trioctahedral micas of the Coe Hill Granite (after Foster, 1960).

$$R^{3+} = Al^{vi} + Fe^{3+} + Ti^{4+}$$

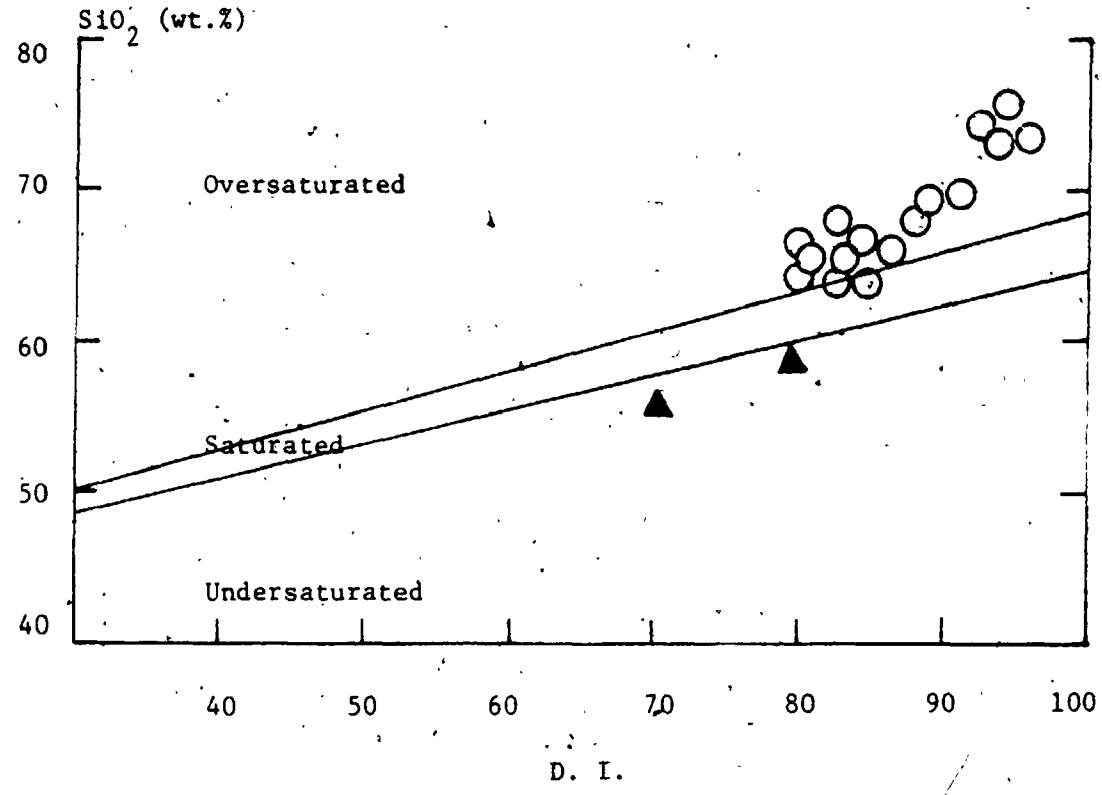

Figure 2-7-4. Variation of SiO_2 as a function of D.I.
Solid-lines separate the oversaturated, saturated and undersaturated fields of Thornton and Tuttle (1960).

○ Granite ▲ Quartz-poor phase

Overall composition of the Coe Hill Granite is metaluminous with average molar $Al_2O_3/(Na_2O+K_2O+CaO)$ ratio of 0.93 and agpaitic index of 0.86. The alkali-lime index (Peacock, 1931) is about 54% SiO_2 indicating ~~an~~ alkali-calcic affinity (Fig. 2-7-5).

The mean compostion of the granitic and monzonitic rocks from the pluton are listed in Table 2-7-3. In general, the average composition of the granitic rocks is similar to those of Loon Lake Pluton (Dostal, 1975) and the average adamellite of Nockolds (1954), except lower in SiO_2 and higher in total iron and Na_2O. Whereas the monzonitic phase is close to the composition of calc-alkali syenite (Nockolds, 1954) and California monzonites (Miller, 1978). This nature is also reflected in the normative Qtz-Plag-Or ternary plot (Fig. 2-7-6) in which the granitic rocks cluster along the side of average adamellite, with less quartz content, and monzonitic rocks associated with the average syenite of Nockolds (1954).

In the normative Ab-An-Or system (Fig. 2-7-7), the granitic rocks of the Coe Hill Granite lie within the granite field, while the quartz-poor ones straddle the boundary between the quartz monzonite and granite fields of O'Connor (1965). Moreover, most samples fall within the low temperature trough of Kleeman (1965). As shown in the Qtz-Ab-An

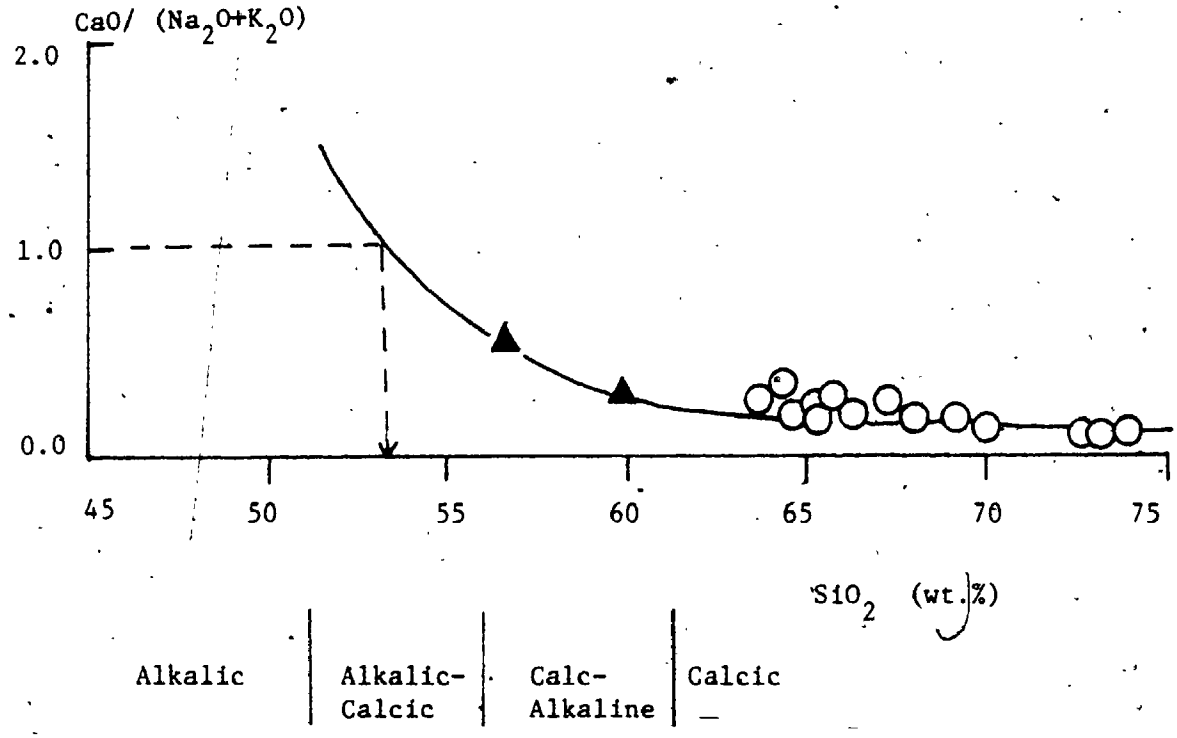

Figure 2-7-5. The alkaline-lime ratios vs. SiO_2 plot of the Coe Hill Granite. Solid-line indicates the chemical variation trend of the pluton. Classification scheme is after Peacock (1931).

○ Granite ▲ Quartz-poor phase

Table 2-7-3. Comparison of average composition of Coe Hill Granite with other similar rock-types

	1 (n=19)	2 (n=12)	3 (n=121)	4 (n=2)	5 (n=12)	6 (n=18)	7 (n=16)
SiO_2 (wt%)	67.65	70.98	69.15	58.32	62.55	59.41	58.80
TiO_2	0.71	0.36	0.65	0.68	0.82	0.83	0.52
Al_2O_3	14.34	14.74	14.63	17.97	18.03	17.12	19.70
TFe_2O_3	4.76	* 2.64	* 3.74	5.00	* 3.69	* 5.33	4.50
Fe_2O_3	1.68	1.20	1.22	2.37	1.81	2.19	-
FeO	2.41	1.30	2.27	2.37	1.69	2.83	-
MnO	0.09	0.03	0.06	0.10	0.07	0.08	0.13
MgO	0.78	0.43	0.99	2.08	0.90	2.02	0.55
CaO	1.54	1.15	2.45	4.09	1.80	4.06	4.44
Na_2O	4.44	3.79	3.35	4.40	4.37	3.92	5.00
K_2O	4.75	5.43	4.58	5.96	6.90	6.53	5.20
P_2O_5	0.17	0.08	0.20	0.34	0.20	0.38	0.17
LOI	0.57	0.51	0.54	0.37	0.46	0.63	0.37
Na_2O/K_2O	0.94	0.70	0.73	0.74	0.69	0.60	0.96
TFe_2O_3/MgO	6.10	6.14	3.78	2.40	4.10	2.64	8.18
		(n=6)					
Sr (ppm)	243	141	-	1675	332	-	1480
Rb	147	137	-	98	70	-	125
Ba	1040	507	-	4033	2125	-	2600
Zr	517	-	-	416	-	-	-
K/Rb	280	329	-	508	818	-	345
Rb/Sr	0.95	0.97	-	0.13	0.06	-	0.08
Ba/Sr	4.16	3.60	-	7.58	2.41	-	1.76
Sr/Ca	214	296	-	485	1302	-	470

1 Average of 19 granite of Coe Hill Granite (this study).
2 Average of 12 quartz monzonite of Loon Lake Pluton (Dostal, 1975).
3 Average of 121 adamellite of Nockolds (1954).
4 Average of 2 monzonitic rocks of Coe Hill Granite (this study).
5 Average of 12 monzonite of Loon Lake Pluton (Dostal, 1975).
6 Average of 18 calc-alkali syenite of Nockolds (1954).
7 Average of 16 monzonite from Granite Mountains (Miller, 1978).
* Total iron as Fe_2O_3 is calculated from reported Fe_2O_3-FeO pair.
n = no. of analyses.

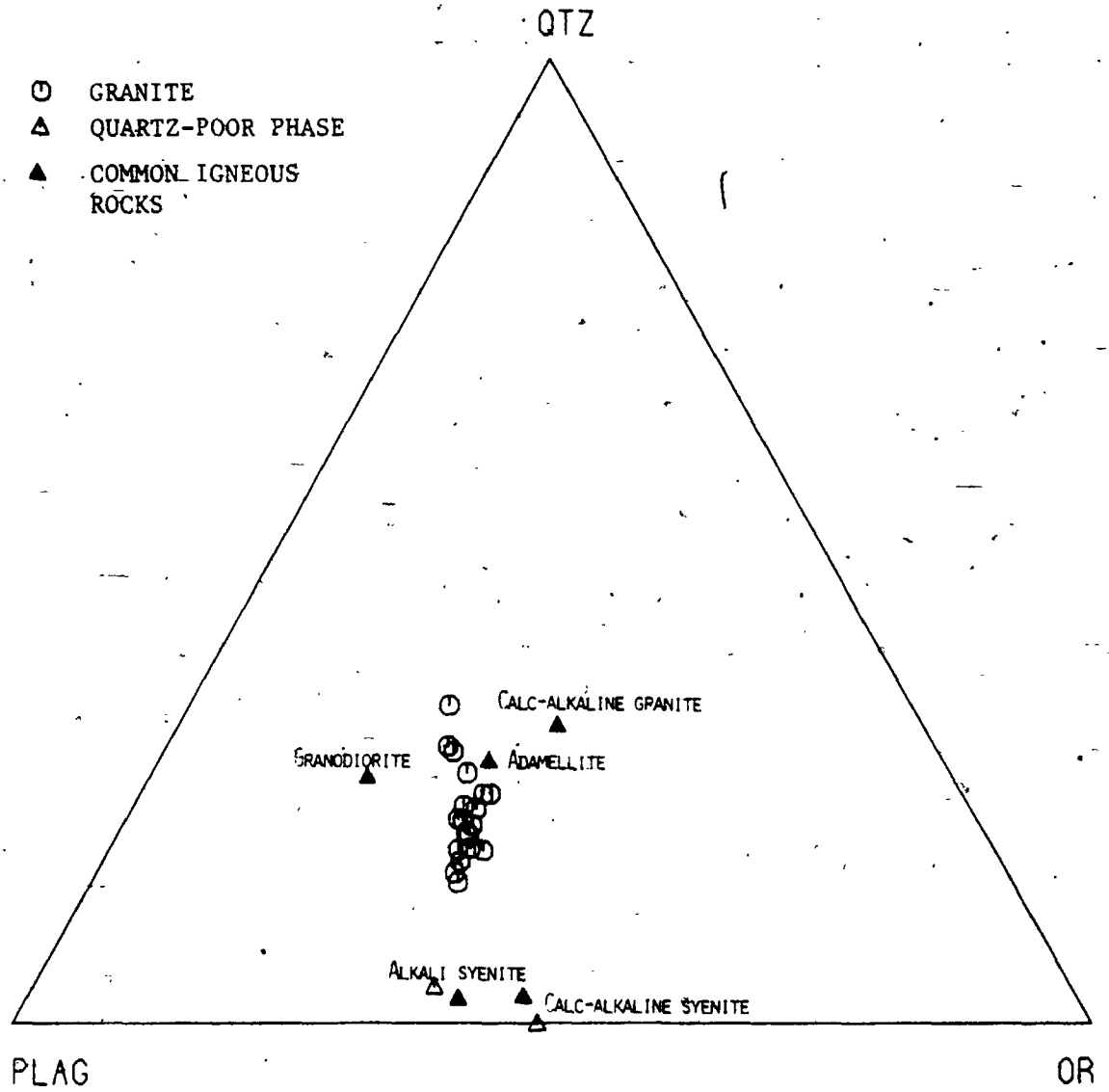

Figure 2-7-6. Normative Qtz-Or-Plag ratios of the Coe Hill Granite and common igneous rocks (calculated from Nockolds, 1954).

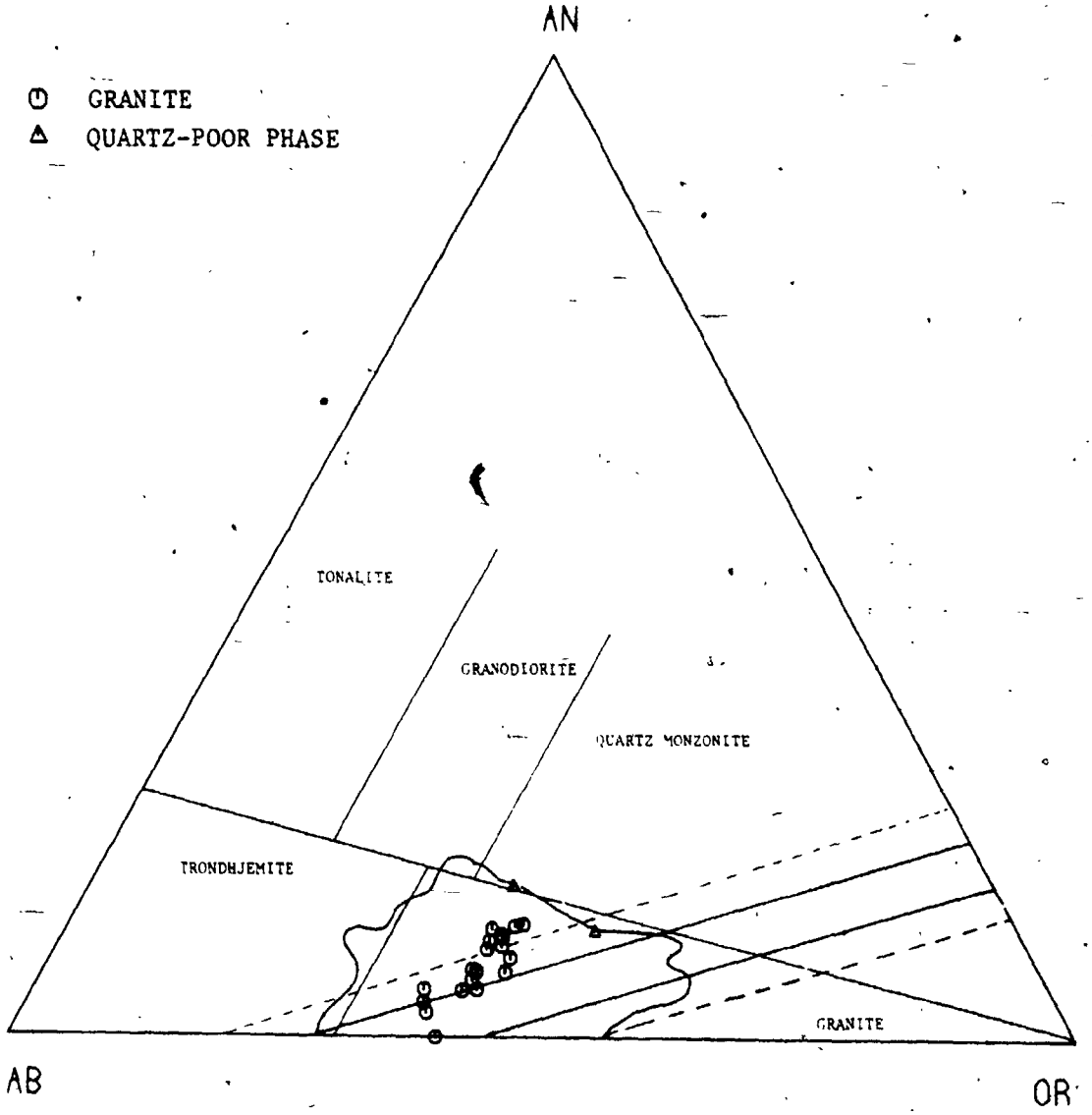

Figure 2-7-7. Normative Ab-An-Or ternary diagram of the Coe Hill Granite. The ireegular solid boundary is the 2% contour of Tuttle and Bowen (1958) enclosing most of granitic rocks that contain more than 80% normative Ab+An+Or+Qtz. The solid-lines indicate the boundary of low temperature trough; dashed-lines show uncertainty due to possibility of analytical error (Kleeman, 1965). Classification scheme is from O'Connor (1965).

projection (Fig. 2-7-8), it is similar to that of Loon Lake Pluton, in which most of the granitic rocks lie within Winkler and Von Platen's granite field (1961), while the rest along with the monzonitic rocks fall in the syenitic field from the Gardar Province of Greenland (Watt, 1966).

Correlation coefficients of major-oxides as a function of SiO_2 for the Coe Hill Granite are given in Table 2-7-4. With the exception of Na_2O giving a mild positive correlation coefficient (R = 0.46), the other major-oxides show negative correlations with SiO_2. It is noted that there are higher correlation coefficients for the granitic rocks alone. Such a difference could be due to either an insufficient sample population of the quartz-poor phase or differential fractionation within each rock type. However, in the Loon Lake Pluton, Dostal (1975) suggested a cogenetic relation for monzonites and granites, despite the varying slopes of variation trends.

In general, the decreases of Al_2O_3, Fe_2O_3, MgO, CaO and K_2O with increasing SiO_2 may result from fractionation of hornblende and feldspars during differentiation of the pluton. The decreases in P_2O_5 and TiO_2 with increasing differentiation reflect fractionation of apatite and sphene or ilmenite, respectively.

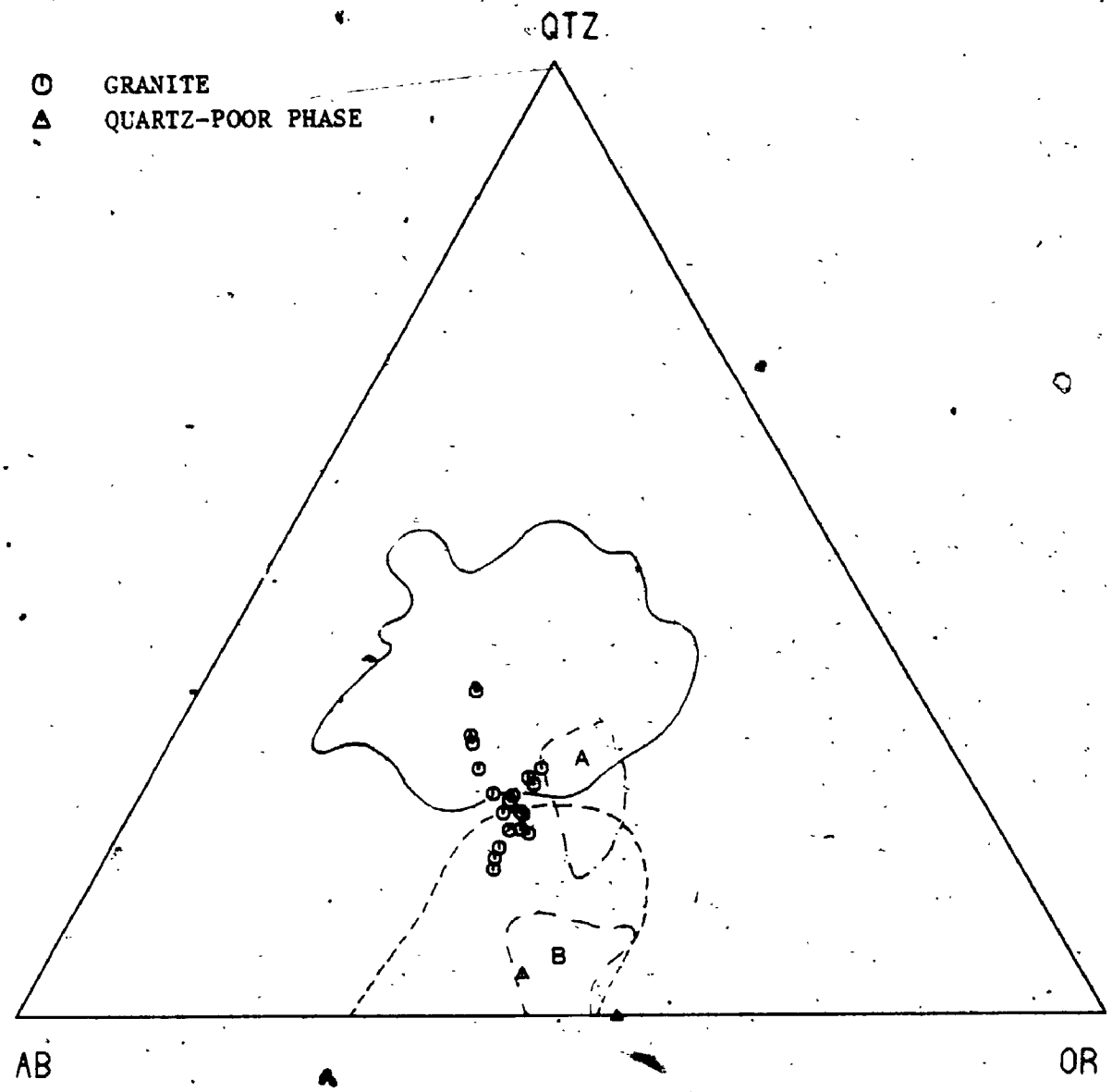

Figure 2-7-8. Normative Qtz-Ab-Or ternary diagram of the Coe Hill Granite. The irregular solid boundary indicates the granite field of Winkler and Von Platen (1961). The irregular dashed-line shows the compositional field of syenitic rocks from Gardar Province of Greenland (Watt, 1966).

Field A : Granite of Loon Lake Pluton

Field B : Monzonite of Loon Lake Pluton (Dostal, 1973)

Table 2-7-4. Correlation coefficients of inter-element variations for the Coe Hill Granite

Correlation		Granite only	Granite + monzonite	Correlation		Granite only	Granite + monzonite
SiO_2 vs.	TiO_2	-0.9749	-0.7181	SiO_2 vs.	U	-0.2273	0.4850
	Al_2O_3	-0.8809	-0.7771		Th	0.7524	0.7630
	Fe_2O_3	-0.9802	-0.7802		F	0.2716	0.2289
	MnO	-0.2893	-0.1789		Cl	-0.0883	-0.0069
	MgO	-0.9666	-0.7860		S	-0.7959	-0.3537
	CaO	-0.9427	-0.9173		Ga/Al	0.0138	0.5362
	K_2O	-0.6299	-0.8099		K/Rb	-0.6330	-0.7723
	P_2O_5	-0.7909	-0.7545		Rb/Sr	0.9512	0.8739
	Na_2O	0.5646	0.4628		Sr/Ba	0.7196	-0.3831
	Rb	0.5253	0.6251		Sr/Ca	-0.6493	-0.6485
	Sr	-0.9650	-0.6701		Zr/Y	-0.7829	-0.5745
	Ba	-0.9552	-0.7746		Y/Ca	0.7209	0.7795
	Zr	-0.9687	-0.5087		Cr/Mg	0.7348	0.5881
	Nb	-0.7322	-0.1212		V/Mg	0.7359	0.5081
	Y	-0.5375	0.0647		Ni/Mg	0.6855	0.5794
	Ga	-0.5754	0.0648		Fe/Mg	0.7597	0.6550
	Pb	-0.5726	-0.6807		Cr/Fe	0.8403	-0.4013
	Zn	-0.8219	-0.3384		V/Fe	-0.4099	-0.6[illegible]5
	Cu	-0.8316	-0.7607		Ni/Fe	-0.7471	-0.2544
	Ni	-0.6655	-0.5739	Nb vs.	Ga/Al	0.2061	0.4638
	Cr	-0.8771	-0.6077	Nb vs.	Y	0.6159	0.7094
	V	-0.7749	-0.7755	Al_2O_3 vs.	Ga	0.5194	-0.3425

In terms of ternary relations among Na_2O-K_2O-CaO (Fig. 2-7-9), there is no "normal" differentiation trend as compared with the Southern California Batholith (Nockolds and Allen, 1953). The granitic rocks of the pluton cluster near the Na_2O-K_2O join at about 5% to 20% CaO, which is compatible with the Loon Lake pluton, whereas the monzonitic rocks are plotted at higher CaO and within the field of Frontenac-type granite (Sauerbrei, 1966). However, from monzonite to granite, it suggests a tendency of decreasing CaO content with increasing Na_2O/K_2O ratio.

On an AFM diagram (Fig. 2-7-10), the Coe Hill Granite shows a similar trend to the Loon Lake Pluton, except that the former has higher total iron content. One monzonitic sample is plotted away from the normal trend and toward the MgO corner, which may be explained by its pyroxene-bearing mineralogy.

7.3.2 Trace-elements -

Average trace-element compositions and element-ratios of both granitic and monzonitic rocks of the pluton are summarized in Table 2-7-3. Comparatively, the monzonite is higher in Sr and Ba and lower in Rb than those of granitic rocks. In addition, in comparison with the equivalents of the

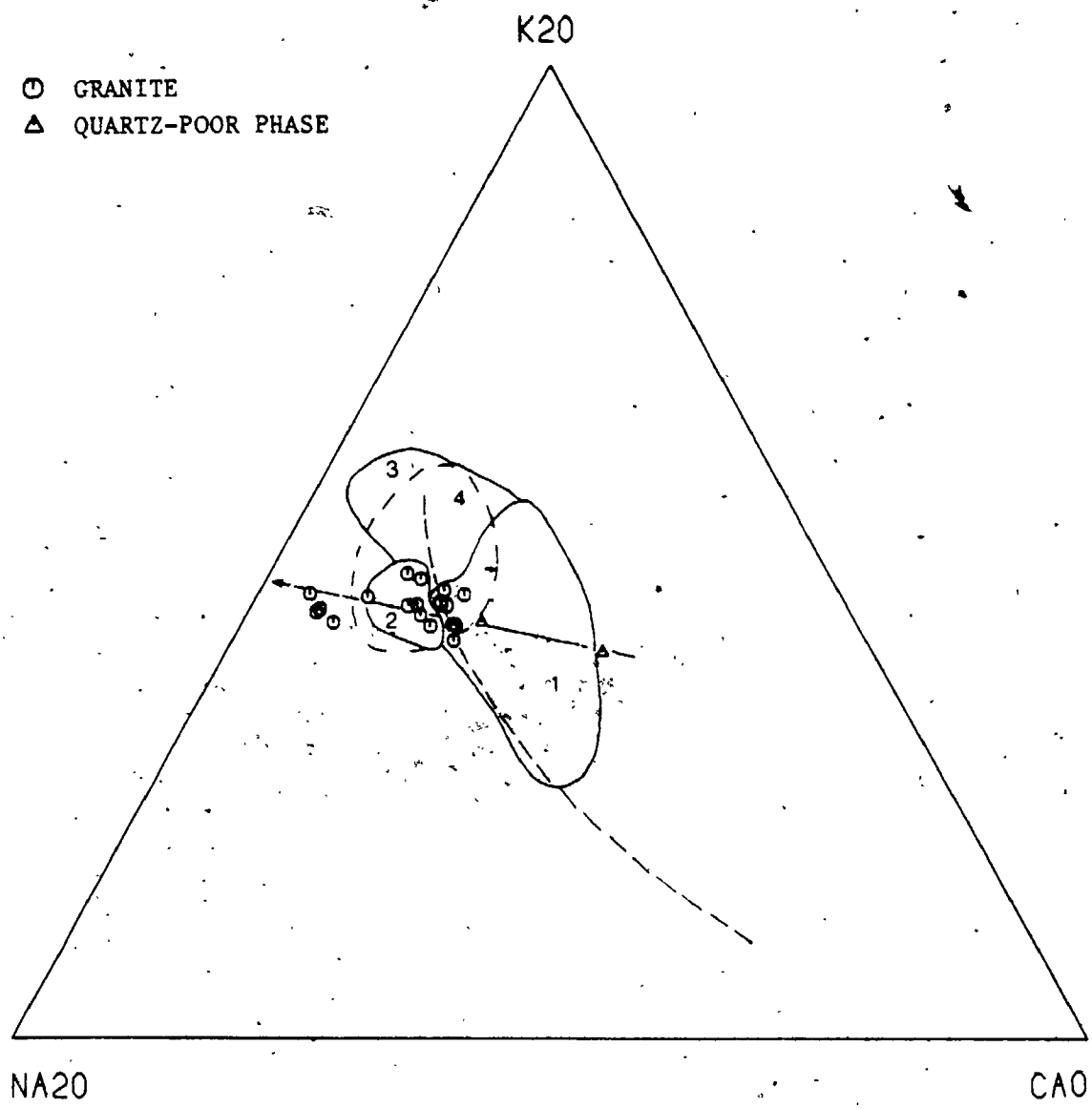

Figure 2-7-9. Na_2O-K_2O-CaO variation diagram of the Coe Hill Granite.

---- Calc-alkaline trend of Southern California Batholith (Nockolds and Allen, 1956).

Field 1 : Frontenac-type granite

Field 2 : Westport-type granite (Sauerbrei, 1966)

Field 3 : Rockport-type granite

Field 4 : Loon Lake Pluton (Dostal, 1973)

⟵ Chemical trend of the Coe Hill Granite (this study)

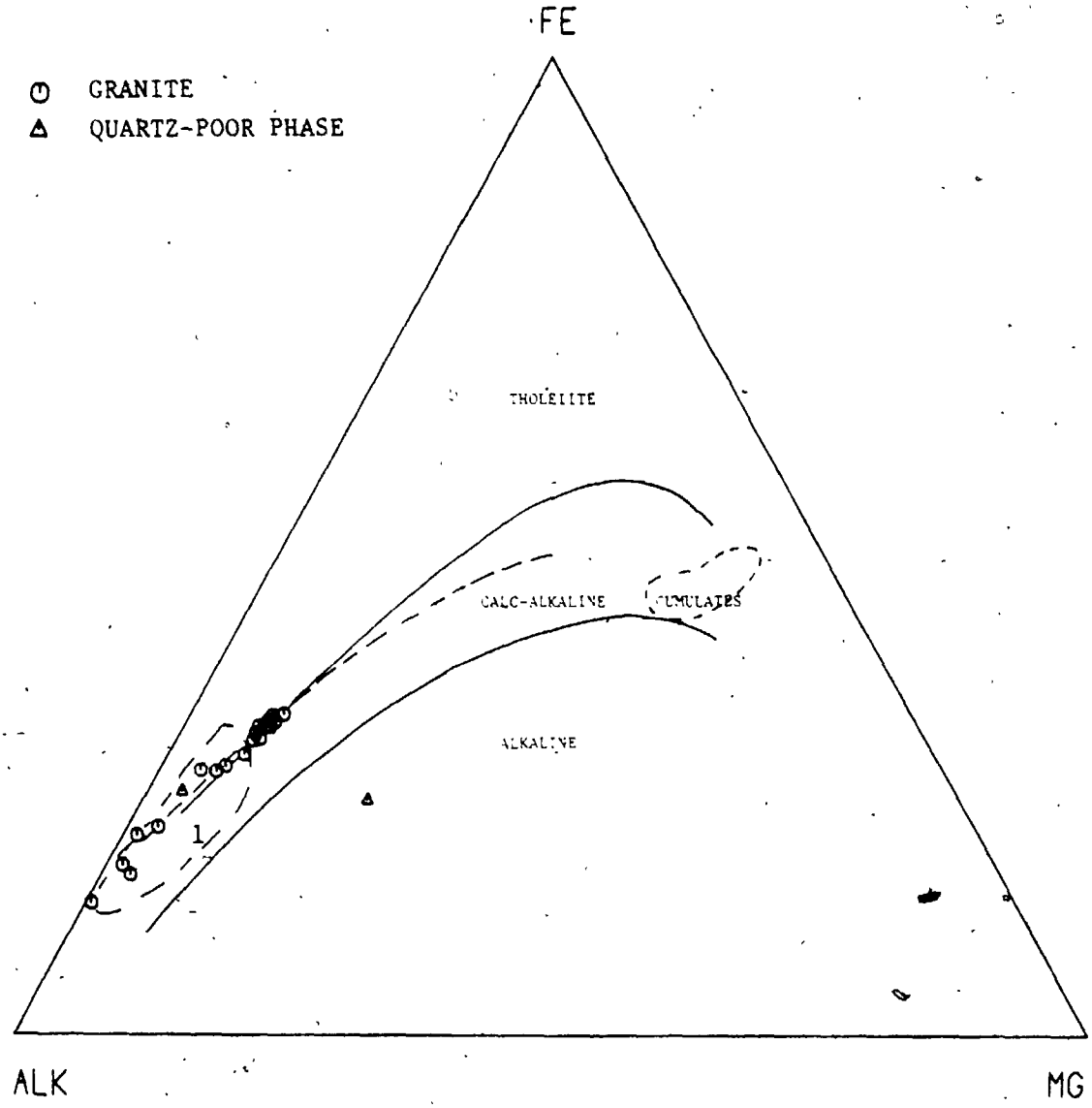

Figure 2-7-10. AFM diagram of the Coe Hill Granite.
Solid-lines separate the tholeiite, calc-alkaline and alkaline fields (Barker and Arth, 1976).

---- Calc-alkaline trend of Southern California Batholith (Nocklods and Allen, 1956).

Field 1 : Loon Lake Pluton (Dostal, 1973)

Loon Lake Pluton, the Coe Hill Granite contains much higher absolute concentrations of alkali-alkali earth elements and lower K/Rb and Sr/Ca ratios (Table 2-7-3). Moreover, the Coe Hill Granite has relatively lower Rb, higher Sr and is more abundant in Ba than the average low-Ca granite (Rb 170 ppm, Sr 100 ppm and Ba 840 ppm, Turekian and Wedepohl, 1961). This leads both the monzonitic and granitic rocks of the pluton to have anomalously higher K/Rb ratios - 280 and 508 respectively - as compared with 230 for average crust (Heier and Adams, 1964). However, such an abnormal K/Rb ratio is also found in the Loon Lake Pluton (Dostal, 1973, 1975) and the Westport-type granite in the Frontenaec Axis (Sauerbrei, 1966).

Similar to major-oxides, the granitic rocks yield significantly higher correlations of trace-elements than those of two rock-types treated as a whole (Table 2-7-4). However, the increase of Rb (R = 0.62) and decreases of Sr (R = -0.67) and Ba (R = -0.77) toward the more felsic rocks is compatible with the differentiation trend of a consanguineous suite. In addition, the smooth trend of the K/Rb ratio as a function of Rb (Fig. 2-7-11A) confirms the comagmatic relation between the quartz-poor phase and the granitic rocks of the pluton. Further, the rather linear relations

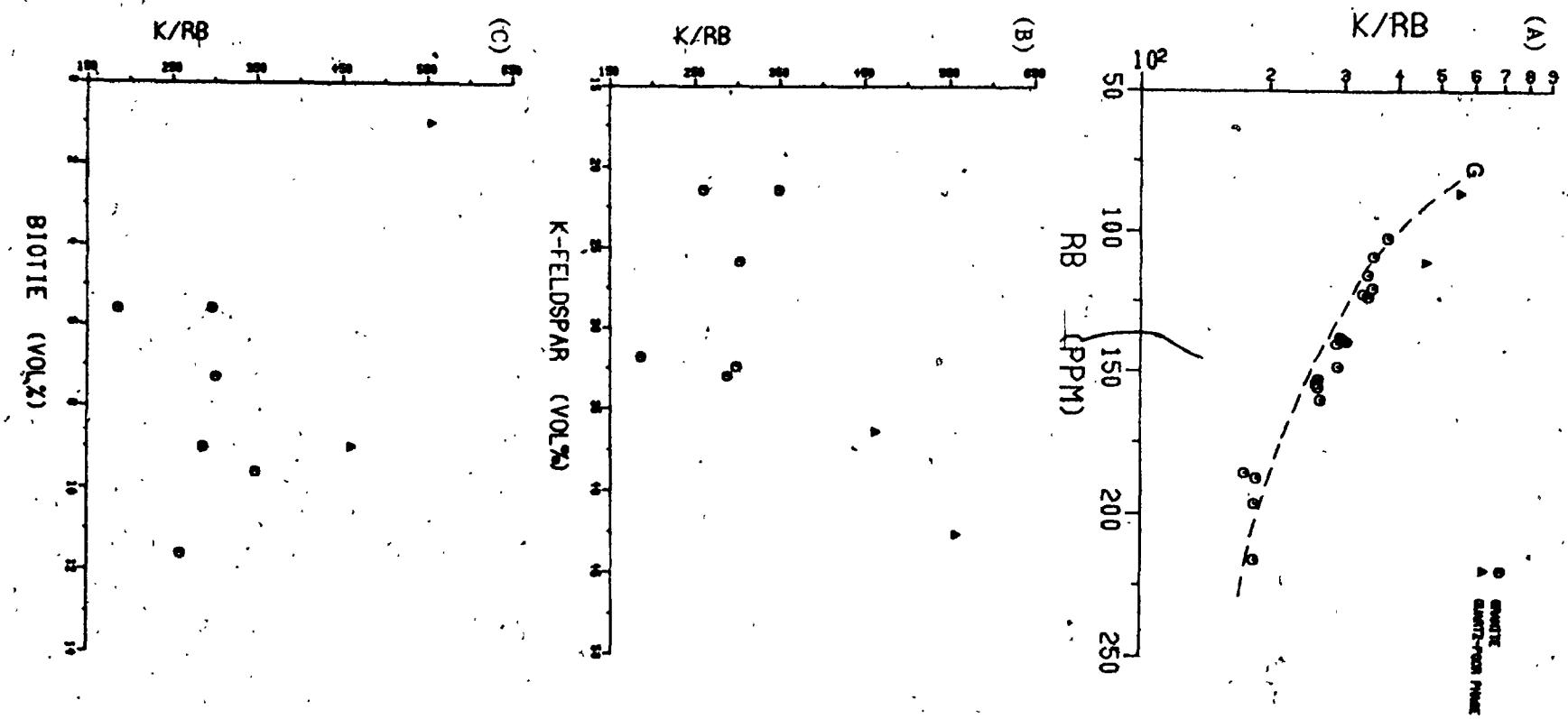

Figure 2-7-11. Variation diagrams of whole-rock K/Rb ratios of the Coe Hill Granite.

(A) K/Rb vs. Rb. G - differentiation trend of the granite.

(B) K/Rb vs. K-feldsapr

(C) K/Rb vs. biotite

between the abundances of biotite and K-feldspar and the whole-rock K/Rb ratios (Fig. 2-7-11B, C) suggest the variation of K/Rb in the melt was mainly controlled by fractionations of the above mineral phases. On the other hand, the strong correlations of Rb/Sr, Sr/Ca and Sr/Ca with SiO_2 support the important role of plagioclase during the evolution of the pluton.

The steep decline of Zr with increasing SiO_2 in the granitic rocks (R = -0.96) may reflect a zircon fractionation. The positive correlations of Cr/Mg, V/Mg, Ni/Mg and Fe/Mg and negative correlations of V/Fe, Ni/Fe with SiO_2 indicate a tendency of increasing Fe and decreasing Mg during differentiation; that is, the Fe/Fe+Mg ratio of the melt increases towards the more silicic rocks.

In terms of Rb-Ba-Sr (Fig. 2-7-12), most of the granitic rocks fall in the anomalous granite field of Bouseily and Sokkary (1975) and the rest are plotted within the range of highly differentiated granite, whereas the monzonites are scattered in the fields of less differentiated and normal granites. Such a relationship may argue against the magmatic origin for some of the granitic rocks of the pluton; however, the enrichment of Sr and/or depletion of Ba can be also due to their source rock.

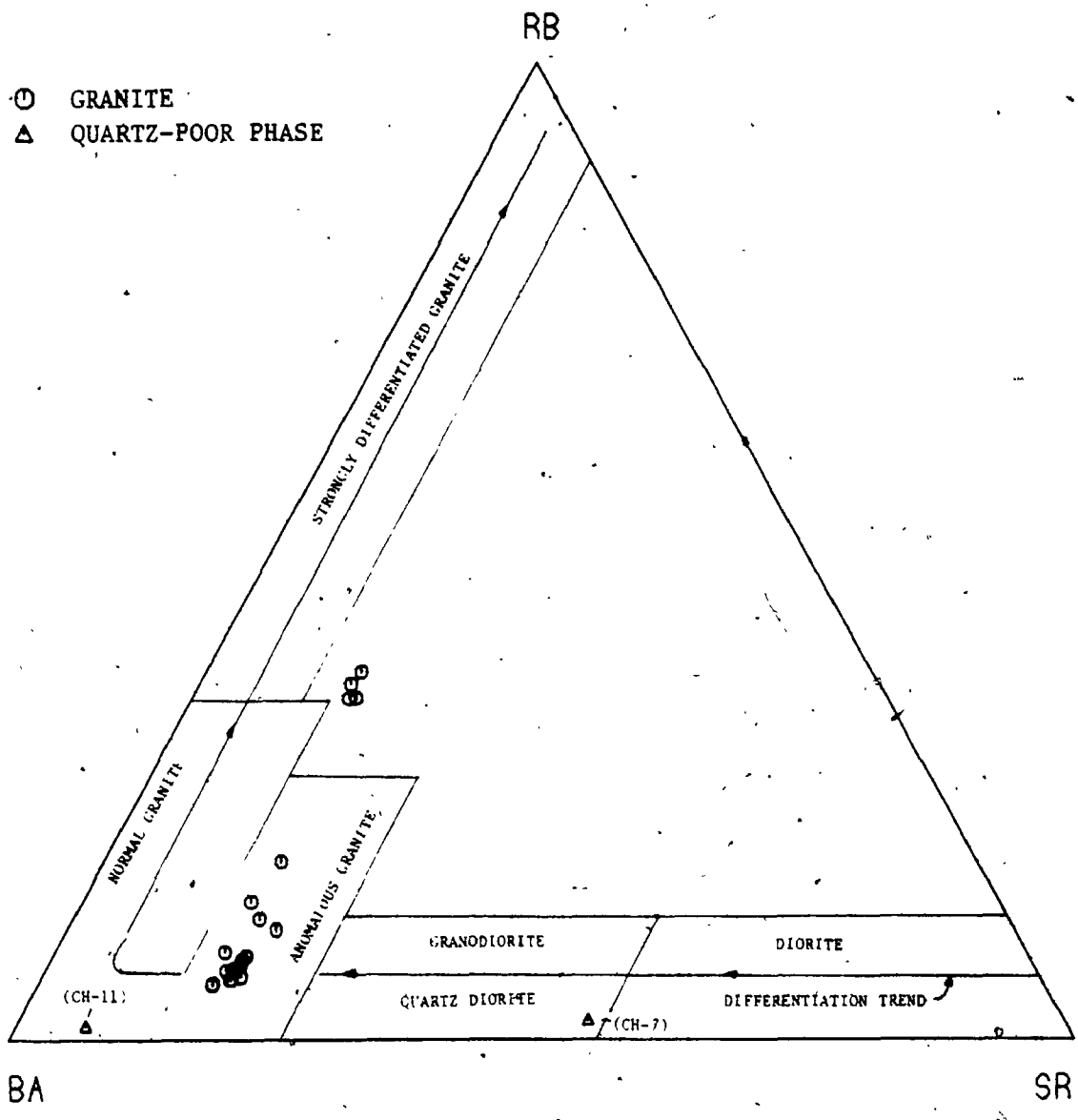

Figure 2-7-12. Rb-Ba-Sr ternary variation diagram of the Coe Hill Granite (after Bouseily and Sokkary, 1975).

7.3.3 Rare-earth Elements -

Rare-earth element data of representative samples from the Coe Hill Granite and similar rock types of the Loon Lake Pluton are listed in Table 2-7-5. Their chondrite-normalized distribution patterns are shown in Figure 2-7-13. Comparatively, the mozonitic rock of the pluton has higher total REE concentration, a well-fractionated curve with steep slope and a small positive Eu-anomaly. While the granitic rocks have lower absolute REE contents and relatively less-fractionated patterns, with or without HREE fractionation, and small negative Eu-anomaly. In general, the normalized REE patterns of the Coe Hill Granite is similar to those of the Loon Lake Pluton, except that the monzonitic rocks of the former show a steeper negative slope than the latter.

The increase of Eu/Eu* value with increasing SiO_2 of the Coe Hill Granite confirms the role of plagioclase fractionation during its evolution. The steep, HREE-depleted pattern of the monzonitic rock may reflect fractionation of pyroxene (hypersthene) or garnet in the residual phase during partial melting. Dostal (1975) argued that in Loon Lake Pluton, the relatively unfractionated HREE patterns of the granitic rocks are probably caused by the accumulation of accessory minerals, which masked

Table 2-7-5. Rare-earth element compositions of the Coe Hill Granite and similar rock-types of the Loon Lake Pluton

	1 CH-7	2 CH-2	3 CH-10-1	4 207	5 98	6 115	7 27
La (ppm)	86.01	63.55	66.21	61.20	229.00	114.00	108.00
Ce	175.78	153.18	85.96	113.00	585.00	224.00	226.00
Sm	15.32	17.53	21.26	13.80	67.00	10.90	15.80
Eu	3.94	3.17	4.51	7.24	14.10	3.10	2.78
Tb	1.10	2.08	1.78	1.64	7.94	1.86	1.49
Yb	1.70	8.68	6.72	2.65	5.30	5.16	5.99
Lu	0.24	1.50	1.19	0.39	0.82	0.84	0.91
7REE	284.09	249.69	187.63	199.92	909.16	379.86	360.97
$(Ce/Yb)_N$	22.20	4.10	2.90	9.80	19.00	4.00	6.60
$(Ce/Sm)_N$	2.40	1.80	1.10	1.70	1.80	2.90	2.90
$(Tb/Yb)_N$	2.60	1.00	0.80	2.70	4.80	1.10	1.00
Eu/Eu^*	1.06	0.63	0.82	1.81	1.05	0.88	0.63
SiO_2 (wt%)	56.67	66.29	65.63	59.41	63.28	72.03	70.44

1. CH-7 (monzonitic rock); CH-2, CH-10-1 (granitic rock), this study.
2. 207, 98 (monzonite); 115, 27 (granite) from Loon Lake Pluton, (Dostal, 1975).
3. Eu^* value is extrapolated graphically from the values of Sm and Tb.
   Eu/Eu^* = the degree of Eu anomaly;
   > 1, positive anomaly;
   < 1, negative anomaly.

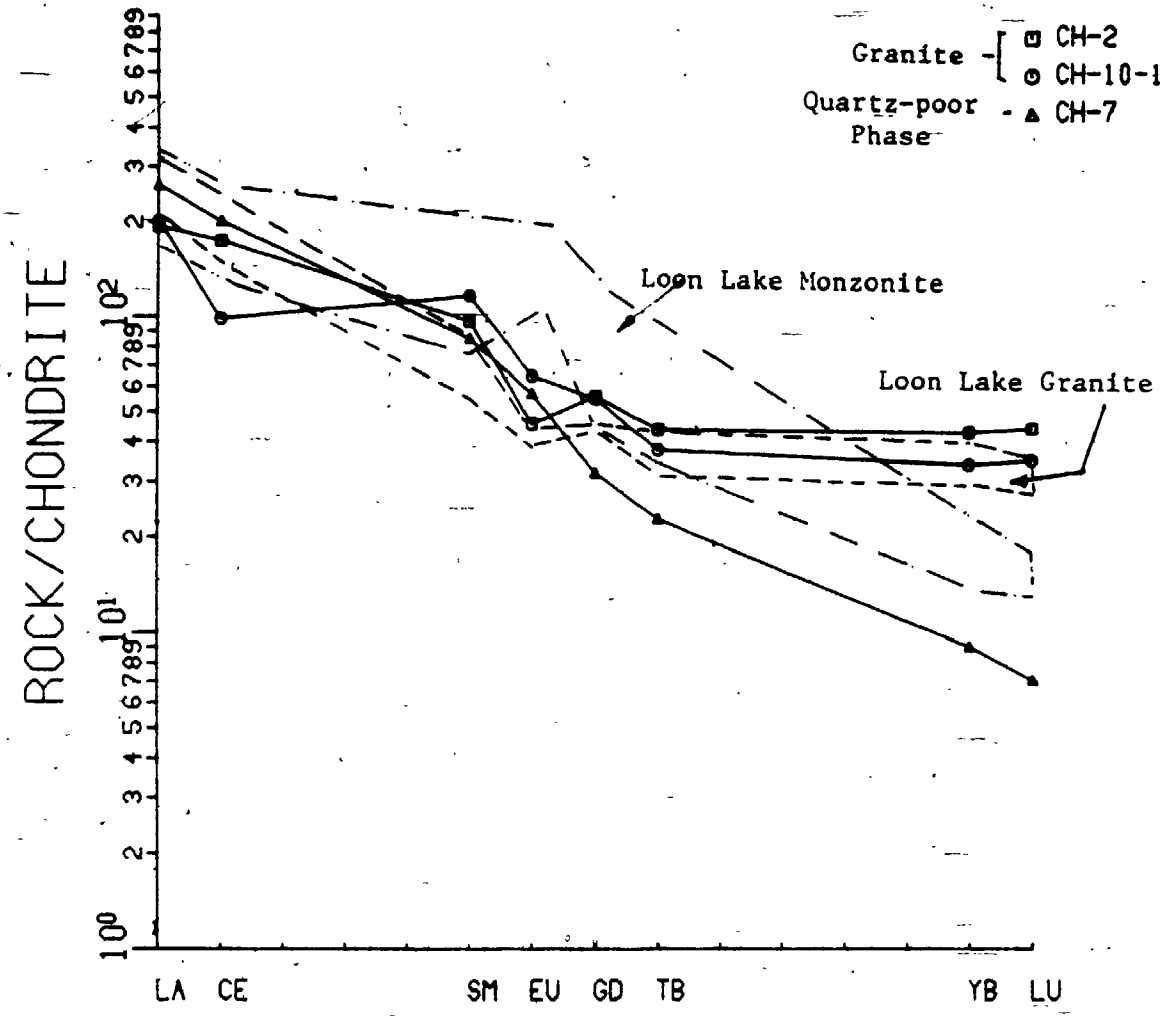

Figure 2-7-13. Chondrite-normalized REE distribution patterns of the Coe Hill Granite. REE fields of Loon Lake granite and monzonite were taken from Dostal (1975).

their inherent REE characters.

7.4 Isotope Geochemistry

Whole-rocks oxygen isotope analyses have been performed on three representative granitic samples from this pluton; the $^{18}O/^{16}O$ ratios are 10.01, 10.00 and 10.74 o/oo. Comparatively, the Coe Hill Granite has a narrower range of $\delta^{18}O$ values than those of the Loon Lake Pluton, ranging from 8.8 to 12.0 o/oo. However, it is in the range of isotopically "normal" granite of Taylor (1978) and is consistent with the intermediate $\delta^{18}O$ granite of the Grenville Province of Ontario (Shieh, 1980; ranging from 9.0 to 12.5 o/oo). The intermediate $\delta^{18}O$ of this pluton may suggest a source of mixed high-^{18}O Grenville metasediments with low-^{18}O basement gneisses of the supercrustal rocks (Shieh, 1980).

The nearby Loon Lake Pluton consists of similar mineral and chemical compositions to the Coe Hill Granite and has been dated by Heaman et al. (1980). The whole-rock Rb-Sr isochron yields an age of 1059 $\pm$ 12 Ma and an initial ratio (R_i) of 0.7035. The relatively low R_i and high $\delta^{18}O$ have led the above authors to conclude that the Loon Lake Pluton can not be isotopically identified as either the S- or I-type granitoids of Chappell and White (1974). However, if only the granitic rocks are considered and a similar low

R_i is assumed, the Coe Hill Granite may be isotopically classified as I-type granite (i.e. R_i = 0.704 - 0.706, $\delta^{18}O$ = 6 - 10).

7.5 Petrogenesis And Source Rocks

Despite of the varying slopes of variation trends in both rock-types, the inter-element and element-ratio variations of alkali and alkaline earth elements suggest that the Coe Hill Granite is a comagmatic suite. In addition, Dostal (1975) indicated that the monzonite and granite of the Loon Lake Pluton are comagmatic but not simply products of continuous fractionation; in other words, they differentiated independently.

From both major- and trace-element data, the variation trends of the granitic rocks of the Coe Hill Granite can be best explained by fractional crystallization of hornblende, feldspars or biotite and accessory minerals (eg. ilmenite, sphene, apatite and zircon). The limited data for the monzonitic rocks do not contribute to a ready understanding of their evolution, especially the K/Rb data.

Such a monzonitic magma may be produced by partial melting of quartz-poor feldspathic material with high K/Rb ratio, or derived from "two-stage" melting processes in the lower crust; firstly, to produce a high K/Rb granulite residuum and then to have a high degree of

partial melting of this material with no feldspar in the residual (Dostal, 1975). Alternatively, it can be derived from extensive fractionation of a more primitive magma (e.g. mantle peridotite).

Miller (1978) proposed that the California monzonites, which are intermediate in SiO_2, metaluminous, high in Na_2O+K_2O, high in LIL-elements with well fractionated REE patterns and contain moderate initial $^{87}Sr/^{86}Sr$ ratios, were most likely derived from the partial melting of alkali eclogite with composition similar to continental tholeiite. However, the California monzonites have moderate K/Rb ratios in comparsion with the equivalents of the Coe Hill Granite and the Loon Lake Pluton. Besides, the California monzonites are considered to be emplaced earlier and are not cogenetic with those calc-alkali granitic batholiths along the west coast of N. America.

Dostal (1975) suggested that in the Loon Lake Pluton the granitic melt was formed by mixing of monzonitic magma with partially fused Grenville basement gneisses, similar to the composition of Apsley biotite gneiss. The Apsley gneisses were interpreted as a series of interstratified silicic volcanic rocks and sandstone horizons (Shaw, 1972) with a reasonable long term crustal history. However, because of the low R_i (0.703) of the Loon Lake Pluton, assimilation processes of such a basement gneiss would not be of a large scale.

Quantitatively, if the differentiation trends are the results of crystal fractionation, then the higher silica rocks should be readily derived from the lower silica ones by extraction of a reasonable hypothetical mineral assemblage. Mass balance calculations (Stormer and Nicholls, 1978) for the granitic rocks of the Coe Hill Granite suggest that crystallize (or substract) a model solid of 11% hornblende, 5% biotite, 40% plagioclase, 35% K-feldspar, 3% sphene, 0.8% apatite and 5% magnetite from sample CH-8 (64.31% SiO_2) is required to form the high silica sample CH-12-3 (73.96% SiO_2). The proportions of removed solid to the evolved magma is about 56:44. The sum of squares for the residuals of this model is about 0.0078, indicating a very good agreement between the model and observed data.

Similar calculations were performed between the monzonitic (CH-11) and granitic (CH-8) rocks but no reasonable results were obtained. This may reflect either the two rock units were not cogenetic or they were cogenetic but differentiated separately. In order to illustrate the possibility of assimilation of partially melted basement gneisses (taken to be the Apsley biotite gneiss of Shaw, 1972) with the monzonitic magma, 5% leucogranite (no. 259) of Dostal (1973) was mixed with sample CH-11. Surprisingly, the resulting magma (the possible proto-granitic melt) gave a reasonable mineral assemblage for magmatic

differentiation. It is suggested that 100 units of mixed-magma = 6% CH-8 + 6% hornblende + 49% plagioclase + 35% K-feldspar + 1% sphene + 3% magnetite.

7.6 Summary

Although no zoning distribution was found in the Coe Hill Granite, the mineral and chemical variations are similar to the nearby, well-dated Loon Lake Pluton.

As shown in the Rb-Ba-Sr ternary diagram, most of the granitic rocks have relatively higher Sr/Ba ratios than those of "normal" granite; this can be explained by either metasomatic reactions or a combination of their higher Sr source rock and/or fractionation of Ba-retaining phases. However, the positions of both rock-types of the pluton in the Qtz-Ab-An-Or-H_2O system indicate a magmatic rather than a metasomatic origin.

The chemical evidences and field relations favour the comagmatic interpretation between the monzonitic and granitic rocks of the pluton, although only limited monzonitic samples have been studied. The preferred model is that of a monzonitic magma which was derived from partial melting of a high K/Rb granulite precursor in the lower crust. Subsequently, that magma assimilated partly fused basement gneisses to form granitic melt. Both magmas differentiated independently during consolidation.

GEOCHEMISTRY AND PETROGENESIS OF SOME GRANITOIDS IN THE GRENVILLE PROVINCE OF ONTARIO AND THEIR TECTONIC IMPLICATIONS

(VOLUME II)

by

Wu Tsai-Way

Department of Geology

Submitted in partial fulfillment
of the requirements for the degree of
Doctor of Philosophy

Faculty of Graduate Studies
The University of Western Ontario
London, Ontario
May, 1984

© Wu Tsai-Way 1984.

TABLE OF CONTENTS

8.0 DELORO PLUTON

8.1 General Characters And Intrusive Relations

The Deloro Pluton is located in the west-central Madoc and southeast corner of Marmora Townships (Fig. 2-8-1). It is a cresent-shaped, composite intrusive body with the maximum dimension of 10 x 6 km^2. The pluton intruded calcareous metasediments, marbles and andesitic to rhyolitic metavolcanic rocks of the Hastings Basin, and it is unconformably overlain by the undeformed Paleozoic limestone sequences.

Three intrusive phases are present in this pluton (Saha, 1959) : (1) a massive, riebeckite-bearing granite with no or rare foliation or lineation; (2) a fine-grained, flinty leucogranite with granophyric texture; (3) a calcic syenite narrow zone limited to the western margin. Besides, aplitic dykes and pegmatitic veinlets are also observed in riebeckite-bearing granite. Rounded to subrounded riebeckite-enriched xenoliths, ranging in size from 30 cm to a few mm long, are considered to be "autoliths" (Fershtater and Borodina, 1977). Larger angular metavolcanic inclusions of the country rocks are also common at the southeastern border zone.

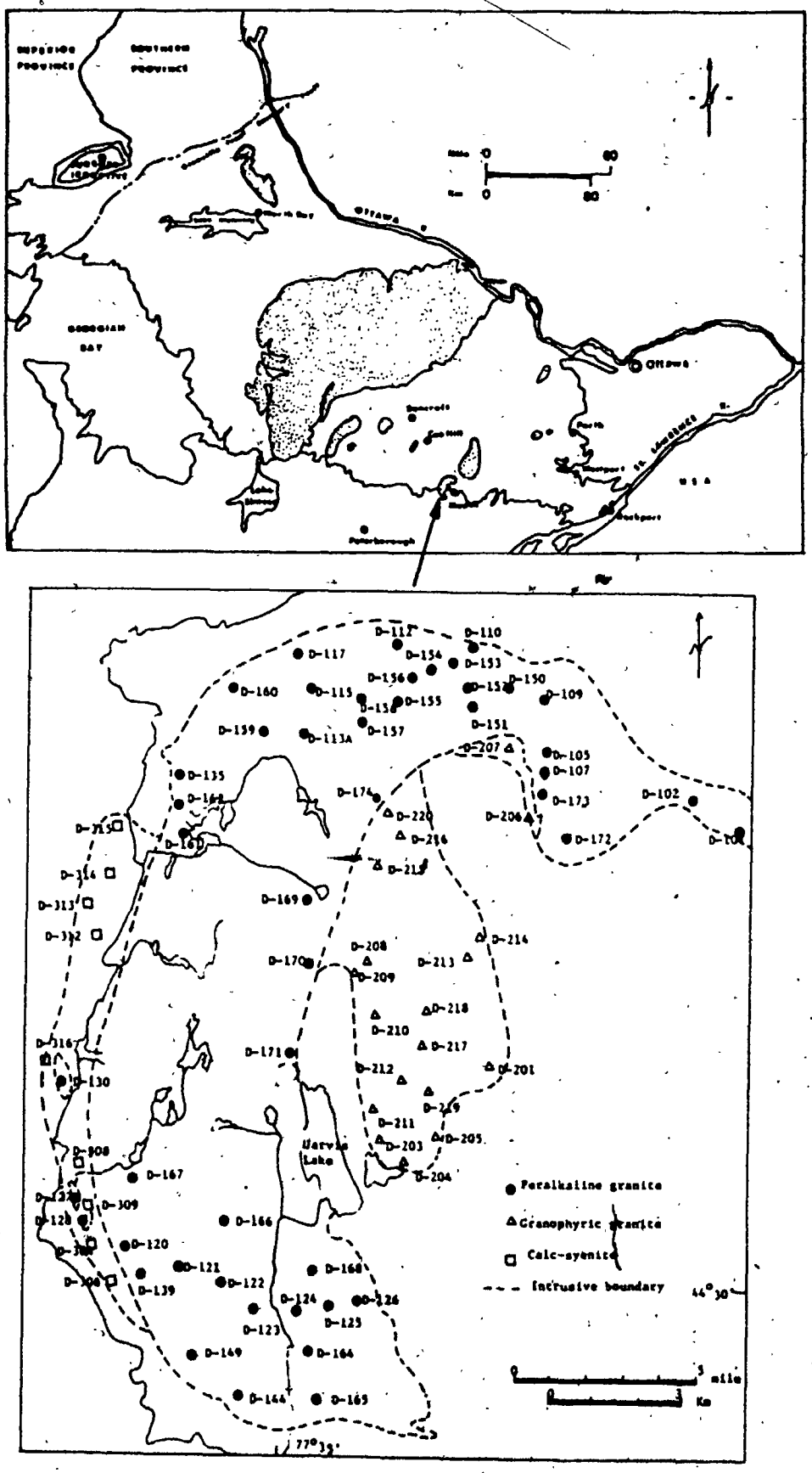

Figure 2-8-1. Sample location map of the Deloro Pluton.

The contact aureole is limited and characterized by the formation of iron ore to the northwest margin; regional metamorphism is in the greenschist facies. Hematization and chloritization are intensively developed along fractures and shear zones.

The occurrence of granophyric texture, the limited contact metamorphism, the lack of foliation and the outward deformation of the country rocks indicate that the Deloro Pluton is an epizonal, forceful intrusion at the wanning stage of the high grade regional metamorphism (Davison et al., 1979). In addition, the presence of perthitic, hypersolvus feldspar, soda amphibole, normative sodium metasilicate and high agpaitic index (> 1) confirmed that the Deloro Pluton is of peralkaline composition (eg. Kuehnbaum, 1973; c.f. Lumbers, 1967).

8.2 Petrography

The Deloro Pluton has been petrographically studied by Saha (1959) and Kuehnbaum (1973); detailed mineral chemistry was also given by the latter author.

8.2.1 Riebeckite-bearing, Hypersolvus Granite -

The riebeckite-bearing granite is mainly composed of hypersolvus feldspar (60%) and quartz (30%), with minor amounts of riebeckite, biotite, zircon, calcite, fluorite, opaques and sphene aggregates. Perthite is the only feldspar; deuteric albitic rims were also found around some perthite grains. Free albite is rare. Euhedral to subhedral quartz grains were strained with wavy extinction; interstitial fine-grained later quartz separates large perthite grains. Riebeckite and biotite form subhedral to anhedral, poikilitic, ragged and inclusion-filled grains; quartz, zircon, fluorite and opaques are common inclusions. The relationship between riebeckite and biotite is considered to be one of mutual equilibrium; the ragged nature of both indicates products of late crystallization. Zircon, calcite, iron oxides, sphene and secondary quartz are clustered along perthite grain boundaries. Ilmenite occurs as individual grains or as exsolution lamellae in the magnetite; sphene aggregates forming rims around ilmentite or magnetite is due to the late stage exsolution of Ti-Fe oxides.

The rounded autoliths (eg. D-124-0) have similar hypersolvus mineralogy to that of the host granite, except for relatively abundant

biotite-riebeckite clusters. Secondary quartz, zircon and calcite are also encountered. Such riebeckite- bearing autoliths are considered to be earlier crystallized host granite which fell back to the residual melt during stoping. Pegmatitic veins with coarse-grained riebeckite and feldspar crystals indicate a late crystallizing phase within a soda-rich fluid.

8.2.2 Granophyric, Subsolvus Granite -

The second phase of the pluton is characterized by its less mafic and leucocratic nature with intensive development of granophyric textures. Feldspars are complex in character and type; microperthite and microcline are frequently intergrown with quartz forming "chessboard" granophyre. Zoned crytoperthitic plagioclase with fine twinning and albitic composition occurs as phenocrysts surrounded by granophyric intergrowth. Anhedral primary muscovite frequently intergrew with chloritized biotite. Opaques and sphene aggregates are associated with biotite. Zircon, fluorite and sulfide minerals are other accessories.

8.2.3 Calc-syenite Suite -

Calc-syenite is considered as a separated body from the Deloro Pluton due to its content of calc-amphiboles (Kuehnbaum, 1973). Subhedral to anhedral green amphiboles form clusters with biotite, zircon, opaques, calcite, sphene and poikilitic fine quartz. Both amphibole and biotite show extensive chloritization in places. Plagioclase phenocrysts are turbid and frequently saussuritized; perthitic alkaline feldspar is still abundant. In sample D-312, it is composed of mainly euhedral epidote crystals and a chlorite - opaques - sphene matrix; sphene corona are well-developed around individual opaque grains. Fluorite and apatite are other accessory minerals.

8.2.4 Other Intrusive Varieties -

In addition to the above three major rock-types, gabbroic and dioritic intrusions are distributed along the western margin beyond the calc-syenite suite; the genetic relation with the Deloro Pluton is unknown at present.

The gabbro is black in clour with laths of well-twinned plagioclase and pyroxene relicts. Hornblende is the most abundant mafic mineral, which is commonly intergrown with biotite; it also occurs

along the edge of pyroxene indicating a replacement relationship. Alkaline feldspar is rare.

Dioritic rocks, ranging from quartz diorite to granodiorite, are mainly composed of hornblende, minor biotite and feldspars. Zircon, apatite, sphene and calcite are accessory phases. Opaques, which are related to mafic minerals, may be due to oxidation.

Later aplitic dyke cutting the ribeckite-bearing granite has fine-grained and leucocratic appearance. In addition to quartz, plagioclase and microcline are predominant constituents; perthitic feldspar crystals are frequently found as phenocrysts. Hematite and ferruginous material are the only mafic components.

8.3 Whole-rock Geochemistry

8.3.1 Major-oxides -

Compositions of both riebeckite-bearing granite and granophyric granite are peralkaline with normative acmite, 0.14 - 6.80 for the former and 1.45 - 6.12 for the latter, and sodium metasilicate. The 0% anorthite in the norms reflects their hypersolvus mineralogy. The agpaitic indices are 1.09 for the riebeckite granite and 1.08 for the

granophyric granite; the calc-syenite suite has a value less than 1.

The average major-oxide compositions of various rock-types from the Deloro Pluton and comparison with other peralkaline granites are given in Table 2-8-1. In general, the riebeckite-bearing phase of the pluton is relatively lower in total iron and higher in Al_2O_3 and Na_2O/K_2O ratio compared to other peralkaline granites. It is however similar to that of peralkaline granite from Saudi Arabia (Radain, 1978) in terms of high Na_2O/K_2O ratio and oxidation index. On the other hand, the granophyric granite is similar to the composition of Quincy Granite, New England (Buma et al., 1971), except that the latter has higher K_2O relative to Na_2O. In the normative Qtz-Plag-Or diagram (Fig. 2-8-2), the hypersolvus granitic rocks cluster around the average peralkaline granite of Nockolds (1954), whereas the calc-syenitic rocks form a distinct group with lower normative quartz content. Rocks of the granophyric granite contain a relatively wide range of composition and higher content of normative plagioclase than those of the riebeckite granite.

In the Qtz-Ab-Or plot (Fig. 2-8-3), both riebeckite and granophyric granites fall within the field of granitic rocks (Winkler and Von Platon, 1961), with a few exceptions; while the syenitic

Table 2-8-1. Average composition of the Deloro Pluton and comparison with other peralkaline granites

(wt.%)	1 (n=55)	2	3 (n=10)	4	5 (n=13)	6 (n=14)	7 (n=7)	8 (n=29)	9 (n=8)	10	11
SiO_2	73.97	73.16	73.05	74.86	73.06	75.51	76.10	74.88	65.22	60.32	51.89
TiO_2	0.19	0.27	0.24	0.20	0.30	0.08	0.19	0.17	0.50	1.35	1.14
Al_2O_3	12.05	12.07	10.62	11.61	11.75	10.99	11.49	12.01	14.21	15.13	15.81
TFe_2O_3	2.60	4.07	6.35	3.68	3.98	3.69	1.69	2.74	6.93	8.69	9.74
Fe_2O_3	1.41	1.86	3.04	2.29	1.73	2.92	-	1.65	3.79	2.59	2.80
FeO	0.99	1.99	2.98	1.25	2.03	0.69	-	1.02	2.73	5.49	6.25
MnO	0.02	0.07	0.21	0.02	0.06	0.04	0.02	0.01	0.07	0.09	0.17
MgO	0.13	tr.	0.10	0.05	0.23	0.01	0.37	0.11	0.80	1.92	6.00
CaO	0.49	0.50	0.60	0.41	0.57	0.18	0.49	0.19	0.93	3.66	11.06
Na_2O	5.32	4.57	4.23	4.30	4.35	4.81	3.72	5.31	6.06	6.11	3.20
K_2O	4.11	4.79	4.48	4.64	4.49	3.98	4.97	4.07	3.67	1.84	0.56
P_2O_5	0.04	0.02	0.37	tr.	0.05	0.02	-	0.03	0.10	0.37	0.23
LOI	0.88	0.46	0.08	0.35	0.74	-	-	0.51	1.09	0.47	0.30
Na_2O/K_2O	1.29	0.95	0.94	0.93	0.97	1.21	0.75	1.30	1.65	3.32	5.71
Oxidation Ind.	74	65	67	79	61	89	-	77	69	48	47
Agpaitic Ind.	1.09	1.05	1.11	1.04	1.02	1.11	1.00	1.08	0.99	0.79	0.37

1 Average of 55 riebeckite-bearing hypersolvus granite of the Deloro Pluton (this study).
2 Arfvedsonite granite of Nigeria-Niger Province (Bowden and Turner, 1974).
3 Average of 10 riebeckite granite (Nockolds, 1954).
4 Average composition of Quincy Granite, New Elngland (Buma et al., 1971).
5 Average of 13 peralkaline granite from Labrador (Collerson, 1982).
6 Average of 14 analyses of Jabal Sayid Riebeckite Granite, Saudi Arabia (Radain, 1978).
7 Average of 7 St. Lawrence peralkaline granite, SE Newfoundand (Teng and Strong, 1976).
8 Average of 29 granophyric granite of the Deloro Pluton (this study).
9 Average of 8 calc-syenite of the Deloro Pluton (this study).
10-11 Analyses of diorite and gabbro from western margin of the Deloro Pluton (this study).

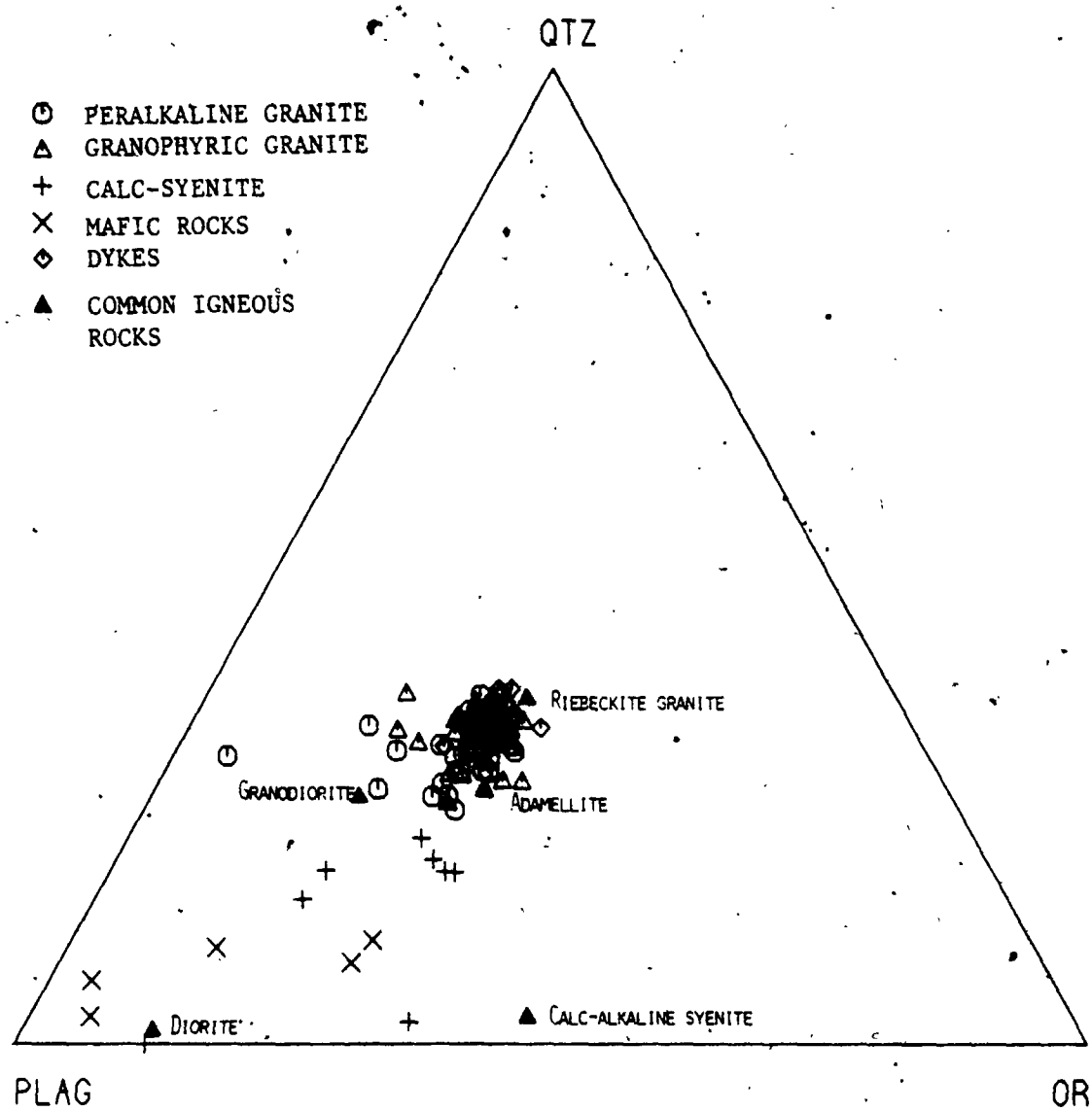

Figure 2-8-2. Normative Qtz-Or-Plag diagram of the Deloro Pluton and common igneous rocks (calculated from Nockolds, 1954).

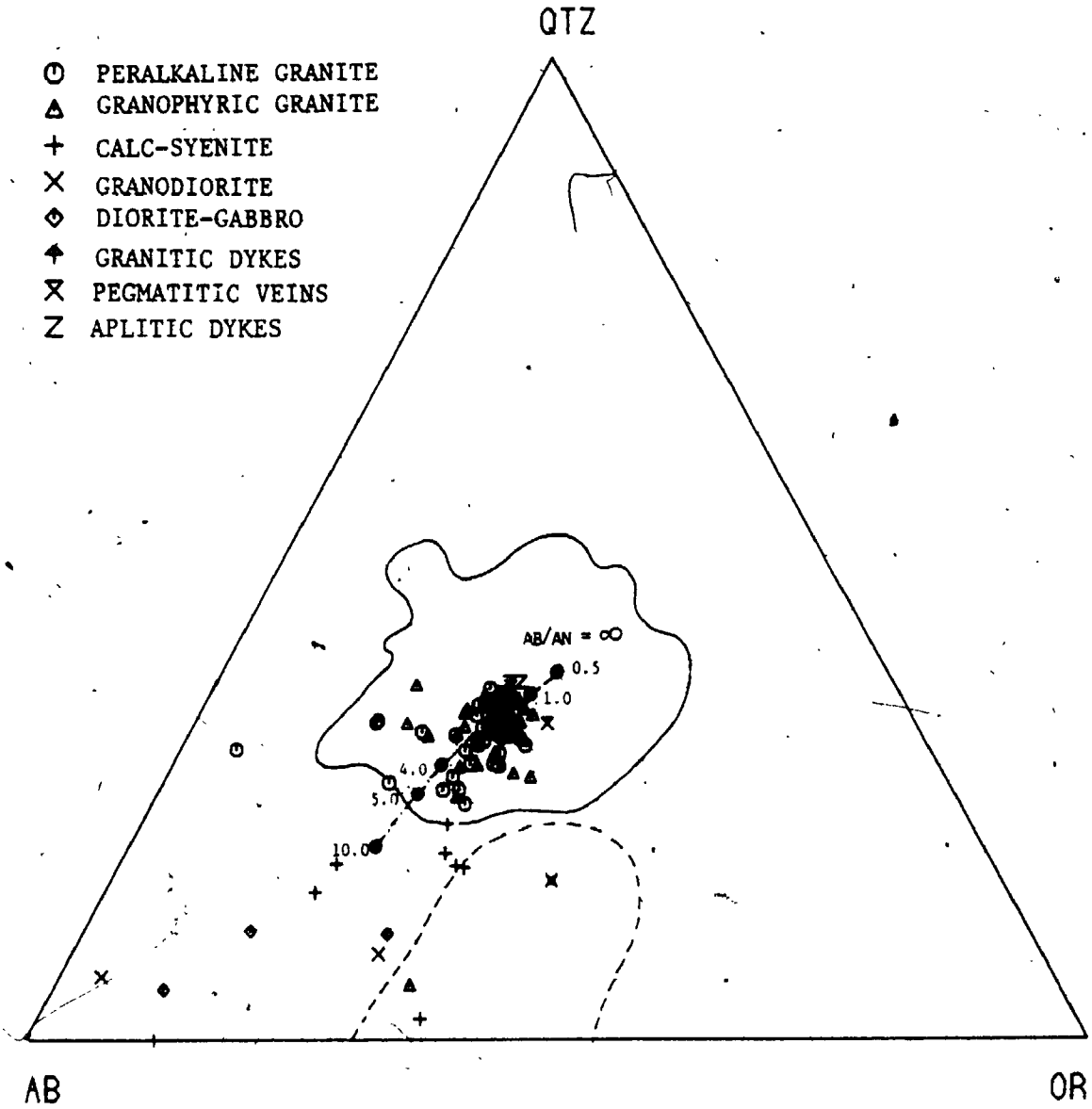

Figure 2-8-3. Normative Qtz-Ab-Or ternary diagram of the Deloro Pluton. The irregular solid boundary indicates the granite field of Winkler and Von Platen (1961). The irregular dashed-line shows the compositional field of syenitic rocks from Gardar Province of Greenland (Watt, 1966). Ternary minima in An-free systems (Tuttle and Bowen, 1958; Luth et al., 1964) are shown by solid circles.

rocks were plotted outside the syenite field of the Gardar Province, Greenland (Watt, 1966). The scatter of data points toward the Ab-apex in the riebeckite granite may reflect the later albitization of the perthite. In addition, rocks of the Deloro Pluton are clustered around the minimum melt compositions of 1 to 3 Kb ($P_{H2O} = P_{Total}$) at the An-free system.

Both Na_2O-K_2O-CaO and AFM diagrams (Fig. 2-8-4, 2-8-5) suggest the Deloro Pluton is a highly differentiated igneous suite following a possible trend similar to Hawaii alkaline basalt (Nocklods and Allen, 1956). Rocks of calc-syenite suite are relatively Na_2O- and iron-enriched, while gabbroic rock fall in the cumulate field of a typical calc-alkaline series (eg. Southern California Bahtolith).

Correlation coefficients of major-oxide variations are given in Table 2-8-2. Although correlation coefficients are higher when the syenite-gabbro is accounted for, the various rock types are not necessarily cogenetic. However, the projections of riebeckite - granophyric granites and calc - syenite in the molecular SiO_2 - Al_2O_3 - total alkali plot (Fig. 2-8-6) are concordant with the formation of peralkaline granite by fractionation of alkali-feldspar from a less siliceous, alkali parent

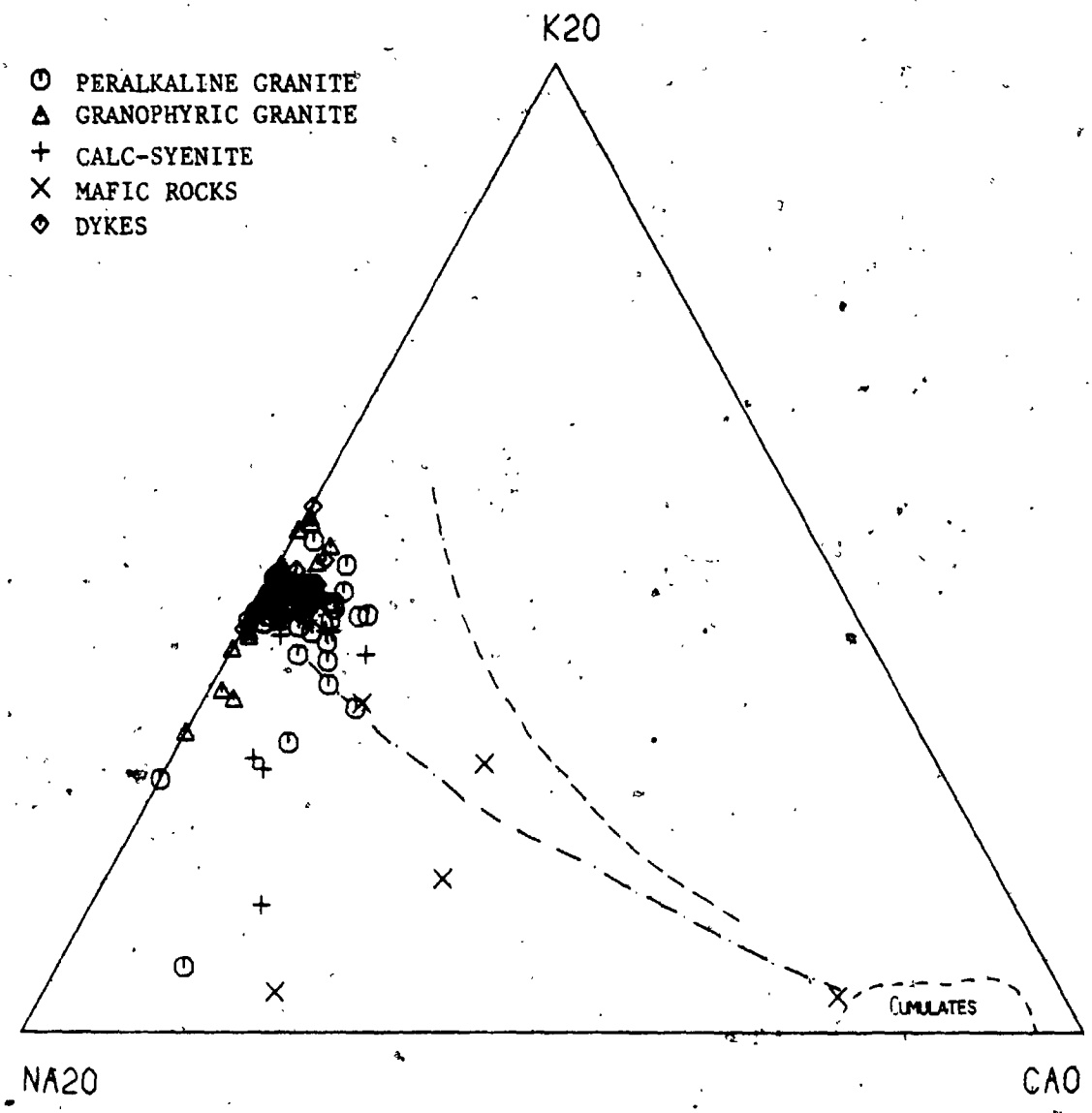

Figure 2-8-4. Na_2O-K_2O-CaO variation diagram of the Deloro Pluton.

—·—·— Calc-alkaline trend of Southern California Batholith (Nockolds and Allen, 1956).

— — — — Differentiation trend of Hawaii alkaline basalt (Nockolds and Allen, 1953)

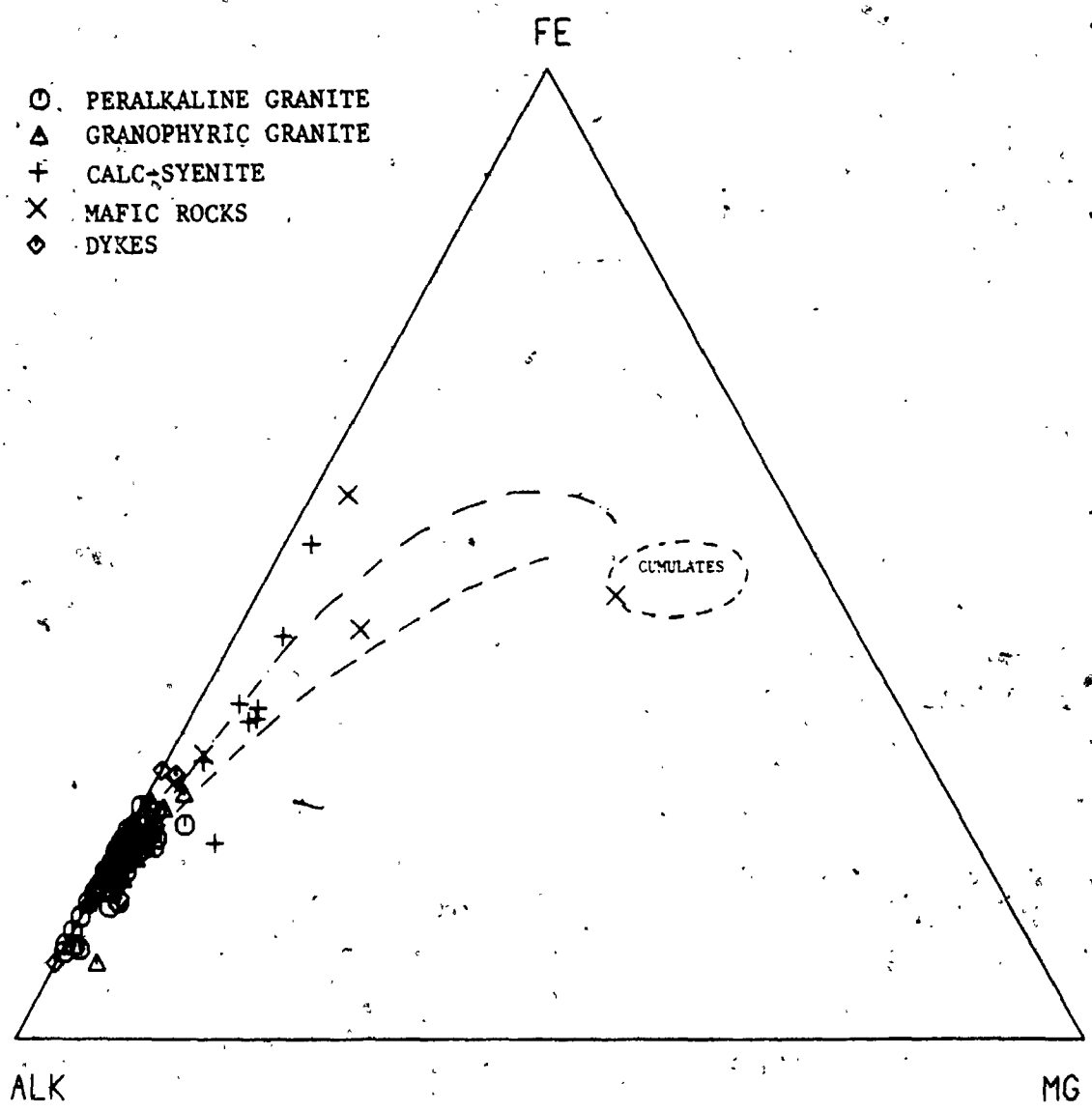

Figure 2-8-5. AFM diagram of the Deloro Pluton.

—·—·— Calc-alkaline trend of Southern California Batholith (Nockolds and Allen, 1956).

– – – – Differentiation trend of Hawaii alkaline basalt (Nockolds and Allen, 1953).

Table 2-8-2. Correlation coefficients of major-oxide variations for the Deloro Pluton

	SiO_2	TiO_2	Al_2O_3	Fe_2O_3	MnO	MgO	CaO	Na_2O	K_2O	P_2O_5
(a) Riebeckite + granophyric granites (84 samples)										
P_2O_5	-0.25	0.34	0.22	0.10	0.15	0.05	0.16	0.15	-0.05	1.00
K_2O	-0.25	-0.09	0.09	0.39	0.04	-0.21	-0.38	-0.89	1.00	
Na_2O	0.16	0.09	0.10	-0.41	-0.11	0.15	0.28	1.00		
CaO	-0.46	0.55	0.29	-0.24	0.06	0.33	1.00			
MgO	-0.42	0.53	0.35	0.15	0.13	1.00				
MnO	-0.21	0.18	-0.08	0.26	1.00					
Fe_2O_3	-0.50	0.27	0.11	1.00						
Al_2O_3	-0.68	0.68	1.00							
TiO_2	-0.76	1.00								
SiO_2	1.00									
(b) Granite + calc-syenite + diorite + gabbro										
P_2O_5	-0.75	0.88	0.67	0.67	0.65	0.62	0.61	0.14	-0.41	1.00
K_2O	0.38	-0.47	-0.40	-0.20	-0.36	-0.47	-0.57	-0.74	1.00	
Na_2O	-0.10	0.12	0.28	-0.01	0.08	-0.08	0.03	1.00		
CaO	-0.75	0.75	0.61	0.52	0.67	0.92	1.00			
MgO	-0.79	0.80	0.65	0.61	0.67	1.00				
MnO	-0.83	0.72	0.64	0.84	1.00					
Fe_2O_3	-0.89	0.77	0.71	1.00						
Al_2O_3	-0.90	0.83	1.00							
TiO_2	-0.90	1.00								
SiO_2	1.00									

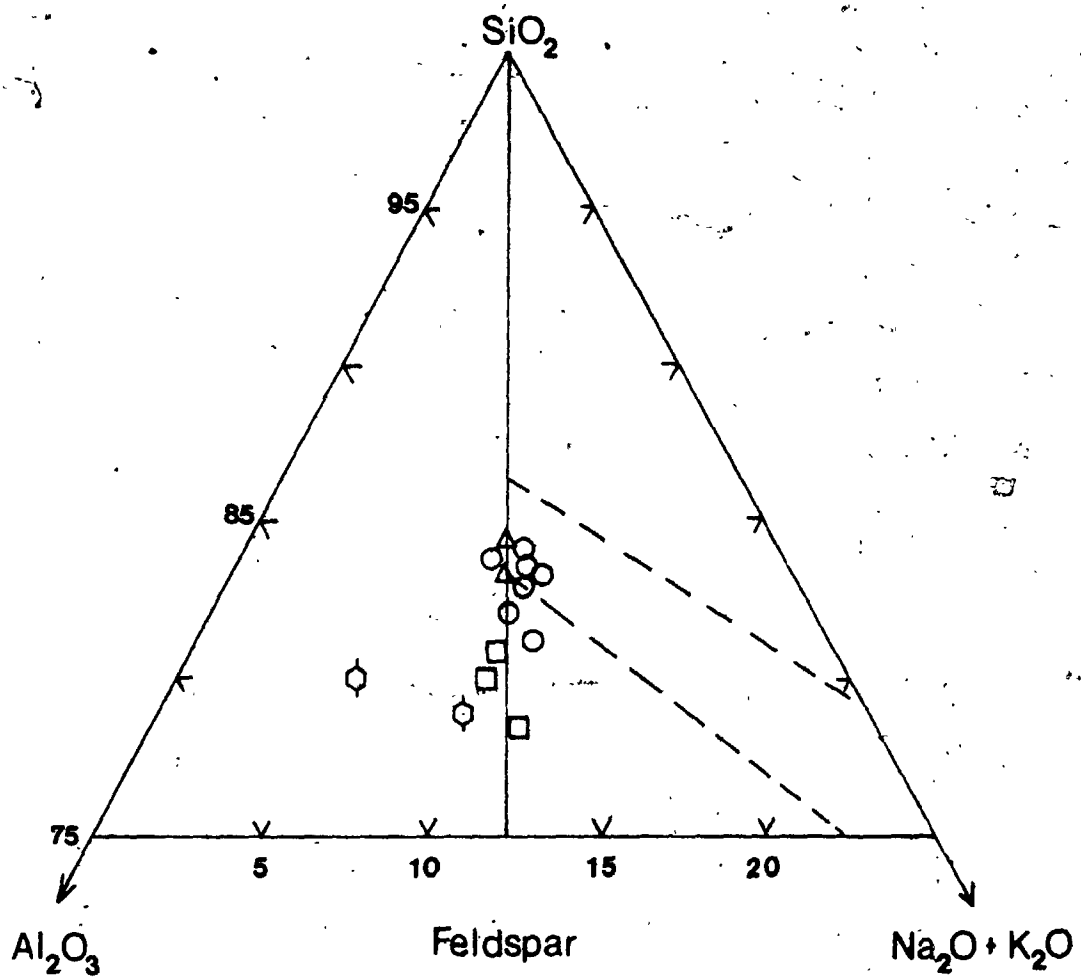

Figure 2-8-6. Molecular proportions of SiO_2-Al_2O_3-total alkali of the Deloro Pluton. Dashed-lines are the quartz-k-feldspar cotectic (upper) and quartz-albite cotectic (lower) plotted by Bailey and Macdonal (1969). For the sake of clarity, only representative samples were plotted.

- ○ Riebeckite-bearing granite
- △ Granophyric granite
- □ Calc-syenite
- ⌀ Diorite-gabbro

(Bailey and Macdonald, 1969).

8.3.2 Trace-elements -

Average trace-elment concentrations of the Deloro Pluton are given in Table 2-8-3. The riebeckite-bearing hypersolvus granite and granophyric granite have similar trace-element compositions, except that the latter has relatively higher Rb/Sr, Sr/Ca and lower K/Rb, which is consistent with normal igneous differentiation. While the calc-syenite suite contains relatively higher Sr, Zr, Zn, K/Rb and Zr/Nb and lower Rb and Nb with respect to riebeckite and granophyric granites.

In comparison with other peralkaline granites, the Deloro Pluton generally has lower Rb, Nb, Zr, Rb/Sr and higher Sr, Ba, femic elements, K/Rb, Sr/Ca. On the other hand, the pluton is enriched in high-field strenghth (HFS) elements (eg. Nb, Zr, Ga, Y) and depleted in alkaline trace-elements (eg. Rb, Sr, Ba) as compared to low-Ca granite (Turekian and Wedepohl, 1961). The anomalous enrichment of HFS elements are characteristic of peralkaline granite (Tauson, 1967; Buma et al., 1971).

Correlation coefficients of trace-element variations in the Deloro Pluton are given in Table

Table 2-8-3. Average trace-element concentrations of the Deloro Pluton and comparison with other peralkaline granite

(ppm)	1 (n=55)	2 (n=33)	3 (n=7)	4	5 (n=13)	6 (n=12)	7 (n=7)	8
Rb	81	97	67	1400	256	356	266	170
Sr	43	43	87	-	20	11	-	100
Ba	253	347	326	-	158	6	160	840
Nb	43	44	38	1500	49	126	-	21
Zr	463	480	652	2160	1046	1653	484	175
Y	93	89	79	585	73[illegible]	201	-	40
Ga	27	26	31	[illegible]	27	-	-	17
Ni	9.5	9.6	6.6	-	4.5	32	-	4.5
Cr	5.7	5.6	7.5	-	7.7	44	-	4.1
V	8.5	7.8	3.8	-	5.6	-	-	44
Zn	36	35	53	-	143	-	39	39
K/Rb	436	348	455	25	241	95	155	247
Rb/Sr	2.01	2.29	0.99	-	12.80	32.30	-	1.70
Sr/Ca	288	[illegible]99	279	-	37	85	-	196
Zr/Nb	11.40	11.80	16.80	1.41	21.30	14.30	-	8.30
Ga/Al	4.20	4.18	4.23	8.42	4.34	-	-	2.36

1 Average of 55 analyses of riebeckite-bearing granite from Deloro Pluton (this study).
2 Average of 13 analyses of granophyric granite from Deloro Pluton (this study).
3 Average of 7 analyses of calc-syenite suite from Deloro Pluton (this study).
4 Albite riebeckite-arfvedsonite granite of the Liruei Complex, Nigeria (Bowden and Turner, 1974).
5 Average of 13 peralkaline granite from Labrador, Newfoundland (Collerson, 1982).
6 Average of 12 Jabal Sayid riebeckite granite, Saudi Arabia (Radain, 1978).
7 Average of 7 St. Lawrence granite, Newfoundland (Teng and Strong, 1976).
8 Average low-Ca granite (Turekian and Wedepohl, 1961).

2-8-4. Except for Sr and V having moderate negative slopes and Zr and Th showing a weak positive correlation with SiO_2, there are no distinctive differentiation trends in the riebeckite-granophyric granites. However, it is noted that there are positive correlations among HFS elements, which is consistent with the behavior of these incompatible trace-elements in an alkaline magma (Barker, 1976). The positive correlation between Nb and Ga/Al (Table 2-8-4) and the expected increase of Ga/Al with differentiation mark these rocks as being residual portions of a strongly fractionated alkaline magma (Siedner, 1965) Although there are weak correlations among alkali element-ratios, they are more or less in accord with the mechanism of fractionation of feldspars.

With a few exceptions, the riebeckite - granophyric granites are plotted as a comagmatic series in the Log K/Rb vs. Rb diagram (Fig. 2-8-7). As expected, the granophyric granite with relatively higher Rb is younger than the riebeckite granite; however, the overlaps between these two granites are marked. The calc-syenitic rocks, on the other hand, form a convex trend which deviates from the trend of those granitic rocks. In terms of Rb-Ba-Sr ternary variation (Fig. 2-8-8), most samples of the granophyric granite fall within the

Table 2-8-4. Correlation coefficients of trace-element variations for the Deloro Pluton

	Nb	Zr	Y	Sr	Rb	Pb	Zn	Cu	Ni	Cr	Ba	V	S	Ga	U	Th	F	Cl
(a) Riebeckite + granophyric granites (84 samples)																		
SiO_2	0.15	0.22	0.05	-0.45	-0.05	0.16	-0.23	-0.02	0.01	-0.19	-0.09	-0.36	-0.11	0.06	0.06	0.23	0.02	-0.09
Nb	1.00	0.16	0.42	0.16	0.24	0.10	0.14	-0.07	0.08	0.04	-0.26	-0.03	0.02	0.40	0.47	0.36	0.18	-0.17
Zr	-	1.00	0.34	-0.34	0.19	0.05	-0.03	0.04	0.23	-0.02	0.04	-0.17	-0.06	0.53	0.15	-0.03	-0.35	0.06
Y	-	-	1.00	-0.03	0.37	0.16	0.36	-0.04	0.53	0.11	-0.06	-0.02	0.02	0.55	0.54	0.49	0.29	-0.27
Th	-	-	0.49	-0.19	0.30	-0.06	0.18	-0.16	0.33	-0.09	-0.16	-0.14	-0.14	0.12	0.77	1.00	0.42	-0.30
(b) Granite + calc-syenite + diorite + gabbro (96 samples)																		
SiO_2	0.27	0.03	0.30	-0.81	0.29	0.03	-0.45	-0.27	0.11	-0.62	-0.11	-0.50	-0.45	-0.19	0.46	0.63	0.36	-0.86
Nb	1.00	0.23	0.49	-0.18	0.30	0.10	0.05	-0.08	0.15	-0.08	-0.32	-0.07	-0.08	0.32	0.52	0.44	0.27	-0.34
Zr	-	1.00	0.43	-0.18	-0.12	0.05	-0.01	0.01	0.16	-0.21	0.01	-0.26	-0.09	0.62	0.21	0.01	-0.15	-0.13
Y	-	-	1.00	-0.29	0.39	0.14	0.18	-0.10	0.52	-0.19	-0.09	-0.18	-0.13	0.45	0.61	0.55	0.37	-0.47
Th	0.44	0.01	0.55	-0.57	0.49	-0.01	-0.13	-0.30	0.24	-0.43	0.05	-0.40	-0.28	0.09	0.84	1.00	0.53	-0.70

	K/Rb	Rb/Sr	Sr/Ba	Sr/Ca	Ga/Al	Zr/Y		Ga/Al
(a) Riebeckite + granophyric granites (84 samples)								
SiO_2	-0.25	0.25	0.13	0.10	0.29	-0.33	Nb	0.46
(b) Granite + calc-syenite + diorite + gabbro (96 samples)								
SiO_2	0.10	0.58	-0.46	0.10	0.35	-0.79	Nb	0.52

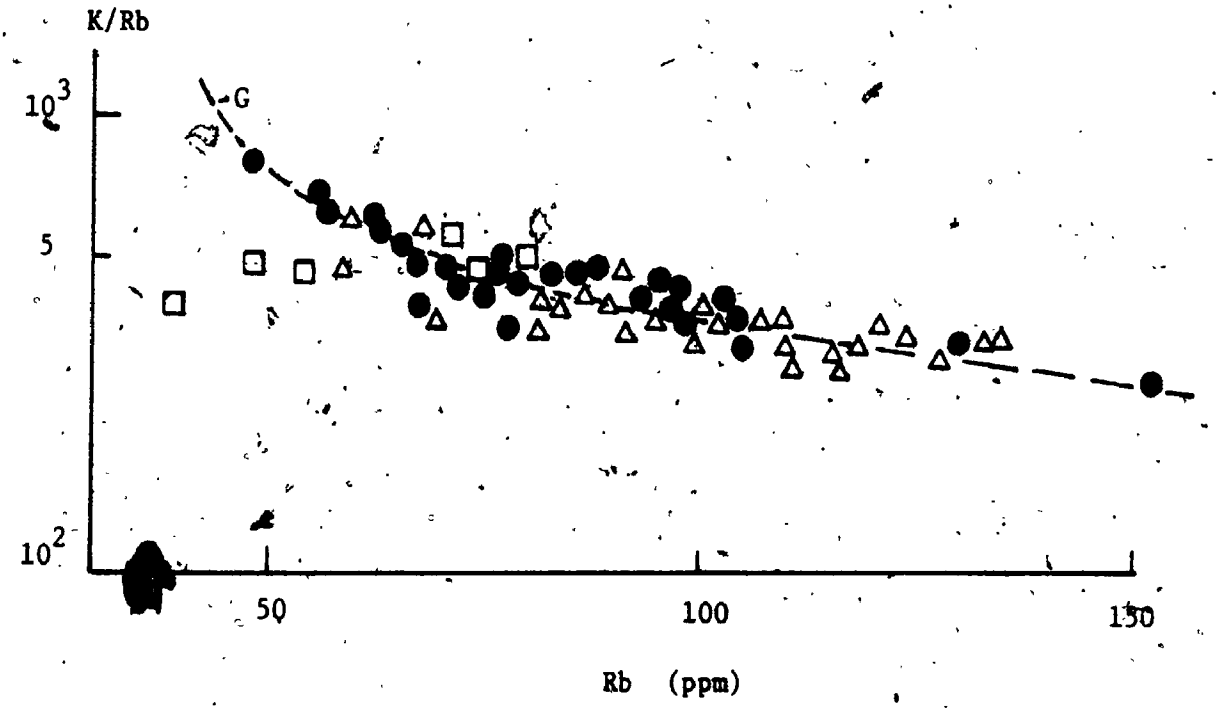

Figure 2-8-7. K/Rb ratio vs. Rb variation diagram of the Deloro Pluton.

G – differentiation trend of the Deloro Pluton

● Riebeckite-bearing granite

△ Granophyric granite

□ Calc-syenite

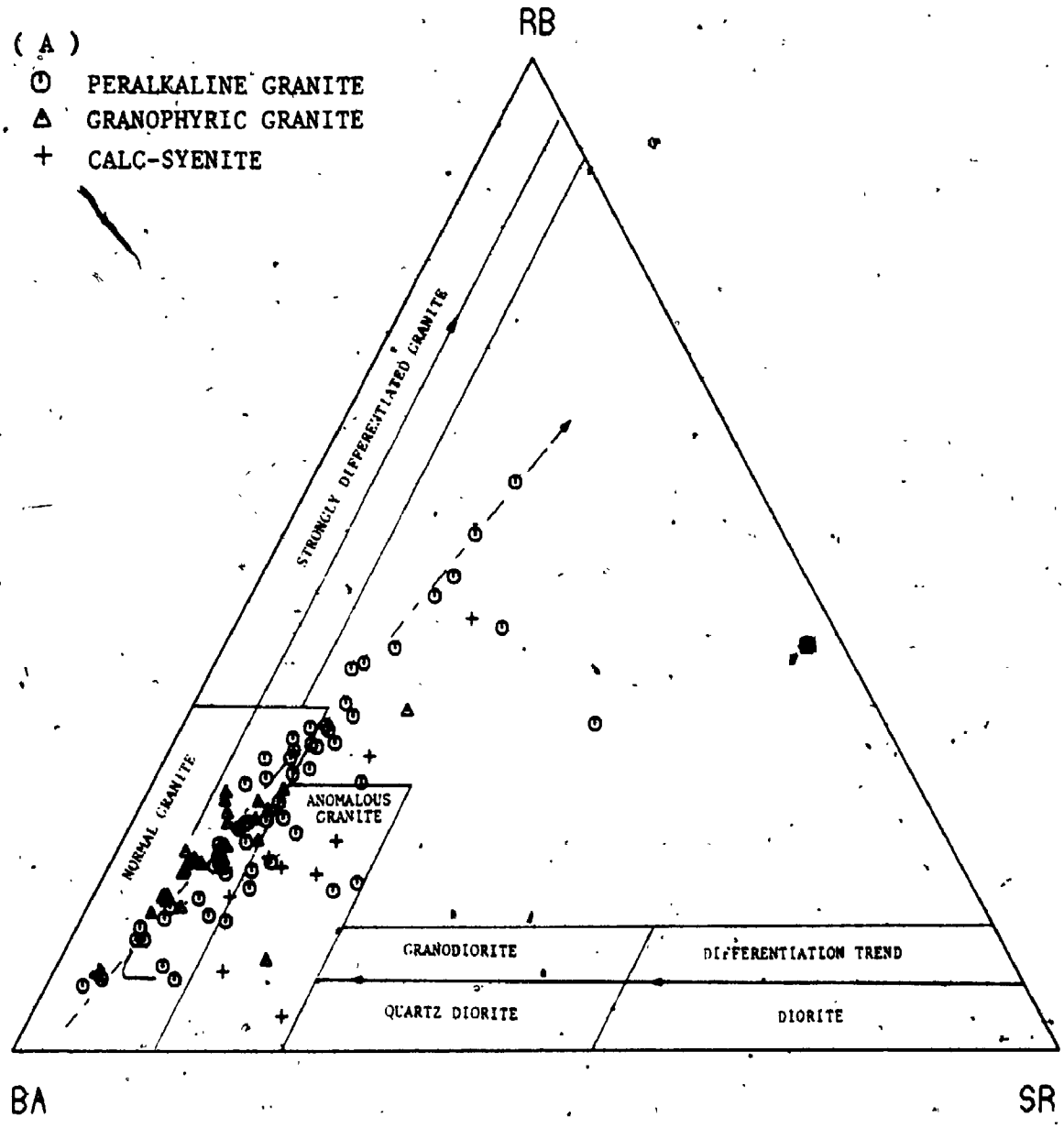

Figure 2-8-8. Rb-Ba-Sr ternary variation diagram of the Deloro Pluton (after Bouseily and Sokkary, 1975).

(A) Riebeckite-bearing granite, granophyric granite and calc-syenite of the Deloro Pluton.
Dashed-line indicates the differentiation trend of the Deloro Pluton.

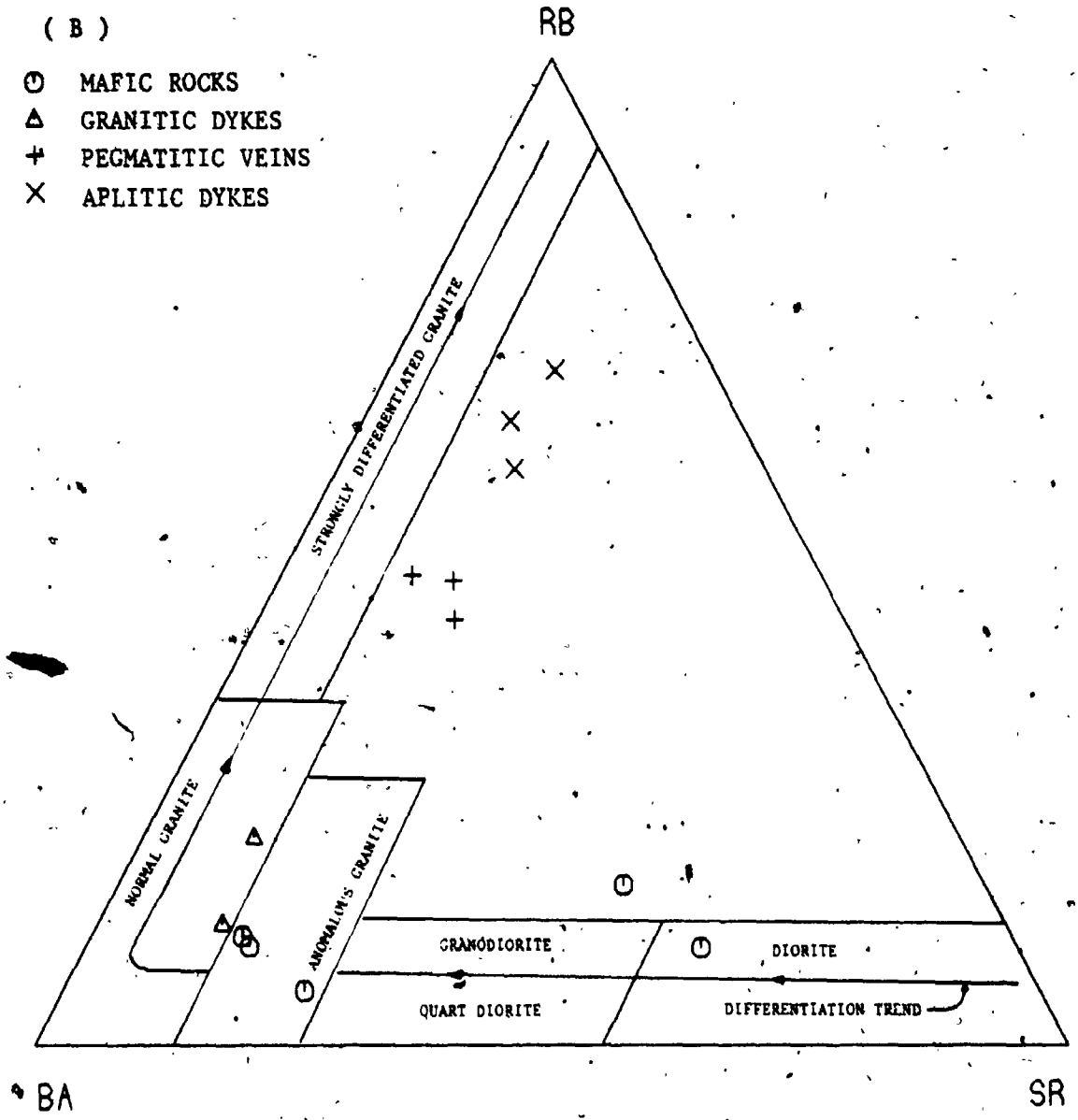

(Figure 2-8~~7~~8. Cont'd)

(B) Mafic rocks and various dykes of the Deloro Pluton.

normal granite field, while the calc-syenitic rocks are plotted in the anomalous granite field indicating a possible metasomatic alteration. The riebeckite granite follows the differentiation trend from the normal granite towards the strongly differentiated granite. The aplitic dykes plotted at the end of granite variation trend (Fig. 2-8-8B), are considered to be differentiates from the riebeckite granite. The autolith, pegmatitic veins and granitic dykes are consistent with compositions of the host hypersolvus granite. On the other hand, except for gabbroic rock having relatively primitive concentration, the dioritic rocks plotted in the anomalous granite field are considered to have a similar origin to the calc-syenitic rocks.

8.3.3 Rare-earth Elements -

Analyses of rare-earth elements, Ta, Hf and Cs for representative samples from the Deloro Pluton are given in Table 2-8-5. Their chondrite - normalized results are plotted in Figure 2-8-9. The range of chondrite - normalized values of peralkaline granites from Nigeria (Bowden and Whitley, 1974) and the metaluminous granite G-2 (USGS standard; Abby, 1980) are also plotted for comparison.

Table 2-8-5. Rare-earth elements, Ta, Hf, Cs compositions of the Deloro Pluton, associated dykes and surrounding volcanic rocks

(ppm)	1 D-166	2 D-135-1	3 D-123	4 D-126-3	5 D-214-3	6 D-201-1	7 D-208-2	8 D-310	9 D-302
La	66.00	41.22	77.19	53.49	64.81	42.21	85.97	77.86	45.48
Ce	148.13	160.69	165.25	205.68	166.95	113.57	189.41	201.07	106.97
Sm	17.76	11.69	21.36	14.80	11.55	9.23	25.68	30.06	11.97
Eu	1.32	2.07	1.69	1.72	1.50	0.96	2.77	2.86	1.57
Tb	3.02	3.50	4.24	4.73	2.95	2.47	4.42	6.01	1.75
Yb	16.58	20.34	18.32	27.84	16.43	16.43	23.44	31.62	8.65
Lu	2.54	2.38	2.38	3.31	1.66	1.77	3.49	4.08	1.34
7REE	255.35	241.79	290.43	311.57	265.35	186.62	335.18	353.56	177.73
Zr	363	544	394	534	349	297	590	909	464
Ta	3.47	3.89	4.41	7.47	2.59	2.67	4.68	4.83	2.72
Hf	14.29	21.19	19.34	26.30	14.11	12.41	26.06	15.14	17.04
Cs	1.08	0.22	0.24	0.53	0.10	0.19	0.16	0.37	0.58
Eu/Eu*	0.22	0.45	0.23	0.28	0.35	0.27	0.32	0.27	0.43
$(Ce/Yb)_N$	2.02	1.81	2.04	1.68	2.32	1.57	1.84	1.44	2.84
$(Ce/Sm)_N$	1.71	2.82	1.59	2.85	2.97	2.53	1.51	1.37	1.85
$(Tb/Yb)_N$	0.77	0.73	0.98	0.73	0.77	0.65	0.80	0.81	0.86
Zr/Hf	25.40	25.60	20.40	20.30	24.70	23.90	22.60	60.00	27.20
SiO_2 (wt%)	71.05	72.69	73.10	74.56	72.33	74.25	75.54	66.89	68.79
F ppm	3660	2084	792	3080	1772	1912	2072	1088	512
Cl ppm	444	336	180	172	120	222	326	660	500

(ppm)	10 D-304B	11 D-163	12 D-124-0	13 D-151-0	14 D-118	15 D-126PG	16 D-421	17 D-423	18 D-425
La	52.01	7.32	75.17	72.94	60.79	23.36	13.39	34.47	18.44
Ce	58.30	24.32	161.76	115.24	134.09	85.61	35.20	119.86	44.10
Sm	17.93	2.36	21.03	10.27	21.17	6.61	4.92	10.49	4.56
Eu	4.25	1.37	1.54	0.58	2.42	0.69	1.67	4.69	0.51
Tb	2.08	0.56	4.18	2.37	3.90	2.88	0.74	2.62	0.61
Yb	10.72	3.37	15.53	8.40	18.52	19.31	4.14	13.16	2.93
Lu	1.97	0.19	1.90	1.02	2.28	2.24	0.65	1.36	0.47
7REE	147.26	39.49	281.11	210.82	243.17	140.70	[illegible]3.28	186.65	91.64
Zr	529	151	189	-	644	278	[illegible]2	511	283
Ta	1.27	0.75	3.68	3.10	4.98	4.67	0.51	1.43	2.85
Hf	7.92	1.34	4.97	0.97	13.78	14.50	1.88	5.56	6.32
Cs	0.99	0.55	1.04	0.10	0.36	0.31	0.10	2.48	0.06
Eu/Eu*	0.84	1.54	0.21	0.15	0.34	0.23	1.04	1.17	0.58
$(Ce/Yb)_N$	1.22	1.65	2.36	3.12	1.63	1.01	1.93	2.06	3.42
$(Ce/Sm)_N$	0.67	2.15	1.59	2.30	1.30	2.69	0.74	2.34	6.25
$(Tb/Yb)_N$	0.81	0.71	1.14	1.19	0.89	0.63	0.76	0.85	0.87
Zr/Hf	66.80	112.60	38.00	-	46.70	19.20	107.50	91.90	44.80
SiO_2 (wt%)	57.75	51.89	73.62	75.56	73.84	75.33	49.60	54.06	69.85
F ppm	1584	552	1948	1060	288	3024	668	1420	183
Cl ppm	872	1440	400	24	314	410	n.d.	n.d.	4.6

1-4: Riebeckite-bearing hypersolvus granite.
5-7: Granophyric subsolvus granite.
8-9: Calc-syenite suite.
10: Dioritic, hybrid rock of the calc-syenite suite
11: Gabbroic rock.
12: Riebeckite-bearing autolith.
13: Late aplitic dyke.
14: Granitic dyke in the syenitic rocks.
15: Riebeckite-enriched pegmatitic vein.
16-17: Metabasalt (n.d. - not determined).
18: Metarhyolite.

Figure 2-8-9. Chondrite-normalized REE distribution patterns of the Deloro Pluton.

(A) REE distributions for riebeckite-bearing peralkaline granite. Field of peralkaline granite of Nigeria is from Bowden and Whiteley (1974).

(B) REE distributions for granophyric granite. Typical granophyry is from Klojonen and Rosenberg (1974).

(C) REE distributions for calc-syenite and mafic varieties.

(D) REE distributions for autolith and various dykes.

(E) REE distributions for metabasalt and rhyolite of the country rocks. (Grenville tholeiite, dacite and andesite are from Condie and Moore, 1977).

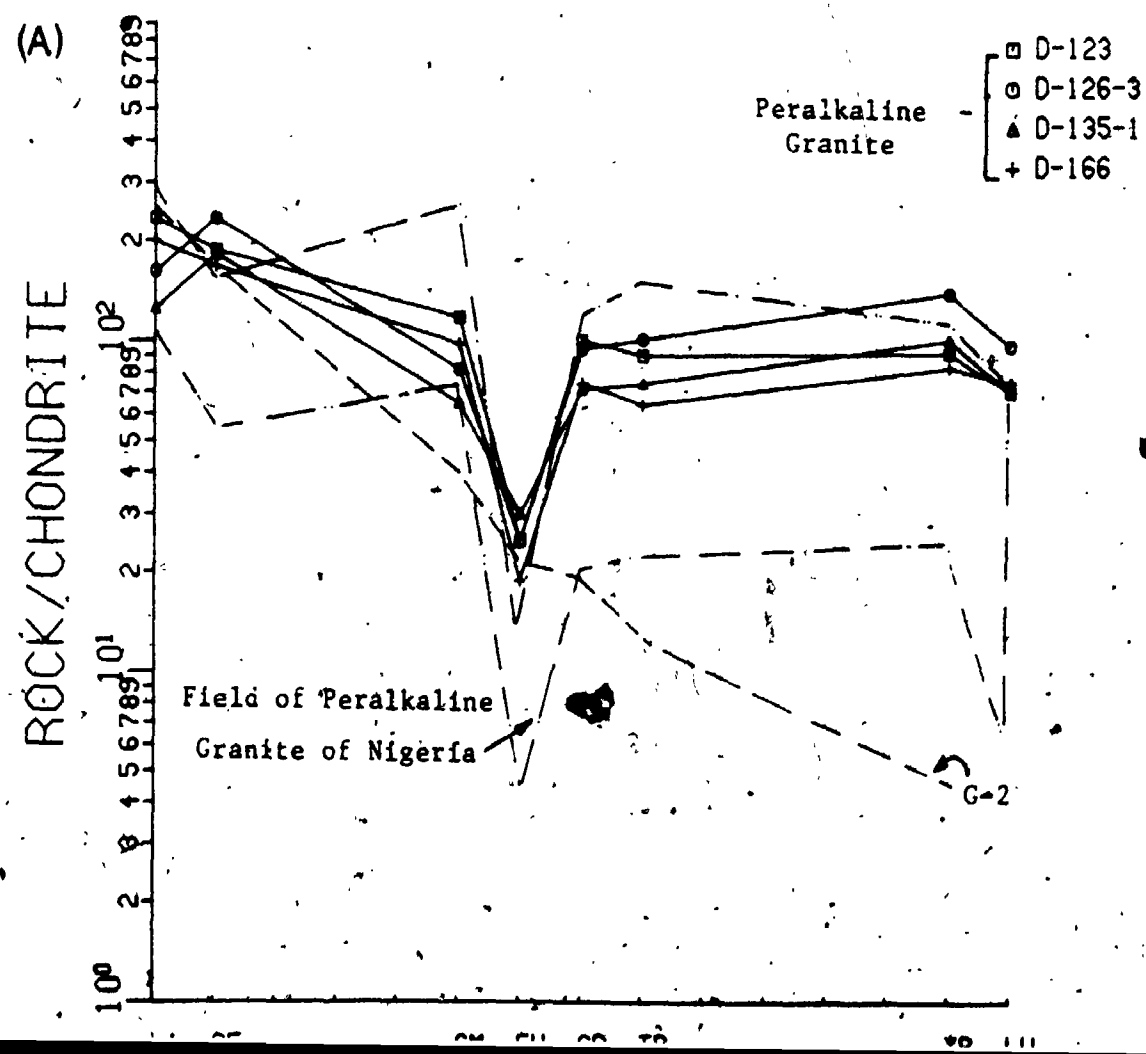

(Figure 2-8-9. Cont'd)

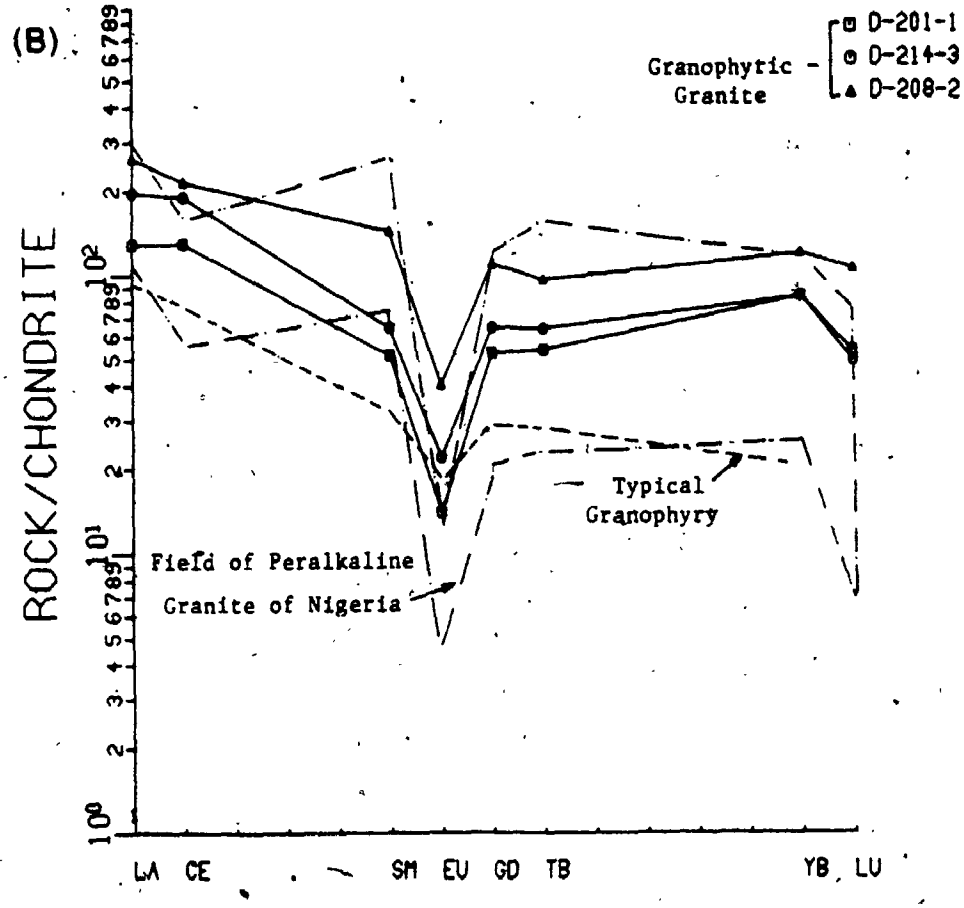

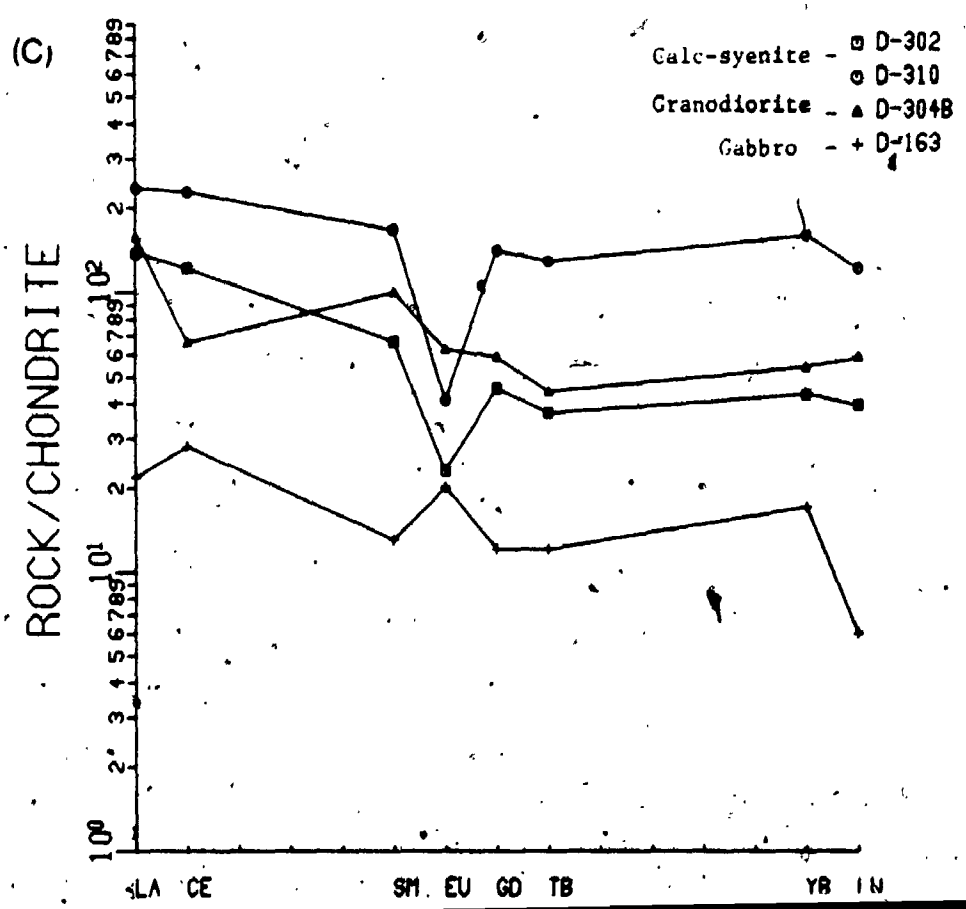

(Figure 2-8-9. Cont'd)

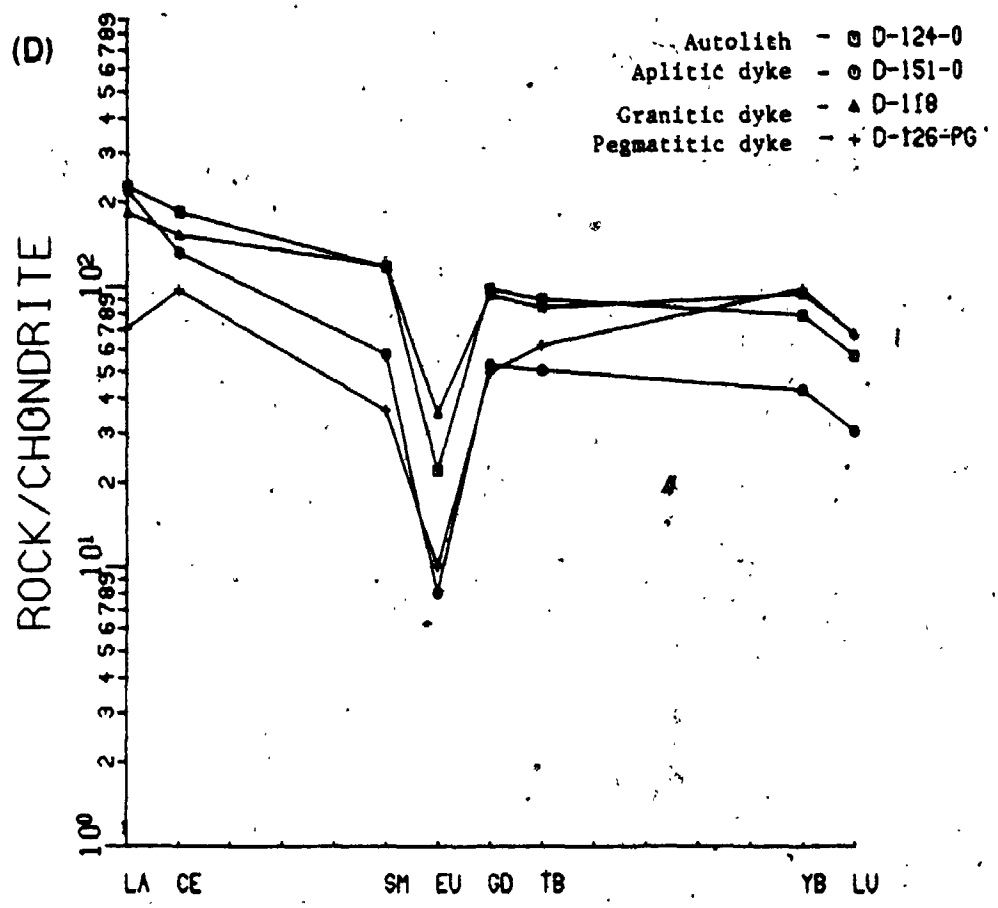

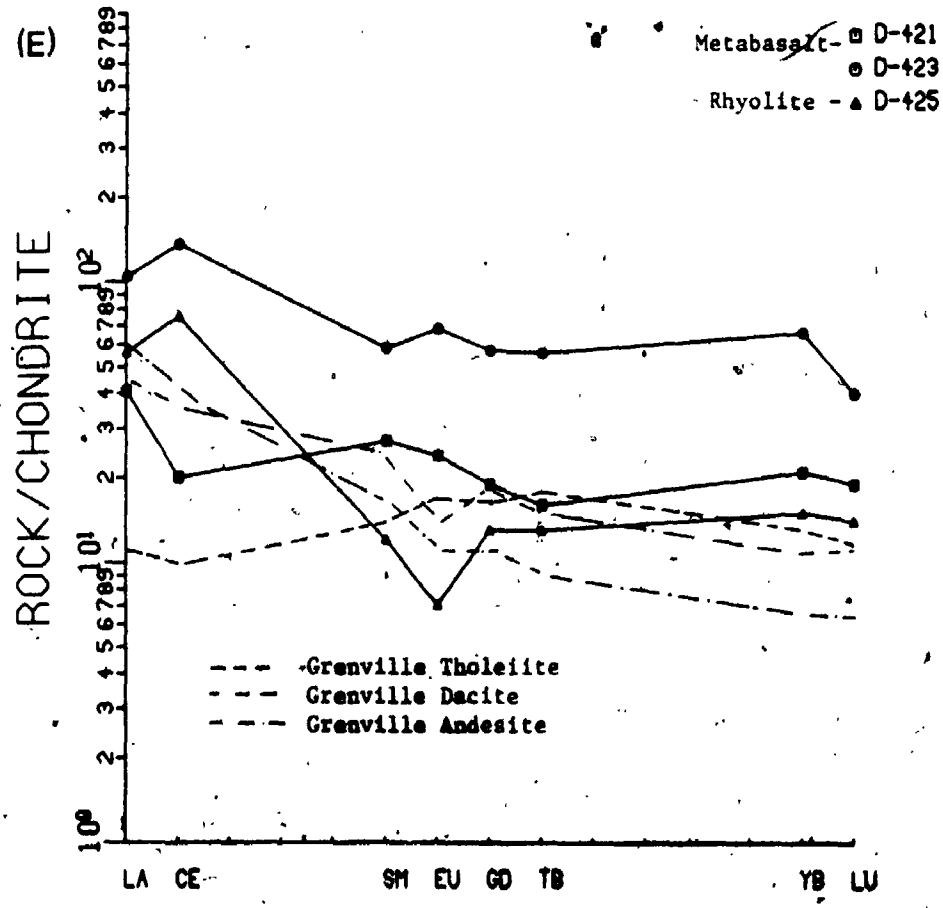

It is apparent that the peralkaline granites are enriched in HREE compared to the metaluminous granite (G-2, agpaitic index = 0.747), and commonly contain higher values for all rare-earth elements. Metaluminous granites commonly show strongly fractionated patterns with $(Ce/Yb)_N$ ratios greater than 20, while the peralkaline granites have relatively flat or concave-up curves with fractionation indices less than 10. The negative Eu-anomaly, on the other hand, is greatly enhanced in the peralkaline granite with a Eu/Eu* ratio less than 0.2 (eg. Harris and Marriner, 1980).

The chondrite-normalized REE patterns for riebeckite granite of the Deloro Pluton, having $(Ce/Yb)_N$ = 1.68 - 2.04, Eu/Eu* = 0.22 - 0.45 (Fig. 2-8-9A), indicate that the HREE is enriched as usual for peralkaline granites, but the negative Eu-anomaly is less marked. The granophyric granite exhibits the similar distribution patterns ($(Ce/Yb)_N$ = 1.57 - 2.32, Eu/Eu* = 0.27 - 0.35; Fig. 2-8-9B) to those of riebeckite granites, except for less abundant total REE. Compared to granophyre of Finland with $(Ce/Yb)_N$ = 3.9 and Eu/Eu* = 0.56 (Koljonen and Rosenberg, 1974), the granophyric granite of this pluton has a less fractionated and concave-up pattern. Syenitic and dioritic rocks show a wide range of REE composition and less

regular patterns. Gabbro (D-163) has the lowest REE contents and a relatively flat curve with a positive Eu-anomaly (Eu/Eu* = 1.54; Fig. 2-8-9C).

The autolith (D-124-0) and granitic dyke (D-128) have similar REE patterns to that of the riebeckite-bearing granite. Late aplitic dyke (D-151-0) exhibits a moderate fractionation pattern ($(Ce/Yb)_N$ = 3.12) and more marked negative Eu-anomaly (Eu/Eu* = 0.15); this may be explained by further fractionation of feldspar accompanied by a smaller amount of mafic and accessory minerals from the Deloro magma. It is interesting to note that the pegmatitic vein (D-126-PG) with abundant euhedral riebeckite megacrystals shows a striking concave curve with anomalous enrichment of HREE (Fig. 2-8-9D). This is indicative of a HREE-enriched melt at the late stage of solidification.

In addition, metabasalts of the country rocks have wide a range of REE concentrations (7REE = 43.2 - 186.6) and less fractionated patterns ($(Ce/Yb)_N$ = 0.95 - 2.06; Fig. 2-8-9E). They are similar to that of Grenville low-K tholeiite ($(Ce/Yb)_N$ = 0.83 and Eu/Eu* = 1.06; Condie and Moore, 1977), except that the former has higher LREE contents. The rhyolite has a well-fractionated pattern ($(Ce/Yb)_N$ = 5.0) with moderate negative Eu-anomaly (Eu/Eu* =

0.58); it is close to the composition of Grenville andesite with $(Ce/Yb)_N$ = 3.57 and Eu/Eu* = 0.6 (Condie and Moore, 1977). However, the rhyolite is more strongly fractionated in LREE ($(Ce/Sm)_N$ = 6.25) than the andesite ($(Ce/Sm)_N$ = 1.41).

The enrichment of HREE in the riebeckite and granophyric granites of the Deloro Pluton is a characteristic feature of peralkaline granite in general. Bowden and Whitley (1974) suggested that this is due to late crystallization of zircon and soda amphibole (HREE-enriched phases) from a fractionating magma. Taylor et al., (1981) argued that a HREE anomaly in the peralkaline granites requires a process other than crystal-liquid equilibria; they prefer a great action of volatiles in controlling the REE distribution. Commonly, the several-fold enrichment of fluorine in the peralkaline granites supports their suggestions. In addition, experimental and empirical evidences also indicate that the light and intermediate REE are concentrated by Cl^- enriched fluids, while the HREE are easily complexed with F^- and/or CO_3^{-2} ions (Kosterin, 1959; Flynn and Burnham, 1977; McLenan and Taylor, 1979). Furthermore, Taylor et al. (1981) suggested that carbonate-complexing is more important than fluorine in terms of the mobility of HREE in the peralkaline magma; it was found that

HREE-carbonate-complexes is much more stable under relatively alkaline and oxidizing state (Kosterin, 1959). For the Deloro Pluton, the four times higher F content and two-fold enrichment of Cl (Table 2-8-5) than those of average low-Ca granite (850 ppm F and 200 ppm Cl) are indications of volatile-complexing during magmatic processes. On the other hand, the presence of primary calcite in the granite supports the high CO_3^{-2} activity in the Deloro magma.

Similar to other peralkaline granites, the HFS elements are also enriched in the Deloro Pluton, although the magnitude may be smaller. The Zr/Hf ranging from 20.3 to 25.6 of the pluton is lower than the common crustal rock ratio of 37 (Brooks, 1970), which may indicate a relative enrichment of Hf over Zr in a peralkaline melt. The high abundances of Zr, Nb, Hf and Ta imply that mineral phases preferentially incorporating these elements (eg. zircon) were not involved in the development of peralkaline granite. It has been found that the increasing fluorine activities in the granitic melt would delay crystallization of zircon (Dietrich, 1968); besides, the presence of alkali cations within the Zr-polymers prevents development of the zircon structure (Watson, 1979). Similarly, the small size and high electronegativity of F^- can form

high-coordination complexes, such as Na_3TaF_8 and Na_2NbF_7, with the large highly-charged cations by the addition of alkali counter ions (eg, Na, K) (Collins et al., 1982).

In other words, the enrichment of HFS elements and HREE in peralkaline granites resulted primarily from deploymerization of the silicate melt by F^- and/or Cl^- ions; the distortion of the melt and crystal structures exhibit the crystallization of HFS-enriched mineral phases, but cumulated in the later more evolved magma.

8.4 Isotopic Geochemistry

Oxygen isotope analyses of whole-rocks and coexisting quartz and feldspar separates of representative samples from various rock-types of the Deloro Pluton are given in Table 2-8-6. Comparatively, the riebeckite and granophyric granites have similar $\delta^{18}O$ values ranging from 9.12 to 10.81 o/op. They are slightly higher than isotopically "normal" granite (Taylor, 1978) and can be classified as the high $\delta^{18}O$ granite of the Grenville Province as defined by Shieh and Schwarcz (1974). However, the isotopic fractionation between co-existing quartz and feldspar (i.e. Δ_{q-f}) ranges from +0.67 to +1.18, indicating a primary magmatic fingerprint (Taylor and Epstein, 1962;

5

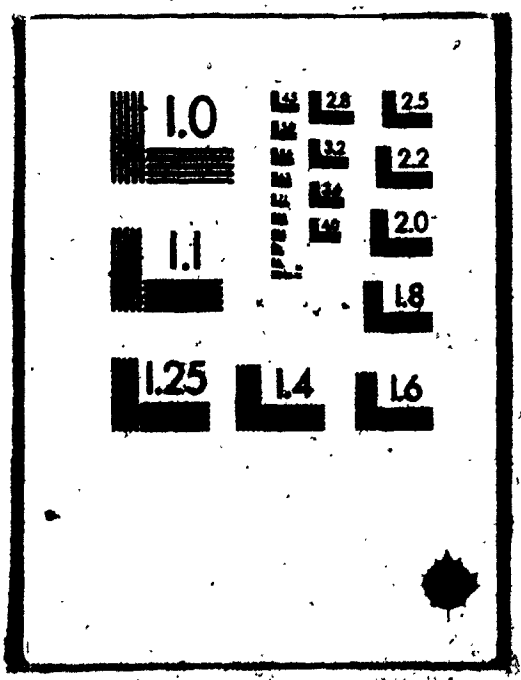

Table 2-8-6. Oxygen isotope analyses of whole-rock and co-existing minerals from the Deloro Pluton

Rock-type	Sample No.	$\delta^{18}O$ whole-rock	$\delta^{18}O$ quartz	$\delta^{18}O$ feldspar	Δ_{q-f}
(a) Riebeckite-bearing Granite	D-109-2	10.81	11.78	10.60	+1.18
	D-122	10.00			
	D-144	9.12			
(b) Granophyric Granite	D-201-2	9.95	10.47	9.80	+0.67
	D-208-1	9.32			
	D-214-1	10.24	10.98	9.83	+1.15
(c) Calc-syenite	D-303	11.14			
(d) Granodiorite	D-315	12.26	12.84	11.00	+1.84
(e) Gabbro	D-163	7.11			

O'Neil and Taylor, 1967; Margaritz and Taylor, 1976; Taylor, 1978); a high-^{18}O parental magma is suggested. The gabbroic rock with the $^{18}O/^{16}O$ ratio of 7.11 o/oo is consistent with a mantle origin.

The calc-syenite and granodiorite, which are not comagmatic with the riebeckite - granophyric granites, have even higher $\delta^{18}O$ values of 11.4 and 12.26 o/oo respectively. The Δ_{q-f} value of +1.84 on granodiorite reflects its high-temperature origin. Such high $\delta^{18}O$ preclude a possible origin for the calc-syenite and granodiorite by assimilation of gabbroic country rocks in the peralkaline magma. Instead, extensive isotope exchange or hybridization with high ^{18}O metasediments is expected.

For the Deloro Pluton as a whole, a Rb-Sr isochron age of 1059 Ma with an initial $^{87}Sr/^{86}Sr$ ratio (R_i) of 0.7036 was reported by Stockwell (1972); Davison et al. (1979) recalculated the age to 1096 Ma. Thus, the Deloro Pluton can be classified as a late-orogenic intrusion. The low R_i eliminates the possibility of significant involvement of crustal material; it is likely derived from partial melting of upper mantle or lower crustal material, or fractionation from a mafic to intermediate syenitic magma.

8.5 An A-type Granite Analogue

Loiseller and Wones (1979) called those granitoids generated along rift-zones and within continental blocks A-type granites due to their anorogenic, alkalic and anhydrous nature. These granitoids form a unique group in the spectrum of granite; characteristic features of A-type granites are summarized in Table 2-8-7 with reference to SE Australia (Collins et al., 1982).

Mineralogically, they are characterized with abundant perthitic alkaline feldspar and granophyric intergrowth, with subordinate zoned plagioclase of oligoclase composition. Interstitial mafic minerals suggest they formed late in the crystallization sequence; iron-rich biotite (annite) and soda amphibole (riebeckite - arfvendsonite) are common. In addition, fluorite, zircon, magnetite and ilmenite are important minor constituents. In contrast to I- and S-type granites (See Chapter IV), A-type granites are free of restite.

Generally, the chemistry reflects their peculiar mineral assemblages. The A-type granites are subalkalic to peralkaline in composition, with lower Al_2O_3, MgO and CaO activities and higher total iron/magnesium and Ga/Al ratios. In particular, A-type granites are anomalously enriched in highly-charged elements, such as Nb, Zr, Y, Ga, REE (except Eu), but depleted in transitional

Table 2-8-7. Characteristics of A-type granitoids and comparison with the Deloro Pluton

A-type *	Deloro Pluton
A. Petrology	
1. Ranging from granite (sensu stricto) to adamellite, including most of hypersolvus granite;	1. hypersolvus granite rim with a subsolvus granite core;
2. near surface intrusion with narrow contact aureole and miarolitic cavities;	2. epizonal, subvolcanic granite with narrow contact aureole;
3. usually intruding rhyolite sequences considered to be comagmatic with the granite;	3. intruding the rhyolitic and andesitic metavolcanic rocks;
4. late in the magmatic cycle and commonly associated with tensional regimes.	4. post- or late-tectonic intrusion.
B. Petrography	
1. K-feldspar is most abundant, forming microperthite and granophyric intergrowth;	1. perthitic feldspar is most abundant, granophyric intergrowth is the major feature of the core;
2. normally zoned plagioclase (An5-30);	2. biotite, lepidomelane in composition, late crystallization phase;
3. biotite, mostly annite, is late in the crystallization sequence;	3. riebeckite is subordinate to biotite, intergrown simultaneously;
4. hastingsite, riebeckite-arfvedsonite are subordinate to biotite but crystallized before it;	4. zircon, fluorite, magnitite-ilmenite and calcite are common accessories.
5. exsolved ilmenite are important accessories.	
C. Chemistry	
1. high $(Na_2O+K_2O)/Al_2O_3$, but not necessary to be peralkaline;	1. peralkaline with molar $(Na_2O+K_2O)/Al_2O_3$ greater than 1;
2. lower Al_2O_3 (12.87-11.49), MgO (0.43-0.03) CaO (1.77-0.01) and high Fe/Fe+Mg;	2. Al_2O_3 (13.32-11.20), MgO (0.56-0.00), and CaO (1.77-0.01);
3. higher abundances of highly-charged cations (eg. HFS elements: Zr, Nb, Y, Hf, Ga, REE, and W, Mo, Sn, Zn);	3. Enrichment of HFS elements and REE;
4. lower abundances of trace elements compatible in mafic silicates (eg. Ni, Co, Cr and Sc) and feldspars (Ba, Sr, Eu).	4. Concentration of F up to 3660 ppm and Cl to 444 ppm.
5. exceedingly high F (> 1000 ppm) and Cl concentrations;	5. average Ga/Al 4.20, anomalously higher HREE with a flat to concave-up pattern, $Eu/Eu^* < 0.45$.
6. high Ga/Al ration (> 3.0) and high, flat REE pattern with large Eu-depletion are diagnostic;	
7. lower H_2O, higher HF and low to moderate oxygen fugacities.	
D. Petrogenesis	
1. Fractional crystallization from a mafic to intermediate syenitic magma (eg. alkaline basalt);	1. 20 to 50% non-model partial melting of the silicic granulite at the lower crust.
2. Partial melting a residual source (i.e. granulite) from a previous partial melting event, which must contain quartz+ K-feldspar+plagioclase and must be F- and/or Cl-rich, but poor in water.	

* The characteristic features of the A-type granitoids are summaried from Collins et. al. (1982) and Loiselle and Wones (1979).

elements (Ni, Co, Cr, Sc) and trace-elements compatible in feldspars (Sr, Ba, Eu). In addition to lower H_2O and low to moderate O_2 fugacities (Loiseeler and Wones, 1979), the A-type granites commonly retain high concentrations of F and Cl. Collins et al. (1982) indicated that the concentration of fluorine in the melt is critical in determining fractionation trends, either metaluminous and peralkaline, in the A-type magma. Furthermore, dissolved volatiles, mainly F^-, Cl^- and CO_3^{-2}, associated with counter-ion effect play a major role in retaining highly-charged cations in alkaline melt.

Based on the initial $^{87}Sr/^{86}Sr$ ratio (0.703 to 0.720), several hypotheses have been considered for the origin of A-type granites: (1) fractional crystallization from a mafic to intermediate syenitic magma (eg. alkaline olivine basalt) by extensive fractionation of feldspars (Bailey and Schairer, 1966; Loiseller and Wones, 1979); (2) partial melting of residual material (eg. granulite) which has undergone previous melting episode (White, 1979; Collins et al., 1982); (3) assimilation of granulite (the lower crust) by alkaline basalt (Loiseller and Wones, 1979); or (4) melting of sodic acid gneisses of crustal origin (Thompson,1969).

Comparison of the Deloro Pluton with the A-type granites is given in Table 2-8-7 and 2-8-8. The

Table 2-8-8. Average compositions of the Deloro Pluton and A-type granites from SE Australia

	1 Riebeckite granite	2 Granophyric granite	3 Calc-syenite	4 Mumbulla granite	5 Gabo granite	6 I-type granite
SiO_2 (wt%)	73.97	74.88	65.22	77.21	73.04	76.03
TiO_2	0.19	0.17	0.50	0.13	0.37	0.11
Al_2O_3	12.05	12.01	14.21	11.79	12.62	12.64
Fe_2O_3	1.41	1.65	3.79	0.36	1.63	0.46
FeO	0.99	1.02	2.73	0.85	1.51	0.70
MnO	0.02	0.01	0.07	0.03	0.08	0.03
MgO	0.13	0.11	0.80	0.04	0.33	0.24
CaO	0.49	0.19	0.93	0.39	0.96	0.80
Na_2O	5.32	5.31	6.06	3.08	3.70	3.43
K_2O	4.11	4.07	3.67	5.00	4.11	4.46
P_2O_5	0.04	0.03	0.10	0.02	0.08	0.02
(Na+K)/Al	1.09	1.05	0.99	0.89	0.83	0.83
Fe^*/Fe^*+Mg	0.95	0.96	0.90	0.97	0.91	0.84
Ga/Al	4.20	4.18	4.25	3.20	3.14	2.09
Rb (ppm)	81	97	67	242	167	212
Sr	43	43	87	43	148	67
Ba	253	347	326	575	767	331
Nb	43	44	38	19	25	11
Zr	463	480	652	170	490	95
Y	93	89	79	90	83	46
Ga	27	26	32	20	21	14
Pb	26	38	34	37	28	24
Zn	36	25	53	122	133	20
Ta	4.8	3.3	3.8	3.1	3.0	-
Hf	20.3	17.5	16.1	6.3	11.6	-
$(Ce/Yb)_N$	1.89	1.91	2.14	3.41	3.82	10

Fe* - Total iron as Fe_2O_3.
1-3 Average compositions of the Deloro Pluton (this study).
4,5 A-type granites from SE Australia (Collins et. al., 1982).
6 I-type granite from the Bega Batholith (Collins et. al., 1982).

subvolcanic intrusion of the riebeckite-biotite (lepidomelane), hypersolvus granite and granophyric, subsolvus granite of the Deloro Pluton are consistent with the petrological and mineralogical characteristics of the A-type granitoids. Geochemically, both riebeckite and granophyric granites are peralkaline in composition; except for higher Na_2O, the Deloro Pluton is closely similar to Australia A-type granites. In terms of trace-element abundances, the Deloro Pluton has relatively lower Sr, Ba, Zn, higher Ga, Hf, Ga/Al and less fractionated REE patterns than those of typical A-type granite. It is also noted that the calc-syenite suite, ranging from hastingsite granite to ferroactinolite syenite (Kuehnbaum, 1973), has compatible trace-element concentrations with the A-type granite. Although it contains higher total iron, MgO and lower SiO_2, the calc-syenite suite could be a metaluminous fraction of the A-type granite (Collins et al., 1982).

8.6 Petrogenesis And Source Rocks

On the basis of field relationships and whole-rock geochemistry (eg. K/Rb vs. Rb), it is suggested that the riebeckite-biotite granite and granophyric granite are comagmatic; while the calc-syenite suite and gabbroic rocks separated from the differentiated trend of the Deloro Pluton.

8.6.1 Origin Of The Peralkaline Granite -

Both riebeckite-biotite and granophyric granites are peralkaline; however, the former contains only hypersolvus feldspar and the latter is subsolvus. The chemical overlaps between these two bodies may indicate two portions of a single magma, and each of them subsequently underwent differentiation along independent but similar routes.

In additon to petrographic evidences and a hypersolvus nature, the internal chemical variations of the riebeckite-biotite granite can be explained by extensive feldspar fractionation (eg. "plagioclase effect"; Bowen, 1945) and later crystallization of mafic and accessory minerals (eg. zircon). The presence of fluorite and calcite in the granite support the enrichment of HREE and HFS elements due to the counter-ion effect, along with F^- and CO_3^{-2} complexing in the peralkaline magma.

By analogy with the peralkaline A-type granites, there appear to be five possible solutions to the origin of riebeckite-biotite granite of the Deloro Pluton:

(1) Fractionation from an alkaline basalt. Because peralkaline rocks are common in the alkaline basalt provinces, Bailey and Schairer (1966)

suggested that the peralkaline granites are fractionates of alkaline basalt. The completely molten nature of the A-type magma (i.e. free-of-restite) and the low R_i of the pluton support the hypothesis of crystal fractionation from a mafic source. However, there is no similar alkaline basalt known in this part of the Grenville Province, although the Deloro Pluton did intrude the Mid-Precambrain (meta)basalt sequences.

(2) Fractionation from an intermediate syenitic magma. The molecular SiO_2-Al_2O_3-total alkali projection (Fig. 2-8-6) suggests the riebeckite-biotite peralkaline granite is derived by alkaline feldspar fractionation from a less siliceous magma similar to that of the calc-syenitic rocks (Bailey and Macdonald, 1969). In addition, the calc-syenite suite may represent a metaluminous trend of the A-type magma. However, the chemical variation trends (eg. K/Rb vs. Rb) preclude the possibility of comagmatism; the disparity of volume also argues against the riebeckite-biotite granite forming as residual liquid from the less siliceous syenitic magma.

(3) Partial melting of fayalite-bearing monzonite source. Bowden (1970) proposed that the peralkaline granites of Nigeria were produced by partial melting of bauchite, a fayalite-bearing

monzonite, by high heat flow from the mantle during the separation of Gondwanaland. In the Hastings Basin area, there is no evidence of bauchite or any other similar metamorphic rocks. In addition, the low initial $^{87}Sr/^{86}Sr$ ratio rules out a source of long term crustal history.

(4) Partial melting of island arc material and marine sediments. Radain (1978) and Radain et al. (1981) suggested that the peralkaline granites of Saudi Arabia, which are closely associated with ophiolite complex, were final products of a long magmatic cycle of a calc-alkaline series. The peralkaline melt could be derived from partial melting of island arc and salty, oxidized marine sediments. Volcanic rocks of the Grenville Supergroup in this part of the Grenville Province have been interpreted as resulting island arc evolution (Condie and Moore, 1977). However, the lack of ophiolitic complex associated with the Deloro Pluton precludes the possible subduction and partial melting of sodium-rich ocean sediments for generating the Deloro magma.

(5) Partial fusion of lower crust or a residual source of previous melting event. In terms of sources of granitic magmas, Chappell and White (1974) proposed two contrasting I- (igneous) and S- (sedimentary) type granites. White (1979) suggested

the A-type granites were derived from another kind of source, which is considered to be a residue from the previous partial melting episode. The residual material known as granulite is the main constituent of the lower crust. The influx of volatiles (F, Cl, CO_2) and the heat flow from deep mantle will initiate the partial fusion of the granulite; its anhydrous nature promotes the high-level intrusion. The higher K/Rb (ave. 436) also favours the residual source.

As aforementioned, the anomalous enrichment of volatiles in the peralkaline or A-type granitic magma depolymerize the melt structure and delay the crystallization of accessory mineral phases which are commonly enriched in highly-charged incompatible trace-elements. Furthermore, at the presence of an immiscible volatile-rich fluid phase, the trace-element partition coefficients differ notably (eg. REE; Cullers et al., 1973). Shaw (1978) illustrated that during anatectic melting the behavior of a trace-element depends not only on the partition coefficients (D^{il}) between mineral i and silicate melt l, but also on the coefficients (D^{if}) between mineral i and the volatile-rich fluid phase f.

In order to quantitatively verify the hypothesis of partial melting of lower crustal rocks

for riebeckite-bearing granite of the Deloro Pluton, the method of Shaw (1978) was adopted for modelling and it is assumed the mineral partition coefficients D^{il} and D^{if} are constant with no influences of P, T and melt composition variations. Non-modal equilibrium melting of a silicic granulite rock (MP-45 of Weaver, 1980) with a norm of 35% quartz, 35% plagioclase, 25% orthoclase and 5% hypersthene was then calculated. The mineral proportions and selected D-values are given in Table 2-8-9.

It was noted that at a constant degree of melting, the total REE and $(Ce/Yb)_N$ ratios decrease, but the Eu/Eu* ratios increase, as the fluid/rock ratios (v) increase. A constant v = 10 was chosen for further calculations - a value reasonable for a H_2O undersaturated magma (Wyllie et al., 1976). Chondrite-normalized REE curves with 20% and 50% partial melting of the silicic granulite are illustrated in Figure 2-8-10A; they fall within the upper half of the REE envelope for the riebeckite-bearing granite with somewhat higher middle REE abundances. It is also interesting that the rhyolitic volcanic rock, which may be the extrusive equivalent of the Deloro pluton, can be derived from 25% partial melting of an intermediate granulite ($Qtz_2Plag_{50}Or_5Opx_{10}Cpx_{10}$) at fluid/rock ratio equal to 0 (Fig. 2-8-10B).

Table 2-8-9. Mineral proportions and selected D-values for non-model equilibrium melting of a silicic granulite

	Proportions		D^{il} (for rhyolitic rocks; Arth, 1976)					
Mineral	P_o^i	P^i	Ce	Sm	Eu	Tb*	Yb	Lu
Qtz	0.35	0.30	0**	0	0	0	0	0
Plag	0.35	0.40	0.27	0.13	2.15	0.075	0.049	0.046
Or	0.25	0.25	0.044	0.018	1.13	0.008	0.012	0.006
Opx	0.05	0.02	0.15	0.27	0.17	0.40	0.86	0.90
Cpx	-	0.03	0.50	1.67	1.56	1.70	1.58	1.54
		D^{sl}	0.1130	0.0635	1.0435	0.0482	0.0631	0.0626
		P^{sl}	0.1370	0.1120	1.1927	0.0910	0.0872	0.0841
		D^{ef}	10	10	10	10	20	20
		D^{sf}	1.130	0.635	10.435	0.482	1.263	1.252
		P^{sf}	1.370	1.120	11.927	0.910	1.744	1.682

* Tb values are extrapolated from Gd and Dy (Arth, 1976).
** Assumed values for quartz.

D^{il} - Partition coefficient between mineral i and silicate melt.
D^{sl} - Partition coefficient between inital rock mass and melt.
D^{sf} - Partition coefficient between inital rock mass and fluid phase.
D^{lf} - Partition coefficient between silicate melt and fluid phase (derived from Shaw, 1978).
P_o^i - Weight fraction of mineral i in the inital rock mass.
- Normative composition of average silicic granulite (Weaver, 1980).
P^i - Weight fraction of mineral i in the melt.
- Normative composition of average riebeckite granite of the Deloro pluton.

Figure 2-8-10. REE modelling of the Deloro Pluton.

(A) Non-modal partial melting of a silicic granulite source at fluid/rock ratio (v) of 10 to produce the peralkaline granitic melt of the pluton.

Non-modal partial melting of a intermediate granulite at fluid/rock ratio (v) about 0 to form the rhyolitic magma.

(B) Fractionation of low-K tholeiite for the calc-syenite.

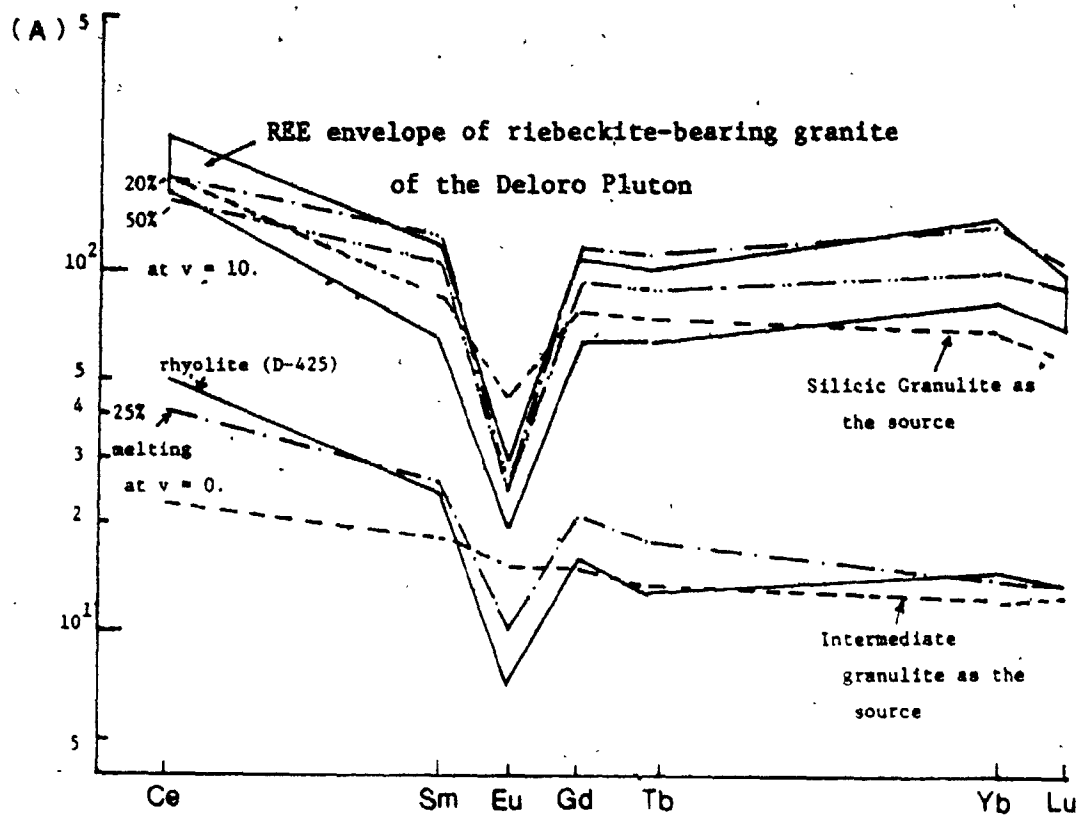
(A)
REE envelope of riebeckite-bearing granite
of the Deloro Pluton
20%
50%
at v = 10.
rhyolite (D-425)
25%
melting
at v = 0.
Silicic Granulite as
the source
Intermediate
granulite as the
source
Ce
Sm
Eu
Gd
Tb
Yb
Lu

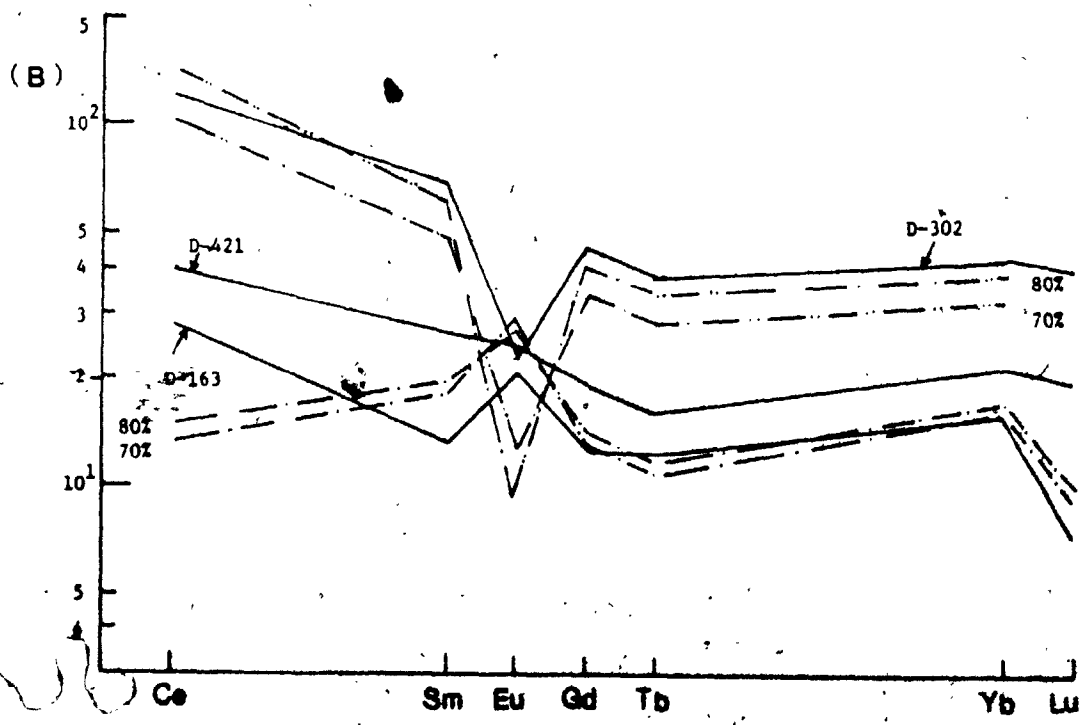
(B)
D-421
D-163
80%
70%
D-302
80%
70%
Ce
Sm
Eu
Gd
Tb
Yb
Lu

In terms of REE distribution patterns and other geochemical characteristics, the granophyric granite is comagmatic with riebeckite-bearing granite. However, the granophyric texture, primary muscovite mineralogy and the presence of two feldspars in the granite require more explanation. The association of hypersolvus and subsolvus granites indicates the change of water or P_{H2O} from anhydrous to H_2O-saturated during the evolution of the Deloro magma. Martin and Bonin (1976) proposed that a late influx of meteoric water would remobilize the nearly crystallized hypersolvus granite to form relatively "wet" subsolvus magma. The similar and relatively higher ^{18}O values in both the hypersolvus and subsolvus granites of the Deloro Pluton preclude the assumption of inducing secondary melting by meteoric water influx. Instead, assimilation of limited amount of metasediments with Al-rich metasilicates may be one of the alternatives for obtaining the extra H_2O and aluminum into the A-type magma; however, further Rb-Sr isotope studies of the granophyric granite are needed to clarify this hypothesis.

8.6.2 Origin Of The Calc-syenite Suite -

Differences between the REE patterns of calc-syenitic rock (D-302) and gabbro (D-163) (Fig. 2-8-9C) could suggest a plagioclase - rich cumulate (gabbro) and a residual melt (calc-syenite) produced by fractional crystallization of a precursor magma with similar $(Ce/Yb)_N$ ratio to both. The low-K tholeiite (D-421) of the country rocks having a similar $(Ce/Yb)_N$ ratio (1.93) and intermediate REE contents is a suitable source magma for this modelling. Figure 2-8-10B illustrates that at 70 - 80% equilibrium crystallization of an assemblage simliar to gabbroic mineralogy ($Plag_{60}Opx_{20}Hb_5$) would give pairs of complimentary patterns which are parallel to the calc-syenitic and gabboric rocks respectively. However, the internal chemical variations are considered to be more complicate, in terms of igneous differentiation of itself, metasomatism and/or hybridization by nearby peralkaline intrusions.

8.7 Summary

The late-orogenic Deloro Pluton is composed of three major intrusive phases: (1) riebeckite - biotite, hypersolvus granite, (2) granophyric biotite-muscovite, subsolvus granite, and (3) calc-amphibole-biotite

syenite suite. They were intruded into the low-K tholeiite, andesite and rhyolite sequences of Mid-Precambrian. The narrow contact metamorphism, the occurrence of granophyre and the association of rhyolite are indications of high-level intrusion; the perthitic, hypersolvus feldspars suggest a high-temperature crystallizing phase at $P_{H2O} < P_{Total}$.

The riebeckite-granophyric granites are peralkaline in composition with anomalously higher concentrations of highly-charged incompatible elements (eg. Nb, Zr, Ta, Hf) and REE. The exceedingly high F content and the presence of calcite and fluorite support the concentrating of HREE and HFS elements in the highly evolved siliceous magma by F^- and CO_3^{-2} complexing and the counter-ion effects. Geochemically and mineralogically, the riebeckite-granophyric granites are analogous with the A-type granites of diagnostic high Ga/Al ratios.

The low R_i precludes the possible crustal origin for the Deloro Pluton; besides, the lack of intermediate to mafic alkaline basalt eliminates the possibility of differentiation by crystal fractionation.

Based on REE modelling, the origin of riebeckite-biotite granite is consistent with 20% to 50% non-modal partial melting of the silicic granulite ($Qtz_{35}Plag_{35}Or_{25}Opx_5$) at a constant fluid/rock ratio of

10. The trace-elements agree with the hypothesis that the riebeckite-granophyric granites are comagmatic; the whole-rocks oxygen isotope argues against the hypothesis of remobilizing the hypersolvus granite by meteoric water flux to form a secondary subsolvus granitic melt. Assimilation of less metamorphosed sediments would supply the extra H_2O and Al_2O_3 by breaking down amphibole-biotite and Al-rich metasilicates, respectively. Rhyolite, probably cogenetic with the Deloro Pluton, is derived from 25% partial melting of intermediate granulite under no fluid influences. Despite the complexity of its internal variations and evolution history, the calc-syenitic rocks are fractionates by 70 - 80% crystallization of the magma with similar composition to that of the low-K tholeiite country rock.

On the basis of petrogenesis, the following sequence of emplacement of the Deloro pluton is suggested: (1) the calc-syenite suite and gabboric rocks were firstly intruded by fractionation of the tholeiitic parent magma; (2) partial melting of granulite lower crustal material by mantle-derived heat-flux and gaseous fluids producing the A-type granitic magma and moving into a crustal level forms riebeckite-biotite, hypersolvus granite of the Deloro pluton; hybridization and metasomatism took place contemporaneously along the margin of the peralkaline

intrusion; (3) assimilation of metasediments producing near H_2O saturated magma intruded into hypersolvus granite.

9.0 BARBER'S LAKE GRANITE

9.1 General Characters And Intrusive Relations

The Barber's Lake Granite outcrops at the southwest corner of Dalhousie Township (Fig. 2-9-1). It has a subrounded shape with a maximum area of about 25 km^2. The granite is well-exposed along the logging roads at its northern and southern margins; Pleistocene fluvial and recent swamp deposits cover most of its interior.

It is composed predominantly of pinkish, medium-grained two-mica granite with no metamorphic fabrics. Locally, pegmatitic phases of the granite occur as "pockets" of mega-K-feldspar, biotite and quartz; a gradational contact was observed between the pegmatitic phase and normal granite. Late aplitic and/or granitic dykes are not found, and the contact aureole is absent. Inclusions of biotite-plagioclase paragneiss and siliceous limestone of the country rocks are present in the border zones. One small gabbroic body with primarily hornblende - plagioclase and pyroxene - relicts was also encountered.

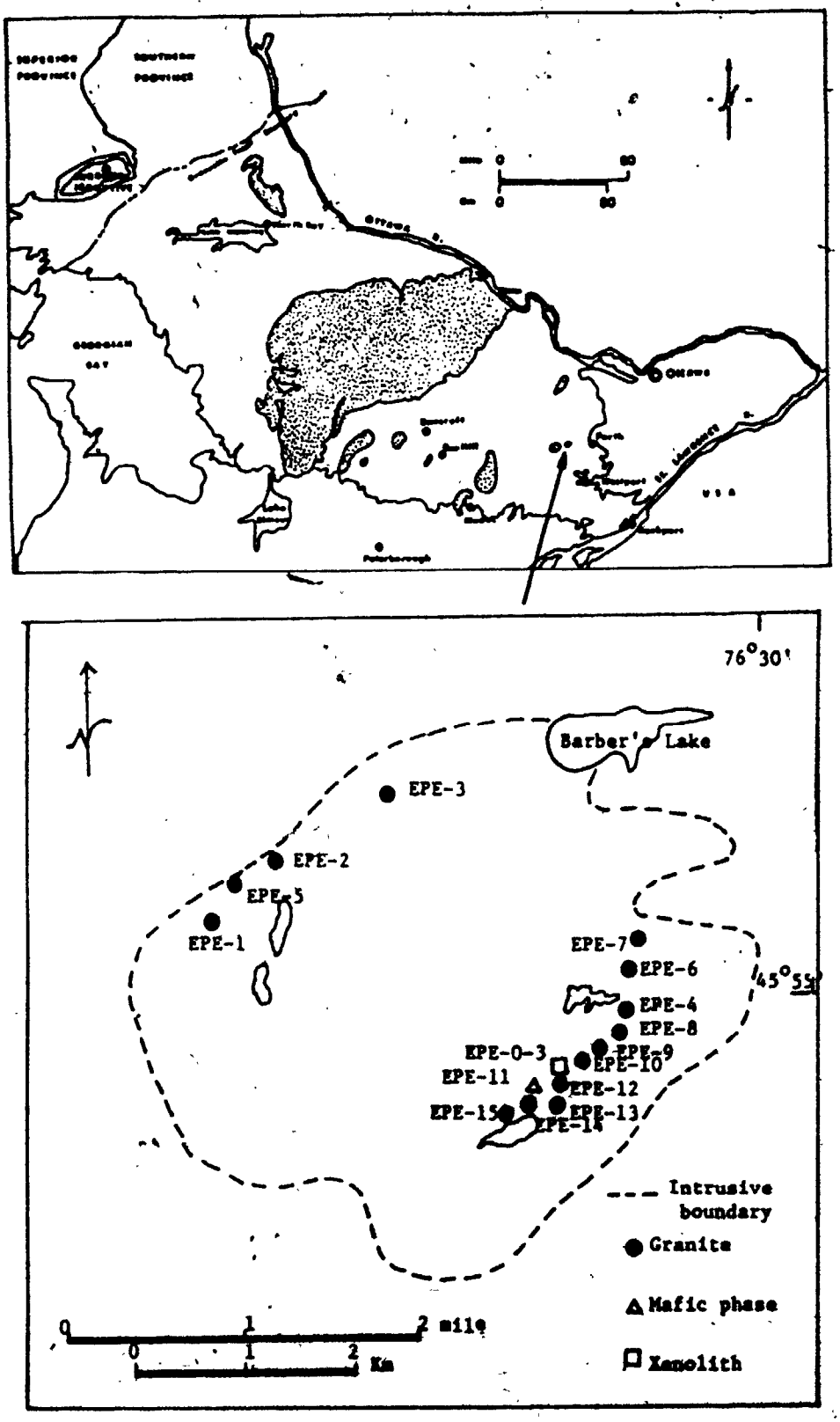

Figure 2-9-1. Sample location map of the Barber's Lake Granite.

In contrast to the heterogeneous nature of the Elphin Granite-Syenite Complex, which is 3 km to the northwest (Fig. 2-9-1), the Barber's Lake Granite contains much more uniform mineralogy and texture. It is thus suggested that they are not consanguineous and different parental magmas are expected (cf. Davison et al., 1979; ODM Map 1956-4). Further, its massive character, discordant contacts and the presence of country rock inclusions may suggest a mesozonal, forceful intrusion after the climax of regional metamorphism.

9.2 Petrography

Samples of the Barber's Lake Granite are characterized by their extremely low content of mafic minerals (C. I. < 5.0) and the presence of primary muscovite. They cluster in the field of granite (adamellite), while the gabbroic, pyroxene-bearing rocks are in the quartz diorite field (Streckeisen, 1976; See Fig. 2-9-2).

9.2.1 Granitic Rcoks -

In addition to the dominant felsic components, biotite, primary muscovite, sphene, zircon and iron oxides are minor constituents. Allanite, apatite, fluorite, secondary carbonate, epidote and spinel

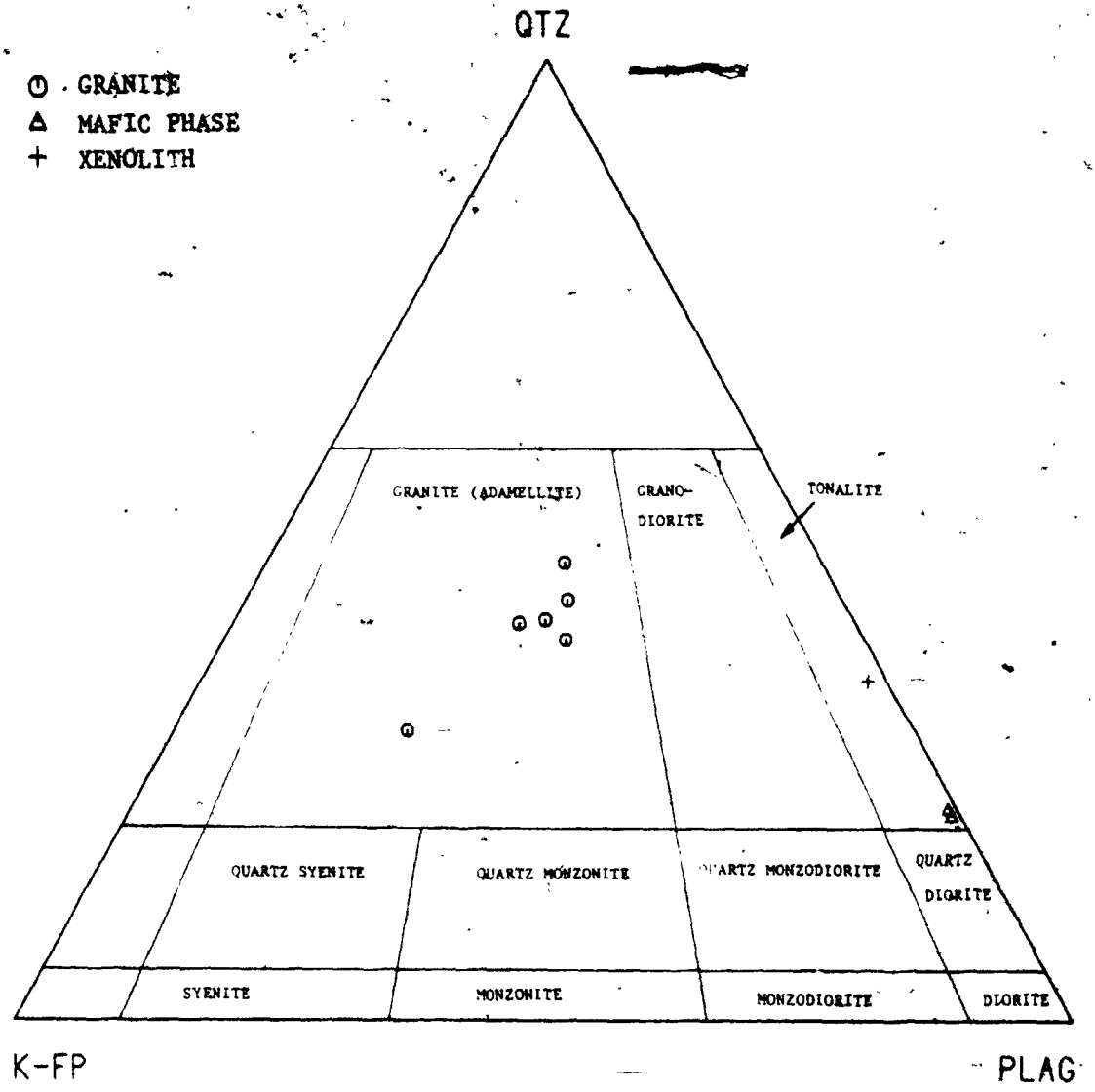

Figure 2-9-2. Modal classification of the Barber's Lake Granite (after Streckeisen, 1976).

are also present in some specimens. Probe analyses of representative feldspars are given in Table 2-9-1. The albitic composition of plagioclase (An_8 to An_{15}) and equal amount of two feldspars (feldsapr ratio = 0.53) are characteristic of alkaline granite of Lumbers (1982).

Plagioclase shows simple albite-twinning without zonal distribution. Euhedral grains are partly sericitized with patches of carbonate and secondary white mica; sphene, zircon and allanite are also commonly enclosed. Microcline with cross-hatch twinning is the major potassium feldspar; perthitic feldspar is also present locally. Quartz forms euhedral to subhedral grains showing undulose extinction and polycrystalline subgrains. Myrmekite or vermicular texture occurs along the contact between microcline and perthitic feldspar.

The only ferromagnesian mineral is biotite (X = straw yellow, Y = Z = yellowish brown with greenish tint to olive green), which is subhedral and partially chloritized. Representative chemical analyses (Table 2-9-2) suggest that it is Fe^{2+}-biotite of Foster (1960; See Fig. 2-9-3). Needle-like spinel and epidote aggregates are commonly enclosed in altered biotite, as well as zircon and sphene. Euhedral to subhedral muscovite

Table 2-9-1. Chemical compositions and calculated formulae of feldspars from the Barber's Lake Granite

(a) Plagioclase			(b) K-feldspar	
Sample No.	1 EPE-3-2	2 EPE-4	1 EPE-3-2	2 EPE-4
(wt%)				
SiO_2	65.56	66.42	64.68	64.69
Al_2O_3	21.81	21.38	18.43	18.54
CaO	2.51	1.78	0.00	0.00
Na_2O	9.69	10.61	0.65	0.60
K_2O	0.30	0.22	15.94	16.06
Total	99.51	100.41	99.70	99.92
Si } Z	11.554	11.616	11.981	11.965
Al } Z	4.529	4.406	4.023	4.041
	16.084	16.022	16.004	16.006
Na } X	3.311	3.598	0.233	0.215
Ca } X	0.406	0.334	0.000	0.000
K } X	0.067	0.049	3.766	3.796
	3.784	3.980	4.000	4.011
O	32	32	32	32
(mol%)				
Ab	87.49	90.39	5.84	5.36
An	10.74	8.38	0.00	0.00
Or	1.78	1.23	94.16	94.64

Table 2-9-2. Chemical composition and calculated formulae of biotite from the rocks of Barber's Lake Granite

Sample No.		EPE-3-2	EPE-4
SiO_2		36.17	35.66
TiO_2		2.37	1.96
Al_2O_3		15.76	14.98
Fe_2O_3		2.92	2.88
FeO		21.44	21.16
MnO		1.01	0.11
MgO		5.33	8.23
CaO		0.05	0.06
Na_2O		0.11	0.07
K_2O		9.73	8.51
Total		94.89	93.62
Si	Z	5.680	5.600
Al^{iv}	Z	2.320	2.400
		8.000	8.000
Al^{vi}	Y	0.594	0.371
Ti	Y	0.280	0.231
Fe^{3+}	Y	0.345	0.340
Fe^{2+}	Y	2.813	2.777
Mg	Y	1.246	1.925
Mn	Y	0.134	0.097
		5.412	5.741
Ca	X	0.008	0.010
Na	X	0.033	0.211
K	X	1.948	1.704
		1.989	1.735
O		22	22
Mg/Fe+Mg+Mn		0.275	0.375
Fe_t/Fe_t+Mg		0.717	0.618
mole of annite		0.469	0.463

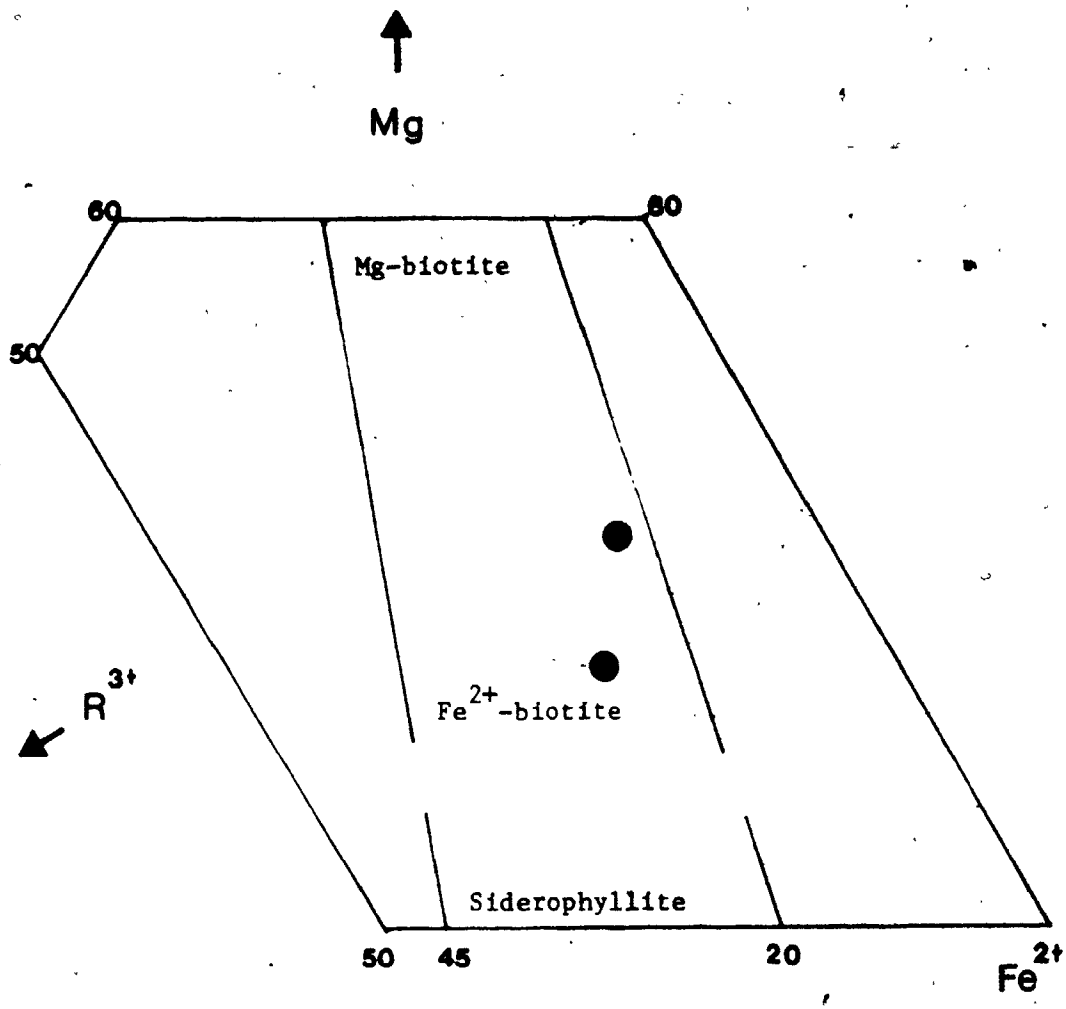

Figure 2-9-3. The $Mg-Fe^{2+}-R^{3+}$ relation in trioctahedral micas of the Barber's Lake Granite (after Foster, 1960).

$$R^{3+} = Al^{vi} + Fe^{2+} + Ti^{4+}$$

forms individual grains or is intergrown with biotite. Poikilitic texture and graphic intergrowth are common. Small flakes of white mica replacing plagioclase and biotite are considered to be secondary.

Sphene, zircon and allanite form as individual grains or inclusions; subhedral zircon is frequently zoned and fractured. One corona-like fluorite grain associated with an altered zircon crystal shows violet colour reaction rim.

9.2.2 Mafic Cumulates -

Mafic cumulates are coarse- to medium-grained with lath-shaped plagioclase and little or no K-feldspar. Quartz content is between 11% to 15% of the mode; and colour index is greater than 35. Hornblende, in addition to biotite and pyroxene, is the chief mafic mineral. Sphene, apatite, zircon, secondary carbonate, chlorite and spinel are accessory minerals.

Plagioclase, oligoclase in composition, occurs as both large lath-shaped crystals and interstitial subhedra. They are well-twinned and partly sericitized. Anhedral quartz and finer plagioclase grains occupy most of the interstitial spaces. Euhedral to subhedral hornblende (X = yellow, Y =

olive green, Z = green to dark green) intergrew with biotite and/or replaced the pyroxene. Poikilitic texture is common with inclusions of quartz grains. Biotite forms smaller, subhedral flakes which are irregularly orientated and interleave with hornblende.

Pyroxene occurs as anhedral relict cores in hornblende or shows symplectic intergrowth texture with surrounding plagioclase. Increasing hornblende and decreasing quartz - spinel inclusions towards the contact of pyroxene and plagioclase suggest a gradational chemical reaction took place during later hydrothermal alteration.

9.2.3 Trondhjemitic Xenolith -

One trondhjemitic xenolith was found in the southern border zone. It is medium-grained with colour index of about 30 and feldspar ratio of 0.95. Subhedral to anhedral quartz grains showing undulose extinction and subgrain boundaries make up 23% of the mode. Plagioclase, the predominant felsic component, ranges in composition from An_{22} to An_{26}. Hornblende and biotite are major mafic constituents. Sphene, apatite and zircon are accessories and occur commonly as inclusions in mafic minerals.

9.3 Whole-rock Geochemistry

9.3.1 Major-oxides -

Composition of the Barber's Lake Granite is peraluminous with normative corundum ranging from 0.0 to 2.47 wt %. The average molar aluminum to total alkaline-lime ratio is about 1.05 and agpaitic index is about 0.896. Except for mafic cumulates and xenolithic rocks, the narrow range composition of this granite (72.9 to 75.9% SiO_2) makes direct measurement of the alkaline-lime index (Peacock, 1931) impossible. However, rocks of the Barber's Lake Granite fall within the alkaline field of Miyashiro (1978; See Fig. 2-9-4).

The mean composition of this granite, related mafic and xenolithic rocks and other similar rock-types are summarized in Table 2-9-3. In general, the chemical composition of the Barber's Lake Granite is similar to that of average muscovite-biotite alkaline granite of Nockolds (1954), except that the former has relatively higher Na_2O/K_2O ratio and oxidation index and lower P_2O_5. In comparison with granitic rocks of the nearby Elphin Complex, Barber's Lake Granite shows more evolved nature with higher SiO_2 and lower Al_2O_3, total iron, MgO and CaO. As shown in the normative Qtz-Plag-Or diagram (Fig. 2-9-5), compositions of

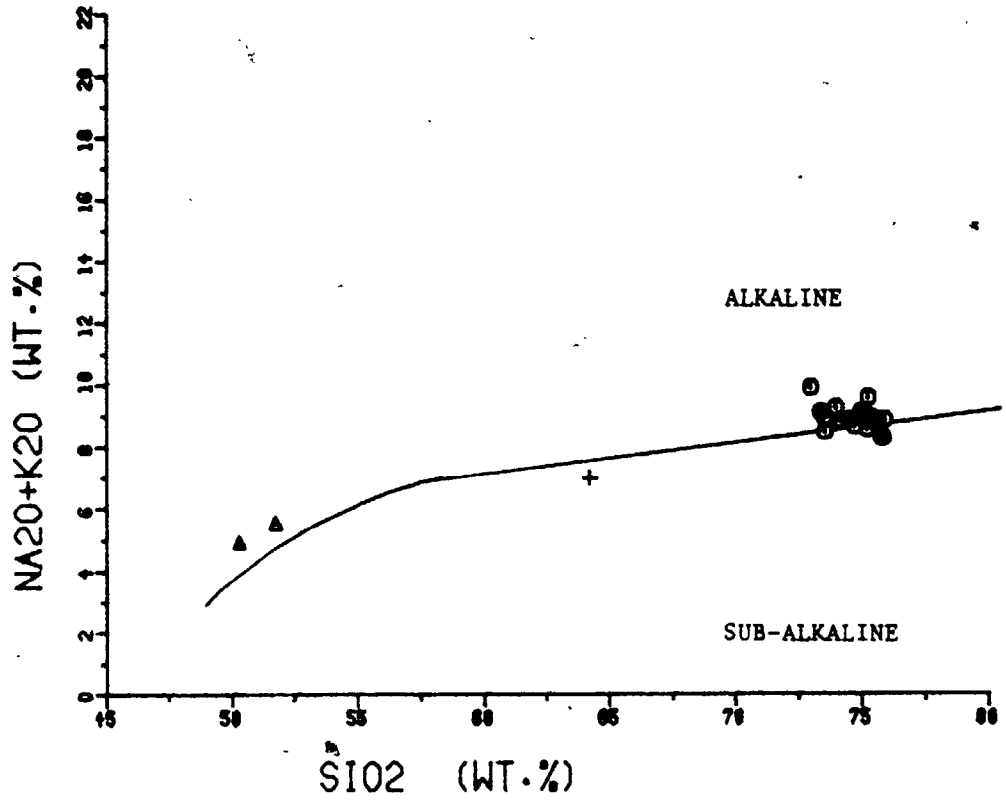

Figure 2-9-4. Na_2O+K_2O vs. SiO_2 plot of the Barber's Lake Granite. Solid-line separates the alkaline and subalkaline fields of Miyashiro (1978).

⊙ GRANITIC ROCKS
▲ GABBROIC ROCKS
+ XENOLITHS

Table 2-9-3. Comparison of average compositions of the Barber's Lake Granite with other similar rock-types

(wt.%)	1 (n=18)	2 (n=13)	3 (n=17)	4 (n=6)	5 (n=37)	6 (n=2)	7 (n=1)		9 (n=18)	10
SiO_2	74.73	68.44	74.63	73.84	73.28	50.98	64.20	Rb	244	150
TiO_2	0.08	0.32	0.14	0.16	0.30	1.35	0.52	Sr	76	285
Al_2O_3	13.30	15.36	13.86	14.29	13.30	18.78	16.40	Ba	194	600
TFe_2O_3	1.40	2.30	*1.51	*1.17	*2.40	8.54	3.82	Nb	26	20
Fe_2O_3	0.60	1.31	0.52	0.34	0.87	2.67	0.94	Zr	131	180
FeO	0.77	0.95	0.89	0.75	1.38	5.29	2.60	Y	18	40
MnO	0.02	0.02	0.04	0.05	0.05	0.11	0.04	Ga	24	18
MgO	0.07	0.76	0.33	0.21	0.50	4.26	2.17	Ni	4.8	10
CaO	0.44	1.21	0.57	0.69	1.17	9.13	4.45	Cr	4.7	4
Na_2O	4.07	5.70	3.05	3.61	2.96	4.24	5.66	V	11	20
K_2O	4.82	4.39	5.16	5.21	5.52	0.98	1.31			
P_2O_5	0.00	0.06	0.18	0.25	0.14	0.12	0.14			
LOI	0.66	1.03	0.63	0.60	0.50	0.95	0.68	Rb/Sr	3.21	0.53
								K/Rb	164	**150-300
Na_2O/K_2O	0.84	1.30	0.59	0.69	0.54	4.33	4.32			
O.I.	58.70	74.50	53.90	47.60	55.80	50.20	41.90			

1. Average of 18 samples from Barber's Lake Granite (this study).
2. Average of 13 granitic rocks from Elphin Granite-Syenite Complex (this study).
3. Average muscovite-biotite alkali granite of Nockolds (1954).
4. Average muscovite alkali granite of Nockolds (1954).
5. Average calc-alkalic biotite granite of Nockolds (1954).
6. Average of 2 mafic cumulates from Barber's Lake Granite (this study).
7. Trondhjemitic xenolith from Barber's Lake Granite (this study).
8. Average composition of Grenville Dacite (Condie and Moore, 1977).
9. The mean trace-element compositions of the Baber's Lake Granite (this study).
10. The mean trace-element concentrations of average granite (Taylor, 1964).

* Total iron calculated from reported FeO and Fe_2O_3.
** Mean K/Rb ratio of "normal" igneous rock (Taylor, 1965).
O.I. = oxidation index.

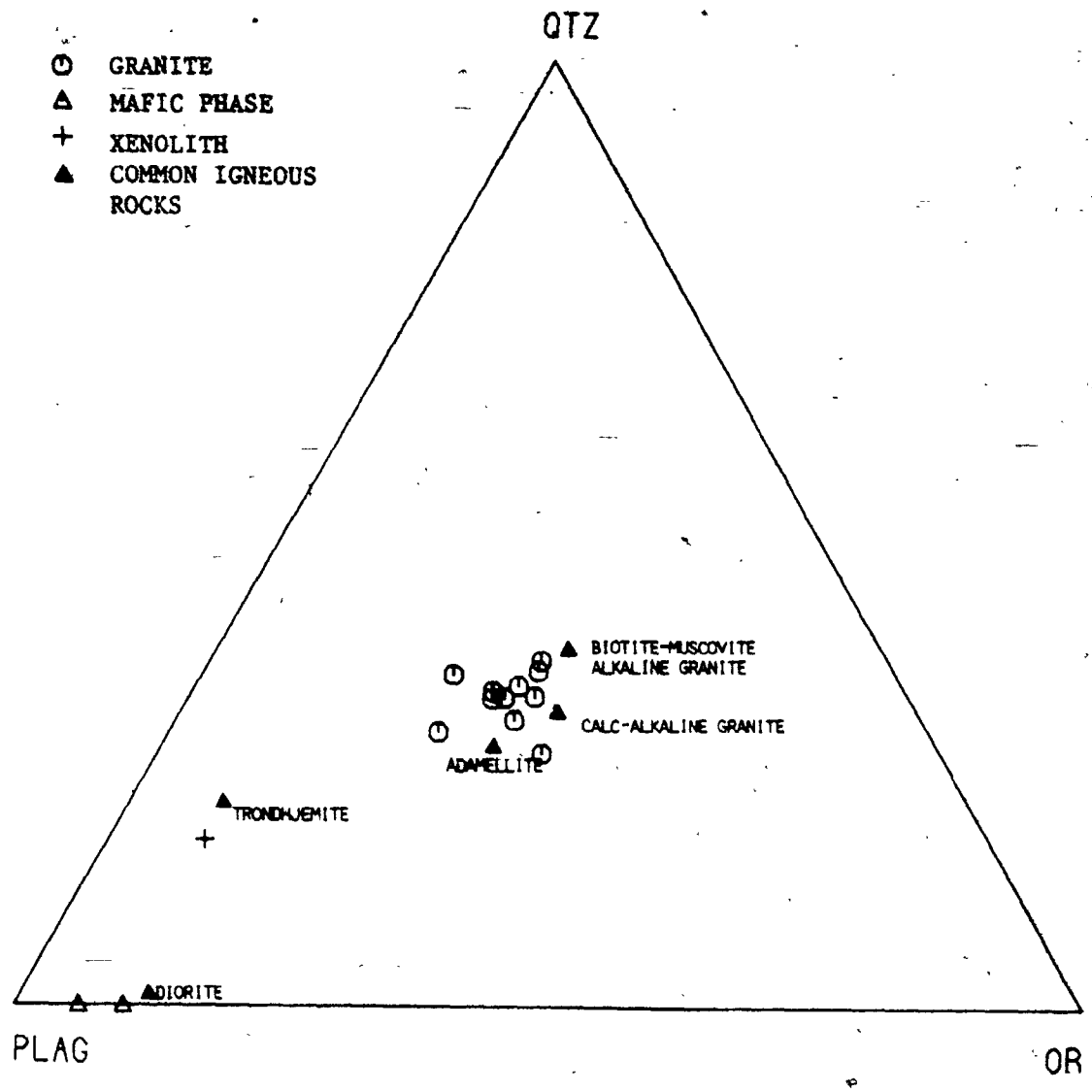

Figure 2-9-5. Normative Qtz-Or-Plag ratios of the Barber's Lake Granite and common igneous rocks (calculated from Nockolds, 1954).

this granite lie between the average adamellite and muscovite-biotite alkaline granite; in addition, the mafic rocks are close to the composition of diorite and xenolithic rock is similar to that of trondhjemite.

In the normative An-Ab-Or plot of O'Connor (1965), the Barber's Lake Granite is in the granite field; the mafic and xenolithic rocks are in the fields of tonalite and trondhjemite, respectively (Fig. 2-9-6). In addition, granitic rocks of this pluton completely fall in the low temperature trough of Kleeman (1965) and granite field of Bowen and Tuttle (1958; See also Fig. 2-9-6). Projections of normative Qtz-Ab-Or and loci of ternary eutectics at various P_{H2O} and Ab/An ratios are given in Figure 2-9-7. Rocks of the Barber's Lake Granite are bracketed by cotectics for P_{H2O} of 0.5 and 5.0 kb at 0% An-content. The composition distribution in the Qtz-Ab-An-Or-H_2O system suggest that the Barber's Lake Granite was of magmatic origin.

Correlation coefficients of major-oxides as a function of SiO_2 are given in Table 2-9-4. For the granitic rocks, Al_2O_3, and Fe_2O_3 show negative correlations with SiO_2, but other elements have no significant trends. However, it was found that most of the correlation coefficients are enhanced as the mafic and xenolithic rocks were included (Table

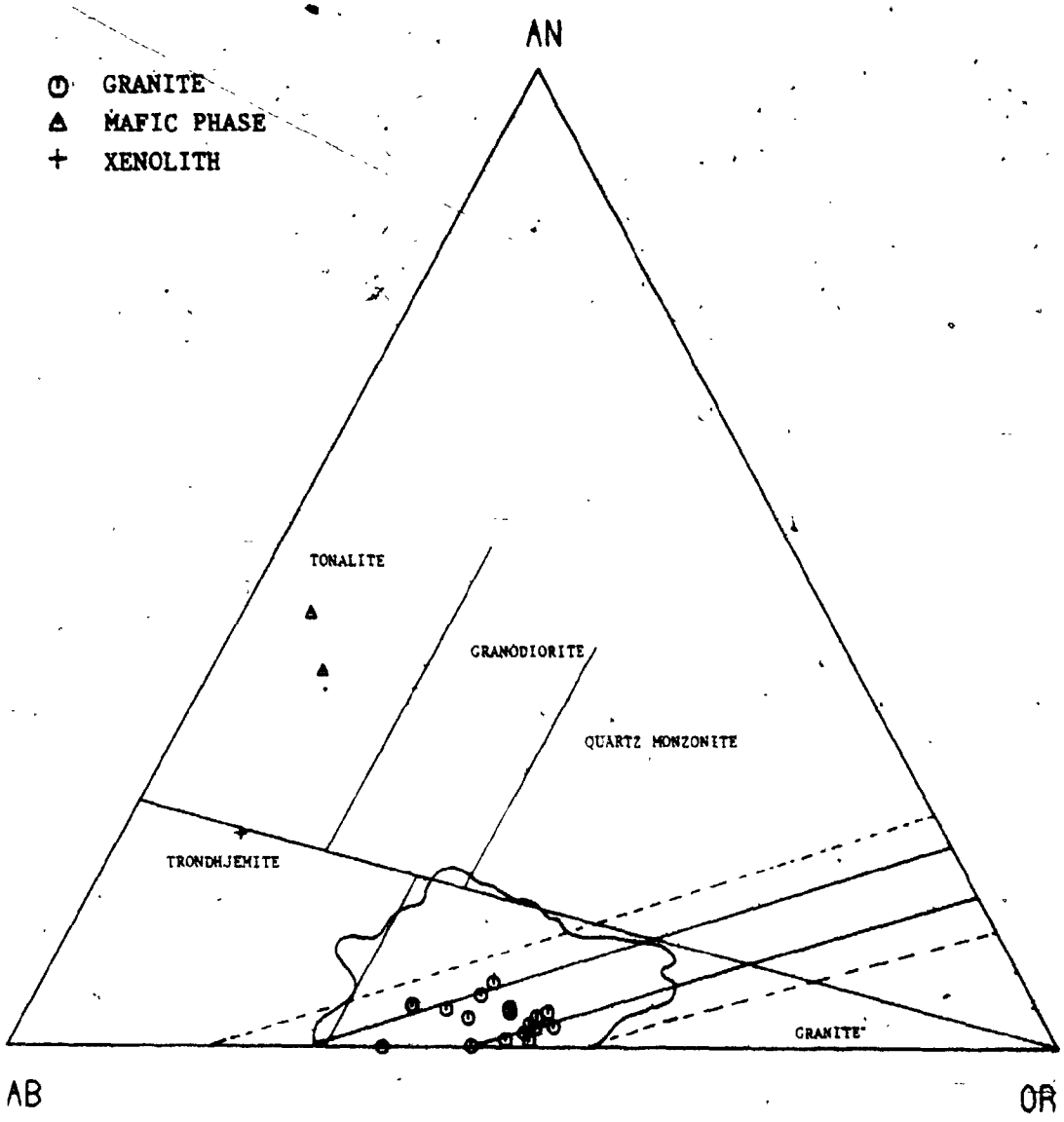

Figure 2-9-6. Normative Ab-An-Or ternary diagram of the Barber's Lake Granite. The irregular solid boundary is the 2% contour of Tuttle and Bowen (1958) enclosing most of granitic rocks that contain more than 80% normative Ab+An+Or+Qtz. The solid-lines indicate the boundaries of low temperature trough; dashed-lines show uncertainty due to analytical error (Kleeman, 1965). Classification scheme is from O'Connor (1965).

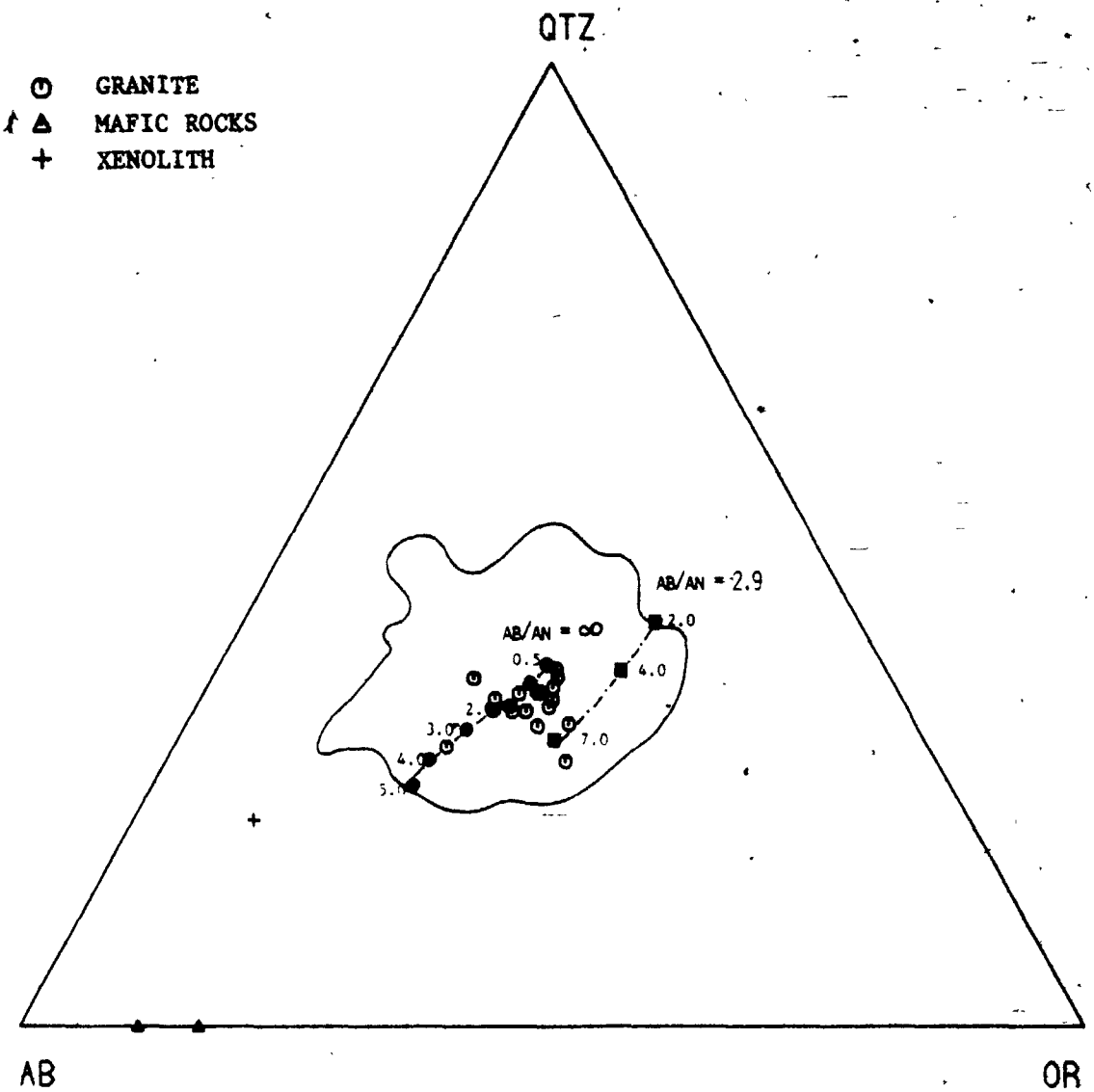

Figure 2-9-7. Normative Qtz-Ab-Or ternary diagram of the Barber's Lake Granite. The irregular solid boundary encloses analyses of 1190 granitic rocks of Winkler and Von Platen (1961). Exeprimentally determined ternary minima Tuttle and Bowen, 1958; Luth et al., 1964) and minima in An-bearing systems (James and Hamilton, 1969) are shown by solid circles and solid squares, respectively.

Table 2-9-4. Correlation coefficients of inter-element variations for the Barber's Lake Granite

Correlation		Granite only	Granite + Mafic + xeno.	Correlation		Granite only	Granite + Mafic + xeno.
SiO_2 vs.	TiO_2	-0.3489	-0.9398	SiO_2 vs.	U	-0.1327	0.5073
	Al_2O_3	-0.7617	-0.9840		Th	-0.4141	0.6497
	Fe_2O_3	-0.4829	-0.9787		F	-0.4224	0.2530
	MgO	-0.4157	-0.9718		Cl	-0.0234	-0.7638
	MnO	-0.1402	-0.9120		S	-0.1343	-0.2902
	CaO	-0.1428	-0.9908		Ga/Al	0.0854	0.1869
	K_2O	-0.3889	0.8697		K/Rb	0.0030	-0.6979
	P_2O_5	-0.4109	-0.8607		Rb/Sr	0.0500	0.6440
	Na_2O	0.0787	-0.2479		Sr/Ba	-0.1911	-0.8113
	Rb	-0.4074	0.8690		Sr/Ca	0.0669	0.1838
	Sr	-0.4658	-0.9133		Zr/Y	-0.4559	0.0853
	Ba	-0.5465	-0.2546		Y/Ca	0.1321	0.2705
	Zr	-0.5423	0.1271		Cr/Mg	-0.1698	0.3055
	Nb	-0.0125	0.4630		V/Mg	-0.2980	0.2255
	Y	-0.1953	-0.0118		Ni/Mg	-0.0756	0.3556
	Ga	-0.1333	-0.7278		Fe/Mg	-0.1879	0.3010
	Pb	-0.3532	0.1735		Cr/Fe	0.0443	-0.7300
	Zn	-0.0804	-0.7543		V/Fe	0.1987	-0.6581
	Cu	-0.3256	-0.6489	Nb vs.	Ga/Al	0.7209	0.7438
	Ni	-0.3274	-0.9850	Nb vs.	Y	0.7116	0.6193
	Cr	-0.4972	-0.9732	Al_2O_3 vs.	Ga	-0.1074	0.6834
	V	-0.0857	-0.8840				

2-9-4). These strong correlations, as a function of SiO_2, may suggest a linear relation among mafic rocks, xenolith and granite as a whole. In terms of K_2O-Na_2O-CaO ternary variation (Fig. 2-9-8), the granitic rocks cluster at the end of the common igneous trend and mafic rocks are near the field of cumulates (Nockolds and Allen, 1953).

9.3.2 Trace-elements -

The Barber's Lake Granite contains relatively lower Sr, Ba, Zr, Y, Ni, Cr, V and higher Rb, Nb, Ga contents than those of average granite (Taylor, 1964; See Table 2-9-3). The mean Rb/Sr is about 3.21 which is much higher than 0.53 of average granite; the K/Rb ratio of 164 is comparable with "normal" igneous values (150 - 300).

Correlation coefficients of trace-element and element - ratio as a function of SiO_2 are given in Table 2-9-4. Rb, Sr, Zr, Ba, Cr, Th and F possess relatively strong negative correlations with SiO_2, but the other elements are comparatively scattered. The increase of Rb as increasing K_2O (Fig. 2-9-9A), and decrease of Ba as decreasing Sr (Fig. 2-9-9B) are consistent with normal differentiation trends. In addition, the steep decrease of Ba as Rb increases (Fig. 2-9-9C) may indicate a late stage

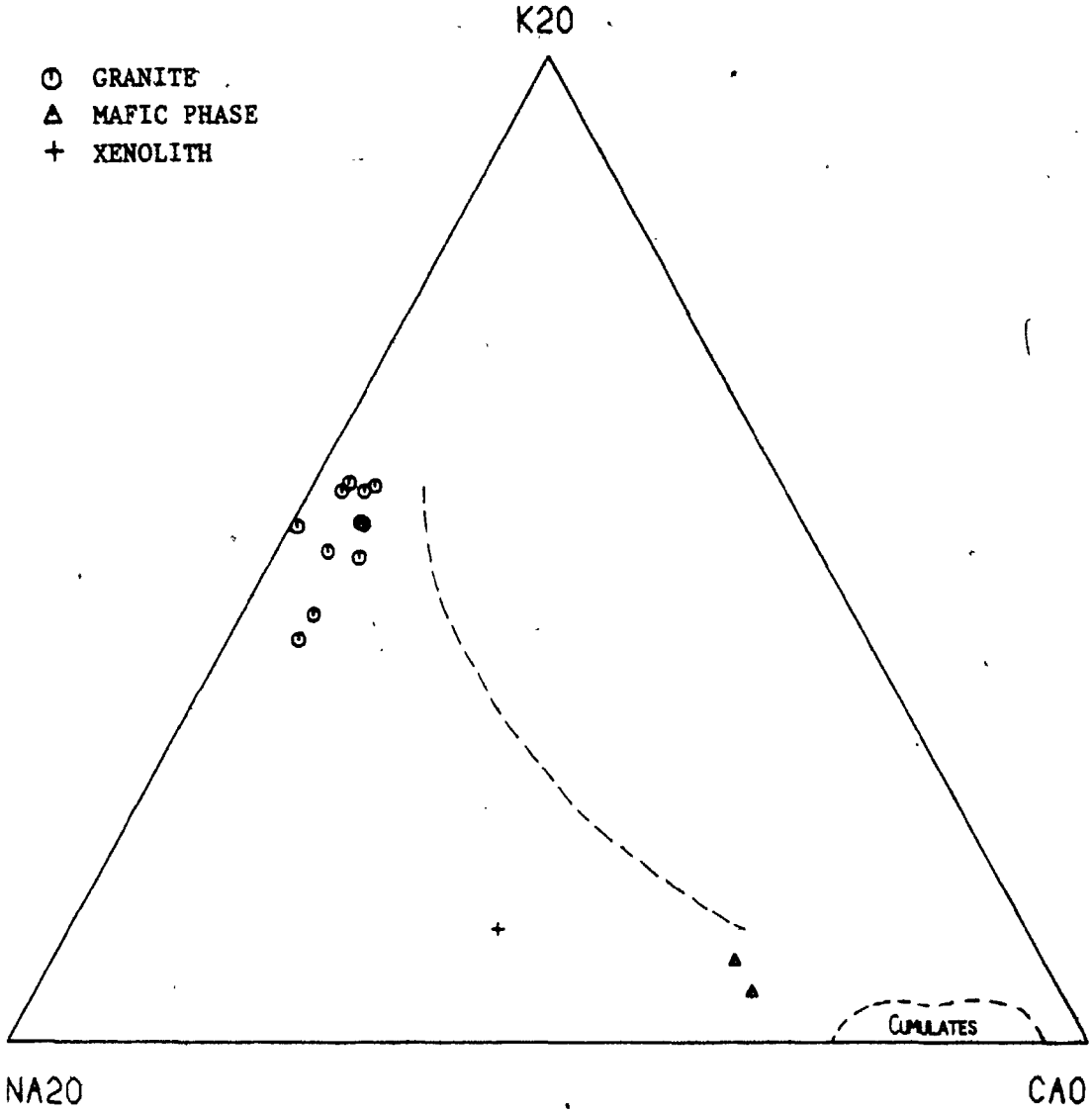

Figure 2-9-8. Na_2O-K_2O-CaO variation diagram of the Barber's Lake Granite.

---- Calc-alkaline trend of Southern California Batholith (Nockolds and Allen, 1956).

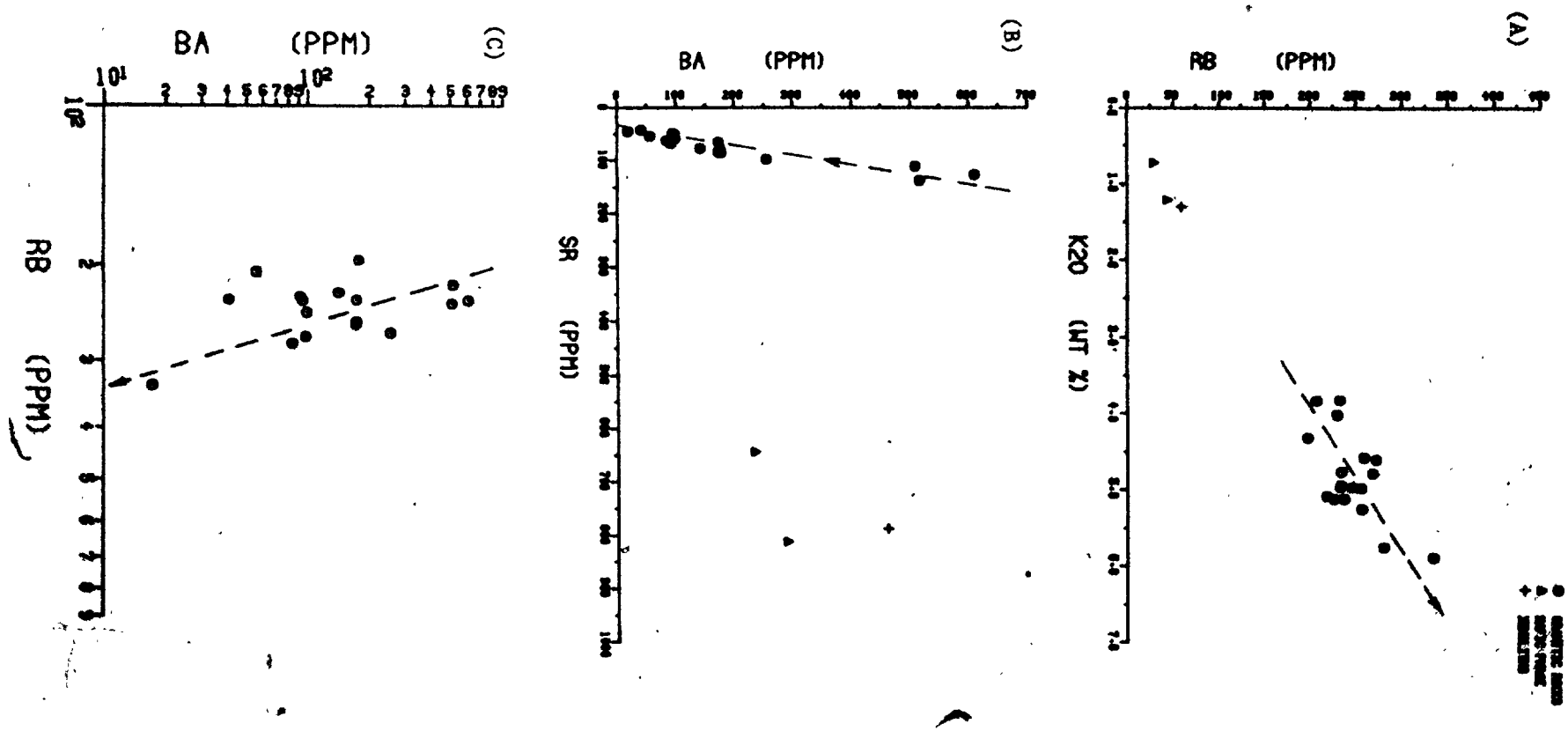

Figure 2-9-9. Variation plots of alkali-alkaline earth elements of the Barber's Lake Granite.

(A) Rb vs. K_2O (B) Ba vs. Sr (C) Ba vs. Rb

Dashed-lines indicate the variation trends of the granite.

differentiation of a highly evolved magma. This is also reflected in the Rb-Ba-Sr ternary diagram of Bouseily and Sokkary (1975, See Fig. 2-9-10), in which most samples of the granite fall outside the field of strongly differentiated granite with some Sr-enrichment. Mafic and xenolithic rocks are in the diorite and anomalous granite fields, respectively.

9.3.3 Rare-earth Elements -

Analyses of rare-earth elements, Ta, Hf and Cs of granitic, mafic and xenolithic rocks from Barber's Lake Granite are presented in Table 2-9-5. Their chondrite-normalized REE distribution patterns are shown in Figure 2-9-11. For the granitic rocks, they show similar shapes with mild fractionation trends and moderate Eu-anomalies. The decrease of Eu/Eu* ratio with increasing SiO_2 can be expected by fractionation of feldspar (esp. plagioclase). It is consistent with gradually increasing Cs and sharply decreasing Ba and Ba/Cs ratio in the granite (Table 2-9-5). Additionally, the sum of LREE (Ce+Sm) decreases from 134 to 76 as SiO_2 increases; such a depletion in the strongly differentiated granitic melt may be due to the fractionation of LREE-enriched minor phases (eg. allanite, sphene and monazite) (Mittlefehldt and Miller, 1983;

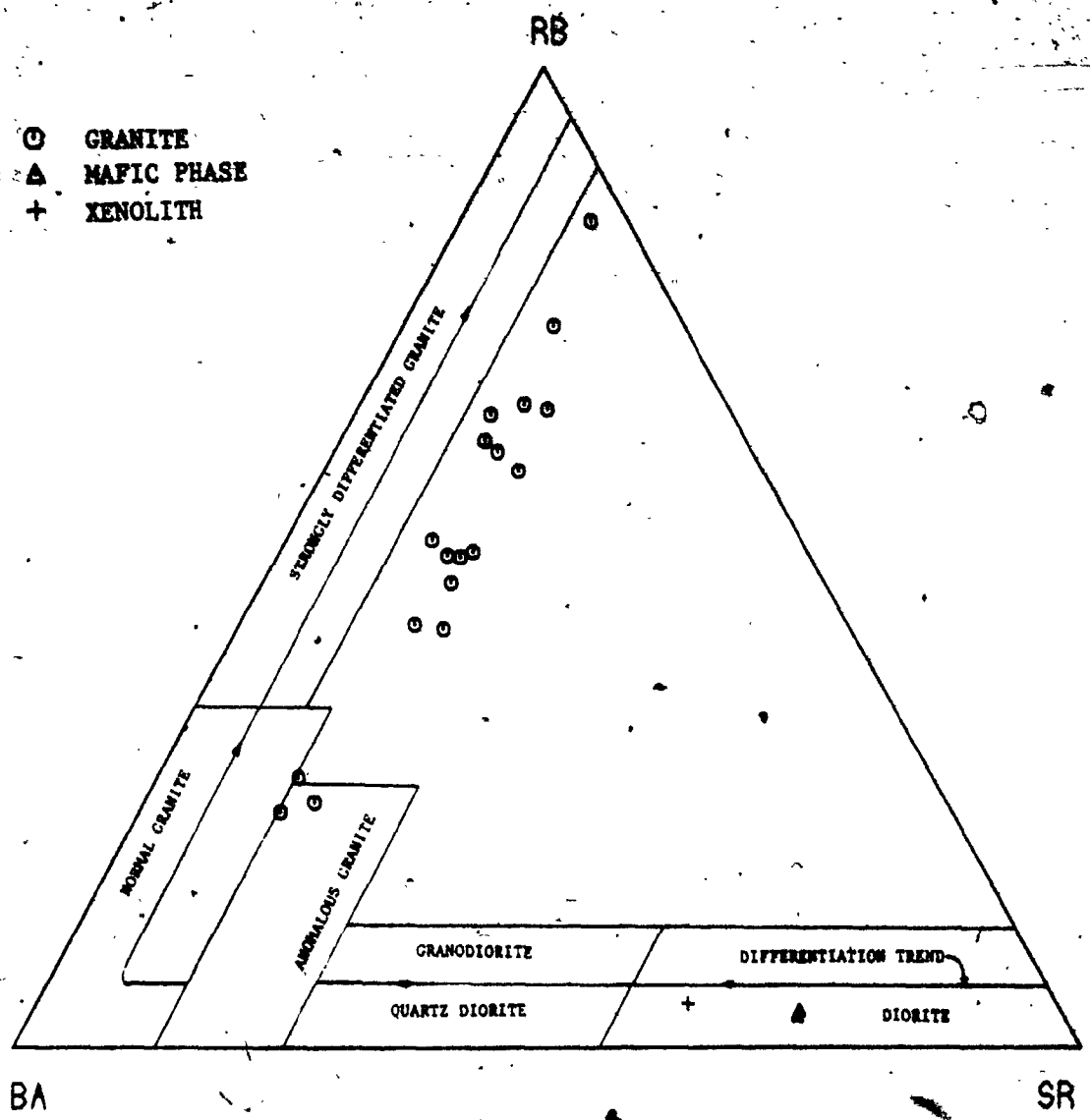

Figure 2-9-10. Rb-Ba-Sr ternary variation diagram of the Barber's Lake Granite (after Bouseily and Sokkary, 1975).

Table 2-9-5. Rare-earth elements, Ta, Hf and Cs compositions of the Barber's Lake Granite and related rocks

(ppm)	1 EPE-1-3	2 EPE-15	3 EPE-4	4 EPE-6	5 EPE-11-A	6 EPE-11-B	7 EPE-0-3	8 EPE-0-1
La	27.82	67.23	65.33	12.50	9.58	11.01	27.36	10.06
Ce	69.49	116.71	126.29	42.99	22.69	32.88	51.05	11.95
Sm	6.89	7.46	7.82	2.57	2.54	3.79	3.94	4.66
Eu	0.58	0.66	0.89	0.28	1.14	1.10	0.90	0.50
Tb	1.10	0.96	0.84	0.54	0.27	0.53	0.52	0.42
Yb	4.47	3.36	2.63	2.63	0.94	1.16	1.87	1.75
Lu	0.78	0.52	0.50	0.38	0.18	0.16	0.26	0.37
ΣREE	111.13	196.90	204.30	61.89	37.34	50.63	85.90	29.71
Ta	4.87	2.81	2.51	3.29	0.56	0.71	2.02	0.39
Hf	5.67	6.19	7.19	1.94	1.69	1.64	6.28	1.27
Cs	3.32	2.66	1.89	2.30	0.97	1.98	2.79	0.12
Eu/Eu^*	0.25	0.31	0.41	0.31	1.45	0.94	0.76	0.25
$(Ce/Yb)_N$	3.59	7.82	11.08	3.77	5.20	5.29	6.44	1.56
$(Ce/Sm)_N$	1.05	1.18	1.38	0.85	1.57	1.57	1.22	1.00
$(Tb/Yb)_N$	2.08	3.24	2.35	3.50	1.76	1.76	2.63	0.54
SiO_2 (wt%)	73.95	73.51	73.34	75.05	50.25	51.70	64.20	48.05
Ba ppm	92.00	610.60	516.60	94.40	-	-	-	-
Ba/Cs	27.70	229.50	273.30	41.00	-	-	-	-

1,2,3 Granitic rocks of the Barber's Lake Granite.
4 Pegmatitic granite of the Barber's Lake Granite.
5,6 Mafic cumulative rocks of the Barber's Lake Granite.
7 Trondhjemitic xenolith of the Barber's Lake Granite.
8 Amphibolite of the country rock.

Figure 2-9-11. Chondrite-normalized REE distribution patterns of the Barber's Lake Granite.

(A) REE distributions for granite.

(B) REE distributions for mafic phase and xenolith.

(A)

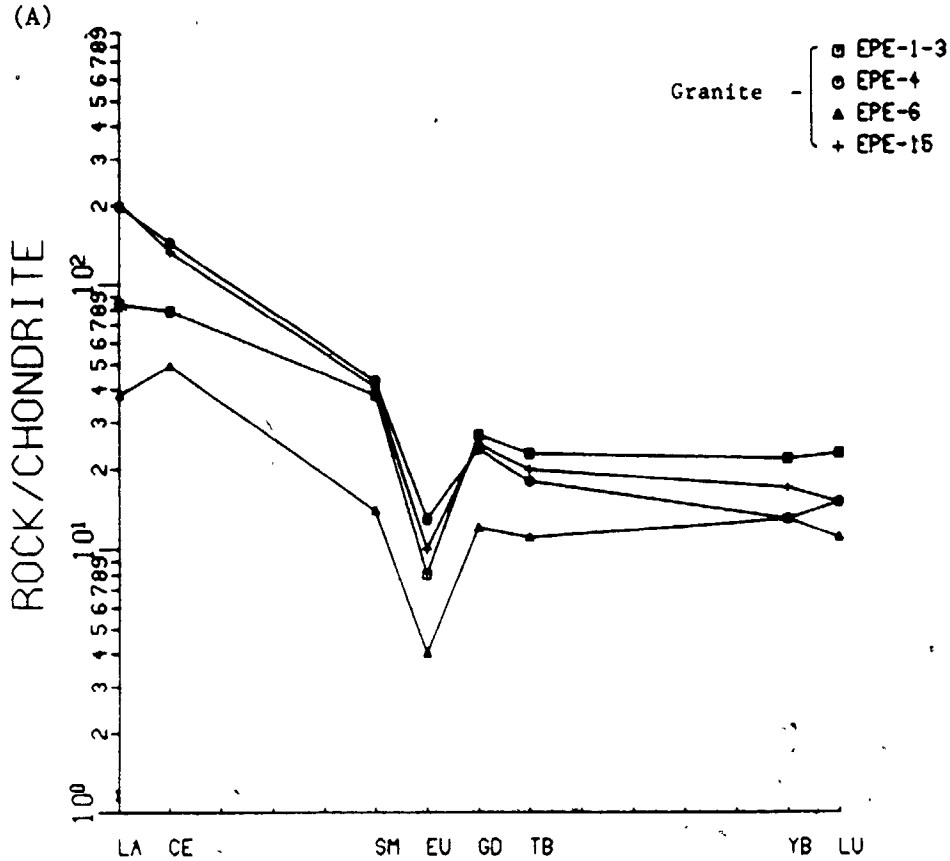
Granite
EPE-1-3
EPE-4
EPE-6
EPE-15
ROCK/CHONDRITE
LA CE SM EU GD TB YB LU

(B)

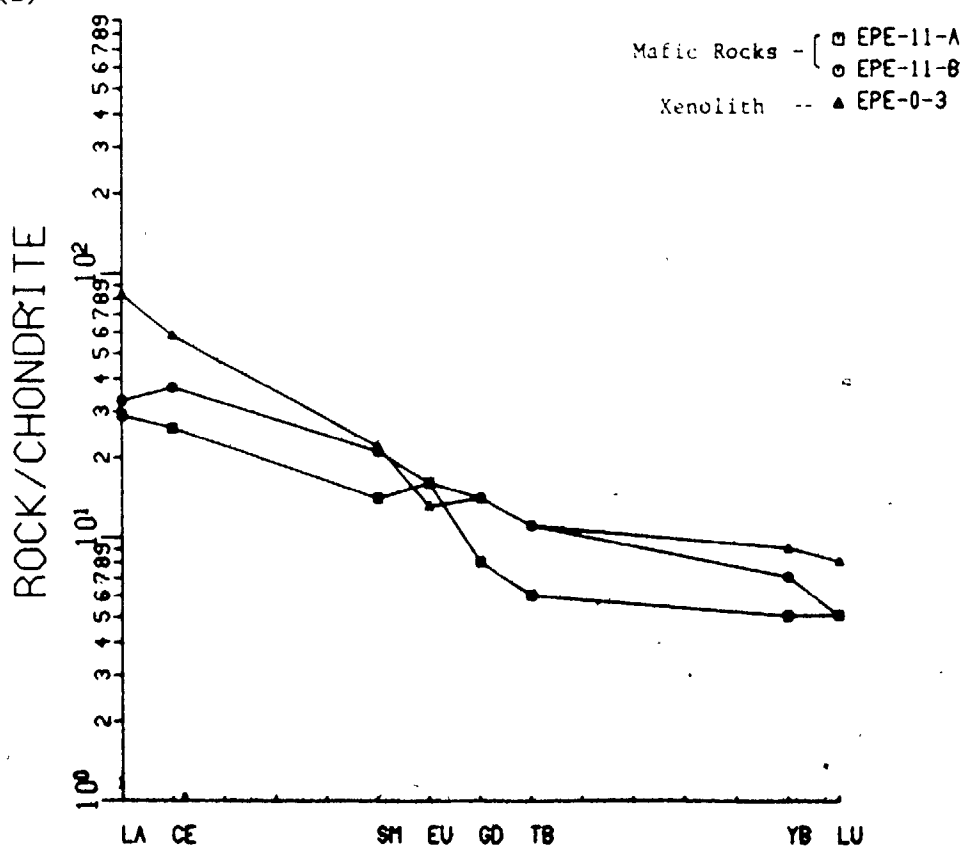
Mafic Rocks
EPE-11-A
EPE-11-B
Xenolith
EPE-0-3
ROCK/CHONDRITE
LA CE SM EU GD TB YB LU

Gromet and Silver, 1983). The LREE and total REE abundances are continuously depleted into the pegmatitic phase (EPE-6), which has similar negative Eu-anomaly (Eu/Eu* = 0.31) but with relative flat pattern ($(Ce/Yb)_N$ = 3.77; See Fig. 2-9-11A).

Chondrite-normalized REE curves of the mafic rocks show less fractionated trends ($(Ce/Yb)'_N$ = 5.2) with or without positive Eu-anomaly, that may indicate their cumulative origin. On the other hand, the trondhjemitic xenolith displays a relatively fractionated pattern with small negative Eu-anomaly. The amphibolite of the country rocks shows a flat curve and contains the lowest total REE abundances (Fig. 2-9-11B).

9.3.4 Uranium And Thorium -

Because of their incompability with early fractionated mineral assemblages, the heat-producing elements - U, Th and K - are concentrated in the residual or more evolved felsic magma during magmatic differentiation (Rogers and Cagland, 1961; Rogers and Adams, 1969a, b). Whether the Th/U ratio increases or decreases with differentiation is mainly controlled by the presence of uranyl ion $(UO_2)^{2+}$, which has greater solibility and mobility than tetravalent uranium (Rogers and Adams, 1969b).

Regarding the distribution of U and Th in whole-rock samples, only a small fraction of these radioactive elements are concentrated in the major rock-forming minerals due to their smaller U and Th distribution coefficients (D^U and D^{TH} << 1). More than 70% of U and Th are in the accessory mineral phases (eg. allanite and monazite for Th; zircon and xenotime for U), which occur as individual mineral grains and/or as microscopic inclusions. Less than 30% of these elements appear as solid solutions in the essential minerals, or as fillings in the interstitial spaces among grains, or as easily leachable substance on the surface of altered products and dispersions throughout the rock.

Concentrations of U, Th, K and their ratios of rocks from the Barber's Lake Granite are given in Table 2-9-6. Uranium and thorium determinations were done by delayed neutron method and instrumental neutron activation analysis, respectively. The precision of these methods can be estimated from the results of duplicate analyses of internal standard UWO-1; it is better than 10% for U (ave. 9.0 ppm) and 3% for ~~Th~~ (ave. 22.2 ppm).

The mean U and Th concentrations of the Barber's Lake Granite are 15.0 and 36.3 ppm respectively, which are comparatively higher than those of average granite (4.8 ppm U and 17 ppm Th,

Table 2-9-6. Uranium, thorium and potassium abundances of the Barber's Lake Granite

Sample No.	U (ppm)	Th (ppm)	K (wt%)	Th/U	U/Kx10^4	Th/Kx10^4	F (ppm)
(A) Granite							
EPE-1-3	30.2	70.1	3.34	2.32	9.04	20.98	592
EPE-2	26.7	59.0	4.89	2.20	5.46	12.06	1440
EPE-3-2	8.0	23.0	4.12	2.88	1.94	5.58	700
EPE-4	5.4	28.1	4.22	5.18	1.28	6.65	736
EPE-5	33.1	37.0	3.82	1.12	8.66	9.69	-
EPE-6	10.9	27.0	3.95	2.48	2.76	6.83	200
EPE-7	16.5	28.0	3.17	1.70	5.21	8.83	432
EPE-15	5.6	18.0	4.10	3.21	1.36	4.39	524
EPE-8	14.2	-	3.18	-	4.46	-	-
EPE-9	11.8	-	4.25	-	2.78	-	276
EPE-10	13.3	-	4.13	-	3.22	-	-
EPE-12	9.1	-	4.12	-	2.21	-	-
EPE-13	17.5	-	4.36	-	4.01	-	-
EPE-14	7.0	-	4.25	-	1.65	-	-
Mean	*(14) 15.0	(8) 36.3	(14) 3.99	2.42	3.76	9.10	612
Ave.**Granite	4.8	17.0	-	***3.5-4.0	-	-	850
(B) Mafic + xenolith							
EPE-11-A	0.5	1.0	0.61	2.00	0.82	1.64	158
EPE-11-B	1.5	1.1	1.01	0.73	1.49	1.09	420
EPE-0-3	2.4	3.0	4.70	1.25	0.51	0.64	292

* No. of analyses.
** Average U and Th of granite (Heier and Rogers, 1963).
*** Average of igneous rocks (Rogers and Adams, 1969).

Heier and Rogers, 1963). In addition, this granite has relatively lower Th/U ratio ranging from 1.0 to 3.0 and average U/K and Th/K ratios of 3.76 and 9.10, respectively. There are no obvious trends in the variations of Th and Th/U as a function of SiO_2. However, it is noteworthy that in the U vs. SiO_2 plot (Fig. 2-9-12A), samples are clustered in three discrete groups; a general enrichment of U with increasing differentiation is illustrated. Rocks of anomalously higher U contents (> 20 ppm) are mainly from the northern margin of the pluton.

The enrichment of uranium in the Barber's Lake Granite can be directly related to: (1) the fixation of U with volatile components (esp. fluorine), (2) the replacing of U with Y - group elements in minor phases (eg. sphene, zircon), (3) the attachment of alteration products during secondary processes (eg. hematization of magnetite or chloritization of biotite). Except for one sample (EPE-2) with 1440 ppm F and 26.7 ppm U, there is no direct relationship between U and F abundances in this granite (Fig. 2-9-12B); In addition, the average F content of the Barber's Lake Granite is far below the average granite value of 850 ppm. The negative correlation between U and Fe_2O_3 as total iron (Fig. 2-9-12C) precludes the enrichment of U by secondary alteration, although chloritization of

Figure 2-9-12. Various U and Th plots of the Barber's Lake Granite. (A) Th vs. SiO_2 (B) U vs. F (C) U vs. Fe_2O_3 and (D) U vs. Y. Solid-lines indicate the visual trends.

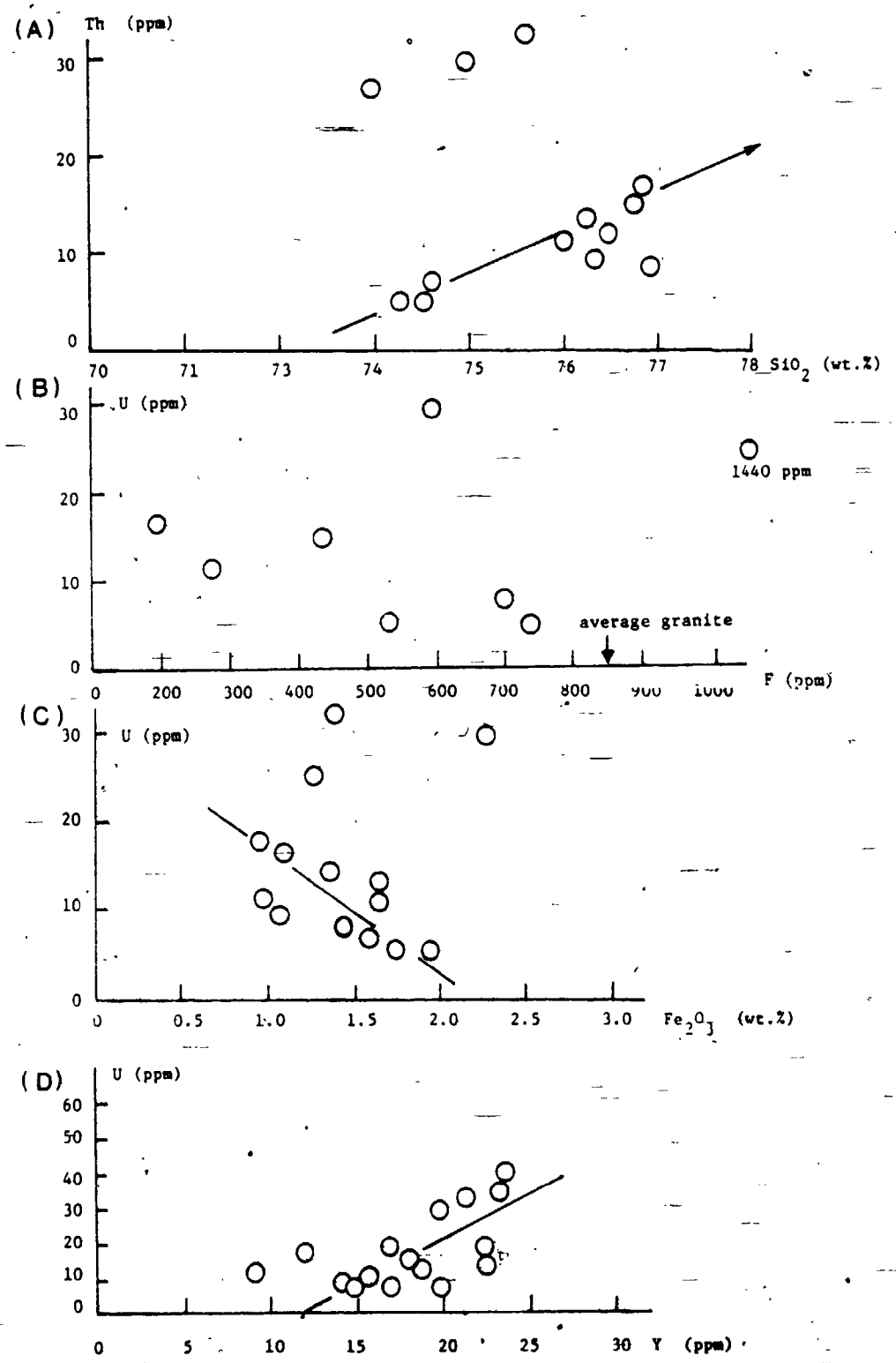
(A)
Th (ppm)
30
20
10
0
70
71
73
74
75
76
77
78
SiO_2 (wt.%)
(B)
U (ppm)
30
20
10
0
1440 ppm
average granite
0
200
300
400
500
600
700
800
900
1000
F (ppm)
(C)
U (ppm)
30
20
10
0
0
0.5
1.0
1.5
2.0
2.5
3.0
Fe_2O_3 (wt.%)
(D)
U (ppm)
60
50
40
30
20
10
0
0
5
10
15
20
25
30
Y (ppm)

biotite does occur in several high U samples. However, variation of U as a function of Y give a positive correlation (Fig. 2-9-12D), which is consistent with the hypothesis that enrichment of U in this granite is a primary feature. In other words, most U are retained by accessory minerals, though fluorine-complexing of uranium ion (U^{4+}) could also occur in the deuteric stage.

9.4 Isotopic Geochemistry

The whole-rock oxygen isotope analyses of the Barber's Lake Granite give the $\delta^{18}O$ values of 10.43 and 10.74 o/oo. Comparatively, they are higher than the isotopically "normal" granite of Taylor (1978) and can be classified as a high-^{18}O granite of Shieh and Schwarcz (1974; $\delta^{18}O > 8.4$) in the Grenville Province of Ontario. Such an O^{18} enrichment in the granite may result from significant isotopic exchange between the granitic melt and surrounding (meta)sedimentary rocks which contain relatively higher ^{18}O (Shieh and Schwarcz, 1974).

Although there are no direct age-date and Rb-Sr isotopic data available for this granite, field evidences and its uraniferous nature suggest that the Barber's Lake Granite was probably temporally related to other uraniferous granites and pegmatites in the

Grenville Province, with an approximate age of 950 ± 30 Ma and initial $^{87}Sr/^{86}Sr$ ratios of 0.703 to 0.705 (Fowler and Doig, 1983). Such low initial ratios preclude the possibilty of crustal origin for this granite.

9.5 Petrogenesis And Source Rocks

For those high U-Th concentrations of granites and pegmatites in this part of the Grenville Province, most authors seem to accept the idea that they were formed by anatexis of a U-Th-rich protolith, either a sedimentary unit (pelite) or the quartzofeldspathic gneisses at the base of the Grenville Supergroup (Robinson, 1961; Evans, 1966; Bright, 1976; Gordon and Masson, 1977). More recently, Fowler and Doig (1983) have used the Rb-Sr isotopic method to test this hypothesis; they found that the uraniferous granites and pegmatites in the Bancroft, Mont Laurier and Johan Beetz areas are some 150 Ma younger than the peak of Grenville Orogeny.

Based on these findings, they precluded the possibility of in-situ anatexis of (meta)sedimentary rock for these granitic rocks. Instead, Fowler and Doig (1983) suggested an origin by partial fusion of peridotite in the mantle by rapid uplift due to isothermal decompression after the Grenville Orogeny. The grantic melt was then generated by water-rich fluid

leaching through a gabbroic crystal mesh to concentrate the silica, alkalis and radioelements.

It is noteworthy that the high $\delta^{18}O$ value, low K/Rb ratio, lower total Sr content, high level of incompatible elements (eg. Nb, Th, Ta, Hf) and possible low initial $^{87}Sr/^{86}Sr$ ratio of the Barber's Lake Granite are comparable to those uraniferous granites of the British Isles (Simpson et al., 1979). They suggested that U-enriched granitic magma of the British Caledonian and Hercynian Provinces are derived from subducted oceanic lithosphere by dehydration of phlogopite at destructive margins. The concentration of U in the granitic magma is attributed to scavenging by ascent of fluorine-enriched fluid phase after the break down of phlogopite.

However, for Barber's Lake Granite, the proper petrogenetic models need to firstly explain the quasi-linear relations of mafic (M), xenolithic (X) and granitic (G) rocks in varioius variation trends. Such straight-line relationships may be interpreted as :

1. Fractional crystallization of M from an initial magma with similar composition to X and leaving the residual liquid G;

2. Partial melting of a protolith with composition X, separating the refractory crystalline residue M and the felsic melt G.

9.5.1 Fractional Crystallization -

The trondhjemitic xenolith (EPE-0-3) of this granite has similar composition to that of the Grenville dacite (Condie and Moore, 1977), except that the former contains higher Na_2O and CaO and lower K_2O (Table 2-9-7). In comparison with other trondhjemite suites of the Grenville Province, the xenolith has relatively higher total iron, MgO, CaO and lower SiO_2; it is intermediate between the typical high-Al_2O_3 trondhjemite of the Elzeivir Batholith and quartz diorite of the Union Lake Pluton (See Table 2-9-7). However, all have similar REE concentrations and parallel chondrite - normalized patterns, though the EPE-0-3 retains higher HREE and a less fractionated curve ($(Ce/Yb)_N$ = 6.4).

The differences of REE distribution patterns among granite, trondhjemitic xenolith and mafic rocks (Fig. 2-9-13) suggest a feldspar-enriched cumulate and a residual melt produced by fractional crystallization of a trondhjemitic precursor. Mass balance calculations by using the least squares method (Stormer and Nicholls, 1978) indicate that differentiation from EPE-0-3 to average composition of the Barber's Lake Granite requires removal of a solid of 72% plagioclase, 20% hornblende, 5% hyperthene, 2% sphene and 0.8% apatite, which is

Table 2-9-7. Comparison of average composition of trondhjemitic rocks in the Grenvill Province

	1	2	3	4	5
SiO_2 (wt.%)	64.20	61.05	70.12	69.17	64.40
TiO_2	0.52	0.74	0.37	0.28	0.44
Al_2O_3	16.40	16.54	15.68	16.36	16.30
TFe_2O_3	3.82	5.53	2.57	2.69	3.84
MnO	0.04	0.08	0.07	0.04	-
MgO	2.17	2.88	0.92	1.11	2.20
CaO	4.45	5.14	2.73	3.38	3.20
Na_2O	5.66	5.50	4.57	5.34	4.00
K_2O	1.31	2.01	0.10	0.03	-
P_2O_5	0.14	0.27	0.10	0.03	-
LOI	0.68	0.54	-	0.58	-
Na_2O/K_2O	4.32	2.74	1.78	4.68	1.67
La (ppm)	27.36	27.02	23.50	20.20	-
Ce	51.05	59.48	45.70	28.70	37.00
Sm	3.94	5.10	3.01	3.11	2.80
Eu	0.90	1.25	1.12	0.81	0.79
Tb	0.52	0.42	0.37	0.32	0.40
Yb	1.87	1.11	0.85	-	1.20
Lu	0.26	0.19	0.13	0.11	0.20
Eu/Eu*	0.76	0.90	1.18	0.96	0.90
$(Ce/Yb)_N$	6.44	11.33	12.09	10.65	7.00
$(Ce/Sm)_N$	1.22	2.43	3.06	1.94	2.69
$(Tb/Yb)_N$	2.63	1.67	1.84	-	1.35

1 Trondhjemitic xenolith (EPE-0-3) of this granite (this study).
2 Average composition of Union Lake Pluton (this study).
3 Average composition of Elzeivir Batholith (Pride and Moore, 1983).
4 Average composition of White Lake Pluton (Somers, 1984, unpub. data).
5 Average composition of Granvill Dacite (Condie and Moore, 1977).

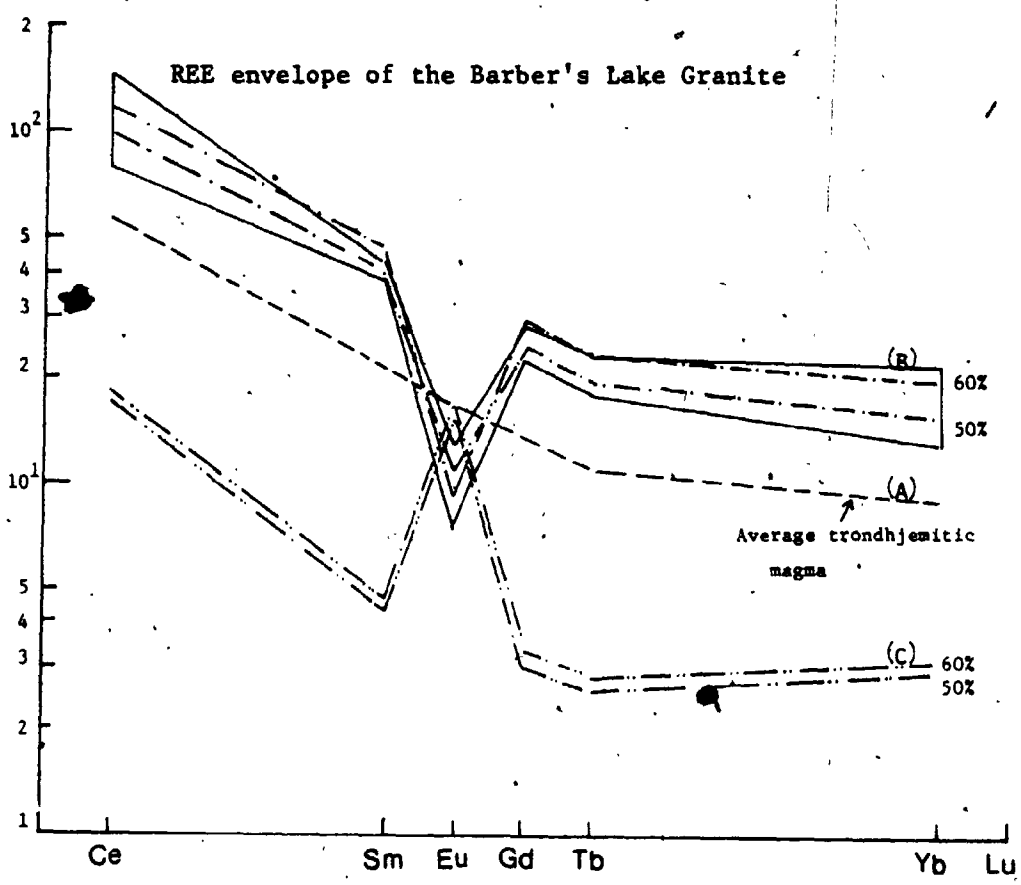

Figure 2-9-13. REE modelling of the Barber's Lake Granite. Fractionation of a trondhjemitic melt (A) to form the Barber's Lake Granite melt (B) and an accumulate (C) (i.e. the mafic phase).

similar to the mineralogy of mafic rocks in this granite. Figure 2-9-13 illustrates that 50 - 60% equilibrium crystalization of an assemblage with 70% plagioclase and 25% orthopyroxene would give two complementary patterns similar to those of granitic and mafic rocks of the pluton. The relatively lower concentration of total REE, especially HREE, in the modelled cumulate rocks could be explained by frationation of REE-enriched minor phases which were not included in this modelling.

The high-Al_2O_3 trodhjemitic rocks in this part of the Grenville Province are considered to be products of equilibrium partial melting of mafic granulite at lower crust (See details in Union Lake Pluton). Although the crystallization of trondhjemitic magma could explain most geochemical characteristics of this granite (eg. low K/Rb and R_i), it is difficult to account for the concomitant enrichment of uranium. However, after high-grade metamorphism, the $CO_{2(g)}$ released from calcite-rich country rocks are easily incorporated into magma; they scavenge the uranium species from the Grenville Supergroup metasediments (Darley et al., 1971) and form uranyl dicarbonate ($UO_2(CO_3)_2^{-2}$) disseminated in the granite magma (Kimberley, 1978) and then replacing the Y-group elements in minor phases. The interpretation of high ^{18}O in the Barber's Lake

Granite by extensive isotopic exchange with surrounding metasediments is a positive indication of scavenging uranium by ascending CO_2-enriched fluid (cf. Fowler and Doig, 1983).

9.5.2 Partial Melting -

With regard to the anatexis hypothesis, granite is essentially a mixture of crystallized melt and assimilated fragments of residual material. If the melt composition is assumed, the composition of residue should be obtainable by mass balance apparoaches (eg. MacRae and Nesbitt, 1980). The compositions of restites, with up to 50% partial melting of a trondhjemitic source (EPE-0-3), are shown in Table 2-9-8. The residue after 50% partial fusion is similar to the composition of mafic rocks (EPE-11-A), except that the former has higher SiO_2, MgO, Na_2O and P_2O_5, but lower total iron and CaO. However, the K_2O concentration is depleted from the residual bulk composition at about 30% partial melting, which indicates the limit for anatexis. Furthermore, 30% partial melting of an assemblage with the average mineralogy of the trondhjemitic xenolith ($Plag_{45}hb_{15}biot_{15}qtz_{25}$) failed to produce the REE patterns as shown in Figure 2-9-11.

Table 2-9-8. Mass balance calculations of partial melting a trondhjemitic source

(wt.%)	EPE-0-3	Ave. of the granite	20% residue	30% residue	40% residue	50% residue	EPE-11-A
SiO_2	64.20	74.73	62.37	60.11	57.02	52.94	50.25
TiO_2	0.52	0.08	0.63	0.72	0.81	0.95	1.80
Al_2O_3	16.40	13.30	17.40	17.85	18.41	19.23	19.21
Fe_2O_3	3.82	1.40	4.48	4.89	5.42	6.16	9.66
MgO	2.17	0.07	2.74	3.09	3.56	4.20	3.50
MnO	0.04	0.02	0.05	0.04	0.05	0.06	0.10
CaO	4.45	0.44	5.52	6.21	7.10	8.35	9.21
Na_2O	5.66	4.07	6.15	6.38	6.69	7.14	4.17
K_2O	1.31	4.82	0.44	(-0.14)*	(-0.62)*	(-1.10)*	0.73
P_2O_5	0.14	0.00	0.18	0.20	0.23	0.27	0.08
H_2O**	0.68	0.66	0.70	0.69	0.69	0.69	0.69

* Depletion of K_2O in the residual material.
** Assuming H_2O content = LOI.

9.6 Summary

The Barber's Lake Granite is a mesozonal, forceful intrusion with inclusions of country rocks along the border zones. It is composed mainly of biotite and primary muscovite in addition to the dominant felsic components. Mafic rocks with igneous pyroxene-relicts are considered to be of cumulative origin.

Chemically, this granite is peraluminous with alkali affinity; both major and trace elements suggest that it is a highly evolved granitic body. Depletion of total REE and LREE with increasing differentiation support fractionation of REE-enriched minor phases in the strongly differentiated magma. In addition, it is characterized by a lower K/Rb and total Sr and higher level of incompatible elements and $\delta^{18}O$.

The two-fold enrichment of U and Th in the Barber's Lake Granite makes it one of the uraniferous granite-pegmatite of the Grenville Province, which intruded after the climax of the Grenville Orogeny. The positive correlation of U and Y is consistent with the replacing of Y-group elements in accessory minerals by U during magmatic differentiation.

Based on the quasi-linear relationships of variation trends and the differences of the REE patterns among the granite, trondhjemitic xenolith and mafic rocks suggest the Barber's Lake Granite resulted from

fractional crystallization of a trondhjemitic magma. The enrichment of uranium is attributed to scavenging by ascending CO_2-rich fluid through the Grenville Supergroup metasediments.

CHAPTER III, GEOCHEMICAL COMPARISONS AMONG SAMPLED GRANITOIDS

1.0 GENERAL STATEMENT

Detailed descriptions of petrology, petrography and geochemistry of sampled granitoids have been given in the foregoing chapter (II). Although there is not sufficient age data available for the sampled granitoids, it is believed that these granites associated with the Grenville Orogeny record a history of 300 or more million years of magmatism in this region; nevertheless, the uraniferous Barber's Lake Granite is considered to be the latest one. Geographically, Mulock and Algonquin Batholiths are in the Ontario Gneiss Segment, while the others with smaller sizes were intruded in the Central Metasedimentary Belt. Discordant intrusive contacts and abundant inclusions of country rocks indicate mesozonal to epizonal (eg. Deloro Pluton) emplacement with forceful injection or stoping mechanism for granitoids of metasedimentary terrain, whereas the Algonquin and Mulock Batholiths are of catazonal character with passive intrusion. The relationship between granitic intrusions and regional deformation and metamorphism led to a classification of :

1. Pre-tectonic -- Algonquin Batholith and Union Lake Pluton;

2. Syn-tectonic -- Elphin Complex, Cheddar Granite and Mulock Batholith;

3. Late-tectonic -- Coe Hill Granite and Deloro Pluton;

4. Post-tectonic -- Barber's Lake Granite.

Modally, compositions of sampled granitoids range from :

1. diorite-gabbro (eg. Algonquin diorite-gabbro and mafic rocks of the Barber's Lake Granite);

2. quartz diorite-tonalite (eg. Union Lake Pluton, hybrid phase of Elphin Complex and tonalite-trondhjemite suite of the Algonquin Batholith);

3. granodiorite (eg. granitic phase of Elphin Complex);

4. monzonite-syenite (eg. monzonite-syenite suite of the Algonquin Batholith, syenitic phase of Elphin Complex, quartz-poor phase of Coe Hill Granite and monzonitic rocks of the Cheddar Granite);

5. granite (adamellite) (eg. Cheddar Granite, Barber's Lake Granite, Coe Hill Granite, Mulock Batholith and granite gneiss of the Algonquin Batholith).

Biotite and hornblende are major mafic minerals for the sampled granitoids, although their proportion varies from one pluton to the other. In addition, pyroxene is present in the mafic and monzonitic-syenitic varieties. For most of the granites, plagioclase is albitic oligoclase to albite ($An_{< 15}$) in composition, while perthite is the major and only feldspar of the main body of the Deloro Pluton. Primary muscovite occurs only in Barber's Lake Granite, whereas riebeckite interleaved with biotite is unique in Deloro Pluton. Apatite, zircon, sphene and magnetite are accessories and commonly included within mafic minerals or form oxidizing rims around them (eg. magnetite and sphene). Myrmekite and vermicular intergrowth of plagiolcase and quartz are frequently encountered in sampled granitoids, whereas granophyric intergrowth of alkaline feldspar and quartz dominates in the younger phase of Deloro Pluton.

Chemically, as expected from the mode, compositions of sampled granitoids are in the range of 45% to 77% SiO_2. Except for the Deloro Pluton and Barber's Lake Granite, most of the sampled granitoids are metaluminous on the basis of Al_2O_3-saturation, with molar Al_2O_3 / (Na_2O+K_2O+CaO) ratios ranging 0.808 to 0.985 (See Table 4-1-2).

The presence of hypersolvus feldspar, soda amphibole, normative sodium metasilicate and high agpaitic index (> 1) reflect the peralkaline origin of the Deloro Pluton. On the other hand, the occurrence of primary muscovite, normative corundum (ave. > 1%) and high molar ratio of aluminum and

total alkali-lime (1.07) suggest a peraluminous nature for the Barber's Lake Granite. It is also noteworthy that all the rest but one are alkalic according to the terms of Miyashiro (1978), while the Union Lake Pluton is calc-alkaline affinity (Peacock, 1931).

2.0 MULTIVARIATE STATISTICAL ANALYSIS

2.1 Q-mode Analysis

In order to separate sampled granitoids into groups of similar chemical character, an average of available chemical analyses was used as representative of each rock-type. For simplicity, nineteen averages were taken for Q-mode analysis.

Q-mode or cluster analysis is a statistical technique that attempts to group samples into a few distinct categories on the basis of mutual linear correlation among samples. A computer programme written by Parks (1970) was modified for this study; similarity between samples is calculated as a simple distance function which is an Euclidean measurement of distance between points in N-space. The calculated distance function ranges from 0.0 (the closest similarity) to +1.0 (the greatest dissimilarity); sample pairs with small distance function (i.e. higher similarity) were chosen to form a distinct group. In this study, lower similarity coefficients were used to identify chemically

similar groups for sampled granitoids (eg. Croudace, 1980).

2.1.1 Major-oxides -

The Q-mode cluster dendrogram based on 10 major-oxides (except P_2O_5) is given in Figure 3-2-1. It forms three distinct groups at similarity level 0.3 corresponding to the granitic (felsic), syenitic-monzonitic (less silicic) and dioritic-gabbroic (mafic) compositions of the sample population. At a similarity coefficient of 0.05, nine groups are further classified. Five groups in the granitic supergroup correspond to :

1. Deloro peralkaline and granophyric granite;

2. Algonquin granite, Barber's Lake Granite, Cheddar Granite and Mulock Batholith;

3. Algonquin granodiorite;

4. Algonquin trondhjemite and Coe Hill Granite;

5. Elphin granitic phase.

Three groups in the syenitic-monzonitic supergroup correspond to :

(top)
Figure 3-2-1. Q-mode cluster dendrogram based on 10 major-oxides.

Figure 3-2-2. Q-mode cluster dendrogram based on 12 trace-elements.
(bottom)

Abbreviations :

Algon-1 - Algonquin granite
Algon-2 - Algonquin granodiorite
Algon-3 - Algonquin monzonite-syenite
Algon-4 - Algonquin syeno-monzo-diorite
Algon-5 - Algonquin tonalite
Algon-6 - Algonquin trondhjemite
Algon-7 - Algonquin diorite-gabbro
UK - Union Lake quartz diorite
Elphin-G - Granite of Elphin Complex
Elphin-S - Syenite of Elphin Complex
Chedd-G - Cheddar granite
Chedd-M - Cheddar monzonite
CH-G - Coe Hill granite
CH-M - quartz-poor phase of Coe Hill Granite
Mulock - Mulock Batholith
Barber - Barber's Lake Granite
Deloro-1 - Riebeckite-bearing granite
Deloro-2 - Granophyric granite
Deloro-3 - Calc-syenite

(top)

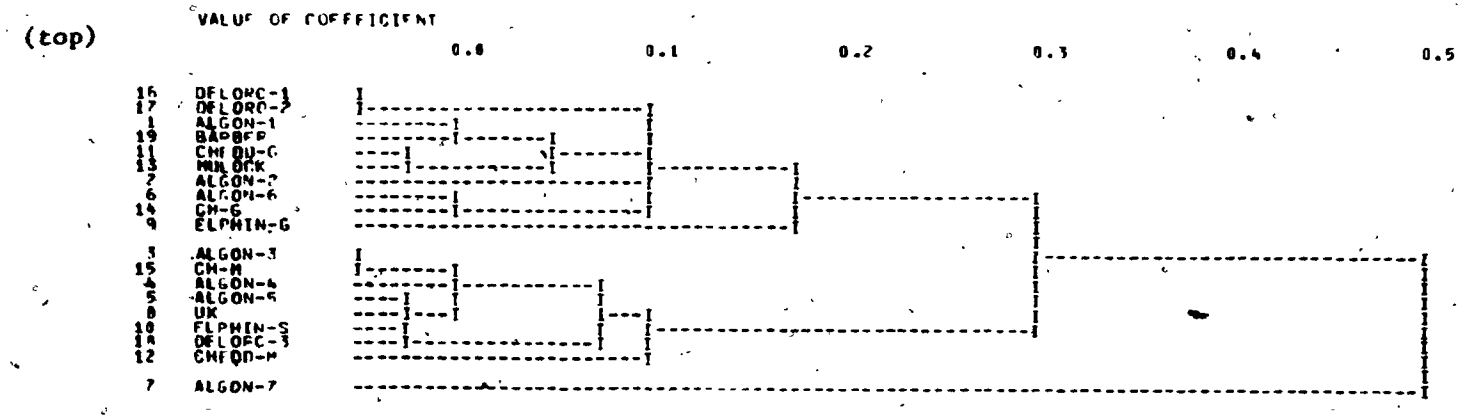
VALUE OF COEFFICIENT
0.0
0.1
0.2
0.3
0.4
0.5
16 DELORO-1
17 DELORO-2
1 ALGON-1
19 BARBER
11 CHEDD-G
13 MULOCK
2 ALGON-2
6 ALGON-6
14 CH-G
9 ELPHIN-G
3 ALGON-3
15 CH-M
4 ALGON-4
5 ALGON-5
8 UK
10 ELPHIN-S
18 DELORO-3
12 CHEDD-M
7 ALGON-7

(bottom)

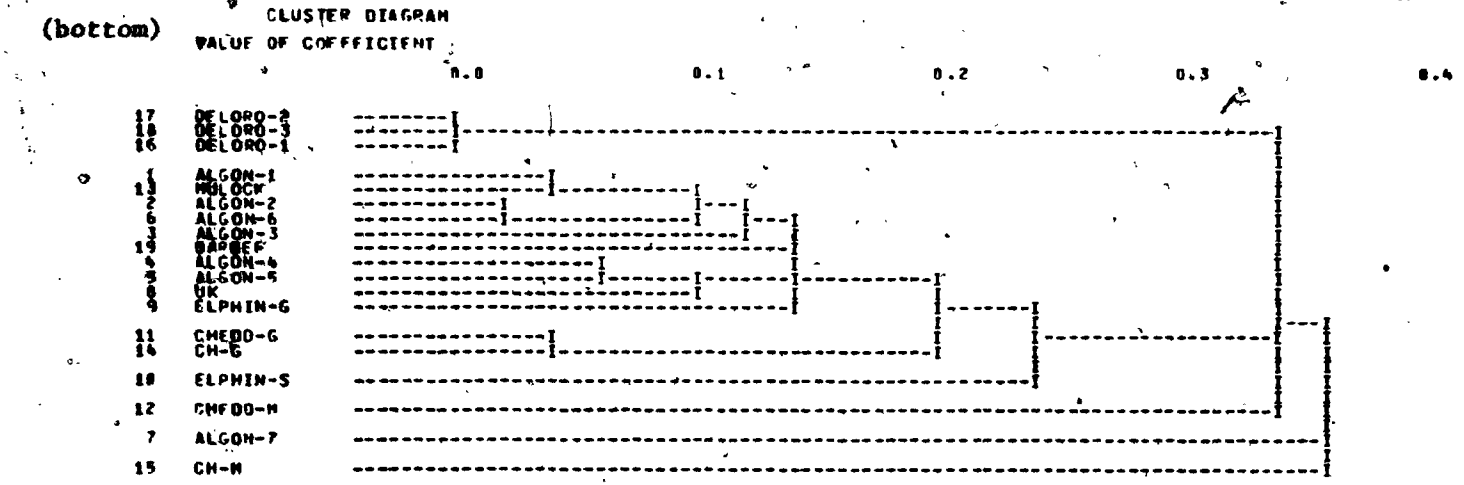
CLUSTER DIAGRAM
VALUE OF COEFFICIENT
0.0
0.1
0.2
0.3
0.4
17 DELORO-2
18 DELORO-3
16 DELORO-1
1 ALGON-1
13 MULOCK
2 ALGON-2
6 ALGON-6
3 ALGON-3
19 BARBER
4 ALGON-4
5 ALGON-5
8 UK
9 ELPHIN-G
11 CHEDD-G
14 CH-G
10 ELPHIN-S
12 CHEDD-M
7 ALGON-7
15 CH-M

1. Algonquin monzonite-syenite, Coe Hill quartz-poor phase, Algonquin syeno-monzo-diorite and tonalite and Union Lake Pluton;

2. Elphin syenitic phase and Deloro calc-syenite suite;

3. Cheddar monzonite.

2.1.2 Trace-elements -

Twelve trace-elements (Nb, Zr, Y, Sr, Rb, Pb, Zn, Ni, Cr, Ba, V and Ga) were used to compute the cluster dendrogram (Fig. 3-2-2). Five groups are classified at the similarity level of 0.3, which separates the Deloro Pluton, Cheddar monzonite, quartz-poor phase of Coe Hill Granite and Algonquin diorite - gabbro from the remaining samples. Members of this latter supergroup were further separated into seven groups at a similarity coefficient of 0.1, which corresponds to :

1. Algonquin granite, granodiorite and trondhjemite and Mulock Batholith;

2. Algonquin monzonite-syenite;

3. Barber's Lake Granite;

4. Algonquin tonalite and syeno-monzo-diorite and Union Lake Pluton;

5. Elphin granitic phase;

6. Cheddar Granite and Coe Hill Granite;

7. Elphin syenitic phase.

2.1.3 Element-ratios -

Element-ratios used to calculate the cluster dendrogram (Fig. 3-2-3) are Na_2O/K_2O, K/Rb, Sr/Ca, Ga/Al. Rb/Sr, Zr/Nb, Zr/Y, Nb/Y, oxidation index (O.I.) and agpaitic index (A.I.). It forms five distinct groups at similarity level of 0.25 corresponding to :

1. Algonquin diorite-gabbro, tonalite, trondhjemite and syeno-monzo-diorite and Union Lake Pluton;

2. Algonquin granite, granodiorite and monzonite-syenite, Mulock Batholith, Coe Hill Granite and Elphin syenitic phase;

3. Deloro Pluton and Cheddar Granite;

(top)

Figure 3-2-3. Q-mode cluster dendrogram based on 10 element-ratios.

(bottom)

Figure 3-2-4. Q-mode cluster dendrogram based on major-, trace-elements element-ratios.

Abbreviations :

Algon-1 - Algonquin granite
Algon-2 - Algonquin granodiorite
Algon-3 - Algonquin monzonite-syenite
Algon-4 - Algonquin syeno-monzo-diorite
Algon-5 - Algonquin tonalite
Algon-6 - Algonquin trondhjemite
Algon-7 - Algonquin diorite-gabbro
UK - Union Lake quartz diorite
Elphin-G - Granite of Elphin Complex
Elphin-S - Syenite of Elphin Complex
Chedd-G - Cheddar granite
Chedd-M - Cheddar monzonite
CH-G - Coe Hill granite
CH-M - quartz-poor phase of Coe Hill Granite
Mulock - Mulock Batholith
Barber - Barber's Lake Granite
Deloro-1 - Riebeckite-bearing granite
Deloro-2 - Granophyric granite
Deloro-3 - Calc-syenite

(top)

CLUSTER DIAGRAM

VALUE OF COEFFICIENT

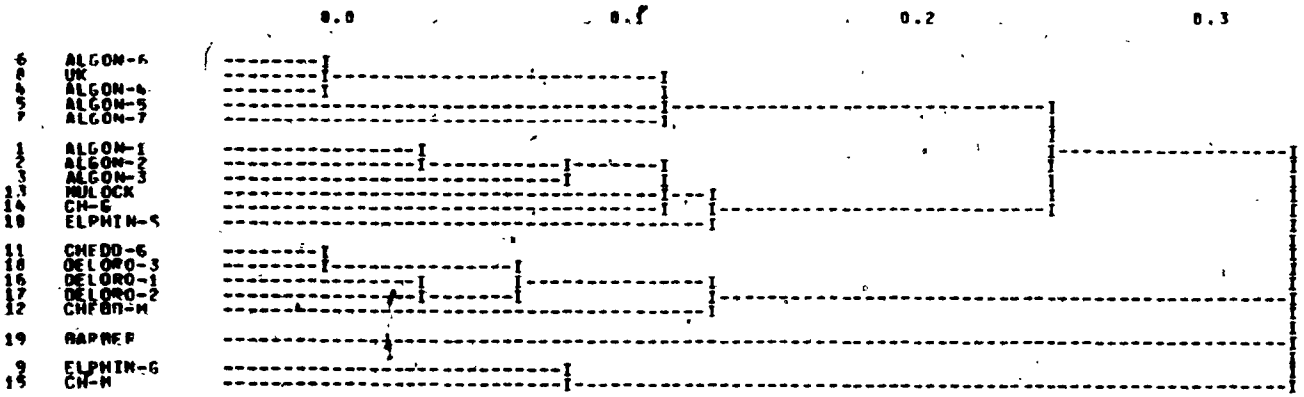

(bottom)

CLUSTER DIAGRAM

VALUE OF COEFFICIENT

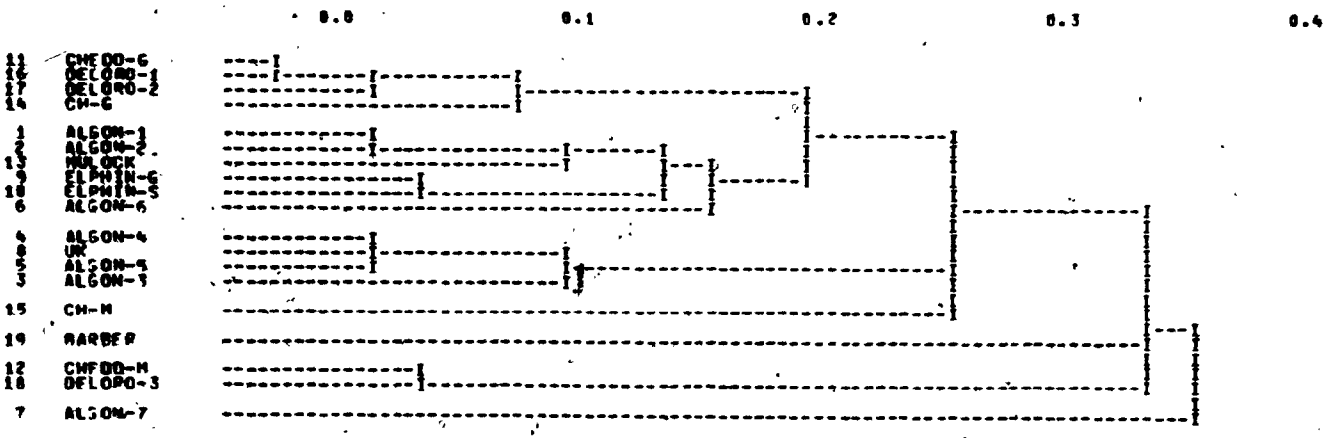

4. Barber's Lake Granite;

5. Elphin granitic phase and quartz-poor phase of Coe Hill Granite.

2.1.4 Major-, Trace-elements And Their Ratios -

The Q-mode cluster dendrogram computed by using 33 variables of the combination of major-, trace-elements and their ratios is given Figure 3-2-4. It reveals four groups at the similarity coefficient of 0.3, that is, (1) Barber's Lake Granite, (2) Cheddar monzonite, (3) Deloro syenite-suite and Algonquin diorite-gabbro and (4) the supergroup of the rest samples. At approximately 0.1 coefficient of similarity, six subgroups are further identified in the supergroup; they are :

1. Deloro Pluton, Cheddar Granite and Coe Hill Granite;

2. Algonquin granite and granodiorite and Mulock Batholith;

3. Elphin Complex;

4. Algonquin trondhjemite;

5. Algonquin monzonite - syenite, syeno - monzo - diorite and tonalite and Union Lake Pluton;

6. quartz-poor phase of Coe Hill Granite.

Although the number of groups and their ordering differ from one dendrogram to another, it is clear that the Q-mode analyses do provide some useful information for grouping of Grenville granitoids in terms of their chemical compositions. Notably, the peralkaline and granophyric granites of the Deloro Pluton and Barber's Lake Granite (peraluminous) form two consistent groups with respect to their trace-elements, element-ratios and overall comparisons. In addition, composition of the Mulock Batholith is closely associated with granite and granodiorite of Algonquin Batholith, while Union Lake Pluton is statistically similar to those of Algonquin tonalite and syeno-monzo-diorite. However, there is no consistent grouping for Elphin Complex, Coe Hill Granite and Cheddar Granite.

2.2 Geochemical Discriminants

In order to understand the mutual relations among variables (i.e. inter-element), factor or R-mode analysis was employed to group variables into a few

independent principal associations (or factors). Varimax rotated factor matrix gave loadings of each variable, which represent the calculated strength (or regression coefficient) for a particular variable in that factor. Five principal factors and factor loadings for 33 variables in the sampled granitoids are given in Figure 3-2-5; low factor loadings (< 0.60) have been omitted for the sake of clarity. Correlation of pair factors can be graphically displayed by two dimensional plots; the direction of a variable in relation to the axes indicates either a positive or a negative loading. Pair correlation of factor 1 and 2 is shown in Figure 3-2-6. Variables 25, 26, 29, 30, 31 are close to the origin, indicating small loadings on both factors, while the cluster of variables 12, 13, 14, 17, 27 has high loadings on factor 2 but low on factor 1. Similarly, variables 3, 5, 7, 8, 11, 15, 20, 22 load high on factor 1; in addition, variable 1 is located at the opposite end of the axis indicating a high negative loading on factor 1. Therefore, as a whole, the graph (Fig. 3-2-6) separates the variables of Nb, Zr, Y, Pb, Ga/Al from Al_2O_3, FeO, MgO, CaO, P_2O_5, Sr, Cr, V and/or SiO_2; in other words, there are discrimination relationships among the above two element-groups.

In addition, factor 1, which accounts for 43% variance of the data, can be interpreted as a " mafic minerals - plagioclase fractionation" factor, because it

Factor Loadings	Factor 1	Factor 2	Factor 3	Factor 4	Factor 5
1.0 (POSITIVE)	Cr				
0.9	MgO	Zr		Zr/Y	
	CaO	Nb	Zn		K_2O
	P_2O_5	Y			
0.8	Ni	Ga			
	V	Ga/Al	MnO	Zr/Nb	
	TiO_2	Pb			
0.7	FeO				
	Al_2O_3				
0.6	Sr	A.I.		Ba	
0.6 (NEGATIVE)			O.I.		
0.7			Sr/Ca		
0.8					Na/K
	SiO_2				
0.9					
1.0					
% Variance	43.1	23.3	14.3	7.3	5.8
Cumulative % Variance	43.1	66.4	80.7	88.0	93.8

A. I. = agpaitic indices.

O. I. = oxidation indices.

Figure 3-2-5, Five principal factors and factor loadings for 33 variables of the sampled Grenville granitoids.

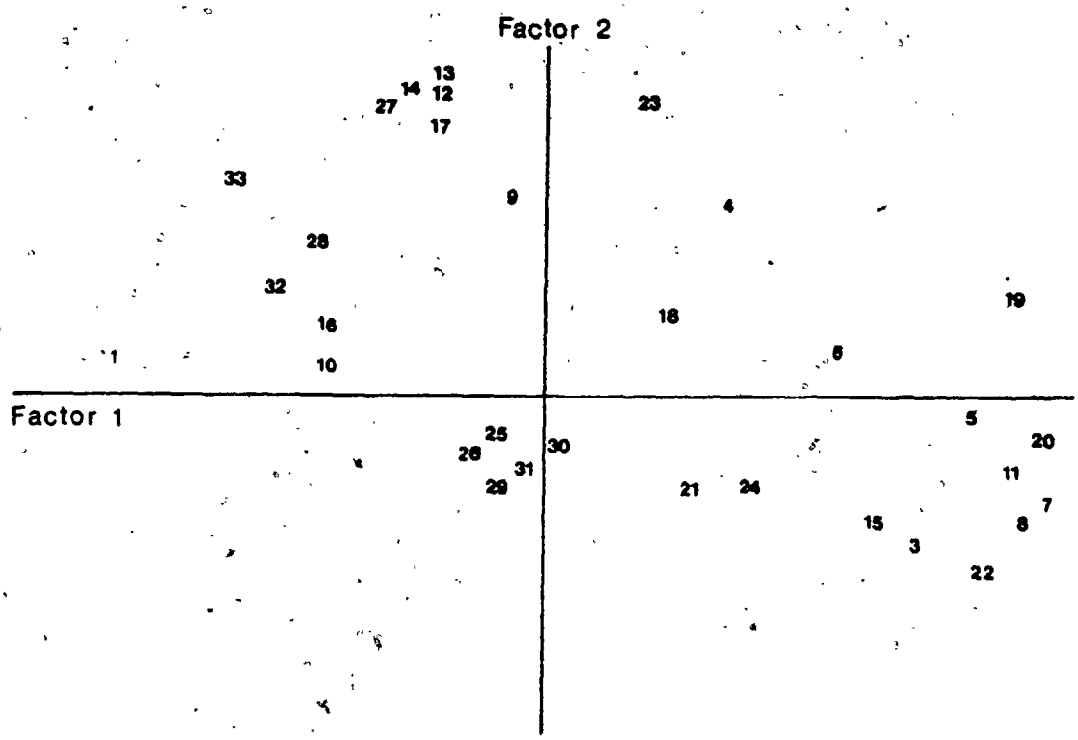

Figure 3-2-6. Graphical presentation of the Varimax rotated factors - pair correlation of factor 1 (horizontal) and factor 2 (vertical).

1. SiO_2	2. TiO_2	3. Al_2O_3	4. Fe_2O_3	5. FeO
6. MnO	7. MgO	8. CaO	9. Na_2O	10. K_2O
11. P_2O_5	12. Nb	13. Zr	14. Y	15. Sr
16. Rb	17. Pb	18. Zn	19. Ni	20. Cr
21. Ba	22. V	23. Ga	24. Na/K	25. K/Rb
26. Sr/Ca	27. Ga/Al	28. Rb/Sr	29. Zr/Nb	30. Zr/Y
31. Nb/Y	32. O.I.	33. A.I.		

is heavily loaded with respect to CaO, MgO, FeO, Al_2O_3 and compatible trace-elements (eg. Cr, Ni). Factor 2 accounts for 23% variance and is interpreted as a "accessory phases fractionation" factor, due to high loadings of the HFS-elements (eg. Nb, Zr, Y).

Selected discrimination diagrams for sampled granitoids are given in Figure 3-2-7. In general, there is a reasonable separation of these granitoids into six groups on the basis of discrimination diagrams as well as the Q-mode cluster dendrograms; they are :

1. Barber's Lake Granite, Coe Hill Granite, Mulock Batholith, Elphin granitic phase and Algonquin trondhjemite;

2. Elphin syenitic phase, quartz-poor phase of Coe Hill Granite and Algonquin syenite-monzonite;

3. Deloro Pluton and Cheddar Granite;

4. calc-syenite suite of Deloro Pluton and Cheddar monzonite;

5. Union Lake Pluton and Algonquin tonalite;

6. dioritic-gabbroic rocks of Algonquin Batholith, hybrid phase of Elphin Complex and mafic cumulates of Barber's Lake Granite.

Figure 3-2-7. Selected discrimination diagrams for sampled granitoids.

(A) Al_2O_3 vs. SiO_2

(B) Na_2O+K_2O vs. SiO_2

(C) Nb vs. SiO_2

(D) Zr vs. SiO_2

(E) Ga vs. Al_2O_3

(F) Zr vs. Al_2O_3

(G) Nb vs. Al_2O_3

Field 1 = Barber's Lake Granite, Coe Hill Granite, Mulock Batholith, Elphin Granite, Algonquin granite and trondhjemite.

Field 2 = Elphin syenite, Coe Hill quartz-poor phase, Algonquin syenite-monzonite.

Field 3 = Deloro Pluton and Cheddar Granite.

Field 4 = Deloro calc-syenite and Cheddar monzonite.

Field 5 = Union Lake Pluton and Algonquin tonalite.

Field 6 = Algonquin diorite-gabbro and mafic cumulates of Barber's Lake Granite.

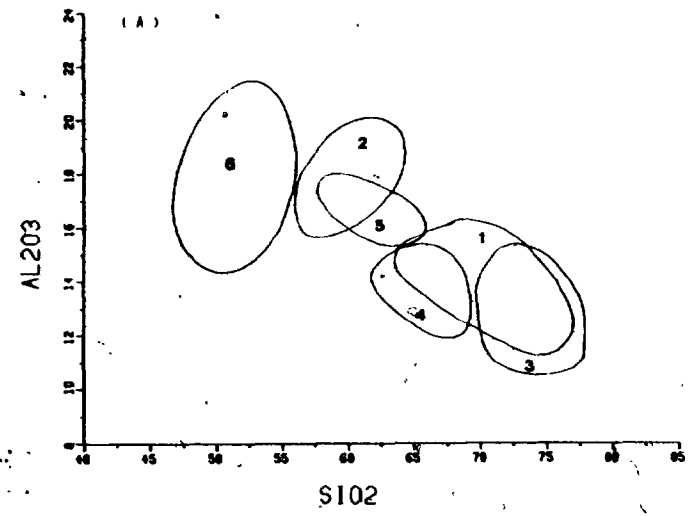
(A)
AL203
SIO2
1
2
3
4
5
6

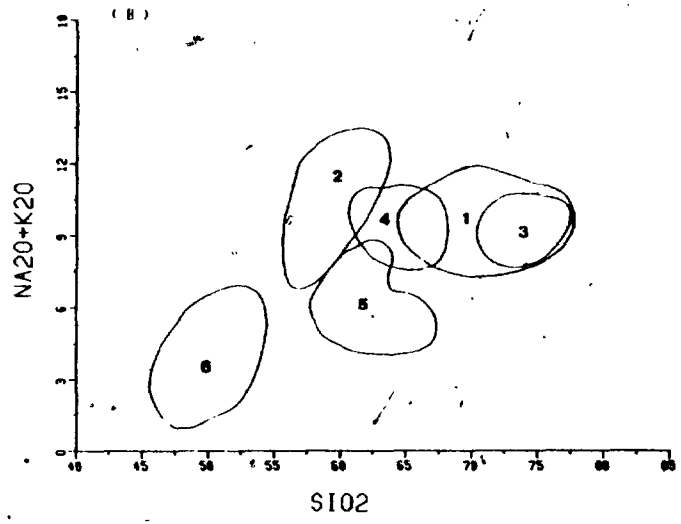
(B)
NA20+K20
SIO2
1
2
3
4
5
6

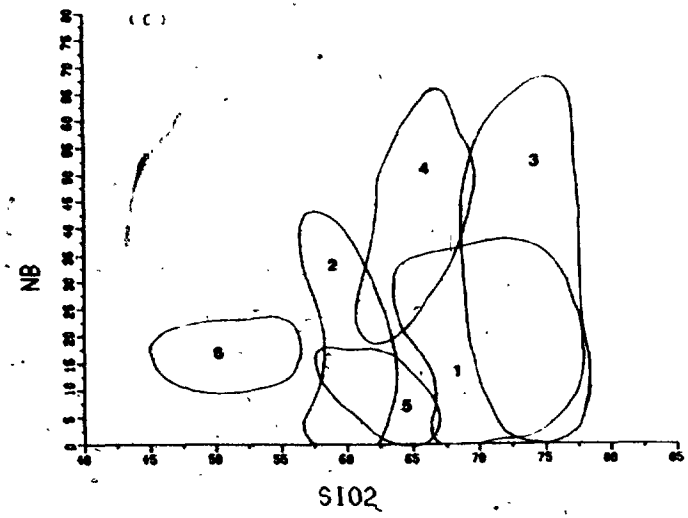
(C)
NB
SIO2
1
2
3
4
5
6

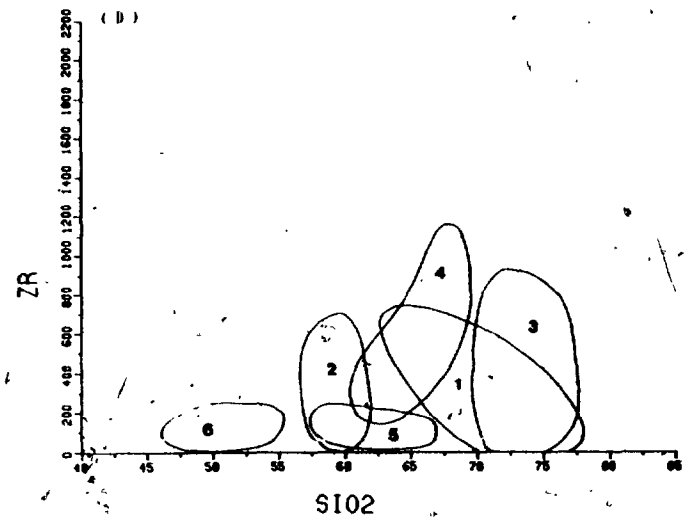
(D)
ZR
SIO2
1
2
3
4
5
6

(Figure 3-2-7. Cont'd)

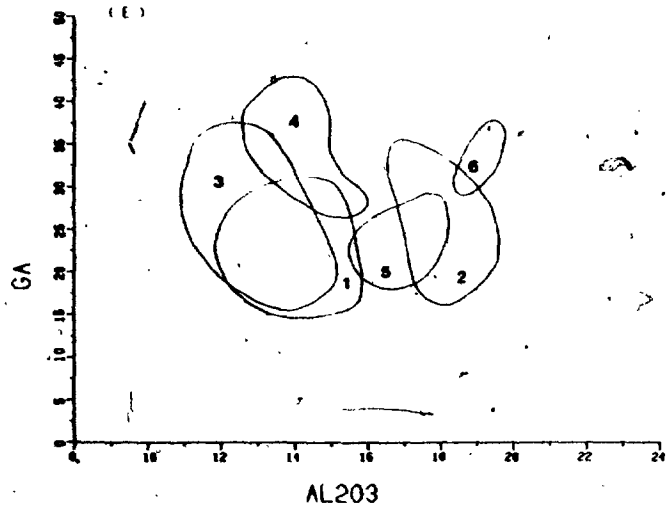

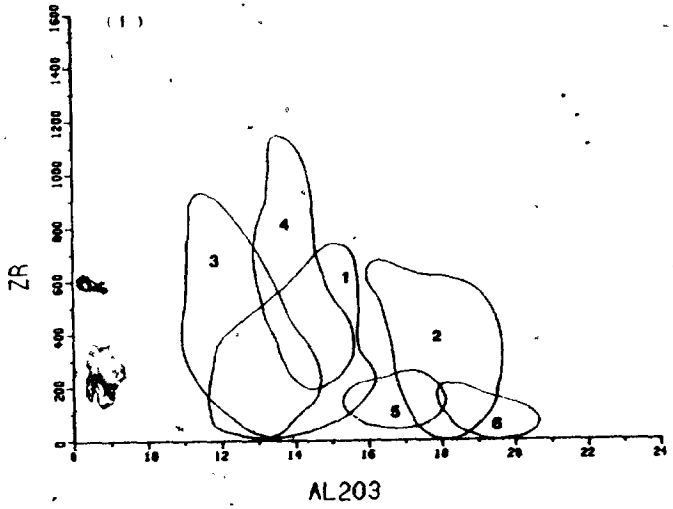

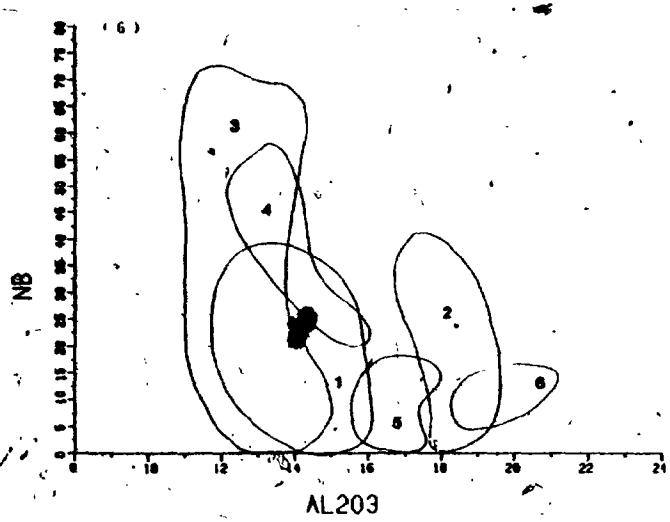

Deloro Pluton and Cheddar Granite with peralkaline and alkaline compositions, respectively, are higher in SiO_2 and lower in Al_2O_3 compared to the majority of studied granitic suites; they are characterized by the anomalous enrichment of HFS-elements (Fig. 3-2-7, D-G). Similar to their granitic counterparts, the calc-syenite suite of Deloro and monzonitic rocks of Cheddar deviate from the common syenitic-monzonitic trend and contain intermediate values of Na_2O+K_2O between the majority of granitic and syenitic rocks (Fig. 3-2-7B). Union Lake quartz diorite and Algonquin tonalite compositionally overlap the syenites but have lower total alkalis (Fig. 3-2-7B). For clarity, syeno-monzo-dioritic rocks of the Algonquin Batholith are not shown in discrimination diagrams; however, they are scattered in the syenite field and/or between the syenite and diorite-gabbro fields. A summary of geochemical compositions for the six groups is given in Table 3-2-1.

As the result of statistical analyses, in spite of age differences, the six-fold classification of sampled Grenville granitoids corresponds to their rock-types in general. Except for Deloro peralkaline granite and alkalic Cheddar Granite, the consistent chemical correlations within each group may be interpreted to have originated from a homogeneous source through a similar evolution path.

Table 3-2-1. Summary of geochemical characteristics for six-fold classification of sampled granitoids

Parameters	Group-1	Group-2	Group-3	Group-4	Group-5	Group-6
SiO_2	77 - 61	68 - 46	78 - 67	72 - 59	66 - 57	66 - 45
Al_2O_3	18 - 11	20 - 12	16 - 11	16 - 11	20 - 15	21 - 13
FeO	3.48 - 0.15	7.79 - 0.95	4.02 - 0.22	5.54 - 1.50	6.21 - 1.99	19.21 - 0.72
MgO	1.87 - 0.0	4.66 - 0.14	0.86 - 0.0	1.16 - 0.27	3.82 - 1.22	12.94 - 0.53
CaO	3.63 - 0.02	7.57 - 1.13	1.77 - 0.0	2.63 - 0.0[illegible]	6.18 - 4.14	9.81 - [illegible].79
Cr	[illegible] - 3.1	64.6 - 4.0	10.6 - 2.7	10.4 - 5.5	40.3 - 5.8	155.1 - 5.6
Ni	9.6 - 1.2	37.1 - 1.6	35.4 - 1.1	14.6 - 1.9	21.0 - 1.8	59.7 - 3.6
V	65.7 - 0.3	268.7 - 11.4	26.5 - 0.0	7.5 - 0.0	133.2 - 18.4	295.9 - 27.9
Nb	52.4 - 0.6	41.5 - 5.1	75.0 - 15.0	65.4 - 19.9	31.1 - 2.8	44.6 - 3.9
Zr	689.0 - 41.2	651.9 - 150.0	1940 - 175	1144 - 209	240.9 - 78.0	535.3 - 44.5
Y	102.7 - 6.3	58.8 - 11.6	179.3 - 42.9	126.8 - 46.6	25.2 - 9.4	41.4 - 13.3
Ga	30.3 - 14.6	36.7 - 21.1	37.1 - 11.8	42.8 - 5.3	36.8 - 19.1	35.2 - 20.5
Pb	53.6 - 5.1	59.2 - 16.5	70.0 - 16.6	43.8 - 17.0	33.2 - 8.3	27.6 - 3.4
Zn	202.2 - 9.8	209.3 - 33.7	274.0 - 11.5	181.3 - 27.8	86.6 - 36.5	141.0 - 15.0
Ga/Al	4.23 - 1.96	5.48 - 2.09	5.74 - 1.97	5.65 - 0.85	3.91 - 2.03	4.09 - 2.08
Zr/Y	26.30 - 3.33	30.8 - 8.95	9.80 - 1.89	10.12 - 1.92	25.63 - 4.73	23.38 - 2.34
A.I.	1.05 - 0.51	0.86 - 0.51	1.30 - 0.86	1.06 - 0.86	0.76 - 0.41	0.99 - 0.13
O.I.	92.0 - 23.0	77.5 - 19.8	86.1 - 38.2	86.1 - 40.8	57.1 - 17.3	57.5 - 21.2

Group-1: Barber's Lake Granite, Coe Hill Granite, Mulock Batholith, granitic phase of Elphin and granite-trondhjemite of Algonquin;
Group-2: syenite phase of Elphin, quartz-poor phase of Coe Hill and syenite-monzonite of Algonquin;
Group-3: Deloro Pluton and Cheddar Granite;
Group-4: calc-syenite of Deloro and Cheddar monzonite;
Group-5: Union Lake Pluton and tonalite of Algonquin;
Group-6: diorite-gabbro of Algonquin, hybrid phase of Elphin and mafic cumulates of Barber's Lake Granite.

Furthermore, whole-rock oxygen isotope ratios of sampled granitoids agree with a two-fold classification of Shieh and Schwarz (1974), in that (1) the high $\delta^{18}O$ granites with $\delta^{18}O > 8.4$ predominate in the Central Metasedimentary Belt, while (2) the low $\delta^{18}O$ granites with $\delta^{18}O < 8.4$ are a characteristic feature of the Ontario Gneiss Segment. Comparison of whole-rock $\delta^{18}O$ of the Grenville granitoids from Ontario and other common igneous rocks is summarized in Figure 3-2-8. The whole-rock $\delta^{18}O$ values of Barber's Lake Granite, Coe Hill Granite, Elphin Complex and Deloro Pluton are consistent with Group-II granites of Shieh (1980), ranging from 9.0 to 12.5. Union Lake Pluton with trondhjemitic affinity is in Group-I granites (7.0 to 9.5) composed of Elzevir, Weslemkoom and Norhtbrook batholiths of the biotite diorite series (Lumbers, 1967). Additionally, the oxygen isotope ratios of Deloro peralkaline granite are considerably higher than those of common hypersolvus granites of Taylor (1968). Shieh and Schwarcz (1974) proposed that extensive oxygen isotopic homogenization and exchange with a deep-seated low ^{18}O reservoir was for low $\delta^{18}O$ granites, while assimilation and exchange with high ^{18}O metasediments was for high $\delta^{18}O$ granites.

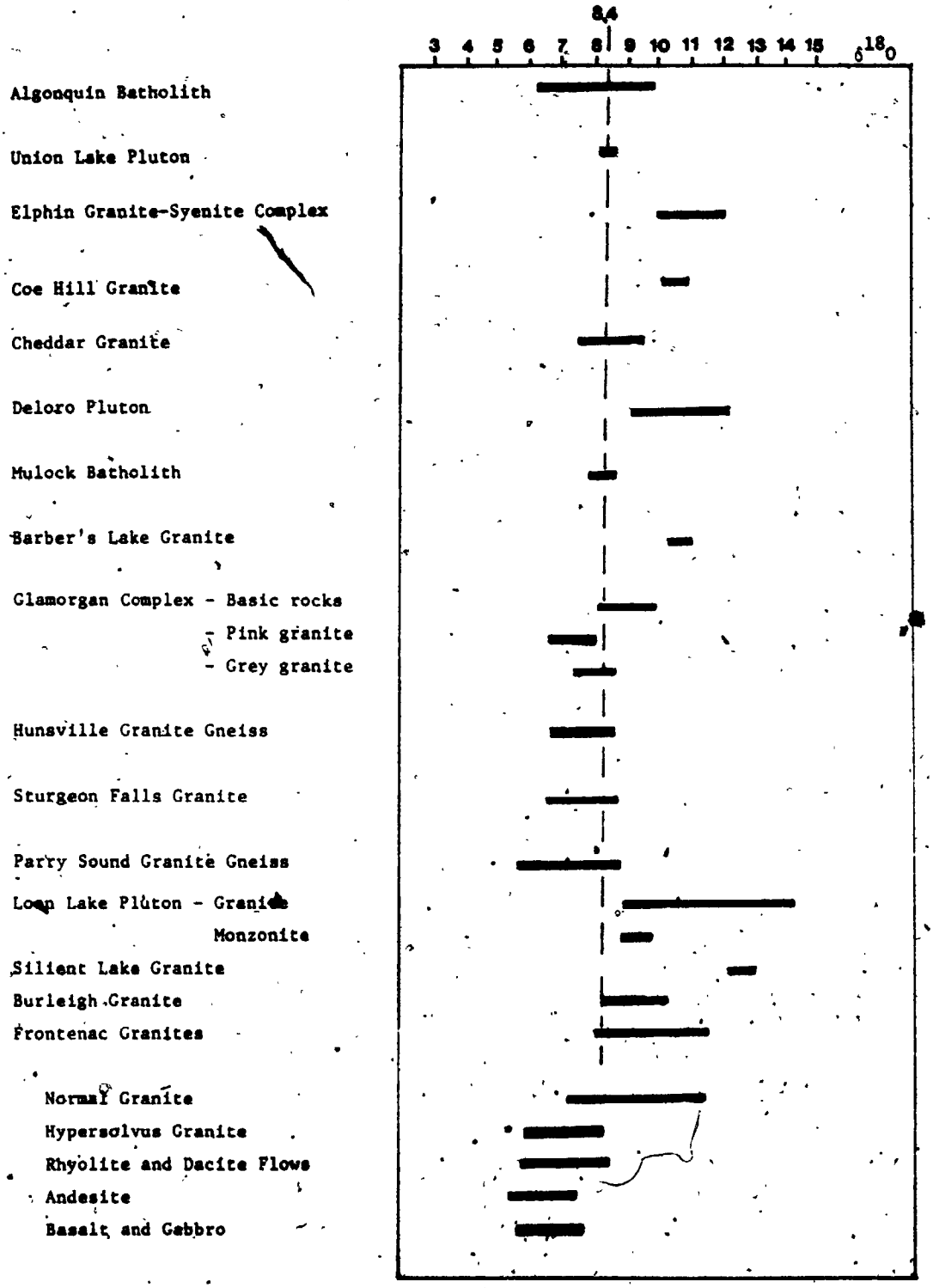

Figure 3-2-8. Comparison of whole-rock $\delta^{18}O$ of the Grenville granitoids of Ontario and common igneous rocks.
(Sources : Shieh and Schwarcz, 1974; Shieh, 1978; Shieh, 1980; Taylor, 1968; and this study)

3.0 COMPARISON OF MINERAL CHEMISTRY FROM SAMPLED GRANITOIDS

Except for the Deloro Pluton, biotite, amphibole and two feldspars from other granites were analyzed by electron microprobe. Whenever possile, biotite separates were obtained for wet chemical determination of ferrous iron concentration.

3.1 Biotite

Biotite data from sampled granitoids are summarized in Figure 3-3-1, 3-3-2 and 3-3-3. In Fe^t/Fe^t+Mg vs. Al^{iv}/Si plot (Fig. 3-3-1), except biotite of xenolith from Cheddar Granite falls within the upper edage of phlogopite field (Deer et al., 1966), all the others are biotite. In terms of octahedral-site occupancy of Mg - R^{3+} ($Al^{iv}+Fe^{3+}+Ti^{4+}$) - Fe^{2+} ($+Mn^{2+}$), the majority of the biotites are in the Mg- and Fe^{2+}-biotite fields of Foster (1960; See Fig. 3-3-2), whereas biotites in TN4G-1a, TS-22G and 648-2G from the Cheddar Granite are in the upper siderophyllite field.

In the ternary Fe^{3+}-Fe^{2+}-Mg diagram (Fig. 3-3-3), which relates the biotite compositions of sampled granitoids to the common oxygen buffers (quartz - fayalite - magnetite, Ni-NiO and Fe_3O_4-Fe_2O_3), biotites from Coe Hill Granite, Barber's Lake Granite and Algonquin granite are equilibrated with buffer Ni-NiO, whereas biotite from Cheddar Granite is similar to the

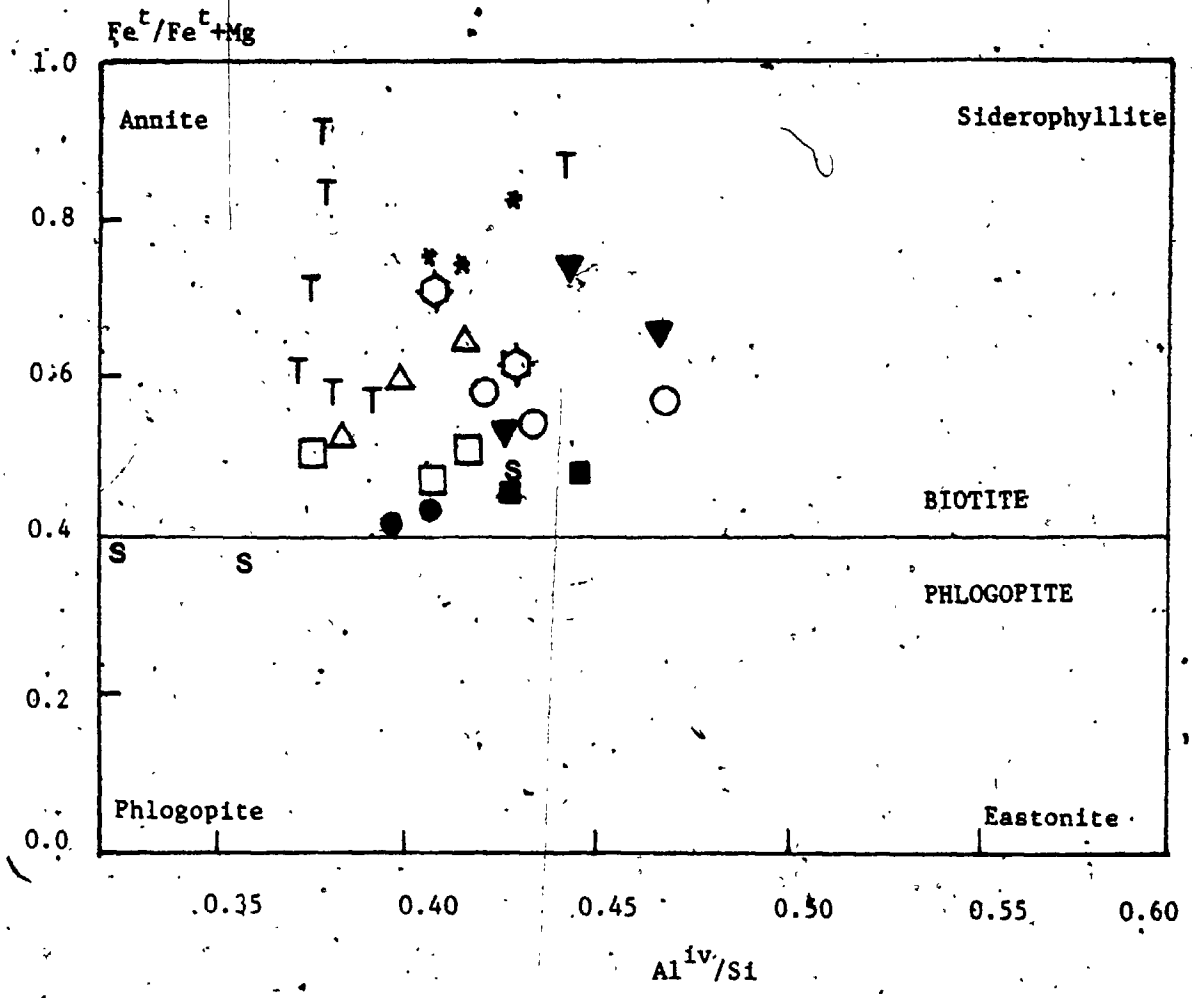

Figure 3-3-1. Fe^t/Fe^t+Mg vs. Al^{iv}/Si plot for phlogopite-biotite compositional fields (from Deer et al., 1966).

- ● Union Lake Pluton
- * Mulock Batholith
- ✡ Barber's Lake Granite
- △ Coe Hill Granite
- □ Elphin Complex
- T Cheddar Granite
- S Cheddar Xenoliths
- ○ Algonquin granite
- ▼ Algonquin monzonite-syenite
- ■ Algonquin tonalite

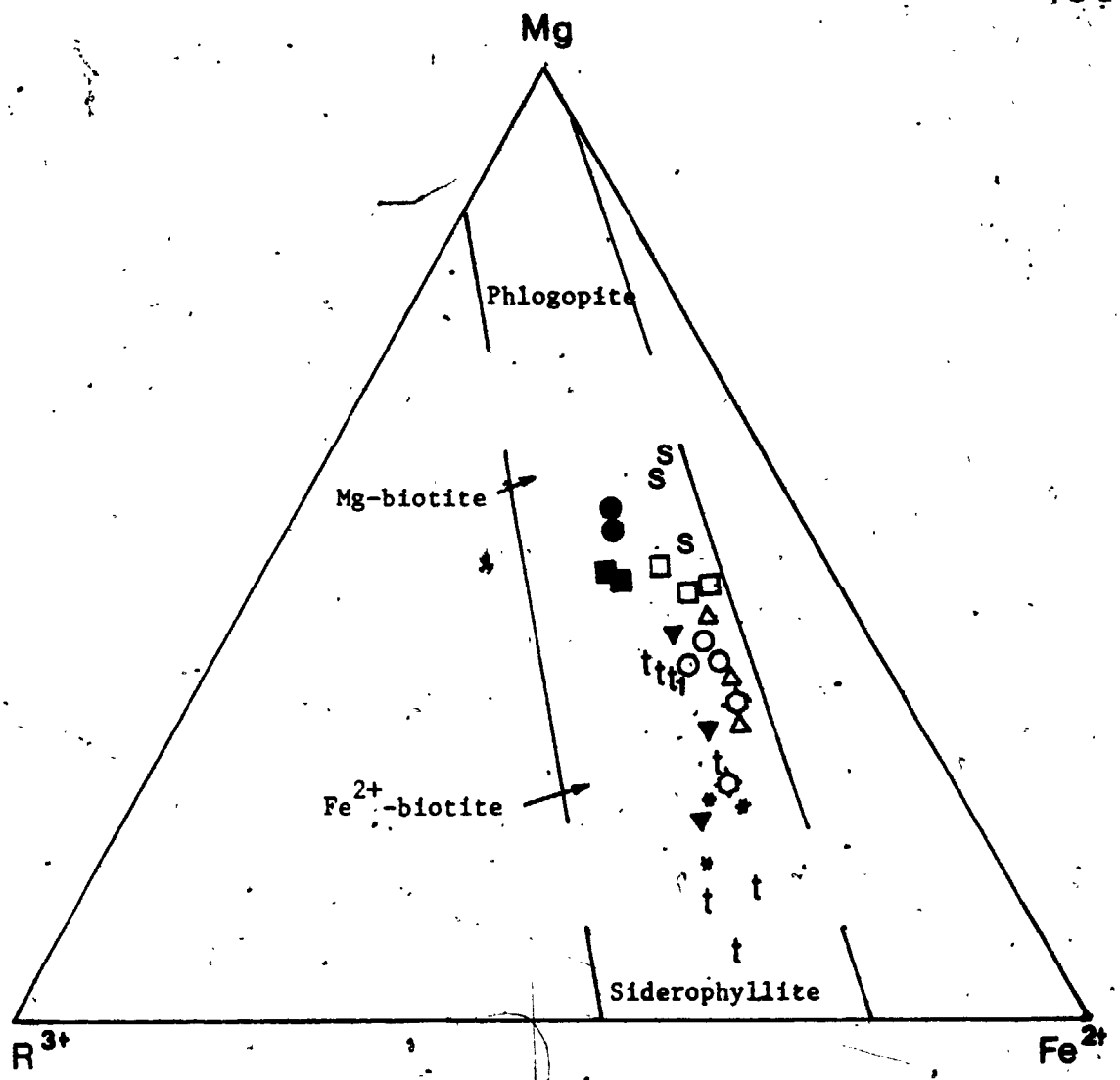

Figure 3-3-2. The $Mg-Fe^{2+}-R^{3+}$ relation in trioctahedral micas of the sampled granitoids (after Foster, 1960).

$$R^{3+} = Al^{vi} + Fe^{3+} + Ti^{4+}$$

- ○ Union Lake Pluton
- * Mulock Batholith
- ⬡ Barber's Lake Granite
- △ Coe Hill Granite
- □ Elphin Complex
- t Cheddar Granite
- t_1 Cheddar monzonite
- S Cheddar Xenoliths
- ○ Algonquin granite
- ▼ Algonquin monzonite-syenite
- ■ Algonquin tonalite

Figure 3-3-3. Fe^{3+}-Fe^{2+}-Mg diagram of biotites from sampled granitoids. Dashed-lines indicate the common oxygen buffers : 1. Fe_3O_4 - Fe_2O_3 2. Ni - NiO 3. Fe_2SiO_4 - SiO_2 - Fe_3O_4

Solid-lines show chemical variation trends of sampled granitoids.

◄- - - - Chemical variation trend of Sierra Nevada Batholith (Dodge et al., 1969).

Compositional field of Japanese Batholiths.

● Union Lake Pluton

★ Mulock Batholith

Barber's Lake Granite

△ Coe Hill Granite

□ Elphin Complex

t Cheddar Granite

t_1 Cheddar Monzonite

○ Algonquin granite

▼ Algonquin monzonite-syenite

■ Algonquin tonalite

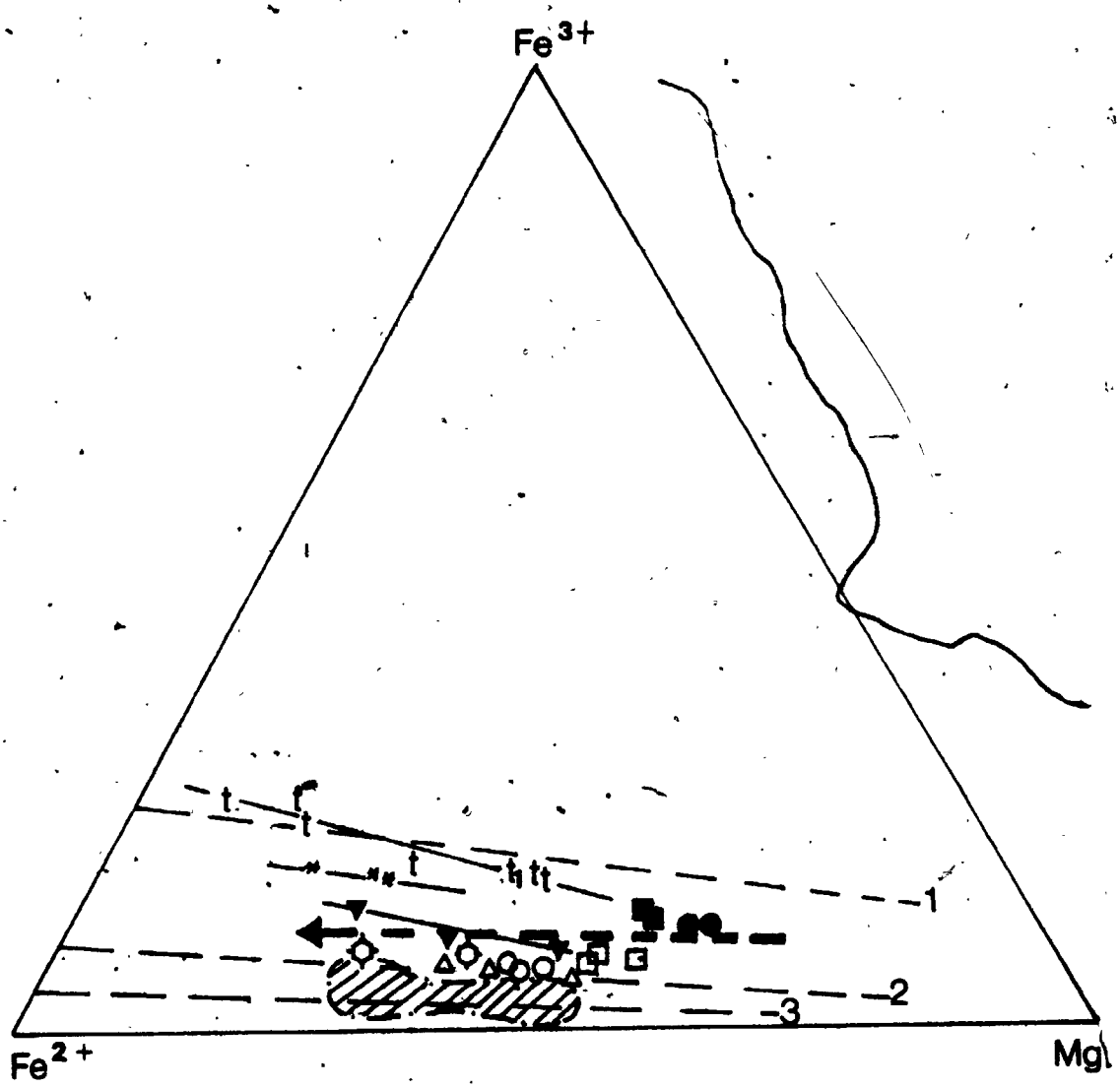
Fe3+
Fe2+
Mg
1
2
3

Fe_3O_4-Fe_2O_3 buffer. In comparison, biotites from Cheddar Granite, Mulock Batholith, Union Lake Pluton and Algonquin tonalite-diorite are more oxidized than those from both the Sierra Nevada Batholith (Dodge et al., 1969) and the Japanese Batholiths (Czamanske et al., 1981). Biotites from Elphin Complex, Coe Hill Granite, Barber's Lake Granite and Algonquin granite are relatively more reduced than those of the Sierra Nevada Batholith but more oxidized than those of the Japanese Batholiths.

Furthermore, in Al_2O_3-MgO-FeO (as total iron) ternary diagram (Fig. 3-3-4), compositional variation of biotites from sampled granitoids shows a well-defined trend with progressively decreasing MgO content from Union Lake quartz diorite and Algonquin tonalite towards Mulock adamellite and Cheddar alkaline granite. In comparison with compositional trends of the the White Mountain Series (Chapman and Williams, 1935) and Caledonian plutonic rocks (Nockolds and Mitchell, 1948), the trend of Grenville granitoids is somewhat a combination of the above trends; however, the variation of Cheddar biotites is consistent with White Mountain Alkaline Series. Notably, the deviation of biotite from Barber's Lake Granite characterized by relatively low silica and high alumina is mainly due to crystallization of primary muscovite (Nockolds and Mitchell, 1948).

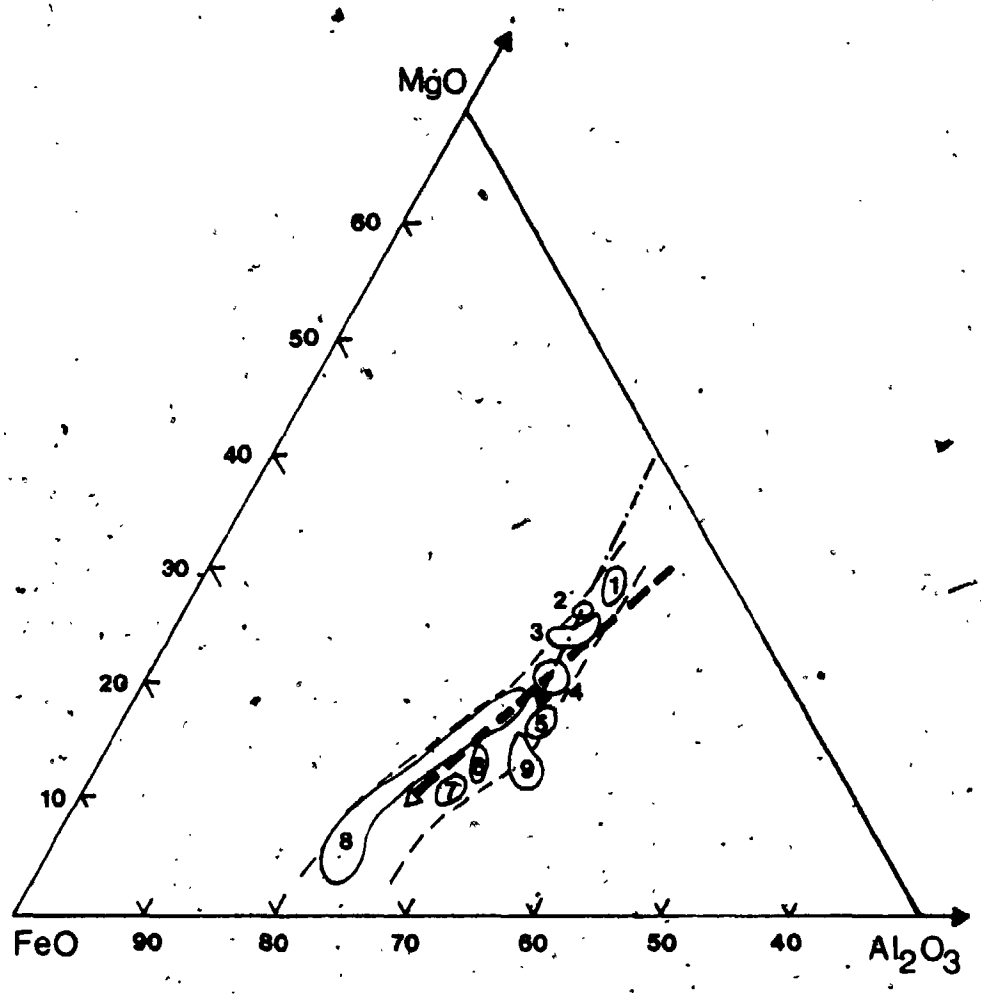

Figure 3-3-4. Portion of Al_2O_3-FeO (total iron)-MgO plot showing variation in compositions of biotites from sampled granitoids.

◁▬▬ Compostional trend of White Mountain Series (Chapman and Williams, 1935).

◀-·-· Compositional trend of Caledonian plutonic rocks (Nockolds and Mitchell, 1948).

---- Compositonal trend of sampled Grenville granitoids (this study).

1. Union Lake Pluton
2. Tonalite of Algonquin Batholith
3. Elphin Complex
4. Algonquin granite
5. Coe Hill Granite
6. Algonquin monzonite-syenite
7. Mulock Batholith
8. Cheddar Granite
9. Barber's Lake Granite

3.2 Amphibole

Modally, except for mafic varieties of sampled granitoids, amphibole is subordinated to biotite and varies in amount from one pluton to another; compositions of amphiboles from the Algonquin Batholith, Union Lake Pluton, Cheddar Granite and Mulock Batholith were chemically analyzed. In the terminology of Leake (1968), all of the studied amphiboles are members of the calcic amphibole group; however, soda amphibole (riebeckite) analyzed by Kuehnbaum (1973) is the major mafic mineral phase of the Deloro peralkaline granite. Chemical variations of analyzed amphiboles are summarized in Figure 3-3-5 and 3-3-6.

Compositions of the studied amphiboles are intermediate between ideal hornblendic amphibole and pargasite - ferrohastingsite (Fig. 3-3-5); however, the Cheddar amphibole is close to that of edenite - ferroedenite end-member, while amphibole from Mulock Batholith is in the range of pargasite - ferropargasite series. Moreover, the main differences among amphiboles can be further explained in terms of ternary variation of Al_2O_3-MgO-FeO (as total iron) (Fig. 3-3-6). For the Algonquin Batholith, with one exception, composition of amphibole form a consistent trend with declining MgO. Similarly, amphiboles from Cheddar Granite show progressively decreasing MgO and Al_2O_3 with increasing FeO, however amphiboles from xenoliths with higher MgO

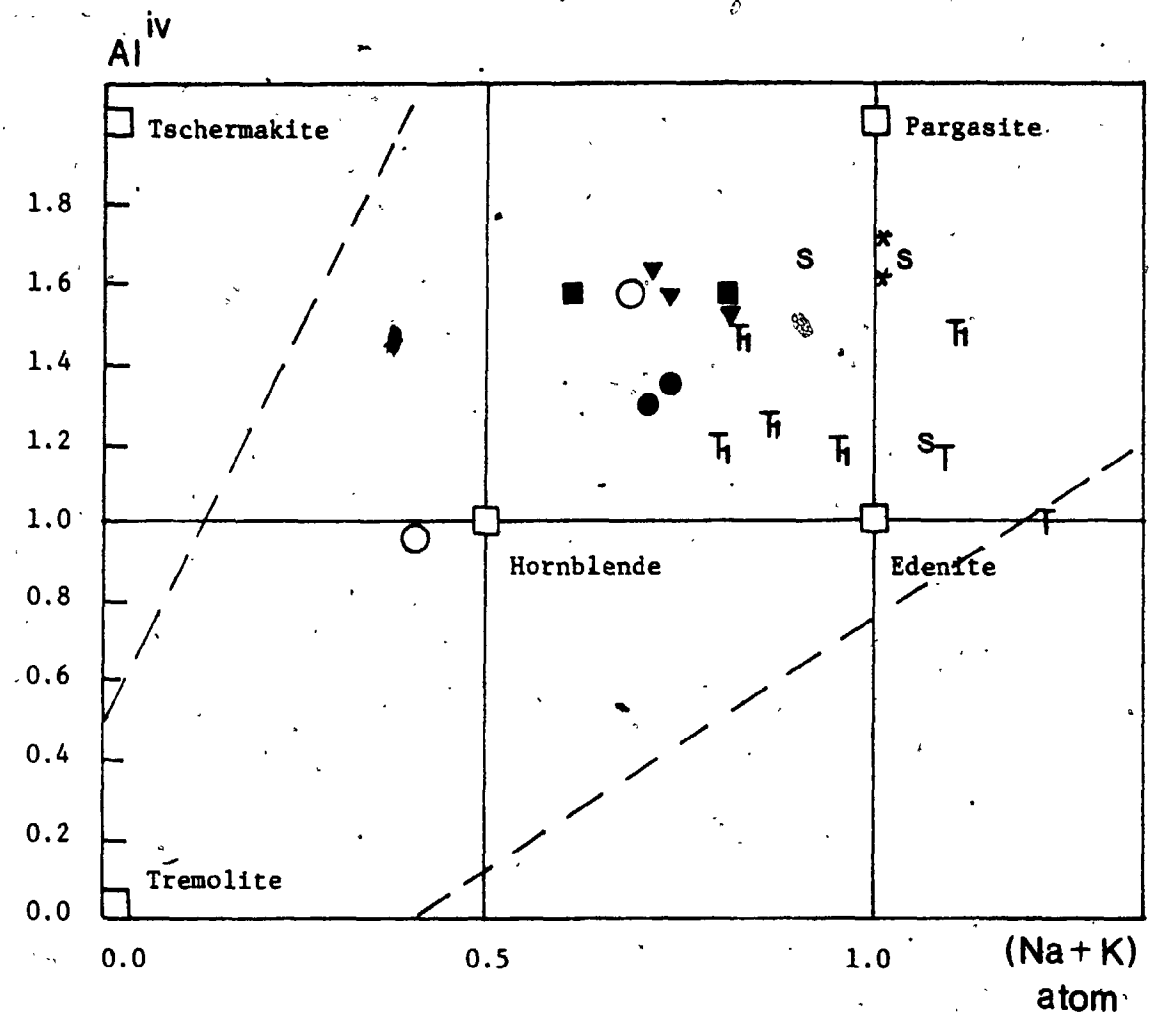

Figure 3-3-5. Chemical variation of calcic amphiboles from sampled granitoids expressed as (Na+K) and (Al^{iv}) atoms per formulae unit (from Deer et al., 1966).

● Union Lake Pluton
* Mulock Batholith
T Cheddar Granite
T_1 Cheddar Monzonite
S Cheddar Xenoliths
O Algonquin granite
▼ Algonquin monzonite-syneite
■ Algonquin tonalite

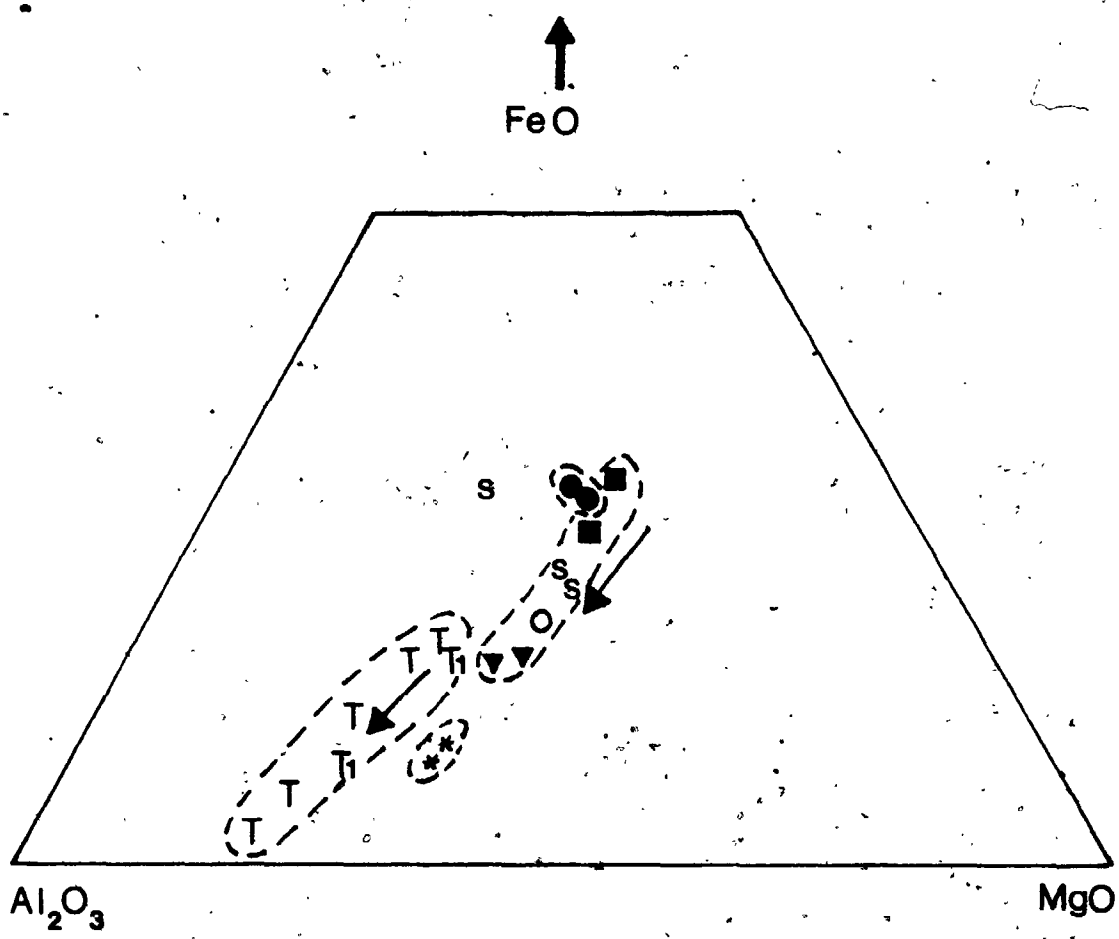

Figure 3-3-6. Al_2O_3-FeO (total iron)-MgO ternary diagram showing Compositional variations of amphiboles from sampled granitoids (from Nockolds and Mitchell, 1948). Dashed-lines enclose the compositional fields of sampled granitoids; arrows indicate the possible differentiation trends.

● Union Lake Pluton
* Mulock Batholith
T Cheddar Granite
T_1 Cheddar Monzonite
S Cheddar Xenoliths
○ Algonquin granite
▼ Algonquin monzonite-syenite
■ Algonquin tonalite

content are separated from this trend. In addition, compositions of amphiboles from Union Lake Pluton and Algonquin tonalite-diorite with the highest MgO contents are similar to those of hornblendite and appinitic diorite from Caledonian granitoids (Nockolds and Mitchell, 1948).

3.3 Feldspars

Data for analyzed feldspars from sampled granitoids are represented in Figure 3-3-7 as fields in relation to isotherms of Stormer (1975); confining pressure of each rock suite has been estimated from the experimental system of Qtz-Ab-Or-An-H_2O (Tuttle and Bowen, 1958; See Fig. 3-3-8). Except for one plagiolcase from Alphin Complex (EPW-7-2) which contains ternary feldspar composition ($Ab_{74}An_8Or_{18}$), all plagiolcase analyzed are unzoned and have Or-content less than 1.5 mole %. On the other hand, all of the alkali feldspars contained some $NaAlSi_3O_8$; 0% An-content of potash feldspars from Union Lake Pluton, Mulock Batholith and Barber's Lake Granite indicate a microcline origin.

The two-feldspar geothermometer of Stormer (1975) was used in an attempt to obtain equilibration temperatures of the late stage crystallization for sampled granitoids (See Fig. 3-3-7). Additionally, the hypersolvus crystallization of single feldspar in Deloro

6

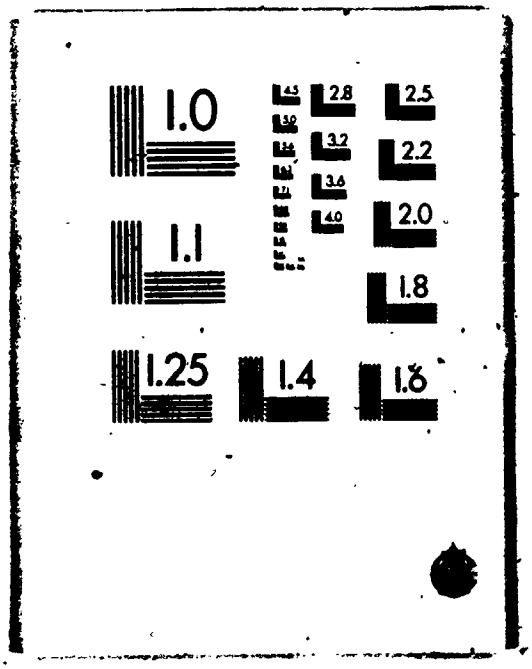

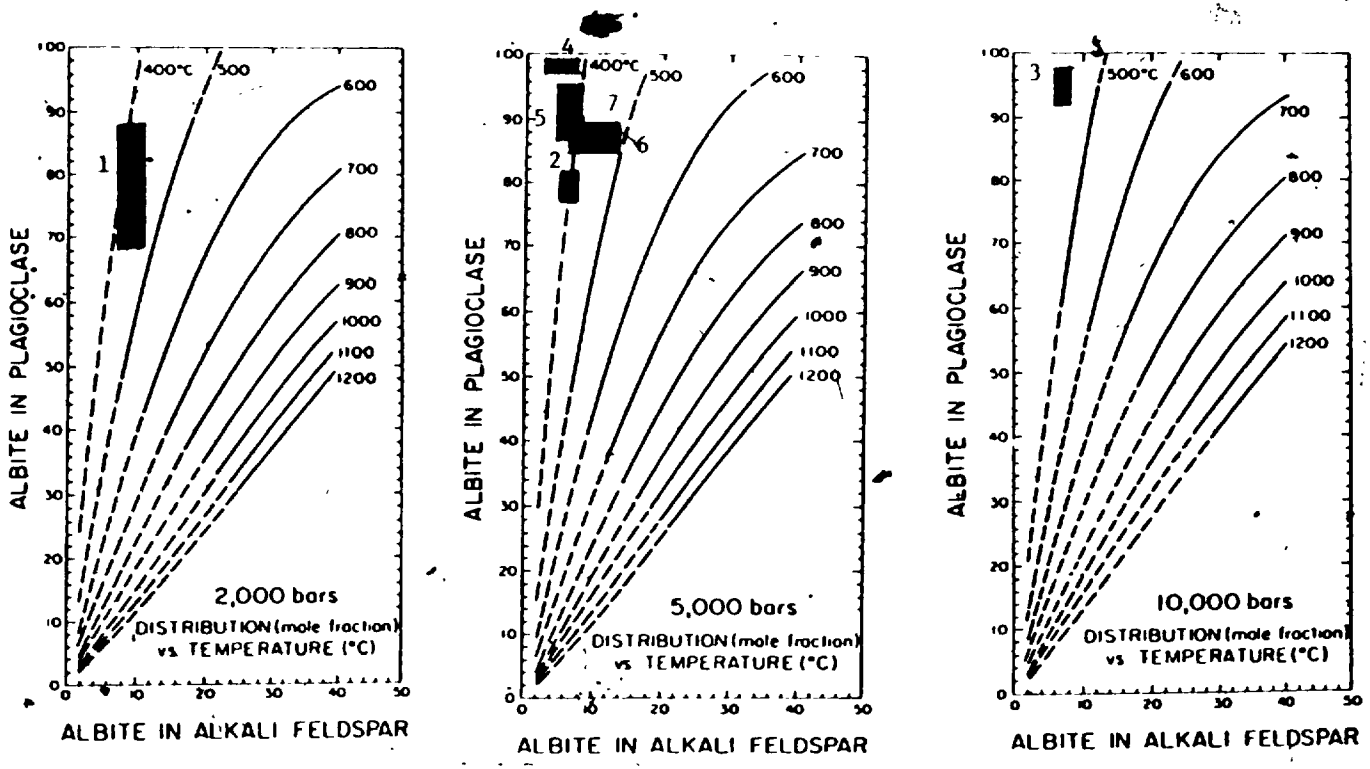

Figure 3-3-7, Representation of alkaline feldspar and piagioclase compositions for individual suites on diagrams for appropriate pressures (from Stormer, 1975).

1. Algonquin Granite 2. Union Lake Pluton 3. Elphin Granite
4. Cheddar Granite 5. Mulock Batholith 6. Coe Hill Granite
7. Barber's Lake Granite

peralkaline granite implies the temperature must exceed 680 °C (Waldbaum and Thompson, 1969).

4.0 THE QTZ-AB-OR-H_2O SYSTEM

The projections of normative proportions of Qtz-Ab-Or for sampled granitoids are shown in Figure 3-3-8. Experimentally determined ternary minima for haplogranite (An-free) system at 0.5 to 10 kb (P_{H2O}) (Tuttle and Bowen, 1958; Luth et al., 1964), minima in An-bearing systems (Winkler, 1967; James and Hamilton, 1969) and anhydrous minima (Luth, 1969) are also indicated in the diagram. Except that the composition of Deloro Pluton is coincident with the minimum melt at 3 kb of An-free system, granitic intrusions of the studied rock suite clearly lie on the feldspathic side of the eutectics, whereas the mafic varieties lie within the field of primary plagioclase precipitation.

In Barber's Lake Granite, the occurrence of primary muscovite indicates a confining pressure above 3-4 kb for stable muscovite at high temperature (Day, 1973). The presence of pegamtitic phases and dykes of the Cheddar Granite suggests a H_2O-saturated magma; the mean compostion with no normative anorthite is plotted between isobars of 5 kb and 10 kb at An-free system, while graodiorite of Algonquin Batholith with 4.17% anorthite located on the eutectics of Ab/An = 2.9 (Winkler, 1967) implies a pressure

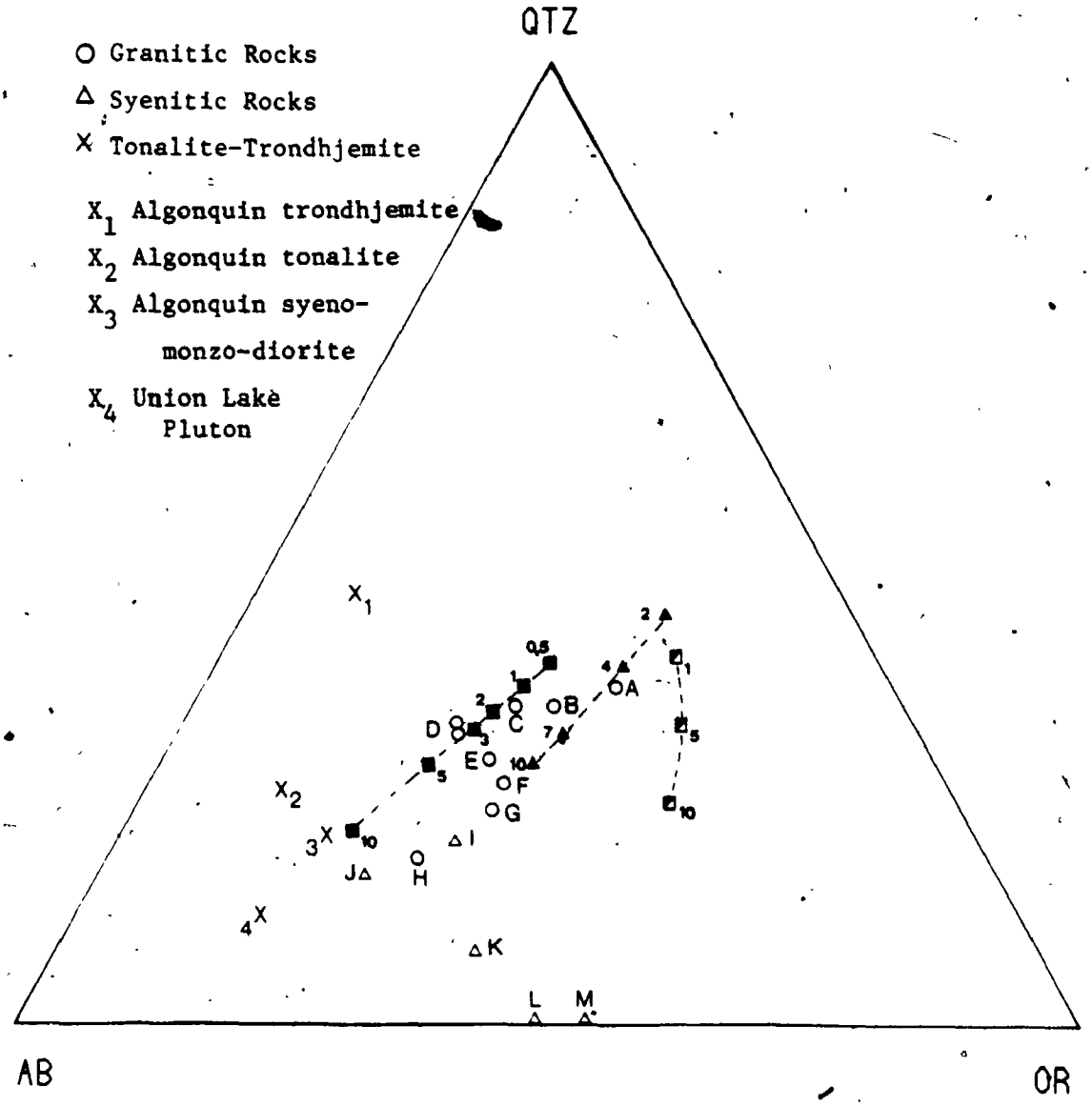

Figure 3-3-8. Normative Qtz-Ab-Or ternary diagram of mean compositions of sampled granitoids. Experimentally determined ternary minima (Tuttle and Bowen, 1958; Luth et al., 1964), minima in An-bearing systems (James and Hamilton, 1969), and anhydrous minima (Luth, 1969) are shown by solid squares, soild triangles and half-filled squares, respectively.

A. Algonquin granodiorite
B. Algonquin granite
C. Barber's Lake Granite
D. Deloro Pluton
E. Cheddar Granite
F. Mulock Batholith
G. Coe Hill Granite
H. Elphin granite
I. Cheddar monzonite
J. Deloro calc-syenite
K. Algonquin syenite-monzonite
L. Coe Hill quartz-poor phase
M. Elphin syenite

range of 4 kb to 7 kb.

Experimental data have revealed that an increase in P_{H2O} shifts the melt minima toward the Ab-apex (Luth et al., 1964), whereas increasing An-content moves the minimum melting point toward the Qtz-Or join (James and Hamilton, 1969). For the majority of sampled granitoids, they are bracketed between eutectics of H_2O-saturated (Tuttle and Bowen, 1958) and anhydrous (Luth, 1969); besides, the normative An-content of them ranges from 3.41 to 5.68%. Thus, it may be interpreted that the disposition of data points of Grenville granitoids on the Qtz-Ab-Or diagram is indicative of H_2O-undersaturated magma generated under pressures greater than 2 kb. However, the pink tint of alkaline feldspar (hematization) and alteration of ferromagnesian minerals (eg. chloritization and oxidation) in sampled granites are indications of late stage H_2O-saturation.

Monzonitic-syenitic rocks of sampled granitoids are believed to have been crystallized at higher confining pressure but lower P_{H2O} conditions than those of granitic rocks. It is consistent with the experimental data which suggest at high pressures low melting fractions tend to be alkali and quartz-poor (Green and Ringwood, 1968). In addition, Condie and Moore (1977) have suggested that the crust would have thickened from < 15 km to about 30 Km while evolving from arc-tholeiite to calc-alkaline volcanism and its intrusive counterpart in SE metasedimentary terrain of

Ontario. In other words, the cogenetic tonalite - trondhjemite (eg. Union Lake Pluton) magma would have generated at pressures about 5 to 10 kb. For simplicity, 2 kb for Algonquin granite, 3 kb for Deloro Pltuon, 5 kb for Barber's Lake Granite, Cheddar Granite, Mulock Batholith, Coe Hill Granite, Union Lake Pluton and Algonquin granodiorite and 10 kb for Elphin Complex were used for quantitative considerations (eg. two-feldspar geothermometry).

CHAPTER IV. GEOCHEMICAL SIGNIFICANCE AND TECTONIC IMPLICATIONS OF THE GRENVILLE GRANITOIDS

1.0 SIGNIFICANCE OF I-TYPE AND S-TYPE CLASSIFICATION FOR GRENVILLE GRANITOIDS

During the study of plutonic rocks of the Lachlan Mobile Belt in eastern Australia, Chappell and White (1974) proposed two contrasting granites with respect to their parental material. They interpreted I-type granite to be derived by partial melting of a mafic igneous source, while S-type granites were generated from a pelitic metasedimentary parent. Characteristic features of both granite types are summarized in Table 4-1-1.

Since then, the designations of I- and S-type granites have been widely applied to similar orogenic belts in other parts of the world (eg. Cordilleran Fold Belt of the west coast of America; Miller and Bradfish, 1980). Although various granites of (meta)sedimentary origin in the Precambrian shield (eg. Arth and Hanson, 1975) may be called S-type granites, little consideration has been given the Grenville granitoids in terms of I- and S-type classification. A summary of characteristic lithology, mineralogy, texture and some chemical indicators of the Grenville granitoids studied here, excluding the A-type Deloro Pluton, is presented in Table 4-1-2.

Table 4-1-1. Characteristics of I-type and S-type granitoids in the orogenic belt

I-type	S-type
A. Petrology	
1. dominantly tonalite and granodiorite;	1. dominantly quartz-rich adamellite and granodiorite;
2. elliptical shape with more regular and sharp boundaries;	2. approximately elliptical in outline but irregular boundaries;
3. mafic hornblende-bearing xenoliths of igneous appearance.	3. mainly metasedimentary inclusions with abundant aluminous-silicates.
B. Petrography	
1. hornblende in mafic varieties, biotite (high Mg/Fe) in felsic varieties;	1. biotite (low Mg/Fe) in mafic variaties, primary muscovite in felsic varieties;
2. no peraluminous minerals;	2. commonly with cordierite, ±sillimanite, ±andalusite, ±garnet;
3. primary sphene, apatite and zircon, as inclusions or tiny individual grains;	3. apatite, zircon, monazite and rutile commonly as larger discrete crystals;
4. magnetite, the major iron-oxide, with lesser ±ilmenite, ±hematite, ±pyrite;	4. ilmenite, the major iron-oxide, with ±pyrrhotite, ±graphite;
5. mafic minerals show a reaction relationship to one another;	5. quartz shows strong undulose extinction and a mosaic texture;
6. plagioclase with much less calcic core is complexly twinned and zoned.	6. plagioclase with higher calcic core is rectangular zoned and sericitized.
C. Chemistry	
1. relatively high sodium, Na_2O > 3.2% in felsic varieties, Na_2O > 2.2% in mafic varieties;	1. relatively low sodium, Na_2O < 3.2% in rocks with 5% K_2O, Na_2O < 2.2% in rocks with 2% K_2O;
2. molar $Al_2O_3/(Na_2O+CaO+K_2O)$ > 1.1;	2. molar $Al_2O_3/(Na_2O+CaO+K_2O)$ < 1.1;
3. normative diopside, or < 1% corundum;	3. > 1% normative corundum;
4. broad spectrum of compositions ranging from felsic to mafic;	4. much more restricted in composition to high SiO_2 type;
5. linear or near-linear variations within plutons;	5. less-regular or irregular variations within plutons;
6. high f_{O2}, high oxidation state and moderate f_{H2O}, high CaO activities;	6. low f_{O2}, low oxidation state and high f_{H2O}, high Al_2O_3 activities;
7. relatively lower in Sc, V, Cr, Ca, Ni, Cu, Zn, Ba, Rb, Th, La, Nd, Ce and Y;	7. relatively higher in Zr, Rb, Th and U, and lower in Sr;
8. REE contents are similar to high-Al basalts;	8. REE contents are similar to average shale;
9. **Ave. Agpaitic Index 0.522, Oxidation Index 49.64 .	9. **Ave. Agpaitic Index 0.595, Oxidation Index 32.34 .
D. Isotopes	
1. linear whole-rock isochrons, with initial $^{87}Sr/^{86}Sr$ ratios of 0.704-0.706;	1. scattered isochrons, with initial $^{87}Sr/^{86}Sr$ ratios > 0.708;
2. lower $\delta^{18}O$, < 10 ;	2. higher $\delta^{18}O$, >10 ;
3. higher $\delta^{34}S$, > +1 (ave. +5).	3. lower $\delta^{34}S$, < 1 (ave. -5).
E. Sources	
1. a fractionated metabasaltic or andesitic source in the lower crust;	1. a (meta) sedimentary pile in the miogeosyncline;
2. or a more primitive, underplating material of an earlier subduction event.	2. or an older peraluminous pelitic or quartzo-feldspathic crustal material.

* Data were compiled from Chappell and White (1974), Griffin et. al. (1978), Hine et. al. (1978), Chappell (1978), Takahashi et. al. (1980), O'Neil and Chappell (1977), Wones (1979), Chappell (1979), Frey and Chappell (1979).

** Averages were taken from Kosciusko Batholith (Hine et. al., 1978) and New England Batholith, Eastern Australia (Chappell, 1978).

Table 4-1-2. Characteristic features of Grenville Granitoids

Granitoid	Algonquin Batholith	Union Lake Pluton	White Lake Pluton	Elphin Complex	Coe Hill Granite
Rock-type	1. Mainly gnessic granite-granodiorites 2. Large units of syenite-monzonite; 3. Small bodies of anorthositic and related mafic rocks.	Quartz-diorite.	Tonalite-trondhjemite.	1. Granodiorite; 2. Calc-alkali syenite.	1. Granite; 2. Monzonitic rocks
Xenolith	Amphibolite and tonalitic rocks of earlier phase (in granitic rocks).	Amphibolite and marble.	Amphibolite.	Dioritic-gabbroic rocks (host).	Amphibolite, gabbro, metasedimentary rocks.
Mineralogy	1. Hb, Biot, ±, in mafic varieties; 2. Biot, ±Hb in felsic varieties; 3. Primary Ap, Zir and Sph 4. Secondary Mus, Ep, ±Gt; 5. Mag, ±Il, ±Sulfates.	1. Hb, Biot, ±Px; 2. Primary Ap, Sph; 3. Mag, ±Hem.	Biot, ±Hb.	1. Biot in granodiorite 2. Biot, Hb in syenite 3. Primary Sph, Ap; 4. Secondary Mus, Ep, and Tm (in syenite); 5. Mag, ±Chalcopyrite	1. Biot, Hb in granite; 2. Px only in monzonite; 3. Primary Sph, Ap, Zir; 4. Mag, ±Il, ±Py.
Texture	1. Undulose extinction and elongation of quartz grains; 2. Vermicular intergrowth of plagioclase and quartz.	1. Pyroxene is often replaced by hornblende; 2. Poikilitic texture in common for hornblende.		1. Quartz-grains show undolose extinction and sugary texture; 2. Myrmekitic texture.	1. Pyroxene forms as relict core surrounded by biotite hornblende; 2. Quartz grains show undulose extinction and serrated boundaries.
Plagioclase composition	1. An_{50-70} in gabbro and anorthositic diorite; 2. An_{10-30} in felsic rock.	An_{15-26}.	An_{25-35}.	1. An < 10 in granodiorite; 2. "Ternary"-feldspar in syenite.	An_{5-15}.
SiO_2 range	45 - 77%	59 - 63%	67 - 72%	57 - 73%	56 - 74%
Al/(Na+K+Ca/2)	0.985 (1.046)*	0.808	1.026	0.949	0.930
Agpaitic Ind.	0.593 (0.788)*	0.697	0.632	0.883	0.863
Oxidation Ind.	50.53 (57.66)*	47.56	46.33	71.95	56.81

* For granite-granodiorite only.

(Table 4-1-2, cont'd)

Granitoid	Loon Lake Pluton	Mulock Batholith	Cheddar Granite	Barber's Lake Granite	Glamorgan Complex
Rock-type	1. Granite; 2. Monzonite (Basic rocks are not comagmatic).	Granite (adamellite)	1. Granite (adamellite); 2. Monzonite.	1. Granite (adamellite); 2. Basic rocks.	1. Trondhjemite (sodic granite); 2. K-rich granite.
Xenolith	Various country rocks.	Metasedimentary rocks.	Tonalitic rocks. (igneous appearance)	Trondhjemitic rocks, amphibolite.	Dioritic rocks in sodic granite.
Mineralogy	1. Biot in granite; 2. Biot, Hb, ±Px in monzonite; 3. Primary Sph, Ap; 4. Mag, ±Il, ±Sulfides.	1. Biot, ±Hb; 2. Primary Ap, Sph, Zir; 3. Mag, ±Il, ±Hem.	1. Biot, Hb (±Px in 2. Primary Ap, Sph, Zir; 3. Mag, ±Il, ±Py.	1. Biot, primary Mus; 2. Primary Sph, Zir; 3. Mag (rare).	1. Biot, ±Hb in trondhjemite; 2. Biot (only) in K-rich granite; 3. Primary Ap, Sph, Zir; 4. Mag, ±Hem.
Texture	1. Cataclasis and mortar texture of quartz; 2. Sphene corona around magnetite-ilmenite grains.	1. Undulose extinction and mosaic texture of quartz; 2. Poikilitic texture in Hb.	1. Undulose extinction of quartz grains; 2. Hornblende replaced by biotite.	1. Undulose extinction and polycrystalline subgrains of quartz; 2. Biotite interleave with primary muscovite (subsolidus phase).	1. Corroded hornblende; 2. Myrmekitic intergrowth.
Plagioclase composition	1. An_{5-15} in granite 2. An_{8-20} in monzonite.	An_{3-15}.	An_{2-15}.	An_{8-11}.	1. An_{15-30} in trondhjemite; 2. An_{5-20} in K-rich granite.
SiO_2-range	59 - 75%	63 - 76%	56 - 77%	73 - 76%	69 - 79%
Al/(Na+K+Ca/2)	1.005	0.960	0.886	1.073	1.082
Agpaitic Ind.	0.841	0.905	0.971	0.887	0.775
Oxidation Ind.	67.06	60.24	67.86	58.77	66.71

(Table 4-1-2, cont'd)

Granitoid	Frontenac - Axis Granites		
	(a) Westport-type	(b) Frontenac-type	(c) Rockport-type
Rock-type	Monzonite.	1. Granite; 2. Monzonite.	Granite.
Xenolith	Gabbro, marble.	Diorite, grabbro, pyroxene - gneiss, quartzite, marble.	Quartzite.
Mineralogy	1. Biot, ±Hb; 2. Primary Sph, Ap, ±Zir.	1. Biot, Hb, ±Py; 2. Primary Sph, Ap, Zir; 3. Mag, ±Py.	1. Biot, ±Hb; 2. Primary Ap, Zir.
Texture	1. Rare myrmekite; 2. Mortar texture absent.	1. Mymekitic texture common; 2. Mortar texture.	1. Some myrmekite; 2. Minor mortar texture.
Plagioclase composition	An_{5-12}.	An_{13-20}.	An_{17-28}.
SiO_2 range	58-62%	57-69%	71-75%
Al/(Na+K+Ca/2)	0.984	0.932	1.083
Agpaitic Ind.	0.838	0.821	0.809
Oxidation Ind.	77.00	75.83	80.04

Data Source:-
1. Loon Lake Pluton (Dostal, 1973).
2. Frontenac-Axis granites (Sauerbrei, 1966).
3. White Lake Pluton (Somers, 1984).
4. Glamorgan Complex (Chesworth, 1967).
5. Other granites from this study.

Abbreviation:-

Biot = biotite,	Mag = magnetite,	Hb = hornblende,	Il = ilmenite,
Px = pyroxene,	Hem = hematite,	Sph = sphene,	Py = pyrite,
Ap = apatite,	Mus = muscovite,	Zir = zircon,	Tm = tourmaline,
Ep = epidote.			

Oxidation Index = 2 x Fe_2O_3 x 100 / (2x Fe_2O_3 + FeO), ave. I-type = 49.64, S-type = 32.34.
Agpaitic Index = (mol.) (Na_2O + K_2O)/Al_2O_3, ave. I-type = 0.522, S-type = 0.595.
(averages calculated from Hine et. al., 1978)

Except for the biotite diorite suite (eg. Union Lake Pluton) and associated trondhjemite (eg. White Lake Pluton), most granitoids in this study contain a monzonitic or syenitic phase - an uncommon feature of the granitic complexes of the Lachlan Fold Belt described by Chappell and White (1974). Biotite and hornblende are the dominant mafic constituents with accessory amounts of magnetite, primary sphene and apatite. Primary muscovite occurs only in the Barber's Lake Granite. In addition, quartz grains commonly show undulose extinction and mortar texture, as are often found in S-type granites. Furthermore, amphibolite, marble and metasedimentary rocks of the envelope are common in the Grenville granitoids; however, xenoliths of tonalitic composition in the Cheddar Granite show evidence of possible restite origin (See Chap. II, Section 5.0). Thus, based on the mineralogy, narrow range of SiO2 and peraluminous nature, only the Barber's Lake Granite could be assigned to the S-type category of Chappell and White (1974).

It is interesting to note that most Grenville granites are metaluminous with alkalic affinity indicated by their high agpaitic indices (0.503 - 0.971). This can be partly explained by their sodic composition of plagioclase (An_{2-35}; excluding the anorthositic rocks). Besides, the Grenville granites, except for the tonalite-trondhjemite suite, have anomalously high oxidation indices (50 - 80) in comparison with average I-type (49.46) and S-type (32.34), which may indicate a relatively higher oxidation state or high f_{O_2} at

the formation of Grenville granites during the Grenville Orogeny.

Geochemically, S-type granites contain relatively low Na_2O and CaO due to sedimentary fractionation. Whereas I-type granites have relatively high ferric iron concentration and O_2 fugacities. Therefore, distinct groupings should be indicated in the plots of Na_2O vs. K_2O, Na_2O vs. CaO and Fe_2O_3 vs. FeO. For standardizing purposes, the typical I- and S-type granitoids of the Kosciusko Batholith in eastern Australia (Hine et al., 1978) are used here.

The Na_2O vs. K_2O variation plots for the Kosciusko Batholith and Grenville granitoids are shown in Figure 4-1-1. Except for some points of the Algonquin Batholith (Fig. 4-1-1D) and Cheddar Granite (Fig. 4-1-1I), granites of the Grenville Province show high Na_2O, typical of I-type affinity. Similarly, in Na_2O vs. CaO plots (Fig. 4-1-2), with few exceptions, Grenville granitoids lie within the I-type field; however, the range of CaO is narrower in the Grenville granitoids than in the Kosciusko Batholith. Consistent with this classification is the Fe_2O_3 vs. FeO variation (Fig. 4-1-3). For the Algonquin Batholith (Fig. 4-1-3D), gabbroic rocks contain relatively higher FeO contents, while tonalite-trondhjemite have variable Fe_2O_3/FeO ratios; the remaining Grenville granitoids are all in the field of I-type granite.

Figure 4-1-1. Na_2O vs. K_2O plots for typical I- and S-type granites and Grenville granitoids.

Data Sources :

Kosciusko Batholith (Hine et al., 1978)

Granites of Frontenac Axis (Sauerbrei, 1966)

Glamorgan Complex (Chesworth, 1967)

Loon Lake Pluton (Dostal, 1973)

Other granitoids (this study)

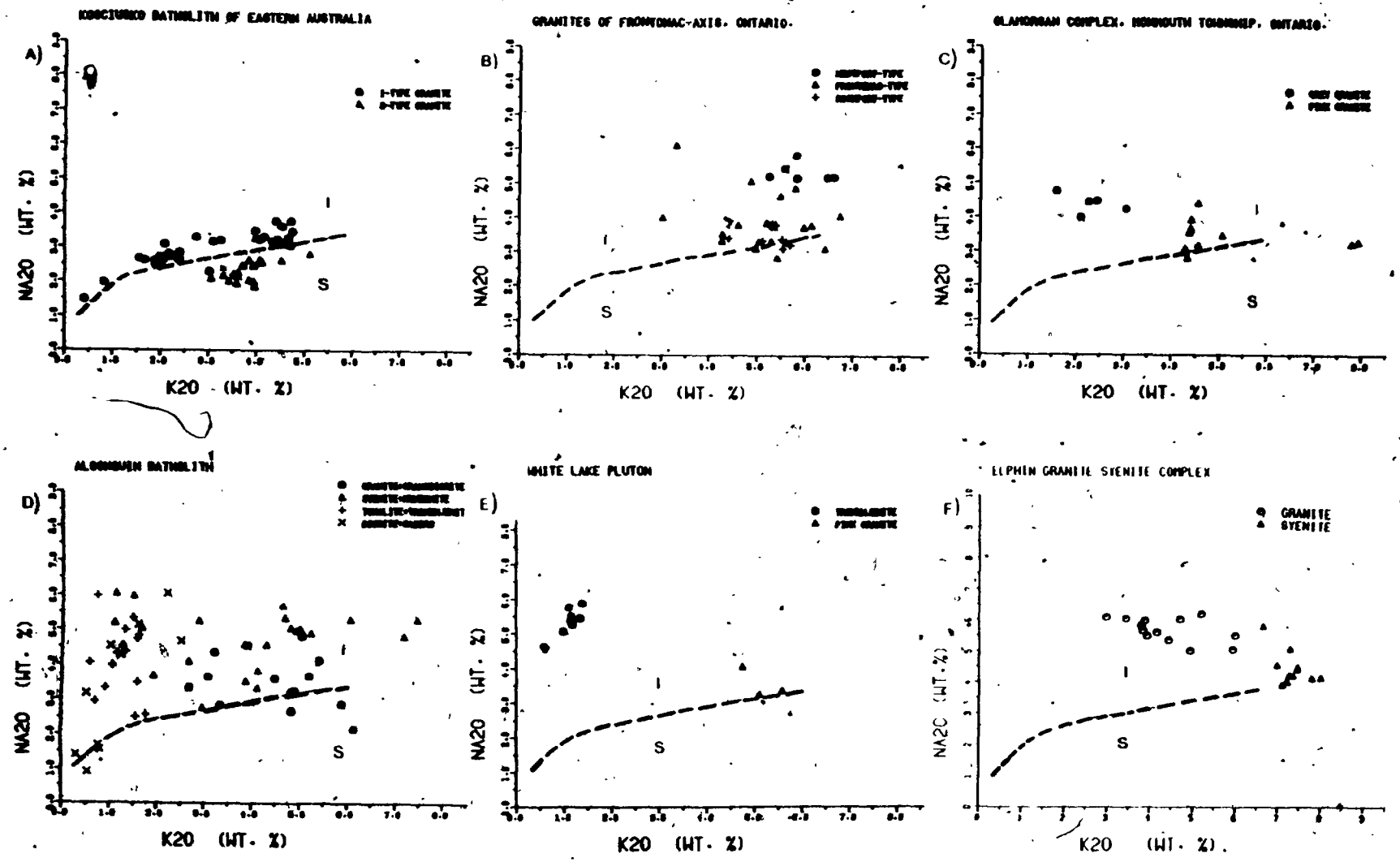
A)
B)
C)
D)
E)
F)
NA2O (WT. %)
K2O (WT. %)
I
S
GRANITE
SYENITE

(Figure 4-1-1. Cont'd)

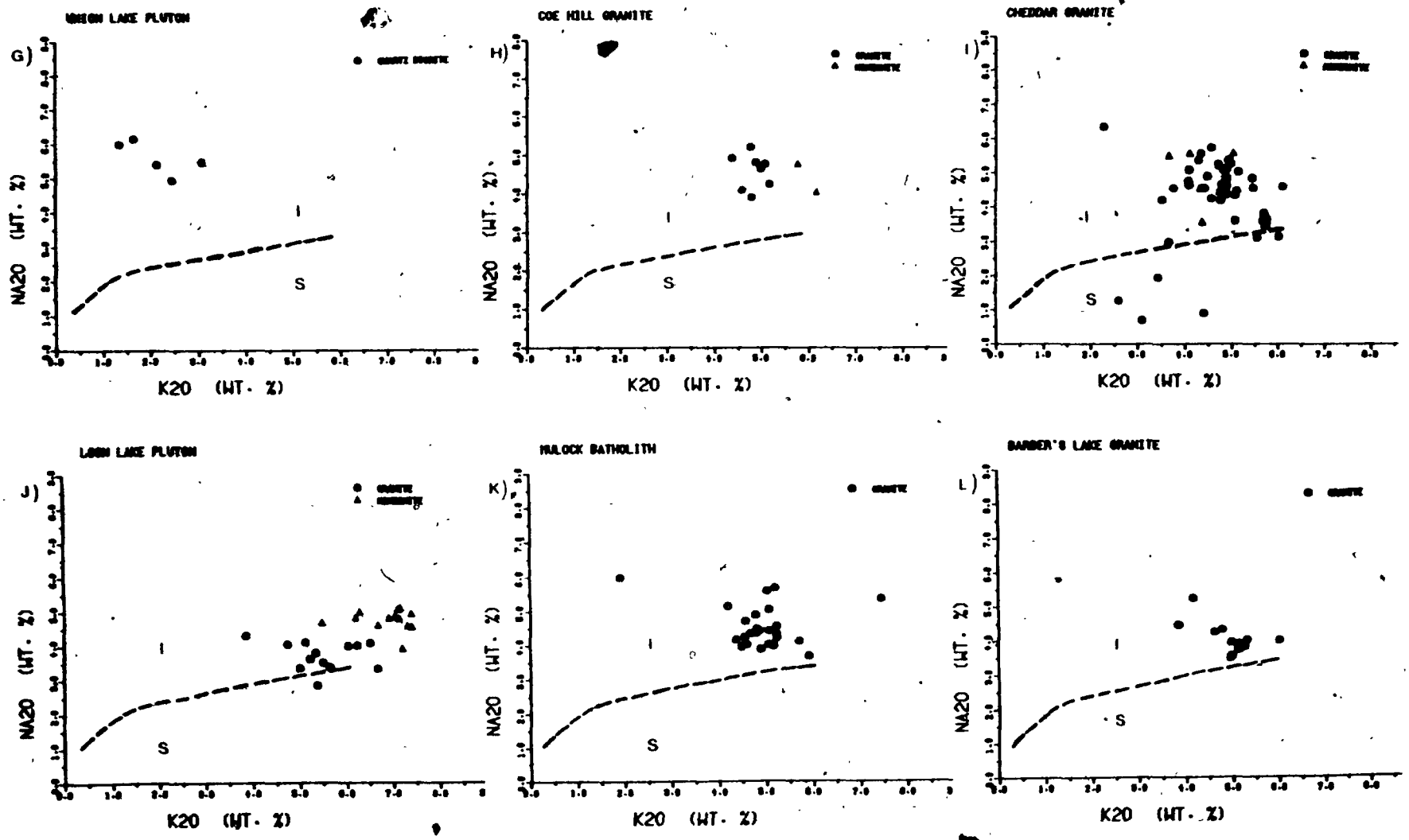

Figure 4-1-2. Na_2O vs. CaO plots for typical I- and S-type granites and Grenville granitoids.

Data Sources :

- Kosciusko Batholith (Hine et al., 1978)
  Granites of Frontenac Axis (Sauerbrei, 1966)
  Glamorgan Complex (Chesworth, 1967)
  Loon Lake Pluton (Dostal, 1973)
  Other granitoids (this study)

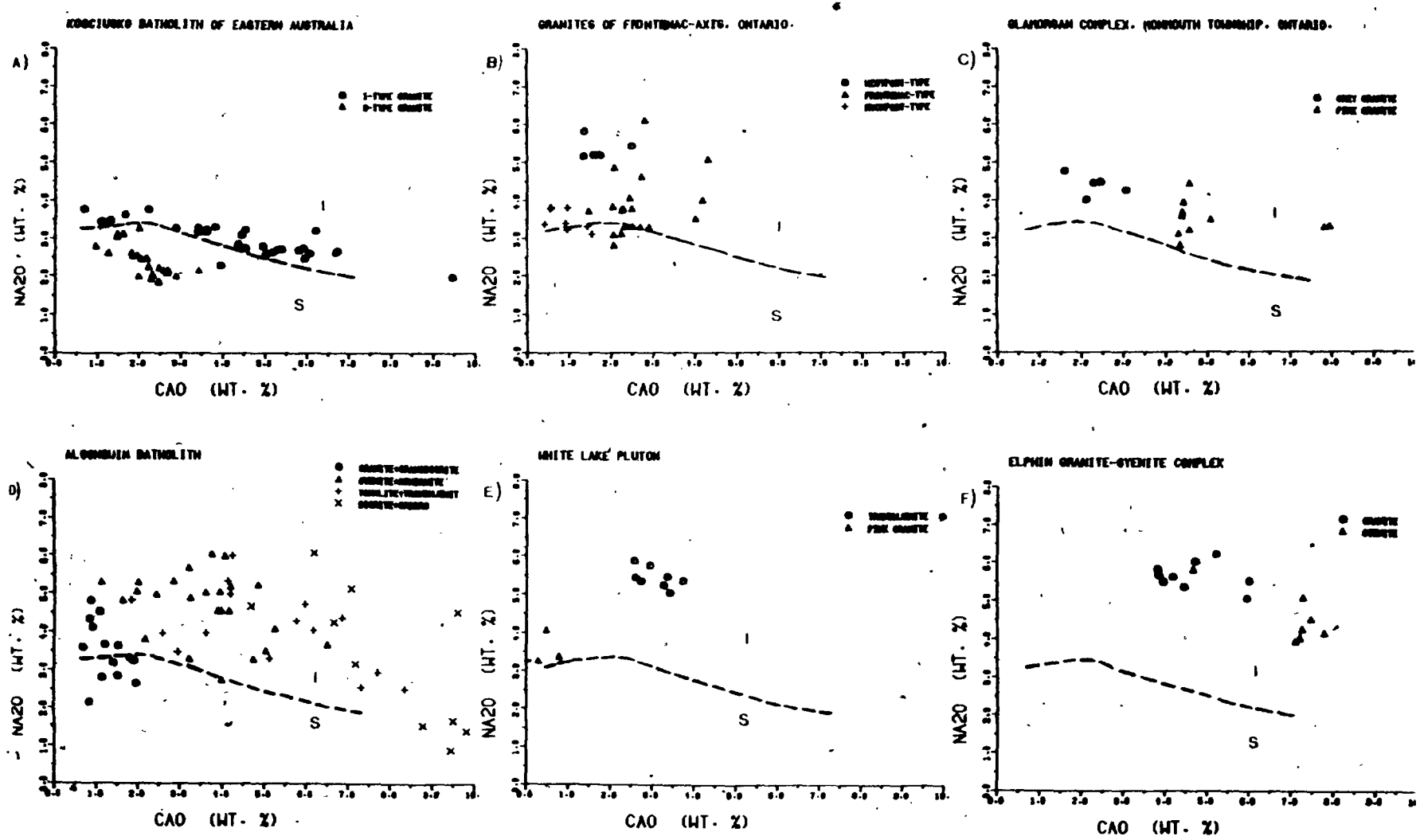
KOSCIUSKO BATHOLITH OF EASTERN AUSTRALIA
A)
GRANITES OF FRONTENAC-AXIS, ONTARIO.
B)
GLAMORGAN COMPLEX, (MONMOUTH TOWNSHIP, ONTARIO.
C)
ALGONQUIN BATHOLITH
D)
WHITE LAKE PLUTON
E)
ELPHIN GRANITE-SYENITE COMPLEX
F)
NA2O (WT. %)
CAO (WT. %)
I
S

(Figure 4-1-2. Cont'd)

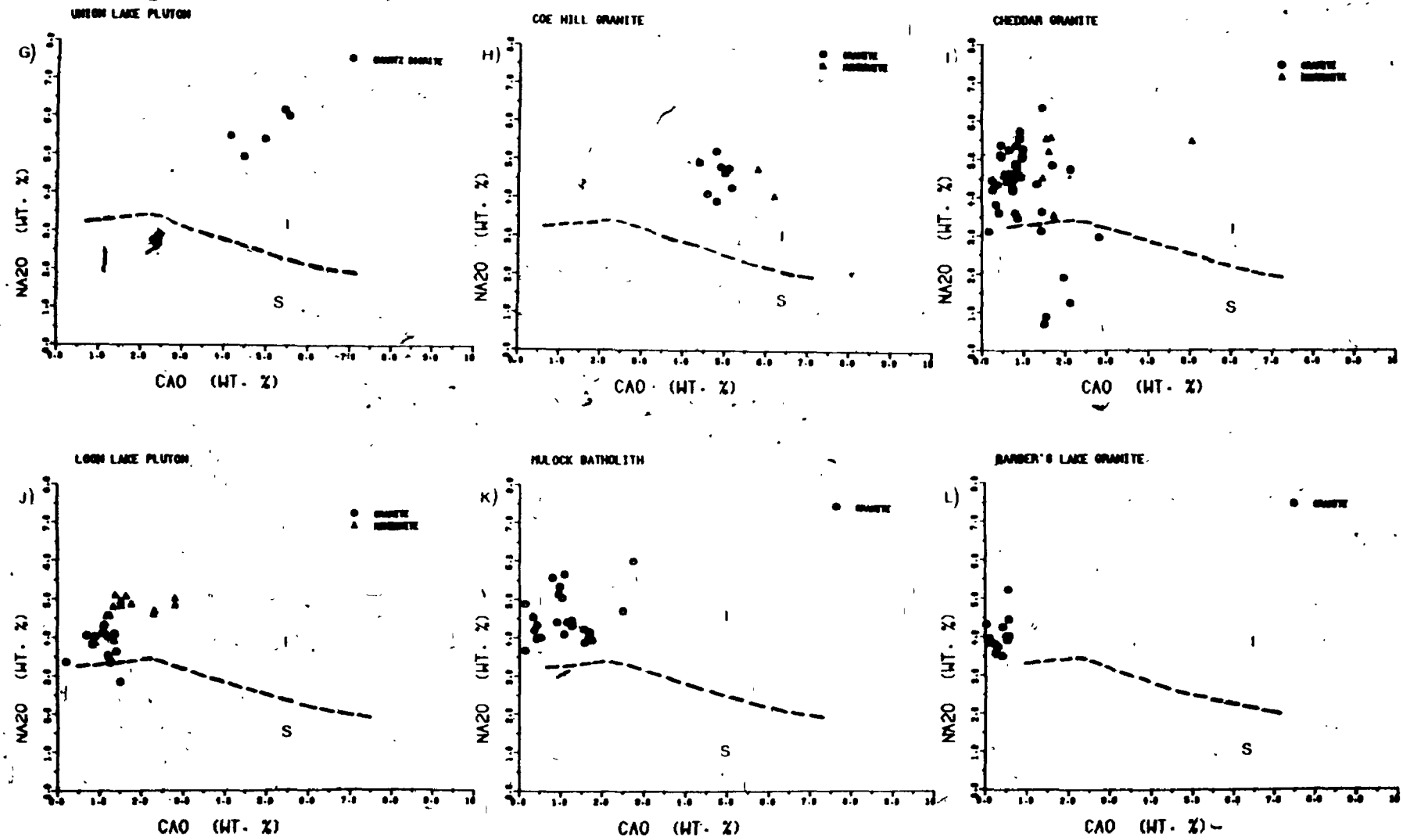

Figure 4-1-3. Fe_2O_3 vs. FeO plots for typical I- and S-type granites and Grenville granitoids.

Data Sources :

Kosciusko Batholith (Hine et al., 1978)

Granites of Frontenac Axis (Sauerbrei, 1966)

Glamorgan Complex (Chesworth, 1967)

Loon Lake Pluton (Dostal, 1973)

Other granitoids (this study)

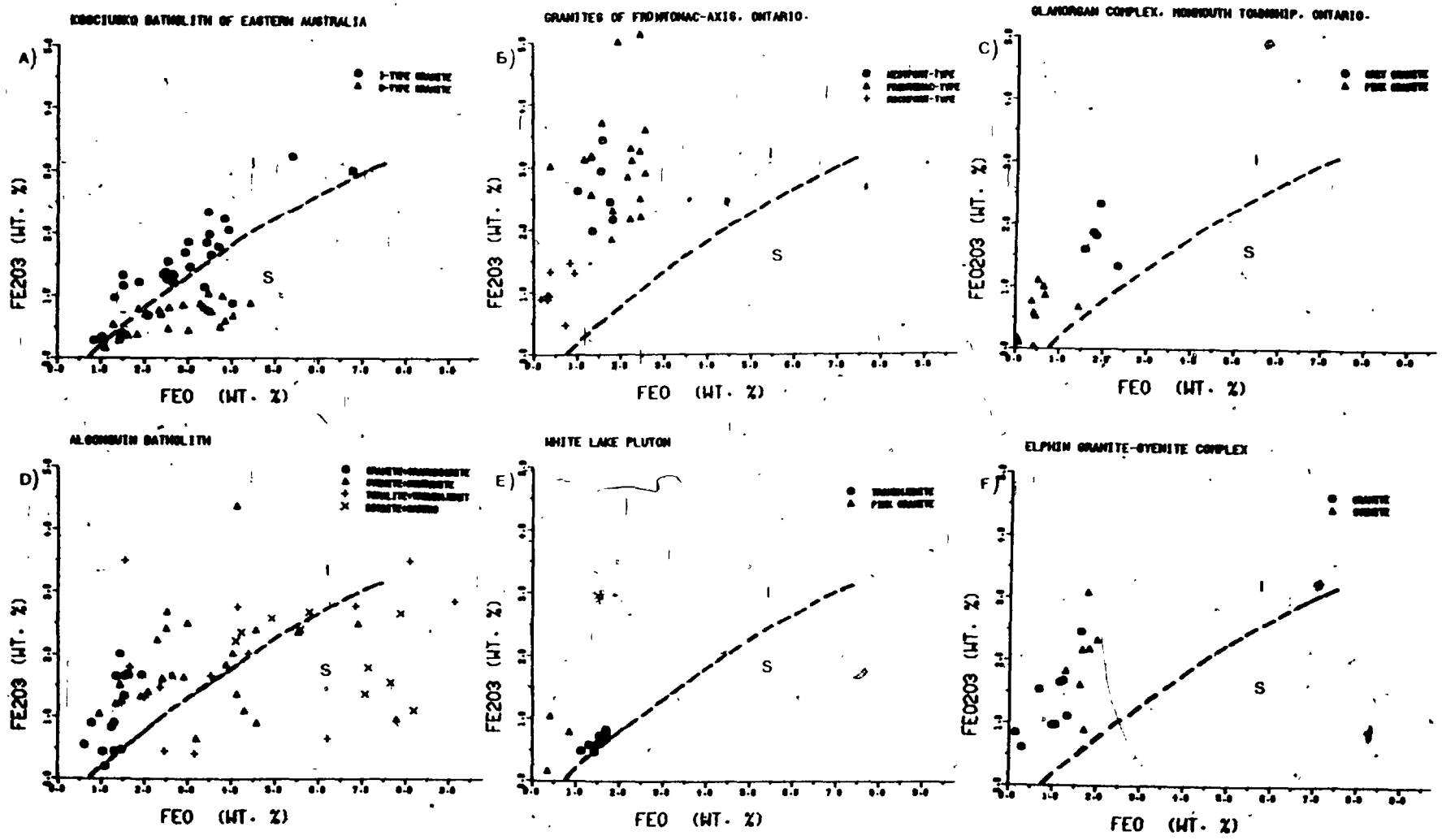
A)
KOSCIUSKO BATHOLITH OF EASTERN AUSTRALIA
I-TYPE GRANITE
S-TYPE GRANITE
S
FE2O3 (WT. %)
FEO (WT. %)
Б)
GRANITES OF FRONTENAC-AXIS, ONTARIO.
S
FE2O3 (WT. %)
FEO (WT. %)
C)
GLAMORGAN COMPLEX, MONMOUTH TOWNSHIP, ONTARIO.
GREY GRANITE
PINK GRANITE
S
FE2O3 (WT. %)
FEO (WT. %)
D)
ALGONQUIN BATHOLITH
S
FE2O3 (WT. %)
FEO (WT. %)
E)
WHITE LAKE PLUTON
TRANSLUCENT
PINK GRANITE
S
FE2O3 (WT. %)
FEO (WT. %)
F)
ELPHIN GRANITE-SYENITE COMPLEX
GRANITE
SYENITE
S
FE2O3 (WT. %)
FEO (WT. %)

(Figure 4-1-3. Cont'd)

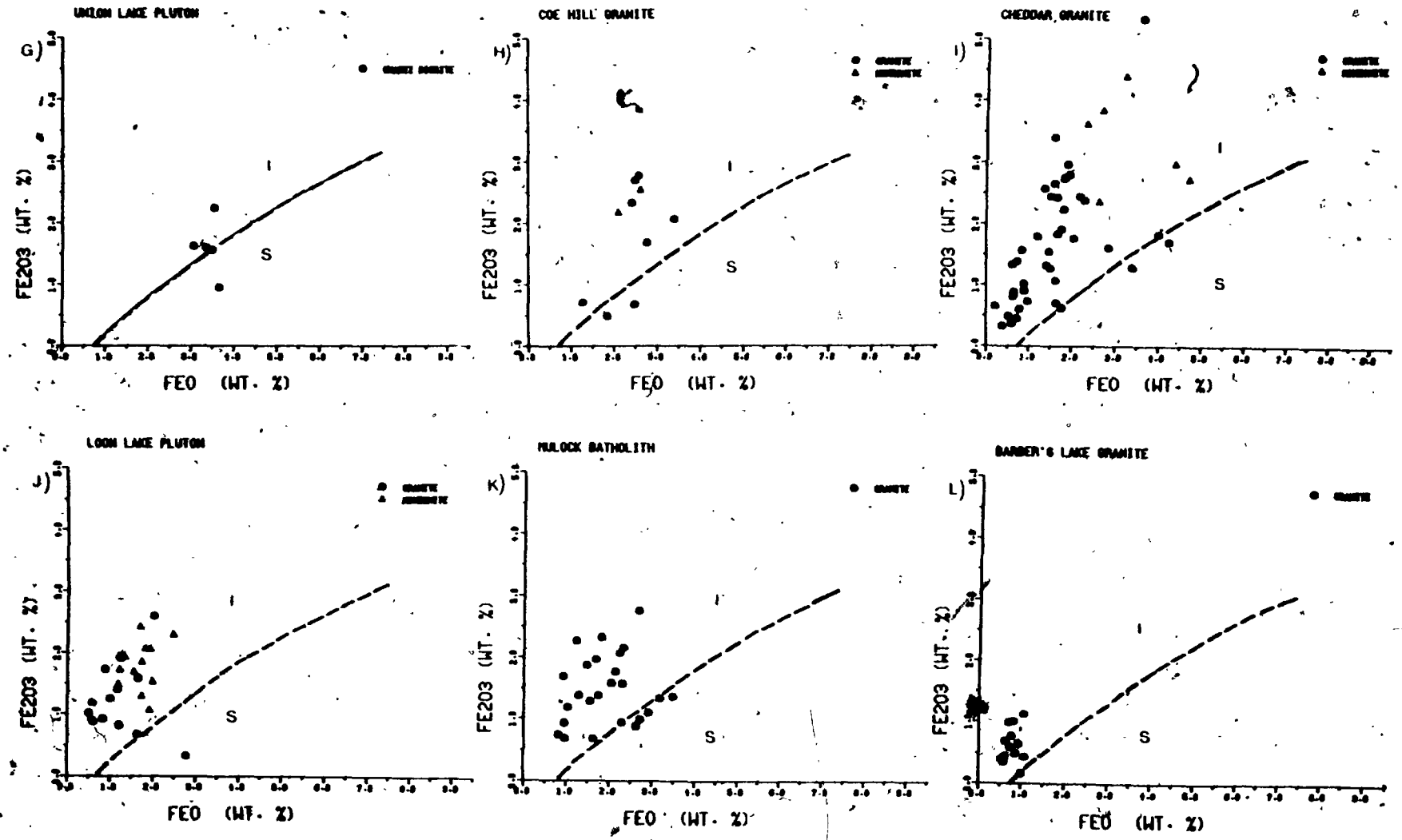

In addition, Takahashi et al. (1980) used ACF plots and molar ratios of $Al_2O_3/(Na_2O+K_2O+CaO)$ and C/ACF as effective parameters for distinguishing I-types from S-types. ACF diagrams for Kosciusko Batholith and Grenville granitoids are shown in Figure 4-1-4. Among these Grenville granitoids, ACF plots indicate that I-types prevail over S-type in the tonalite-trondhjemite suite of southeastern Ontario (eg. Union Lake and White Lake Plutons), whereas the S-types predominate in the Glamorgan complex, Loon Lake Pluton, Mulcok Batholith and Barber's Lake Granite. Both I-types and S-types appear in the Frontenac Axis Granites, Algonquin Batholith, Elphin Complex, Coe Hill Granite and Cheddar Granite. It is noteworthy that monzonite in the Coe Hill and Cheddar Granites are of I-types, while the Westport-type monzonite of the Frontenac Axis Granites and some syenitic rocks of the Algonquin Batholith are of S-types. The syenite phase of the Elphin Complex straddles both fields.

Histograms of C/ACF ratios of the Grenville granitoids and typical I- and S-type granites of Australia are presented in Figure 4-1-5 .. In general, the S-type granitoids contain relatively low ratios with a mode of 0.225, whereas the I-types are grouped at the higher end with a mode of 0.325. Except for the tonalite-trondhjemite suite which shows a positive I-type affinity, rocks of the Glamorgan Complex, Coe Hill Granite (mode 0.275), Loon Lake Pluton (mode 0.250), Mulock Batholith (mode 0.225) and

Figure 4-1-4. ACF ternary diagrams for typical I- and S-type granites and Grenville granitoids.

Data Sources :

Kosciusko Batholith (Hine et al., 1978)
Granites of Frontenac Axis (Sauerbrei, 1966)
Glamorgan Complex (CHesworth, 1967)
Loon Lake Pluton (Dostal, 1973)
Other granitoids (this study)

KOSCIUSKO BATHOLITH OF EASTERN AUSTRALIA

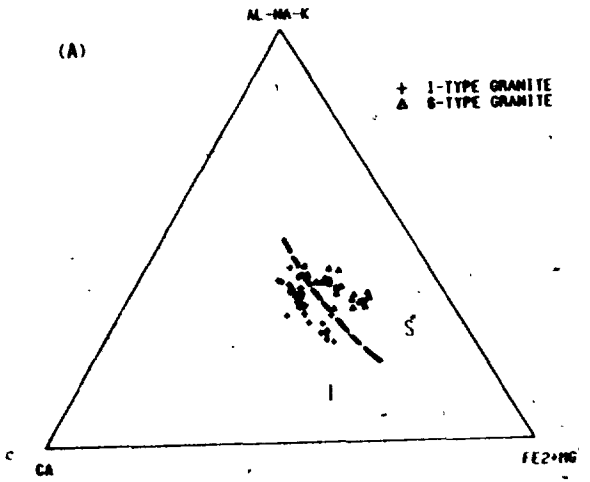

GRANITES OF FRONTENAC-AXIS, ONTARIO.

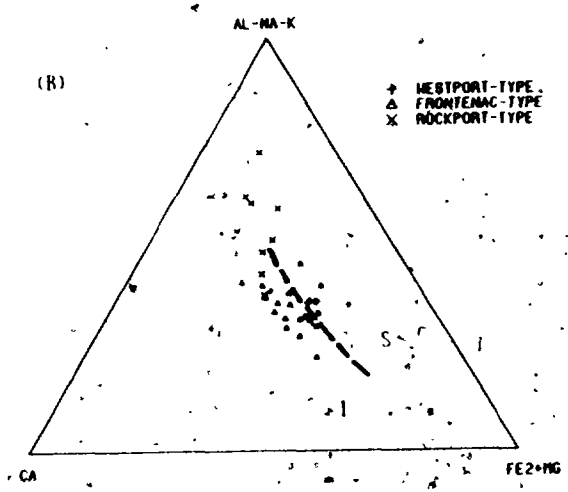

GLAMORGAN COMPLEX, MONMOUTH TOWNSHIP, ONTARIO.

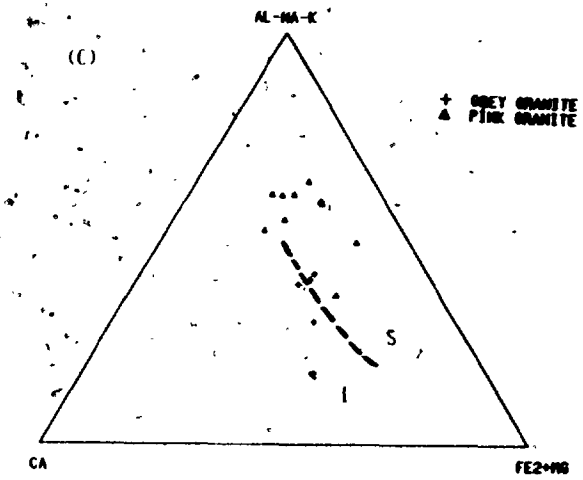

ALGONQUIN BATHOLITH

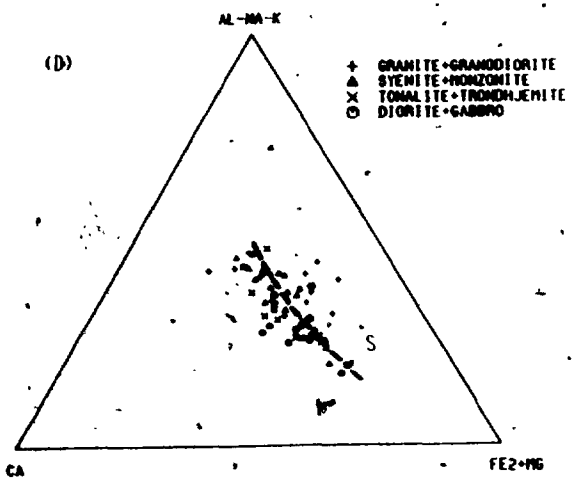

WHITE LAKE PLUTON

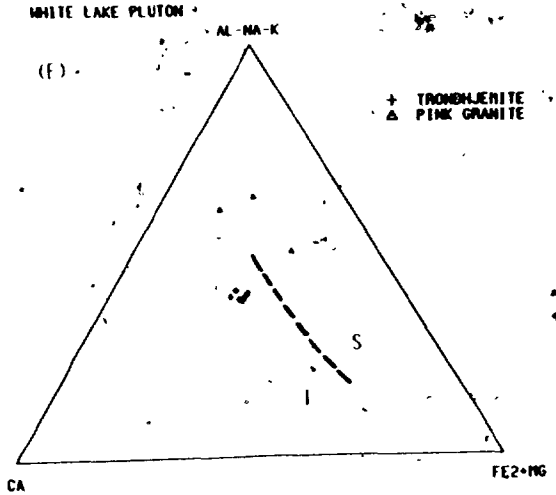

ELPHIN GRANITE-SYENITE COMPLEX

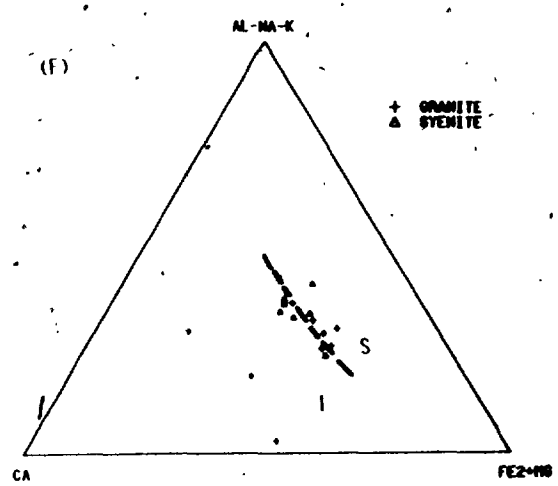

(Figure 4-1-4. Cont'd)

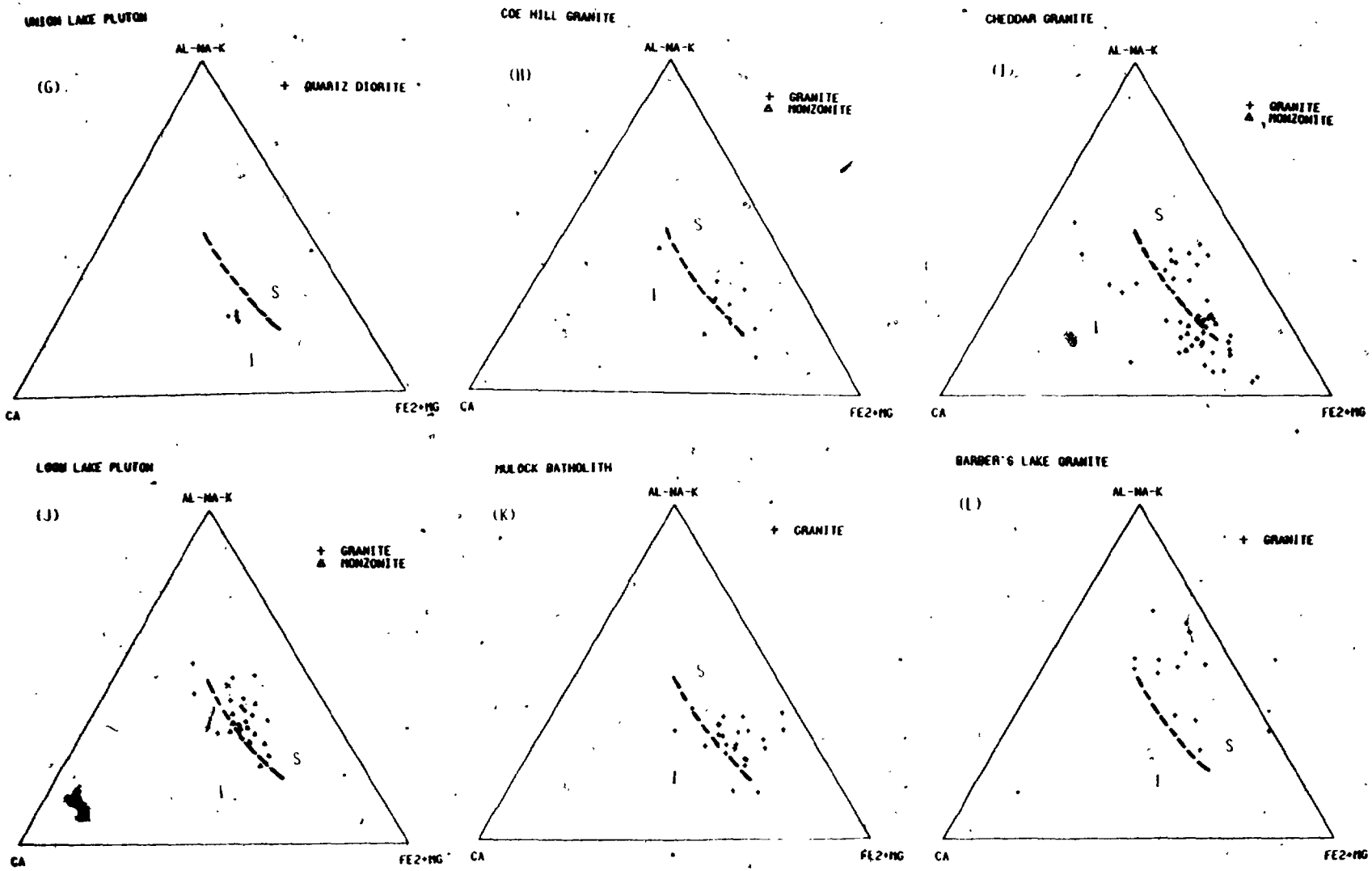

Figure 4-1-5. Histograms of C/ACF for typical I- and S-type granites and Grenville granitoids.

Data Sources :

Kosciusko Batholith (Hine et al., 1978)
Granites of Frontenac Axis (Sauerbrei, 1966)
Glamorgan Complex (Chesworth, 1967)
Loon Lake Pluton (Dostal, 1973)
Other granitoids (this study)

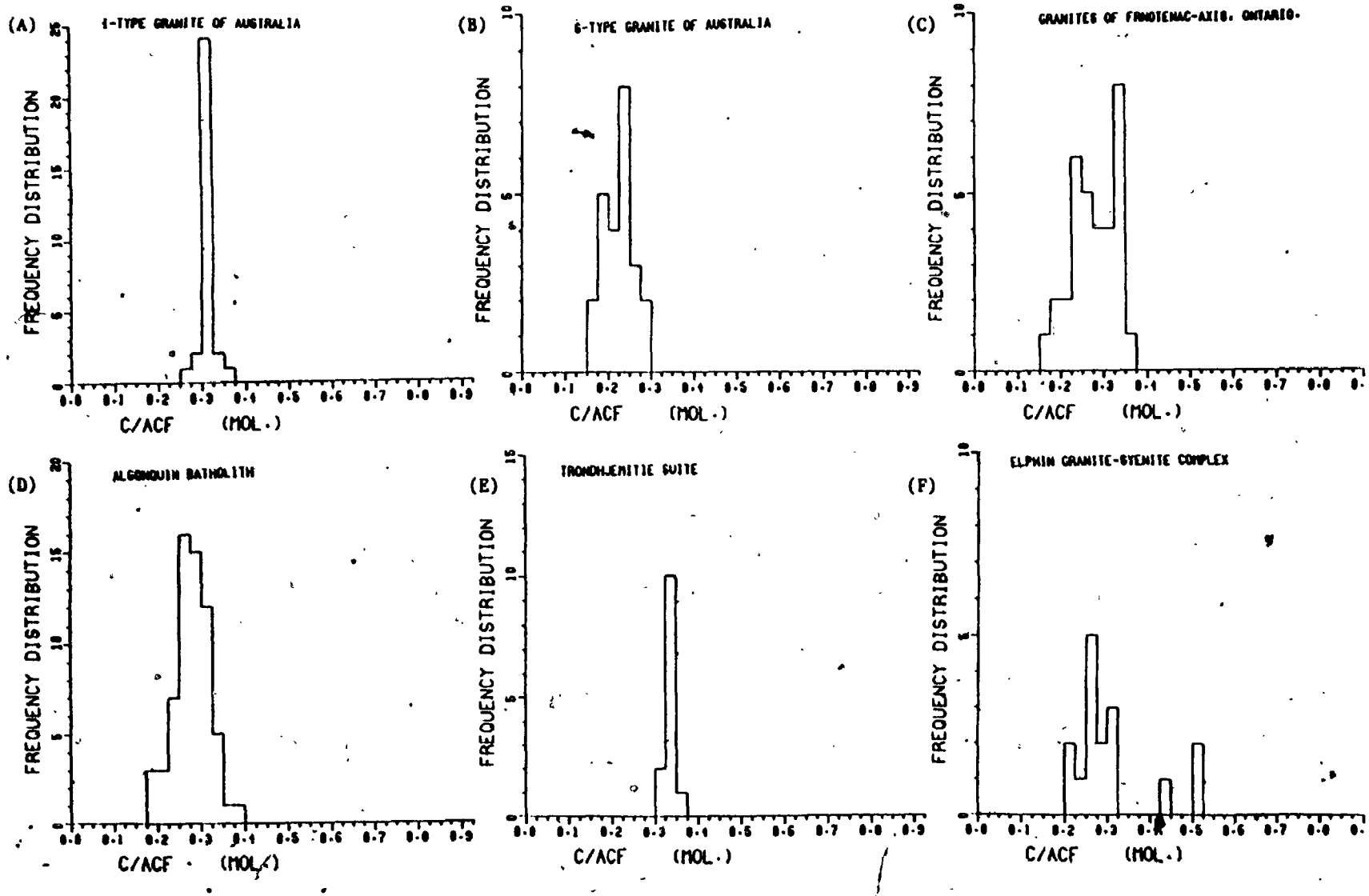
(A)
I-TYPE GRANITE OF AUSTRALIA
(B)
S-TYPE GRANITE OF AUSTRALIA
(C)
GRANITES OF FRONTENAC-AXIS, ONTARIO.
(D)
ALGONQUIN BATHOLITH
(E)
TRONDHJEMITIE SUITE
(F)
ELPHIN GRANITE-SYENITE COMPLEX
FREQUENCY DISTRIBUTION
C/ACF (MOL.)

(Figure 4-1-5. Cont'd)

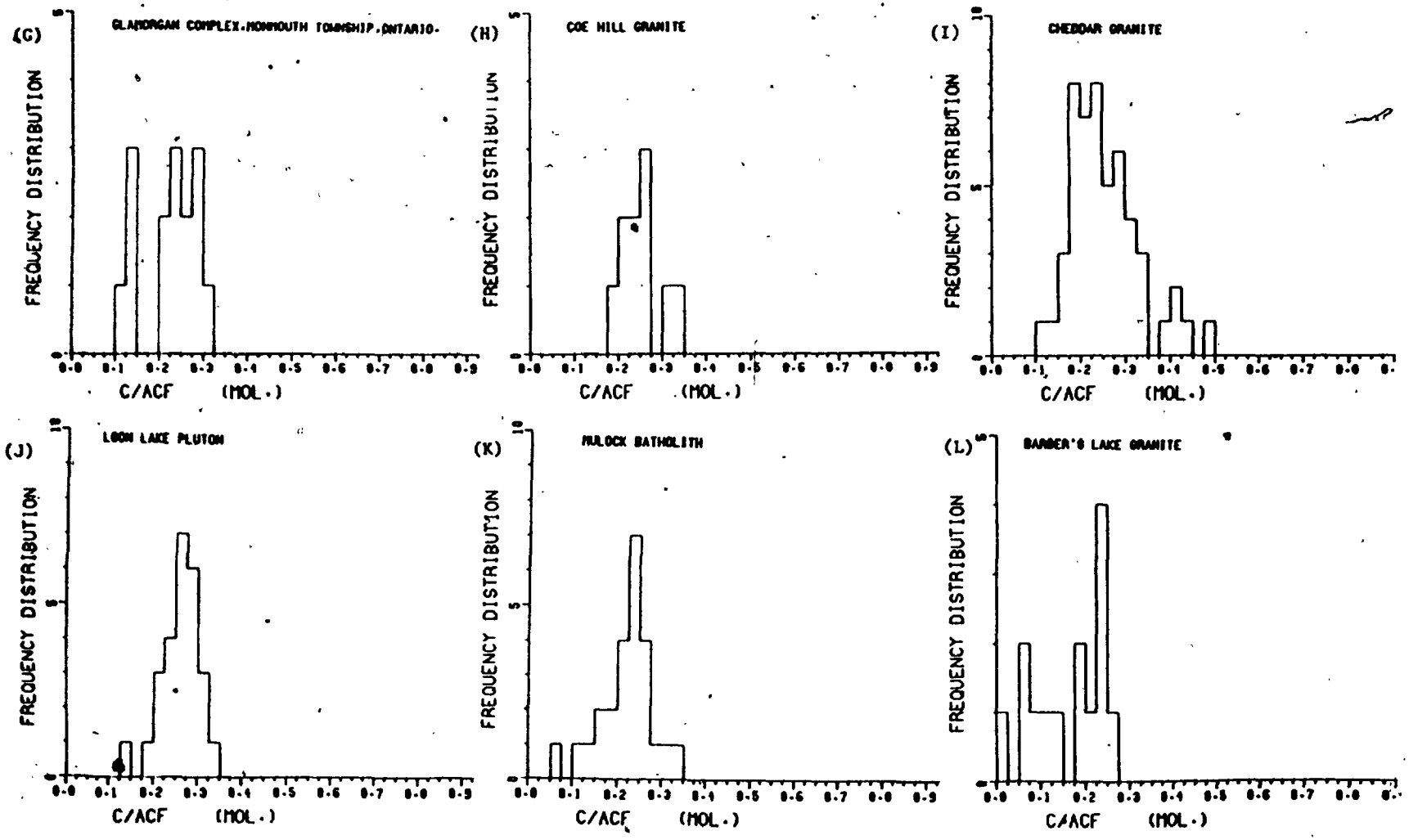

Barber's Lake Granite (mode 0.225) are considered to be S-type granitoids, based on their C/ACF ratios. Using the same criteria, both I- and S-types are common in the rest of Grenville granitoids, for example, the bimodal distribution in the Frontenac Axis Granites and Cheddar Granite. The Algonquin Batholith (Fig. 4-1-5D) forms a unimodal distribution between the two types with a median of 0.275.

In their original definition, Chappell and White (1974) defined the distinguishing boundary between I-type and S-type granitoids at about 1.1 in terms of molar ratio of aluminum to total alkali-lime. Frequency distributions of molar $Al_2O_3/(Na_2O+K_2O+CaO)$ for the Grenville granitoids are shown in Figure 4-1-6. There is some overlap between the felsic I-types and mafic S-types. Surprisingly, except for Barber's Lake Granite, several granitoids assigned to S-type granitoids by ACF plots and C/ACF ratios, now lie in the I-type granitoids (eg. Loon Lake Pluton and Mulock Batholith). It is also interesting to note that the tonalite-trondhjemite suite forms two distinct groups (See Fig. 4-1-6E) in the I-types field. Similarly, the Frontenac Axis Granites show bimodal distribution (Fig. 4-1-6C) and the Algonquin Batholith contains both types (Fig. 4-1-6D).

Because many sedimentary rocks are enriched in ^{18}O, relative to the mantle high ^{18}O values for plutonic rocks are considered to reflect crustal involvment or isotopic exchange during magma generation (Taylor, 1978). O'Neil and

Figure 4-1-6. Historgrams of molar $Al_2O_3/(Na_2O+K_2O+CaO)$ for typical I- and S-type granites and Grenville granitoids.

Data Sources :

Kosciusko Batholith (Hine et al., 1978)

Granites of Frontenac Axis (Sauerbrei, 1966)

Glamorgan Complex (Chesworth, 1967)

Loon Lake Pluton (Dostal, 1973)

Other granitoids (this study)

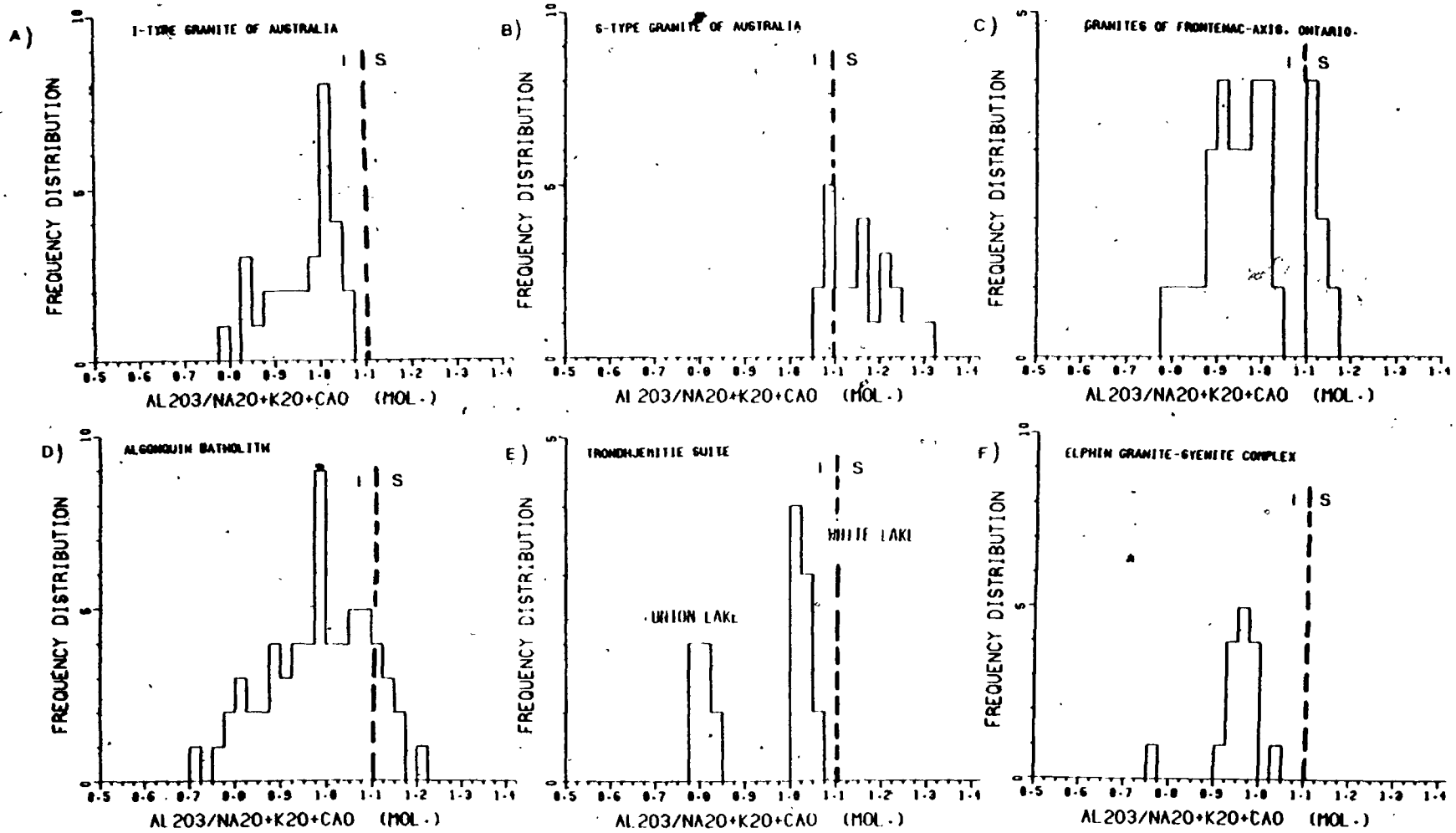
A)
I-TYPE GRANITE OF AUSTRALIA
B)
S-TYPE GRANITE OF AUSTRALIA
C)
GRANITES OF FRONTENAC-AXIS, ONTARIO.
D)
ALGONQUIN BATHOLITH
E)
TRONDHJEMITIE SUITE
UNION LAKE
WHITE LAKE
F)
ELPHIN GRANITE-SYENITE COMPLEX
I
S
FREQUENCY DISTRIBUTION
AL203/NA2O+K2O+CAO (MOL.)

(Figure 4-1-6. Cont'd)

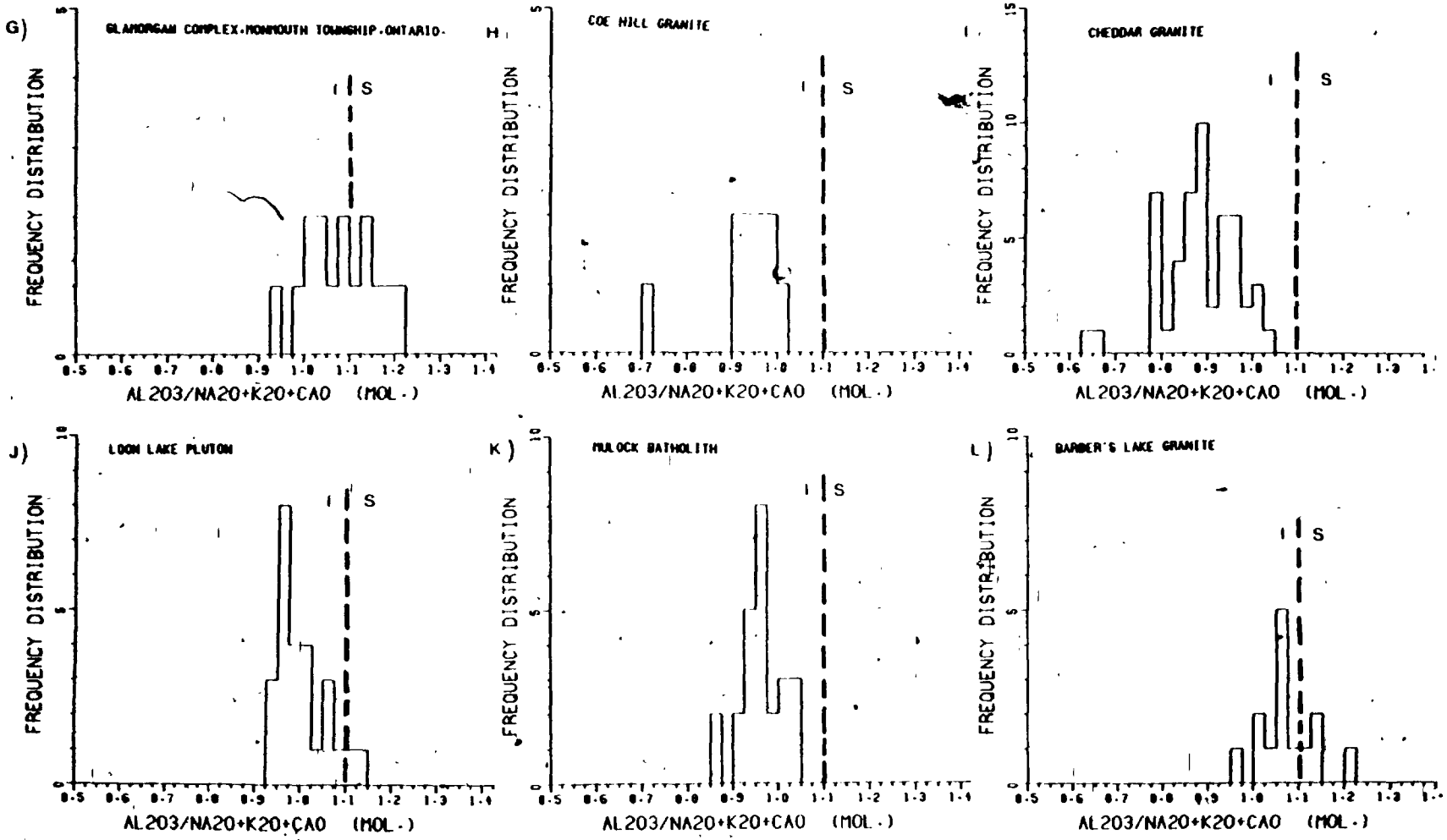

Chappell (1977) and O'Neil et al. (1977) proposed that it is possible to distinguish I- and S-type granites in the Lachlan Mobile Belt of Australia on the basis that S-type granites have $\delta^{18}O > +10$ o/oo whereas I-types have lesser values. Whole-rock $^{18}O/^{16}O$ ratios of the Grenville granitoids studied here together with the values of typical I- and S-type granites from Australia and isotopically "normal" granite from Taylor (1978) are summarized in Figure 4-1-7. Using these criteria, the Barber's Lake Granite, Coe Hill Granite and Frontenac-type granites have strong S-type oxygen isotope fingerprints, but most of the granitoids of the Grenville Province would be considered I-types. Both I- and S-type granites are present in the Loon Lake Pluton, Elphin Complex and Westport-type granites of Frontenac Axis. The isotopically "normal" granite (Taylor, 1978) should be classified as I-type.

In addition to oxygen isotope compositions, higher initial $^{87}Sr/^{86}Sr$ ratios of the plutonic rocks are also used to infer magma generation in the continental crust. Lower $^{87}Sr/^{86}Sr$ ratios are expected from the I-type granitoids (0.704 - 0.706, Chappell and White, 1974), reflecting an origin from mafic igneous sources. However, S-type granitoids may also have low initial ratios when they have originated by partial melting of younger volcanogenic sediments (eg. Flood and Shaw, 1977). Distribution of initial $^{87}Sr/^{86}Sr$ ratios from 31 determinations in the Grenville Province are given in Figure 4-1-8. Except for

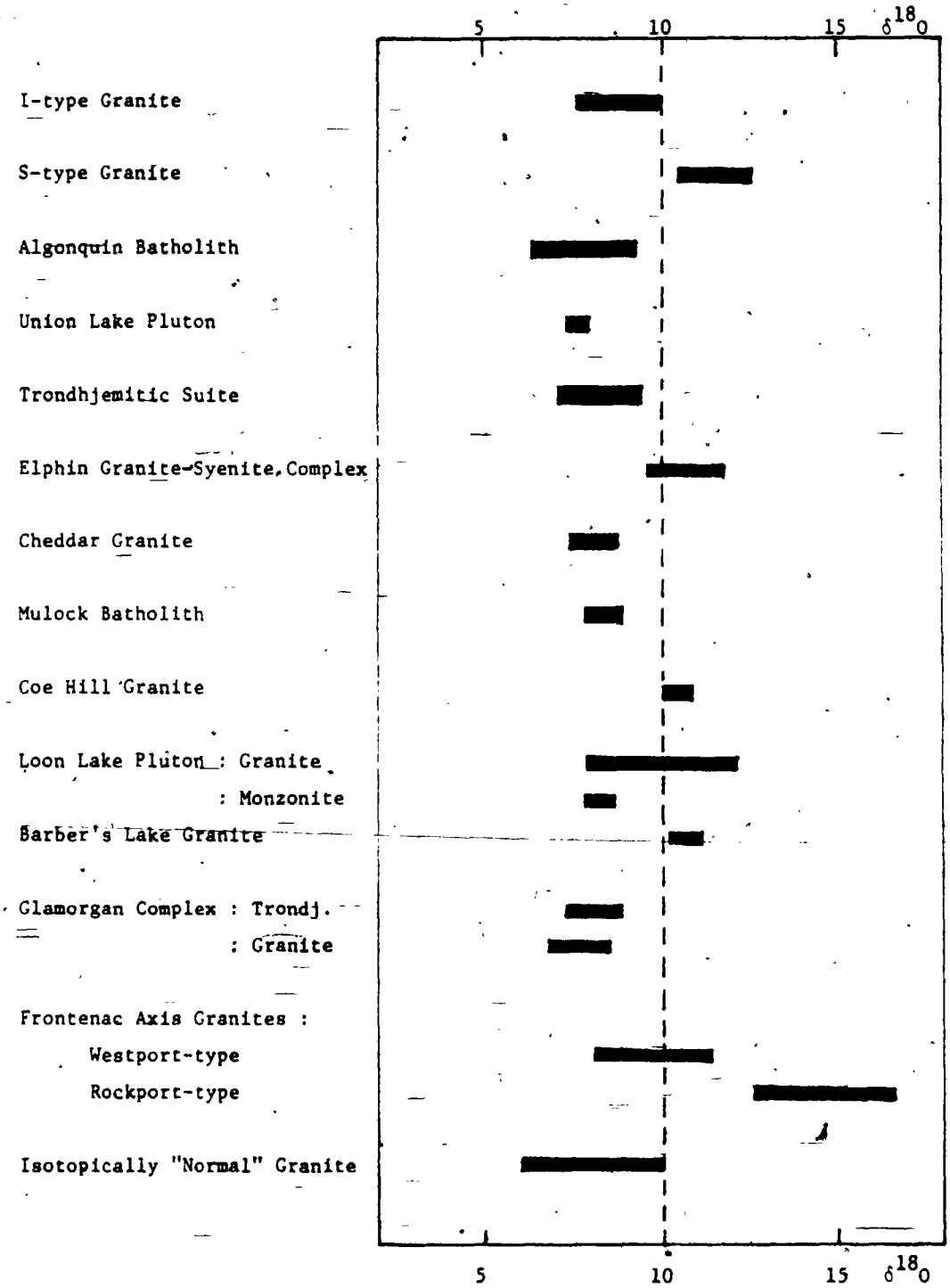

Figure 4-1-7. Comparison of the whole-rock $\delta^{18}O$ of the Grenville granitoids and I- and S-type granites of eastern Australia.

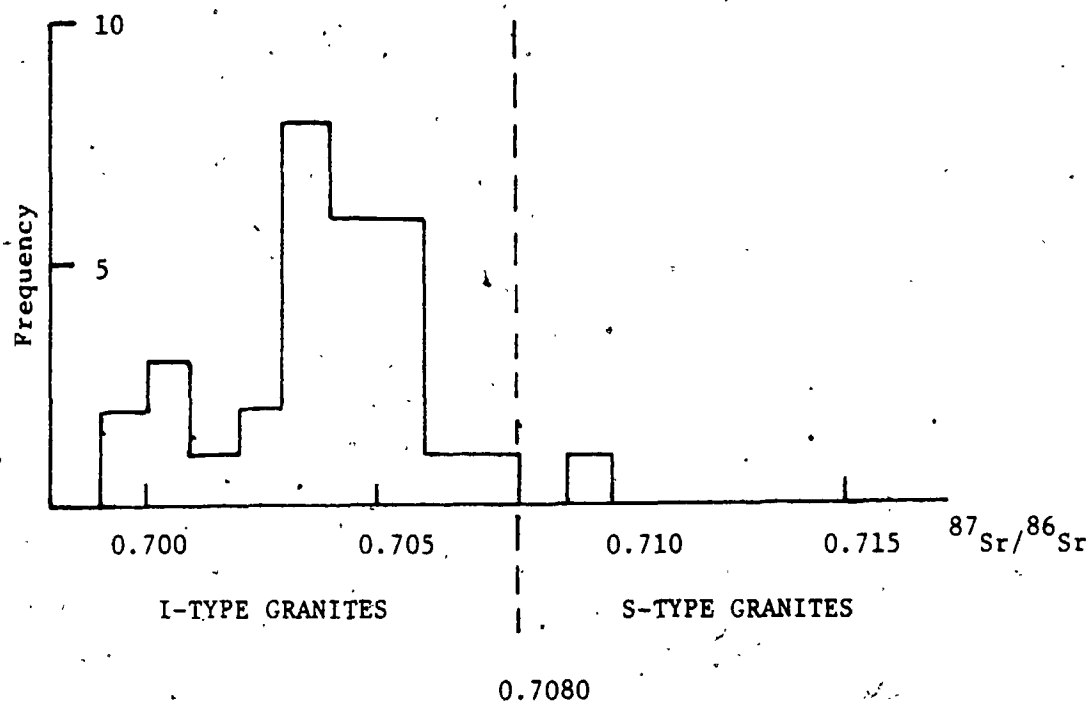

Figure 4-1-8. Distribution of initial $^{87}Sr/^{86}Sr$ ratios of the Grenville granitoids. (Data were compiled from : Bell and Blenkinsop, 1980; Davis et al., 1967; Doig, 1977; Fowler and Doig, 1983; Heaman et al., 1980; Krogh and Hurley, 1968; Krogh and Davis, 1969, 1970).

one granitoid which has $^{87}Sr/^{86}Sr$ ratio > 0.708 (Turgeon Lake Granite; Fowler and Doig, 1983), the remaining granitoids of the Grenville would be considered I-types.

In distinguishing between I- and S-type granitoids from the Grenville granites, emphasis has been placed on lithology, mineral assemblage, whole-rock chemistry and isotopic composition. A summary of correlations between Grenville granitoids and typical Australian I- and S-type granites using these chemical parameters are presented in Table 4-1-3. Except for the biotite diorite suite and associated trondhjemitic rocks (Union Lake and White Lake Pluton) which consistently fall within the I-type definition (Chappell and White, 1974), the remaining granitoids from the Grenville give both I- and S-type characteristics. There is no significant concordance between I- and S-type classification and the Grenville granitoids studied.

Sasaki and Ishihara (1978) and Czamamske et al. (1981) have pointed out that the discrepancies between the Cretaceous-Paleocene Inner Zone batholith of southwestern Japan and the I- and S-type granitoids originally defined in eastern Australia may result from diversities in chemical and isotopic characteristics of source regions. In other words, the granitic terranes of Australia and Japan each have their own "unique" geological features. The anomalously high oxidation indices, the alkalic affinity and consistent low initial $^{87}Sr/^{86}Sr$ ratios of the Grenville granitoids may indicate an unusual environment for

Table 4-1-3. Summary of correlations between Grenville Granitoids and typical I- and S- type granites in eastern Australia

Parameters / Granitoids	Mineralogy	ACF Plot	Al/(Na+K+Ca/2) (molar)	C/ACF (molar)	$Fe^{3+}/Fe^{3+}+Fe^{2+}$ (atom)	K/Na+K (atom)	$\delta^{18}O$
Algonquin Batholith	I	I + S	I + S	I + S	I + S	I	I
Union Lake Pluton	I	I	I	I	I	I	I
White Lake Pluton	I	I	I	I	I	I	I
Elphin Complex	I	I + S	I	I + S	I	I + S	I + S
Coe Hill Granite	I	I + S	I	S	I + S	I	S
Loon Lake Pluton	I	S	I	S	I	S	I + S
Mulock Batholith	I	S	I	S	I	I	I
Cheddar Granite	I	I + S	I	I + S	I	I + S	I
Barber's Lake Granite	S	S	S	S	I	I	S
Glamorgan Complex	I	S	I + S	S	I	I + S	I
Frontenac-Axis Granites:							
1. Westport-type	I	S	I	I + S	I	I + S	I + S
2. Frontenac-type	I	I	I	I + S	I	I + S	S
3. Rockport-type	I	I	S	I + S	I	I + S	S

a. I - I-type affinity.
b. S - S-type affinity.
c. $Fe^{3+}/Fe^{3+}+Fe^{2+}$ (atom) and K/Na+K (atom) are other chemical parameters for distinguishing I and S-type granitoids (Takahashi et. al., 1980)

generation of granitic magmas beneath the Grenville Province. Besides, a great deal of tectonic mobility has occurred during formation of Phanerozoic batholiths in terms of subduction along a destructive plate boundary.

2.0 COMPARISONS OF CONTINENTAL MARGIN SUITES AND GRENVILLE GRANITOIDS

2.1 Geochemical Characteristics Of Marginal Batholiths

Recent studies indicate that the majority of batholithic granitoids are products of orogenic activities along plate boundaries, either generated in the subduction zones at ocean-continent boundaries (eg. Andean-type) by partial melting of upper mantle wedge and/or subducted oceanic slab, or produced in the collision zones at continent-continent boundaries (eg. Himalaya-type) by partial fusion of the thickened continental crusts. In terms of geochemical studies, only limited data are available for the collision-type igneous suites, whereas both major- and trace-element concentrations and their distributions of the continental margin batholiths associated with andesitic magmatism have been broadly investigated at a variety of locations. For further discussions, data from (1) typical continental margin suites: Klamath Mountains (Hotz, 1971), East-Central Sierra Neveada (Bateman et

al., 1963), Toulumne Intrusive Series (Bateman and Chappell, 1979), Eastern Alaska Range Batholith (Richter et al., 1975), Guichon Creek Batholith (Olade, 1976), Ben Ghnema Batholith (Rogers et al., 1980), (2) magmatic-arc plutonic rocks: intrusive rocks of New Guinea (Hine and Mason, 1978), plutonic rocks of Antarctic Peninsula (Saunders et al., 1980), and (3) Kangdese Magmatic Belt of Tibet (Academia Sinica, 1980), were used for illustrations and comparisons.

The marginal batholithic rocks range in composition from gabbro, diorite, tonalite, granodiorite to true granite, which is commonly parallel to their extrusive counterparts; however, the former has a higher proportion of intermediate silicic rocks relative to basic ones. Chemically, the igneous rocks from convergent plate boundaries are characterized by calc-alkaline composition. However, with increasing maturity of convergence with respect to the degree of envolvement of continental basement, the calc-alkaline marginal magmatism may migrate to alkalic-calcic or alkalic affinity (Brown, 1979, 1982).

In the AFM diagrams (Fig. 4-2-1), typical calc-alkaline series show smooth variation trends with low to moderate iron-enrichment relative to MgO and total alkalis. Such compositional variations can be explained by fractional crystallization of Fe-Mg-rich mineral phases (eg. olivine, pyroxene and amphibole)

Figure 4-2-1. AFM diagrams for batholithic suites from various tectonic settings.

(A) Continental margin batholiths :

A1. Klamath Mountain Series (Hotz, 1971)

A2. East-Central Sierra Nevada (Bateman et al., 1963)

A3. Tuolumne Intrusive Series (Bateman and Chappell, 1979)

A4. Eastern Alaska Range (Richter et al., 1975)

A5. Guichon Creek Batholith (Olade, 1976)

A6. Ben Ghnema Batholith (Rogers et al., 1980)

(B) Magmatic arc plutons :

B1. Intrusive rocks of New Guinea (Hine and Mason, 1978)

B2. Plutonic rocks of Antarctic Peninsula (Saunders et al., 1980)

(C) Collision-type plutonic rocks (Kangdese Magmatic Belt of Tibet)

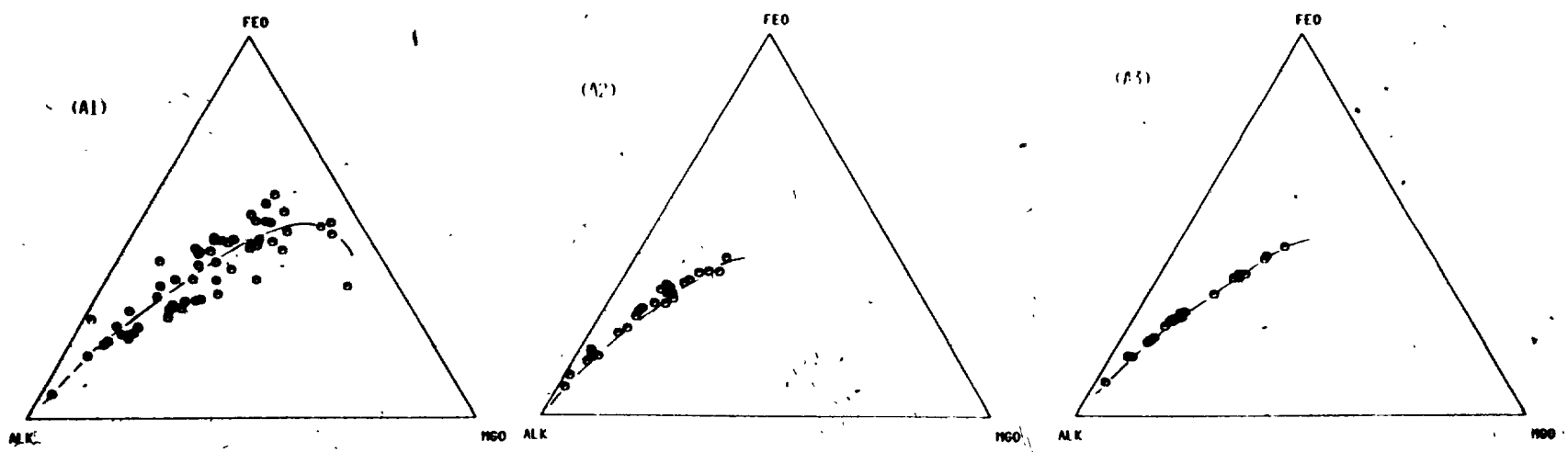

(Figure 4-2-1. Cont'd)

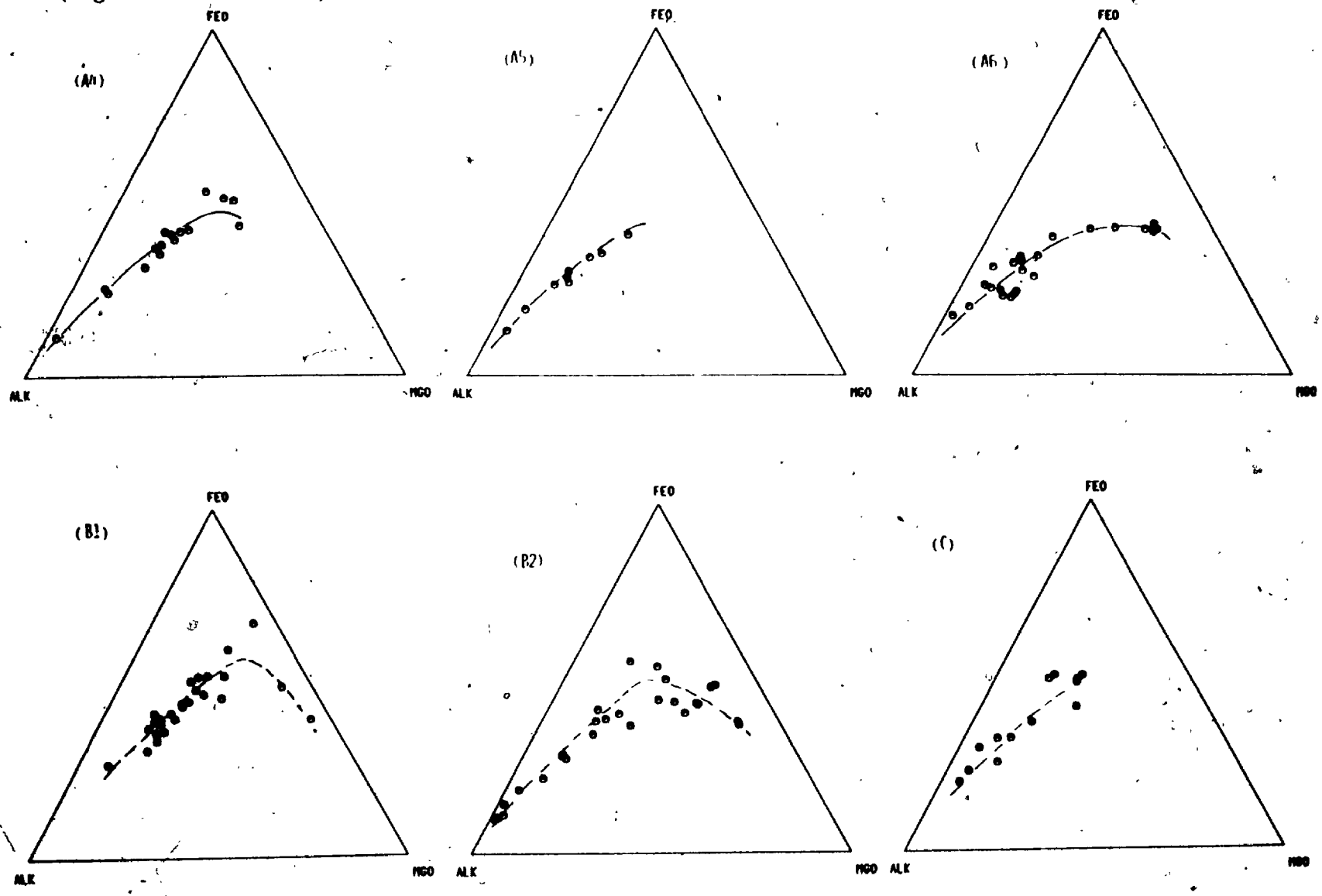

(Brown, 1982); this may also explain the general depletion of Cr and Ni abundances in the calc-alkaline suite. Notably, rocks from modern magmatic-arcs (Fig. 4-2-1, B1 and B2) show distinct convex patterns with relatively stronger iron-enrichment and higher initial MgO contents, suggesting their primitive nature and less involvement of crustal component. This difference between marginal batholiths and magmatic-arc plutons is also shown in the MgO vs. Fe_2O_3 (as total iron) variation plots (Fig. 4-2-2). The former shows a trend of exponentially increasing total iron with increasing MgO, while the latter, similar to those of island-arc tholeiites (Dixon and Batiza, 1979), forms an arc distribution with a high at about 12% Fe_2O_3 and decreasing Fe_2O_3 towards the high MgO end-member (Fig. 4-2-2, B1 and B2). In contrast, there is a linear relationship for rocks of the Kangdese suite of Tibet (Fig. 4-2-2C).

In addition to AFM diagrams, the relationships between K_2O and SiO_2 (the so-called "K-h" variation) in andesitic volcanic suites have been widely adopted for tectonic interpretations in terms of depth to the subduction zone and crustal thickness (Dickison, 1975). The K_2O - SiO_2 relations for batholithic suites from convergent boundaries are shown in Figure 4-2-3. It is noted that there is a general linear trend of increasing K_2O with increasing SiO_2 for granitoids from continental

Figure 4-2-2. MgO vs. Fe_2O_3 (total iron) plots for batholithic suites from various tectonic settings.

(A) Continental margin batholiths :

A1. Klamath Mountains Series (Hotz, 1971)

A2. East-Central Sierra Nevada (Bateman et al., 1963)

A3. Tuolumne Intrusive Series (Bateman and Chappell, 1979)

A4. Eastern Alaska Range (Richter et al., 1975)

A5. Guichon Creek Batholith (Olade, 1976)

A6. Ben Ghnema Batholith (Rogers et al., 1980)

(B) Magmatic arc plutons :

B1. Intrusive rocks of New Guinea (Hine and Mason, 1978)

B2. Plutonic rocks of Antarctic Peninsula (Saunders et al., 1980)

(C) Collision-type plutonic rocks (Kangdese Magmatic Belt of Tibet)

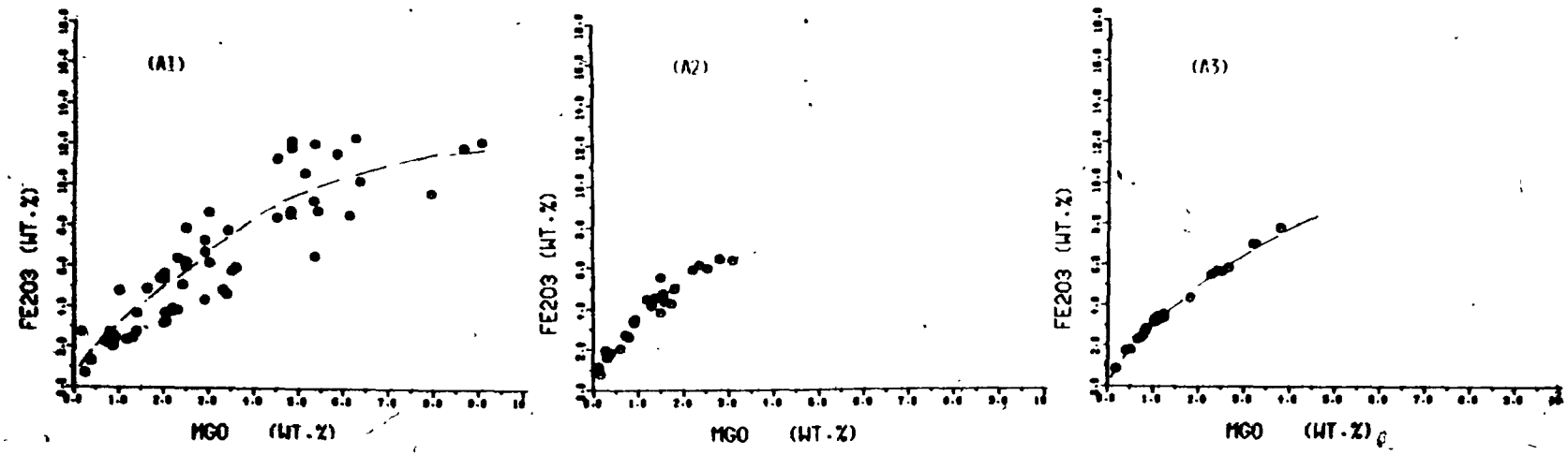

(Figure 4-2-2. Cont'd)

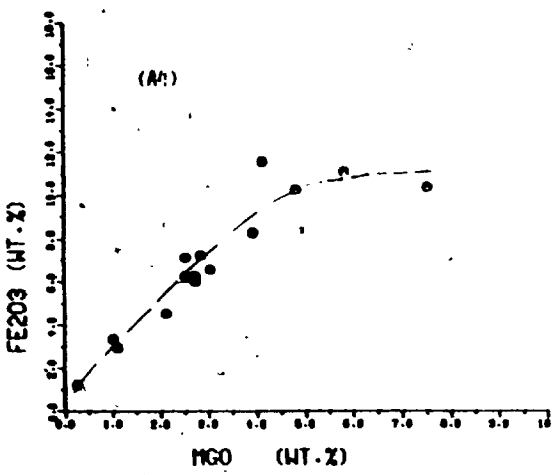

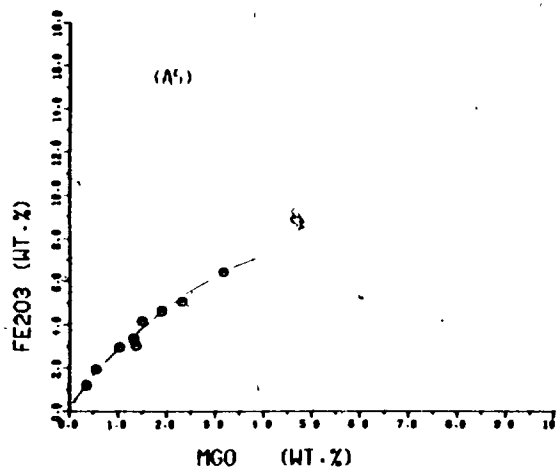

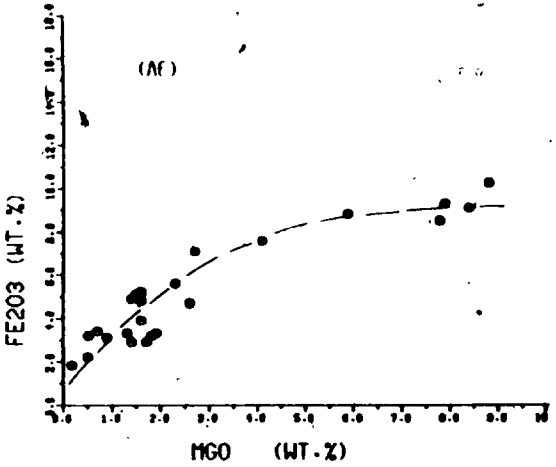

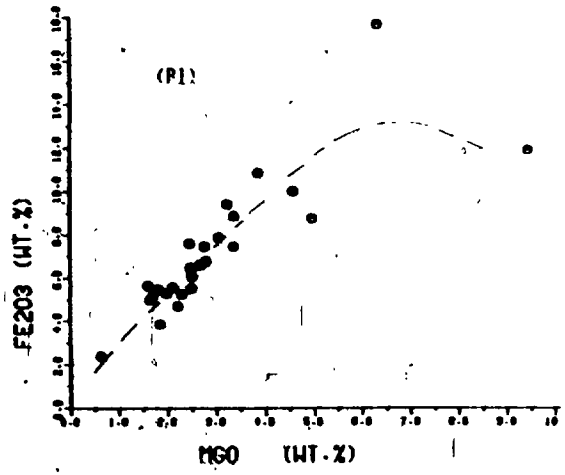

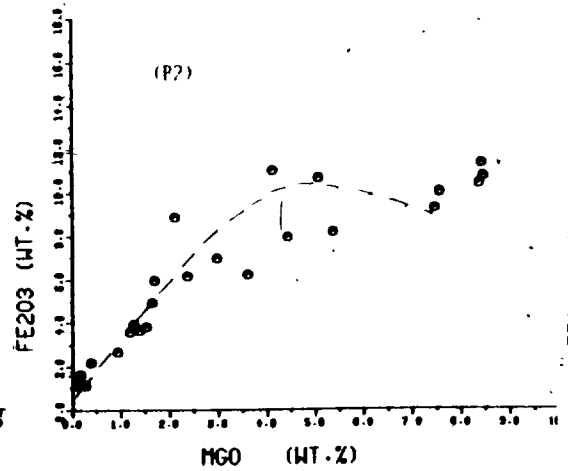

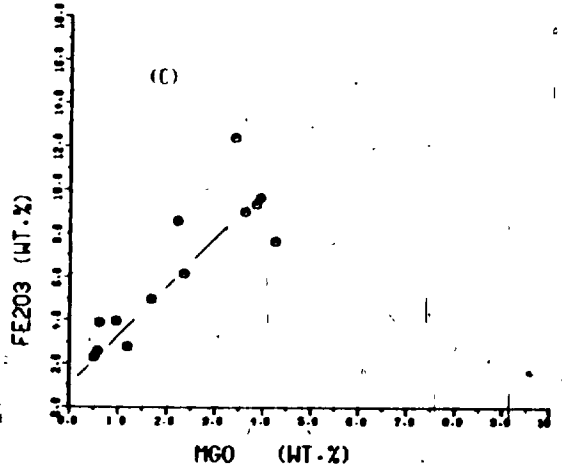

margins (Fig. 4-2-3, A1-A6), whereas K_2O concentrations increase exponentially with respect to SiO_2 for plutonic rocks from modern magmatic-arcs (Fig. 4-2-3, B1 and B2). Commonly, the K_2O content at 60% SiO_2 was used as an indicator for depth to subduction and thickness of continental crust; that is, the latter ones are linear proportional to the former (Rogers and Novitsky-Evans, 1977). For continental margin suites (Fig. 4-2-3, A1-A6), the K_2O contents at 60% SiO_2 range from 1.5 to 3.0 wt%, while it is less than 1% for magmatic-arc suites. By extrapolation from Rogers and Novitsky-Evans (1977), estimates of depth to subduction zone lie between 180 and 125 km for continental margin batholiths, but less than 100 km for magmatic-arc suites. Similarly, estimates of crustal thickness are 20 to 65 km for marginal batholiths and < 15 km for arc suites. However, data from Kangdese suite of continental collision zone are somewhat scattered (Fig. 4-2-3C); it is believed that both the depth to subduction and thickness of crust are much greater than those of marginal suites.

During the past decade, systematic studies of trace-element variations in the batholithic granitoids along converging boundaries were also carried out (eg. Rodgers et al., 1980; Saunders et al., 1980). Although variations of individual trace-element may differ from one pluton to another, there are general trends of

Figure 4-2-3. K_2O vs. SiO_2 relationships for batholithic suites from various tectonic settings.

(A) Continental margin batholiths :

A1. Klamath Mountains Series (Hotz, 1971)

A2. East-Central Sierra Nevada (Bateman et al., 1963)

A3. Tuolumne Intrusive Series (Bateman and Chappell, 1979)

A4. Eastern Alaska Range (Richter et al., 1975)

A5. Guichon Creek Batholith (Olade, 1976)

A6. Ben Ghnema Batholith (Rogers et al., 1980)

(B) Magmatic arc plutons :

B1. Intrusive rocks of New Guinea (Hine and Mason, 1978)

B2. Plutonic rocks of Antarctic Peninsula (Saunders et al., 1980)

(C) Collision-type plutonic rocks (Kangdese Magmatic Belt of Tibet)

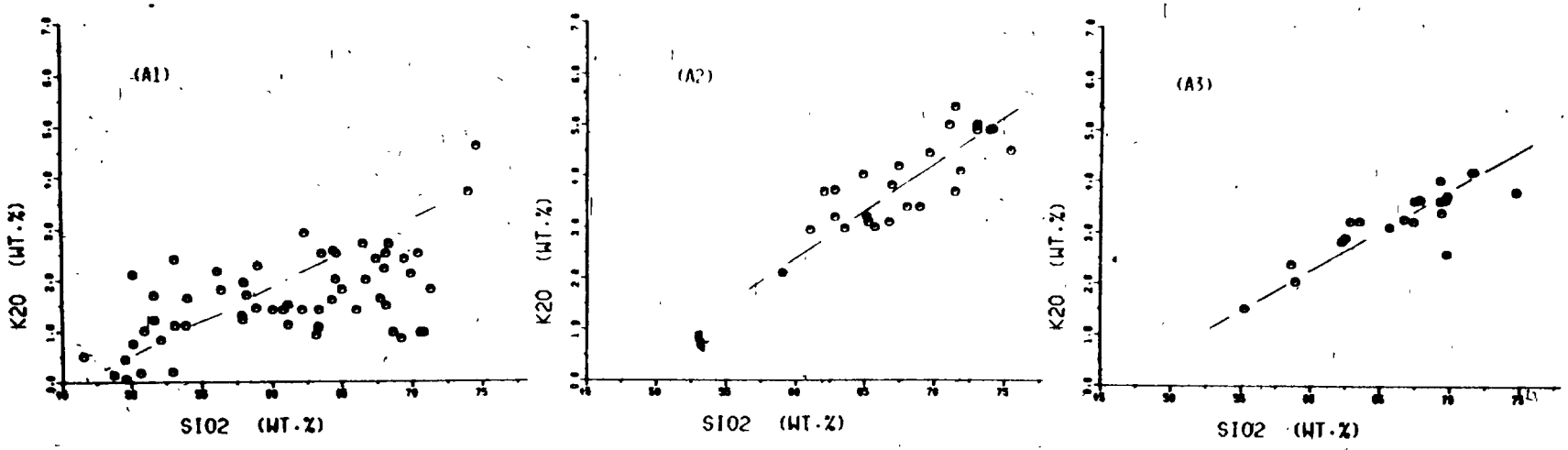

(Figure 4-2-3. Cont'd)

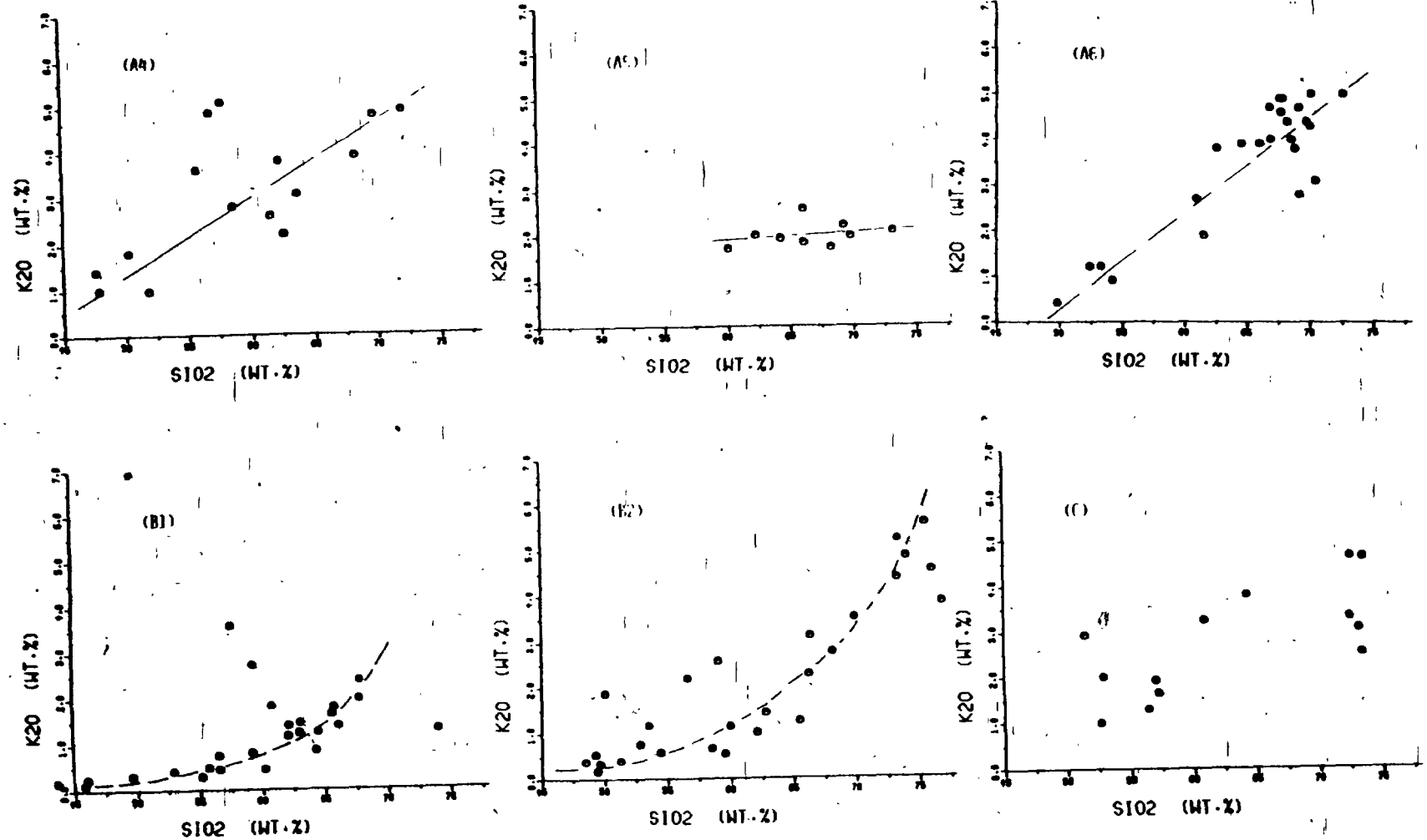

increasing large-ion-lithophile (LIL) elements (eg. Rb, Ba, Th, U), decreasing abruptly compatible elements (eg. Cr, Ni, V) and constant or decreasing high-field strength (HFS) elements (eg. Zr, Nb, Y) toward the more silicic end-members. Saunders et al. (1980) proposed that the high LIL/HFS element ratios in the calc-alkaline magma along the continental margins are primary features due to dehydration processes of the subducted slab in which the HFS-retaining phases (eg. rutile, zircon, apatite) remain as residue. Moreover, REE are moderately fractionated with low $(Ce/Yb)_N$ ratios about 2-10 and chondrite-normalized Yb values < 25. Negative Eu-anomalies are commonly developed in the more silicic rocks (Rogers et al., 1980; Croudace, 1980).

2.2 Comparison Of Algonquin Batholith And Marginal Batholithic Rocks

Geochemically, the Algonquin Batholith is composed of two compositional and comagmatic trends, that is, the diorite - tonalite - trondhjemite association and syenite - granite association (See Chap. II Section 2.0). The alkali-lime index of the former is about 59% SiO_2 indicating a calc-alkaline affinity, while the latter is alkali-calcic in composition. In the AFM diagram (Fig. 4-2-4A), the sodic rocks show a moderate iron-enrichment trend, whereas the potassic ones tend to

Figure 4-2-4. (A) AFM diagram (B) Fe_2O_3 vs. MgO (C) K_2O vs. SiO_2 plots of the Algonquin Batholith

(A1) Potassic differentiation association

(A2) Sodic differentiation association

Dashed-lines show chemical variation trends within each rock-association.

(A1)

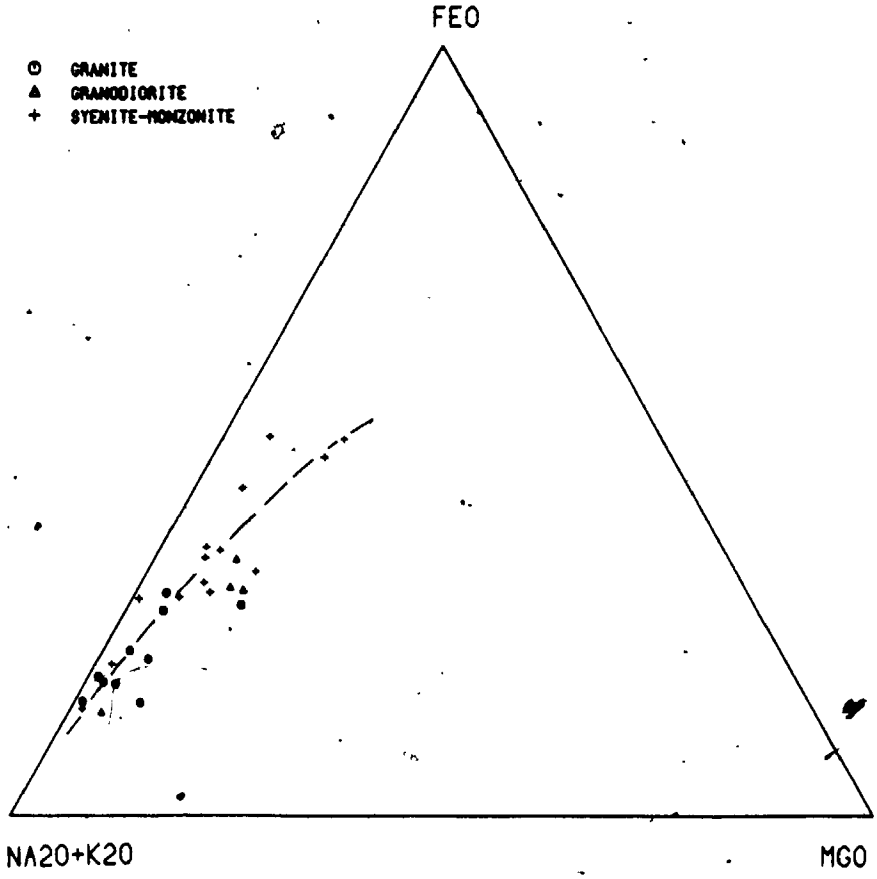
FEO
GRANITE
GRANODIORITE
SYENITE-MONZONITE
NA2O+K2O
MGO

(A2)

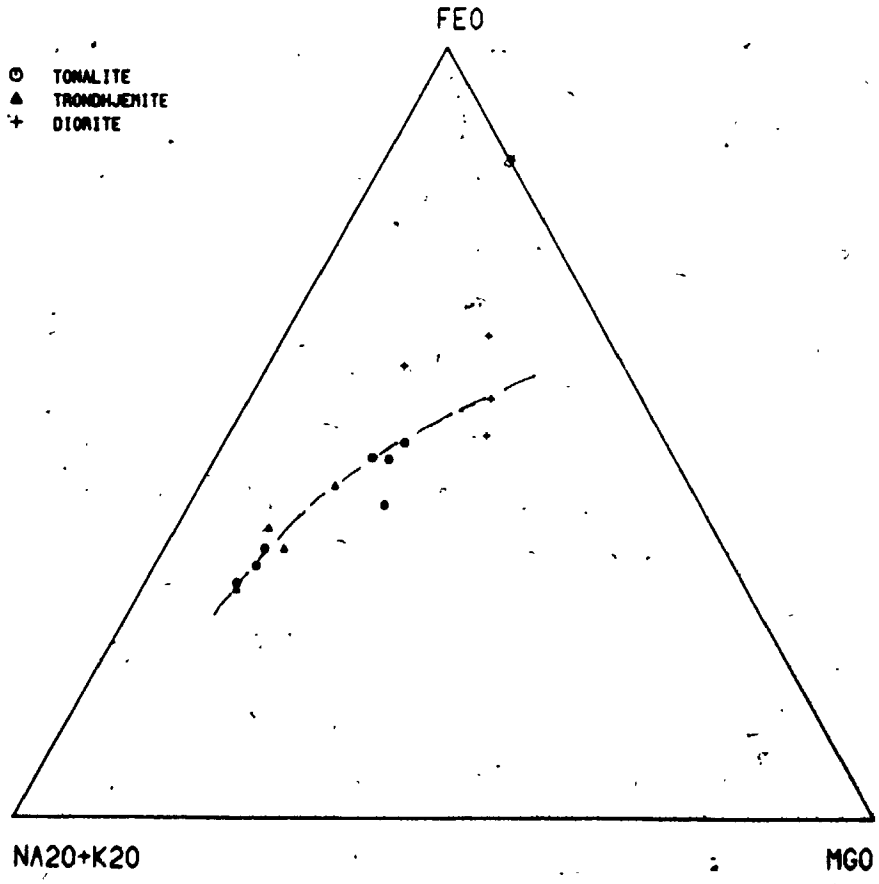
FEO
TONALITE
TRONDHJEMITE
DIORITE
NA2O+K2O
MGO

(Figure 4-2-4. Cont'd)

(B1) ALGONQUIN BATHOLITH - POTASSIC DIFFERENTIATION ASSOCIATION

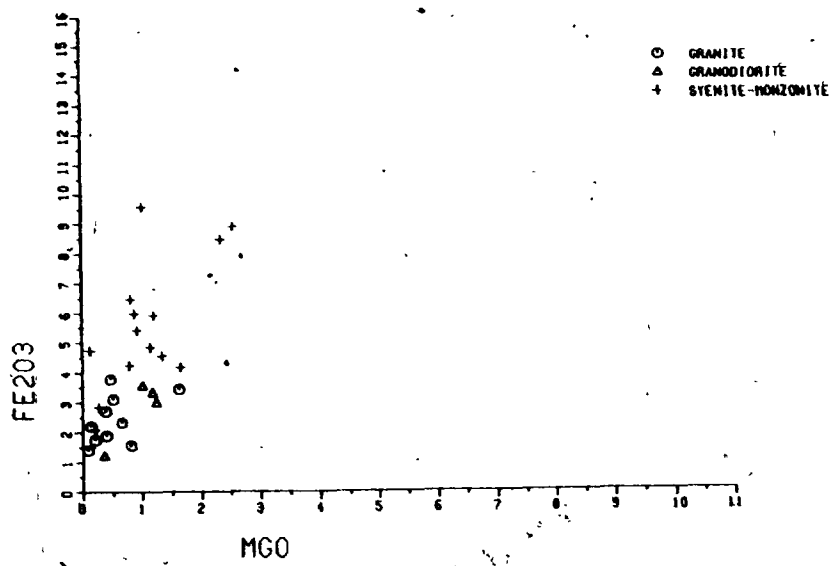

(B2) ALGONQUIN BATHOLITH - SODIC DIFFERENTIATION ASSOCIATION

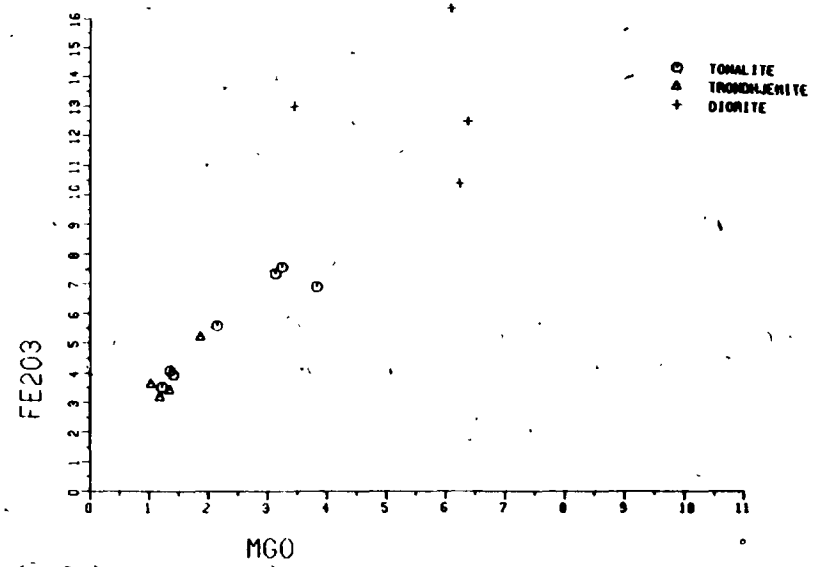

(C1)

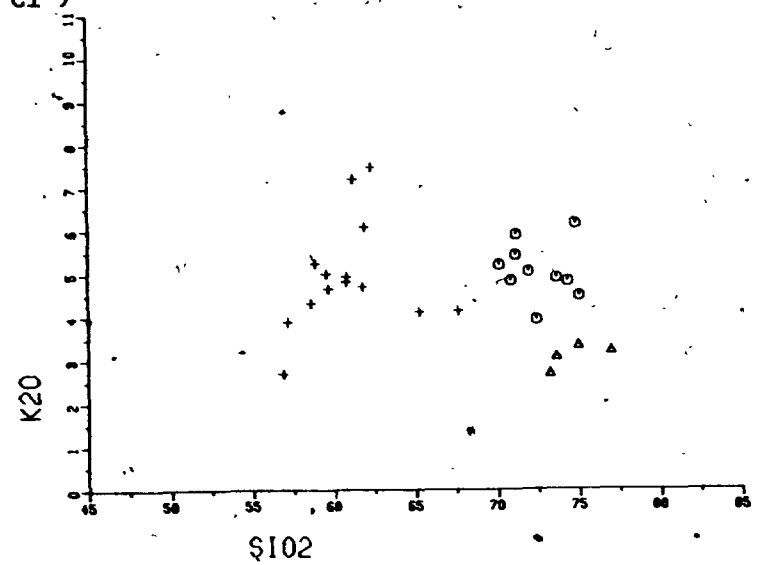

(C2)

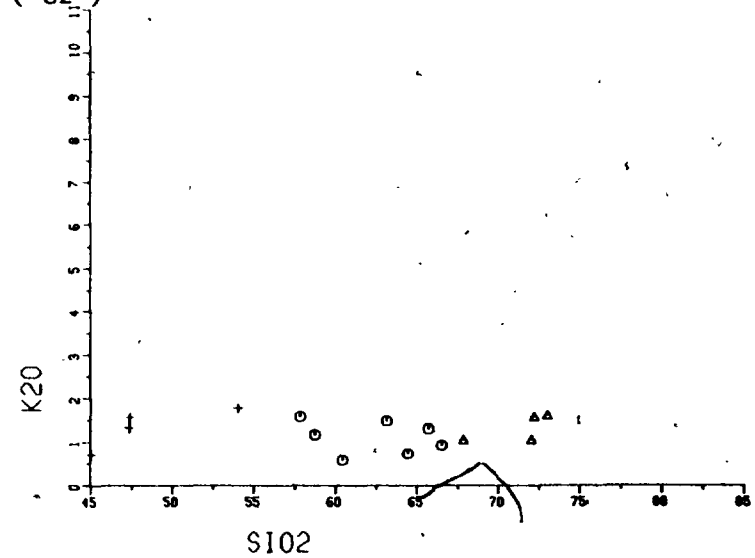

cluster towards the alkali apex. Similarly, in Fe_2O_3 vs. MgO and K_2O vs. SiO_2 plots (Fig. 4-2-4 B,C), the diorite - tonalite - trondhjemite suite shows comparable trends to continental margin batholithic rocks, while the syenitic - granitic rocks are scattered and show opposite trends to each other.

Lumbers (1982) suggested that the Algonquin Batholith intruded the shallow watwr facies of trough sedimentary sequences of Huronian age. The resemblance of REE normalized patterns of sodic rocks with the Proterozoic gabbro - diorite - tonalite - trondhjemite suite of SW Finland suggests an early age of emplacement, possibly a continuation of Archean calc-alkaline magmatism, while the later potassic intrusions are probably related to the major transcontinental anorogenic (within-plate) plutonic magmatism at about 1.4 to 1.5 Ga (Silver et al., 1977). There is no physical evidence of an existing craton margin at the time of emplacement of Algonquin diorite - tonalite - trondhjemite suite; however, the calc-alkaline affinity and some geochemical parameters support at least the contention that they were intruded in a similar environment.

2.3 Comparison Of New England Granites And Grenville Granitoids

Except for the Algonquin Batholith, most of the sampled Grenville granitoids have a narrow range of composition. This makes it difficult to compare Grenville granitoids with plutonic rocks from plate boundaries by using the foregoing geochemical parameters. Nevertheless, comparisons were made between the Paleozoic plutonic rocks of New England, U.S.A. and sampled Grenville granitoids, excluding the Deloro peralkaline granite, in terms of regional and plutonic geology, petrography and chemical data.

2.3.1 Intrusive Styles And Regional Metamorphism -

New England granites are frequently found as thin (< 2 km) horizontal plutonic masses. They are not commonly zoned but closely associated with pegmatites (Neilson et al., 1976; Wones, 1980). The existence of pegmatites may suggest a relatively high water content and less viscous magma with faster settling rates which led the plutons to have a more homogeneous appearance.

With respect to regional deformation, the New England plutons can be classified into four "Magma Series": Highlandcroft (the pre-Silurian),

Oliverian (a pre-tectonic), New Hampshire (syn-tectonic) and White Mountain (post-tectonic) (Wones, 1980). Although regional metamorphism is irregular and mainly fault-controlled, there is a general trend from high pressure in the southwest to low pressure in the northeast (Thompson and Norton, 1968).

Granitoids of the Grenville Province are commonly of mesozonal to catazonal emplacement with the exceptions of peralkaline granite and later intrusions. Most plutons are marked by sharp intrusive contacts, although gradational contacts are also encountered locally. Pegmatitic phases are not common for Grenville granitoids which supports P_{H2O} - undersaturated conditions during crystallization. In addition, compositionally zoned plutonic complexes are uncommon ; however, inclusions of country rocks are usually found in the contact zones. Pinkish colour, mainly due to oxidation of feldspar, and medium-grained, homogeneous appearance, due to recrystallization by metamorphism, are characteristic of the Grenville granitoids.

As regards the climax of Grenville Orogeny, the granitoids can be grouped into: pre-tectonic, syn-tectonic, late-tectonic and post-tectonic intrusions. Except for the Hastings Basin with

greenschist facies, regional metamorphism in the Grenville Province is realtively uniform with a prevailing amphibolite facies; however, a regional gradient may exist from the upper amphibolite facies in the northwest to the granulite facies in the southeast (the Frontenac Axis).

2.3.2 Petrographic Comparisons -

Most of New England plutons are alkaline granites with low plagioclase contents; 47.6% of these plutons are muscovite-bearing, 33.6% hornblende-bearing and 18.7% biotite-bearing only (Wones, 1980). Except for the diorite - tonalite - trondhjemite suite, the majority of Grenville granitoids are alkaline or sub-alkaline with moderate plagioclase contents. However, in contrast, biotite and hornblende are the predominant mafic minerals in Grenville granitoids; primary muscovite is only present in the late, uraniferous Barber's Lake Granite.

The plagioclase/total feldspar ratio and colour index (=biot.+hb.+px.+sph.+opques) are fundamental parameters for illustrating the modal characteristics of granitoids. Histograms of feldspar ratio and colour index for sampled Grenville granitoids and New England granites are

shown in Figure 4-2-5, A and B, respectively. Although the Grenville granitoids have relatively higher feldspar ratios with a mode of 0.5, the marked bimodal distribution pattern is closely similar to those post-Silurian granites in New England (Fig. 4-2-5A). On the other hand, sampled Grenville granitoids retain less mafic components with a mode of colour index < 5, while those of New England plutons have a mode of about 6 (Fig. 4-2-5B).

2.3.3 Chemical Compositions -

For simplicity, three chemical parameters, SiO_2, CaO and the $K_2O/(K_2O+Na_2O)$ ratio (Wones, 1980), were chosen for comparisons. Histograms of these parameters for both sampled Grenville granitoids and New England granites are shown in Figure 4-2-6. The SiO_2 contents of both granites are bimodal, 59% and 74%. for Grenville granitoids and 69% and 75% for the New England ones (Fig. 4-2-6A). For CaO contents, the Grenville granitoids have a mode about 0.5% and strongly skew to the high CaO side (Fig. 4-2-6B), whereas the New England Plutons have a mode of about 0.8%. Again, the $K_2O/(K_2O+Na_2O)$ values of rocks from the two areas show great similarities with a unimodal distribution (Fig. 4-2-6C); however, the New England granites

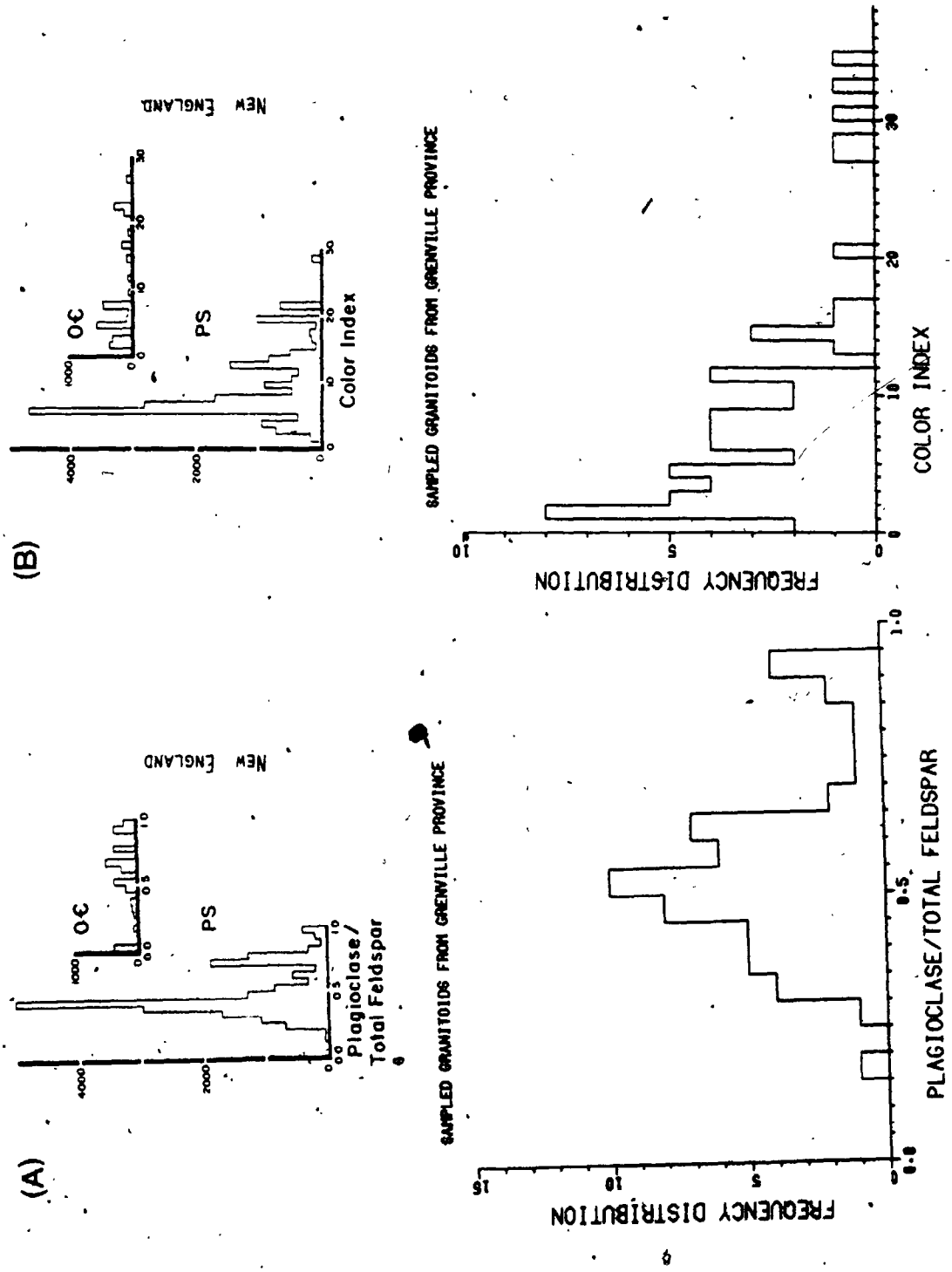

Figure 4-2-5. Comparison of feldspar ratios and colour indices of sampled Grenville granitoids with those of New England plutonic rocks (from Wones, 1980; PS = Silurian through Permian age; OЄ = Pre-Silurian age).

Figure 4-2-6. Comparison (A) SiO_2 (B) CaO and (C) $K_2O/(K_2O+Na_2O)$ of sampled Grenville granitoids with those of New England plutonic rocks (from Wones, 1980).

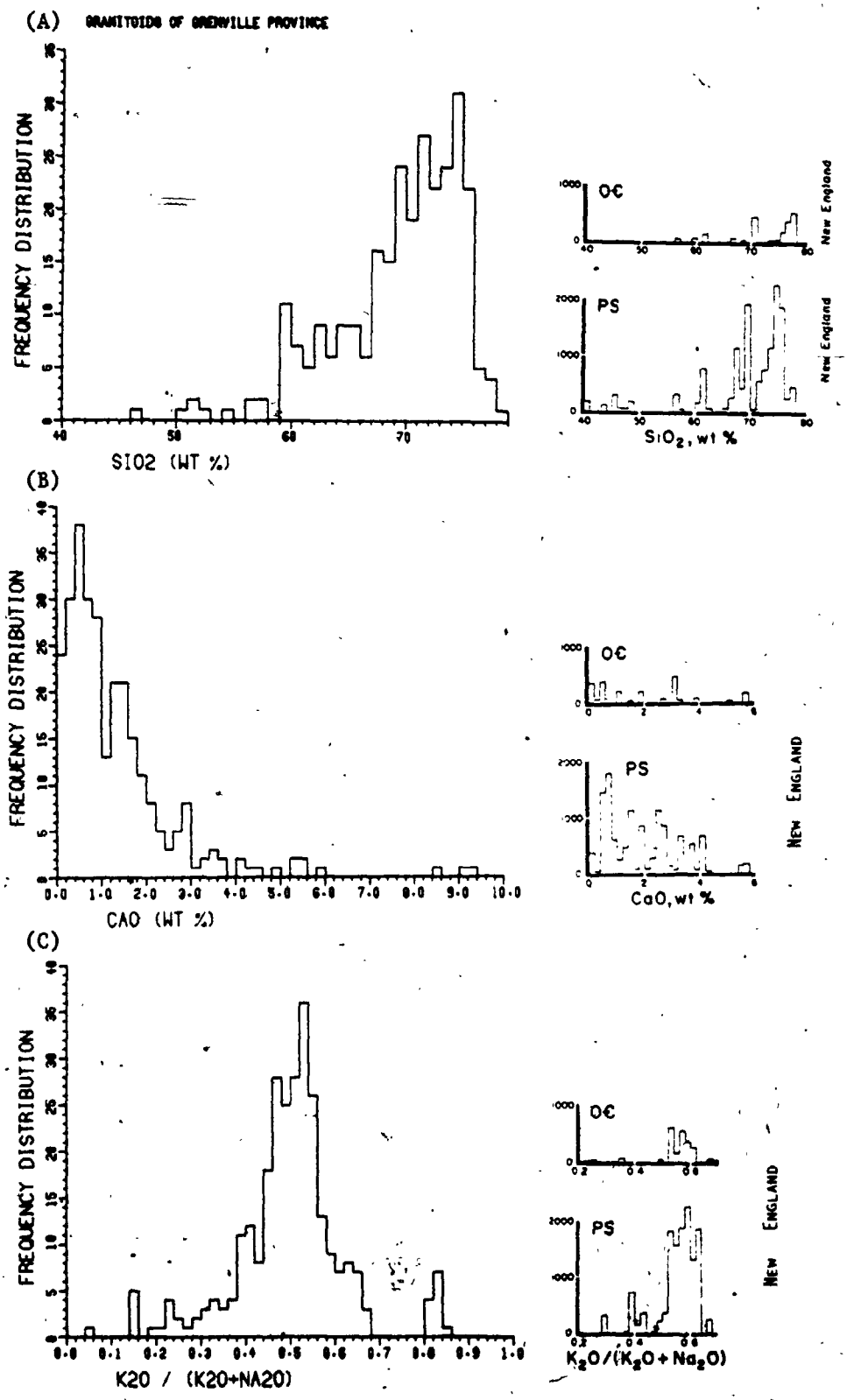
(A) GRANITOIDS OF GRENVILLE PROVINCE
FREQUENCY DISTRIBUTION
SIO2 (WT %)
OC
PS
New England
SiO_2, wt %
(B)
FREQUENCY DISTRIBUTION
CAO (WT %)
OC
PS
New England
CaO, wt %
(C)
FREQUENCY DISTRIBUTION
K20 / (K20+NA20)
OC
PS
New England
$K_2O/(K_2O+Na_2O)$

contain relatively higher K_2O than those of the Grenville.

In addition to low CaO, high SiO_2 and the presence of primary muscovite, the initial $^{87}Sr/^{86}Sr$ ratios for New England granites ranging from 0.703 to 0.710 indicate a high proportion of sedimentary source material, though some have a clear igneous origin (Wones, 1980). For Grenville granitoids, the presence of hornblende and initial $^{87}Sr/^{86}Sr$ ratios less than 0.706 indicate that they predominantly crystallized from magmas derived mainly from upper mantle and lower crust.

Despite the differences of intrusive styles, regional metamorphism and Sr-isotopes, there are petrographic (eg. feldspar ratio and colour index) and chemical similarities between New England granitic plutons and Grenville granitoids, which may suggest a comparable geological setting.

Siliceous plutons along eastern North America are believed to be associated with closure of the Iapetus Ocean by subduction of oceanic crust beneath the North America continent. Early models suggested plutonic rocks of Paleozoic age in New England intruded the continent and continental shelves along both sides of the suture (Osberg, 1978). However, recent studies of plutonism indicate that the suture zones were not zones

of subduction but zones of transform faults (Thomas, 1977) or zones of oblique subduction (Wones, 1980). Further investigations of Ordovician and Silurian volcanic rocks of the area (Aleinikoff, 1977; Moench and Gates, 1976) showing bimodal chemistry and absence of calc-alkaline volcanism suggest rift zones rather than zones of subduction. It is also suggested that New England is possibly of allochthonous origin due to the unrelated stratigraphy and plutonism to the surroundings (Wones, 1980).

2.4 Grenville Magmatism And Tectonic Settings

The past two decades of geological research have clearly shown that the Earth is dynamic. Interrelationships of mobile lithospheric plates define two distinct tectonic settings each characterized by diagnostic magmatism. That is, (1) the orogenic (calc-alkaline) magmatism associated with compressional environments along convergent plate boundaries characterized by subduction of oceanic crust; (2) the anorogenic (alkalic-peralkaline) magmatism associated with tensional environment along divergent plate boundaries characterized by deep fractures and rift zones.

Martin and Piwinskii (1972) first quantitatively evaluated the relation between plutonic rock chemistry

and their tectonic settings. Petro et al., (1979) further indicated that D.I. (differentiation index of Thornton and Tuttle, 1960), composition of normative plagioclase, CaO content, total alkalis, $CaO/(Na_2O+K_2O)$ and FeO* (total iron)/(FeO*+MgO) ratios are suitable for distinguishing granitic plutons from compressional and extensional environments. Similarly, Brown (1982) using calc-alkali ratio against silica separated the alkali-calcic, anorogenic suites from the calc-alkaline, orogenic suites.

Frequency distributions of D.I. and normative plagioclase composition for typical compressional (Sierra Nevada Batholith) and extensional (Iceland, Younger Granites of Nigeria) suites, Algonquin Batholith and other Grenville granitoids are shown in Figure 4-2-7 and 4-2-8, respectively. It indicates that the compressional suite has an unimodal distribution with intermediate mode, while the extensional suites have bimodal distributions. However, plutonic rocks of Iceland (Fig. 4-2-7B and 4-2-8B) clearly illustrate the acidic-basic mode, whereas the Younger Granites of Nigeria (Fig. 4-2-7C and 4-2-8C) give a marked silicic rock enrichment with a less distinct basic mode. Comparison of Algonquin Batholith and other Grenville granitoids with typical compressional and extensional suites shows that the distribution patterns of Grenville granitoids are very similar to those of the Younger

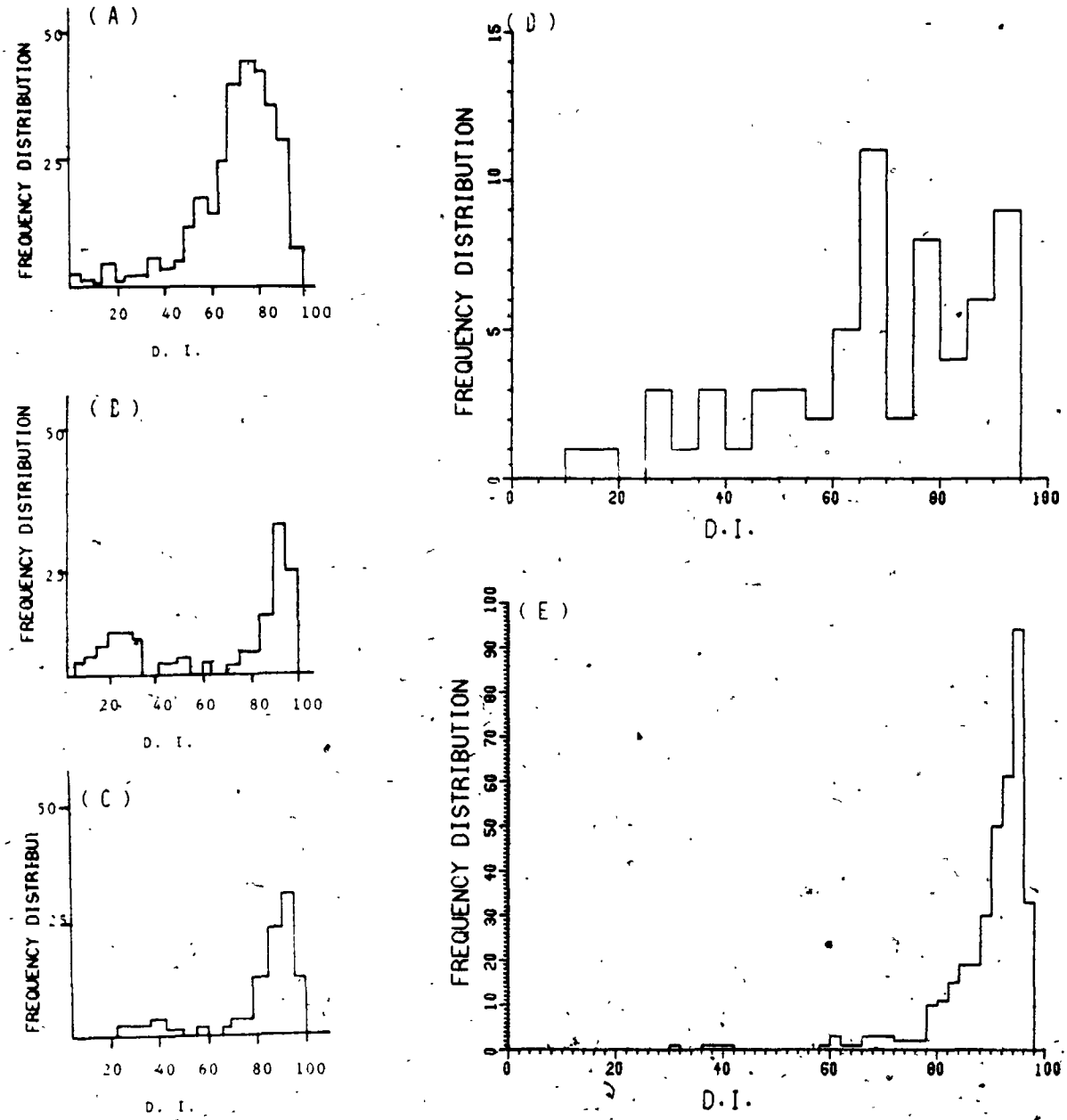

Figure 4-2-7. Frequency distributions of D.I. of the Grenville granitoids and typical compressional and extensional suites.

(A) Sierra Nevada Batholith - typical compressional suite.

(B) Plutonic rocks of Iceland - typical extensional suite.

(C) Younger Granites of Nigeria - extensional suite (?).

(D) Algonquin Batholith (this study).

(E) Other Grenville granitoids (this study).

(A - C from Petro et al., 1979)

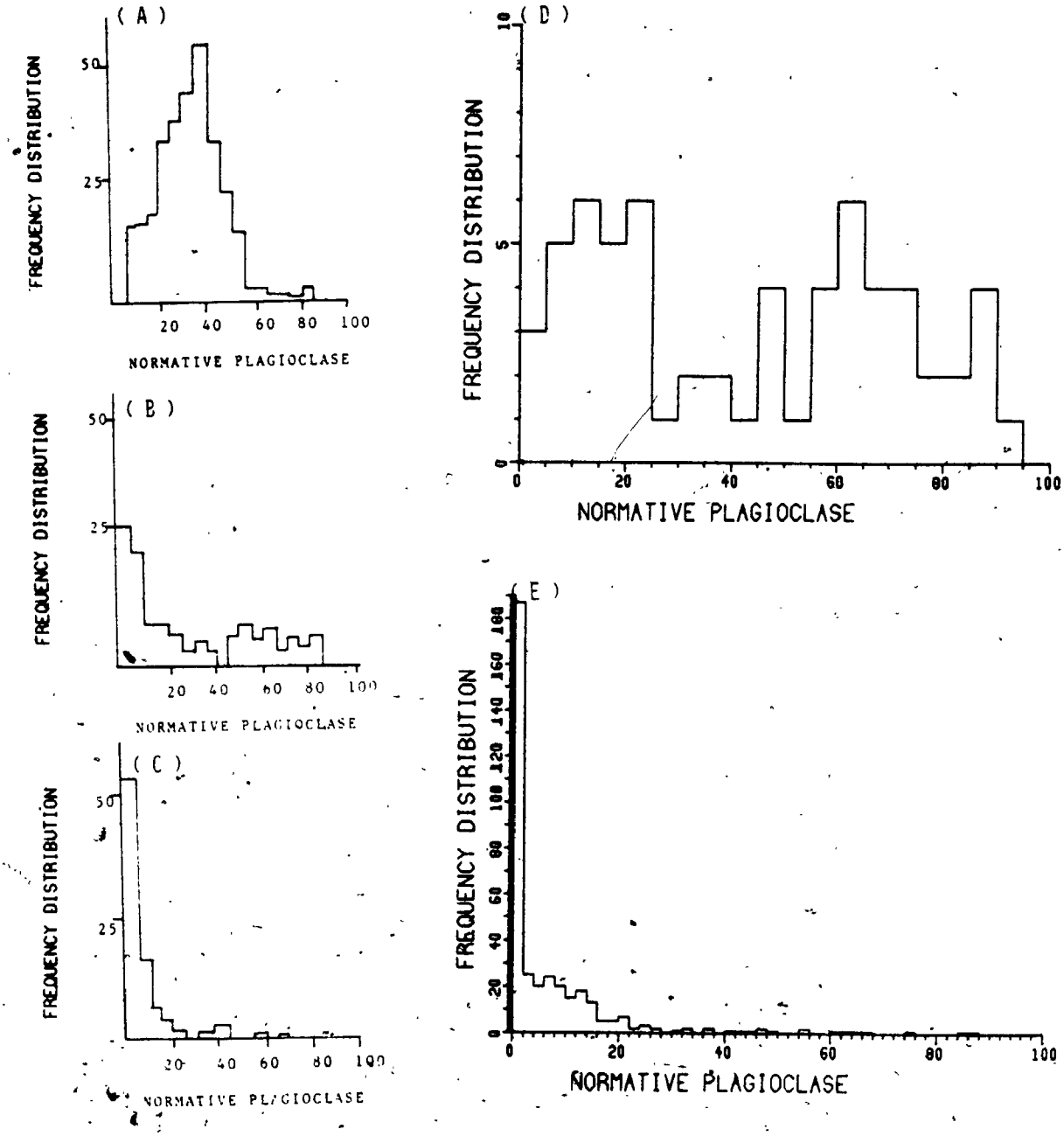

Figure 4-2-8. Frequency distribution of normative plagioclase composition of the Grenville granitoids and typical compressional and extensional suites.

(A) Sierra Nevada Batholith - typical compressional suite.
(B) Plutonic rocks of Iceland - typical extensional suite.
(C) Younger Granites of Nigeria - extensional suite (?).
(D) Algonquin Batholith (this study).
(E) Other Grenville granitoids (this study).
(A - C from Petro et al., 1979)

Granites of Nigeria of an extensional tectonic setting. The Algonquin Batholith shows a bimodal distribution for normative plagioclase but the distribution is unclear for D.I.; the higher frequency at intermediate range (60-70) of D.I. (Fig. 4-2-7D) may be due to its hybrid phases (eg. syeno - monzo - diorite).

Calc-alkaline ratio vs. silica plot for sampled Grenville granitoids is shown in Figure 4-2-9; plots for plutonic suites of Proterozoic and Phanerozoic ages with separation of compressional (calc-alkaline) and extensional (alkali-calcic) environments (adopted from Brown, 1982) is also given for comparison (Fig. 4-2-9A). It clearly shows that the extensional, alkaline suites with low CaO and high alkalis have logarithmic calc-alkali ratios < 0, while the compressional suites have ratios > 0 but decrease with increasing SiO_2. For sampled Grenville granitoids, except for the diorite - tonalite - trondhjemite suite of Algonquin Batholith and Union Lake Quartz Diorite having similar trends to compressional suites (Fig. 4-2-9B, 1 and 9), all the other granites of the Grenville Province give similar trends to extensional suites (Fig. 4-2-9B, 2-8).

Although the frequency distributions for Grenville granitoids show no bimodal patterns of typical extensional suites, there are close simiarities to those of the Younger Granites of Nigeria. Black (1969) has

Figure 4-2-9. Calc-alkaline ratios vs. SiO_2 plots for sampled Grenville granitoids.

(A) Fields of calc-alkaline, compressional suite (field A1) and alkali-calcic, extensional suite (field B1) (modified from Brown, 1982).

(B) Variation trends of sampled Grenville granitoids.

1. Algonquin sodic rock-association
2. Algonquin granite
3. Elphin Complex
4. Coe Hill Granite
5. Mulock Batholith
6. Cheddar Granite
7. Barber's Lake Granite
8. Algonquin monzonite-syenite
9. Union Lake Pluton

(A)

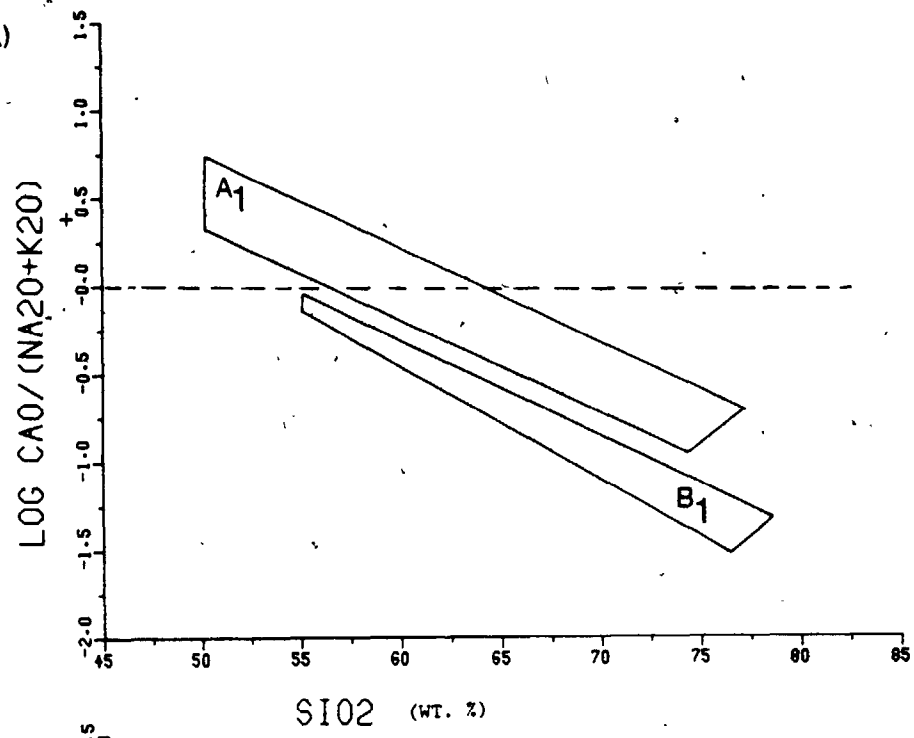
LOG CAO/(NA2O+K2O)
SIO2 (WT. %)
A1
B1

(B)

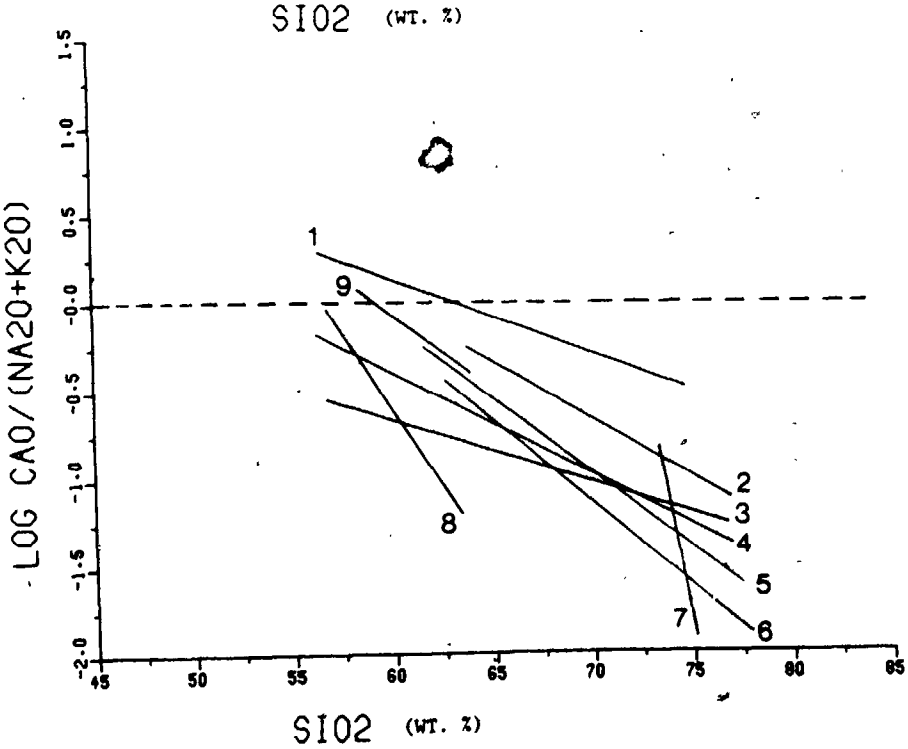
LOG CAO/(NA2O+K2O)
SIO2 (WT. %)
1
2
3
4
5
6
7
8
9

proposed that the development of Nigeria - Niger Younger Granite Province may be related to the disruption of the Gondwanaland Supercontinent in the Mesozoic; the linear distribution of alkaline ring-complexes reflects the zones of high heat flow from the mantle. In addition, Brown (1982) emphasized that the abundance of alkali-calcic and alkaline magma series in mid-Proterozoic sequences may indicate the importance of within-plate, extensional rift magmatism at that time.

CHAPTER V. EVOLUTION OF GRENVILLE CRUST (ONTARIO) DURING THE LATE PRECAMBRIAN : CONCLUSIONS

Descriptions, comparisons and discussions in each of the foregoing chapters concerning the origin of Grenville granitoids and their tectonic implications assist in constructing the evolutionary history of Grenville granitic terrain during the late Precambrian. The inability to separate Grenville granitoids, which are characterized by high oxidation indices and an abundance of syenite - monzonite phases, into I- and S-type categories indicates a deeper source for generation of Grenville magma. Trace element models for the origin of sampled granitoids suggest that the major Grenville granitoids crystallized from magmas generated at upper mantle and/or lower crust (granulite facies) with a limited crustal component; it is consistent with the prevailing low initial $^{87}Sr/^{86}Sr$ ratios for granites of this region.

Similarities between some New England plutons (mainly alkaline granites) and Grenville granitoids suggest a comparable geological environment (either zones of transform fault, oblique subduction, or zones of rifting). In addition, the close resemblances with the Younger Granites of the Nigerian extensional tectonic setting confirm the existence of a long term extensional regime during the development of Grenville plutonism.

Tectonically, the Grenville Structural Province has been recognized as one of the high-grade "mobile belts" in the North Atlantic Shield (Laurentian Supercontinent) during the mid-Proterozoic period 1800 - 1000 Ma (Windley, 1977). Prior to 1800 Ma, a prolongation of the Huronian Supergroup was unconformably deposited along the perimeter of the Archean proto-continent and was subjected to Hudsonian deformations at about 1950 ± 100 Ma ago.

The calc-alkaline, diorite - tonalite - trondhjemite suite of the Algonquin Batholith intruded along the margin of the Huronian "sedimentary basin" (Brown, 1980) about 1500 Ma. The major transcontinental, anorogenic (within-plate) magmatism associated with intrusions of anorthosite massif, rapakivi granite (not common in Ontario) and mangerite took place between 1500 and 1400 Ma (Silver et al., 1977); syenitic - monzonitic and anorthositic intrusions of the Algonquin Batholith and Ontario Gneiss Segment were part of this event.

At about 1300 Ma, a "proto-Atlantic Ocean" was developed to the southeast of the present Grenville Belt; dyke swarms (eg. Mackenzie dyke swarm), rift zones (eg. Keweenawan rift) and Bancroft - Renfrew aulacogen (graben-type trench) occurred on the continental plate associated with this extensional episode (Baer, 1976). Deposition of Grenville Supergroup and major volcanism characteristic of within-plate ocean floor basalt (Tudor metavolcanics, Holm et al., 1984) did not occur until after

1300 Ma; finally, the nepheline-bearing alkaline complexes intruded as a linear belt at the northwest side of the aulacogen (Bancroft region, 1285 - 1187 Ma). The Grenville Supergroup was continuously deposited in the depositional "sea" and lay unconformably on the Algonquin Batholith and gneiss complexes (now the Ontario Gneiss Segment) to the north and northwest. Associated with this extensional environment, subalkaline and alkalic plutonism (mainly the quartz monzonite suite of Lumbers, 1982) and minor anorthositic units were dominant in the sedimentary and volcanic "basin" (now the Central Metasedimentary Belt) during the period of 1200 - 1050 Ma.

The trondhjemite - sodic granite suite (known as the biotite diorite series of Lumbers, 1982) associated with calc-alkaline volcanism of island-arc assemblages at the southeast corner of the Central Metasedimentary Belt (or the Elzevir Terrain of Moore, 1982) may represent a local compressional environment at the southeast side of the depositional trough, which in turn may be related to a southward subduction on a regional scale.

The final closure of the depositional "sea", resulting in reactivation and deformation of the whole Grenville Province (known as Grenville Orogeny), was about 1000 $\pm$ 100 Ma. Calc-alkaline syenite and monzonite were dominant in the post-tectonic intrusions. A summary of evolution events for the Grenville crust is given in Table 5-1; the Grenville granitic terrain is likely a product of

Table 5-1. Summary of the evolution of Grenville crust during the Late Precambrian

Tectonic Regime	Event	Approximate Time
	Deposition of older accumulation (Huronian Supergroup).	prior to 1800 Ma
Compression (Contraction)	Hudsonian Orogeny.	1950 ± 100 Ma
	Intrusion of calc-alkaline, diorite-tonalite-trondhjemite suite of Algonquin Batholith.	about 1500 Ma
Extension	Transcontinental anorogenic magmatism: intrusion of anorthosite-rapakivi granite-mangerite assemblage.	1500 - 1400 Ma
	Intrusion of syenite-monzonite suite of Algonquin Batholith.	
	Developing a "proto-Atlantic Ocean" and associated dyke swarms and rift-zones.	1300 Ma
	Opening Bancraft-Renfrew aulacogen: deposition of Grenville Supergroup and ocean floor basalt volcanism.	1300 Ma
	Intrusion of nepheline-bearing alkaline complexes along inner northwest side of the aulacogen (Bancroft region).	1285 Ma
(Local compression)	Southeastward subduction and developing of island-arc assemblages (Bishop Conner); instrusion of calc-alkaline, trondhjemite-sodic granite (the biotite-diorite series).	1250 Ma
Extension	Extensive subalkaline-alkalic plutonism with minor anorthositic units (within the "sedimentary trough").	1200 - 1050 Ma
Compression	Grenville Orogeny: Morin Event and Grenvillian Event associated with the closure of depositional "sea"; reactivation and deformation of both younger and older accumulations.	1100 Ma 950 Ma
Extension	Initiation of St. Lawrence Rift System.	900 Ma

Proterozoic "extension - contraction" cycles (Wousen et al., 1984).

Although the proposed evolution model for the Grenville Province of Ontario is over-simplified based upon only magmatic events, it agrees well with the general geological settings, depositional sequences and structural features of the Province. In addition, the model may also favour two orogenic events for deformation of the Grenville Province (Baer, 1981b): (1) the Morin Event (1100 Ma) restricted to Central Metasedimentary Belt, (2) the Grenvillian Event (900 Ma) which extended to the whole province. However, conclusions reached in this study may not be valid for the Grenville Belt as a whole, it certainly inputs additional information for understanding the Grenville geology of Ontario and, to some extent, of Quebec.

APPENDIX A. BEHAVIOR OF TRACE-ELEMENTS DURING MAGMATIC PROCESSES

1.0 GENERAL STATEMENT

Over the past decade, great advances have been made in understanding the geochemistry of trace-elements during magmatic processes - particularly of granitic melt generation and their differentiation (eg. Condie and Lo, 1971; Arth and Hanson, 1975; McCarthy and Hasty, 1976; Hanson, 1978; McCarthy and Kable, 1978; Miller and Mittlefehldt, 1982; Mittlefehldt and Miller, 1983).

Among elements, the large-ion and highly-charged elements are most interesting in this study. Their incompatibility and strong affinity with the more siliceous end members of a comagmatic series make them more important in the study of petrogenesis of granitic rocks. However, only a brief account of the behavior of the following elements will be presented here:

1. Alkali-metal and alkaline-earth elements,
2. Rare-earth elements (REE),
3. High-field strength elements (HFS).

Whether an element will be treated as a trace-element or not depends upon whether the element behaves in

accordance with Henry's dilution law and whether it is a stoichiometric constituent in the phases considered.

Several terms have been commonly used in the literature to describe the behavior of trace-elements during igneous processes :

1.1 Distribution Coefficient (K_d) And Bulk Distribution Coefficient (D)

Since trace-elements form dilute solid solution and are distributed between phases at equilibrium or quasi-equilibrium condition, the Nernst distribution coefficient for a given trace-element between a mineral and a co-existing melt is defined as the ratio of weight fractions between these two phases (i.e. K_d (min/melt) = C (min)/ C (melt), C = concentration). It is highly dependent upon temperature, pressure, bulk composition of the mineral and melt, and crystal structure of the mineral. These parameters may vary widely in nature.

The bulk distribution coefficient (D) is therefore determined as the summation of the product of weight fraction of individual mineral and its mineral/melt distribution coefficient (i.e. $D = X * K_d$, X = weight fraction of a given mineral).

Such partitioning data have been obtained from both the phenocryst-matrix pairs of volcanic rocks and

synthetic charges. But our knowledge of trace-element partitioning in granitic melt is still limited. Recent studies have indicated that :

1. the effect of melt composition on trace-element partitioning becomes "extremely important" in a high silica magma (eg. Mahood and Hildreth, 1983);

2. the potential fractination of minor phases for controlling trace-element behavior in the granitic melt may restrict the use of these elements in the calculation of petrogenetic models, such as allanite and monazite for LREE depletion in highly differentiated silicic rocks (Mittlefehdlt and Miller, 1983; Gromet and Silver, 1983).

Although there are problems and uncertainties, trace-element modelling of melting and fractionation trends in granitic suites is still a powerful and effective tool to put constrains on its evolution history by cautiously selecting the proper distribution coefficients.

1.2 Incompatible And Compatible Elements

An incompatible element preferentially partitions into the melt over the co-existing crystalline phases; in other words, it has a lower bulk distribution coefficient, generally $D < 1$. On the contrary, the compatible element is readily incorporated into crystallizing minerals (eg. Ni, Co, Cr for olivine); that is, $D > 1$.

However, the terminology used is closely related to the system investigated. For instance, the rare earth elements are considered to be incompatible in mafic and intermediate melts, but if accessory mineral phases (eg. apatite, zircon or allanite) are present as a late crystallizing phase or as a residual phase during partial melting, they may behave as compatible elements and are completely partitioned into the accessories.

1.3 Large-ion-lithophile (LIL) And High-field strength (HFS) Elements

Goldschmidt geochemically classified the elements into : siderophile, chalcophile, lithophile and atmophile classes. Although there are overlaps in the first three categories, the lithophile elements, especially the ones with large ionic radii, are thought to overwhelmingly participate in silicates rather than

metal or sulphide phases. Because of this strong affinity with silicates, the large-ion-lithophile (LIL) elements are considered to be useful indicators for magmatic evolution.

Elements with a higher charge/radius ratio (Z/R > 1.4) are called the high-field strength (HFS) elements (eg. Nb, Zr, Ta, Hf, etc); whereas the low-field strength elements (Z/R <1.4) are converse of this.

1.4 Rules For Interchanging Ions

By definition, trace-elements are the diodochic impurities of rock-forming minerals and are dispersed throughout the rock. They usually do not form their own minerals and are not present in high concentrations in the minerals. Thus their distribution during crystallizing of magma is largely controlled by crystal-chemical factors (eg. coordinate number, electronegativity and the form of coordination polyhedra, etc., Povarennykh, 1972).

Goldschmidt (1937) first formulated certain specific rules for interchanging of ions (elements) among crystal lattices, based on their size and charge : (from Tauson, 1965)

1. for two interchangeable ions in a crystal structure their ionic radii should not differ by

more than 15%;

2. for two ions having the same charge and similar ionic size, the ion with smaller radius will be preferentially incorporated in the crystal (eg. $K^+ > Rb^+$ in K-feldspar);

3. for two ions having the same ionic radii but different charges, the ion with higher charge will be preferentially incorporated in the mineral (eg. $Ba^{2+} > K^+$ in K-feldspar).

Later geochemists (Ahrens, 1953; Ringwood, 1955; Burns and Fyfe, 1967) have noted that in addition to the magnitude of the ionic size and charge, the ionization potential, electronegativity, type of bonding and the condition of mineral crystallization all control the diadochic distribution of trace-elements during crystallization of magma.

2.0 GEOCHEMICAL CHARACTERISTICS OF SOME TRACE-ELEMENTS

2.1 Alkali-metals And Alkaline-earths

(Rb, Cs, Sr and Ba)

The alkali-metals (Li, Na, K, Rb, Cs) are the Group IA elements in the periodic table. They are characterized by relatively larger size and their

readiness to lose one valence electron from the outermost shell of the atom. Thus, the alkali-metals are geochemically "oxyphile" and markedly concentrated in the upper crust of the earth (Heier and Adams, 1964).

The alkaline-earths (Be, Mg, Ca, Sr, Ba) are the Group IIA elements with lesser ionic character than that of alkali-metals. They are easily oxidised and occur commonly with a 2+ charge.

Among these two groups, Na, K, Mg, Ca are major constituents of the common rock-forming minerals (eg. Na-Ca solid solution in plagioclase; K in K-feldspar; Ca and Mg in mafic minerals). Differences in geochemical behavior of these "major" elements are eventually related to the behavior of their specific minerals during differentiation. In addition, little is known about the behavior of Li and Be during igneous processes and no crystal-chemical relations are expected between them and the other alkali-metals and alkaline-earths. Therefore, no further discussions of Li and Be will be considered in this study.

2.1.1 Rubidium (Rb^+, R=1.47) -

Its chemical characters are entirely coherent with potassium (K^+, r=1.33) because of their geochemical similarity; the distribution of Rb in all rock-types always parallels K.

Although Rb preferentially enters the K position in micas, whose content increases from biotite, muscovite to lepidolite, the bulk concentration of Rb in the rock is contained in feldspars. The slight enrichment of Rb relative to K results in a decrease of the K/Rb ratio towards the more differentiated granitic rocks.

Crustal abundance of Rb is about 90 ppm and the average K/Rb ratio is around 230. Rb ranges from 110 to 170 ppm in Ca-poor and Ca-rich granite,respectively; while the "normal" K/Rb ratio for igneous rocks is considered to be within the range of 150 to 300 (Taylor, 1965; Turekian and Wedepohl, 1961). For late-stage differentiated granites, a K/Rb ratio of less than 100 was reported by Taylor et al. (1956) However, Taylor (1965) indicated that the abnormally high K/Rb ratio of a rock series may be caused by the deficiency of Rb due to accumulation of early feldspars or removal of biotite. Heier and Adams (1964) also suggested that the strong coherence between K and Rb in igneous fractionation makes it difficult to use this ratio for tracing moderate fractionation processes.

2.1.2 Cesium (Cs^+, R=1.67) -

Cesium is the largest cation among these elements and forms the strongest ionic bond with any other elements. Because of its large ion size and substitution only for K in common rock-forming minerals, Cs is an ideal indicator of fractional crystallization path. Taylor (1965) suggested that Ba/Cs ratio would be suitable for this purpose, because Ba^{2+} is enriched in the earlier fractions of K-bearing minerals and Cs^+ in later ones. In common with Rb^+, Cs^+ enters the 12-fold coordination position in micas in preference to the smaller sites in feldspars.

The average of Cs in granite is in the range of 2 to 4 ppm; and the average of K/Cs ratio in granite is between 1000 to 7000 (Heier and Adams, 1964). Frey (1980) reported that in southeast Australia, granites derived from (meta)sedimentary origin (S-type) have relatively higher Cs contents than those derived from igneous origin (I-type granites).

2.1.3 Strontium (Sr^{2+}, R=1.18) -

Because Sr has intermediate ionic size between Ca^{2+} (r=0.99) and K^+ (r=1.33), the Ca-sites in plagioclase and the K-sites in K-feldspar are

suitable for substituting for Sr^{2+}. Although Sr^{2+} preferentially enters K-positions in K-feldspar, the bulk concentration of Sr in the rock is controlled by plagioclase. The average of Sr in granite is about of 440 ppm to 100 ppm depending on CaO-content.

During the processes of differentiation, Sr may behave in two different ways. It increases gradually to a maximum concentration in the intermediate rocks and then decreases towards the highly differentiated felsic ones. In other words, in mafic rocks, Sr increases with decreasing CaO; whereas in felsic rocks it decreases as CaO-content decreases.

The increase of Sr/Ca ratio during magmatic differentiation is an indication of the plagioclase fractionation. In addition, the Rb/Sr ratio also increases during differentiation, in which Rb is enriched in the late differentiates and Sr is incorporated in the early crystallized Ca-silicates (e.g. plagioclase).

2.1.4 <u>Barium</u> (Ba^{2+}, R=1.34) -

The geochemical behavior of barium is comparatively simple; like Cs^{+}, Ba^{2+} substitutes only for K^{+} in the common minerals and enters

K-feldspar more readily than biotite. Although Ba enters the early formed K-bearing phases, it will not be completely depleted from the magma until very late in a differentiation sequence (Taylor, 1965). Thus, the ratio of Sr/Ba serves as a sensitive index for fractionation of feldspars; it is expected to decrease during magmatic differentiation. In addition, the Rb/Ba ratio would increase during fractionation. Bouseily and Sokkary (1975) reported that in granite the Ba-content seems also to govern the Rb/Sr ratio during differentiation. The average concentration of Ba are 420 and 840 ppm in the Ca-poor and Ca-rich granites, respectively.

The effects of major rock-forming minerals on K, Rb, Cs, Sr and Ba contents during magmatic differentiation are summarized in Table A-1. In brief, the variation trends of the alkali-metals and alkaline-earths and their inter-element ratios appear to depend upon whether the minerals, which retain these elements, remain in the residue;

1. K/Rb ratio of the melt is affected only by the presence of K-feldspar and/or biotite; it decreases in the melt if K-feldspar remains in the residue.

2. Rb/Sr ratio increases with differentiation; if biotite remains in the residue, the Rb/Sr ratio of the melt will decrease.

3. Sr/Ba ratio of the melt will decrease if plagioclase, which retains Sr, remains in the residue; it will increase if K-feldspar and biotite, which retain Ba, remain in the residue.

2.2 Rare-earth Elements (The Lanthanides)

In this study, the rare-earth elements (REE) are considered to be the lanthanide group only, from lanthanum to lutetium (Z = 57-71). They may be subgrouped into the "Cerium Earths" or light rare-earths (LREE, La-Eu) and the "Yttrium Earths" or heavy rare-earths (HREE, Gd-Lu). The REEs comprise a uniquely coherent group due to their similar ionization potential and electronegativity; for instance, all the members share a common 3+ oxidation state under most natural conditions, except Ce^{4+} and Eu^{2+} which occur in an extremely oxidizing and reducing environment, respectively. The only difference among them would be the gradual decrease of ionic radii with increasing atomic number (known as "lanthanide contraction").

Ca^{2+} (r=0.99) is the common cation closest in size to those of the REE, which are strongly electropositive and readily form complexes. However, the REE are strictly lithophile and largely retained by minor phases in highly differentiated siliceous magma (eg. Burma et al., 1971; Vinogradov and Vinogradova, 1973; Mahood and Hildreth, 1983; Gromet and Silver, 1983). Taylor (1965) also indicated that minerals containing Sr, Ba and K tend to concentrate the larger ions of the "Cerium group", while those containing Sc and Zr concentrate the "Yttrium group" of smaller ionic radii.

The REE are not really rare; they are much more abundant in the lithosphere than Au and Ag, and about as abundant as Sn, Pb and Co (Haskin et al., 1966). There are a wide variety of REE abundances in granitic rocks; but only little differences were found between the I- and S-type granites in southeast Australia (Frey, 1980).

In spite of diversity of the absolute concentrations of REE in the igneous rocks, the rock/chondrite normalized ratios or graphic patterns (Haskin et al., 1968) are commonly ultilized to describe their behavior during the magmatic processes. Generally, in granitic rocks with intermediate SiO_2 composition, the LREE are enriched relative to the HREE with a negative Eu anomaly; that is, a steep,

negative slope distribution curve. However, the same may not be true for the very felsic end members of a comagmatic series (Emmerman, 1975; Miller and Mittlefehdt, 1982).

Like other trace-elements, the variation and relative abundances of REE in granitic melt depend upon the distribution of minerals, in this case, whether likely accessory minerals remain in the residue or fractionally crystallized from the melt. McCarthy and Kable (1978) have studied the behavior of REE during partial melting of granitic rocks in some detail. They concluded that :

1. with increasing partial melting of granitic gneisses, the LREE were partitioned into the melt (D < 1); while Eu and HREE were retained by the solid (D >1).

2. when the partial melt successively underwent fractional crystallization, Eu and LREE were partitioned into the crystals (D > 1); whereas the HREE were concentrated in the residual melt (D < 1).

Furthermore, Arth (1976) and Hanson (1978) summarized the relative abundances and K_ds for REE of common mineral phases in felsic rocks (See Table A-2). Relative to the other REE, the HREE are preferentially

retained by garnet, zircon, hornblende and less so by clinopyroxene; while the LREE are mainly concentrated in apatite, allanite, monazite and possibly sphene (Mittlefehldt and Miller, 1983; Gromet and Silver, 1983).

It was also indicated that though the K_d of REE for a given mineral may vary with composition of the melt, temperature, pressure and other variables, the shape of the distribution pattern is constant (eg. Figure A-1, from Hanson, 1978; Frey, 1980). Therefore, a given mineral will have a characteristic effect on REE distribution pattern of the melt which allows us to monitor the role of the mineral during magmatic differentiation. For example, the anomalous behavior of Eu in granitic magma may be due to a combination effect of various minerals. A negative Eu anomaly pattern may result from plagioclase or K-feldspar remaining in the residue (solid) during partial melting or due to intensive segregation of feldspars (esp. plagioclase) from the melt during fractional crystallization, whereas the positive Eu anomaly pattern may derive from garnet, apatite, hornblende, clinopyroxene and hypersthene remaining in the residue (Hanson, 1978). However, the nature of the REE distribution curve of the melt is mainly dependent upon the initial mineralogy of the parental source as well as the extent of REE equilibration

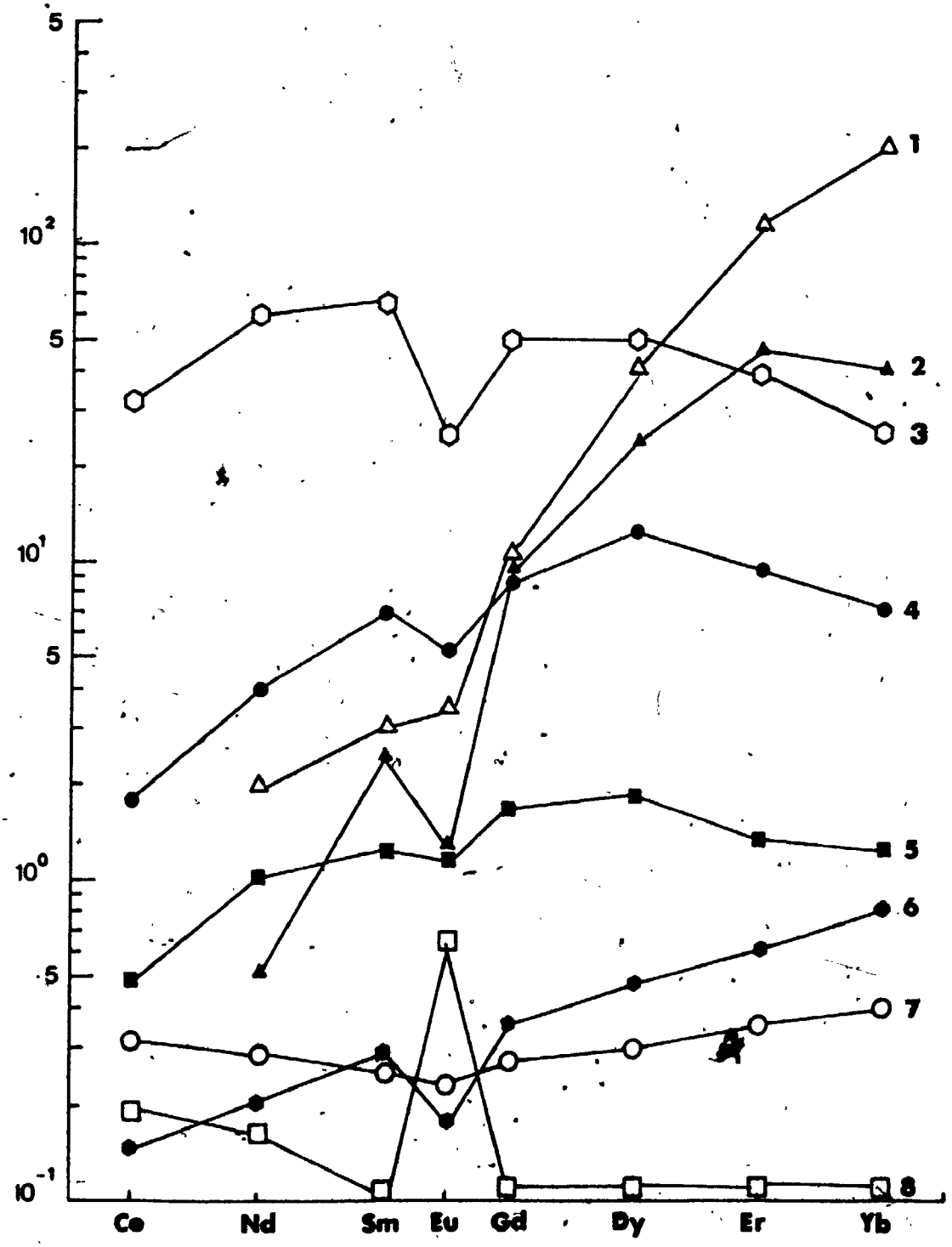

Figure A-1. Chondrite-normalized REE distribution patterns for minerals of acidic rocks (Frey, 1980). Estimated REE partition coefficients are primarily based on phenocryst/matrix data. (1) zircon (2) garnet (3) apatite (4) hornblende (5) clinopyroxene (6) hypersthene (7) biotite (8) feldspar

between melt and residue (eg. zircon during partial melting, Watson, 1979).

2.3 High-field Strength Elements

(Nb, Zr, Ta, Hf, Y and Ga)

The high-field strength elements (Z/R > 1.4) used in recent petrogenesis studies are those highly charged transition metals of the second and third series (i.e. Group IVB and VB), such as Ti, Zr, Hf, Nb and Ta. Because of their "near-ideal" incompatibility (i.e., for major rock-forming minerals their bulk distribution coefficients D --> 0, Frey, 1980) and immobility during geological processes, they are good indicators for the degree of fractionation or partial melting in a genetically related rock suite. In addition, their inter-element ratios are commonly used to infer samples which are related to a common source (eg. Ti-Zr-Y triangle variation diagram to distinguish basaltic rocks from different tectonic settings, Pearce and Cann, 1973).

2.3.1 Zirconium And Hafnium -

(Zr^{4+}, r=0.79; Hf^{4+}, r=0.78)

The pairs Zr-Hf and Nb-Ta have similar ionic size and coherent geochemical behavior. Zr^{4+}

either forms its own mineral phase, zircon ($ZrSiO_4$), or substitutes for Ti^{4+} in the early formed mafic minerals. The Ti/Zr is expected to increase during differentiation.

The ratio of Zr/Hf is not readily changed by alteration processes; for most of crustal rocks it is close to a contant 37 (Brooks, 1970) and about 50 for average of the upper crust (Taylor, 1965). The crustal average abundance of Zr and Hf are 165 ppm and 3 ppm, respectively. The average granite is 180 ppm for Zr and 4 ppm for Hf (Taylor, 1964).

For plutonic rocks, the Zr/Hf ratio tends to decrease as increasing acidity, especially as the rocks become progressively undersaturated (Brooks, 1970). However, there is no systematic change of Zr throughout the differentiation sequence of the calc-alkaline series (Rogers et al., 1980).

The major Ti-bearing phases, hornblende, biotite, (titano)magnetite and ilmenite, associated with rutile, sphene, zircon and apatite accessory minerals are the main HFS element contenders. Tarney and Saunders (1979) in their study of the origin of the Cordilleran Batholith suggested that the variation of HFS elements (i.e., Zr, Hf, Nb, Ta) in the calc-alkaline magma

could be due to the fractionation of minor phases, such as rutile, ilmenite, sphene, etc. (similar to REE in the siliceous melt).

2.3.2 Niobium And Tantalum -

(Nb^{5+}, r=0.69; Ta^{5+}, r=0.68)

Like Zr-Hf, Nb-Ta is another coherent pair of elements with close geochemical similarity. The Nb/Ta ratio for the average crust is about 10, based on their abundance in the crust of about 20 ppm for Nb and 2 ppm for Ta.

On the basis of ionic radii, Nb and Ta may substitute for Ti^{4+}, Zr^{4+}, Sn^{4+}, Mo^{6+} and W^{6+}. Formation of the complex ions will depend on the availability of halogen (volatile)-rich fluid in the magma (Taylor, 1965); concentrations of these highly-charged cations in the peralkaline site and some undersaturated rocks (eg. nepheline syenite) are believed to be the result of volatile-rich fluid decreasing the degree of polymerization in the more differentiated magma (Bowden, 1974; Collerson, 1982). Under extreme fractionation, Nb will be readily incorporated into the melt relative to Ta; thus the Nb/Ta ratio will increase with differentiation.

Taylor (1965) stated that the bulk of Nb and Ta in granites appears to be retained by biotite; and the Nb/Ta ratio in the minerals decreases in the sequence of biotite (12.6), ilmenite (6.6) and zircon (0.64) infering a definite relations between Ti-Nb and Zr-Ta.

2.3.3 Yttrium (Y^{3+}, R=0.92) -

Yttrium, scandium and the lanthanides are the Group IIIB elements in the periodic table. All have ionic size close to Ca^{2+} (r=0.99). In contrast to Sc, Y behaves as a heavy lanthanide; Y^{3+} is expected to substitute in early Ca-positions in intermediate to felsic magma. On the other hand, it concentrates in later apatite and titanite due to the more covalent character of the Y-O bond compared with the Ca-O bond (Taylor, 1965).

Y behaves more complexly than the HREE, although there are similar geochemical characteristics. For mafic magma, Y is enriched in the residual melt during fractional crystallization, whereas for intermediate and felsic magma, crystallization of minor amounts of hornblende and clinopyroxene (early Ca-bearing phases) will tend to deplete the Y content in the

residual; later crystallizing apatite would sharply reduce or even completely deplete Y from the melt (Pearce and Norry, 1979).

Because of its higher charge/radius ratio (Z/R > 3) and incompatibility during igneous processes, in modern literature Y is considered to be one of the HFS elements rather than REE. The crustal average abundance of Y is about 33 ppm, and about 40 ppm for average granite (Taylor, 1964).

2.3.4 Gallium (Ga^{3+}, R=0.67) -

Gallium is commonly considered to have a close coherent relation with Al (Al^{3+}, r=0.61) in igneous geochemistry. It has a relatively simple geochemical behavior, either entering Al^{3+} sites or substituting in the Fe^{3+} position of common rock-forming minerals.

Ga is expected to be enriched relative to Al in the later differentiates of a comagmatic suite; the Ga/Al ratio will increase during magmatic differentiation. However, Albuquerque (1971) reported a constant Ga/Al ratio in a suite of differentiated granitic rocks from northern Portugal. They have interpreted this as the effect of differential partition of Ga among the

co-existing mineral phases (eg. Ga is relatively depleted in K-feldspar).

Recently, Collerson (1983) found that Ga associated with other HFS elements was strongly enriched in syenite and peralkaline granite from Larbrador. Collins et al., (1982) also determined that a significant enrichment of Ga relative to Al (i.e. high Ga/Al ratio) is one of the chemical characteristics of the A-type granites of Loiseller and Wones (1979) because they are alkalic, anorogenic and anhydrous.

The effects of major mineral phases in granite on HFS elements during igneous differentiation are outlined in Table A-1. In summation, the behavior of the HFS elements is more complex and irregular than those of REE and alkali-metals and alkaline-earths. Tarney and Saunders (1979) reported that in the calc-alkaline suite of Antarctic Peninsular Plutons, the HFS elements do not show any systematic variation with increasing SiO_2 contents. For example, Zr increases until SiO_2 reaches 60 - 65% then decreases sharply; Nb increases slowly in basaltic rocks but remains relatively constant in felsic plutonic rocks. Such variations are interpreted as due to the removal of minor HFS element-retaining phases or due to the heterogenity of the source and the composition of the

Table A-1. The effects of major rock-forming minerals on K, Rb, Cs, Sr, Ba, REE and HFS elements contents during magmatic processes

Common Mineral	Alkali Metals and Alkaline Earths Elements	Rare Earth Elements	High-field Strength Elements
Plagioclase	1. Major Sr-bearing mineral with typical Kd > 4 for rhyolite. 2. The absolute Kd values for K and Rb are so low that the presence of plagioclase in the residue does not affect K/Rb ratio greatly. 3. Sr/Ba ratio in the melt is reduced and Rb/Sr ratio is increased.	1. Except Eu (Kd > 2), the other REE are little affected by plagioclase; that is, a relative flat distribution pattern with a striking Eu positive anomaly. 2. The degree of Eu anomaly decreases as the An-content of plagioclase increases.	1. Little effect on the HFS distribution due to its relatively smaller Kd.
K-feldspar	1. K is the stoichiometric constituent; with high Kd for Ba and Sr, and fair amount of Rb and Cs. 2. K/Rb and K/Ba are greatly reduced in the melt; while Sr/Ba and Rb/Sr are increased (to a lesser extent compared with the presence of residual biotite).	1. Similar to plagioclase, retaining large Kd for Eu and with a relative LREE enrichment than that of HREE. 2. The fractionation of feldspar, both K-feldspar and plagioclase, leads a pronounce depletion of Eu in the melt .	1. Similar to plagioclase.
Biotite	1. K is the stoichiometric constituent; with higher Kd for Ba and Rb. 2. Rb and Cs are enriched relatively to the co-existing K-feldspar due to its larger coordination number (12 - fold). 3. Maintaining a constant K-content in a melt; reducing the Rb/Sr and K/Rb ratios and increasing the Sr/Ba ratio sharply.	1. Little effect on the REE distribution due to its relatively smaller Kd for REE (that is, a relative flat distribution pattern).	1. Major Ti-bearing phase with relatively larger Kd for HFS. 2. Accept Zr more readily than Hf; Nb than Ta.
Hornblende	1. Low Kds for K, Rb, Sr and Ba, thus it has little effect on these elements in the melt. 2. The presence of residual Hb may lower K/Rb ratio slightly.	1. Relatively larger Kd for middle REE (Gd-Er) and lesser for HREE. 2. Resulting a depletion of middle and lesser heavy REE and a positive Eu anomaly in the melt.	1. Major Ti-bearing mineral with higher Kd for HFS than those of biotite and major Y-contender. 2. Alkaline amphiboles may uptake Zr (and Hf) in the peralkaline melt.
Hypersthene	1. Relatively lower Kd for the alkali and alkaline-earth elements and does not affect the ratios of these elements.	1. Larger Kd for HREE with a positive slope distribution curve and an Eu depletion. 2. Resulting the melts with more LREE enrichment than HREE and a positive Eu anomaly.	1. Relatively smaller Kd for HFS.

(Table A-1, cont'd)

Clinopyroxene	1. Relatively higher Kd for Sr than those for K, Rb and Ba.	1. Larger Kd for middle REE (Gd-Dy) and smaller Eu depletion pattern. 2. Leading to melts with relative depletion of middle REE and less depletion of the HREE.	1. Relatively larger Kd for HFS, and major Y-bearing mineral. 2. Preferential uptake Y than Zr.
Garnet	1. Very small Kd for K, Rb, Sr and Ba; no major effects on the melts.	1. Very large Kd for HREE and relatively smaller Kd for LREE, with an Eu depletion. 2. Leading to melts with relative depletion of HREE and a positive Eu anomaly.	1. Larger Kd for Ti, Zr and Y, especially for Y, Kd ~35.0 (a stoichiometric constituent).
Zircon	1. Do not contain significant alkali-metals and alkaline-earth elements	1. Large Kd for REE in general, especially the HREE. 2. The presence of zircon in the residue leads to the depletion of HREE in the melt dramatically.	1. Zr-bearing mineral (a stoichiometric constituent) and higher Kd for Hf, Ta. 2. Zircon saturation level is strongly dependent upon the alkalinility of the melt.
Apatite	1. Relatively larger Kd for Sr; resulting depletion of Sr in the melt after crystallizing apatite.	1. Large Kd for REE in general, especially middle REE (Sm-Dy), with a distinctive Eu depletion curve. 2. The presence of apatite in the residue leads to relative depletion of the middle REE and a positive Eu anomaly.	1. Except Y (Kd >40), the other other HFS have little effect by apatite.
Allanite + Monazite	1. Do not contain significant alkalic-metals and alkaline-earth elements.	1. Larger Kd for LREE and resulting a relative depletion of LREE in the melt .	
Sphene - titanite	1. Do not contain significant alkalic-metals and alkaline-earths.	1. Larger Kd for LREE, resulting a relative depletion of LREE in the melt.	1. Relatively larger Kd for Zr and Y.
Magnitite - ilmenite	1. Do not contain significatn alkalic-metals and alkaline-earths.	1. Do not contain significant REE with a flat linear distribution curve.	1. Relatively larger Kd for Nb, Y and Zr (Kd for Ti > 12, a stoichiometric constituent).

(information from: Heier and Adams, 1964; Taylor, 1965, Brooks, 1970; Arth and Hanson, 1975; Hanson, 1978; Pearce and Norry, 1979; Frey, 1980)

7 7

OF / DE

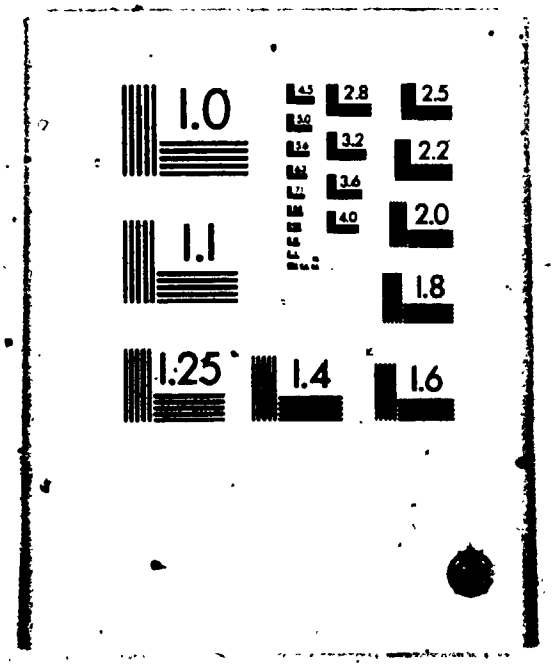

melt itself.

In general, a solid crystallized from a basic magma will contain lesser amount of HFS elements than that crystallized from an acid melt (Watson, 1976). Besides, the HFS elements have the tendency to be enriched in the alkalic-peralikaline felsic melts : (1) Nb-Ta enrichment by complexing with halogen-rich fluids (Taylor, 1965); (2) Zr enrichment due to the retardation of zircon fractionation (Watson, 1979).

The Zr/Y ratio is expected to increase during differentiation, due to crystallization of early Ca-phases of hornblende and clinopyroxene which retain most of Y in the rock. It will then sharply decrease due to zircon fractionation from the more siliceous magma. In addition, the Zr/Y ratio will fractionate more effectively by partial melting processes rather than fractional crystallization (Pearce and Norry, 1979).

3.0 QUANTITATIVE PETROGENESIS MODELLING FOR GRANITIC ROCKS

Based on our understanding of the geochemical behavior of trace-elements during magmatic processes, the goal of our research has been shifted from qualitative description to quantitative modelling of the evolution of

igneous rocks. This was partly accelerated by great advances in rapid and precision analytical techniques for determinations of both trace-elements and their mineral/melt partition coefficients (K_d).

Mathematic equations for petrogenetic modelling have been developed by Rayleigh (1896), Gast (1968), Shaw (1970), Hertogen and Gijbels (1976), and Allegre and Minster (1978); their applications for granitic rocks were also studied by Arth (1976) and Hanson (1978). Under the assumption that the rock is to represent the melt (liquid) fraction during differentiation, two major hypotheses are widely accepted for solving petrogenetic problems: (a) fractional crystallization, (b) partial melting.

3.1 Fractional Crystallization

Fractional crystallization implies that rock is consolidated from the residual liquid which has undergone differential segregation of mineral phases (cumulates).

3.1.1 Rayleigh Equilibrium Crystallization -

Rayleigh equilibrium crystallization is a likely mechanism for a fast cooling magma, where the settling mineral phase is quickly covered by

the next layer of crystals and only a temporary equilibrium between the melt and the mineral surface is reached.

3.1.2 Total Equilibrium Crystallization -

Total equilibrium crystallization is considered to be a mechanism for slowly cooling magma, in which the crystallizing mineral phase is gradually covered and an overal equilibrium is maintained by diffusion of the element

3.2 Partial Melting

Because the rock represents the liquid portion of a crystallizing magma, such melt can be generated by partial fusion of a multiphase solid assemblage under a proper pressure and thermal gradient within the lower crust and/or upper mantle. Therefore, the initial composition of the melt is mainly dependent upon whether mineral phases, which retain the trace-elements, remain in the residual (solid) or not.

Under equilibrium conditions, two types of mechanisms are commonly considered in the natural environment:

1. Batch melting - where the liquid and the solid maintain continual eqilibrium, until enough

melt has been accumulated leading to removal from the magma chamber. This is probably a more realistic model for common igneous fusion processes (Hanson, 1978).

2. Fractional melting - where small fractions of the melt are continuously removed from the residual, so that only surface equilibrium with solid phases is achieved.

Furthermore, a successful use of quantitative modelling is strongly dependent on accurately determing partition coefficients for various trace-elements. In addition, as Hanson (1978) pointed out, due to large variations in P - T conditions, possible parental composition and the sluggish reactions in the granitic magma system, it may not be possible to restrict the number of plausible petrogenetic models.

At present, only alkali-alkali earths, REE and some HFS elements were chosen for trace-element modelling, due to availability of their K_d for various minerals in granitic rocks. The partition coefficients of trace-elements for rhyolitic or acidic rocks are listed in Table A-2, which is taken from Arth (1976), Hanson (1978) and Pearce and Norry (1979). Besides, partition coefficients for

Table A-2. Distribution Coefficients for Rhyolitic or Acidic Rocks

Element \ Mineral	Hypersthene	Clino-pyroxene	Hornblende	Biotite	Phlogopite	Plagio-clase	K-feldspar	Apatite	Zircon	Garnet	Magnetite
K	0.0023	0.037	0.081	(5.63)*	-	0.100	(1.49)*	-	-	0.020**	-
Rb	0.0027	0.032	0.014	3.26	0.94	0.041	0.659	-	-	0.0085	-
Sr	0.0850	0.516	0.022	0.12	0.672	4.400	3.870	-	-	0.015	-
Ba	0.0029	0.131	0.044	6.36	15.30	0.308	6.120	-	-	0.017	-
Ce	0.15	0.50	1.52	0.32	0.23	0.270	0.044	34.7	2.64	0.35	-
Nd	0.22	1.11	4.26	0.29	0.34	0.210	0.025	57.1	2.20	0.53	-
Sm	0.27	1.67	7.77	0.26	0.39	0.130	0.018	62.8	3.14	2.66	-
Eu	0.17	1.56	5.14	0.24	0.50	2.150	1.13	30.4	3.14	1.50	-
Gd	0.34	1.85	10.00	0.28	0.35	0.097	0.011	56.3	12.00	10.50	-
Dy	0.46	1.93	13.00	0.29	0.20	0.064	0.006	50.7	45.70	28.60	-
Er	0.65	1.66	12.00	0.35	0.17	0.055	0.006	37.2	135.00	42.80	-
Yb	0.86	1.58	8.38	0.44	0.17	0.049	0.012	23.9	270.00	39.90	-
Lu	0.90	1.54	5.50	0.33	0.21	0.046	0.006	20.2	323.00	29.60	-
Ti	0.4	0.7	7.0	1.5**	2.5	0.05	(similar	0.1	-	1.2	12.5
Zr	0.2	0.6	4.0	1.2	2.0	0.1	to	0.1	-	1.2	0.8
Y	1.0	4.0	6.0	1.2	2.0	0.1	plagio-	40.0	-	35.0	2.0
Nb	0.8	0.8	4.0	1.8	3.0	0.06	clase)	0.1	-	-	2.5

* K is an essential structural constituent in biotite and K-feldspar.
** K, Rb, Sr, Ba and REE for garnet are taken from dacitic rocks (Nagasawa and Schnetzler, 1971).
Ti, Zr, Y and Nb for biotite are taken from intermediate rocks (Pearce and Norry, 1979).

(Alkali-Alkaline Earths and REE are taken from Arth 1976 and Hanson, 1978;
HFS elements are taken from Pearce and Norry, 1979)

high-silica (> 75% SiO_2) felsic rocks of Mahood and Hildreth (1983) are also listed in Table A-3.

In this study, the proto-models were qualitatively determined by variation trends of major- and trace-elements and then quantitatively verified by the mass balance calculation of Stormer and Nicholls (1978). For example, to simulate possible trends resulted from crystal fractionation in a granitic body, appropriate compositions were chosen from chemical analyses, representing typical compositions at either end. All reasonable mineral phases identified in the granite were initially included in the calculation; mineral compositions were either analyzed by electron microprobe or selected from the literature (Deer et al., 1966). Where solutions indicated addition rather than subtraction of minerals, those mineral were rejected and the solution recalculated until only subtracted minerals were obtained (eg. Strong and Minatidis, 1975). This calculation was then checked by trace-element modelling.

Table A-3. Distribution coefficients for high-silica felsic magma

Element \ Mineral	Allanite	Ferro-hedenbergite	Augite	Hypersthene	Biotite	Sanidine a.	Sanidine b.	Ilmenite	Titano-magnetite	Zircon
La	2362	3.5	13.1	10.8	2.59	0.057	0.071	1.31	17.5	26.6
Ce	2063	4.0	11.3	9.0	2.15	0.043	0.041	1.19	15.4	23.5
Nd	1400	5.9	11.1	7.8	1.80	0.044	0.021	0.96	10.9	22.0
Sm	756	6.21	11.75	6.47	1.61	0.0288	0.014	0.684	8.25	17.7
Eu	122	5.5	5.4	2.4	1.00	2.000	3.500	0.40	3.1	12.0
Tb	235	4.0	10.5	4.7	1.30	0.023	0.035	0.36	6.4	37.0
Dy	123	n.d.	10.3	3.3	1.05	0.025	0.150	0.37	-	95.0
Yb	24.5	4.5	5.0	2.1	0.60	0.016	0.006	0.55	-	490.0
Lu	22	6.1	4.8	2.1	0.65	0.015	0.050	0.74	-	635.0
Th	420	0.77	6.56	5.30	1.43	0.0208	0.0149	0.427	10.3	62.4
U	14	0.33	0.35	0.31	0.18	0.018	0.037	0.063	-	298.0
Sc	49.4	109.00	96.00	18.10	13.10	0.049	0.024	18.500	9.3	60.3
Hf	9.8	0.39	0.00	0.00	0.47	0.015	0.023	0.650	0.0	2645.0
Ta	1.9	0.101	0.72	0.98	1.36	0.0184	0.029	18.000	0.74	54.8
Cr	391	-	-	-	5.30	-	-	-	-	119.0
Co	44	17.0	56.0	84.0	79.00	0.290	0.090	26.00	113.0	9.0
Zn	30	7.2	19.0	19.0	13.00	0.065	0.090	7.80	36.0	n.d.
Mn	17.1	30.0	31.3	57.0	7.90	0.018	0.016	27.00	21.6	1.78
Ca	-	-	-	-	1.2	0.009	0.061	-	-	4.4
Rb	-	-	-	-	3.0	0.360	0.640	-	-	-
Sr	-	-	-	-	-	-	-	-	-	-
Ba	-	-	0.5	0.3	5.4	-	6.7	-	-	-

(Compiled from Mahood and Hildreth, 1983)

APPENDIX B. ANALYTICAL METHODS

1.0 SAMPLE PREPARATION

More than 400 samples were collected from eight selected granitoids, including granitoid itself, related dykes, xenoliths and country rocks. Initially, 5 to 10 kg of least weathered sample was split by hydraulic splitter into about fist-size blocks. Leached surfaces, fracture fillings and possible mineralized veinlets were sawed out and discarded.

Except for a representative handspecimen and a piece for thin sectioning, the bulk sample was coarsely crushed by jaw crusher. About 250 gm of coarse material was pulverized by a tungsten-carbide coated Bleuler mill for less than 30 sec. This portion was taken as representative of the bulk sample.

In addition to X-ray fluorenscence spectrometer analysis (XRF), powdered rocks (< 250 mesh) were also used for instrumental neutron activation analysis (INAA), ferrous iron (FeO) determination and fluorine-chlorine analysis. The remaining coarse material were then used for mineral separation processes.

2.0 X-RAY FLUORESCENCE SPECTROMETER ANALYSIS (XRF)

X-ray fluorescence analyses were performed by a Philips PW-1450 Automatic Sequential Spectrometer with selectable Cr, W and Rh targets and five changeable crystals. Instrumental settings and running conditions are listed in Table B-1. Data counts obtained from the spectrometer were punched onto 8-channel paper tape by an on-line Teletype (before Feb. 1983), or stored in a floppy disk by a 32k RAM microcomputer. The data was then read into CDC Cyber-170 computer for further reduction.

2.1 Major-oxide Determination

Except for Na_2O and LOI (Loss of Ignition), nine major-oxide (SiO_2, TiO_2, Al_2O_3, Fe_2O_3, MnO, MgO, CaO, K_2O, P_2O_5) concentrations were determined by using the heavy absorber fusion technique of Norrish and Hutton (1969). Fusion beads were prepared following the method of Harvey et al. (1973) by mixing the sample with commercially available Spectroflux-105 (lithium tetraborate 47.03%, lithium carbonate 36.63% and lanthanum oxide 16.34%). The major-oxide concentrations were calculated against the monitor FS-94 supplied by Dr. Norrish from CSIRO, S. Australia.

Na_2O was determined on pressed powder pelletes calibrated against various international standards. Loss of ignition, including H_2O, CO_2, S and other

Table B-1. Instrumental setting and running conditions for X-ray fluorescence analysis

Element	Line	Analysing 2θ	Crystal	X-ray Tube Target	Kv	mA	Detector/ Collimator*	Interfering element
Major Oxide (on fusion disc)								
SiO_2	K_α	109.40	PET	Cr	60	40	F/c	
TiO_2		86.29	LiF-200		40	30	F/f	
Al_2O_3		145.47	PET		60	40	F/c	
Fe_2O_3		57.62	LiF-200				F/f	
MnO		63.07	LiF-200	W			F/f	
MgO		136.90	ADP	Cr			F/c	Ti,Fe,Ca and K K_β
CaO		61.77	GE				F/f	
K2O		69.78					F/f	
P_2O_5		140.90					F/c	Ca K_α
(on powder pellet)								
Na_2O	K_α	55.01	TLAP	Cr	60	40	F/c	
Bkg		53.51						
Trace Element (on powder pellet)								
Nb	K_α	21.37	LiF-200	Rh	60	40	S/f	Y K_β
Bkg		21.05						
Zr	K_α	22.55						Sr K_β
Bkg		23.00						
Y	K_α	23.80						Rb K_β
Bkg		24.00						
Sr	K_α	25.13						
Bkg		25.50						
Rb	K_α	26.60						
Bkg		26.35						
Pb	$L_{\beta 1+2}$	34.01					F/f	
Bkg		34.50						
Zn	K_α	41.82					F+S/f	
Bkg		42.50						
Cu	K_α	45.05						
Bkg		45.65						
Ni	K_α	48.70						Co K_β
Bkg		48.10						
Co	K_α	52.83						Fe K_β
Bkg		53.50						
Cr	K_α	69.41					F/f	V K_β
Bkg		69.95						
Ba	L_α	87.30						Ti K_α
Bkg		88.00						
V	K_α	76.98						Ti K_β
Bkg		78.00						
S	K_α	75.96					F/c	
Bkg		77.00						
Ga	K_α	38.94					S/f	
Bkg		39.25						

* Detector/Collimator combinations used:
- F/c = Flow proportional counter with coarse collimator;
- F/f = Flow proportional counter with fine collimator;
- S/c = Scintillation counter with coarse collimator;
- S/f = Scintillation counter with fine collimator;
- F+S = Combination of flow and scintillation counter.

** In general, the pulse height selectors were set at 250-750 for flow counter and 150-850 for scintillation counter.

*** 40 sec. was used for all major oxides; whereas for trace element analyses, 100 sec. and 40 sec. were used for background and peak, respectively.

volatiles was calculated from the weight loss after roasting 2 hrs. at 1100 °C.

During the course of analysis, the international and internal standards were analyzed in association with the samples. The precision and accuracy of major-oxide determinations can be suggested from the duplicate analyses of these standards (See Table B-2). The interlaboratory comparison is also shown in Table B-2. In general, the reproducibility of all determinations is better than 5%, except ±20% for P_2O_5 < 0.2 wt.%, ±15% for MnO < 0.1 wt.% and about ±10% for MgO.

2.2 Trace-element Determination

A rapid and routine determination of 15 geologically interesting trace-elements (Nb, Zr, Y, Sr, Rb, Pb, Zn, Cu, Ni, Co, Cr, Ba, V, S and Ga) was developed during this study.

If a major-oxide composition of the sample is known, the backgrounds beneath spectral peaks can be interpolated mathematically or graphically from a "synthetic background working curve" based on the method of Feather and Willis (1976, the background scattering is inversely proportional to bulk mass absorption coefficeint of the sample). Interference corrections for X-ray line overlaps (eg. Sr on Zr, Rb on Y, Y on Nb, etc.) were carried out by measuring synthetic

Table B-2. XRF analyses of major-oxides for standard rocks and interlaboratory comparison

Standard	Statistics	SiO_2	TiO_2	Al_2O_3	Fe_2O_3	MnO	MgO	CaO	K_2O	P_2O_5	Na_2O	LOI
	R.V.	69.22	0.48	15.40	2.69	0.03	0.75	1.96	4.46	0.13		
G-2	mean (15)*	69.50	0.49	15.44	2.68	0.03	0.75	1.84	4.50	0.12		
(Granite)	S.D.	0.25	0.01	0.11	0.03	0.005	0.08	0.07	0.07	0.025		
	C.V. (%)	0.36	2.26	0.69	1.20	15.15	10.47	3.52	1.47	20.16		
	R.V.	59.61	1.06	17.19	6.78	0.10	1.52	4.94	2.92	0.51		
AGV-1	mean (14)	59.53	1.07	17.36	6.78	0.10	1.48	4.99	3.05	0.49		
(Andesite)	S.D.	0.17	0.01	0.12	0.07	0.003	0.12	0.13	0.04	0.02		
	C.V. (%)	0.28	1.21	1.67	0.97	3.03	7.96	2.56	1.25	3.27		
	R.V.	54.53	2.26	13.72	13.41	0.18	3.48	6.97	1.70	0.36		
BCR-1	mean (9)	54.31	2.27	13.82	13.38	0.19	3.37	7.15	1.87	0.35		
(Basalt)	S.D.	0.19	0.04	0.10	0.12	0.005	0.26	0.10	0.03	0.01		
	C.V. (%)	0.35	1.85	0.75	0.93	2.67	7.65	1.41	1.33	3.12		
	R.V.										3.35	
G-A	mean (20)										3.59	
(Granite)	S.D.										0.10	
	C.V. (%)										2.78	
	ILC (3)***	68.23	0.44	15.33	2.52	0.07	1.14	2.21	4.54	0.23	3.77	1.26
UWO-1	mean (8)	68.69	0.43	15.17	2.63	0.08	0.94	1.93	4.13	0.17	3.66	1.15
(Granite)	S.D.	0.36	0.01	0.22	0.05	0.01	0.08	0.06	0.10	0.05	0.12	0.20
	C.V. (%)	0.52	2.32	1.45	1.90	12.50	8.51	3.11	2.42	29.4	3.27	17.39

* Number of duplicate analyses;
** Total iron as Fe_2O_3;
*** ILC, interlab comparison from X-ray Assay, Toronto.

R.V. = Recommanded values from Abbey (1980);
S.D. = Standard deviation;
C.V. (%) = Coefficient of variation, i.e. relative deviation from mean.

interference standards to obtain the stripping factors (eg. Nisbet et al., 1979). The typical background working curve and the composition of interference standards are shown in Figure B-1 and Table B-3, respectively.

Calculation of trace-element concentration was carried out by comparing the corrected peak intensity of unknown sample with the standard. It is simply expressed as:

$$C_{unk} = (I_{unk}/I_{std}) * (u_{unk}/u_{std}) * C_{std}$$

C = concentration in ppm;

I = intensity of radiation measured in cts/sec.;

u = total mass absorption coefficient of rock matrix at given wavelength.

The lower limit of detection (LLD) of this synthetic background mehtod may be calculated from Norrish and Chappell (1977) as:

$$LLD = 6/m\ (Bkg\ /\ T)^{1/2}$$

m = no. of cts/sec/ppm for the standard;

Bkg = no of background cts/sec calculated from working curve;

T = analytical time used (e.g. 100 sec.).

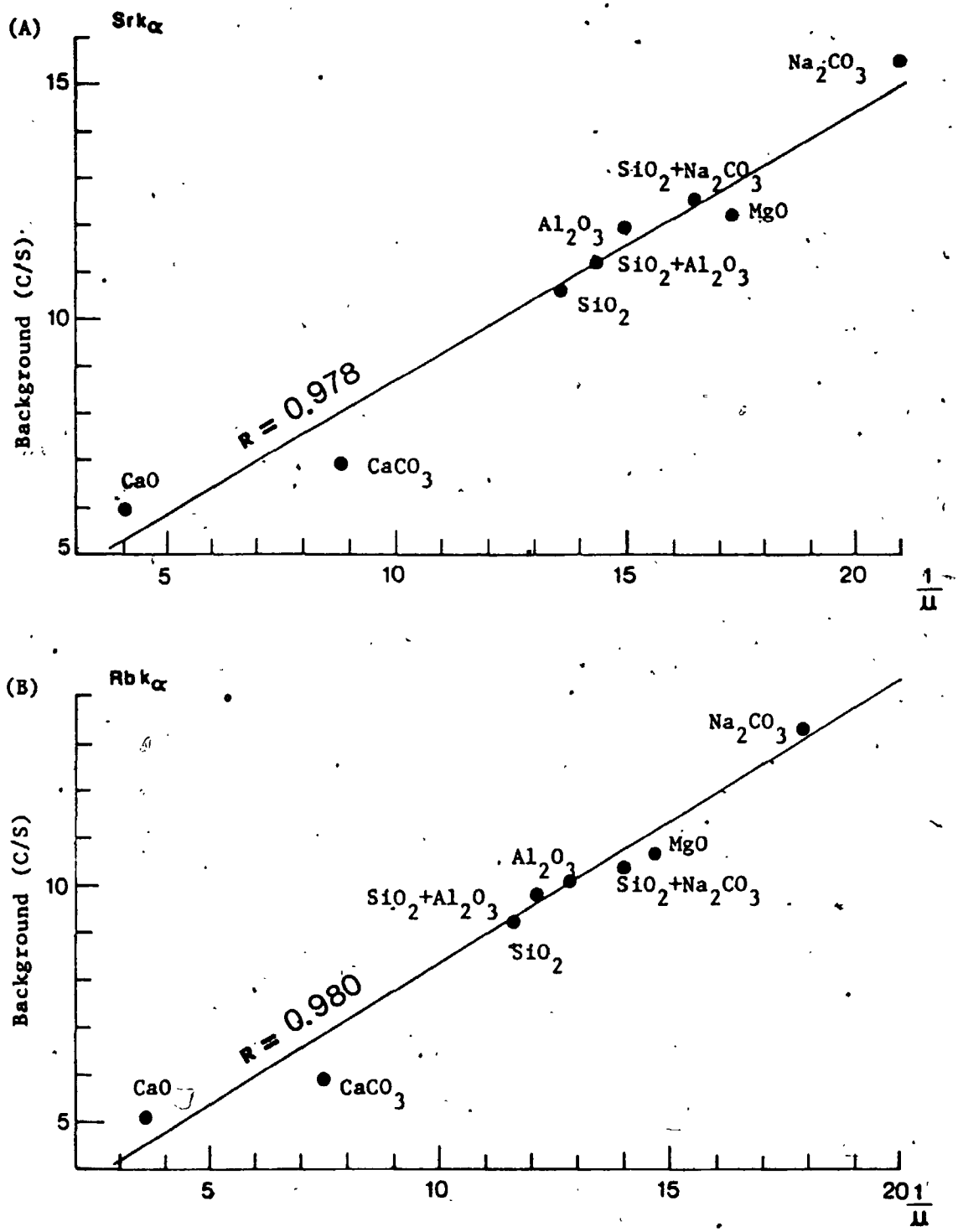

Figure B-1. Typical background working curves for trace-element analysis. (A) for Sr (B) for Rb. u = mass absorption coefficient.

Table B-3. Compositions of synthetic standards for trace-element analysis

(A) Mass absorption correlation standards (for background working curve):

Name	Oxide composition
MAC-1	100% SiO_2
MAC-2	100% Al_2O_3
MAC-3	100% Na_2CO_3
MAC-4	100% $CaCO_3$
MAC-5	100% CaO
MAC-6	98% MgO
MAC-7	50% SiO_2 + 50% Al_2O_3
MAC-8	50% SiO_2 + 50% Na_2CO_3
MAC-9	100 Fe_2O_3
MAC-10	100% ZnO

(B) Interference standards (for calculating interference factors):

Name	Composition
1. Rb-Y	99.97% SiO_2 + 0.03% $RbCO_3$
2. Fe-Co	97.0% SiO_2 + 3.0% Fe_2O_3
3. Sr-Zr	99.97% DTS-1 (USGS std) + 0.03% $SrCO_3$
4. Y-Nb	99.97% DTS-1 (USGS std) + 0.03% YO_3
5. Co-Ni	99.97% SiO_2 + 0.03% Co-metal
6. Ti-Ba	97.0% SiO_2 + 3.5% TiO2
7. V-Cr	99.0% SiO_2 + 1.0% V_2O_5

Except that Ba was calibrated against standard AGV-1 (andesite), the other elements were calculated against standard G-2 (granite). The accuracy, precision and detection limit of trace-element determinations are given in Table B-4 and the data reduction programme is listed in Appendix C-4.

During interlaboratory cross examination, it was obvious that samples pulverized by the tungsten-carbide coated Bleuler led to a Co contamination amounting 5 to 10 times that of average granite; the Co analyses were thus discarded.

3.0 FERROUS IRON DETERMINATION

About half the samples were analyzed for ferrous iron (FeO) using the method of Wilson (1955). Exact 0.25 gm sample and 0.05 gm ammonium metavanadate (AMV) were dissolved in 5 ml cold 40% HF. The ferrous iron present in the sample was oxidized quantitatively by AMV, and the excess amount was then titrated against the standardized ferrous ammonium sulfate (FAS) solution. The amount of FeO in the sample was thus equal to the initial AMV minus the AMV titrated.

The reproducibility and accuracy of this analysis was found to be dependent on the procedure of standardization of FAS; for instance, whether the ceric sulfate 0.05N solution has been precisely made up. However, GSC standard SY-2 and

Table B-4. Precision, accuracy and detection limits for trace-element analysis

	UWO-1				G-2			
Element	Mean(10)*	S.D.	C.V.(%)	R.V.	Mean(5)	S.D.	C.V.(%)	LLD
Nb	22.8	1.78	7.8	13	12.9	1.17	9.07	2.0
Zr	240.7	1.27	0.5	300	299.1	1.75	0.59	2.0
Y	27.1	0.70	2.6	11	11.1	0.21	1.90	1.5
Sr	210.7	3.00	1.4	480	478.7	1.33	0.28	3.0
Rb	198.0	1.50	0.8	170	170.7	2.42	1.42	3.0
Pb	32.7	2.73	8.4	30	30.2	2.16	7.16	5.0
Zn	50.1	2.39	4.8	84	85.7	3.10	3.62	2.0
Cu	9.3	0.40	4.3	10	10.2	0.40	3.92	0.5
Ni	7.7	1.57	20.3	3.5	3.9	1.07	26.88	1.0
Co	24.9	3.32	13.4	5	5.1	0.77	15.16	2.5
Cr	13.3	1.72	13.0	8	7.8	1.28	16.45	1.5
Ba	566.1	16.83	3.0	1900	1784.5	30.15	1.69	8.0
V	42.1	3.61	8.4	36	38.7	4.82	12.45	4.5
Ga	21.4	2.36	11.0	23	22.9	1.63	7.10	4.5

* Number of analyses;
R.V. = Recommanded values from Abbey (1980);
S.D. = Standard deviation;
C.V. = Coefficient of variation;
LLD = Lower limit of detection (in ppm).

internal standard UWO-1 were analyzed along with each batch of samples for monitoring the preparation procedures. The results of duplicate analyses of the standards are given in Table B-5.

4.0 INSTRUMENTAL NEUTRON ACTIVATION ANALYSIS (INAA)

4.1 Instrumentation And Analytical Procedures

REE, Ta, Hf, Cs, Sc and Th were analyzed by INAA, after the method of Gordon et al. (1968) and modified by Gibson and Jagam (1980). An INAA lab was newly assembled and put into operation during this study.

Approximate 0.25 gm of powdered sample was weighed and sealed into a small polyethylene vial. Usually, 18 samples and two standards (G-2) were packed in two plastic dishes and irradiated simutaneously for 6 hrs. under a flux of about 10^{12} n/cm^2.sec at McMaster Nuclear Reactor Centre. To ensure a uniform neutron flux, the rock samples were rotated during irradiation.

The irradiated samples were then cooled for at least 6 days before counted by an Ortec co-axial lithium-drifted germanium (Ge(Li)) gamma-ray detector and analyzed by a 1024-channel Canberra Model 8180 multichannel analyser (MCA). Instrumental specifications of the detector and analyzing systems are listed in Table B-6. The FWHM of ^{60}Co 1332 kev

Table B-5. The FeO-determinations for various standard rocks

	MRG-1 (4)*	Sy-2 (11)	AGV-1 (1)	UWO-1 (14)
Mean	8.50	3.63	2.09	1.64
Range	8.38-8.70	3.53-3.70	-	1.41-1.71
S.D.	0.14	0.05	-	0.11
C.V. (%)	1.70	1.29	-	6.70
R.V.	8.63	3.62	2.03	-

* Number of analyses;
S.D. = Standard deviation;
C.V. = Coefficient of variation;
R.V. = Recommanded values from Abbey (1980).

Table B-6. Instrumental specifications for INAA systems

(A) The Detector System

1. Ge (Li) detector - an Ortec coaxial Ge(Li) semiconductor detector.

Diameter	42.9 mm
Length	31.0 mm
Detector volume	45.89 c.c.
Total active volume	39.30 c.c.
Drift depth	17.5 mm
Diffusion depth	1.1 mm
Window-to-detector distance	5.0 mm
Absorbing layers:-	Aluminum 0.5 mm
	Teflon 1.0 mm
Resolution	2.7kev FWHM at 1.33mev
Input voltage	2.2 kv

2. Bias voltage unit - an Ortec-459 bias voltage unit provides a voltage from 0 to ±5 kv with min. noise.

3. Cryostate assembly - it is designed to keep the detector under vaccum and at liquid nitrogen temperature (77°K) continuously.

4. Preamplifier - Ortec 120-4 preamplifier.

(B) The Analysing System

1. Multichannel analyser - Canberra Model-8180 Multichannel Analyser (MCA).

   (a) Pulse amplifier
   (b) Analog to Digital Converter unit (ADC)
   (c) Memory unit - full memory (1024 chs.) may be subdivided into halves or quarters via nine memory control rotary switch
   (d) Cathode Ray Tube display unit (CRT)

2. Build-in microprocessor - including energy calibration, peak location, peak gross and net area computation, 1.65 σ counting statistic calculation and spectrum stripping.

gamma-ray peak observed was 2.7 kev, that is, the resolution of the system was better than 0.2%.

Three counting stages were setup for different target isotopes; in general, the shorter half-life nuclides were counted earlier with less counting time, while the longer ones were counted after irradiation about 6 to 10 weeks in order to decrease interferences. The combinations of ^{109}Cd (88.2 kev), ^{232}Th (^{233}Pa, 311.8 kev), ^{137}Cs (661.6 kev) and ^{60}Co (1173.2 kev) energy sources were used to calibrate the system at different stages. Based on the linear relations between channel number and the energy calibrated, each channel was approximately 0.45 to 0.6 kev wide. Dead time set to be < 10% for all counting stages, which can be corrected by adjusting the distance between the detector and analyzing sample. Counting scheme and MCA settings used in this study are summarized in Table B-7 and B-8, respectively.

Since energy lines of gamma-ray for those geologically interested isotopes have been well-documented (eg. Gordon et al., 1968; Crouthamel et al., 1970; Jacobs et al., 1977; Gibson and Jagam, 1980), the photopeaks of elements can be easily identified to within ± 1 kev after proper energy calibration. About 10 channels, in some cases 15 channels, around each analyzing peak were chosen for later integration of peak area.

Table B-7. Counting scheme for instrumental neutron activation analysis in this study

Count stage	Element	Target isotope	Product nuclide	Half-life*	Analysed photopeak (kev)	Interfering peak (kev)
I. (After irradiation 7-10 days)	Sm	^{152}Sm	^{153}Sm	46.0 h	103.2	1. During the first few days after irradiation the peak in the vicinity of 100 kev is essentially due to Sm-103.
	La	^{139}La	^{140}La	40.22 h	328.8	
II. (After irradiation 15-18 days)	Lu	^{176}Lu	^{177}Lu	6.71 d	208.4	
	Hf	^{180}Hf	^{181}Hf	42.50 d	482.0	
IIIA. (After irradiation 40-45 days)	Ce	^{140}Ce	^{141}Ce	33.00 d	145.4	1. Severe interference from ^{59}Fe-143 kev; can be corrected from ^{59}Fe-1099 kev.
	Yb	^{168}Yb	^{169}Yb	32.00 d	177.2	
	Ta	^{181}Ta	^{182}Ta	115.10 d	222.1	2. Considerable interference from ^{181}Ta-179 kev; can be corrected from ^{181}Ta-222 kev.
	Tb	^{159}Tb	^{160}Tb	72.10 d	298.5	
	Th	^{232}Th	^{233}Pa	27.00 d	311.9	3. Interference from ^{233}Pa(Th)-300 kev; can be corrected from ^{233}Pa-312 kev.
	Cr	^{50}Cr	^{51}Cr	27.80 d	320.0	4. Not severe interference from ^{169}Yb-308 Kev; no correction was made in this study.
IIIB. (After irradiation 50-55 days)	Eu	^{151}Eu	^{152}Eu	12.00 y	778.9	
	Cs	^{133}Cs	^{134}Cs	2.05 y	795.8	
	Sc	^{45}Sc	^{46}Sc	83.90 d	889.2	
	Fe	^{58}Fe	^{59}Fe	45.00 d	1099.2	
	Co	^{59}Co	^{60}Co	5.26 y	1173.2	

* The values of half-life of analyses isotopes are taken from Gorden et al. (1968) and used for later calculating decay constants ($\lambda = 0.693/t^{1/2}$, $t^{1/2}$ = days).

Table B-8. The running conditions and MCA settings* for INAA

Parameters	Count - I	Count - II	Count - IIIA	Count - IIIB
Cooling period (days)	7 - 10	15 - 18	40 - 45	50 - 55
Distance from detector(cm)	5 - 8	3 - 4	1 - 2	1 - 2
Preset time (sec)	4×10^3	1×10^4	3×10^4	3×10^4
AMP coarse gain	300	300	300	100
AMP fine gain	4.79	0.50	4.79	5.15
ADC conv. gain	1024	1024	1024	2048
Digital offset	(off)	256	(off)	1024
Energy calibration	^{109}Cd 88.0 kev at ch.242. ^{233}Th 311.8 kev at ch. 799.	^{233}Th 311.8 kev at ch. 284. ^{137}Cs 661.6 kev at ch. 864.	^{109}Cd 88.0 kev at ch. 242. ^{233}Th 311.8 kev at ch. 799.	^{137}Cs 661.6 kev at ch. 136. ^{60}Co 1173.2 kev at ch. 991.
Spectrum stored	13 kev - 401 kev	140 kev - 706 kev	13 kev - 401 kev	613 kev - 1224 kev
Approx. kev/ch.	0.437	0.606	0.437	0.598

* Other parameters (used) for all analyses:-

FUNCTION : PHA	SCA-LLD : 0.20	I/O device : TTY-out
DATA : ADD	ULD : 10.00	
Pile up rejection : off	Time constant : 2μs	
Base line restorer: off	ADC baseline : 3.00	
Memory control : 1/1	ADC gate : off	

The total area which integrated from a full energy peak was used for the measurement of intensity of the isotope, Background was estimated by making a linear fit between the lowest pairs of channel on either side of the peak maximum. The net area was equal to total integrated area subtracting the estimated background (See Figure B-2). For standards and samples, the same number of channels have been integrated; however, minor adjustment was required if the peak shape had been significantly altered.

Although the Ge(Li) semiconductor detector gave an excellent resolution, the ^{59}Fe 142.5 kev peak, ^{182}Ta 179 kev peak and ^{233}Pa 300 kev peak were not totally resolved from the ^{141}Ce 145.5 kev peak, ^{169}Yb 177 kev peak and ^{160}Tb 298.5 kev peak, respectively. Interference factor was determined by the ratio between the interfered photopeak and another clean energy line of the same isotope; the amount of interference was then calculated from the latter peak area by multiplying this factor. Interference factors were obtained from duplicate measurements of silica-based, synthetic Ta and Th monitors and a piece of Fe-wire; they are: Fe-142/Fe-1099 = 0.2036, Ta-179/Ta-222 = 0.5887 and Th-300/Th-312 = 0.1885.

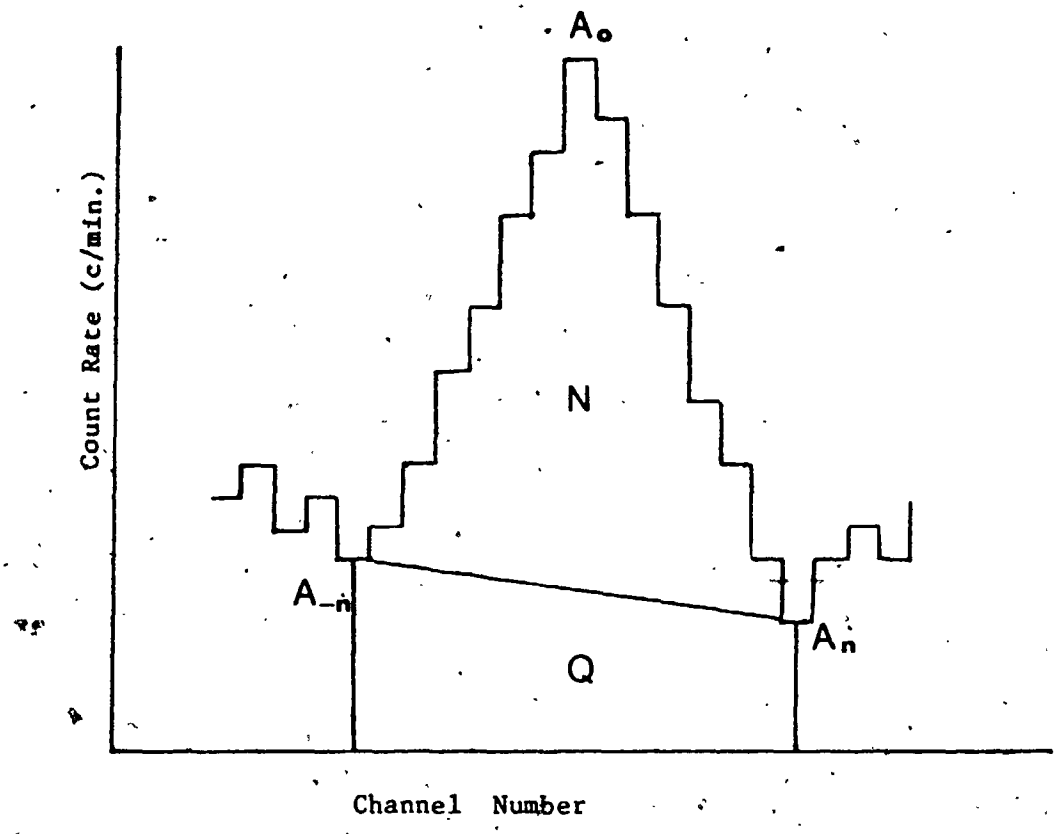

Figure B-2. Datermination of a peak area.

$$P \text{ (total area)} = A_0 + \sum_{1}^{n} A_i + \sum_{-1}^{-n} A_i$$

$$Q \text{ (background)} = (A_n + A_{-n}) * n / 2$$

$$N \text{ (net area)} = P - Q$$

4.2 Quantitative Computation

Theoretically, the number of neutron interactions (X_i) occurring in a unit time is directly proportional to the number of target nuclei (N) in a sample and to the neutron flux ( ), that is :

$$X_i = \sigma_i \phi N$$

σ_i = cross-section of a given type of interaction.

Thus, increase in the number of radiation nuclei (N*) with time from the beginning of irradiation is defined as :

$$\frac{dN^*}{dt} = \sigma\phi N - \lambda N$$

σ = the activation cross-section;

dN* = the decay rate of the same nuclei;

λ = the decay constant.

After integration,

$$N^* = \sigma\phi N (1 - e^{-\lambda t_i}) .$$

t_i = the irradiation time.

The number of radioactive nuclei remaining after a cooling period (t_d) from the end of irradiation can be calcualted as :

$$N^* = \sigma\phi N (1 - e^{-\lambda t_i}) e^{-\lambda t_d}$$

The counts measured during each counting interval (t_c) is expressed as :

$$N^* = \sigma\phi N (1 - e^{-\lambda t_i}) e^{-\lambda t_d} (1 - e^{-\lambda t_c}) I_r \varepsilon_r$$

I_r = the intensity of emitted gamma-ray of a given energy;

ε_r = the efficiency of the detector.

In a comparative analytical method, the activity measured from the unknown sample was compared with the activity of the reference standard which has similiar matrix and activation cross-section. Therefore, with the same neutron flux and irradiation time, and analyzing the same energy line with the same counting time, the calculation equation can be simplified as :

$$\frac{N^*_{unk}}{N^*_{std}} = \frac{N_{unk}}{N_{std}} * \frac{e^{-\lambda t_d(unk)}}{e^{-\lambda t_d(std)}}$$

that is,

$$Conc_{(unk)} = Conc_{(std)} * \frac{W_{std}}{W_{unk}} * \frac{PA_{(unk)}}{PA_{(std)}} * \frac{e^{-\lambda t_d(std)}}{e^{-\lambda t_d(unk)}}$$

W = weight of the powdered rock analysed;

PA = net peak area of a given energy r-ray;

t_d = decay period after irradiation.

Before quantitative calculation, the net peak counts were checked with Currie's "working expressions" criteria (1968) and the "paired observations" (the true mean of background counts) were used for computing. Only those ones with net peak areas greater than the "determinative limit" (L_Q) were processed quantitatively.

Based on the results of 5 replicates of G-2 and UWO-1, the accuracy and precision of the analyses for most samples may be taken as : Ce, Th, Sc = ±3%, La, Sm, Hf = ±5%, Eu, Lu, Cs = ±10%, Tb, Yb, Ta = ±15%. Results obtained on UWO-1 and RHY-1 also show excellent agreement between laboratories (i.e. Nuclear Activation Service, McMaster University and Geology Dept., University of Ottawa). Details are summarized in Table B-9.

Table B-9. The duplicate analyses of G-2, UWO 1 and RHY-1 by INAA and interlaboratory comparison

Standard	Statistics	La	Ce	Sm	Eu	Tb	Yb	Lu	Ta	Hf	Cs	Th	Sc
	R.V.	92.00	160.00	7.20	1.40	0.50	0.86	-	0.80	8.00	1.40	25.00	3.50
G-2	mean (5)	94.02	160.96	7.10	1.31	0.48	0.67	0.12	0.71	8.41	1.44	24.58	3.54
(Granite)	S.D.	1.43	3.01	0.21	0.09	0.05	0.12	0.01	0.09	0.25	0.17	0.80	0.13
	C.V. (%)	1.52	1.87	2.98	7.07	9.59	18.46	5.89	12.32	2.99	11.86	3.25	3.88
	NAS*	48.00	95.00	10.00	1.30	1.50	4.10	0.58	-	-	-	24.00	-
UWO-1	mean (3)	45.82	91.18	8.63	1.10	1.13	4.00	0.60	4.32	8.47	7.40	22.19	6.97
(Granite)	S.D.	2.73	3.19	0.44	0.09	0.13	0.28	0.03	0.52	0.44	0.36	0.52	0.06
	C.V. (%)	5.95	3.50	5.08	8.00	11.83	7.00	5.65	11.95	5.19	4.87	2.33	0.86
RHY-1	Western*	-	-	-	0.98	-	-	-	-	5.14	-	3.01	8.22
(Rhyolite)	Ottawa*	-	-	-	0.99	-	-	-	-	5.78	-	3.14	8.39

* NAS - results from Nuclear Activation Service, McMaster University, Hamilton, Ontario.
Western - results from this study.
Ottawa - results from Geolofy Dept., University of Ottawa. (Dr. C. Pride, personal comm.)

5.0 IN-SITU GAMMA-RAY SPECTROMETER ANALYSIS

In-situ U and Th measeurements were performed with an Exploranium Model DISA-400A Portable gamma-ray Differential Spectrometer, which is equiped with a 76 mm diameter x 76 mm thick standard NaI(Tl) scintillation detector.

Three differential channels were used for gamma-ray energy emission of ^{40}K (1.46 Mev), ^{214}Bi (1.76 Mev, equivalent ^{238}U) and ^{208}Tl (2.62 Mev, equivalent ^{232}Th) with window widths 200, 200 and 400 Kev, respectively. A ^{137}Cs energy source (approx. 1 micro curie) was used to adjust internal energy calibration for proper window settings. The resolution of the detector was about 9% at ^{60}Co 1.33 Mev energy line.

Each station chosen required a flat surface (Doig, 1968) with an area over 3 min diameter. The detector was held about 2 cm above the surface. In order to obtain better than 10% of counting statistics, a minimum of 120 counts in each window was required (i.e. 2 to 4 min. for each measurement); average of 3 measurements is considered as the representative reading of that station.

Background radiations were measured from the open water of the Paudash Lake, near Bancroft. Two measurements were taken each morning and evening during a two-week period. Average measurements are 10, 19 and 48 cts/min for Th, U and K respectively.

For quantitative determinations of eU and eTh from the field, it has to be assumed that the secular equilibrium between parent radioelements (U and Th) and their daughter decay products was retained (eg. no loss of radon or removal of radium) due to a huge sample volume. Besides, the count rate detected in any one channel of the spectrometer was dependent mainly on (Cassidy, 1981) :

1. the concentration of the parent radioisotope;
2. the sensitivity of the detector;
3. the presence of interfering isotopes;
4. the background count rate;
5. the energy of the emitted gamma-ray.

Thus, equations for calculation of in-situ K, eU and eTh determinations considering the above parameters are given as Killeen and Carmicheal (1970):

$$eTh = F_1 \, (Th_{cpm} - B_{th})$$

$$eU = F_2 \, (U_{cpm} - B_u - S_1 * (Th_{cpm} - B_{th}))$$

$$K = F_3 \, (K_{cpm} - B_k - S_2 * (Th_{cpm} - B_{th}) - S_3 * (U_{cpm} - B_u - S_1 * (Th_{cpm} - B_{th})))$$

where F_1, F_2, F_3

= the sensitivity or calibration factors of the detector;

S_1, S_2, S_3

= the stripping factors for contribution from neighbor interfering radioisotpes;

B_{th}, B_u, B_k

= the background count rate.

Since these factors are unique to each scintillator, quantitative determinations of K, eU and eTh can be obtained if they have been properly calibrated.

For this study, the sensitivity and stripping factors were calibrated from measurements done at the Geological Survey of Canada radiometric calibration facilities at Bell's Corner (Ontario), using the computer programme of Dr. P.G. Killeen (GSC). The nine factors for the detector (Serial no. 133753) are :

Sensitivities: F_1 = 8.7 cpm/ppm eTh

F_2 = 24.0 cpm/ppm eU

F_3 = 180.0 cpm/ % K

Stripping Factors: S_1 = 0.93 cts (from Th in U)

S_2 = 0.86 cts (from Th in K)

S_3 = 0.95 cts (from U in K)

Background (calculated):

B_1 = 5.3 cpm

B_2 = 23.0 cpm

B_3 = 36.0 cpm

(Note: The measured backgrounds were used for final computing.)

6.0 FLUORINE AND CHLORINE DETERMINATIONS

6.1 Preparation Of Sample Solution

The method of Haynes (1978) for joint analysis of fluorine and chlorine with a single sample fusion and the ion-selective electrode technique was adopted in this study.

An Orion Model 407A/F specific ion meter was used in conjunction with 4 Orion ion-selective electrodes, namely 94-09 fluoride electrode, 94-17 chloride electrode, 94-16 silver sulfide electrode and 90-02 double-junction reference electrode. The reference electrode was filled with filling solutions, (1) inner soultion of KCl saturated with AgCl,and (2) outer solution of 10% KNO3. The typical analytical assembly for fluorine analysis is shown in Figure B-3.

The oxidizing flux, mixture of two parts (by weight) of reagent-grade Na_2CO_3 and one part of zinc

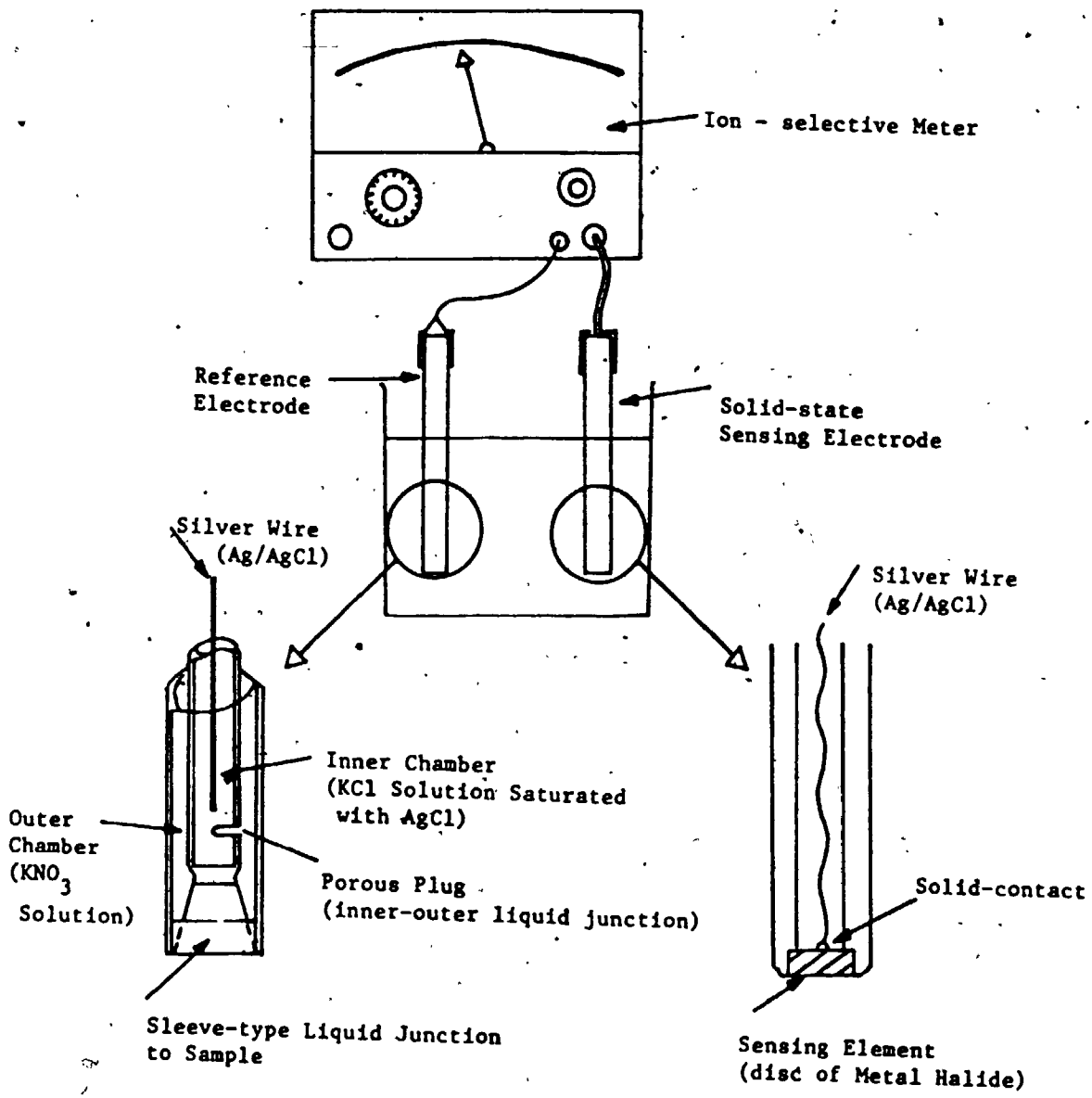

Figure B-3. Schematic representation of analytical assembly for fluorine and chlorine analyses.

oxide, was used for fusion process. About 0.5 gm of powdered rock and 2.0 gm of flux were weighed in a 30 ml Pt-crucible and thoroughly mixed. Sample-flux mixture was then fused in the furnace at about 1000±10 °C for 30 min.. The detail procedures for sample dissolution and preparation for fluorine-chlorine determinations are summarized in Haynes (1978).

The use of Na_2CO_3 - ZnO flux and additional acid, 8 ml of 10% citric acid for F and 1.5 ml nitric acid for Cl, during sample dissolution was to eliminate or reduce the interference and complexing with other ions. For instance, the fluorine electrode can be seriously interfered by OH^- due to its similar ionic size to F^-. Thus the PH of the sample solution was maintained between 5.5 and 5.6 in order to eliminate the OH^- interference and the complexing HF or HF_2^-. In addition, polyvalent cations such as Al^{3+}, Fe^{3+} and Si^{4+} in the rock readily form complexes with fluorine ion; the oxidizing flux allows them to be retained as insoluble residue in the filler (Huang and Johns, 1967). The additional polyvalent cations will be removed by complexing with citrate ions from the citric acid.

The 1% (10,000 ppm) F^- and Cl^- stock solutions were made by dissolving 22.1018 gm NaF and 16.4853 gm NaCl in 1,000 ml deionized water, respectively. Subsequently, the 1,000, 100 and 10 ppm standard solutions were diluted from this stock solution. In order to calibrate

the ion meter, appropriate volumes of standard solutions were mixed with 1 gm flux (as total ion adjust buffer) and proper amount of (citric or nitric) acid and treated as for the samples.

For example, 10 ppm F^- calibration solution was made by 10 ml of 100 ppm standard solution mixed with 1 gm oxidizing flux and 50 ml of deionized water. About 10 ml citric acid were added, mixed thoroughly and CO_2 gases were allowed to escape. After standing for at least 1 hour, the PH of the solution was adjusted to 5.5 to 6.5 by adding extra citric acid. The solution was then made up to 100 ml with deionized water and ready for calibration.

6.2 Quantitative Determination

When the ion selective electrodes are placed in an appropriate sample solution, there is a flux of ions across the disc membrane (eg. LaF_3 of the fluoride electrode, AgCl of the chloride electrode and Ag2S of the silver sulfide electrode) in the direction of the lowest activity. Since the ions carry a charge, an electric potential is then set up. This electric potential can be measured by connecting the ion-selective electrode (internal reference electrode) via a voltmeter with an external reference electrode which is also placed in the same sample solution.

The potential across the voltmeter is given by the Nernst equation :

$$E = E_o + (2.3RT / nF) \log A$$

where E = the total potential developed between the ion electrode and the reference electrode;

E_o = a constant potential relative to the type of reference electrode and its filling solutions;

n = the charge(s) on the ion;

A = the activity of the ion being measured;

T = temperature;

R, F = constants.

The function 2.3RT/nF is termed the Nernst Factor (S); for any given ionic charge this factor is only dependent on temperature. Hence, for a given temperature, the calibration curve with E plotted against logA can be constructed on standard 4-cycle semi-logarithmic paper. The electrode potential can be read from a regular PH/mv meter by using the Rel Mv function. Since the Orion 407A/F specific ion meter incorporates a slope control and log activity scale, the meter can be directly calibrated against solutions of known activity at a given temperature; the activity of rock sample solution can thus be measured.

However, the activity of the sample solution is only a measurement of amount of ions available for reaction. At low concentration in pure solutions, the activity is essentially equal to the concentration. But in rock sample solution, the activity is usually lower than its concentration because of complexing with other ions in the solution. That is, the concentration is equal to the free ions (activity) plus the bonded ions (complexes), which was then converted to ppm in the rock. It is expressed as:

$$\text{ppm in rock} = C * V / W$$

where C = concentration in sample solution;
V = volume of sample solution (ml);
W = sample weight analyzed (gm).

for this study,

$$\begin{aligned} &\text{ppm in rock} \\ &= \text{concentration measured} * 100 / 0.25 \\ &= \text{concentration measured} * 400 \end{aligned}$$

The precision obtained from replicates of UWO-1 indicating within 15% for fluorine analyses and about 10% for chlorine determinations.

7.0 ELECTRON MICROPROBE ANALYSIS

Biotite, amphibole and feldspars of representative samples were analyzed by means of a Material Analysis Company (MAC-400) three-spectrometer electron microprobe with KRISEL automation control. Data were reduced on-line with the MAGIC reduction software. An accelerating potential of 15 Kv and sample current of 500 and 250 uA were used for mafic silicates and feldspars, respectively. 30 sec. count-interval or 20,000 preset counts was used, whichever came first.

Three to five points per grain, six to ten grains per thin section were analyzed in order to establish homogeneity and to probe for any zonation. The Fe_2O_3 contents and Fe^{3+}/Fe^{2+} ratios of biotite were determined on selected mineral separates by titration; the conversion factors were then calculated for other samples of the same pluton. The structural formulae were calculated by computer programme SUPERCAL based on 6, 23, 22 and 32 oxygen for pyroxene, amphibole, biotite and feldspars, respectively. Average of analyses for each mineral per sample is reported. Analytical precision for the system has been determined by Fleet and Barnett (1978) and listed in Table B-10.

8.0 OXYGEN ISOTOPE ANALYSIS

Oxygen isotope abundances of whole-rocks and co-existing quartz - feldspar fractions were analyzed by Dr. R. Kerrich of this department. Oxygen isotopes were extracted from the sample by means of fluorination and then converted to CO_2 for high precision mass spectrometric determination.

Table B-10. Analytical presicion of microprobe analysis

Si ± 0.6%	Ti ± 1.8%	Ca ± 0.7%
Al^{iv} ± 1.6	Fe ± 1.2	Na ± 4.3
Al^{vi} ± 9.9	Mg ± 1.9	K ± 1.9

Number of analyses > 100

Appendix C. Analytical Results

C-1. Modal composition of sampled granitoids (in pocket).

C-2. Normative composition of sampled granitoids (in pocket).

C-3. Chemical composition of sampled granitoids (in pocket).

C-4. Trace-element data reduction programme.

```
      PROGRAM TRACE (INPUT,OUTPUT,TAPE5=INPUT,TAPE6=OUTPUT)
C
C
C     THIS IS A RAPID AND ROUTINE DATA REDUCTION PROGRAMME FOR 15
C    GEOLOGICALLY INTERESTING TRACE-ELEMENTS, NAMELY NB, ZR, Y, SR,
C    RB, PB, ZN, CU, NI, CO, CR, BA, V, S AND GA.
C     TOTAL INTENSITIES OF ANALYZING ELEMENTS WERE CORRECTED FOR
C    INTERFERENCE FROM THE OVERLAP X-RAY LINES AND ABSORPTIONS FROM
C    MAJOR OXIDES.
C     BACKGROUNDS WERE INTERPOLATED MATHEMATICALLY FROM A "SYNTHETIC
C    BACKGROUND WORKING CURVE".
C
C
      DIMENSION TITLE(8),HEAD(3),OXIDE(14),ATWT(13),OXWT(14),
     1          OXMA(15,15),NEL(15),NL(15),LT(15),SNAM1(10),TB(15),
     2          SB(15),CMA(15),SSCO(15,20),A(20,30),B(20,2),SCT(15),
     3          SLP(15),SNAM2(7),UCO(15,8),TP(15),SP(15),SSP(8,15),
     4          SMA(15,8),FINT(8),MDC(15),SNAM3(15),SPPM(15,15),
     5          TMA(15),TMA1(15,15),SPT1(15,15),STD(15),SP1(15),
     6          SNAM4(250),UMA(15),UMA1(15,250),SPT2(250,15),
     7          SP2(15),CONC1(15,15),CONC2(250,15) ,SPSTD(15),PPM(15),
     8          SNAM(15),CCO(250,15),UKO(250,15),CCO1(15),UKO1(15)

      DATA HEAD/"TRACE","ELEMENT","ANALYSIS"/
C
      DATA NEL/"NB","ZR","Y","SR","RB","PB","ZN","CU","NI","CO","CR",
     1         "BA","V","S","GA"/
C
      DATA FSIGN/"INT F"/
C
      DATA OXIDE/"SIO2","TIO2","AL2O3","FE2O3","MNO","MGO","CAO","K2O",
     1           "P2O5","NA2O","H2O","ZNO","CACO3","NA2CO3"/
C
C
C     ATOMIC WEIGHTS OF SI, TI, AL2, FE2, MN, MG, CA, K2, P2, NA2,
C    H2, ZN, C.
C
C
      DATA (ATWT(J),J=1,13)/28.086, 47.90, 53.963, 111.694, 54.933,
     1                      24.312, 40.08, 78.104,  61.948, 45.980,
     2                      2.016, 65.40, 12.00/
C
C
C     OXIDE WEIGHTS OF SIO2, TIO2, AL2O3, FE2O3, MNO, MGO, CAO, K2O,
C    P2O5, NA2O, H2O, ZNO, CACO3, NA2CO3.
C
C
      DATA (OXWT(J),J=1,14)/60.085, 79.899, 101.962, 159.693, 70.932,
     1                      40.311, 56.079, 94.203, 141.943, 61.979,
     2                      18.015, 81.400,100.080, 105.980/
C
C
C     MASS ABSORPTION COEFFICIENTS FOR SI, TI, AL, FE, MN, MG, CA, K,
C    P, NA, O, ZN, C  (HEINRICH, 1966).
C
```

```
C
      DATA (OXMA(J,1),J=1,13)/8.2,27.9,6.6,43.2,39.1,5.2,21.7,19.0,
     1      10.0,4.0,1.7,62.6,0.6/
      DATA (OXMA(J,2),J=1,13)/9.5,32.3,7.6,49.9,45.2,6.0,25.1,22.0,
     1     11.6,4.6,1.9,72.3,0.7/
      DATA (OXMA(J,3),J=1,13)/11.0,37.3,8.9,57.7,52.2,7.0,29.0,25.5,
     1     13.4,5.4,2.2,83.4,0.8/
      DATA (OXMA(J,4),J=1,13)/12.8,43.3,10.3,66.6,60.5,8.1,33.7,29.5,
     1     15.6,6.3,2.6,96.5,0.9/
      DATA (OXMA(J,5),J=1,13)/15.0,50.5,12.0,78.0,70.5,9.5,39.3,34.5,
     1     18.2,7.3,3.1,112.5,1.1/
      DATA (OXMA(J,6),J=1,13)/17.6,59.1,14.1,91.2,82.5,11.2,46.1,40.4,
     1     21.4,8.6,3.6,131.4,1.3/
      DATA (OXMA(J,7),J=1,13)/50.4,166.8,40.7,256.3,232.0,32.4,130.5,
     1     115.0,61.3,24.8,10.5,49.0,3.8/
      DATA (OXMA(J,8),J=1,13)/61.4,202.6,49.6,311.1,281.6,39.5,158.6,
     1    139.8,74.7,30.3,12.9,59.5,4.6/
      DATA (OXMA(J,9),J=1,13)/75.2,247.3,60.7,379.6,343.6,48.4,193.7,
     1     171.0,91.4,37.2,15.8,72.7,5.7/
      DATA (OXMA(J,10),J=1,13)/92.8,304.4,75.0,57.6,422.5,59.8,238.6,
     1     210.7,112.9,45.9,19.6,89.4,7.1/
      DATA (OXMA(J,11),J=1,13)/183.8,597.0,149.0,144.0,128.1,119.1,
     1     469.2,415.4,223.6,91.4,39.4,223.6,14.2/
      DATA (OXMA(J,12),J=1,13)/312.6,113.6,253.9,190.6,169.5,203.3,
     1      793.2,703.7,380.2,156.1,67.6,296.1,24.5/
      DATA (OXMA(J,13),J=1,13)/253.2,85.8,190.8,144.0,128.1,152.7,
     1     598.6,530.4,286.0,117.2,50.6,223.6,18.3/
      DATA (OXMA(J,14),J=1,13)/1949.3,689.6,1593.4,1157.5,1029.5,
     1     1284.8,502.4,424.6,2370.7,986.2,435.5,1797.9,160.0/
      DATA (OXMA(J,15),J=1,13)/41.7,138.3,33.6,212.8,192.6,26.7,
     1      108.1,95.2,50.7,20.5,8.7,40.7,3.1/
C
C
C     SYNTHETIC COMPOUNDS FOR CALCULATING BACKGROUND WORKING CURVES.
C
C
      DATA SNAM1/"SIO2","AL2O3","NA2CO3","CACO3","CAO","MGO",
     1     "SIO2+AL2O3","SIO2+NACO3","FE2O3","ZNO"/
C
C
C     OXIDE COMPOSITIONS OF SYNTHETIC COMPOUNDS.
C
C
      DATA (SSCO(J,1),J=1,14)/100.0,0.0,0.0,0.0,0.0,0.0,0.0,0.0,0.0,0.0,
     1      0.0,0.0,0.0,0.0,0.0/
      DATA (SSCO(J,2),J=1,14)/0.0,0.0,100.0,0.0,0.0,0.0,0.0,0.0,0.0,0.0,
     1      0.0,0.0,0.0,0.0,0.0/
      DATA (SSCO(J,3),J=1,14)/0.0,0.0,0.0,0.0,0.0,0.0,0.0,0.0,0.0,0.0,
     1      0.0,0.0,0.0,0.0,100.0/
      DATA (SSCO(J,4),J=1,14)/0.0,0.0,0.0,0.0,0.0,0.0,0.0,0.0,0.0,0.0,
     1      0.0,0.0,0.0,100.0,0.0/
      DATA (SSCO(J,5),J=1,14)/0.0,0.0,0.0,0.0,0.0,0.0,100.0,0.0,0.0,0.0,
     1      0.0,0.0,0.0,0.0,0.0/
      DATA (SSCO(J,6),J=1,14)/0.0,0.0,0.0,0.0,0.0, 98.0,0.0,0.0,0.0,0.0,
     1      0.0,0.0,0.0,0.0,0.0/
```

```
      DATA (SSCO(J,7),J=1,14)/50.0,50.0,0.0,0.0,0.0,0.0,0.0,0.0,0.0,
     1      0.0,0.0,0.0,0.0,0.0/
      DATA (SSCO(J,8),J=1,14)/50.0,0.0,0.0,0.0,0.0,0.0,0.0,0.0,0.0,
     1      0.0,0.0,0.0,0.0,50.0/
      DATA (SSCO(J,9),J=1,14)/0.0,0.0,100.0,0.0,0.0,0.0,0.0,0.0,0.0,
     1      0.0,0.0,0.0,0.0,0.0/
      DATA (SSCO(J,10),J=1,14)/0.0,0.0,0.0,0.0,0.0,0.0,0.0,0.0,0.0,
     1      0.0,100.0,0.0,0.0,0.0/
C
C
C     INTERFERENCE CORRECTION STANDARDS.
C
C
      DATA SNAM2/"RB-Y","FE-CO","SR-RB","Y-NB","CO-NI","TI-BA","V-CR"/
C
C
C     OXIDE COMPOSITIONS OF INTERFERENCE STANDARDS.
C
C
      DATA (UCO(I,1),I=1,14)/100.0,0.0,0.0,0.0,0.0,0.0,0.0,0.0,0.0,0.0,
     1      0.0,0.0,0.0,0.0/
      DATA (UCO(I,2),I=1,14)/96.5,0.0,0.0,3.5,0.0,0.0,0.0,0.0,0.0,0.0,
     1     0.0,0.0,0.0,0.0/
      DATA (UCO(I,3),I=1,14)/40.61,0.0,0.25,8.70,0.12,49.80,0.14,0.0,
     1    0.0, 0.01,0.42,0.0,0.0,0.0/
      DATA (UCO(I,4),I=1,14)/40.61,0.0,0.25,8.70,0.12,49.80,0.14,0.0,
     1    0.0, 0.01,0.42,0.0,0.0,0.0/
      DATA (UCO(I,5),I=1,14)/100.0,0.0,0.0,0.0,0.0,0.0,0.0,0.0,0.0,0.0,
     1     0.0,0.0,0.0,0.0/
      DATA (UCO(I,6),I=1,14)/97.0,3.0,0.0,0.0,0.0,0.0,0.0,0.0,0.0,0.0,
     1     0.0,0.0,0.0,0.0/
      DATA (UCO(I,7),I=1,14)/99.0,0.0,0.0,0.0,0.0,0.0,0.0,0.0,0.0,0.0,
     1      0.0,0.0,0.0,0.0/
C
C
C     READ INPUT DATA.
C
C
      READ(5,100) TITLE
  100 FORMAT(8A10)
      WRITE(6,110) (HEAD(I),I=1,3)
  110 FORMAT(1H1,36X,3A10)
      WRITE(6,120) TITLE
  120 FORMAT(1H0,8A10)
C
C     INPUT NO. OF ELEMENTS ANALYZED (I2), NO. OF STANDARDS USED
C    TO CONSTRUCT BACKGROUND WORKING CURVE (I2), NO. OF STANDARDS
C    FOR CALCULATING CONCENTRATIONS (I2) AND NO. OF SAMPLES (I3).
C
      READ(5,130) NE,NMCA,NSTD,NS
  130 FORMAT(3I2,I3)
C
C     INPUT ELEMENT LIST.
C
      READ(5,140) (LT(I),I=1,NE)
```

```
  140 FORMAT(15(A2,2X))
C
C     INPUT SELECTIONS FOR CALCULATION STANDARDS.
C
      READ(5,150)(MDC(I),I=1,NE)
  150 FORMAT(15I2)
C
C     INPUT OXIDE COMPOSITIONS OF STANDARDS.
C
      DO 180 I=1,NSTD
      READ(5,160) SNAM3(I),(CCO(I,J),J=1,14)
  160 FORMAT(A10,14F5.2)
C
C     INPUT TRACE-ELEMENT CONCENTRATIONS OF STANDARDS.
C
      READ(5,170) (SPPM(I,K),K=1,15)
  170 FORMAT(10F8.2)
  180 CONTINUE
C
C     INPUT OXIDE COMPOSITIONS OF UNKNOWN SAMPLES.
C
      DO 200 I=1,NS
      READ(5,190) SNAM4(I),(UKO(I,J),J=1,14)
  190 FORMAT(A10,14F5.2)
  200 CONTINUE
C
C     CALCULATE BULK MASS ABSORPTION COEFFICIENTS.
C
      DO 220 I=1,NE
      DO 210 J=1,12
      OXMA(J,I)=OXMA(J,I)*ATWT(J)/OXWT(J) + (OXWT(J)-ATWT(J))/OXWT(J)
     1          *OXMA(11,I)
  210 CONTINUE
      OXMA(13,I)=OXMA(7,I)*ATWT(7)/OXWT(13) + OXMA(13,I)*ATWT(13)/
     1           OXWT(13) + OXMA(11,I)*(OXWT(13)-ATWT(13)-ATWT(7))/
     2           OXWT(13)
      OXMA(14,I)=OXMA(10,I)*ATWT(10)/OXWT(14) + OXMA(13,I)*ATWT(13)/
     1           OXWT(14) + OXMA(11,I)*(OXWT(14)-ATWT(13)-ATWT(10))/
     2           OXWT(14)
  220 CONTINUE
      WRITE(6,230)
  230 FORMAT(1H0,30X,"OXIDE MASS ABSORPTION COEFFICIENTS")
      WRITE(6,240) (OXIDE(I),I=1,14)
  240 FORMAT(1H0,8X,14A8)
      DO 250 I=1,NE
  250 WRITE(6,260) NEL(I), (OXMA(J,I),J=1,14)
  260 FORMAT(1H0, 2X, A2, 14F8.2)
C
C
C     CALCULATE AND CONSTRUCT BACKGROUND WORKING CURVES.
C
C
      DO 320 I=1,NMCA
      READ(5,270)NUM
  270 FORMAT(21X,I2)
```

```
      DO 290 J=1,NE
      READ(5,280) TB(J),SB(J)
  280 FORMAT(8X,F7.3,F8.0)
      IF(TB(J).EQ.0.0) TB(J)=1.0
      SB(J)= SB(J)/TB(J)
  290 CONTINUE
      M1=-1
      DO 310 K=1,NE
      CMA(K)=0.0
       DO 300 J=1,14
  300 CMA(K)=CMA(K) + SSCO(J,I)*OXMA(J,K)/100.0
      M1=M1+2
       M2=M1+1
      A(I,M1)=1.0/CMA(K)
      A(I,M2)=SB(K)
  310 CONTINUE
  320 CONTINUE
  330 N1=0
      NN=2*NE
      DO 370 I=1,NN,2
      DO 340 K=1, NMCA
      B(K,1)=A(K,I)
      B(K,2)=A(K,I+1)
  340 CONTINUE
      N1=N1+1
      WRITE(6,350)LT (N1)
  350 FORMAT(1H1,"CALIBRATION FOR ",2X,A2)
      CALL LINFIT(SNAM1,B,NMCA,20,2,SCT(N1),SLP(N1))
      WRITE(6,360) SCT(N1), SLP(N1)
  360 FORMAT(1H0,"THE CALIBRATION LINE : BKG(I) =",F18.5," +",F18.5,
     1            " 1/MAC")
  370 CONTINUE
C
C     SWITCH TO PEAK POSITION
C
      DO 410 J=1,7
      READ(5,270)NUM
      DO 400 K=1,NE
      READ(5,380) TP(K),SP(K)
  380 FORMAT(8X,F7.3,F8.0)
         IF(TP(K).EQ.0.0) TP(K)=1.0
      SSP(J,K)=SP(K)/TP(K)
      DO 390 I=1,14
  390 SMA(K,J)=SMA(K,J)+UCO(I,J)*OXMA(I,K)/100.0
  400 CONTINUE
  410 CONTINUE
C
C
C     CALCULATE INTERFERENCE FACTORS.
C
C
      CPSY=SSP(1,3)-(1/SMA(3,1)*SLP(3)+SCT(3))
      CPSRB=SSP(1,5)-(1/SMA(5,1)*SLP(5)+SCT(5))
      FINT(1)=CPSY/CPSRB
      CPSCO=SSP(2,10)-(1/SMA(10,2)*SLP(10)+SCT(10))
```

```
      FINT(2)=CPSCO/UCO(4,2)
      CPSSR=SSP(3,4)-(1/SMA(4,3)*SLP(4)+SCT(4))
      CPSZR=SSP(3,2)-(1/SMA(2,3)*SLP(2)+SCT(2))
      FINT(3)=CPSZR/CPSSR
      CPSNB=SSP(4,1)-(1/SMA(1,4)*SLP(1)+SCT(1))
      CPSY1=SSP(4,3)-(1/SMA(3,4)*SLP(3)+SCT(3))
      CPSRB1=SSP(4,5)-(1/SMA(5,4)*SLP(5)+SCT(5))
      CPSY2=CPSY1-CPSRB1*FINT(1)
      FINT(4)=CPSNB/CPSY2
      CPSNI=SSP(5,9)-(1/SMA(9,5)*SLP(9)+SCT(9))
      CPSCO1=SSP(5,10)-(1/SMA(10,5)*SLP(10)+SCT(10))
      CPSCO2=CPSCO1-UCO(4,5)*FINT(2)
      FINT(5)=CPSNI/CPSCO2
      CPSBA=SSP(6,12)-(1/SMA(12,6)*SLP(12)+SCT(12))
      CPSV=SSP(6,13)-(1/SMA(13,6)*SLP(13)+SCT(13))
      FINT(6)=CPSBA/UCO(2,6)
      FINT(7)=CPSV/UCO(2,6)
      CPSCR=SSP(7,11)-(1/SMA(11,7)*SLP(11)+SCT(11))
      CPSV1=SSP(7,13)-(1/SMA(13,7)*SLP(13)+SCT(13))
      CPSV2=CPSV1-UCO(2,7)*FINT(7)
      FINT(8)=CPSCR/CPSV2
C
C
C     CALCULATE CONCENTRATIONS OF UNKNOWN SAMPLES.
C
C
      DO 440 I=1,NSTD
      READ(5,270)NUM
      DO 420 K=1,NE
         TMA(K)=0.0
      DO 420 J=1,14
      TMA(K)=TMA(K)+CCO(I,J)*OXMA(J,K)/100.0
      CCO1(J)=CCO(I,J)
  420 CONTINUE
      CALL CORR (LT,NEL,NE,FINT,TMA,CCO1,SLP,SCT,SP1)
      DO 430 K=1,NE
      TMA1(K,I)=TMA(K)
      SPT1(I,K)=SP1(K)
  430 CONTINUE
  440 CONTINUE
      DO 450 J=1,NE
      M=MDC(J)
      STD(J)=SPPM(M,J)/(TMA1(J,M)*SPT1(M,J))
  450 CONTINUE
      WRITE(6,460)     (NEL(K),K=1,NE)
  460 FORMAT(1H1,20X," OXIDES MASS ABSORPTION ON STDS AND SAMPLES",
     1       //,1x,"SAMPLE",2X,15(2X,A2,2X))
      DO 470 I=1,NSTD
  470 WRITE(6,480)SNAM3(I),(TMA1(K,I),K=1,NE)
  480 FORMAT(1H0,A8,15F6.1)
      DO 490 J=1,7
  490 WRITE(6,480)SNAM2(J),(SMA(K,J),K=1,NE)
C
      DO 520 I=1,NS
      READ(5,270)NUM
```

```
      DO 500 K=1,NE
      UMA(K)=0.0
      DO 500 J=1,14
      UMA(K)=UMA(K)+UKO(I,J)*OXMA(J,K)/100.0
      UKO1(J)=UKO(I,J)
  500 CONTINUE
      CALL CORR(LT,NEL,NE,FINT,UMA,UKOI,SLP,SCT,SP2)
      DO 510 K=1,NE
      UMA1(K,I)=UMA(K)
      SPT2(I,K)=SP2(K)
  510 CONTINUE
  520 CONTINUE
      DO 530 L=1,NS
  530 WRITE (6,480)SNAM4(L),(UMA1(K,L),K=1,NE)
      DO 540 I=1,NE
      K=MDC(I)   $  SPSTD(I)=SPT1(K,I)  $  PPM(I)=SPPM(K,I)
      SNAM(I)=SNAM3(K)
  540 CONTINUE
      WRITE(6,550)(NEL(K),K=1,NE)
  550 FORMAT(1H1,20X,"NET PEAK (CPS) ON STDS AND SAMPLES",//,1X,
     1       "SAMPLE",15(3X,A2,3X),/)
      WRITE(6,560)(SNAM(I),I=1,NE)
  560 FORMAT(2X," STDS ",3X,15A8)
      WRITE(6,570)(SPSTD(J),J=1,NE)
  570 FORMAT(1H0,9X,15F8.2)
      DO 590 I=1,NSTD
      WRITE(6,580)SNAM3(I),(SPT1(I,K),K=1,NE)
  580 FORMAT(1H0,A8,15F8.2)
  590 CONTINUE
      DO 600 J=1,NS
  600 WRITE(6,580)SNAM4(J),(SPT2(J,K),K=1,NE)
C
C
C     OUTPUT THE RESULTS.
C
C
      WRITE(6,110)(HEAD(I),I=1,3)
      WRITE(6,120)TITLE
      WRITE(6,610) FSIGN, (FINT(I),I=1,8)
  610 FORMAT(1H0,A5,4X,"RB ON Y ",2X,"FE ON CO",4X,"SR ON ZR",2X,
     1       " Y ON NB",5X,"CO ON NI",2X,"TI ON BA",2X,"TI ON V ",
     2       2X, " V ON CR",/,8X,8(F9.4,2X))
      WRITE(6,620)(LT (K),K=1,NE)
  620 FORMAT(1H0," SAMPLE ",15(3X,A2,3X),/)
      WRITE(6,560)(SNAM(I),I=1,NE)
      WRITE(6,630)(PPM(I),I=1,NE)
  630 FORMAT(1H0,9X,15F8.1)
      WRITE(6,640)
  640 FORMAT(1H0," CONCENTRATION OF SAMPLES ...",//)
      WRITE(6,620)(LT (K),K=1,NE)
      DO 660 I=1,NSTD
      DO 650 K=1,NE
  650 CONC1(I,K)=STD(K)*SPT1(I,K)*TMA1(K,I)
  660 WRITE(6,670) SNAM3(I), (CONC1(I,K),K=1,NE)
  670 FORMAT(1H0,A8,15F8.1)
```

```
      DO 690 I=1,NS
      DO 680 K=1,NE
  680 CONC2(I,K)=STD(K)*SPT2(I,K)*UMA1(K,I)
      WRITE(6,670) SNAM4(I), (CONC2(I,K),K=1,NE)
  690 CONTINUE
C
  700 WRITE(6,710)
  710 FORMAT(1H0,"PROGRAM BY TSAI-WAY WU",/,12X,
     1        "GEOLOGY DEPARTMENT",/,12X,
     2        "UNIVERSITY OF WESTERN ONTARIO",/,12X,
     3        "SEPTEMBER, 1982")
      STOP
      END
C
C
C     SUBROUTINE CORR CALCULATE THE NET INTENSITIES BY SUBTRACTING
C    BACKGROUNDS AND INTERFERENCES FROM TOTAL COUNTS.
C
C
         SUBROUTINE CORR (LT,NEL,NE,FINT,TMA,CCO,SLP,SCT,SSP)
      DIMENSION NEL(15),LT(15),FINT(8),TMA(15),SLP(15),SCT(15),
     1          SP(15),BKG(15),CCO(15),SSP(15),TP(15)
      DO 110 I=1,NE
      READ(5,100) TP(I),SP(I)
  100 FORMAT(8X,F7.3,F8.0)
      IF(TP(I).EQ.0.0) TP(I)=1.0
      SP(I)=SP(I)/TP(I)
      BKG(I)=1/TMA(I)*SLP(I)+SCT(I)
      SSP(I)=SP(I)-BKG(I)
  110 CONTINUE
      DO 120 J=1,NE
      IF (LT(J).EQ.NEL(2)) SSP(J)=SSP(J)-FINT(3)*SSP(4)
      IF (LT(J).EQ.NEL(12)) SSP(J)=SSP(J)-FINT(6)*CCO(2)
      IF (LT(J).EQ.NEL(3))  SSP(J)=SSP(J)-FINT(1)*SSP(5)
      IF (LT(J).EQ.NEL(10)) SSP(J)=SSP(J)-FINT(2)*CCO(4)
      IF (LT(J).EQ.NEL(13)) SSP(J)=SSP(J)-FINT(7)*CCO(2)
  120 CONTINUE
      DO 130 J=1,NE
      IF (LT(J).EQ.NEL(1)) SSP(J)=SSP(J)-FINT(4)*SSP(3)
      IF (LT(J).EQ.NEL(9)) SSP(J)=SSP(J)-FINT(5)*SSP(10)
      IF (LT(J).EQ.NEL(11)) SSP(J)=SSP(J)-FINT(8)*SSP(13)
  130 CONTINUE
      RETURN
      END
C
C
C     SUBROUTINE LINFIT CONSTRUCTS LINEAR REGRESSION LINES FOR
C    BACKGROUND WORKING CURVES.
C
C
         SUBROUTINE LINFIT (TTL,A,N,N1,M1,C1,C2)
      DIMENSION A(N1,M1), B(2,2), C(2),D(20,5),TTL(20)
      DO 110 I=1,2
      C(I)=0.0
      DO 100 J=1,2
```

```
      B(I,J)=0.0
  100 CONTINUE
  110 CONTINUE
      DO 120 I=1,N
      B(1,1)=B(1,1)+1.0
      B(1,2)=B(1,2)+A(I,1)
      B(2,2)=B(2,2)+A(I,1)*A(I,1)
      C(1)=C(1)+A(I,2)
      C(2)=C(2)+A(I,1)*A(I,2)
  120 CONTINUE
      B(2,1)=B(1,2)
      CALL SLE(B,C,2,2,1.0E-08)
      SUMC=0.0
      SUMI=0.0
      SUM1=0.0
      SUM2=0.0
      SUM3=0.0
      DO 130 I=1,N
      D(I,1)=A(I,1)
      D(I,2)=A(I,2)
      D(I,3)=(D(I,2)-C(1))/C(2)
      D(I,4)=D(I,1)-D(I,3)
      D(I,5)=C(1)+D(I,1)*C(2)
      SUMC=SUMC+D(I,1)
      SUMI=SUMI+D(I,2)
  130 CONTINUE
      WRITE(6,140) N
  140 FORMAT(1H0,I2,"MAC STANDARDS HAVE BEEN USED.",//," STANDARDS",
     1        5X,"RECIPROCAL OF MAC",2X," BKG (C/S)",5X,
     2        " CALCULATED MAC ",5X,"DIFFERENCE")
      AVEC=SUMC/FLOAT(N)
      AVEI=SUMI/FLOAT(N)
      DO 150 I=1,N
  150 WRITE(6,160)TTL(I),(D(I,J),J=1,4)
  160 FORMAT(1H0,A10,5X,F10.6,4X,F16.6,2X,F10.6,10X,F10.6)
      SY=0.0
      SY2=0.0
      SYC=0.0
      SYC2=0.0
      DO 170 I=1,N
      SY=SY+D(I,2)
      SY2=SY2+D(I,2)**2
      SYC=SYC+D(I,5)
      SYC2=SYC2+D(I,5)**2
      SUM1=SUM1+(D(I,2)-AVEI)**2
      SUM2=SUM2+(D(I,1)-AVEC)**2
      SUM3=SUM3+(D(I,2)-AVEI)*(D(I,1)-AVEC)
  170 CONTINUE
      SST=SY2-SY*SY/FLOAT(N)
      SSR=SYC2-SYC*SYC/FLOAT(N)
      SSD=SST-SSR
      R2=SSR/SST
         R=SQRT(R2)
      C1=C(1)
      C2=C(2)
```

```
      WRITE(6,180)N,SST,SSR,SSD,R2,R
  180 FORMAT(1H0," NO. OF STANDARDS USED : ",I2,/
     1          " TOTAL SUM OF SQUARES : ",F20.4,/,
     2          " SUM OF SQUARES DUE TO REGRESSION : ", F20.4,/,
     3          " SUM OF SQUARES DUE TO DEVIATION : ",F20.4,/,
     4          " GOODNESS OF FIT : ", F15.6,/,
     5          " CORRELATION COEFFICIENT : ",F15.6)
      RETURN
      END
C
C
         SUBROUTINE SLE(A,B,N,N1,ZERO)
      DIMENSION A(N1,N1),B(N1)
      DO 150 I=1,N
      DIV=A(I,I)
      IF(ABS(DIV)-ZERO) 160,160,100
  100 DO 110 J=1,N
      A(I,J)=A(I,J)/DIV
  110 CONTINUE
      B(I)=B(I)/DIV
      DO 140 J=1,N
      IF(I-J) 120,140,120
  120 RATIO=A(J,I)
      DO 130 K=1,N
      A(J,K)=A(J,K)-RATIO*A(I,K)
  130 CONTINUE
      B(J)=B(J)-RATIO*B(I)
  140 CONTINUE
  150 CONTINUE
      RETURN
  160 WRITE(6,170)
  170 FORMAT(1H0," FAIL TO PASS THE TEST IN SUBROUTIN SLE")
      STOP
      END
```

REFERENCES

Abby, S., 1980, Studies in "standard samples" for use in general analysis of silicate rocks and minerals. Part 6: 1979 edition of "usable" values. Geol. Surv. Can., Paper 80-14, 30pp.

Academia Sinica, 1980, Kangdese granitoid belt. In: Field excursion guidebook, 45-49. Symposium on Qing-Xizang (Tibet) Plateau, Beijing.

Adams, F.D. and Barlow, A.E., 1910, Geology of the Haliburton and Bancroft areas, Province of Ontario. Geol. Surv. Can. Mem. 6.

AGI, 1972, Glossary of Geology (M. Gary, R. McAfee Jr. and C.L. Wolf eds.). Am. Geological Institute, Washington, D.C., 805 pp.

Ahrens, L.H., 1953, The use of ionization potentials, Part II. Geochim. Cosmochim. Acta, 3, 1-29.

Albuquerque, C.A.R. de, 1971, Petrochemistry of a series of granitic rocks from Northern Porturgal. Geol. Soc. Am. Bull., 82, 2783-2798.

Aleinikoff, J.N., 1977, Petrochemistry and tectonic origin of the Ammonoosuc Volcanics. New Hampshire - Vermont. Geol. Soc. Am. Bull., 88, 1546-1552.

Allegre, C.J. and Minster J.F., 1978, Quantitative models of trace element behavior in magmatic processes. Earth Planet. Sci. Lett., 38, 1-25.

Amstrong, R.L., 1966, K-Ar dating of plutonic and volcanic rocks in orogenic belt. In: Potassium Argon Dating (O.A. Schaeffer and J. Zahringer eds.). Springer-Verlag, Heidelberg, 117-131.

Arth, J.G., 1973, Geochemistry of early Precambrian igneous rocks, Minnesota-Ontario. Unpubl. Ph.D. thesis, State University of New York at Stony Brook, 152pp.

Arth, J.G., 1976, Behavior of trace elements during magmatic processes - a summary of theoretical models and their applications. Jour. Res. U.S. Geol. Surv., 4, 41-47.

Arth, J.G., 1979, Some trace elements in trondhjemites - their implications to magma gneiss and paleotectonic setting. In: Trondhjemites, dacites and related rocks (F. Barker ed.). Elsevier Scientific Publishing Company, Amsterdam, 123-131.

Arth, J.G. and Barker, F., 1976, REE partitioning between hornblende and dacitic liquid and implications for the genesis of trondhjemite - tonalitic magmas. Geology, 4, 534-536.

Arth, J.G., Barker, F., Peterman, Z.E. and Friedman, I., 1978, Geochemistry of the gabbro - diorite - tonalite - trondhjemite suite of southwest Finland and its implications for the origin of tonalitic and trondhjemitic magmas. Jour. Petrol., 19, 289-316.

Arth, J.G. and Hanson, G.N., 1975, Geochemistry and origin of the early Precambrian crust of northeastern Minnesota. Geochim. Cosmochim. Acta, 39, 325-362.

Baer, A.J., 1976, The Grenville Province in Helikian time: a possible model of evolution. Phil. Trans. Roy. Soc. London, A280, 499-515.

Baer, A.J., 1977, The Grenville Province as a shear-zone. Nature, 267, 337-338.

Baer, A.J., 1980, Foliated and recrystallized granites from the Timber Lake Pluton, Ontario. Geol. Surv. Can. Paper 80-1C, 201-205.

Baer, A.J., 1981a, A Grenvillian Model of Proterozoic plate tectonics. In: Precambrian plate tectonics (A. Kroner, ed.). Elsevier Scientific Publishing Company, Amsterdam, 353-385.

Baer, A.J. 1981b, Two orogenies in the Grenville Belt? Nature, 290, no. 5802, 129-131.

Bailey, D.K. and Schairer, J.F., 1966, The system Na_2O - Al_2O_3 - Fe_2O_3 - SiO_2 at 1 atmorsphere and the petrogenesis of alkaline rocks. Jour. Petrol., 7, 114-170.

Bailey, D.K. and Macdonald, R., 1969, Alkali feldspar fractionation trends and the derivation of peralkaline liquid. Am. Jour. Sci., 267, 242-248.

Bailey, D.K. and MacDonald, R., 1970, Petrochemical variation among mildly peralkaline (comendite) obsidians from the oceans and continents. Contr. Mineral. Petrol., 28, 340-351.

Baird, A.K., McIntyre, D.B., Welday, E.E. and Madlem, K.W., 1964, Chemical variations in granitic pluton and its surrounding rocks. Science, 146, 258-259.

Baird, A.K., McIntyre, D.B. and Welday, E.E., 1967, Geochemical and structural studies in batholithic rocks of southern California: part II, sampling of the Rattlesnake Mountain Pluton for chemical composition, variability, and trend analysis. Geol. Soc. Am. Bull., 78, 191-222.

Bandurkin, G.A., 1961, Behavior of the rare earths in fluorine-bearing media. Geochemistry, 1961 vol, 159-167.

Barker, B.H., 1976, A note on the behavior of incompatible trace elements in alkaline magms. In: Petrology and geochemistry of continental rifts (E.R. Neumann and I.B. Ramberg eds.), 15-25.

Barker, F. and Arth, J.G., 1976, Generation of trondhjemitic - tonalitic liquids and Archean bimodal trondhjemite - basalt suites. Geology, 4, 596-600.

Barker, F., Wones, D.R., Sharp, W.N. and Desborough, G.A., 1975, The Pikes Peak Batholith, Colorado Front Range, and a model for the origin of the gabbro -

anorthosite - syenite - potassic granite suite. Precambrian Res., 2, 97-160.

Barker, F., Friedman, I., Hunter, D.R. and Gleason, J.D., 1976, Oxygen isotopes of some trondhjemites, acidic gneisses and associated mafic rocks. Precambrian Res., 3, 547-557.

Basaltic Volcanic Study Project, 1981, Basaltic volcanism on the terrestrial planets. Pergamon Press, Inc., New York, 1286pp.

Barton, J.M. and Doig, R., 1977, Sr-isotopic studies of the origin of the Morin anorthosite complex, Quebec, Canada. Contr. Mineral. Petrol., 61, 219-230.

Bateman, P.C., Clack, L.D., Huber, N.K., Moore, J.G. and Rinehart, C.D., 1963, The Sierra Nevada Batholith - a synthesis of recent work across the central part. U.S. Geol. Surv. Prof. Paper. 414-D, 46pp.

Bateman, P.C. and Chappell, B.W. 1979, Crystallization, fractionation, and solidification of the Tuolome Intrusive Series, Yeosemite National Park, California. Geol. Soc. Am. Bull., 90, 465-482.

Bell, K. and Blenkinsop, J., 1980, Whole rock Rb-Sr studies in the Genville Province of Southeastern Ontario and Western Quebec - a summary report. Geol. Surv. Can. Paper 80-1C, 152-154.

Black, R., 1969, Field occurrences of Niger peralkaline acid rocks. Conference of Petrology of peralkaline rocks, University of Reading. Abstracted in Mineral Mag. 37, xliii-xliv.

Bouseily, A.M. and Sokkary, A.A., 1975, The relation between Rb, Ba and Sr in granitic rocks. Chem. Geology, 16, 207-219.

Bowden, P., 1970, Origin of the younger granites of northern Nigeria. Contr. Mineral. Petrol., 25, 153-162.

Bowden, P., 1974, Oversaturated alkaline rocks, granites, pantellerite and comendites. In: The alkaline rocks (H. Sorensen ed.). John Wiley and Sons, New York, 109-123.

Bowden, P. and Turner, D.C., 1974, Peralkaline and associated ring-complexes in the Nigeria-Niger Province, West Africa. In: The alkaline rocks (H. Sorensen ed.). John Wiley and Sons, New York, 330-354.

Bowden, P. and Whitley, J.E., 1974, Rare-earth patterns in peralkaline and associated granites. Lithos, 7, 15-21.

Bowen, N.L., 1945, Phase equilibria bearing on the origin and differentiation of the alkaline rocks. Am. Jour. Sci., 243A, 75-89.

Bright, E.G., 1976, Cavendish and Anstruther Townships, Peterborough County. In: Summary of field work 1976 (O.G. Milne, W.R. Cowan, K.D. Card and J.A. Robertson eds.). Ontario Division of Mines, Toronto, Ont., Rept. MP-67, 122-126.

Bright, E.G., 1980, Eels Lake Area, Southern Onterio. Ontario Geol. Surv., Preliminary map p-2205.

Brooks, C.K., 1969, On the distribution of zirconium and hafnium in the Skaergaard intrusion, East Greenland. Geochim, Cosmochim. Acta, 33, 357-374.

Brown, G.C. 1979, The changing pattern of batholith emplacement during Earth history. In: Origin of granite batholith: geochemical evidence, (M.P. Atherton and J. Tarney, eds.). Shiva Publishing, Orpington, 106-115.

Brown, G.C., 1980, Calc-alkaline magma genesis: the Pan-African contribution to crustral growth? In: Evolution and mineralization of the Arabian-Nubian Shield (A.M.A. Al-shanti, ed.). IAG Bull. no. 3, 19-29.

Brown, G.C., 1982, Calc-alkaline intrusive rocks: their diversity, evolution, and relation to volcanic arcs. In: Andesites-orogenic andesites and related rocks (R.S. Thorpe ed.). John Wiley and Sons, New York, 437-461.

Brown, R.L., Chappell, J.F., Moore, J.M. Jr. and Thompson, P.H., 1975, An ensimatic island arc and ocean closure in Grenville Province of southeastern Ontario, Canada. Geosci. Can., 2, 141-144.

Burma, G., Frey, F.A. and Wones, D.R., 1971, New England granites: trace element evidence regarding their origin and differentiation. Contr. Mineral. Petrol., 31, 300-320.

Burns, R.G. and Fyfe, W.S., 1967, Trace element distribution rules and their significance: a review. Chem. Geol., 2, 89-104.

Cassidy, J., 1981, Techniques of field gamma-ray spectrometry. Mineral. Mag., 44, 391-398.

Chapman, R.W. and Williams, C.R., 1935, Evolution of the White Mountain Magma Series. Am. Mineral., 20, 502-.

Chappell, B.W., 1978, Granitoids from the Moonbi District, New England Batholith, eastern Australia. Jour. Geol. Soc. Australia, 25, 267-283.

Chappell, B.W., 1979, Granites as images of their source rocks (abs.). Geol. Soc. Am., Abstr. with Prog., 11, 400.

Chappell, B.W. and White, A.J.R., 1974, Two contrasting granite types. Pacific Geology, 8, 173-174.

Chayes, F., 1970, On deciding whether trend surfaces of progressively higher order are meaningful. Geol. Soc. Am. Bull., 81, 1273-1278.

Chesworth, W., 1967, The origin of certain granitic rocks occurring in Glamorgan Township, southwestern Ontario. Unpubl. Ph.D. thesis, McMaster

University, Hamilton, Ontario.

Collerson, K.D., 1982, Geochemistry and Rb-Sr geochronology of associated Proterozoic peralkaline and subalkaline anorogenic granites from Labrador. Contr. Mineral. Petrol., 81, 126-147.

Collins, W.J., Beams, S.D., White, A.J.R. and Chapell, B.W., 1982, Nature and Origin of A-type granites with particular reference to southeastern Australia. Contr. Mineral. Petrol., 80, 189-200.

Compston, W. and Chappell, B.W., 1979, Sr-isotope evolution of granitoid source rocks. In: The Earth: its origin, structure and evolution (M.W. McElhinny ed.). Academic Press, London, 377-424.

Condie, K.C., 1976, Trace element geochemistry of Archean greenstone belts. Earth Science Reviews, 12, 393-417.

Condie, K.C. and Lo, H.J., 1971, Trace element geochemistry of the Louis Lake Batholith of early Precambrian age, Wyoming. Geochim. Cosmochim. Acta, 35, 1099-1119.

Condie, K.C. and Moore, J.M. Jr., 1977, Geochemistry of Proterozoic volcanic rocks from the Grenville Province, eastern Ontario. In: Volcanic regimes in Canada (W.R.A. Baragar, L.C, Coleman and J.M. Hall, eds.). Geol. Assoc. Can., Spec. Paper 16, 149-168.

Cox, F.G., Bell, J.D. and Pankhurst, R.J., 1979, The interpretation of igneous rocks. George Allen and Unwin, London, 450pp.

Croudace, I.W., 1980, The geochemistry and petrogenesis of the Lower Paleozoic granitoids of North Wales. Unpubl. Ph.D. thesis, University of Birmingham, England.

Crouthamel, C.E., Adams, F. and Dams, R., 1960, Applied gamma-ray spectrometry. Pergamon Press. New York, 752pp.

Cullers, R.L., Medaris, L.G. and Haskin, L.A., 1973, Experimental studies of the distribution of rare earths as trace elements among silicate minerals and liquid and water. Geochim. Cosmochim. Acta, 37, 1499-1512.

Currie, K.L., 1976, The alkaline rocks of Canada. Geol. Surv. Can. Bull., 239, 228pp.

Currie, L.A., 1968, Limits for qualitative detective and quantitative determination: application to radiochemistry. Anal. Chem., 40, 586-593.

Czamanske, G.K., Ishihara, S. and Atkin, S.A., 1981, Chemistry of rock-forming minerals of the Cretaceous-Paleocene Batholith in southwestern Japan and implications for magma genesis. Jour. Geophys. Res., 86, no. B-11, 10431-10469.

Darley, A.G., Charbonneau, B.W. and Richardson, K.A., 1977, The distribution of uranium in rocks as a guide to the recognition of uraniferous region. Symposium on Recognition and Evaluation of Uraniferous Areas, Internatinal Atomic Energy Agency, Vienna, Austria, IAEA TC15/9, 55-86.

Davis, G.L., Hart, S.R., Aldrich, L.T., Krogh, T.E. and Manizaga, F., 1967, Geochronology of the Grenville Province in Ontario, Canada. Carnegie Inst. Washington, Yearbook, 1965, 379-386.

Davis, G.L., Krogh, T.E., Hart, S.R., Brooks, C. and Erlank, A.J., 1970, The age of metamorphism in the Grenville Province, and the age of the Grenville Front. Carnegie Institute of Washington Yearbook 67, 224-230.

Davis, J.C., 1973, Statistics and data analysis in Geology. John Wiley and Sons, New York.

Davison, A., Britton, J.M., Bell, K. and Blenkinsop, J., 1979, Regional synthesis of the Grenville Province of Ontario and Western Quebec. Geol. Surv. Can., Paper 79-1B, 153-172.

Davison, A. and Morgan, W.C., 1981, Preliminary notes on the geology east of Georgian Bay, Grenville structural Province, Ontario. Geol. Surv. Can. Paper 81-1A, 291-298.

Davison, A., Culshaw, N.G. and Nadeau, L., 1982, A tectono-metamorphic framework for part of the Grenville Province, Parry Sound Region, Ontario. Geol. Surv. Can. Paper 82-1A, 175-190.

Day, H.W., 1973, The high temperature stability of muscovite plus quartz. Am. Mineral., 58, 255-262.

Deer, W.A., Howie, R.A. and Zussman, 1966, An introduction to the rock-forming minerals. Longman Group Limited, London, 528pp.

Dewey, J.F. and Burke, K.C.A., 1973, Tibetan, Variscan and Precambrian basement reactivation: products of continental collision. Jour. Geol., 81, 683-692.

Dickison, W.R., 1975, Potash-depth (k-h) relations in continental margin and intra-oceanic magmatic arcs. Geology, 3, 53.

Dietrich, R.V., 1968, Behavior of zirconium in certain artifical magmas under diverse P.T. conditions. Lithos, 1, 20-29.

Dodge, F.C.W., Smith, V.C. and Mays, R.E., 1969, Biotites from granitic rocks of the Central Sierra Nevada Batholith, California. Jour. Petrol., 10, 250-271.

Doig, R., 1968, The natural gamma-ray flux: in-situ analysis. Geophysics 33, 311-328.

Doig, R., 1977, Rb-Sr geochronology and evolution of the Grenville Province in northwestern Quebec, Canada. Geol. Soc. Am. Bull., 88, 1843-1856.

Donaldson, J.A. and Irving, E. 1972, Grenvill front and rifting of the Canadian Shield. Nature, 237, 139-140.

Dostal, J., 1973, Geochemistry and petrology of the Loon Lake Pluton, Ontario. Unpubl. Ph.D. thesis. McMaster University, Hamilton, Ontario, 328pp.

Dostal, J., 1975, Geochemistry and Petrology of the Loon Lake Pluton, Ontario. Can. Jour. Earth Sci., 12, 1331-1345.

Emmerman, R., 1975, Petrologic significance of rare earths in granites. Contr. Mineral. Petro., 52, 267-283.

Ermanovics, I.F., McRitchie, W.D. and Houston, W.N., 1979, Petrochemistry and tectonic setting plutonic rocks of the Superior Province of Manitoba. In: Trondhjemite, dacite and related rocks (F. Barker ed.). Elsevier Scientific Publishing Company. Amsterdam, 323-358.

Evans, A.M., 1966, The development of lit par lit gneiss at the Bicroft uranium mine, Ontario. Can. Mineral., 8, 593-609.

Feather, C.E. and Willis, J.P., 1976, A simple method for background and matrix correction of spectral peaks in trace element determination by X-ray fluorenscence spectrometry. X-ray spectrometry, 5, 41-48.

Fershtater, G.B. and Borodina, N.S., 1977, Petrology of autolith in granitic rocks. Internat. Geology Rev., 19, 458-468.

Fleet, M.E. and Barnett, R.L., 1978, AL^{IV}/AL^{VI} partitioning in calciferous amphiboles from the Frood mine, Sudbury, Ontario. Can. Mineral., 16, 527-532.

Flood, R.H. and Shaw, S.E., 1977, Two "S-type" granite suites with low initial $^{87}Sr/^{86}Sr$ ratios from the New England Batholith, Australia. Contr. Mineral. Petrol. 61, 163-173.

Flynn, T. and Burnham, 1978, An experimental determination of rare earth partition coefficients between a chloride containing vapour phase and silicate melts. Geochim. Cosmochim. Acta, 42, 685-701.

Foster, M.D., 1960, Interpretation of the composition of trioctahedral micas. U.S. Geol. Surv. Prof. Paper 354-B.

Fowler, A.D. and Doig, R., 1979, Origin of uraniferous granitoids, Granville Province, Quebec and Ontario (abs.). Geol. Assoc. Can., Abstr. with Prog., 4, 50.

Fowler, A.D., 1980, The age, origin, and rare-earth-element distributions of Grenville Province uraniferous granites and pegmatites. Unpubl. Ph.D. thesis. McGill University, Montreal, Qubec. 137pp.

Fowler, A.D. and Doig, R., 1983, The age and origin of Grenville Province uraniferous granites and pegmatites. Can. Jour. Earth Sci., 20, 92-104.

Frey, F.A., 1980, Applicatins of neutron activation analysis in mineralogy and petrology. In: Newtron activatin analysis in the geosciences, short course (G.K. Muecke, ed.). Mineral. Assoc. Can., 167-210.

Fryer, B.J. and Edgar, A.D., 1977, Significance of rare earth distributions in coexisting minerals of peralkaline undersaturated rocks. Contr. Mineral. Petrol., 61, 35-48.

Fyfe, W.S., 1973, The granulite facies, partial melting and the Archean crust. Philo. Trans. Roy. Soc. London, A273, 457-461.

Fyson, W.K., Baer, A.J. and Habib, M.K., 1980, Structural fabric and uranium distribution in shear zones near Cardiff, Ontario. Ontario Geol. Surv., Miscel. Paper 93, 83-85.

Gast, P.W., 1968, Trace element fractionation and the origin of tholeiitic and alkaline magma types. Geochim. Cosmochim. Acta, 32, 1057-1086.

Gibson, I.L. and Jagam, P., 1980, Instrumental neutron activation analysis of rocks and minerals. In: neutron activation analysis in the geosciences (G.K. Muecke ed.). Short course. Mineral.

Assoc. Can., 109-131.

Gittins, J., 1967, Nepheline rocks and petrological problems of the Haliburton-Bancroft area. In: Guidebook - geology of parts of eastern Ontario and western Quebec. (S.E. Jenness ed.). Geol. Assoc. Can. / Mineral. Assoc. Can. / Mineral. Assoc. Am., 31-57.

Goldschmit, V.M., 1937, The principles of distribution of chemical elements in minerals and rocks. Jour. Chem. Soc., 655-672.

Gordon, E.E., Randle, K., Coles, G.G., Corlis, J.B., Beeson, M.H. and Oxley, S.S., 1968, Instrumental activation analysis of standard rocks with high resolution gamma-ray detectors. Geochim. Cosmochim. Acta, 42, 725-742.

Gordon, J.B. and Masson, S., 1977, Uranium and thorium deposits in Ontario. Ontario Geol. Surv., Miscel. Paper 75, 192-194.

Green, T.H. and Ringwood, A.E., 1968, Genesis of the calc-alkaline igneous rock suite. Contr. Mineral. Petrol., 18, 105-162.

Griffin, T.J., White, A.J.R. and Chappell, B.W., 1978, The Moruya Batholith and geochemical contrast between the Moruya and Jindabyne suite. Jour. Geol. Soc. Australia, 25, 235-247.

Gromet, L.P. and Silver, L.T., 1983, Rare earth element distributions among minerals in a granodiorite and their petrogenetic implications. Geochim. Cosmochim. Acta, 47, 925-939.

Hanson, G.N., 1978, The application of trace elements to the petrogenesis of igneous rocks of granitic composition. Earth Planet. Sci. Lett., 38, 26-43.

Harper, C.T., 1967, On the interpretation of potassium-argon ages from Precambrian Shields and Phanerozoic Orogens. Earth Planet. Sci. Lett., 3, 128-132.

Harris, N.B.W. and Marriner, G.F., 1980, Geochemistry and petrogenesis of a peralkaline granite complex from Midian Mountains, Saudi Arabia. Lithos 13, 325-337.

Harvey, P.K., Taylor, D.M., Hendry, R.D. and Bancroft, F., 1973, An accurate fusion method for the analysis of rocks and chemically related materials by X-ray fluorescence spectrometry. X-ray spectrometry, 2, 33-44.

Haskin, L.A., Frey, F.A., Schmitt, R.A. and Smith, R.H., 1966, Meteoritic solar and terrestrial rare earth distributions. In: Physics and chemistry of the Earth (L.H. Ahrens, F. Press, S.K. Runcorn and H.C. Urey eds.). Pergamon Press Ltd., Oxford, v.5, 167-322.

Haskin, L.A., Haskin, M.A., Frey, F.A. and Wildeman, T.R., 1968, Relative and absolute terrestrial abundances of the rare earths. In: Origin and distribution of the elements (L.H. Ahrens ed.). Pergamon, New York, 889-912.

Haynes, S.J., 1978, Joint determination of fluorine and chlorine in granitic rocks with ion-selective electrodes. Talanta, 25, 85-89.

Heaman, L.M., Shieh, Y.N., McNutt, R.H. and Shaw, D.M., 1980, Interpretation of strontium and oxygen isotope data from the Loon Lake Pluton and the Apsley gneiss, Grenville Province, Ontario, EOS, 81, no. 17, 387.

Heier, K.S. and Adams, J.A.S., 1964, The geochemistry of the alkali metals. In: Physics and chemistry of the Earth (L.H. Ahrens, F. Press and S.K. Runcorn eds.). v.5, 253-381.

Heier, K.S. and Rogers, J.J.W., 1963, radiometric determination of thorium, uranium and potassium in basalts and in two magmatic differentiation series. Geochim. Cosmochim. Acta, 22, 137-154.

Hertogen, J. and Gijbels, R., 1976, Calculation of trace element fractionation during partial melting. Geochim. Cosmochim. Acta, 40, 313-322.

Hewitt, D.F., 1962, Wallaston Township. Ontario Dept. Mines, Geol. Rept. 11, 29-55.

Hewitt, D.F. and James, W., 1955, Geology of Dungannon and Mayo Townships. Ontario Dept. Mines, 64, pt.8, 65pp.

Hine, R. and Mason, D.R., 1978, Intrusive rocks associated with porphyry copper mineralization, New Britain, Papua New Guinea. Economic Geology, 73, 749-760.

Hine, R., Williams, I.S., Chappell, B.W. and White, A.J.R., Contrasts between I- and S-type granitoids of the Kosciusko Batholith. Jour. Geol. Soc. Australia, 25, 219-234..

Holm, P., Smith, T., Huang, C., Gerasimoff, M., Grant, B., Filbey, B. and McLauglin, K., 1984, Geochemistry of Grenville meta-igneous rocks from a portion of the Hastings Lowland (abs.). Geol. Assoc. Can. / Miner. Assoc. Can., Abstr. with Prog., 9, 74.

Hotz, P.E., 1971, Plutonic rocks of the Kamath Mountains, California and Oregon. U.S. Geol. Surv. Prof. Paper, 684-B.

Hung, W.H. and Johns, W.D., 1967, Simultaneous determination of fluorine and chlorine in silicate rocks by rapid spectrophotometric method Anal. Chim. Acta, 37, 508.

Ingham, W.N. and Keevil, N.B., 1951, Radioactivity of Bourlamaque, Elzevir and Cheddar Batholiths, Canada. Geol. Soc. Am. Bull., 62, 131-148.

Irving, E., Emslie, R.F. and Ueno, H., 1974, Upper Proterozoic paleomagnetic poles from Laurentia and the history of the Grenville Structural Province. Jour. Geophys. Res., 79, 5491-5502.

Jacobs, J.W., Korotev, R.L., Blanchard, D.P. and Haskin, L.A., 1977, A well-tested procedure for instrumental neutron activation analysis of silicate rocks and minerals. Jour. Radioanal. Chem., 40, 93-114.

James, R.S. and Hamilton, D.R., 1969, Phase relations in the system $NaAlSi_3O_8$ - $KAlSi_3O_8$ - $CaAl_2Si_2O_8$ - SiO_2 at 1 kilobar water vapour pressure. Contr. Mineral. Petrol, 21, 111-141.

Killeen, P.G. and Carmichael, C.M., 1970, Gamma-ray spectrometer calibration for field analysis of thorium, uranium and potassium. Can. Jour. Earth Sci., 7, 1093-1098.

Kimberley, M.M., 1978, High-temperature uranium geochemistry. In: short course in Uranium deposits: their mineralogy and origin (M.M. Kimberley ed.). Mineral. Assoc. Can., 101-104.

Kleeman, A.W., 1965, The origin of granitic magmas. Jour. Geol. Soc. Australia, 12, 35-52.

Koljonen, T. and Rosenberg, R.J., 1974, Rare earth elements in granitic rocks. Lithos, 7, 249-261.

Kosterin, A.V., 1959, The possible modes of transport of the rare earths by hydrothermal soloutions. Geochemistry, 1959 vol, 381-387.

Krogh, T.E. and Hurley, P.M., 1968, Strontium isotope variation and whole-rock isochron studies, Grenville Province of Ontario. Jour. Geophys. Res., 73, 7107-7125.

Krogh, T.E. and Davis, G.L., 1969, Geochronology of the Grenville Province. Carnegie Institute of Washington Yearbook, 67, 224-230.

Krogh, T.E. and Davis, G.L., 1970, Isotopic ages along the Grenville Front in Ontario. Carnegie Institute of Washington Yearbook 68, 309-313.

Krogh, T.E. and Davis, G.L., 1973, The significance of inherited zircons on the age and origin of igneous rocks - an investigation of the Labrador adamellites. Carnegie Institute Washington Yearbook 72, 610-613.

Krumbein, W.C. and Slack, H.A., 1958, Statistical analysis of low-level radioactivity of Pennsyvanian black fissile shale in Illinois. Geol. Soc. Am. Bull., 67, 739-762.

Kuehnbaum, R.M., 1973, Petrology of the Deloro Pluton and associated country rocks, near Madoc, Ontario. Unpubl. M.Sc. thesis, Univerisity of Toronto, Toronto, 173pp.

Leake, B.E., 1968, A catalog of analyzed calciferous and subcalciferous ampohiboles together with their nomenclature and associated minerals. Geol. Soc. Am. Spec. Paper 98, 210pp.

Loiselle, M.C. and Wones, 1979, Characteristics and origin of anorogenic granites (abs.). Geol. Soc. Am., Abstr. with Prog., 11, 48.

Lumbers, S.B., 1967, Stratigraphy, plutonism, and metamorphism in the Ottawa River Remnant in the Bancroft-Madoc Area of the Grenville Province of southeastern Ontario, Canada. Unpubl. Ph.D. thesis, Princeton University, 331pp.

Lumbers, S.B., 1968, Geology of Cashel Township, Ontario Dept. Mines, Geol. Rept., 71, 54pp.

Lumbers, S.B., 1971, Geology of the North Bay Area, District of Nippissing and Parry Sound. Ontario Div. Mines and Northern Affairs, Geol. Rept., 94, 104pp.

Lumbers, S.B., 1975, Geology of the Burwash Area, Districts of Nipissing, Parry Sound and Sudbury. Ontario Division of Mines, Geol. Rept. 116, 160pp.

Lumbers, S.B., 1978, Geology of the Grenville Front Tectonic Zone between Sudbury and Timagami, Ontario. Geol. Assoc. Can. / Geol. Assoc. Am., Annual meeting, Guidebook, 347-361.

Lumbers, S.B., 1982, Summary of metallogeny - Renfrew county area. Ontario Geol. Surv., Rept. 212, 53pp.

Lumbers, S.B. and Krong, T.E., 1977, Distribution and age of anorthosite suite intrusions in the Grenville province of Ontario (abs.). Geol. Assoc. Can. / Mineral. Assoc. Can., Abstr. with Prog.,

Luth, W.C., Jahns, R.H. and Tuttle, O.F., 1964, The granite system at pressure of 4 to 10 kilobars. Jour. Geophys. Res., 69, 759-773.

Luth, W.C., 1969, The sysetem $NaAlSi_3O_8$ - SiO_2 to 20 Kb and the relationship between H_2O content, P_{H2O} and P_{total} in granitic magmas. Am. Jour. Sci., 267A, 325-341.

MacIntyre, R.M., York, D. and Moorhouse, W.W., 1967, Potassium-argon age determinations in the Madoc-Bancroft area in the Grenville Province of the Canadian Shield. Can. Jour. Earth Sci., 4, 815-828.

MacRae, N.D. and Nesbitt, H.W., 1980, Partial melting of common metasedimentary rocks: a mass balance approach. Contr. Mineral. Petrol., 75, 21-26.

Magaritz, M. and Taylor, H.P. Jr, 1976, Isotopic evidence for meteoric - hydrothermal alteration of plutonic igneous rocks in the Yakutat Bay and Skagway areas, Alaska. Earth Planet. Sci. Lett., 30, 179-190.

Mahood, G. and Hildreth, W., 1983, Large partition coefficients for trace elements in high-silica rhyolites. Geochim. Cosmochim. Acta, 47, 11-30.

Martin, R.F. and Bonin, B., 1976, Water and magma genesis: the association hypersolvus granite - subsolvus granite. Can. Mineral., 14, 228-237.

Martin, R.F. and Piwinski, A.J., 1972, Magmatism and Tectonic Settings. Jour. Geophys. Res., 77, no.2, 4966-4975.

Mason, B., 1966, Principles of Geochemistry. John Wiley and Sons, New York, 3rd edition, 329pp.

McCarthy, T.S. and Groves, D.I., 1979, The Blue Tier Batholith, northeastern Tasmania, a cumulate-like product of fractional crystallization. Contr. Mineral. Petrol., 71, 193-209.

McCarthy, T.S. and Hasty, R.A., 1976, Trace element distribution patterns and their relationship to the crystallization of granitic melt. Geochim. Cosmochim. Acta, 40, 1351-1358.

McCarthy, T.S. and Kable, E.J.D., 1978, On the behavior of rare-earth elements during partial melting of granitic rock. Chem. Geol., 22, 21-29.

McCrank, G.F.D., Misiura, J.D. and Brown, P.A., 1980, Plutonic rocks in Ontario. Geol. Surv. Can., Paper 80-23, 171pp.

McLennan, S.M. and Taylor, S.R., 1979, Rare earth element mobility associated with uranium mineralization. Nature, 282, 247-250.

McLennan, S.M., Fryer, B.J. and Young, G.M., 1979, Rare earth elements in Huronian (Lower Proterozoic) sedimentary rocks: composition and evolution of the post-Kenoran upper crust. Geochim. Cosmochim. Acta, 40, 375-388.

Miller, R.R. and Gittins, J., 1982, Geochronology and Petrology of the Grenville Nepheline-bearing suite: a metamorphosed rift environment (abs.). Ottawa-Carleton Centre for Geosciences Studies, Grenville Workshop, Prog. and Abstr., p.7.

Miller, C.F., 1977, Early alkalic plutonism in the calc-alkalic batholithic belt of California. Geology, 5, 685-688.

Miller, C.F., 1978, Monzonitic plutons, California, and a model for generation of alkali-rich, near silica-saturated magmas. Contr. Mineral. Petrol., 67, 349-355.

Miller, C.F. and Bradfish, L.J., 1980, An inner Cordilleran Belt of muscovite-bearing plutons. Geology, 8, 412-416.

Miller, C.F. and Mittlefehldt, D.W., 1982, Depletion of light rare-earth elements in felsic magmas. Geology, 10, 129-133.

Miller, C.F., Stoddard, E.F., Bradfish, L.J. and Dollase, W.A., 1981, Composition of plutonic muscovite: genetic implications. Can. Mineral., 19, 25-34.

Mittlefehldt, D.W. and Miller, C.F., 1983, Geochemistry of the Sweetwater Wash Pluton, California: implications for "anomalous" trace element behavior during differentiation of felsic magmas. Geochim. Cosmochim. Acta, 47, 109-124.

Miyashiro, A., 1978, Nature of alkalic rock series. Contr. Mineral. Petrol., 66, 91-104.

Moench, R.H. and Gates, O., 1976, Bimodal volcanic suites of Silurian and early Devonian age, Machias - Eastport area, Maine. Geol. Soc. Am., Abstr. and Prog., 8, 232.

Moore, J.M. Jr., 1982, Stratigraphy and tectonics of the Grenvillian Orogen in eastern Ontario. Ottawa-Carleton Centre for Geoscience Studies, Grenville Workshop, Prog. and Abstr., p.7.

Moore, J.M. Jr. and Thompson, P.H., 1972, The Flinton Group, Grenville Province, eastern Ontario. 24th International Geological Congress, Proceedings, sec. 1, 221-229.

Morris, W.A. and Roy, J.L., 1977, Discovery of Hadrynian polar track and the Grenville problem revisited. Nature, 266, 689-692.

Nagasawa, H.H. and Schnetzler, C.C., 1971, Partitioning of rare earth, alkalie and alkaline earth elements between phenocrysts and acidic igneous magma. Geochim. Cosmochim. Acta, 35, 953-968.

Neilson, D.L., Clark, R.G., Lyons, J.B., Englund, E.J., and Borns, D.J., 1976, Chronology and styles of multiple deformation, plutonism, and polymetamorphism in the Merrimack synclinorium of Western Maine. Geol. Soc. Am. Mem., 146,

203-238.

Nisbet, E.G., Dietrich, V.J. and Esenwein, A., 1979, Routine trace elemet determination in silicate minerals and rocks by X-ray fluorescence. Fortschr. Miner., 57, 264-279.

Nockolds, S.R., 1954, Average chemical compositions of some igneous rocks. Geol. Soc. Am. Bull., 65, 1007-1032.

Nockolds, S.R. and Mitchell, R.L., 1948, The geochemistry of some Caledonian plutonic rocks: a study in the relationship between the major and trace elements of igneous rocks and their minerals. Trans. Roy. Soc. Edinburg, 6, 533-575.

Nockolds, S.R. and Allen, R., 1953, The geochemistry of some igneous rock series. Geochim. Cosmochim. Acta, 4, 105,142.

Nockolds, S.R. and Allen, R., 1956, The geochemistry of some igneous rock series, Part III. Geochim. Cosmochim. Acta, 9, 34-77.

Norrish, K. and Hotton, J.T., 1969, An accurate X-ray spectrographic method for the analysis a wide range of geological samples. Geochim. Cosmochim. Acta, 33, 431-453.

O'Connor, J.T., 1965, A classification for quartz-rich igneous rocks based on feldspar ratios. U.S. Geol. Surv. Prof. Paper 525-B, 79-84.

Olade, M.A., 1976, Geochemical evolution of copper-bearing granitic rocks of Guichon Creek Batholith, British Columbia, Canada. Can. Jour. Earth Sci., 13, 199-209.

O'Leary, M., Lippert, R.H. and Spitz, O.T., 1966, FORTRAN IV and map program for computation and plotting of trend surfaces for degree 1 through 6. Computer Contribution no. 3, State Geol. Surv., The university of Kansas, Lawrence, 47pp.

O'Neil, J.R. and Chappell, B.W., 1977, Oxygen and hydrogen isotope relations in Berridale Batholith. Jour. Geol. Soc. London, 133, 559-571.

O'Neil, J.R., Shaw, S.E. and Flood, R.H., 1977, Oxygen and hydrogen isotope compositions as indicators of granite genesis in the New England Batholith, Australia. Contr. Mineral. Petro. 62, 313-328.

O'Neil, J.R. and Taylor, H.P. Jr., 1967, The oxygen isotope and cation exchange chemistry of feldspars. Am. Mineral., 52, 1414-1437.

Osberg, P.H., 1978, Synthesis of the geology of the northeastern Appalachians, U.S.A. Geol. Surv. Can. Paper 78-13, 137-148.

Palmer, H.C. and Carmichael, C.M., 1973, Paleomagnetism of some Grenville Province rocks. Can. Jour. Earth Sci., 14, 1876-1887.

Parks, J.M., 1970, FORTRAN IV program for Q-mode cluster analysis on distance function with printed dendrogram. Computer Contribution. no.46, State Geol. Surv., The University of Kansas, Lawrence.

Peacock, M.A., 1931, Classification of igneous rock series. Jour. Geol., 85, 383-393.

Pearce, J.A. and Cann, J.R., 1973, Tectonic setting of basic volcanic rocks determined using trace element analyses. Earth planet. Sci. Lett., 19, 290-300.

Pearce, J.A. and Norry, M.J., 1979, Petrogenetic implications of Ti, Zr, Y and Nb variations in volcanic rocks. Contr. Mineral. petrol., 69, 33-47.

Petro, W.L., Vogel, T.A. and Wilband, J.T., 1979, Major-element chemistry of plutonic rock suites from compressional and extensional plate boundaries. Chem. Geology, 26, 217-235.

Povarennykh, A.S., 1972, The role of crystallo-chemical factors in the distribution of rare elements in minerals. 24th Internat. Geol. Congress, sec. 10, 85-92.

Pride, C. and Moore, J.M. Jr., 1983, Petrogenesis of the Elzevir batholith and related trondhjemitic intrusions in the Grenville Province of eastern Ontario, Canada. Contr. Mineral. Petrol., 82, 187-194.

Pride, C. and Muecke, G.K., 1980, Geochemistry and origin of granitic rocks, Scourian Complex, NW Scottand. Contr. Mineral. Petrol., 80, 379-385.

Radain, A.A.M., 1978, petrogenesis of some peralkaline and non-peralkaline post-tectonic granites in the Arabian Shield, Kingdom of Saudi Arabia. Unpubl. Ph.D. thesis, University of Western Ontario, London, Ontario, 246pp.

Radain, A.A.M., Fyfe, W.S. and Kerrich, R., 1981, Origin of peralkaline granites of Saudi Arabia. Contr. Mineral. Petrol., 78, 358-366.

Rayleigh, J.W.S., 1896, Theoretical considerations respecting the separation of gases by diffusion and similar processes. Philos. Mag., 42, 77-82.

Richter, D.H., Lanphere M.A. and Matson, N.A. Jr., 1975, Granitic plutonism and metamorphism, eastern Alaska Range, Alaska. Geol. Soc. Am. Bull., 86, 819-829.

Ringwood, A.E., 1955, The principles governing trace element distribution during magmatic crystallization, Part I and II. Geochim. Cosmochim. Acta, 7, 189-242.

Rogers, J.J.W. and Novitsky-Evans, J.M., 1977, The Clarno Formation of Central Oregon, U.S.A. - volcanism on a thin continental margin. Earth Planet. Sci. Lett., 34, 56-66.

Rogers, J.J.W., Hodges, K.V. and Ghuma, M.A., 1980, Trace elements in continental-margin magmatism: Part II; trace elements in Ben Ghnema Batholith and

nature of the Precambrian crust in central North Africa. Geol. Soc. Am. Bull., 91, 1742-1788.

Rogers, J.J.W. and Ragland, P.C., 1961, Variation of thorium and uranium in selected granitic rocks. Geochim. Cosmochim. Acta, 25, 99-109.

Rogers, J.J.W. and Adams, J.A.A., 1969a, Thorium, In: Handbook of geochemistry, v.11/4, sec.90 (K.H. Wedepohl ed.). Springer Verlag, Berlin.

Rogers, J.J.W. and Adams, J.A.s., 1969b, Uranium, In: Handbook of geochemistry, v.11/4, sec.92 (K.H. Wedepohl ed.). Springer Verlag, Berlin.

Robinson, S.C., 1961, Economic uranium deposits in granitic dykes, Bancroft District, Ontario. Can. Mineral., 6, 513-521.

Saha, A.K., 1957, The mode of emplacement of some granitic plutons in southeastern Ontario. Unpubl. Ph.D. thesis, University of Toronto, Toronto.

Saha, A.K., 1959, Emplacement of three granitic plutons in southeastern Ontario, Canada. Geol. Soc. Am. Bull., 70, 1293-1326.

Sampson, G.A., 1972, Petrology of some Grenville volcanic and pelitic rocks from near Madoc, southeastern Ontario. Unpubl. Ph.D. thesis, University of Toronto, Toronto, Ontario, 218pp.

Sasaki, a. and Ishihara, S., 1979, Sulfur isotopic composition of the magnetite-series and ilmenite-series granitoids in Japan. Contr. Mineral. Petrol. 68, 107-115.

Sauerbrei, J.A., 1966, The granitic rocks of the Frontenac Axis. Unpubl. M.Sc. thesis, Queen's Univeristy, Kingston, Ontario, 115pp.

Saunders, A.D., Tarney, J. and Weaver, S.D., 1980, Transverse geochemical variations across the Antarctic Peninsula: implications for the genesis of calc-alkaline magmas. Earth Planet. Sci.

Lett., 46, 344-360.

Schwerdtner, W.M. and Lumbers, S.B., 1980, Major diapiric structures in the Superior and Grenville Provinces of the Canadian Shield. In: the continental crust and its mineral deposits (D.W. Strangway ed.). Geol. Assoc. Can., Spec. Paper 20, 149-180.

Sethuraman, K. and Moore, J.M. Jr., 1973, Petrology of metavolcanic rocks in the Bishop Corners - Donaldson area, Grenville Province, eastern Ontario. Can. Jour. Earth Sci., 10, 589-614.

Shaw, D.M., 1970, Trace element fractionation during anatexis. Geochim. Cosmochim. Acta, 34, 237-243.

Shaw, D.M., 1972, Origin of the Apsley gneiss. Can. Jour. Earth Sci., 9, 18-35.

Shaw, D.M., 1978, Trace element behavior during anatexis in the presence of a fluid phase. Geochim. Cosmochim. Acta, 42, 933-943.

Shieh, Y.N., 1978, High ^{18}O granitic plutons from the Frontenac Axis, Grenville Province of Ontario (abs.). Geol. Assoc. Can. / Mineral. Assoc. Can., Abstr. with Prog., 10, no. 7, 493.

Shieh, Y.N., 1980, Oxygen isotope compositions of granitic and syenitic plutons in the Central Metasedimentary Belt, Grenville Province of Ontario. EOS, 61, no. 17, 410.

Shieh, Y.N., and Schwarcz, H.P., 1974, Oxygen isotope studies of granite and migmatite, Grenville Province of Ontario, Canada. Geochim. Cosmochim. Acta, 38, 21-45.

Siedner, G., 1965, Geochemical features of a strongly fractionated alkali igneous suite. Geochim. Cosmochim. Acta, 29, 113-137.

Silver, L.T., 1969, A geochronologic investigation of Adirondack Complex, Adirondack Mountains, New York. In: origin of Anorthosite and related rocks (Y.W. Isachsen ed.): N.Y. State Museum Service, Mem. 18, 233-251.

Silver, L.T. and Lumbers, S.B., 1965, Geochronologic studies in the Bancroft-Madoc area of the Grenville Province, Ontario, Canada (abs.). Geol. Soc. Am., Abstr. with Prog., 153.

Silver, L.T. and Lumbers, S.B., 1966, Geochronologic studies in the Bancroft-Madoc area of the Grenville Province, Ontario, Canada (abs.). Geol. Soc. Am. Spec. Publ. no. 87.

Silver, L.T., Bickford, M.E., Van Schmus, W.R., Anderson, J.L., Anderson, T.H. and Madaris, L.G. Jr., 1977, The 1.4-1.5 b.y. transcontinental anorogenic plutonic perforation of North America (abs.). Geol. Soc. Am., Abstr. with Prog., 9, no. 7, 1176-1177.

Simpson, P.R., Brown, G.C., Plant, J. and Ostle, D., 1979, Uranium mineralization and granite magmatism in the British Isles. Phil. Trans. Roy. Soc. London, A-291, 385-412.

Somers, G, 1984, Geochemistry and petrogenesis of White Lake pluton, southeast Ontario. Unpubl. M.Sc. thesis, University of Western Ontario (in preparation).

Stockwell, C.H., 1972, Deloro stock - southeastern Ontario. (rubidium - strontinum isochron age studies). Geol. Surv. Can., Paper 72-23, 49-52.

Stormer, J.C. Jr., 1975, A practical two-feldspar geothermometer. Am. Mineral., 60, 667-674.

Stormer, J.C. Jr. and Nicholls, J., 1978, XLFRAC: a program for the interactive testing of magmatic differenciation models. Computer and Geosciences, 4, 143-159.

Streckeisen, A., 1976, To each plutonic rock its proper name. Earth Science Reviews, 12, 1-33.

Strong, D.F. and Minatidis, D.G., 1975, Geochemistry and tectonic setting of the late Precambrian Holyrood plutonic series of eastern Newfoundland. Lithos, 8, 283-295.

Takahashi, M., Aramaki, S. and Ishihara, S., 1980, Magnetite - series / Ilmenite - series vs. I-type / S-type granitoids. Mining Geol. Special Issue, 8, 13-28.

Tarney, J. and Saunders, A.D., 1979, Trace element constraints on the origin of Cordilleran Batholiths. In: Origin of Granite Batholiths: Geochemical evidence (M.P. Atherton and J. Tarney eds.). Shiva Publishing Limited, 90-105.

Tarney, J. and Windly, B.F., 1977, Chemistry, thermal gradients and evolution of the lower continental crust. Jour. Geol. Soc. London, 134, 153-172.

Tauson, L.V., 1965, Factors in the distribution of the trace elements during the crystallization of magmas. In: Physics and chemistry of the Earth (L.H. Ahrens, F. Press, S.K. Runcorn and H.C. Urey eds.). Pergamon Press, Oxford, v.6, 215-249.

Tauson, L.V., 1967, Geochemical behaviour of rare earth elements during crystallization and differentiation of granitic magmas. Geochem. Int., 4, 1067-1074.

Taylor, H.P., 1968, The oxygen isotope geochemistry of igneous rocks. Contr. Mineral. Petrol., 19, 1-71.

Taylor, H.P. Jr., 1978, Oxygen and hydrogen isotope studies of plutonic granitic rocks. Earth Planet. Sci. Lett., 38, 177-210.

Taylor, H.P. Jr. and Epstein, S., 1962, Relationship between $^{18}O/^{16}O$ ratios in coexisting minerals of igneous and metamorphic rocks, I. principles and experimental results. Geol. Soc. Am. Bull.,

73, 461-480.

Taylor, H.P. and Turi, B., 1976, High-^{18}O igneous rocks from Tuscan magmatic province, Italy. Contr. Mineral. Petrol., 55, 33-54.

Taylor, R.P., Strong, D.F. and Fryer, B.J., 1981, Volatile control of contrasting trace element distributions in peralkaline granitic and volcanic rocks. Contr. Mineral. petrol., 77, 267-271.

Taylor, S.R., 1964, Abundance of chemical elements in the continental crust: a new table. Geochim, Cosmochim. Acta, 28, 1273-1285.

Taylor, S.R., 1965, The application of trace element data to problems in petrology. In: physics and chemistry of the Earth (L.M. Ahrens, F. Press, S.K. Runcorn and H.C. Urey eds.). v.6, 133-214.

Taylor, S.R., Emeleus, C.H. and Exley, C.S., 1956, Some anomalous K / Rb ratios in igneous rocks and their petrological significance. Geochim. Cosmochim. Acta, 10, 224-229.

Teng, H.C. and Strong, D.F., 1976, Geology and geochemistry of the St. Lawrence peralkaline granite and associated fluorite deposits, southeast Newfoundland. Can. Jour. Earth Sci., 13, 1374-1385.

Thomas, W.A., 1977, Evolution of Appalachian-Ouachita salients and recesses from reentrants and promontories in the continental margin. Am. Jour. Sci., 277, 1233-1278.

Thompson, J.B. Jr., and Norton, S.A., 1968, Paleozoic regional metamorphism in New England and adjacent areas. In: studies of Appalachian Geology, Northern and Maritime (Zen, E-an ed.). Interscience, New York, 319-327.

Thompson, R.N., 1969, Ternary granites and associated rocks of the Marsco area, Island of Skye. Quat. Jour. Geol. Soc. London, 124, 349-385.

Tilley, C.E. and Gittins, J., 1961, Igneous nepheline-bearing rocks of the Haliburton-Bancroft, province of Ontario. Jour. Petrol., 2, 38-48.

Tindle, A.G. and Pearce, J.A., 1981, Petrogenetic modelling of in situ fractionational crystalization in the zoned Loch Doon pluton, Scotland. Contr. Mineral. Petrol., 78, 196-207.

Thornton, C.P. and Tuttle, O.F., 1960, Chemistry of igneous rocks. I. Differentiation index. Am. Jour. Sci.,258, 664-684.

Turekian, K.K. and Wedepohl, K.H., 1961, Distribution of elements in some major units of the Earth's crust. Geol. Soc. Am. Bull., 72, 175-192.

Turner, F.J. and Verhoogen, J., 1969, Igneous and metamorphic petrology. McGraw-Hill Book Co., New York, 694pp.

Tuttle, O.F. and Bowen, N.L., 1958, Origin of granite in light of experimental studies. Geol. Soc. Am. Mem. 74, 153pp.

Upton, B.G.J., 1960, The Alkaline igneous complex of Kungnat Fjeld, South Greenland. Medd. om Gronland, 123, no.4, 145pp.

Waldbaum, D.R. and Thompson, J.B., 1969, Mixing properties of sanidine crystalline solutions: IV. Phase diagrams from equation of state. Am. Mineral., 54, 811-838.

Watson, E.B., 1976, Two liquid partition coefficients: Experimental data and geochemical implications. Contr. Mineral. Petrol., 56, 119-134.

Watson, E.B., 1979, Zircon saturation in felsic liquids: experimental results and application to trace element geochemistry. Contr. Mineral. Petrol., 70, 407-419.

Watt, W.S., 1966, Chemical analyses from the Gardar igneous province, South Greenland. Grönlands Geol. Unders., Rapp. Nr. 6, 92pp.

Weaver, B.L., 1980, Rare earth element geochemistry of Madras granulites. Contr. Mineral. Petrol., 71, 271-279.

Whalen, J.B., 1983, The Ackley City Batholith, southeastern Newfoundland: evidence for crystal versus liquid-state fractionation. Geochim. Cosmochim. Acta, 47, 1443-1457.

White, A.J.R., 1979, Sources of granite magmas (abs.) Geol. Soc. Am., Abstr. with Prog., 539.

White, A.J.R. and Chappell, B.W., 1977, Ultrametamorphism and granitoid gensis, Tectonophysics, 43, 7-22.

Wilson, A.D., 1955, A new method for determination of ferrous iron in rocks and minerals. Bull. Geol. Serv. Gt. Britain, 9, 56-68.

Windley, B.F., 1977, The evolving continents. John Wiley and Sons, London, 384pp.

Winkler, H.G.F., 1961, Genesen von graniten und migmatiten auf grund neuer experimente. Geol. Rund., 51, 347-364.

Winkler, H.G.F., 1967, Petrogenesis of metamorphic rocks. Springer-Verlag, 2nd edition, 237pp.

Winkler, H.G.F., and Von Platen, H., 1961, Experimentelle Gesteins metamorphose, V. Experimentelle anatektischer schmelzen und ihre petro-genetische Bedeutung. Geochim. Cosmochim. Acta, 24, 250-259.

Wones, D.R., 1979, Intensive parameters during the crystallization of granitic plutons. Geol. Soc. Am., Abstr. with Prog., 11, 543.

Wones, D.R., 1980, A comparison between granitic plutons of New England, U.S.A. and the Sierra Nevada Batholith, California. In: the Caledonides in the USA, proceedings (D.R. Wones ed.). Dept. Geological Sci., Virginia Polytechnic Institute and State University, memoir 2, 123-130.

Wousen, G., Roy, D.W., Dimroth, E., Chown, E.H., 1984, The Grenville Province as a Proterozoic extension-contraction cycle (abs.). Geol. Assoc. Can. / Miner. Assoc. Can. Abstr. with Prog., 9, 117.

Wyllie, P.J., 1963, Applications of high pressure studies to the earth sciences. In: high pressure physics and chemistry (R.S. Bradly ed.). v2, 1-89, Academic Press, London.

Wyllie, P.J., Huang, W.L., Stern, C.R. and Maaloe, S., 1976, Granitic magmas: possible and impossible sources, water contents, and crystallization sequences. Can. Jour. Earth Sci., 13, 1007-1019.

Wynne-Edwards, H.R., 1967, The Grenville Province, In: guidebook - geology of parts of eastern Ontario and western Quebec, 1-4. Annual meeting, Geol. Assoc. Can. / Mineral. Assoc. Can. / Mineral. Assoc. Am., Kingston, Canada.

Wynne-Edwards, H.R., 1972, The Grenville Province. Geol. Assoc. Can. Spec. Paper 11, 263-334.

Wynne-Edwards, H.R., 1976, Proterozoic ensialic orogenies: the millipede model of ductile plate tectonics. Am. Jour. Sci., 276, 927-953.

The University of Western Ontario

Faculty of Graduate Studies
Stevenson-Lawson Building
London, Canada
N6A 5B8

TO WHOM IT MAY CONCERN:

THIS IS TO ADVISE THAT APPENDIX C (1, 2 and 3) IN THE THESIS OF DR.TSAI-WAY WU WHICH IS TO BE INSERTED IN A POCKET ON THE BACK COVER OF VOLUME II, IS IN MICROFICHE FORM AND IS AVAILABLE TO THE READER THROUGH INTERLIBRARY LOANS ALONG WITH THE THESIS

END

1	2	6	0	3	8	5

FIN